Wisconsin Highway Research Program

Construction Vibration Attenuation with Distance and its Effect on the Quality of Early-Age Concrete

SPR # 0092-06-04

John Siwula, PE, MS
Sam Helwany, PE, PhD, Richard Lyons, PE, MS

HNTB Corporation

University of Wisconsin-Milwaukee
Department of Civil Engineering and Mechanics

September 2011

WHRP 11-02

Disclaimer

This research was funded through the Wisconsin Highway Research Program by the Wisconsin Department of Transportation and the Federal Highway Administration under Project 0092-06-04. The contents of this report reflect the views of the authors who are responsible for the facts and accuracy of the data presented herein. The contents do not necessarily reflect the official views of the Wisconsin Department of Transportation or the Federal Highway Administration at the time of publication.

This document is disseminated under the sponsorship of the Department of Transportation in the interest of information exchange. The United States Government assumes no liability for its contents or use thereof. This report does not constitute a standard, specification or regulation.

The United States Government does not endorse products or manufacturers. Trade and manufacturers' names appear in this report only because they are considered essential to the object of the document.

Technical Report Documentation Page

1. Report No. WHRP 11-02	2. Government Accession No	3. Recipient's Catalog No
4. Title and Subtitle Construction Vibration Attenuation with Distance and its Effect on the Quality of Early-Age Concrete		5. Report Date June 2011 6. Performing Organization Code Wisconsin Highway Research Program
7. Authors John Siwula, PE, MS, HNTB Corporation, Sam Helwany, PE, PhD, UW-Milwaukee Richard Lyons, PE, MS, HNTB Corporation		8. Performing Organization Report No.
9. Performing Organization Name and Address HNTB Corporation West Park Place, Suite 300 Milwaukee, WI 53224-3526		10. Work Unit No. (TRAIS) 11. Contract or Grant No. WisDOT SPR# 0092-06-04
12. Sponsoring Agency Name and Address Wisconsin Department of Transportation Division of Business Services Research Coordination Section 4802 Sheboygan Ave. Rm 104 Madison, WI 53707		13. Type of Report and Period Covered Final Report, 2005-2011 14. Sponsoring Agency Code
15. Supplementary Notes		

16. Abstract

Damage to structures due to vibrations from pile driving operations is of great concern to engineers. This research has stemmed from the need to address potential damage to concrete-filled pipe piles and recently placed concrete structures that could be affected by pile driving vibrations. The study will focus on two topics: (1) The attenuation of potentially damaging pile driving vibrations with distance from the source, and (2) The effects of distance and curing time of concrete on the quality (unconfined compressive strength) of recently-placed concrete exposed to pile driving vibrations. The effects of pile driving vibrations did not cause problems with concrete compressive strength except for the case where concrete had only cured for 4 to 6 hours before vibration.

17. Key Words	18. Distribution Statement
Pile driving, vibrations, peak particle velocity, concrete strength, cure time, scaled distance, beams, cylinders.	No restriction. This document is available to the public through the National Technical Information Service 5285 Port Royal Road Springfield VA 22161

19. Security Classif.(of this report)	19. Security Classif. (of this page)	20. No. of Pages	21. Price
Unclassified	Unclassified	455	

Acknowledgements

This research was sponsored by the Wisconsin Department of Transportation through the Wisconsin Highway Research Program. The authors acknowledge staff from both organizations and individuals from HNTB for assistance provided during this project. Thanks to the Technical Oversight Committee members Jeffrey Horsfall (Chair), Robert Arndorfer, Daniel Reid, and Andrew Zimmer for help through the process. Also thanks to Steve Maxwell for performing PDA testing as part of the field study. Wisconsin Department of Transportation field crews directed by Timothy Stoikes provided drilling services which were a great benefit. David Jaromin, Jintae Lee, Therese Koutnik, Scott Miller, and Sara Padarath of HNTB were instrumental in various aspect of the research. The Edward E. Gillen Company performed pile driving services which were necessary for the field study and Meyer Materials provided concrete for both the laboratory and field study. Giles Engineering Associates performed excavations to construct field concrete block samples and drilled the borings for below grade vibration monitor placement. Lastly, the research team is grateful to the Port Authority of Milwaukee, particularly Larry Sullivan for allowing the field study to be performed on their property.

Executive Summary

Project Summary

The research consisted of a laboratory and field study that focused on vibration effects on concrete strength and the attenuation of potentially damaging pile driving vibrations with distance from the source. Concrete samples with variable cure times were exposed to vibrations of different magnitudes based on distance from a pile driving hammer source. The quality (compressive strength) of concrete exposed to the vibrations was tested to see what effect the cure time and/or vibration magnitude had on the material.

Damage to structures due to vibrations from pile driving operations is of great concern to engineers and contractors. The concern relates to potential liability for reported damage claims. This research has stemmed from the need to address potential damage to concrete-filled pipe piles and recently placed concrete structures that could be affected by pile driving vibrations.

The Wisconsin Department of Transportation has requirements for pile driving operations. For Cast In Place Concrete pipe piles pile driving activities are restricted. If concrete cylinder tests are being used where field operations are not controlled by cylinder tests, the contractor must wait at least 14 days to drive pile shells within 15 feet of recently cast piles in an effort to reduce damage to piles. Concrete strength testing can be used to attempt to reduce the time before driving other piles. These requirements can delay foundation construction and completion of transportation projects. These delays can also negatively impact the travelling public. The research was performed to determine if vibrations could affect concrete strength and what vibration levels were associated with strength reductions. It was desired to determine the relationship between vibration attenuation with distance from the pile driving source such that the current pile driving requirements may be reduced.

Background

Damage to structures from vibrations has been a concern for a long time. The former United States Bureau of Mines has performed extensive research related to blast induced vibrations over a period

of at least 50 years. Research has also been performed by others to attempt to identify the main factors that result in vibration damage. The research has shown that certain vibration levels can result in damage to structures. However, the extent of damage depends on many variables including distance from the vibration source, energy of the source, structure condition and construction materials, surface topography, and subsurface conditions.

The vibration effect on structures is also a perception problem because of human sensitivity to vibrations. Humans can detect very low levels of vibrations and vibrations that would be considered unpleaseant to an individual are typically not of sufficient magnitude to create structural problems. However, the layperson does not understand the relationship between vibration magnitude and the effect on structural condition. Claims that structure damage has occurred are often made even though the condition of a structure before and after a vibration event are unchanged. This happens because individuals typically do not inventory cracks in structures until vibrations from an outside source occur and they notice things that previously went unnoticed.

Due to the many variables that affect vibration transmission and the human perception problem, pre- and post-construction structure condition surveys are performed to provide a record of conditions. This process helps with unwarranted damage claims but also adds time and cost to construction projects.

Process

The process consisted of two separate phases of study. A laboratory and desktop analysis phase and a field study phase. The analysis work was performed to evaluate variables affecting vibrations and the laboratory testing of concrete looked at concrete strength based on variable curing times and the effect of different magnitudes of vibration. The field study phase used a pile driving hammer to create vibrations at various distances from concrete samples with variable cure times. Instrumentation was installed to monitor vibrations and sound.

A finite element analysis was carried out to investigate the effects of varying pile sizes, pile types, and hammers on ground surface vibrations. The finite element results were compared with: (1) Common empirical equations used for vibration predictions, and (2) Limited number of field tests that include vibration measurements caused by pile driving operations. To investigate the effects of

distance and curing time of concrete on the quality of recently-placed concrete exposed to pile driving vibrations, a comprehensive laboratory testing program for 90 concrete cylinder and 36 concrete beam samples subjected to various peak particle velocities and various curing times was carried out.

A comprehensive field testing program was performed to monitor pile driving induced vibrations. A Vulcan 08 air pile driving hammer was used to generate vibrations at two pile locations. Vibration and noise were monitored using seismographs. Geophone monitors were placed on the surface and at 10 feet below grade to collect vibration data at prescribed distances from the pile hammer which allowed attenuation equations to be generated. Pile Driving Analyzer measurements were also taken to measure pie driving energy. A total of 72 concrete cylinders and 24 concrete beams were constructed, extracted from the field and tested in the laboratory for strength.

Findings and Conclusions

The results of the study indicate that the vibrations levels had little effect on the concrete unconfined compressive strength of both the laboratory and field samples. The variable cure time also had little effect on the concrete strength with the exception of laboratory beam samples cured for 4 to 6 hours prior to vibration. The results are consistent with previous research.

The vibrations measured in the field at the surface were greater than those measured at a 10-foot depth. The lower vibrations at depth are due to material damping below ground. Geometric damping resulted in attenuation of vibrations with distance from the source. The field data exhibited more data variability than the laboratory data.

Based on the results of this study, the current Wisconsin Department of Transportation specifications for driving Cast In Place pipe pile are too restrictive. Consideration should be given to modifying the requirements to reduce pile construction time.

Additional research topics that should be considered are:

1. Pile driving vibration related settlement in soil profiles

2. Freeze-thaw effect on early age concrete after pile driving
3. Microstructure inspection of concrete and air voids of concrete
4. Durability, workability and other concrete strength properties for different curing times and vibrations
5. Test other concrete mixes (e.g. different admixtures such as mid-range and high range water reducers, silica fume, corrosion inhibitors, etc) and types of concrete mixes (e.g. high early strength, CLSM, cellular foamed concrete, etc)
6. Determine if a maturity meter application can reliably be used to develop a reliable correlations related to concrete strength subjected to vibrations
7. Shear bond strength for reinforcing steel

Table of Contents

Disclaimer i
Technical Report Documentation Page ii
Acknowledgements iii
Executive Summary iv
Project Summary iv
Background iv
Process v
Findings and Conclusions vi
List of Figures x
List of Tables xiv
CHAPTER 1 1
1.0 INTRODUCTION 1
1.1 PROBLEM STATEMENT 1
1.2 OBJECTIVES 2
1.3 BACKGROUND 3
1.4 METHOD OF INVESTIGATION 7
CHAPTER 2 8
LITERATURE REVIEW OF WAVE MOTION AND GROUND VIBRATION 8
2.0 FUNDAMENTAL OF WAVE PROPAGATION AND VIBRATION 8
2.1 WAVE PROPAGATION 14
2.2 ATTENUATION OF ELASTIC WAVES 21
2.3 PILE DRIVING VIBRATION 30
CHAPTER 3 50
NUMERICAL MODELING 50
3.0 THE NUMERICAL MODEL 50
CHAPTER 4 71
FINITE ELEMENT ANALYSIS FOR PREDICTING PILE-INDUCED GROUND VIBRATIONS 71
4.0 INTRODUCTION 71
4.1 FINITE ELEMENT ANALYSIS OF CASE STUDY 1 72
4.2 FINITE ELEMENT ANALYSIS OF CASE STUDY 2 81
4.3 FINITE ELEMENT PARAMETRIC ANALYSIS 89
4.4 CONCLUSIONS 98

CHAPTER 5 100
5.0 DETERMINING THE QUALITY OF CONCRETE STRENGTH OF LABORATORY SAMPLES WITH VARIABLE CURE TIMES SUBJECTED TO VERTICAL VIBRATIONS 100
5.1 LABORATORY TESTING OF CONCRETE CYLINDRICAL SPECIMENS 100
5.2 LABORATORY TESTING OF CONCRETE BEAM SPECIMENS 113
CHAPTER 6 120
6.0 VIBRATION FIELD STUDY 120
6.1 FIELD MONITORING PROGRAM 120
6.2 FIELD SITE DETERMINATION 121
6.3 FIELD TESTING PROTOCOL 127
6.4 FIELD TESTING 131
CHAPTER 7 140
7.0 DETERMINING THE QUALITY OF CONCRETE STRENGTH OF FIELD SAMPLES WITH VARIABLE CURE TIMES SUBJECTED TO PILE DRIVING INDUCED VIBRATIONS 140
7.1 CONCRETE CYLINDERS 140
7.2 VIBRATION ATTENUATION AT MARQUETTE INTERCHANGE 151
7.3 CONCRETE BEAMS 152
CHAPTER 8 161
8.0 SUMMARY AND CONCLUSIONS 161
8.1 RECOMMENDATIONS FOR FURTHER STUDY 164
REFERENCES 168

List of Figures

Figure 2.1 Characters of free vibration (Das, 1992)

Figure 2.2 Terms describing harmonic motion (Richart et al., 1970)

Figure 2.3 Three types of vibratory wave motion (Richart et al., 1970)

Figure 2.4 Vibration nomograph for harmonic motion (Richart et al., 1970)

Figure 2.5 Compression waves (Geology and Geophysics at University of Wyoming, 2003)

Figure 2.6 Shear waves (Geology and Geophysics at University of Wyoming, 2003)

Figure 2.7 Rayleigh wave (Geological Sciences at Brown University, 2006)

Figure 2.8 Relation between Poisson's ratio and velocities of compression, shear, and Rayleigh waves in a semi-infinite elastic medium (Richart et al., 1970)

Figure 2.9 Relation of variations of amplitude at different depth for Rayleigh wave with various Poisson's ratios (Richart et al., 1970)

Figure 2.10 Love wave (Geological Sciences at Brown University, 2006)

Figure 2.11 Wave propagation (Das, 1992)

Figure 2.12 Various wave motions in elastic medium (Lamb, 1904)

Figure 2.13 Surface wave motions at 10, 20,30m from vibration source (Attwell et al. 1973)

Figure 2.14 Attenuation of particle velocity at the ground surface with distance from pile (Attwell et al., 1973)

Figure 2.15 Particle velocity attenuation with distance for various energy sources (Attwell et al., 1973)

Figure 2.16 Scaled distance versus peak vertical particle velocity (Wiss, 1981)

Figure 2.17 Spring-mass-dashpot systems (Parola, 1970)

Figure 2.18 End bearing pile (School of Engineering and Built Environment, Napier University, 1999 and Das, 1999)

Figure 2.19 Friction pile (School of Engineering and Built Environment, Napier University, 1999 and Das, 1999)

Figure 2.20 Steel pipe piles

Figure 2.21 Precast concrete piles

Figure 2.22 Section of the precast concrete piles (Das, 1999)

Figure 2.23 Cast-in-situ (cast-in-place) concrete piles (Das, 1999)

Figure 2.24 Timber piles

Figure 2.25 Combination pile made of concrete and timber piles for protecting timber piles from decay (School of Engineering and Built Environment, Napier University, 1999)
Figure 2.26 Drop hammer and members (Das, 1999)
Figure 2.27 Steam hammer and the members of the single-acting and double-acting steam hammer (Das, 1999)
Figure 2.28 Diesel hammers and operation principle (Das, 1999)
Figure 2.29 Hydraulic hammers
Figure 2.30 Standard vibrodriver and the principle of the driver (Das, 1999)
Figure 3.1 Benchmark Problem 1
Figure 3.2 Waves Absorbed by Infinite Elements
Figure 3.3 Propagation of the waves generated by the impulse load
Figure 3.4 Particle path of Rayleigh wave
Figure 3.5a Movement of body and surface waves at t=0.1 second
Figure 3.5b Movement of body and surface waves at t=0.3 second
Figure 3.5c Movement of body and surface waves at t=0.6 second
Figure 3.5d Movement of body and surface waves at t=1.2 second
Figure 3.5e Movement of body and surface waves at t=1.6 second
Figure 3.6 Vertical displacements at Nodes 626 and 648
Figure 3.7 Poisson's ratio versus wave velocity (Knopoff, 1952)
Figure 3.8 Foundation on the surface of soil layer (Chouw et al., 1991)
Figure 3.9 Finite element discretization
Figure 3.10 Element type and boundary condition
Figure 3.11 Applied harmonic displacements
Figure 3.12 Surface waves in the elastic half space
Figure 3.13 Displacement emanating from the center of foundation
Figure 3.14 Displacements traveling along the ground surface
Figure 3.15 Movement of displacement in different types of elements
Figure 3.16 Comparison of amplitude of surface waves with distance from source
Figure 3.17 Falling Weight Deflectometer (Al-Khoury et al., 2001)
Figure 3.18 Dimensions of ground geometry and finite element meshes
Figure 3.19 Applied pulse load (Al-Khoury et al., 2001)
Figure 3.20 Vertical displacements at the center of ground geometry with stiff subgrade

Figure 3.21 Vertical displacements at the center of ground geometry with soft subgrade
Figure 4.1 Schematic Presentation of Case Study 1
Figure 4.2 Finite element discretization of Case Study 1
Figure 4.3 Hammer-Pile Soil Interaction
Figure 4.4 Ground Surface Free Vibration (Study Case 1)
Figure 4.5 Measured Versus Computed Peak Particle Velocities at station 1 (5.5 m from pile) (a) Field Observation, (b) FEM
Figure 4.6 Measured Versus Computed Peak Particle Velocities at station 2 (16.5 m from pile) (a) Field Observation, (b) FEM
Figure 4.7 Schematic Presentation of Case Study 2
Figure 4.8 Finite element discretization of Case Study 2
Figure 4.9 Sample Input and Output Vibrations (a) Source Vibration (b) Ground Surface Vibration 1.62 m from Pile
Figure 4.10 Ground Surface Free Vibration (Study Case 2)
Figure 4.11 Measured Versus Computed Peak Particle Velocities (Case Study 2)
Figure 4.12 Schematic Presentation of "Base Case" for the Parametric Analysis
Figure 4.13 Finite element discretization of "Base Case" for the Parametric Analysis
Figure 4.14 Hammer-Pile Soil Interaction
Figure 4.15 Sample Output Ground Surface Vibrations (a) at 4.5 m from Pile (b) at 3 m from Pile (c) at 1.5 m from Pile
Figure 4.16 Effects of Embedded Pile Length on Ground Surface Vibration
Figure 4.17 Effects of Soil Stiffness on Ground Surface Vibration
Figure 4.18 Effects of Hammer Energy on Ground Surface Vibrations
Figure 5.1 Laboratory Vibration Test Apparatus (for Cylindrical Specimens)
Figure 5.2 Close-up: Laboratory Vibration Test Apparatus
Figure 5.3 MTS Control System
Figure 5.4 Laboratory Test Vibrations
Figure 5.5 Effects of PPV on Cylinder 3-day Strength
Figure 5.6 Effects of PPV on Cylinder 3-day Stiffness
Figure 5.7 Ultimate Strength/Stiffness Test Apparatus
Figure 5.8 Effects of PPV on Cylinder 7-day Strength
Figure 5.9 Effects of PPV on Cylinder 7-day Stiffness
Figure 5.10 Effects of PPV on Cylinder 28-day Strength

Figure 5.11 Effects of PPV on Cylinder 28-day Stiffness
Figure 5.12 Laboratory Vibration Test Apparatus (for Beam Specimens)
Figure 5.13 Close-up of the Laboratory Vibration Test Apparatus (for Beam Specimens)
Figure 5.14 Simple beam with third-point loading (AASHTO Designation: T97-03, ASTM Designation: C78-02)
Figure 5.15 Simple beam with third-point loading (close-up)
Figure 5.16 Effects of PPV on Beam 3-day flexural strength
Figure 5.17 Effects of PPV on Beam 7-day flexural strength
Figure 6.1 Field Study Location
Figure 6.2 Aerial Photograph of Research Site
Figure 6.3 Orientation of Field Test Site Piles
Figure 6.4 CIPPOC Mold
Figure 6.5 Schematic of below Grade Geophone in PVC pipe
Figure 6.7 Schematic of Test Pile Location
Figure 6.8 View of Edward E. Gillen Co. Pile driving hammer, crane and compressor during vibration monitoring at Test Pile #1
Figure 6.9 View of Test Pile # 1 after completion of driving
Figure 6.10 View of Test Pile # 2 after completion of driving, note pile leads/hammer
Figure 6.11 View of Block 8 at Test Pile #2 Location
Figure 7.1 Concrete Strength versus Curing Time (Wiss, 1981)
Figure 7.2 Test Pile # 1 Concrete CIPPOC Test Results
Figure 7.3 Scaled Distance versus Peak Particle Velocity at Surface for Test Pile # 1
Figure 7.4 Scaled Distance versus Peak Particle Velocity at 10 feet Depth at Test Pile # 1
Figure 7.5 Test Pile # 2 Concrete CIPPOC Test Results
Figure 7.6 Scaled Distance versus Peak Particle Velocity at Surface at Test Pile # 2
Figure 7.7 Distance versus Peak Particle Velocity From Marquette Interchange
Figure 7.8 Beam Strength Results for Test Pile # 1
Figure 7.9 Beam Strength Results for Test Pile # 2
Figure 7.10 Beam and CIPPOC Strength versus Curing Time at Test Pile #1
Figure 7.11 Beam and CIPPOC Strength versus Curing Time at Test Pile #2

List of Tables

Table 2.1 Distribution of the elastic waves at the ground surface (Miller and Pursey, 1955)

Table 2.2 Ground vibration measurements (Attwell et al., 1973)

Table 2.3 Attenuation coefficient corresponding to various classifications of material (Woods and Jedele, 1985)

Table 2.4 Advantages and disadvantages of steel piles

Table 2.5 Advantages and disadvantages of concrete piles

Table 2.6 Advantages and disadvantages of the timber piles

Table 2.7 Impact pile hammer data (Vesic, 1977)

Table 2.8 Comparison of energies released (Dowding, 1996)

Table 3.1 Amplitude of applied load

Table 3.2 Soil Parameters

Table 3.3 Problem Parameters (Chouw et al., 1991)

Table 3.4 Material properties (Al-Khoury et al., 2001)

Table 5.1 Laboratory Vibration Tests on Young Concrete Cylinders

Table 5.2 WisDOT A-FA Concrete Mix Information Per Cubic Yard

Table 5.3 Laboratory Vibration Tests on Young Concrete Beams

Table 6.1 Weather Data During Field Study

Table 6.2 Maximum Recorded Vibration Levels

Table 6.3 Sound Levels at Test Site

Table 7.1 Concrete Cylinder Matrix per Site

Table 7.2 Concrete Beam Matrix per Site

Table 7.3 Concrete Beam Modulus of Rupture Data

CHAPTER 1

1.0 INTRODUCTION

1.1 PROBLEM STATEMENT

Potential damage to structures due to construction-induced vibrations from operations such as pile driving and blasting is of great concern to engineers. Vibrations associated with blasting are regulated by the Department of Commerce COMM 7 of Wisconsin Administrative Code. COMM 7 established vibration limits such that blasting does not cause injury or excessive annoyance to people or damage to structures. Nevertheless, COMM 7 does not specifically address ground vibration resulting from pile driving.

The Wisconsin Department of Transportation (WisDOT) typically requires pre-construction surveys and/or inspections prior to construction to provide data for potential vibration-induced damage claims. Damage claims from property owners who believe their structure was damaged due to construction vibrations can be legitimate but also can be due to the fact that humans are sensitive to vibrations and think that cracks have occurred because they felt vibrations. The magnitude of vibrations that can cause damage to a structure are a function of many factors including distance from the vibration, structure condition, vibration energy, subsurface conditions and frequency of vibrations. Regardless of the vibration magnitude, contractors are required to monitor construction-induced vibrations. The WisDOT Standard Specifications sets limits on the timing and distance of concrete placement and distance of driving pile shells adjacent to concrete-filled piles. The Specifications only address pile driving vibrations with respect to the concrete placed within pile shells and not with respect to other recently placed

concrete structures such as footings. The approach is perceived as unnecessarily restrictive in some cases and may contribute to longer construction periods and increased project costs. This research has stemmed from the need to address potential damage to concrete-filled pipe piles and recently placed concrete structures that could be affected by pile driving vibrations. The study will focus on two research topics:

1. The attenuation of potentially damaging pile driving vibrations with distance and depth from the source. Pile driving was performed using an impact hammer and evaluation of vibration attenuation from vibratory pile installation is beyond the scope of this research.
2. The effects of distance and curing time of concrete on the quality of recently-placed concrete exposed to pile driving vibrations. Quality of concrete as discussed in this study is limited to the compressive strength of samples.

1.2 OBJECTIVES

The objectives of this research were: (1) investigate the attenuation of potentially-damaging pile driving vibrations with distance and depth and (2) investigate the effects of distance and age on the quality of concrete exposed to pile driving vibrations. To attain the first objective, finite element analysis modeling of varying pile sizes, pile types, and hammers was performed. The finite element results were compared to common empirical equations used for vibration predictions. The finite element results were also compared to a limited number of field tests that include vibration measurements. To

attain the second objective, testing of laboratory concrete samples subjected to various peak particle velocities (PPVs) was carried out.

Recommendations that lead to better definition of how pile-induced vibrations from different hammers affect the quality of concrete with distance were desired from this research. An additional want of this research was that recommendations for specifying acceptable ground vibrations and/or distances for recently-placed concrete based on curing time and/or compressive strength could be provided.

1.3 BACKGROUND

Previous investigation objectives by others have included determining threshold levels of human perception and annoyance from steady state and transient vibrations as well as preventing and assessing damage to structures and equipment. Much of the literature on pile- and blast-induced vibrations discussed attenuation of vibrations with distance and how they are related to the damage of *existing* structures.

The United States Bureau of Mines (now defunct) performed many studies on blast-induced damage to structures and numerous publications have been generated. Bulletin 636 (Nichols, Johnson, and Duvall, 1971) provided details on blast-induced vibrations and gave limits on vibrations that should not cause damage to residential structures. A peak particle velocity of less than 2 inches per second was provided as a value that would be considered safe while a value greater than 2 inches per second could damage a structure. Bulletin 8507 (Siskind, Stagg, Knopp, and Dowding, 1980) discussed

vibration levels that cause damage to structures and included recommendations for monitoring both within and around structures. The concept of structure age and condition affecting structure response to vibrations were presented. This research also indicated that structural resonance response to low frequency ground vibrations was a serious problem. For vibration frequencies of less than 40 Hertz, the bulletin recommended maximum vibrations levels of 0.75 in/sec for drywall homes and 0.5 in/sec for plaster homes. At frequency levels above 40 Hertz, the recommendation was to maintain vibrations levels to no more than 2 in/sec. The research indicated that these safe values and unlikely to produce interior cracking or other damage.

The text "Rock Blasting and Overbreak Control" by Konya and Walters (1991) presents data on the mechanics of blast induced vibrations and methods that can be used to reduce vibrations. The text gives details on research and theory behind blast vibration generation including the concept of charge weight related to vibration control. Scaled distance is presented as an effective way to control blast vibration. It takes the form of the following equation: $D_s = d/W^{1/2}$

where D_s is scaled distance, d is the distance from a blast to a structure and W is the maximum charge weight per blast delay in pounds.

The phenomenon of wave attenuation and the associated ground surface vibration caused by pile driving operations is well understood. Nevertheless, relatively few researchers have addressed the effects of vibrations on the behavior of early-age concrete. Tawfiq and Abichou (2003) referenced a study by Woods (1997) that indicated that only 9 of 26

state highway agencies surveyed had Standard Specifications for controlling vibrations from pile driving operations. Tawfiq and Abichou indicated that the specified vibration measurements varied from state to state and that vibration criteria for "green" concrete were hardly addressed by many state agencies.

The Committee of Deep Foundations concluded that "there are no detrimental effects due to vibration of concrete during its setting and curing period. There is evidence that beneficial effects may even be derived" (ASCE, 1984). On the contrary, in another ASCE publication (ASCE, 1993) it is recommended that pile driving should not be allowed within 100 feet of concrete which has not attained its design strength.

NCHRP Synthesis 253 Report (Woods, 1997) includes excerpts from a draft version of ACI 231-97, Chapter 5 under consideration, which states that a threshold of failure has not yet been reported in test programs cited, and that establishing PPV criteria in the 5 to 10 inch/sec range for 2 to 7 day-old concrete should easily be demonstrable with limited compressive cylinder testing.

Bastian (1970) describes three case histories in which compressive strength was found to be greater for concrete subjected to pile-driving vibrations compared to cylinders cured under normal conditions. One of the studies cited was from a 1929 Michigan Highway Department Report that is one of the first documented cases where tests were conducted specifically to determine the effect of pile driving vibrations on fresh concrete in nearby cast-in-place piles.

Oriard (1999) provides guidelines for maximum allowable particle velocity for different curing ages of concrete. His guidelines indicate acceptable particle velocities in the range of 5 to 20 in/sec for curing concrete.

Wiss (1981) has indicated that additional studies to evaluate the effects of vibration on "young" concrete are recommended. Literature dated after the Wiss (1981) recommendation, however, does not consistently address or conclude the effect of vibrations on curing concrete. Reddy et al. (2000) stated that although enough has been learned about concrete vibration during the past 50 years to insure that low slump concrete can be placed successfully, a better understanding of the interaction of vibration and fresh concrete is still desirable.

Hulshizer (1996) performed testing on field and laboratory concrete samples with variable ages that were subjected to vibrations as part of work performed for the Seabrook Nuclear Station project in Seabrook, New Hampshire. The testing compared concrete compressive strength, shear and reinforcement bond strength. Field testing was also done on four concrete wall sections. The field samples were subject to vibrations from blasting while the lab samples were vibrated using a shake table. Vibration levels ranged from 8 to 12 inches/second with some levels up to 16 inches/second. The results of the compressive strength testing were essentially the same for the field and laboratory specimens. For concrete subjected to the maximum vibration levels of the study at curing ages less than 24 hours after concrete placement, there was no reported reduction in

compressive strength below the design value when compared to samples not subject to vibrations. The study concluded that there was no evidence that vibrated "green" concrete would not attain the specified 28-day strength design values.

Due to the varying opinions and recommendations on this subject, it appears imperative that an additional research study be conducted to address the effects of vibrations caused by pile driving on early-age concrete.

1.4 METHOD OF INVESTIGATION

This study presents a review of wave motion and ground vibration (Chapter 2), finite element analyses (Chapters 3 and 4), an extensive laboratory testing program (Chapter 5), and a field vibration study (Chapter 6). The laboratory program will evaluate the influence of a wide range of peak particle velocities of vibration and how that affects the short-term and long-term compressive strength. Test results will be compared with control sets not subjected to vibrations. In addition, a finite element model will be developed to predict induced ground vibrations due to pile driving considering various pile driving equipment and excitation mechanisms. The model will take into consideration the heterogeneity of the soil. After calibrating the numerical model to site-specific behavior, the model will be used to analyze various conditions of interest (Chapter 4) that will complement the experimental results obtained from laboratory vibration tests. The field study (Chapter 6) information will be used to compare the compressive strength data (Chapter 7) and summary and conclusions will be presented along with recommendations for further study (Chapter 8).

CHAPTER 2

LITERATURE REVIEW OF WAVE MOTION AND GROUND VIBRATION

2.0 FUNDAMENTAL OF WAVE PROPAGATION AND VIBRATION

2.0.1 Fundamental Definitions

To help understand the characteristics of waves and vibrations, some fundamental definitions are given below with respect to a simple harmonic vibration as shown in Figure 2.1.

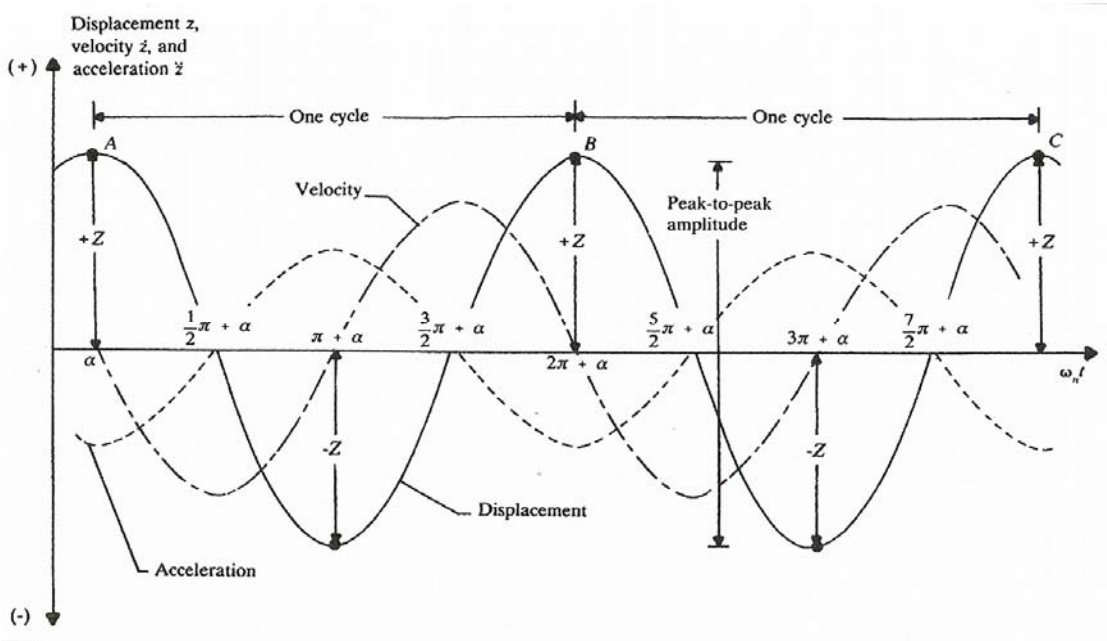

Figure 2.1 Characters of free vibration (Das, 1992)

- Wave: disturbance traveling from one point to another transferring energy but not particles.

- Vibration: particle disturbance about its equilibrium position in a repetitive fashion.
- Free vibration: vibration in system under the action of forces inherent in the system itself and in the absence of external impressed forces.
- Forced vibration: vibration of a system caused by an external force.
- Degree of freedom: number of independent coordinates required to describe the solution of a vibrating system.
- Amplitude: magnitude of maximum displacement. This is referred to as the single amplitude. The peak-to-peak displacement amplitude is equal to 2A, which is sometimes referred to as the double amplitude.
- Period: time required for the motion to repeat itself. This is called cycle. The period of repeating motion can be given by

$$T = \frac{2\pi}{\omega_n} \tag{2.1}$$

- Frequency: number of cycles in a given period, and can be represented by

$$f = \frac{1}{T} = \frac{\omega_n}{2\pi} \tag{2.2}$$

- Resonance: resonance occurs when the applied frequency to the system coincides with its natural frequency, so resulting in a high level of vibration.
- Wave length: distance between any two identical parts of adjacent vibration cycles. Wave length is proportional to the wave velocity and inversely proportional to the frequency, and can be expressed as follows.

$$\lambda = \frac{c}{f} \tag{2.3}$$

- Angular velocity: ratio of the change in angular position $\Delta\theta$ to the change in

time Δt .

$$\omega = \frac{\Delta \theta}{\Delta t} \tag{2.4}$$

- Wave velocity: ratio of the change in the distance position Δx to the time change Δt .

$$c = \frac{\Delta x}{\Delta t} \tag{2.5}$$

- Particle velocity: ratio of change in vibration displacement with respect to time.

2.0.2 Vibratory Wave Motion

Harmonic or sinusoidal motion is the simplest form of vibratory motion and can be described with respect to displacements by the equation 2.6.

$$Z = A \sin(\omega t - \alpha) \tag{2.6}$$

where, Z=Displacement

A=Displacement amplitude from the mean position

ω =Circular frequency (rad/sec)

t =Time

α =Phase angle

Equation 2.6 defines the vibratory wave motion as a cyclic movement of displacement with respect to time variation as shown in Figure 2.2.

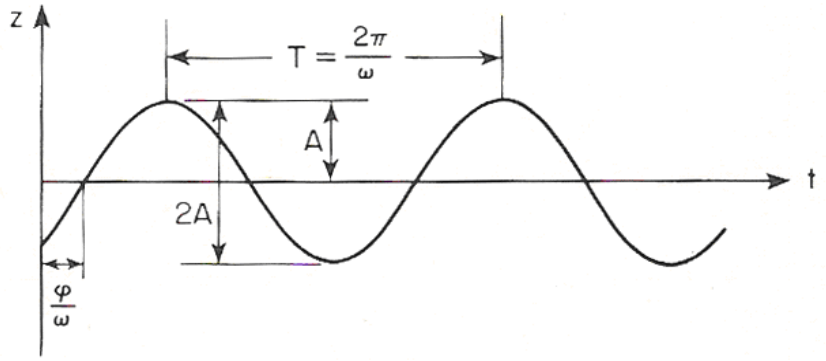

Figure 2.2 Terms describing harmonic motion (Richart et al., 1970)

From Figure 2.2, it can be seen that amplitude and frequency are required to define the harmonic motion. The phase angle α in some cases is necessary to specify the time relationship between amplitude and frequency. In fact, all vibratory wave motions cannot be completely harmonic and sinusoidal. Harmonic motion of vibration is only obtained under controlled laboratory conditions. Figure 2.3 shows three types of vibratory wave motions.

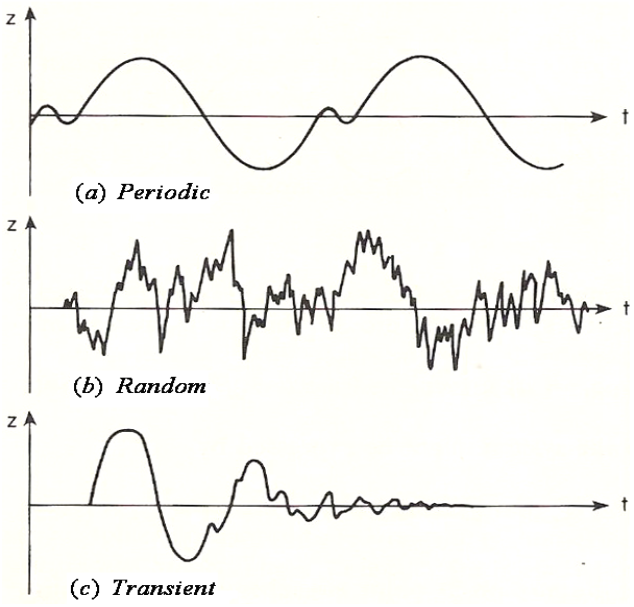

Figure 2.3 Three types of vibratory wave motion (Richart et al., 1970)

Repeat motion of displacement versus time is called Periodic motion; whereas in Random motion the displacement-time pattern does not repeat. Transient motion is related to impulsive load or disturbance applied to damped system for a very short time. After the impulse load or disturbance has disappeared, the vibrations decay gradually until the damped system returns to repose.

2.0.3 Derivatives of Displacement of Vibrating Medium

The amplitude of vibration may be expressed in terms of particle displacement, velocity or acceleration. These quantities are the most significant factors to evaluate the nature of vibratory wave motion, and are associated with the relationship of derivatives. In mathematical expression, displacement could be described as the first and second, or third derivatives with respect to time. The quantities obtained from the derivatives of equation 2.6 are

$$\text{Displacement, } Z = A\sin(\omega t - \alpha) \tag{2.7}$$

$$\text{Velocity, } \frac{dz}{dt} = \dot{Z} = \omega A\cos(\omega t - \alpha) \tag{2.8}$$

$$\text{Acceleration, } \frac{d^2z}{dt^2} = \ddot{Z} = -\omega^2 A\sin(\omega t - \alpha) \tag{2.9}$$

For a harmonic vibration, all quantities could be obtained by the use of a vibration nomograph as shown in Figure 2.4. The vibration nomograph provides for convenience of conversion and calculation to obtain the velocity for frequency.

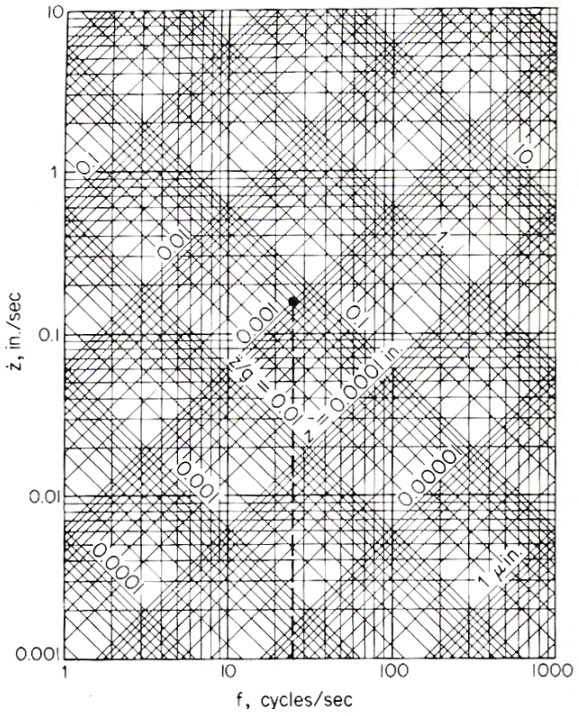

Figure 2.4 Vibration nomograph for harmonic motion (Richart et al., 1970)

In the field, because the amplitude of a harmonic or sinusoidal vibration produced by an earthquake or construction equipment does not depend on the sine or cosine, displacement, velocity and acceleration could be simply converted with A and ω

$$\text{Displacement, } Z = A \tag{2.10}$$

$$\text{Velocity, } \dot{Z} = \omega A \tag{2.11}$$

$$\text{Acceleration, } \ddot{Z} = -\omega^2 A \tag{2.12}$$

These equations all have combinations with each other. The amplitude of displacement is obtained with the inverse relationship of velocity and expressed as the inverse relationship of acceleration as follows,

$$A = \frac{\dot{Z}}{\omega} = Z \tag{2.13}$$

$$A = \frac{\ddot{Z}}{\omega^2} = Z \qquad 2.14$$

2.0.4 Interference of Wave Propagation, Damping

Theoretically, the vibratory wave motion without friction can be explained as the undamped free vibration theory of soil dynamics. However, in practice, friction causes the vibration to be damped. All vibrations undergo a gradual decrease of vibration amplitude with time and distance. This phenomenon is referred to as damping. The damping degree depends on the presence of the fiction forces. The friction force is proportional to the wave velocity of a medium having lower wave velocity such as loose granular soil. The frictional force is proportional to the square root of the wave velocity of a medium having higher wave velocity such as dense sand. The damping is classified with three damped conditions depending on the effect of the friction forces. Under the weakly damped condition, the effect of the friction forces is little, but is greater in the overdamped condition. When the vibrating system returns to the equilibrium position in the shortest possible time, this condition is referred to critical damping. Damping has a considerable effect on limiting the vibration amplitude at resonance.

2.1 WAVE PROPAGATION

The propagation of a wave is generally affected by the type of wave, ground condition, and boundaries between the soil layers, especially at the surface of the ground.

2.1.1 Types of Waves

The elastic waves are classified as body waves and surface waves according to the medium of propagation. Body waves include the compression waves and shear waves, and Rayleigh wave is a representative surface wave. Love wave is another surface wave.

2.1.1.1 Compression wave

The compression wave is one of the body waves, and also called Primary, Longitudinal, or Dilatational waves. The ground is alternately compressed and dilated in the direction of propagation as shown in Figure 2.5. The compression waves travel slightly less than twice as fast as shear waves, and can travel through any type of material. The velocity of compression waves (C_p) in a rod and in an infinite medium can be represented as

$$C_p = \sqrt{\frac{E}{\rho}} \quad \text{(In a rod)} \qquad 2.15$$

$$C_p = \sqrt{\frac{E(1-\nu)}{\rho(1-2\nu)(1+\nu)}} \quad \text{(In an infinite medium)} \qquad 2.16$$

where, E : Young's modulus

ν : Poisson's ratio

ρ : Density

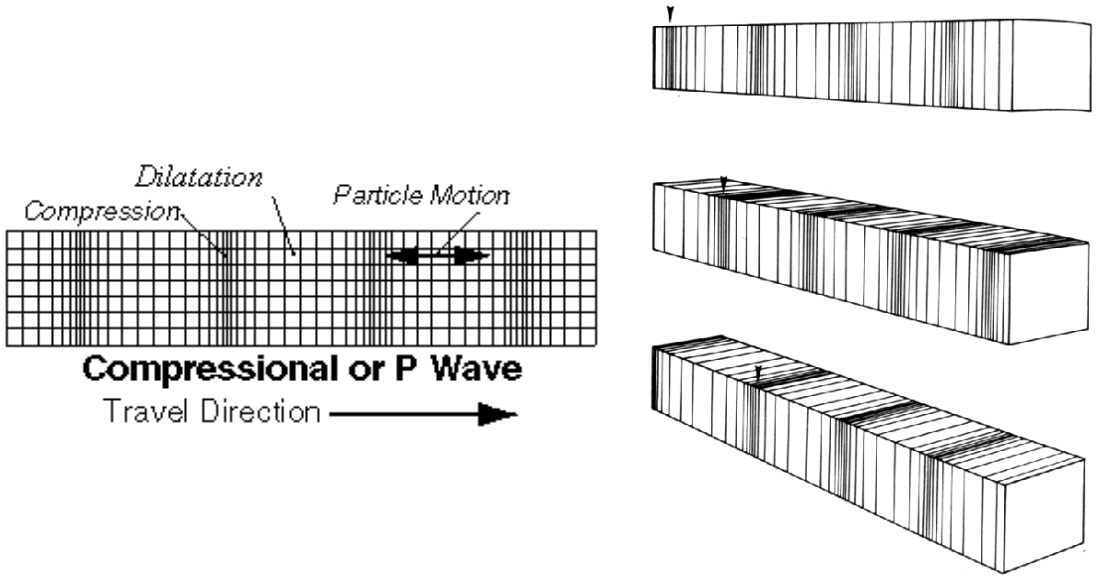

(a) Wave motion of compression waves (b) 3-dimensional view of P-wave motion

Figure 2.5 Compression waves (Geology and Geophysics at University of Wyoming, 2003)

According to these equations, the velocity of compression wave in an infinite medium is faster than that in a rod since the lateral displacement is constrained in an infinite medium, whereas it is free in a rod.

2.1.1.2 Shear waves

The shear wave is one of the body waves, and is called Transverse, Distortional, or Secondary waves. The shear waves cause a particle to vibrate perpendicularly to the direction of wave propagation as shown in Figure 2.6. The shear waves cause the change in the shape of an element in the medium but no change in the volume as the waves go through. The velocity of the shear wave in a rod and in an infinite medium can be expressed by

$$C_s = \sqrt{\frac{G}{\rho}} \qquad 2.17$$

where, G : shear modulus of medium

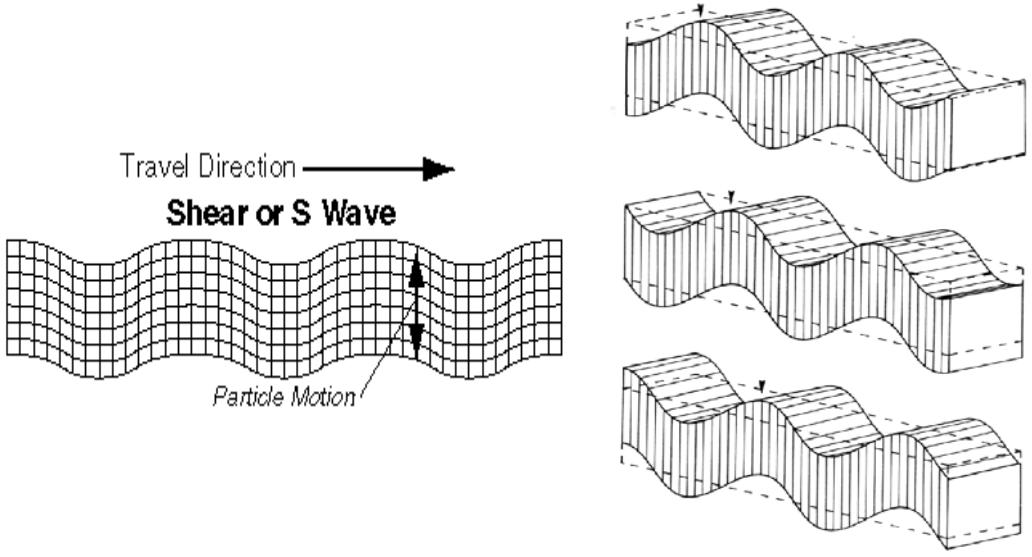

(a) Wave motion of shear waves

(b) 3-dimensional view of S-wave motion

Figure 2.6 Shear waves
(Geology and Geophysics at University of Wyoming, 2003)

2.1.1.3 Rayleigh waves

The Rayleigh wave was found in 1885 by Lord Rayleigh. Rayleigh waves are distinct from other types of waves, such as P-waves and S-waves, which are body waves, or Love waves, another type of surface wave. Rayleigh waves are generated by the combination of compression and shear waves with no horizontal component. The Rayleigh wave travels with a velocity that is lower than the compression, shear, and Love wave velocities. Rayleigh waves are also called Rayleigh-Lamb wave or Ground roll because

this wave moves along the surface of the ground making circle or ellipse particle motion toward the direction of propagation as presented in Figure 2.7.

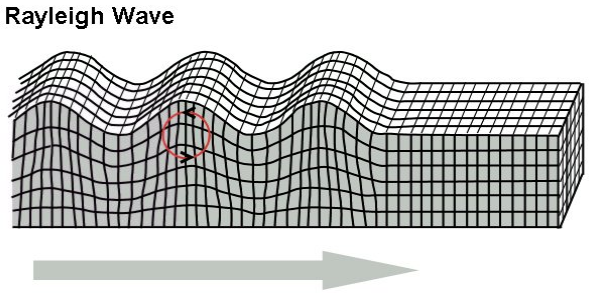

Figure 2.7 Rayleigh wave (Geological Sciences at Brown University, 2006)

Particles move inversely to the direction of the wave propagation at the top of the ellipse of a circle. The Rayleigh waves move along the surface and the motion of Rayleigh wave is confined to a zone near the boundary of two continuous media. The amplitude of Rayleigh waves decrease with increasing distance under the surface. The Rayleigh waves are slightly slower than the shear waves.

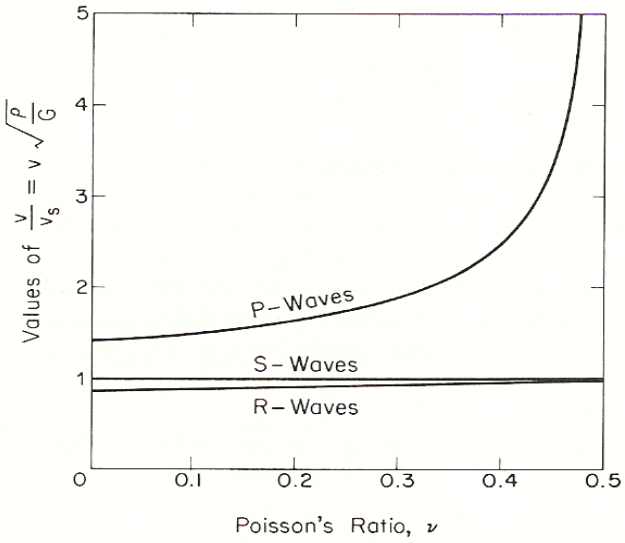

Figure 2.8 Relation between Poisson's ratio and velocities of compression, shear, and Rayleigh waves in a semi-infinite elastic medium (Richart et al., 1970)

In Figure 2.8, Poisson's ratio could be plotted as the range from 0 to 0.5, and for all values of Poisson's ratio, V/V_S is always greater than 1. For homogeneous soil, the velocity of Rayleigh wave (C_r) is proportional to the shear wave velocity(C_s) (equation 2.18):

$$C_r = kC_s \qquad 2.18$$

According to Jaeger and Cook (1979), the maximum value of k is 0.9553 when the Poisson's ratio is 0.5, and the value of k is 0.919 when the Poisson's ratio is 0.25. Figure 2.9 represents the value of U and W versus the distance of wave lengths of Rayleigh waves for Poisson's ratios.

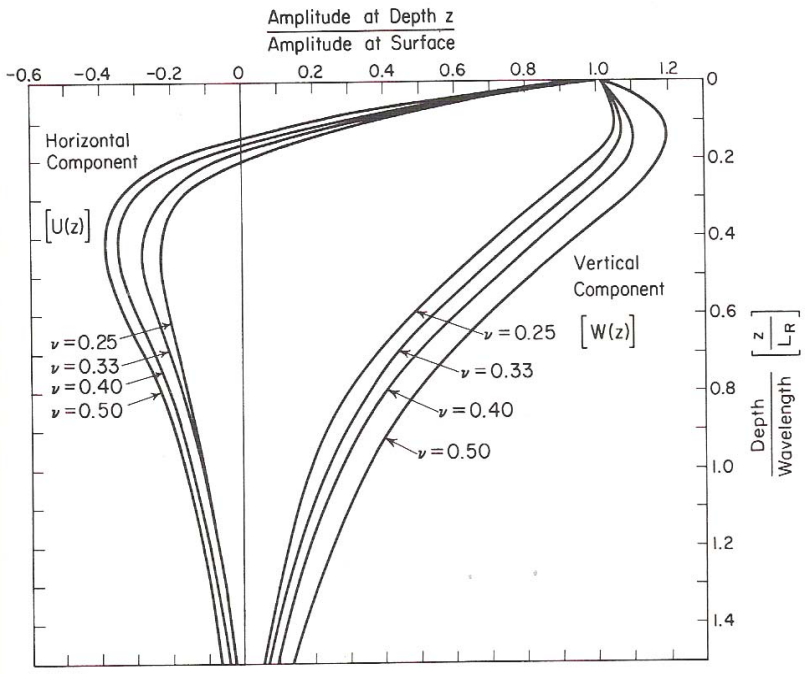

Figure 2.9 Relation of variations of amplitude at different depth for Rayleigh wave with various Poisson's ratios (Richart et al., 1970)

where, U and W : Special variation of displacements u and w.

2.1.1.4 Love waves

A British scientist, A.E.H. Love named the waves that induce the horizontal shearing of the ground as Love waves in 1911. The Love waves are formed by the constructive interference of multiple reflections of S_h waves at the free surface, and usually travel faster than Rayleigh waves, about 90% of the S wave velocity. The particle motion of the Love wave is parallel to the ground, and is perpendicular to the direction of the wave propagation.

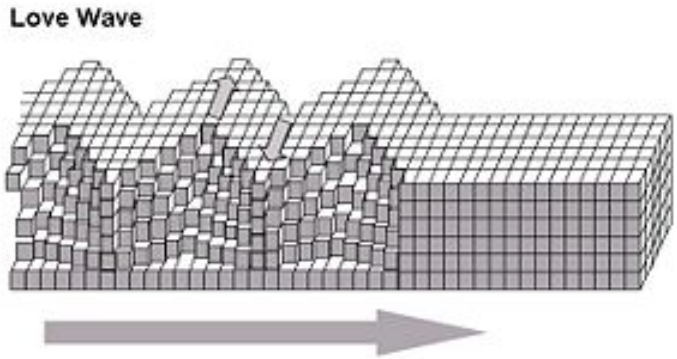

Figure 2.10 Love wave (Geological Sciences at Brown University, 2006)

2.1.2 Wave Equations

Richart et al. (1970) presented the property of traveling waves in his elastic theory. The vibration is one of the factors that make waves move or travel. The wave motion in all elastic bodies or mediums can be explained by the partial-differential equation, which is called the wave equation:

$$\frac{\partial^2 u}{\partial t^2} = v^2 \frac{\partial^2 u}{\partial x^2} \qquad 2.19$$

The symbol v is the wave propagation velocity. The wave equations for the body and surface waves can be solved in one or three dimensions to represent the wave propagation in a rod and in an elastic infinite medium and the wave equations for the surface can be solved in a plane at the surface of an elastic half space.

2.2 ATTENUATION OF ELASTIC WAVES

Provided that wave energy is generated in the ground by means of the pile driving, blasting or any other dynamic vibration source, the vibration will be propagated in the ground in the form of body waves and on the surface of the ground as surface waves. As the waves created by a source of vibration at the surface of an elastic half space travel toward the infinite medium, they encounter the ground having greater volume and suffer reduction of amplitude and wave energy depending on their distance from the source. Figure 2.11 shows the wave front originated from vibration source A. The energy of propagating body waves distributes over an area that increases with the square of the radius. The amplitude of source is proportional to square root of energy per unit area as:

$$\text{Amplitude of source} \propto \sqrt{E} \tag{2.20}$$

The symbol E represents the energy per unit area. The amplitude of body waves is inversely proportional to the distance as:

$$\text{Amplitude of body waves} \propto \frac{1}{r} \tag{2.21}$$

The symbol r represents the distance from the source. The amplitude of body waves at the surface of the half space only is inversely proportional to the distance as

$$\text{Amplitude of body waves} \propto \frac{1}{r} \tag{2.22}$$

The symbol r represents the distance from the source. While the amplitude of surface waves will decrease with the distance as:

$$\text{Amplitude of surface waves} \propto \frac{1}{r^2} \qquad 2.23$$

where r is the distance from the source.

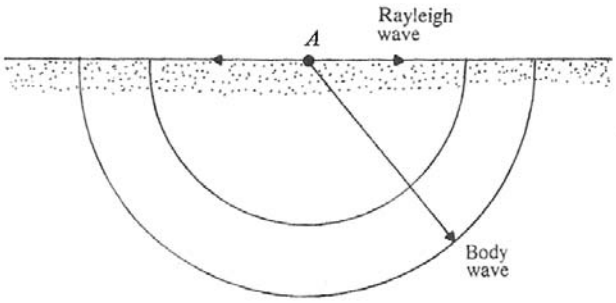

A : Source of disturbance

Figure 2.11 Wave propagation (Das, 1992)

Since the compression waves are the fastest, they will arrive first, followed by shear waves and then surface waves, such as Rayleigh waves as shown in Figure 2.12.

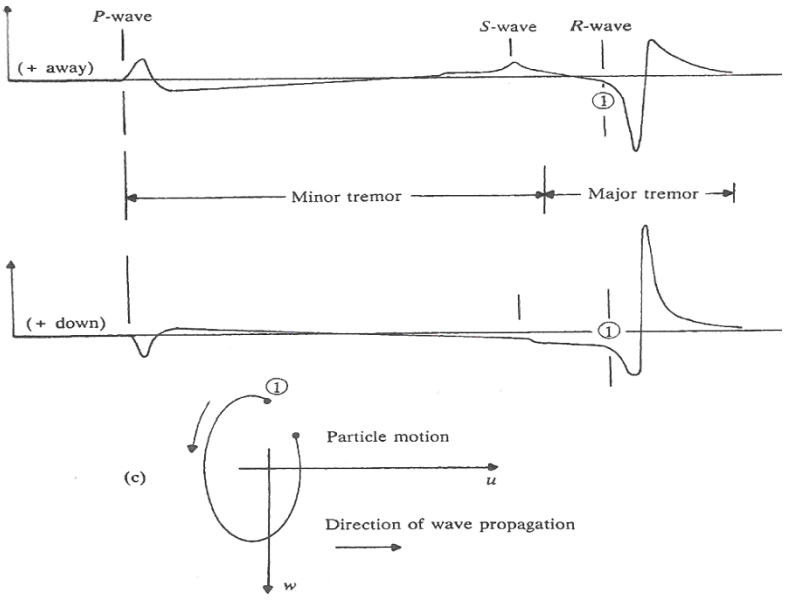

Figure 2.12 Various wave motions in elastic medium (Lamb, 1904)

Miller and Pursey (1955) calculated the distribution of total input energy of the elastic waves at the surface of the ground as shown in Table 2.1.

Table 2.1 Distribution of the elastic waves at the ground surface (Miller and Pursey, 1955)

Compression Waves	**Shear Waves**	**Rayleigh waves**
7%	**26%**	**67%**

From the data, it can be deduced that Rayleigh waves dominate the particle movements at the ground surface, and cause the most damage to nearby structures. Attwell et al. (1973) studied the attenuation of ground vibrations from sheet pile driving, and suggested graphically plotted surface wave motions shown in Figure 2.13. The amplitude of the

surface waves decrease with distance from the driven sheet pile, and the direction of wave motion is almost a retrograde ellipse as described in Figure 2.13.

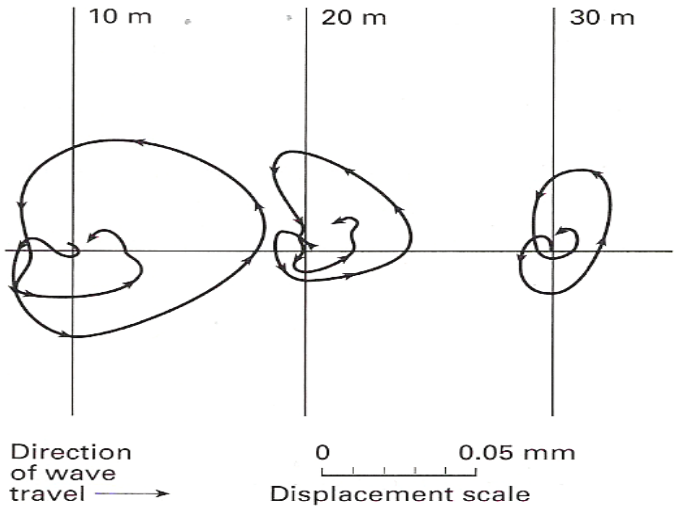

Figure 2.13 Surface wave motions at 10, 20,30m from vibration source (Attwell et al. 1973)

Attwell et al. (1973) presented the attenuation of particle velocity (mm/s) at ground surface with distance (r) from pile and for various energy sources as shown in Figures 2.14 and 2.15.

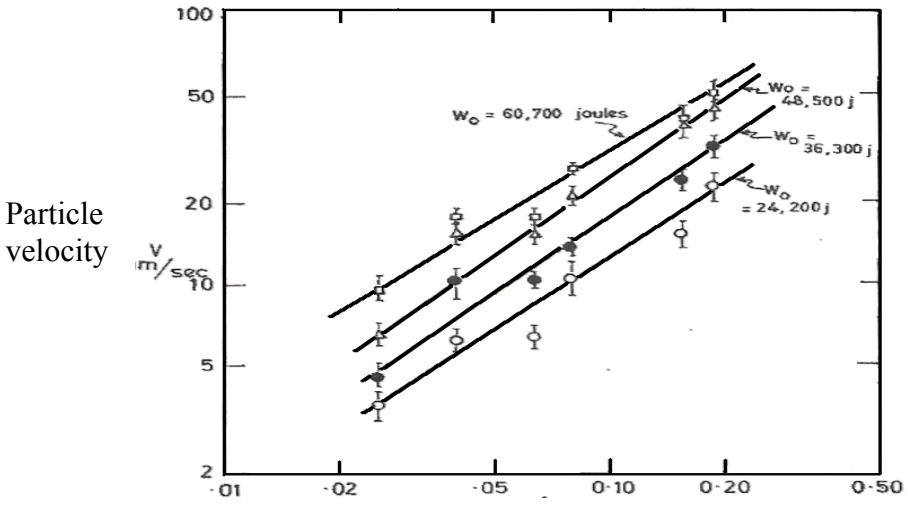

Figure 2.14 Attenuation of particle velocity (mm/s) at the ground surface with distance from pile (Attwell et al., 1973)

Particle velocity, V (mm/s)

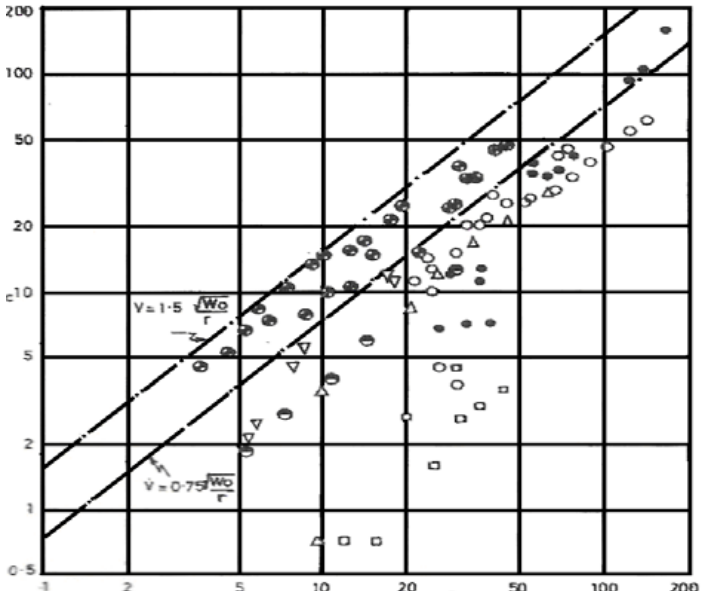

$(W_o)^{-1/2}/r$ Joules^{-1}/m

Figure 2.15 Particle velocity (mm/s) attenuation with distance for various energy (W_o) sources, (Attwell et al., 1973)

Symbols of Figure 2.15 are given in Table 2.2.

Table 2.2 Ground vibration measurements (Attwell et al., 1973)

Case No.	Vibration Source	Symbol Figure 5	Soil type	Range of Energy inputs (Jules) (drop hammer height × drop hammer weight)	Range of radial distances (r) from vibration source (m)
1	Shell boring	⊡	Coarse and stiff clay base	1050-10500	1.5 to 3
2	Driven H-piles	⊙	Layered medium sand and silt	9100-36500	1.5 to 7.5
3	Driven sheet piles	⊕	Stiff silty clay on firm laminated clay	24000-60700	5 to 40
4	Diesel hammer	⊖	Laminated clay	20000	5 to 40
5	Driven circular mandrel	●	Layered coarse sand and gravel	127000-212000	3 to 15
6	Wet vibroflotation	△	Fine sand	1350 per cycle	1 to 4.5
7	Dry vibroflotation	▽	Uncompacted fill	2700 per cycle	1 to 6

The loss of the amplitude of waves due to spreading out is referred to geometrical damping, and the loss from the absorption in the soil material is called material damping. These two types of damping and the vertical amplitude of Rayleigh waves can be explained by the relation.

$$\bar{w}_m = w_1 \sqrt{\frac{r_1}{r_n}} \exp[-\beta(r_n - r_1)] \qquad 2.24$$

where $\bar{w}_n$ and w_1 are the vertical amplitudes at distances r_n and r_1, and β is the absorption coefficient. The magnitude of β is based on the soil type.

Richart et al. (1963) suggested Equation 2.25 that shows the relationship of distance and wave attenuation. The waves decay geometrically with distance; that is, the geometrical damping could be expressed as

$$A_2 = A_1 \left(\frac{r_1}{r_2} \right)^n \qquad 2.25$$

where r_1 is the distance from vibration source to point of known amplitude

r_2 is the distance from vibration source to point of unknown amplitude

A_1 is the amplitude of motion at distance r_1 from source

A_2 is the amplitude of motion at distance r_2 from source

n is a power depending on type of wave:

$n = \frac{1}{2}$ for Rayleigh waves

n =1 for body waves

n =2 for body waves at the surface

The material damping can be combined with the geometrical damping as suggested by Bornitz (1931), and shown by Woods and Jedele (1985):

$$A_2 = A_1\left(\frac{r_1}{r_2}\right)^n \exp[-\alpha(r_2 - r_1)] \qquad 2.26$$

The symbol α is a coefficient of attenuation. The coefficient α depends on soil. Woods and Jedele (1985) presented the attenuation coefficient for various soil types in Table 2.3.

Table 2.3. Attenuation coefficient corresponding to various classifications of material (Woods and Jedele, 1985)

Class	Attenuation Coefficient α (1/ft) 5 Hz	Attenuation Coefficient α (1/m) 5 Hz	Description of Material
Ⅰ	0.003 to 0.01	0.01 to 0.033	Weak or Soft Soils-loesy soils, dry or partially saturated peat and muck, mud, loose beach sand, and dune sand, recently, plowed ground, soft spongy forest or jungle floor, organic soils, topsoil. (shovel penetrates easily) (N<5)
Ⅱ	0.001 to 0.003	0.0033 to 0.01	Competent Soils-most sands, sandy clays, silty clays, gravel, silts, weathered rock. (can dig with shovel)(5<N<15)
Ⅲ	0.0001 to 0.001	0.00033 to 0.0033	Hard Soils-dense compacted sand, dry consolidated clay, consolidated glacial till, some exposed rock. (cannot dig with shovel, need pick to break up)(15<N<50)
Ⅳ	〈 0.0001	〈 0.00033	Hard, Competent Rock-bedrock freshly exposed hard rock. (difficult to break with hammer)(N>50)

Since α is a frequency dependent value, α is represented as

$$\alpha_2 = \alpha_1 \left(\frac{f_2}{f_1} \right) \qquad 2.27$$

When α_1 is assumed as a known value at frequency f_1, the unknown value of α_2 at frequency f_2 can be calculated with Equation 2.27. As early as 1912, Gollitsin (1912) suggested Equation 2.28 to calculate the amplitude reduction of Rayleigh waves:

$$A_2 = A_1 \sqrt{\frac{r_1}{r_2}} e^{-\gamma(r_2 - r_1)} \qquad 2.28$$

where A_1 is the amplitude of vibration at an unknown distance r_1 from the disturbance source.

A_2 is the amplitude of vibration at a known distance r_2 from the disturbance source.

γ is the attenuation coefficient

In equation 2.28, $\sqrt{\frac{r_1}{r_2}}$ represents geometric damping, and the exponential $-\gamma(r_2 - r_1)$ is the material damping. Wiss (1981) suggested pseudo-attenuation model (Equation 2.29):

$$v = kD^{-n} \qquad 2.29$$

where v is the peak particle velocity

k is the value of velocity at one unit of distance

D is the distance from disturbance source

n is the attenuation rate

Wiss (1981) also suggested the Equation 2.30 to include source energy in an attenuation equation. This equation is called scaled-distance equation, and is expressed as

$$v = k\left[\frac{D}{\sqrt{E_n}}\right]^{-n} \qquad 2.30$$

Figure 2.16 shows the relationship of peak vertical particle velocity versus scaled distance. The ground type is considered by the value of n. The sloping line with $n = 1.5$ is applied to class I soils, and $n = 1.1$ can be applied to the class II soils of Woods and Jedele (1985).

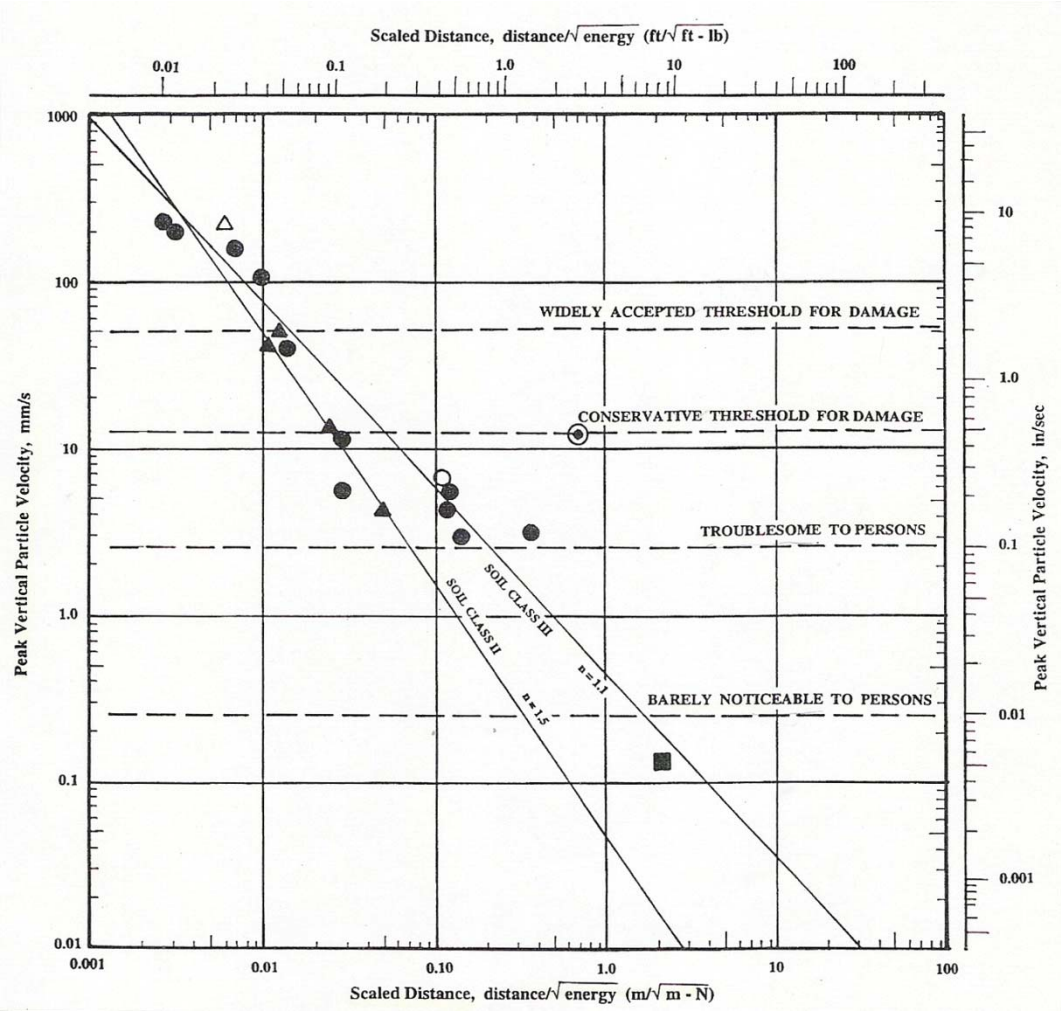

Figure 2.16 Scaled distance versus peak vertical particle velocity (Wiss, 1981)

2.3 PILE DRIVING VIBRATION

Ground vibration can be generated by natural and artificial sources. The natural vibration sources such as earthquakes can cause severe damage to the buildings and structures. On the other hand, artificial vibration sources such as construction equipment and construction activities including piling driving operations have relatively less damaging effects on structures. Also, artificial vibration sources are potentially controllable.

Pile driving operations frequently form one of the main vibration sources, particularly in urban areas, where the recent development trends toward high-rise structures and structures requiring deep foundations have led to increasing use of pile foundations. Piles are usually driven into the ground by means of driving hammers. During pile driving, a hammer transfers energy into the pile head at impact and pushes the pile into the ground. The magnitude of vibration caused by piling operation is controlled primarily by the hammer and pile type, and ground conditions. The FHWA manual "Design and Construction of Driven Pile Foundations (Hannigan et al.1996)" presents detailed information on piling including equipment, construction considerations, design equations, and specifications.

2.3.1 Pile Driving Equipment and Impacting System

The pile driving mechanism can be idealized as an imposition of the hammer force on top of the pile as shown in Figure 2.17. Cushion blocks function as a transmitting medium.

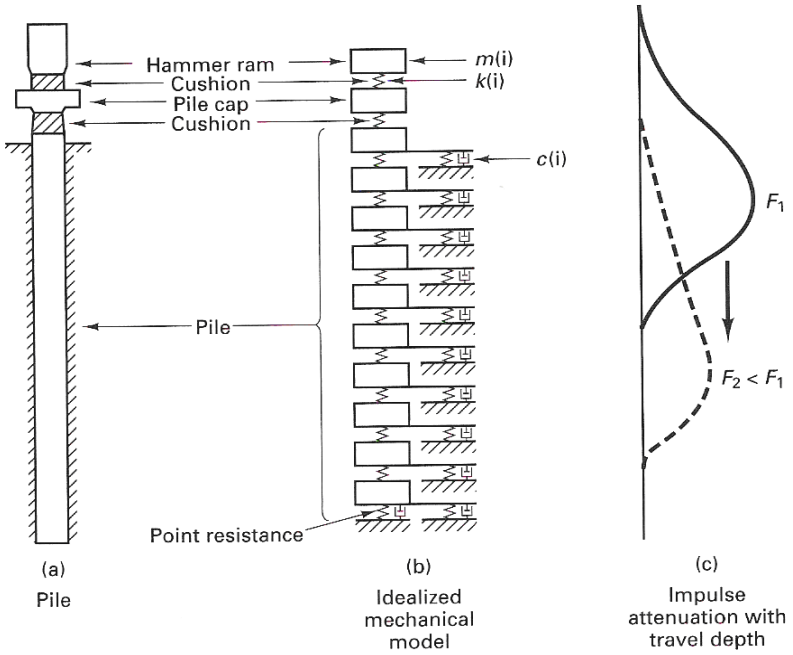

Figure 2.17 Spring-mass-dashpot systems (Parola, 1970)

2.3.2 Types of Piles

Different types of piles have been developed to suit the construction conditions such as the type of load to be carried, subsoil condition, and ground water level. Piles may be generally classified with respect to the way in which the load is transferred to the soil as either end bearing piles or friction piles. According to the material, piles may be divided into steel piles, concrete piles, timber and composite piles.

2.3.2.1 Classification of Pile with respect to Load Transmission and Functional

Behavior

- End bearing piles (point bearing piles)

When bedrock or rocklike materials are located at a reasonable depth from the ground, end-bearing piles can be extended into these hard soil layers. Figure 2.18 shows the mechanism of the end bearing pile.

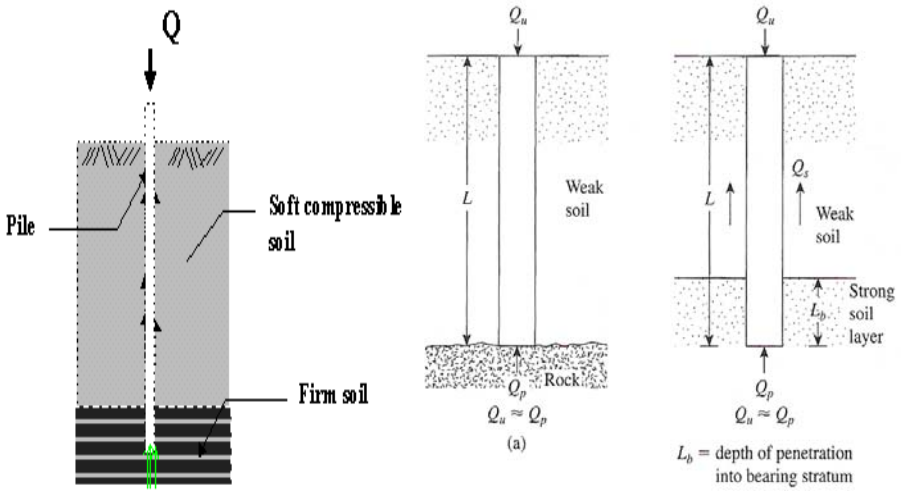

Figure 2.18 End bearing pile (School of Engineering and Built Environment, Napier University, 1999 and Das, 1999)

The ultimate pile load is

$$Q_u = Q_p + Q_s \qquad \text{(if } Q_s \text{ is very small, } Q_u = Q_p\text{)} \qquad 2.31$$

where Q_p is the pile bearing load

Q_s is the load carried by skin friction generated at the surface of the pile

- Friction piles

If there is no bedrock or rocklike materials at a reasonable depth from the ground, the use of the end bearing piles is uneconomical; thus in this case piles are driven into the softer material to a specific depth. Since the resistance of a pile is originated from the skin friction, these types of piles are called friction piles. The principle of this application is given in Figure 2.19.

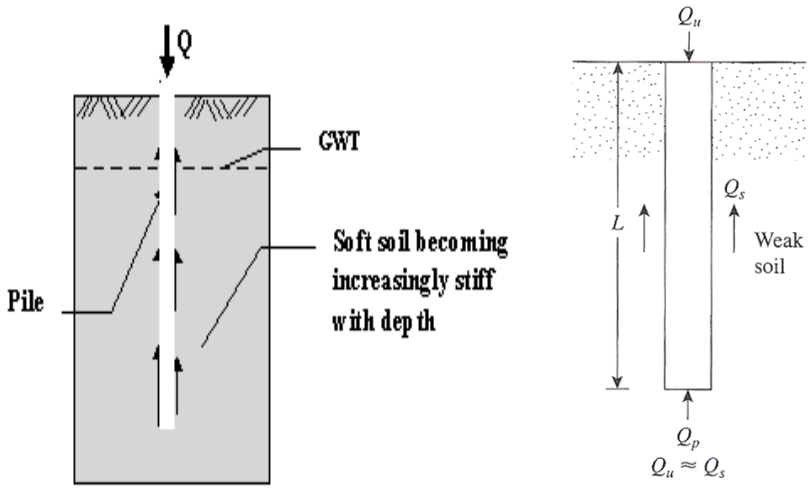

Figure 2.19 Friction pile (School of Engineering and Built Environment, Napier University, 1999 and Das, 1999)

The ultimate pile load is

$$Q_u = Q_p + Q_s \qquad (\text{if } Q_p \text{ is very small, } Q_u = Q_s) \qquad 2.32$$

- Compaction piles

So-called compaction piles are used in the certain case in which piles are driven into granular soils to get the appropriate compaction of the soil located at the ground surface. The length of the compaction piles depend on

(a) Relative density of the soil before compaction

(b) Desired relative density of the soil after compaction

(c) Required depth of compaction

2.3.2.2 Classification of Pile with respect to Type of Material

- **Steel Piles**

Figure 2.20 Steel pipe piles

Steel piles include pipe piles and H-section piles made up of steel or iron materials. Wide-flange and I-section beams can also be used as piles. However, H-section piles are preferred because the web and flange thicknesses are equal. Steel piles are proper for handling and driving in long lengths. The allowable capacity of steel pile can be obtained by

$$Q_{all} = A_s f_s \qquad 2.33$$

Where A_s is the cross-sectional area of the steel pile

f_s is the allowable stress of the steel pile

The advantages and disadvantages of steel piles are given in Table 2.4.

Table 2.4 Advantages and disadvantages of steel piles

Advantages	Disadvantages
• **Easy to handle and cut to desired length** • **Possible to drive the steel piles into dense soil layers** • **Easy to splice and bolt** • **Can withstand high driving stresses** • **Can make long length piles** • **Proper for heavy loads** • **Can be anchored in sloping rock**	• **Corrosion problem** • **Relatively easy to deviate during installation** • **Relatively expensive** • **High level of noise during driving**

- **Concrete Piles**

Figure 2.21 Precast concrete piles

Concrete piles can be classified into two basic categories: (a) precast concrete piles and (b) cast-in-situ or cast-in-place concrete piles. Reinforcement is provided to enable the pile to resist the bending moment during transportation, and to resist vertical loads and bending moments caused by structure vertical and lateral loads. Precast piles are made to the desired lengths, and cured before being transported to

the site for the pile driving operation. Figure 2.22 shows square and octagonal cross-section precast concrete piles.

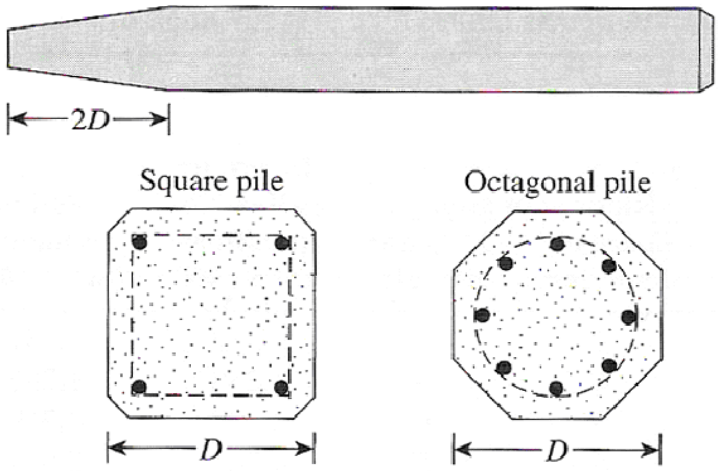

Figure 2.22 Section of the precast concrete piles (Das, 1999)

Cast-in-situ or cast-in-place concrete piles are made in the field by making a hole in the ground and filling with concrete. Cast-in-situ concrete piles are divided into two categories: (a) cased and (b) uncased. Cased piles are made by driving a steel casing with a mandrel into the ground. This mandrel is a tool that helps in driving, and is withdrawn after the filling of the concrete into the steel casing. A Cast-in-situ concrete pile can have a pedestal at its tip, which is an expanded concrete bulb. Various types of cast-in-situ concrete piles are shown in Figure 2.23.

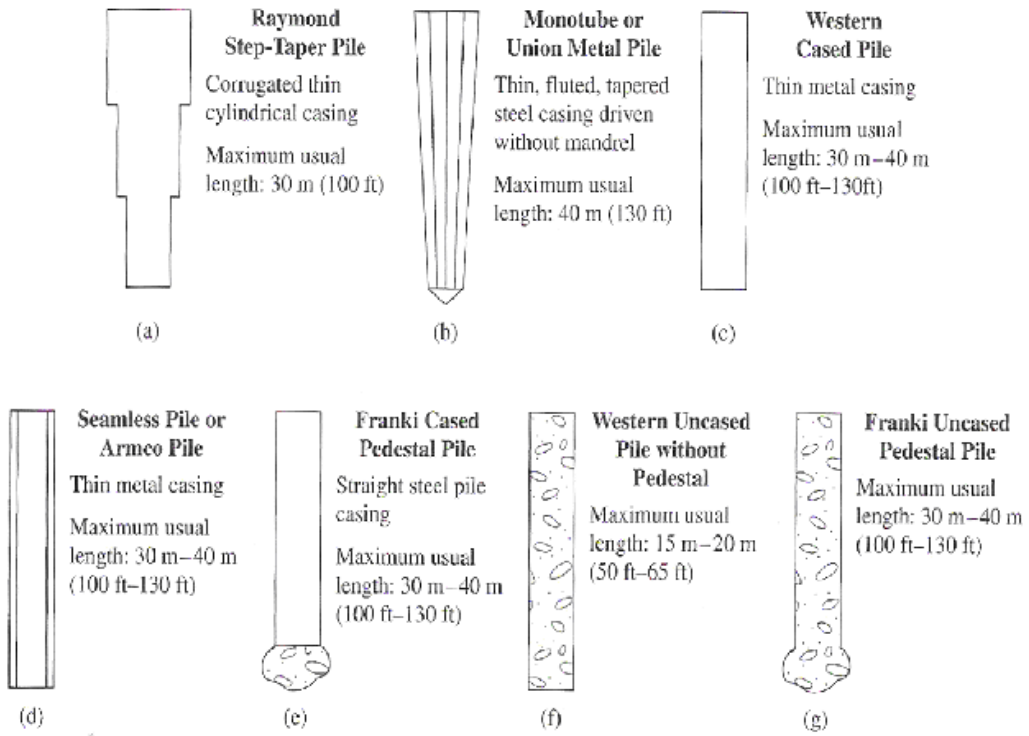

Figure 2.23 Cast-in-situ (cast-in-place) concrete piles (Das, 1999)

The allowable capacity of a cast-in-situ concrete pile is obtained by the Equation 2.34 and 2.35:

- **Cased Pile**

$$Q_{all} = A_s f_s + A_c f_c \qquad 2.34$$

- **Uncased Pile**

$$Q_{all} = A_c f_c \qquad 2.35$$

Where A_s is the cross sectional area of the steel casing

A_c is the cross sectional area of the concrete pile

f_s is the allowable stress of the steel casing

f_c is the allowable stress of the concrete pile

The advantages and disadvantages of concrete piles are given in Table 2.5.

Table 2.5 Advantages and disadvantages of concrete piles

	Advantages	Disadvantages
Precast concrete piles	• **Does not corrode as easily as steel** • **Easy to splice** • **Relatively inexpensive** • **Stable in squeezing ground** • **Makes long length piles** • **Increase the relative density of a granular founding stratum**	• **Relatively difficult to cut** • **Possible for displacement, heave, and disturbance of the soil during driving.** • **Possible to be damaged during driving** • **Noise and vibration problem** • **Difficult to drive for the large diameter**
Cast-in-situ concrete piles	• **No risk of ground heave** • **Install in conditions of very low headroom** • **Relatively low effect of noise and vibration** • **Makes long length piles** • **Not dependent on handling or driving conditions for the material of piles** • **Install in very large diameters** • **Inspect soil removed in boring** • **Possible for sample or in- situ test** • **Flexible length for the varying ground conditions** • **Possible to enlarge the end of the pile up to two or three diameters in clay**	• **Difficult to place the concrete under adverse conditions and to inspect subsequently** • **Difficult to form the enlarged ends in cohesionless materials without special techniques** • **Difficult to extend the piles above ground level especially in river and marine structures** • **Possible to loosen sandy and gravely soils requiring base grouting to achieve economical base resistance by boring methods**

- **Timber Piles**

Timber piles are tree trunks without branches and bark as shown in Figure 2.24.

The maximum length of most timber piles is 30 to 65ft (10 to 20m). The use of timber piles is decreasing because of the increasing popularity of steel and concrete piles.

Figure 2.24 Timber piles

The allowable capacity of the timber piles is:

$$Q_{all} = A_p f_w \qquad 2.36$$

where A_P is the average cross sectional area of the pile

f_w is the allowable stress for the timber pile

The advantages and disadvantages of timber piles are presented in Table 2.6.

Table 2.6 Advantages and disadvantages of the timber piles

Advantages	Disadvantages
• **Easy to handle** • **Relatively inexpensive (In plentiful area)** • **Easy to remove excess length**	• **Easily rots above the ground level** • **Limited bearing capacity** • **Easy to be damaged during driving** • **Difficult to splice** • **Easy to be attacked by marine borers in salt water.**

- **Composite Piles**

Composite piles are made of several materials. Different types of materials are used for the upper and lower parts of the pile. For instance, composite piles may be made of steel and concrete or timber and concrete. The combination of the materials for the piles can be varied depending on the ground condition and bearing capacity. Figure 2.25 shows a combination of concrete and timber piles that accounts for the level of water table.

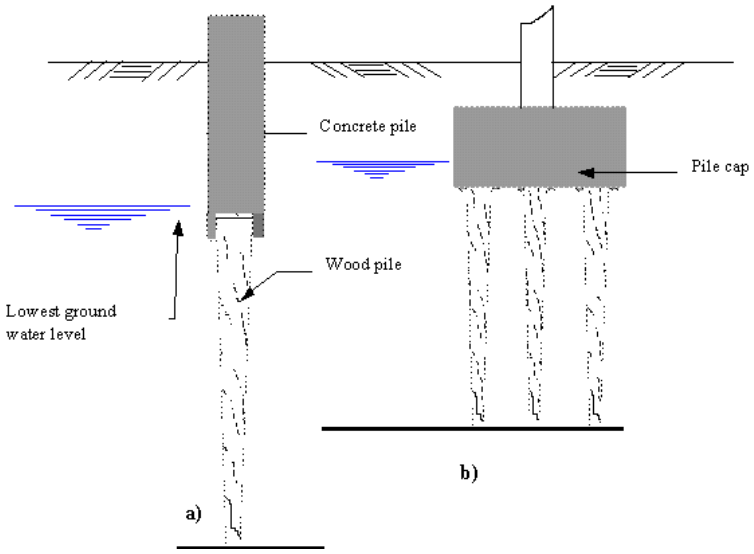

Figure 2.25 Combination pile made of concrete and timber piles for protecting timber piles from decay (School of Engineering and Built Environment, Napier University, 1999)

2.3.3 Types of Hammers

Piles are driven into the ground by means of a hammer. Hammer is equipment used to input energy to the pile in order to drive it into the ground. Many types of hammers are available for driving different types of piles in different ground conditions. Hammers are classified into two main types: (a) Impact hammers and (b) vibratory hammers.

2.3.3.1 Impact hammer

An impact hammer causes an impact by a weight falling through a certain height on the pile head. The simplest type of impact hammer is the drop hammer but other types of driving hammers have been developed using different types of power sources such as diesel, steam, air and hydraulics to speed up the number of strikes.

● Drop Hammer

The drop hammer is the traditional and oldest driving method which has been used for driving piles since ancient times. The drop hammer consists of a solid mass made of steel, ranging in weight between 0.5 ton and 5 tons. The piles are driven by the drop of the ram, or striking part, from a falling height H . One disadvantage is the slow rate of blows. Figure 2.26 shows a drop hammer, and describes the pile/hammer materials and operating principle.

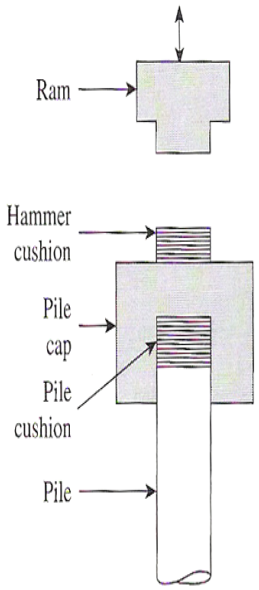

Figure 2.26 Drop hammer and members (Das, 1999)

● Steam and Air Hammer

Steam and air hammers are another type of the impact hammer which employ steam or compressed air for operation. There are two types of steam & air hammers: (a) single-acting steam & air hammer (b) double-acting and differential steam and air hammer. In the single –acting steam & air hammer, the ram is raised by the air or steam pressure, and is dropped by gravity. The ram of the double-acting and differential steam and air hammer is raised and pushed downward by the steam and air. Figure 2.27 shows the steam hammer, and operating principle of the single-acting, and double-acting and differential steam and air hammers.

(a) Steam hammer

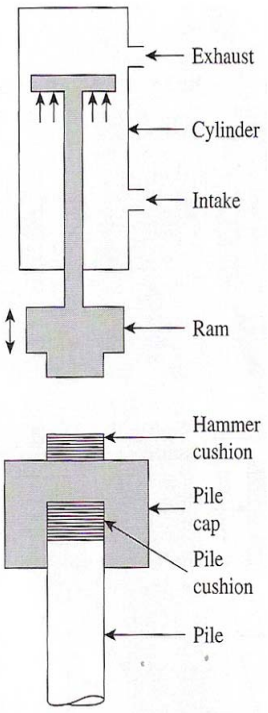

(b) Operating principle of the single-acting steam and air hammer

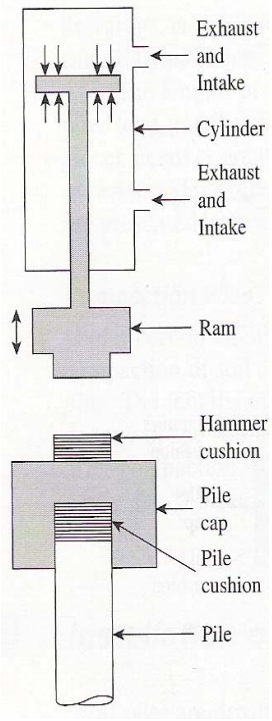

(c) Operating principle the double-acting and differential steam air hammer

Figure 2.27 Steam hammer and the members of the single-acting and double-acting steam hammer (Das, 1999)

●Diesel Hammer

The diesel hammer is a form of impact hammer which uses air and atomized diesel fuel to provide the energy to drive the pile. The hammer has a fuel tank and driving ram, so that no additional power pack is needed, and it can be easily mobilized. Diesel hammers are made of three major parts: (a) Ram, (b) Anvil, and (c) fuel-injection system. The raised ram in the hammer ignites the air-fuel mixture when it falls. The repetition of this action pushes the pile into the ground and raises the ram again. The diesel hammer is especially effective in hard driving conditions. Figure 2.28 shows the two types of diesel hammers and principle of operation.

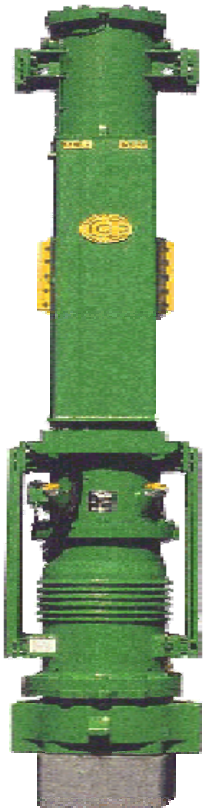

(a) Single-acting diesel hammer

(b) Double-acting diesel hammer

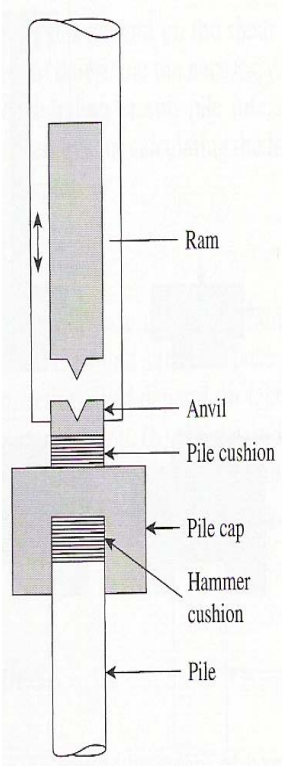

(c) Operating principle of diesel hammer

Figure 2.28 Diesel hammers and operation principle (Das, 1999)

● **Hydraulic Hammer**

The hydraulic hammer consists of a hydraulic actuator, ram weight, support cage, power source and control panel. The piston in the hydraulic actuator is connected to the ram weight and lifts the ram upwards hydraulically to a selected height which then drops under free fall conditions. This type of hammer is suitable for driving long and heavy piles for deep penetration. There are also two types of hydraulic hammers: (a) single-acting hydraulic hammer, and (b) double-acting hydraulic hammer. Figure 2.29 shows the types of hydraulic hammers.

(a) Single-acting hydraulic hammer

(b) Double-acting hydraulic hammer

Figure 2.29 Hydraulic hammers

2.3.3.2 Vibratory Hammer

The vibratory hammer, or vibrodriver, is a type of hammer which introduces continuous sinusoidal vibration into the pile and ground during its operation. This type of hammer essentially consists of two counter-rotating weights. The piles are driven into the ground by the sinusoidal dynamic vertical force of two counter-rotating weights. The hammer is suitable for driving piles in granular or cohesionless soils. The vibrodrivers are classified according to the driving power as standard vibrodriver and hydraulic

vibrodriver. Figure 2.30 describes the standard vibratory hammer and the operation principle.

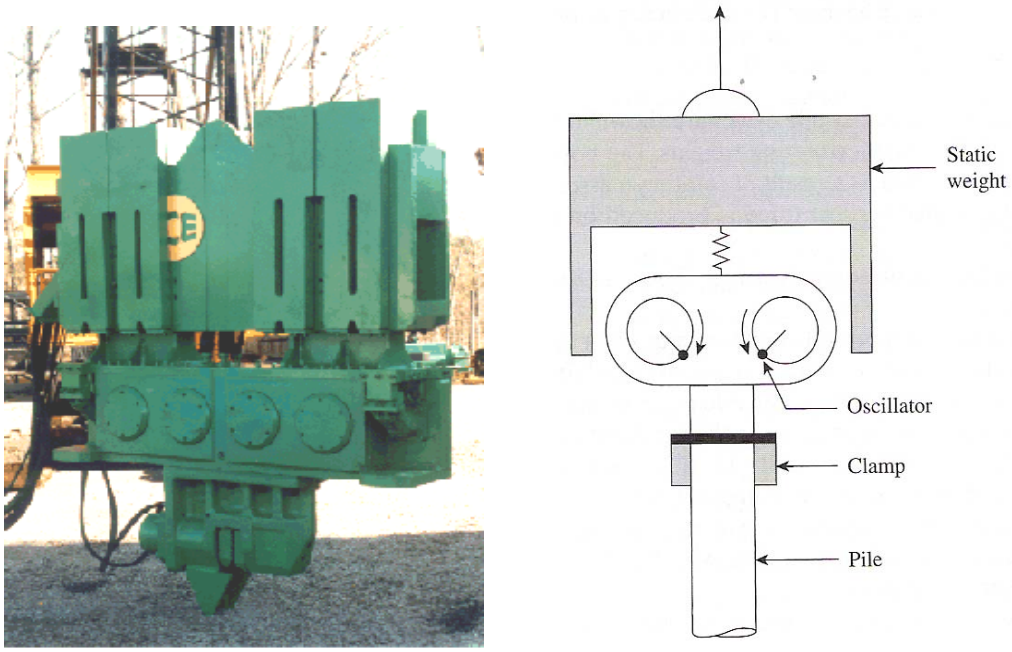

(a) Standard vibrodriver (b) Operating principle of the driver

Figure 2.30 Standard vibrodriver and the principle of the driver (Das, 1999)

Vesic (1977) presented the data in Table 2.7 for impact hammers.

Table 2.7 Impact pile hammer data (Vesic, 1977)

Rated Energy (*kip – ft*)	*Make of Hammer*	*Model Number*	*Type*[1]	*Blows per Minute* (max/min)	*Stroke at Rated energy* (*in*)	*Weight of Striking part* (*kips*)	*Total Weight* (*kips*)
1800	**Vulcan**	**6300**	**S-A**	**38**	**72**	**300**	**838**
300	**Delmag**	**D100-13**	**Dies.**	**45/34**	**NA**	**44.894**	**70.435**
225	**Delmag**	**D80-23**	**Dies.**	**45/36**	**NA**	**37.275**	**58.704**
200	**Raymond**	**RU-200**	**-**	**40/30**	**40**	**60**	**-**
180	**Vulcan**	**060**	**S-A**	**62**	**36**	**60**	**121**
165	**Delmag**	**D62-22**	**Dies.**	**50/36**	**-**	**27.077**	**42.834**
150	**Vulcan**	**530**	**S-A**	**42**	**60**	**30**	**141.82**
149.6	**Mitsubishi**	**MH80B**	**Dies.**	**60/42**	**-**	**17.6**	**43.9**
130	**MKT**	**S-40**	**S-A**	**55**	**39**	**40**	**96**
127	**MKT**	**DE-150**	**Dies.**	**50/40**	**129**	**15**	**29.5**
120	**Vulcan**	**040**	**S-A**	**60**	**36**	**40**	**87.5**
113.5	**Vulcan**	**400c**	**Dies.**	**100**	**16.5**	**40**	**83**
107.18	**Delmag**	**D46-32**	**Dies.**	**53/37**	**NA**	**19.58**	**30.825**
97.5	**MKT**	**S-30**	**S-A**	**60**	**39**	**30**	**86**
83.88	**Delmag**	**D36-32**	**Dies.**	**53/36**	**NA**	**17.375**	**26.415**
79.6	**Kobe**	**K42**	**Dies.**	**52**	**98**	**9.2**	**22**
70	**ICE**	**1072**	**Dies.**	**68/64**	**72**	**10**	**25.5**
68.898	**Delmag**	**D30-32**	**Dies.**	**52/36**	**NA**	**13.472**	**20.704**
60	**Vulcan**	**020**	**S-A**	**60**	**36**	**20**	**39**
60	**MKT**	**S20**	**S-A**	**60**	**36**	**20**	**38.6**
58.248	**Delmag**	**D25-32**	**Dies.**	**52/37**	**NA**	**12.37**	**18.5**
50.2	**Vulcan**	**200C**	**Diff.**	**98**	**15.5**	**20**	**67.815**
48.75	**Raymond**	**150C**	**Diff.**	**115/105**	**18**	**15**	**32.5**
48.7	**Vulcan**	**016**	**S-A**	**60**	**36**	**16.2**	**30.2**
48.7	**Raymond**	**0000**	**S-A**	**46**	**39**	**15.2**	**23**
44.5	**Kobe**	**K22**	**Dies.**	**52**	**98**	**4.8**	**10.6**
44	**MKT**	**MS-500**	**S-A**	**50/40**	**48**	**15.5**	**-**
42	**Vulcan**	**014**	**S-A**	**60**	**36**	**14**	**27.5**
40.6	**Raymond**	**000**	**S-A**	**50**	**39**	**12.5**	**21**
39.8	**Delmag**	**D-22**	**Dies.**	**52**	**NA**	**4.8**	**10**
39.366	**Delmag**	**D16-32**	**Dies.**	**52/36**	**NA**	**7.166**	**11.079**
37.5	**MKT**	**S14**	**S-A**	**60**	**32**	**14**	**31.6**
36	**Vulcan**	**140C**	**Dies.**	**103**	**15.5**	**14**	**27.9**
33	**Vulcan**	**33D**	**Dies.**	**50/40**	**120**	**7.94**	**-**
32.5	**MKT**	**S10**	**S-A**	**55**	**39**	**10**	**22.2**

32.5	Vulcan	010	S-A	50	39	10	18.7
32.5	Raymond	00	S-A	50	39	10	18.5
32	MKT	DE-40	Dies.	48	96	4	11.2
30.2	Vulcan	OR	S-A	50	39	9.3	16.7
30	ICE	520	Dies.	84/80	71	5.07	17.04
28.1	Mitsubishi	MH15	Dies.	60/42	-	3.31	8.4
28	MKT	DE-33B	Dies.	50/40	126	3.3	7.75
26.3	Link-Belt	520	Dies.	82	43.2	5	12.5
26	MKT	C-8	D-A	81	20	8	18.7
26	Vulcan	08	S-A	50	39	8	16.7
26	MKT	S8	S-A	55	39	8	18.1
25	Vulcan	505	S-A	46	60	5	29.5
24.4	Vulcan	80C	Diff.	111	16.2	8	17.8
24.4	Vulcan	8M	Diff.	111	NA	8	18.4
24.3	Vulcan	0	S-A	50	39	7.5	16.2
24	MKT	C-826	D-A	90	18	8	17.7
22.6	Delmag	D-12	Dies.	51	NA	2.7	5.4
22.4	MKT	DE-30	Dies.	48	96	2.8	9
19.8	Union	K13	D-A	110	24	3	14.5
19.8	MKT	11B3	D-A	95	19	5	14.5
19.5	Vulcan	06	S-A	60	36	6.5	11.2
19.2	Vulcan	65C	Diff.	117	15.5	6.5	14.8
18.2	Link-Belt	440	Dies.	88	36.9	4	10.3
18	Delmag	D8-22	Dies.	52/38	NA	4	6.147
17	MKT	DE-20B	Dies.	50/40	126	2	6.4
16.2	MKT	S5	S-A	60	39	5	12.3
16	MKT	DE-20	Dies.	48	96	2	6.3
16	MKT	C5	Comp.	110	18	5	11.8
15.1	Vulcan	50C	Diff.	120	15.5	5	11.7
15.1	Vulcan	5M	Diff.	120	15.5	5	12.9
15	Vulcan	1	S-A	60	36	5	10.1
15	Link-Belt	312	Dies.	100	30.9	3.8	10.3
13.1	MKT	10B3	D-A	105	19	3	10.6
12.7	Union	1	D-A	125	21	1.6	10
9	Delmag	D5	Dies.	51	NA	1.1	2.4
9	MKT	C-3	D-A	130	16	3	8.5
9	MKT	S3	S-A	65	36	3	8.8
8.75	MKT	9B3	D-A	145	17	1.6	7
8.8	MKT	DE-10	Dies.	48	96	11	3.5
8.7	MKT	9B3	D-A	145	17	1.6	7
8.2	Union	1.5A	D-A	135	18	1.5	9.2
8.1	Link-Belt	180	Dies.	92	37.6	1.7	4.5
8.1	ICE	180	Dies.	95/90	57	1.725	5.208
7.2	Vulcan	2	S-A	70	29.7	3	7.1

7.2	Vulcan	30C	Diff.	133	12.5	3	7
7.2	Vulcan	3M	Diff.	133	NA	3	8.4
6.5	Link-Belt	105	Dies.	94	35.2	1.4	3.8
0.4	Vulcan	DGH100A	Diff.	303	6	0.1	0.8
0.4	MKT	3	D-A	400	5.7	0.06	0.7
0.3	Union	7A	D-A	400	6	0.08	0.5

Dowding (1996) compared the magnitude of energies originating from different sources for comparison purposes as shown in Table 2.8.

Table 2.8 Comparison of energies released (Dowding, 1996)

Source	Energy released ($10^3 J$)
Earthquake RM 7.1	**16,000,000,000,000**
Nuclear explosion 1megaton	**5,400,000,000**
TNT $\frac{1}{2} kg$	**5400**
Franki drop weight $11{,}000 - 15{,}000 kg$	**27-190**
Diesel hammer MKT DE 70B	**57-85**
Tomen vibratory Extractor VM2	**7**

CHAPTER 3

NUMERICAL MODELING

3.0 THE NUMERICAL MODEL

A numerical model for predicting ground surface vibrations caused by pile driving will be developed in Chapter 4. The numerical model is based on the finite element method embodied in the computer program Abaqus. This finite element computer program is a commercial general-purpose code developed by Abaqus, Inc. In this Chapter, three numerical models of three benchmark dynamic problems of interest are established and verified by comparing their numerical results with the benchmark problem solutions reported in the literature.

3.0.1 Benchmark Problem 1: Velocity of Rayleigh Wave

Since Rayleigh wave is a surface wave and the area of wave motion is confined to the surface of the ground, the amplitude of Rayleigh wave is affected by the depth of disturbance source, and is inversely proportional to the square root of the distance from the source. The Rayleigh wave is slower than the compression wave at the surface of the ground. The analysis of Rayleigh wave traveling along the ground surface is important because the greatest damage potential to above-ground structures is caused by Rayleigh waves that carry most of the destructive energy emanating from the vibration source.

The finite element method is used to predict the velocity of Rayleigh wave traveling along the surface of an elastic half space that is excited by an impulse load (applied at the

surface). A two-dimensional plane strain elastic half space is used for the analysis as shown in Figure 3.1.

"Infinite" elements and "Finite" elements are used to establish the mesh shown in Figure 3.1. The infinite elements are used to minimize wave reflection from the boundary of the soil continuum. As shown in the Figure, an impulse load of 100 kN and duration of 0.005 seconds (see Table 3.1) is applied at the origin. The soil is assumed to be linear elastic with the parameters given in Table 3.2.

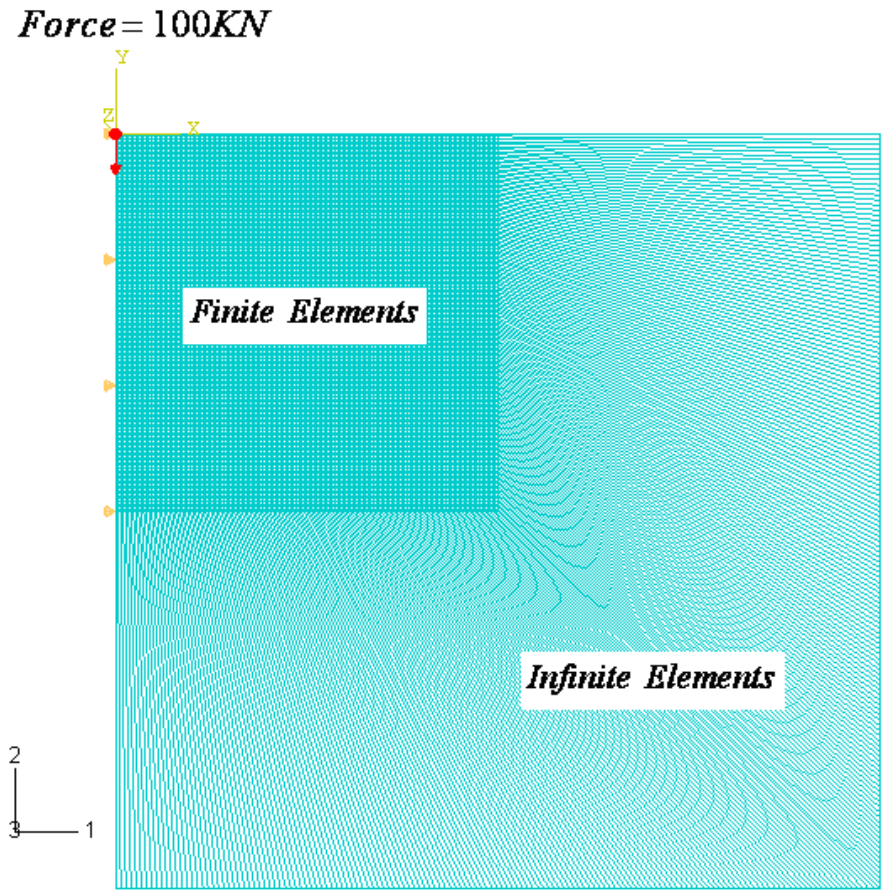

Figure 3.1 Benchmark Problem 1

Table 3.1 Amplitude of applied load

Time (second)	Force (KN)
0	**0**
0.0025	**100**
0.005	**0**
1	**0**

Table 3.2 Soil Parameters

Parameters	Value
γ, *unit weight*	**19.6** kN/m^3
E, *Young's* mod*ulus*	**1000** kN/m^2
ν, *Poisson's ratio*	**0.25**

Figure 3.2 shows the benefit of using infinite elements--the surface waves are absorbed by the infinite elements and reflection of the stress wave is prevented. Figure 3.3 describes the movement of waves from the impulse load. It is noted that the surface waves, displayed with the yellow and red, are visible along the ground surface. Also noted from the Figure is that the body waves precede the surface waves since the body waves are faster than the surface waves as mentioned in the literature review.

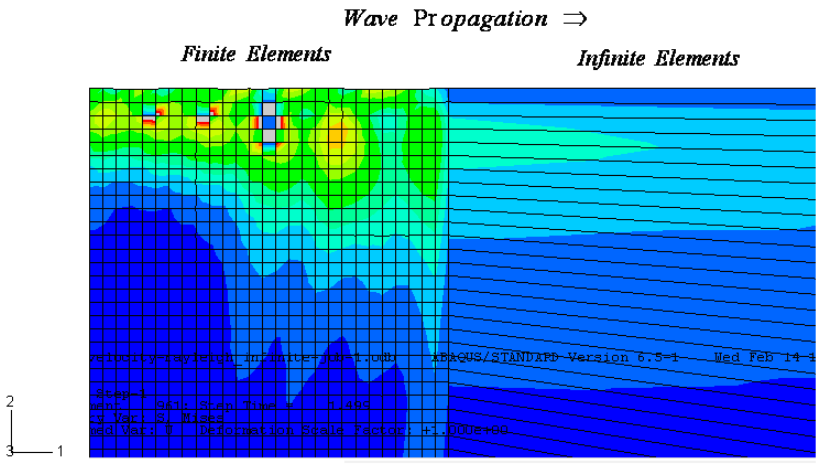

Figure 3.2 Waves Absorbed by Infinite Elements

According to Dowding (1996), on the ground surface, a combination of geometrical spreading and frequency dependence explains why Rayleigh waves predominate at large distances. First, Rayleigh waves travel only on the ground surface and their energy only spreads over a cylindrical surface rather than the spherical surface of the body waves. Second, the lower frequency Rayleigh waves will have traveled fewer deformational cycles and lost less energy than the higher frequency body waves. The Rayleigh wave propagates away from the vibration source forming a particle motion of a retrograde ellipse. This retrograde ellipse motion distorts the surface of the ground, and can cause damage to structures on the ground surface. From the results of the present finite element analysis, a "particle path" of a surface point can be plotted as shown in Figure 3.4. It is noted from the Figure that the particle traverses an elliptical path in its movement. Figures 3.5a to 3.5e illustrate the propagation of body and surface waves at different time interval.

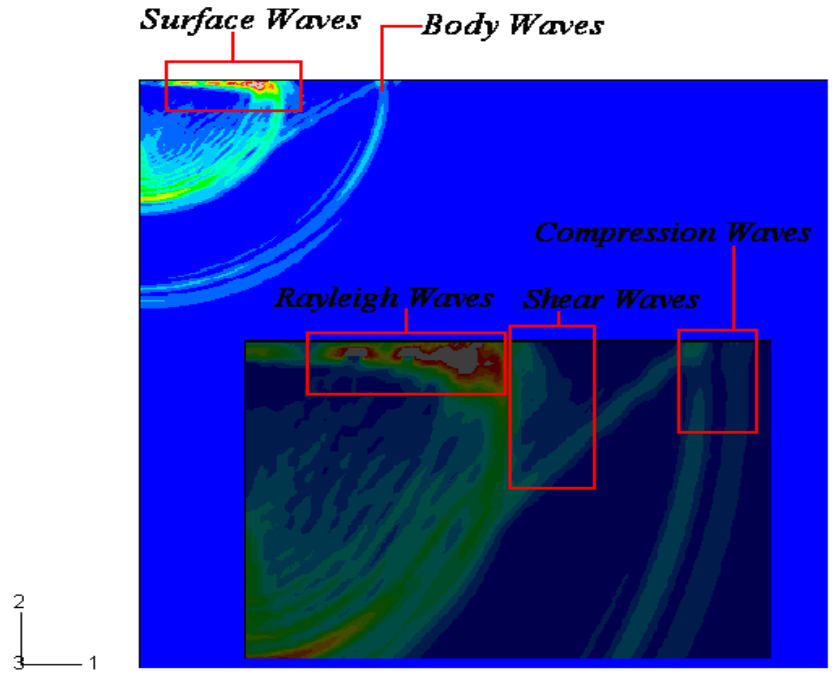

Figure 3.3 Propagation of the waves generated by the impulse load

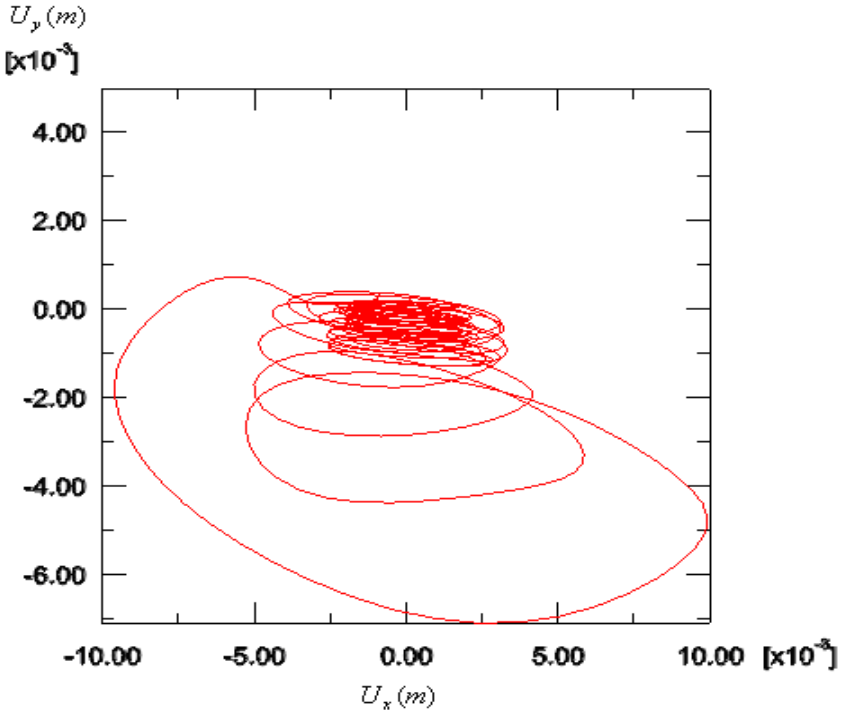

Figure 3.4 Particle path of Rayleigh wave

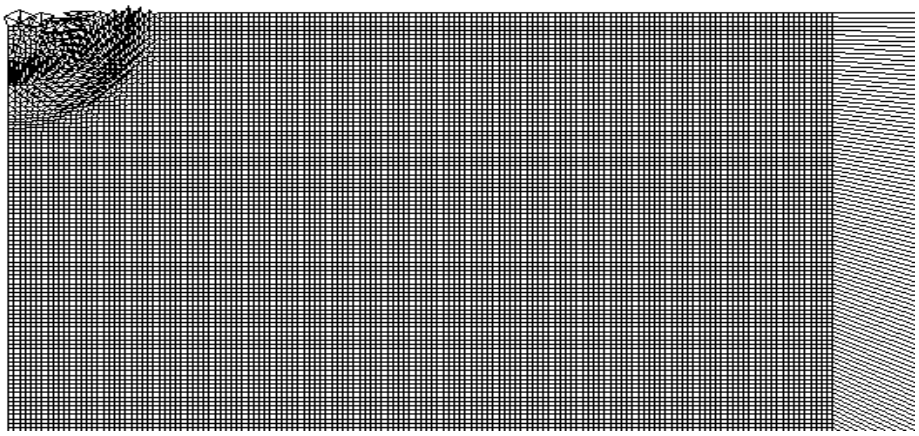

Figure 3.5a Movement of body and surface waves at t=0.1 second

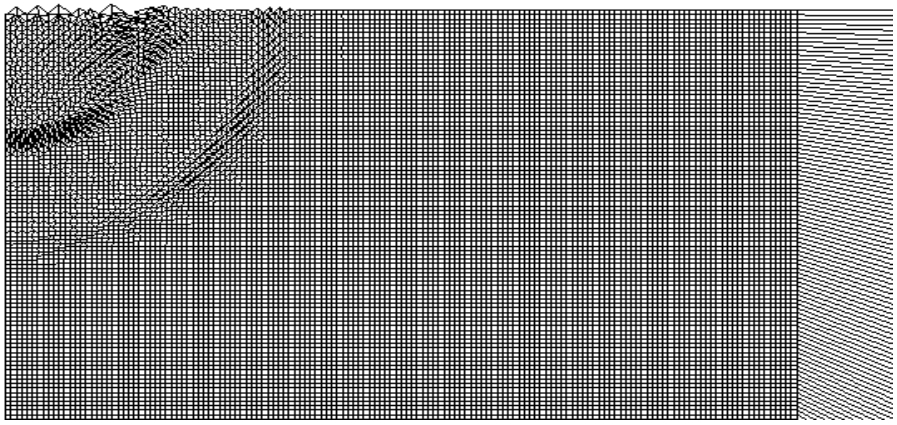

Figure 3.5b Movement of body and surface waves at t=0.3 second

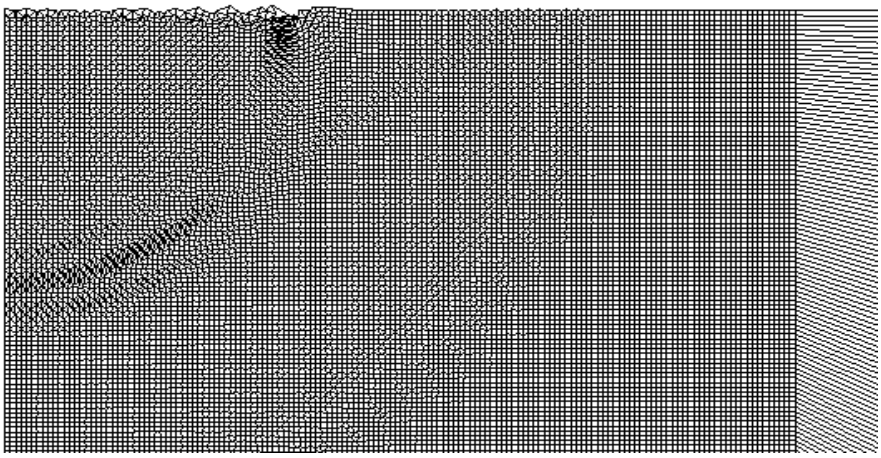

Figure 3.5c Movement of body and surface waves at t=0.6 second

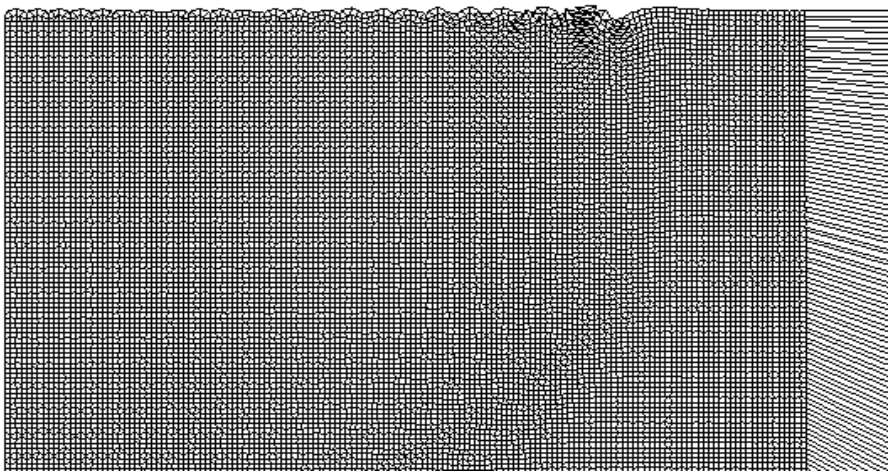

Figure 3.5d Movement of body and surface waves at t=1.2 second

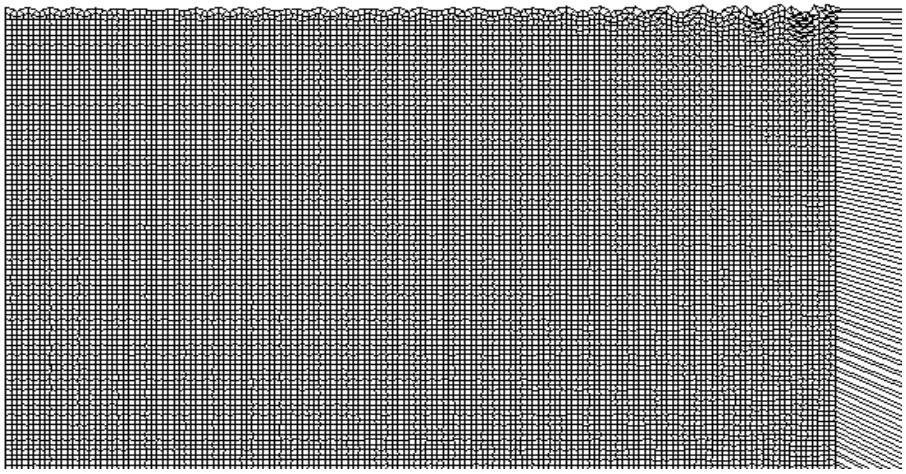

Figure 3.5e Movement of body and surface waves at t=1.6 second

Two points are selected at the ground surface for calculating the model velocities of the compression and Rayleigh waves to compare with the theoretical values. Nodes 626 and 648 are selected as shown in Figure 3.6, and they are located at 39.527 m and 32.095 m away from the impulse load. The velocity between the two points is:

$$V = \frac{D}{T} \tag{3.1}$$

Where D is the distance between the two points (Nodes 626 and 648),

T is the time required for the wave to travel from one point to the other point as estimated from Figure 3.6.

Thus,

$$V_P = \frac{D_{(node626-648)}}{T} = \frac{39.527m - 32.095m}{0.65472s - 0.54072s} = 65.2m/s$$

$$V_R = \frac{D_{(node626-648)}}{T} = \frac{39.527m - 32.095m}{1.15672s - 0.95272s} = 36.4m/s$$

In Figure 3.6, the vertical component of the shear wave is small compared with that of the compression wave, and is masked by the Rayleigh wave which posses a considerable amplitude. The shear wave is lost in the oscillatory tail of the compression wave, and the overwhelming presence of the Rayleigh wave.

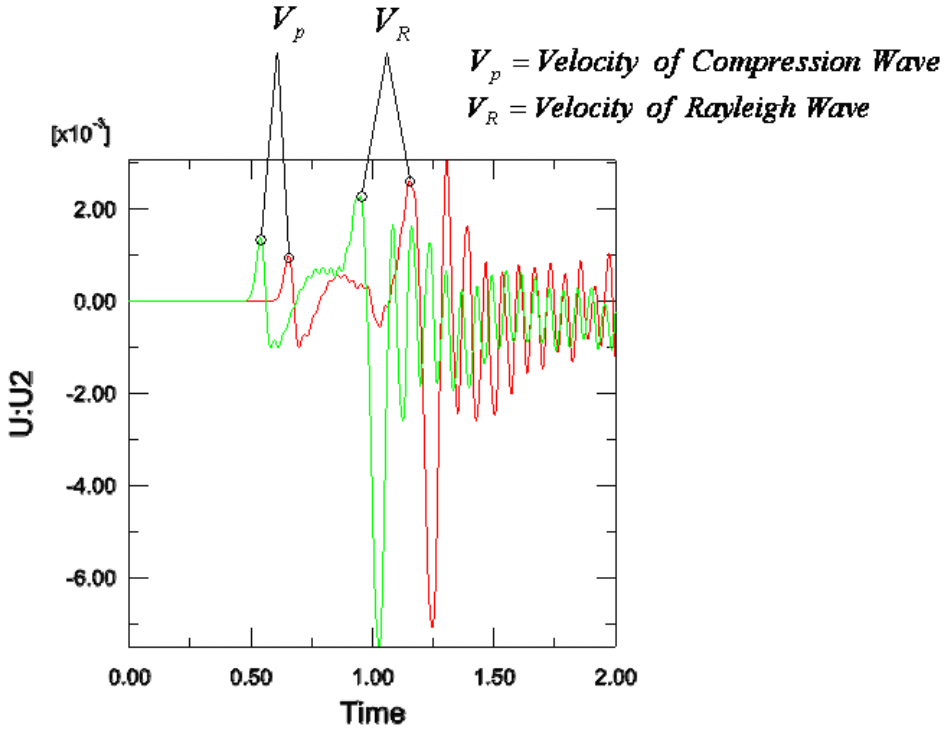

Figure 3.6 Vertical displacements at Nodes 626 and 648

The velocity of Rayleigh wave can be theoretically calculated from the Equation 3.2 suggested by Knopoff (1952).

$$1-8\left(\frac{V_S}{V_R}\right)^2+\left[24-16\left(\frac{V_P}{V_S}\right)^2\right]\left(\frac{V_S}{V_R}\right)^4-16\left[1-\left(\frac{V_P}{V_S}\right)^2\right]\left(\frac{V_S}{V_R}\right)^6=0 \qquad 3.2$$

Figure 3.7 shows the relationship of V_p, V_s and V_R versus Poisson's ratio.

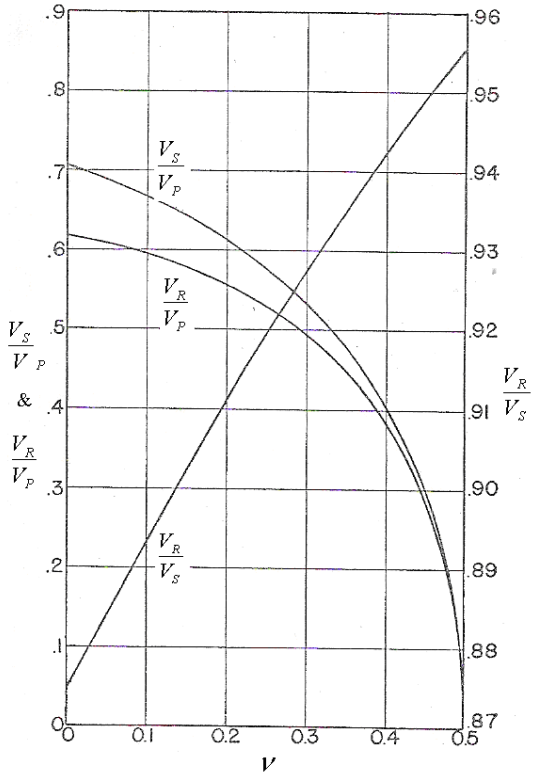

Figure 3.7 Poisson's ratio versus wave velocity (Knopoff, 1952)

From Knopoff's equation, the following relationship can be obtained.

$$V_R = 0.5308\ V_P \qquad 3.3$$

Where, $V_P = \sqrt{\dfrac{(1-\nu)E}{(1+\nu)(1-2\nu)\rho}}$ 3.4

$$\rho = \frac{\gamma}{g} \qquad 3.5$$

Where γ is the total unit weight

g is the acceleration of gravity, $9.8\, m/s^2$

Since $\frac{V_R}{V_S} = 0.9194$ ($from\ \ Figure\ \ 2.9,\ \ Poisson's\ ratio\ \ \nu = 0.25$)

and $V_P = \sqrt{3}\ V_S$.

Therefore, the velocities of compression and Rayleigh wave are:

$$V_P = \sqrt{\frac{(1-\nu)E}{(1+\nu)(1-2\nu)\rho}} = \sqrt{\frac{(1-0.25)7{,}000{,}000\ \ N/m^2}{(1+0.25)(1-2\times 0.25)2000\ \ kg/m^3}} = 64.8\ \ m/s$$

$$V_R = 0.9194\ \ V_S = 0.9194 \times \sqrt{\frac{E}{2(1+\nu)\rho}} = 0.9194 \times \sqrt{\frac{7{,}000{,}000\ \ N/m^2}{2(1+0.25)2000\ \ kg/m^3}} = 34.4\ \ m/s$$

Where, $E = 7{,}000{,}000\ \ N/m^2$

$$\rho = \frac{\gamma}{g} = \frac{19.6\ \ kN/m^3}{9.81\ \ m/s^2} \approx 2000\ \ kg/m^3$$

The theoretical values of the compression and Rayleigh wave velocities, calculated above, are in good agreement with those estimated from the finite element analysis.

3.0.2 Benchmark Problem 2: Displacement Comparison of the Surface Waves

Chouw et al. (1991) used the boundary element method to calculate the vertical displacement on the surface an elastic half space (infinitely thick soil layer) subjected to a 3-m-wide strip foundation with a sinusoidal load. The sinusoidal load has displacement

amplitude of 0.48 m and a frequency of 5 Hz. The problem configuration is shown in Figure 3.8 (use H=∞), and the half space elastic parameters are given in Table 3.3.

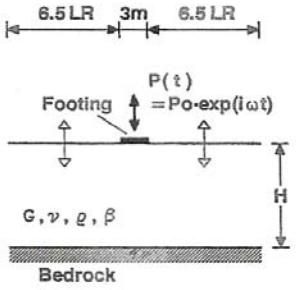

Figure 3.8 Foundation on the surface of soil layer (Chouw et al., 1991)

Table 3.3 Problem Parameters (Chouw et al., 1991)

Material type		**values**
Footing	**Width**	**3m**
	Unit vertical excitation (frequency)	**5Hz**
	Amplitude	**0.48 m**
Soil	**Mass density,** ρ	**1800** kg/m^3
	Poisson's ratio, ν	**0.33**
	Shear modulus, G	**53.28** $\times 10^3 kPa$
	Elastic modulus, E	**142** $\times 10^3 kPa$

"Infinite" elements and "Finite" elements are used to establish the mesh shown in Figure 3.9. The infinite elements (see Figure 3.10) are used to minimize wave reflection from the boundary of the soil continuum. A sinusoidal load with 0.48-m amplitude and 5-Hz frequency is applied on a 1.5-m wide strip located at the ground surface as shown in

Figure 3.11. The soil is assumed to be linear elastic with the parameters given in Table 3.3. Only half of the geometry is analyzed because of symmetry.

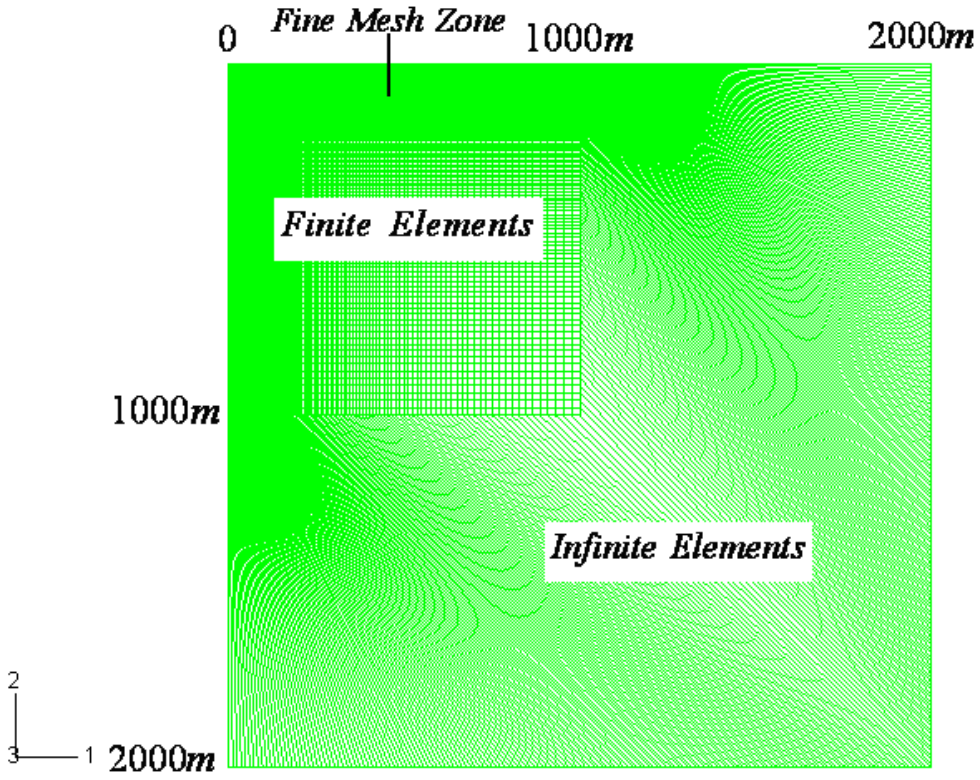

Figure 3.9 Finite element discretization

Figure 3.12 shows the resulting waves traveling in a three dimensional elastic half space. Figure 3.13 to 3.15 show the wave propagation originating from the source and traveling toward the infinite elements.

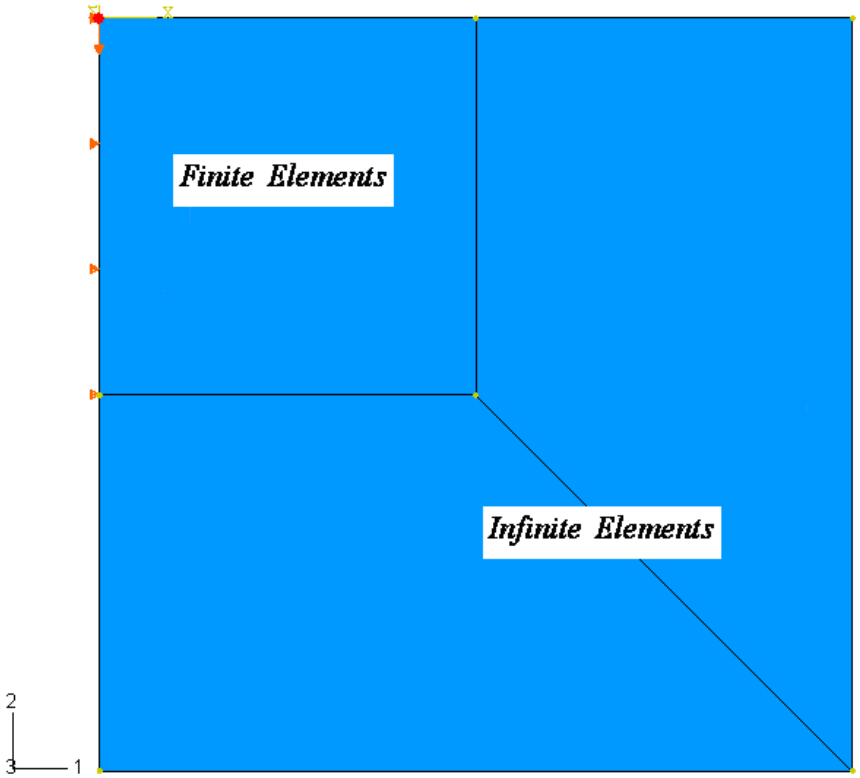

Figure 3.10 Element type and boundary condition

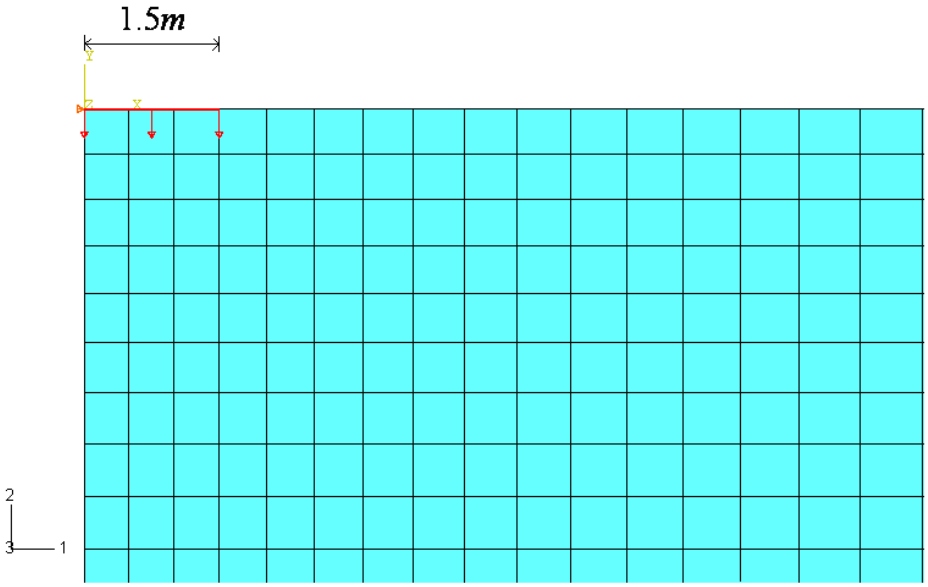

Figure 3.11 Applied harmonic displacements

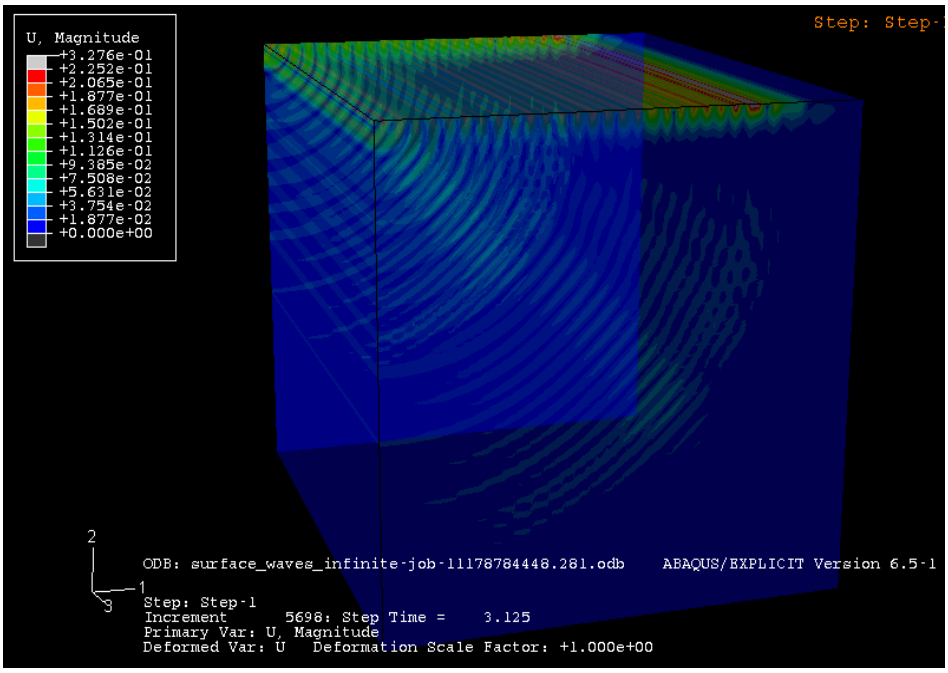

(a) Wave propagation in the elastic half space

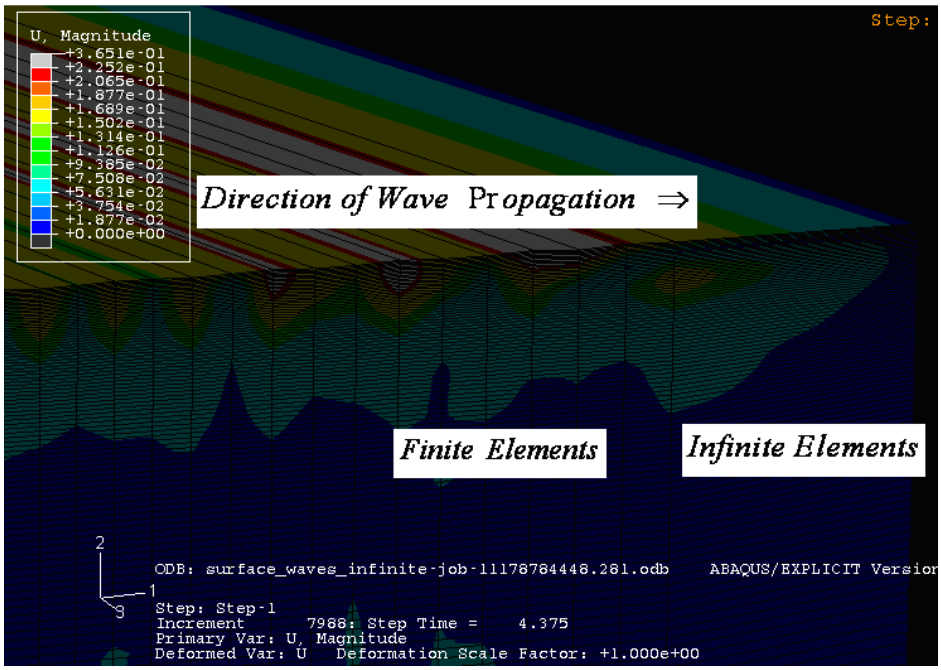

(b) Surface waves propagating from finite elements to infinite elements in the elastic half space

Figure 3.12 Surface waves in the elastic half space

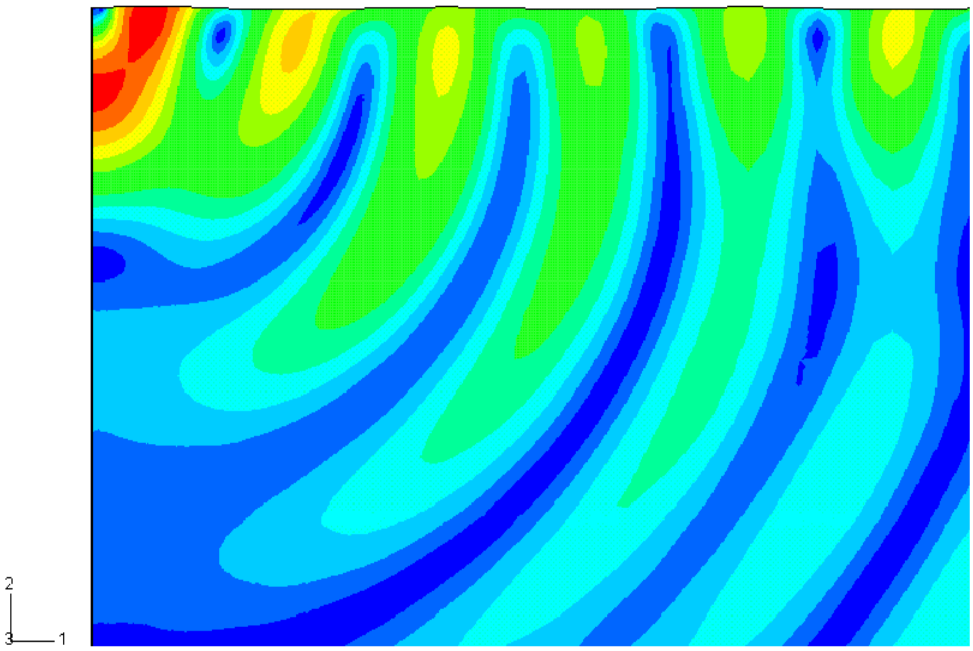

Figure 3.13 Displacement emanating from the center of foundation

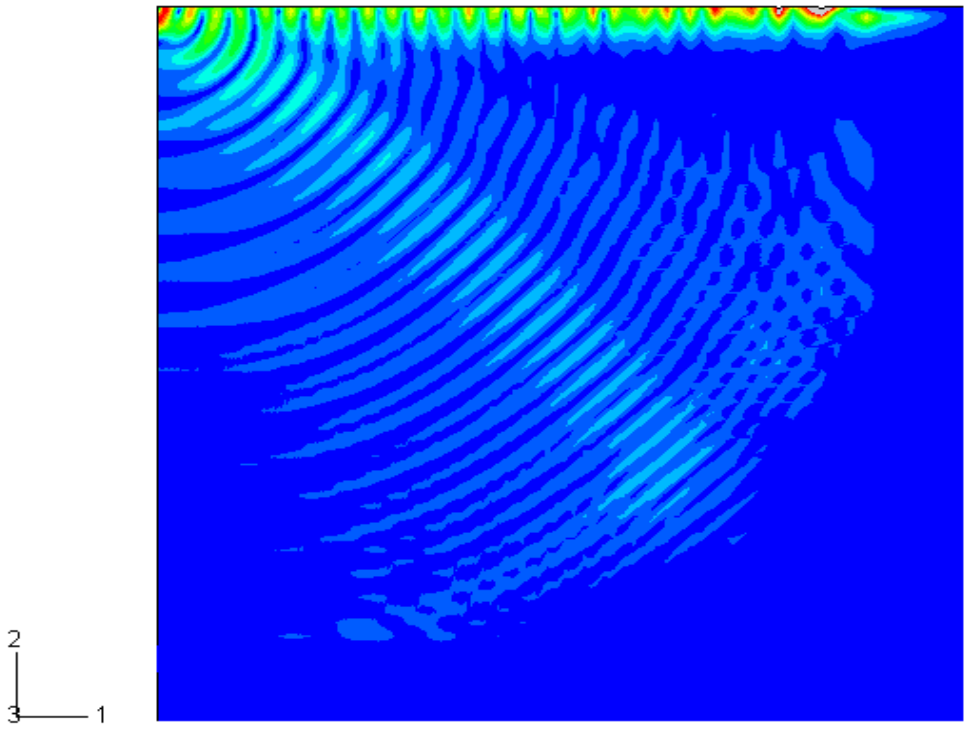

Figure 3.14 Displacements traveling along the ground surface

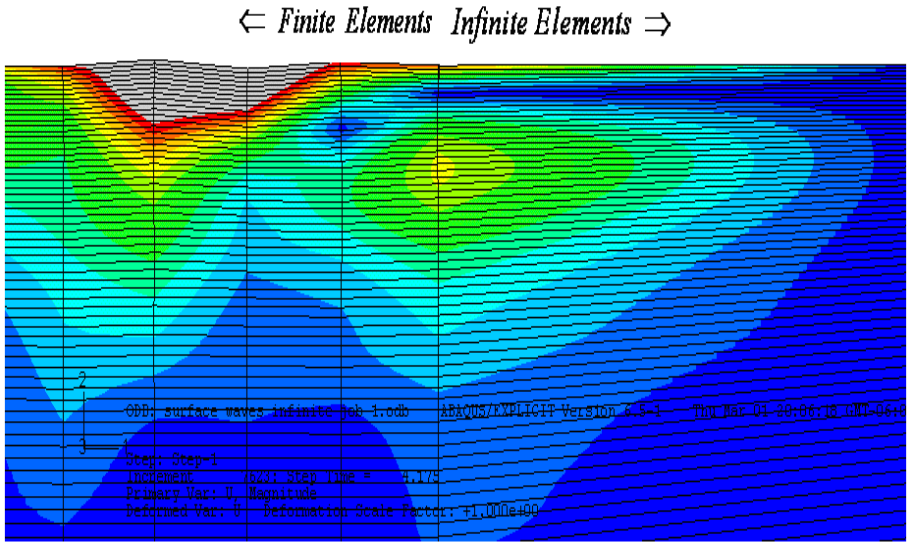

Figure 3.15 Movement of displacement in different types of elements

Figure 4.16 shows the amplitude of surface waves with distance predicted by the boundary element method as provided by Chouw et al. (1991). The Figure also shows the amplitude of surface waves calculated using the present finite element analysis. Good agreement between the predictions by the two methods is noted in the Figure.

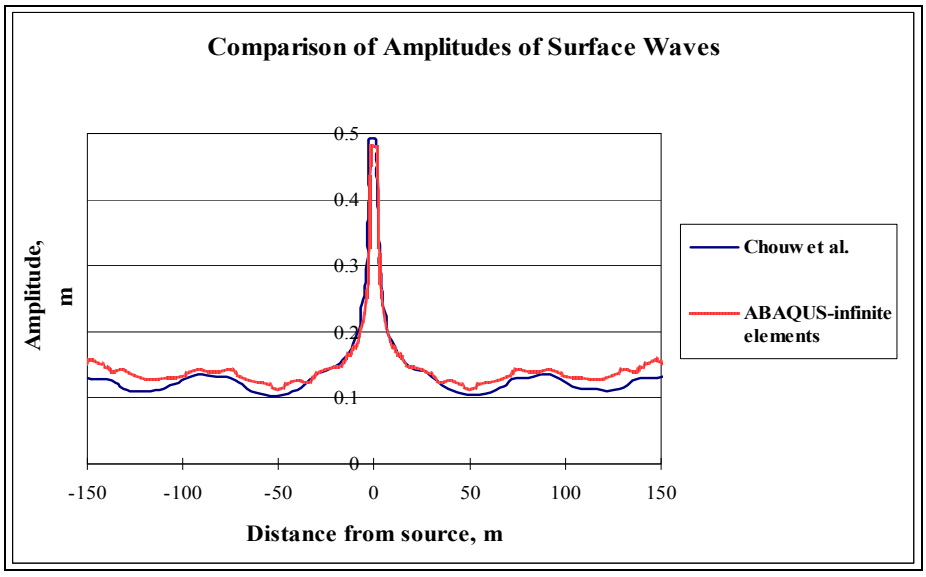

Figure 3.16 Comparison of amplitude of surface waves with distance from source

3.0.3 Benchmark Problem 3: Falling weight deflectometer Simulation

In this section the dynamic response of a multi layer system due to a transient load pulse is considered. For such a layered system, there is no available analytical solution. For verification, the computational results of Abaqus are compared with those obtained from a semi-analytical technique using the spectral element method (Al-Khoury et al, 2001). The problem involves the Falling Weight Deflectometer (FWD) which is a non-destructive dynamic test used commonly for the evaluation of pavement structures. Figure 3.17 is a schematic illustration of FWD.

The geometry is modeled using axisymmetry. The finite element mesh is shown in Figure 3.18. The geometry is 100 m wide and 100 m deep, as presented in the Figure. A three-layered system representing pavement structure and consisting of asphalt, subbase and subgrade layers is considered. Two cases are evaluated: First, the pavement structure is based on a stiff subgrade. Second, the pavement structure is based on a soft subgrade. The properties of the layers are listed in Table 3.6. Infinite elements are used to simulate silent boundaries. A distributed load with 0.15 m radius is used to simulate a typical Falling Weight Deflectometer (FWD) load pulse. Figure 3.19 shows the load pulse in time. The load starts at t = 0.052 s and ends at t = 0.076 s.

Figure 3.20 and Figure 3.21 show the vertical displacements at the centre directly under the load for both stiff and soft subgrade structures. The results shown in the Figures

indicate that calculations by both Abaqus (finite element method) and Al-Khoury et al. (spectral element method) are in good agreement.

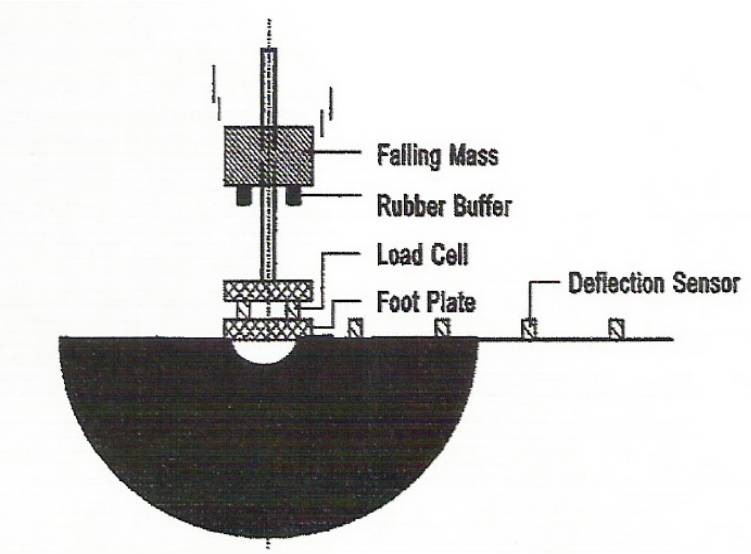

Figure 3.17 Falling Weight Deflectometer (Al-Khoury et al., 2001)

Table 3.4 Material Properties (Al-Khoury et al., 2001)

properties	Asphalt	Subbase	Soft subgrade	Stiff subgrade
Unit weigh of soil	**23** kN/m^3	**19** kN/m^3	**15** kN/m^3	**15** kN/m^3
Young's modulus	**1E**10^6 kN/m^2	**2E**10^5 kN/m^2	**1E**10^5 kN/m^2	**2.5E**10^4 kN/m^2
Poisson's ratio	**0.35**	**0.35**	**0.35**	**0.35**
Thickness	**150 mm**	**250 mm**	**Very thick**	**Very thick**

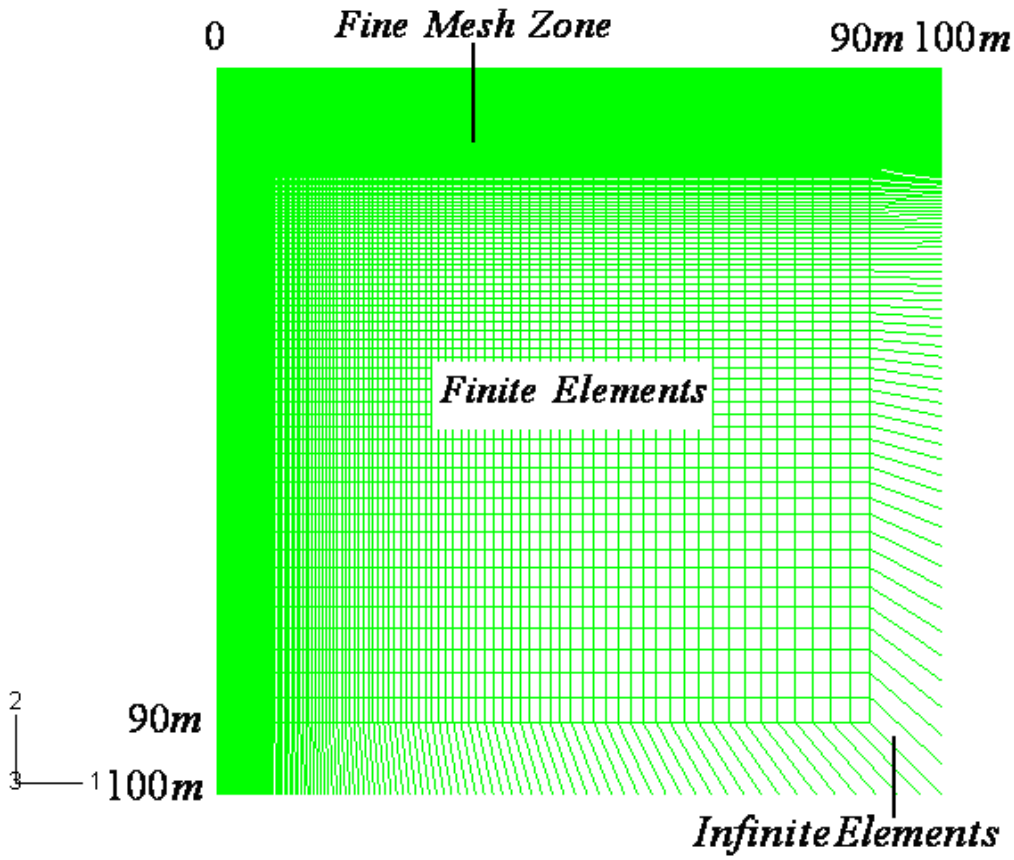

Figure 3.18 Dimensions of ground geometry and finite element meshes

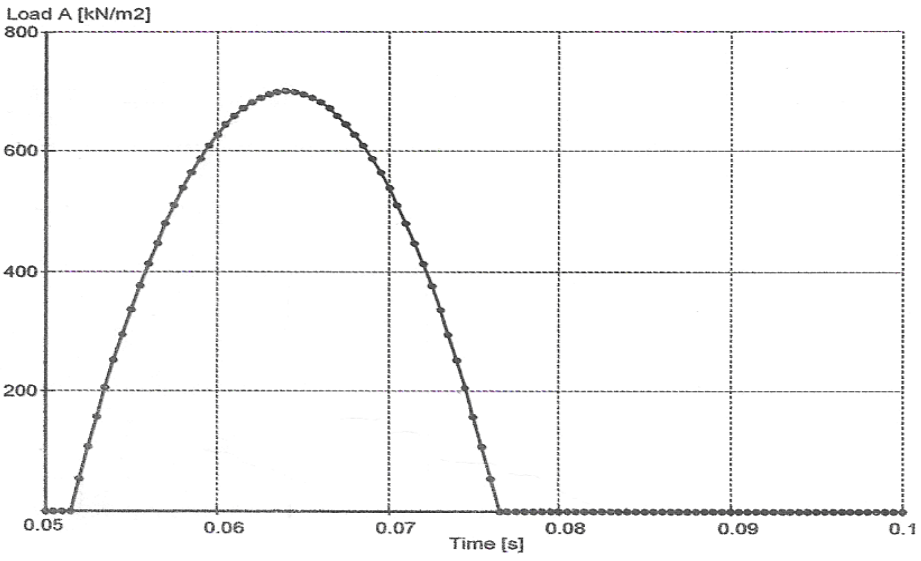

Figure 3.19 applied pulse load (Al-Khoury et al., 2001)

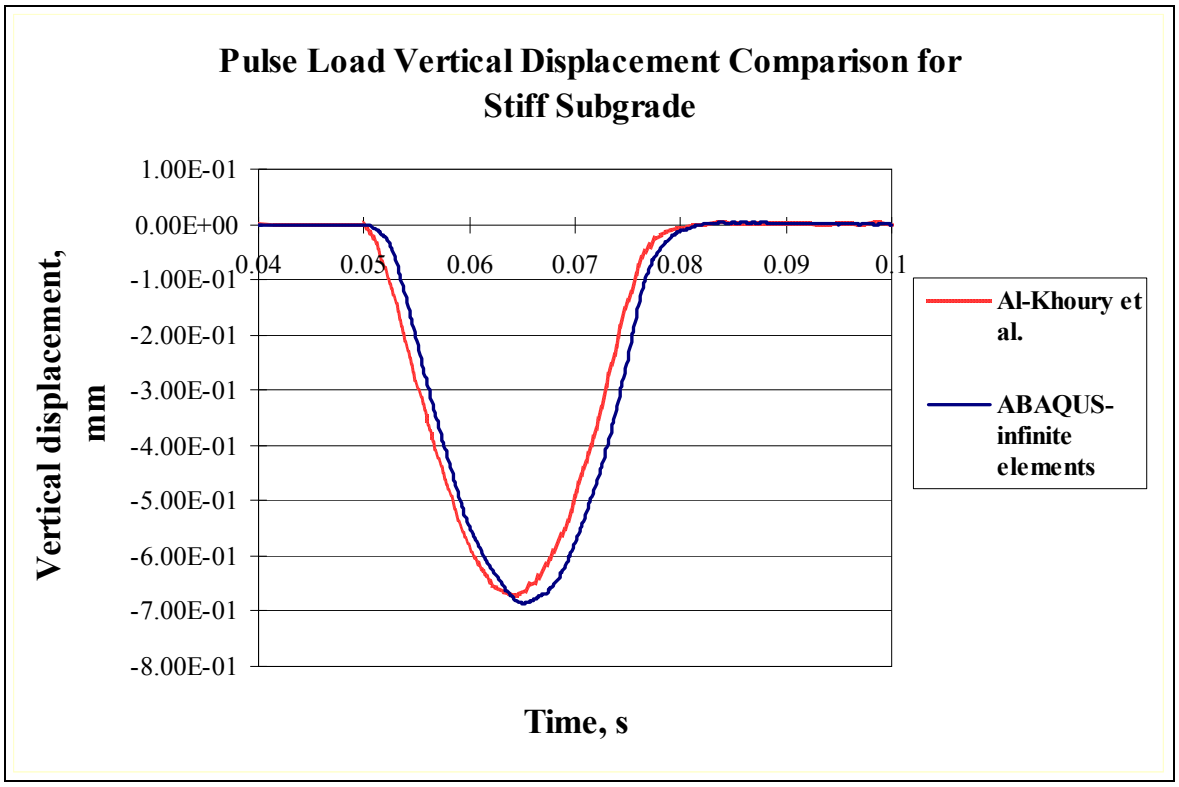

Figure 3.20 Vertical displacements at the center of ground geometry with stiff subgrade

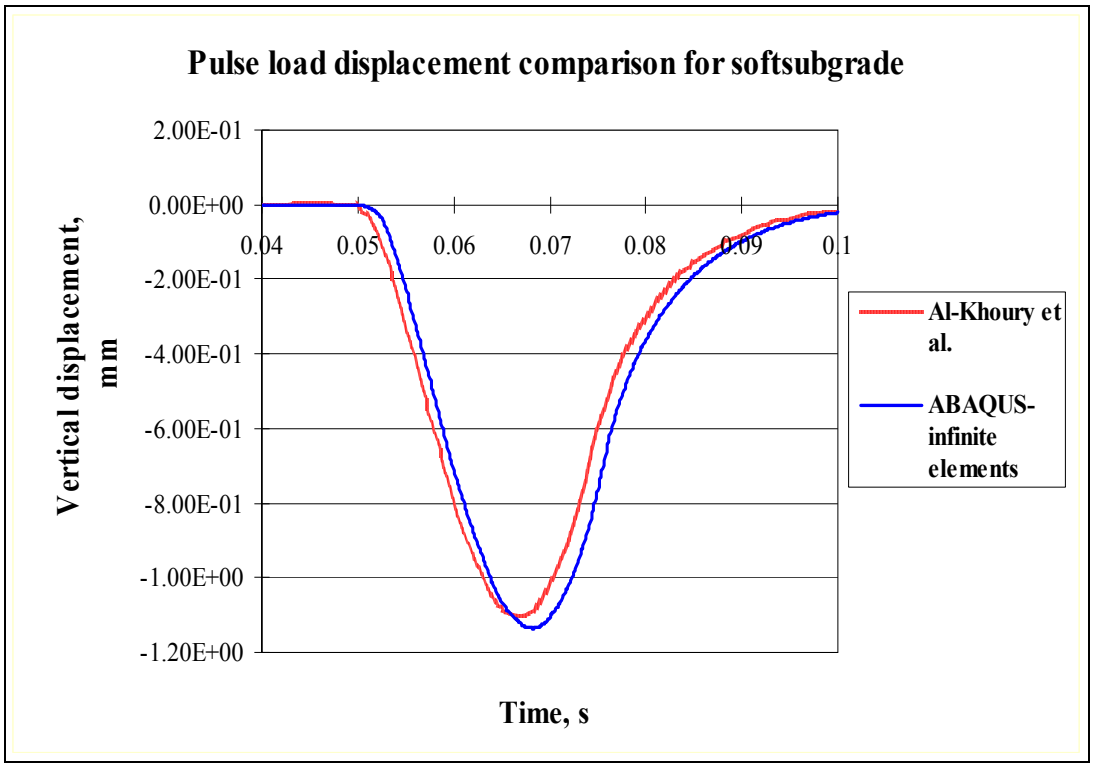

Figure 3.21 Vertical displacements at the center of ground geometry with soft subgrade

CHAPTER 4

FINITE ELEMENT ANALYSIS FOR PREDICTING PILE-INDUCED GROUND VIBRATIONS

4.0 INTRODUCTION

The developed finite element model for predicting induced ground vibrations due to pile driving must consider three main aspects: (1) pile configuration and pile driving equipment or excitation mechanism, (2) dynamic soil-pile interaction, and (3) surface and subsurface vibrations in the soil. First, driving equipment and accessories in both impact and vibratory driving techniques are considered and the excitation mechanisms in both techniques are modeled. The pile-soil interaction problem is investigated using a carefully-constructed numerical model that includes the pile and the soil with interface elements in between. The model can take into consideration the heterogeneity of the soil. Using the model, the field vibration due to impact and vibratory pile driving are studied in a homogeneous medium (one soil layer) and in a heterogeneous medium (multi layered soil). The analysis of such complex systems cannot be attained by closed-form analytical solutions, and that necessitates the use of numerical techniques such as the finite element method and the finite difference method.

The finite element model is calibrated using the results of two field tests. This is done by comparing the measured vibrations at different points (at some distance from the vibration source) with those calculated from the finite element model using the same

value of excitation (energy and frequency) of the hammers used in the field tests. The material properties of the soil are estimated based on the soil type at each testing site.

After calibrating the numerical model to site-specific behavior, the model is used to analyze various conditions of interest that will complement the experimental results. This includes (1) the effects of input (source) energy; (2) effects of the embedded pile length; and (3) effects of soil stiffness. The results of the finite element analysis will clarify the effects of the above factors on ground surface vibration and the propagation and attenuation of the stress waves caused by pile driving.

4.1 FINITE ELEMENT ANALYSIS OF CASE STUDY 1

This case history was analyzed to illustrate the capability of the finite element method in solving such a complicated problem. One of the reasons of selecting this case for analysis is that it is a well-documented case where the pile configuration and soil properties were provided. Even though this case study is representative of "bored" piles, it can also represent a driven pile that has reached a certain depth, 21.5 m in this example, when the measurements were taken due to one hammer blow. Case study 1 (Ramshaw et al., 1998) involves a 21.5-m-long, 0.75-m-diameter bored-cast-in-situ pile subjected to one blow of a 2.2 ton hammer dropped through 1.2 m distance. Measurements of ground surface vibrations, using geophones, and pile head force/time records were carried out simultaneously. The soil consists of 10.5-m-thick firm to stiff silty clay layer underlain by a very thick dense fine to medium sand layer. The unit weight of the silty clay soil is 19.70 kN/m^3, its elastic modulus is 26×10^3 kPa, and its Poisson's ratio is 0.35. The unit

weight of the sandy soil is 21 kN/m^3, its elastic modulus is 50×10^3 kPa, and its Poisson's ratio is 0.3. Figure 4.1 shows a schematic presentation of the soil-pile-hammer system.

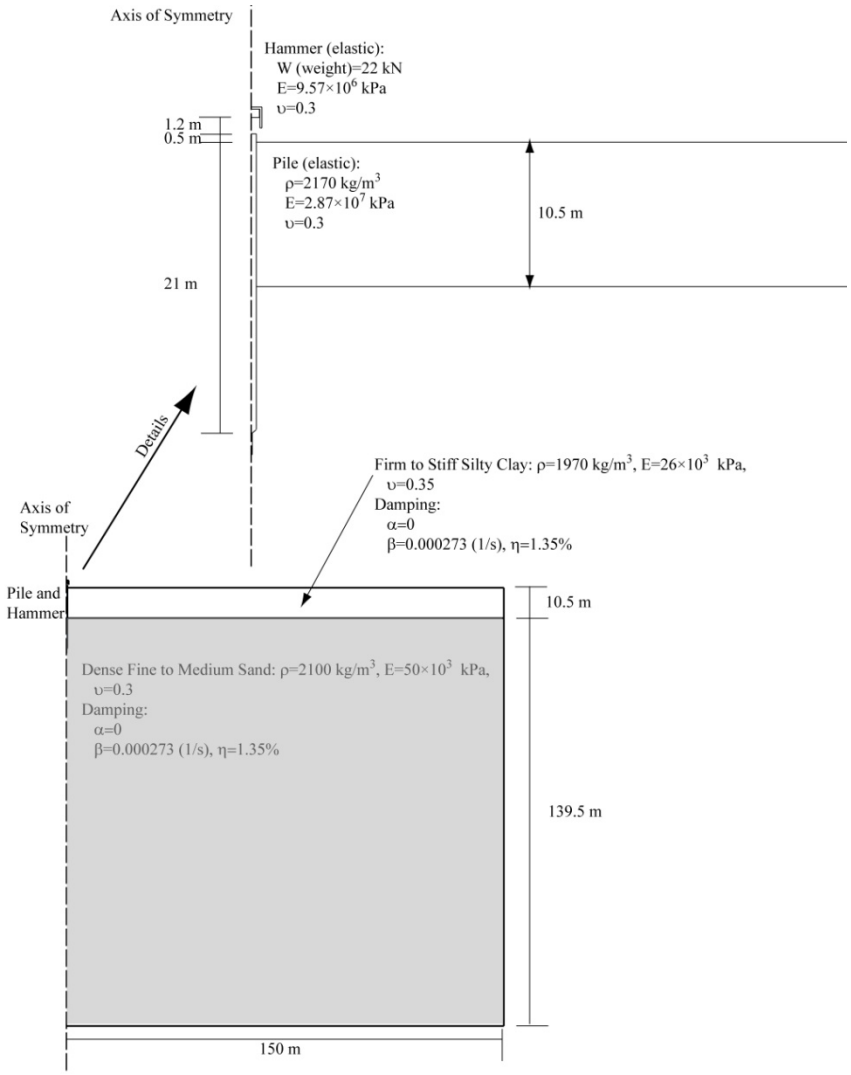

Figure 4.1: Schematic Presentation of Case Study 1

In this finite element analysis a dynamic solution is sought for a layer of silty clay underlain by a layer of sand loaded by a 21.5-m long concrete-filled pipe pile with D=0.75 m. The pile is subjected to one blow by a 2.2 ton hammer falling a distance of 1.2 m. The problem geometry and materials are shown in Figure 4.1.

The pile in this example is cylindrical in shape and loaded in the axial direction only, therefore, the finite element mesh of the pile and the surrounding soil can take advantage of this axisymmetric condition. It should be noted that the finite element mesh of a soil-pile-hammer system must include interface elements that are capable of simulating the frictional interaction between the pile surface and the soil. Also, since this is a bored pile it is assumed to be embedded in perfect contact with the soil before applying pile loads. The ground water table is deep and the soil is assumed to be dry.

The two-dimensional axisymmetric finite element mesh analyzed is shown in Figure 4.2. The finite element mesh is 150 m deep and 150 m wide. The model considers only one half of the pile and the hammer taking advantage of symmetry as indicated in the Figure. The pile is initially in perfect contact with the soil. The interaction between the pile and the soil is simulated using penalty-type interface between the pile and the soil with a friction factor of 0.9. This type of interface is capable of describing the frictional interaction between the pile surface and the soil in contact.

Three-node linear axisymmetric triangular elements are used for the soil, the pile, and the hammer. The base of the soil is free in the horizontal direction and fixed in the vertical direction. The vertical boundary on the left side is a symmetry line, and the vertical boundary on the right side is fixed in the horizontal direction but free in the vertical direction. It is noted that the mesh is finer in the vicinity of the pile and near the ground surface since that zone is a zone of stress concentration. No mesh convergence studies

have been performed. However, the dimensions of the finite element mesh are chosen in a way that the boundary effect on the dynamic pile behavior is minimized—it takes approximately 2 s for the p-wave, due to a hammer blow, to travel from the pile to the mesh boundary and back to the vicinity of the pile. This time is greater than 0.5 s which is the time needed to capture the surface vibration at 5.5 m and 16.5 m from the pile.

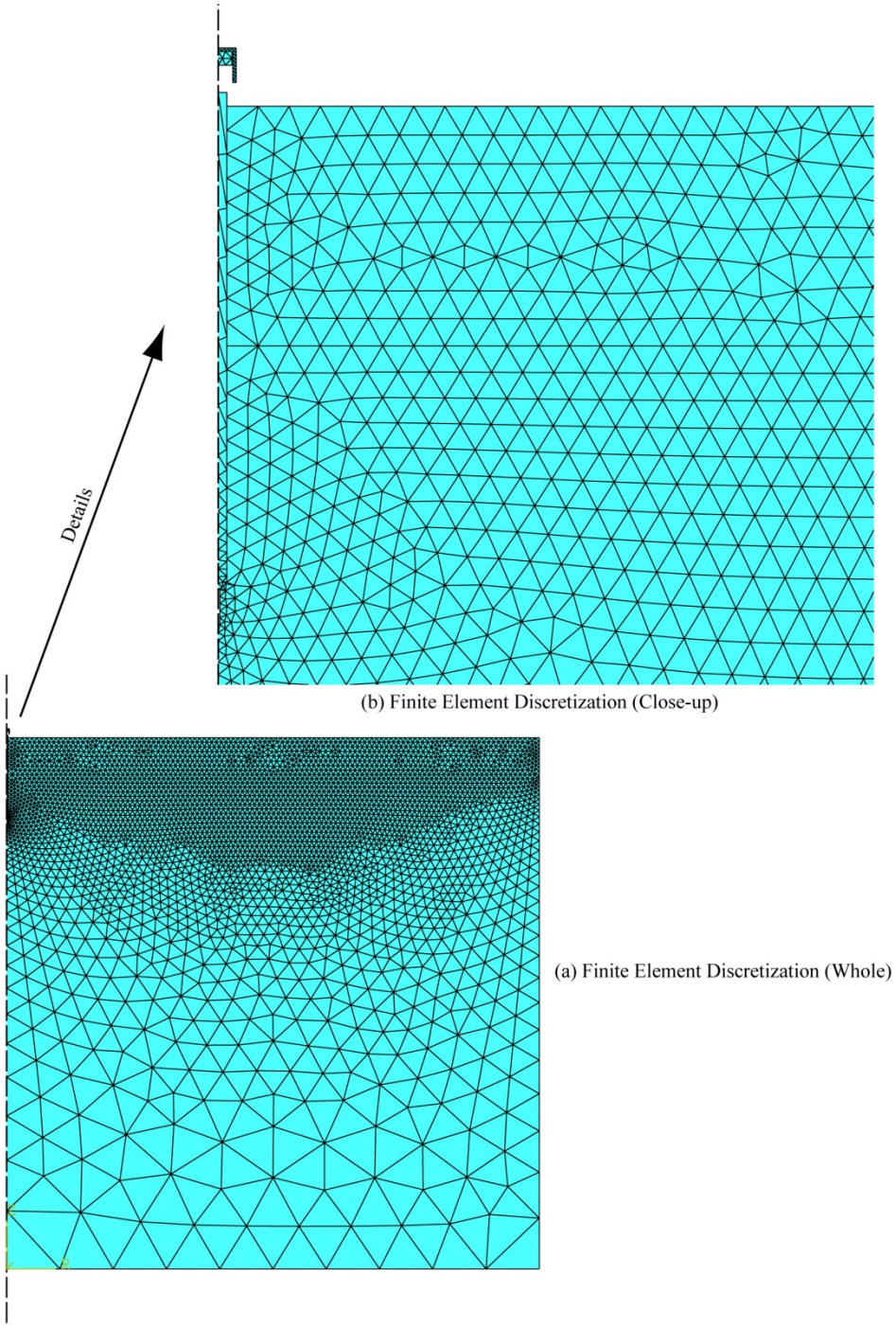

Figure 4.2: Finite Element Discretization of Case Study 1

The soil response (both layers) is assumed to be linear elastic and isotropic. The assumption of linear elasticity is justified in this particular case since the objective is to predict surface vibrations due to pile loading rather than the penetration of the pile. The soil strains associated with vibrations are very small in most of the soil domain. This justifies the assumption of linear elasticity. The soil immediately in contact with the pile, especially at the tip of the pile, is subject to greater strains and may traverse to its plastic region. This, however, may have small effects on soil surface vibration.

The problem is run in one step with a total duration of 1 s. In this step, a gravity load is applied to the 2.2-ton-hammer causing it to fall freely a distance of 1.2 m before colliding with the end of the pile. Interface elements with penalty formulation are used between the hammer and the end of the pile to prevent the hammer from penetrating the pile. For simplicity, no pile cap or anvil is used at the top of the pile. Figure 4.3 shows the hammer displacement and velocity during its free fall, at impact with the pile, and after impact where the hammer is raised about 1 m above the end of the pile.

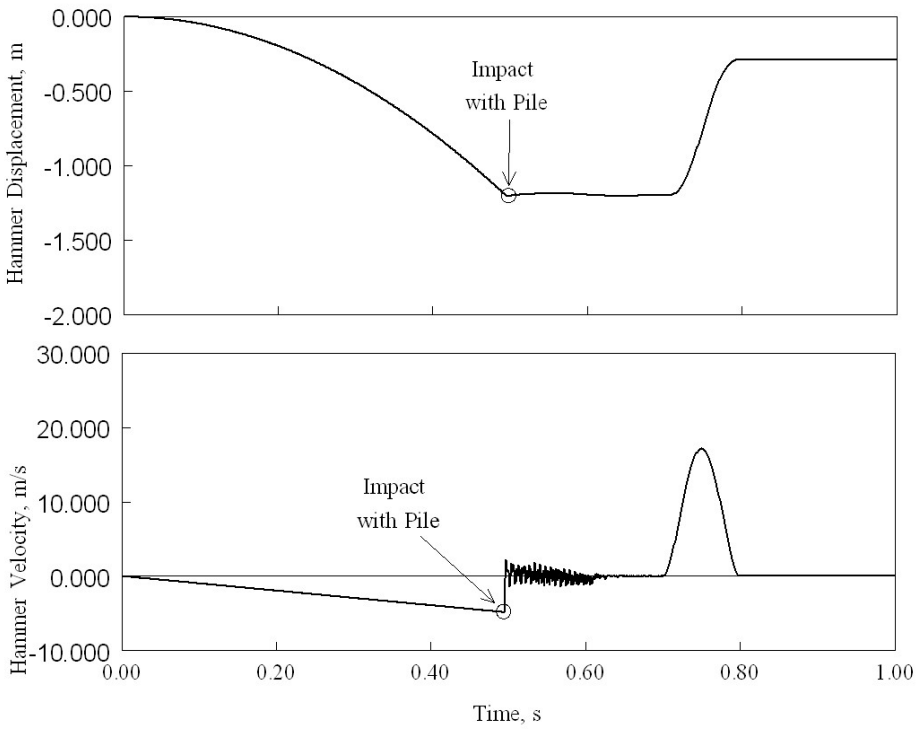

Figure 4.3: Hammer-Pile-Soil Interaction

At impact, a stress wave is generated at the top of the pile traversing through the body of the pile towards its tip. During that time most of the energy generated by the impact is transmitted to the surrounding soil along the sides and the tip of the pile generating compression and shear waves in the soil. The compression and shear waves travel through the soil towards the ground surface where another wave, called a Rayleigh wave, is generated near the ground surface. Ground surface vibrations are produced by these three waves combined.

It is widely accepted that the damping ratio of soil is function of soil's shear strain. The study by Seed et al. (1984) indicates that the damping ratio for sand is less than 2% when

the sand is subjected to very small shear strains less than 10^{-3}%. In the present analysis the material damping properties are tuned to provide approximately 1.35% fraction of critical damping for the first mode of vibration of the two-layer soil system shown in Figure 4.1. Assuming Rayleigh stiffness proportional damping, the factor β required to provide a fraction ζ_1=1.35% of critical damping for the first mode is given as $\beta = 2\xi_1/\omega_1$. The first frequency of the two-layer soil system is obtained by a separate analysis in which the system is subjected to a uniform impulse load (pressure) at the ground surface. The system is then allowed to oscillate. Figure 4.4 shows the free vibration of a point at the ground surface. The natural frequency $f_1 \approx 15.75$ Hz is extracted from Figure 4.4. This is used to calculate $\omega_1 = 98.91$ radian/s. Based on this, β is chosen to be 2.73×10^{-4} s.

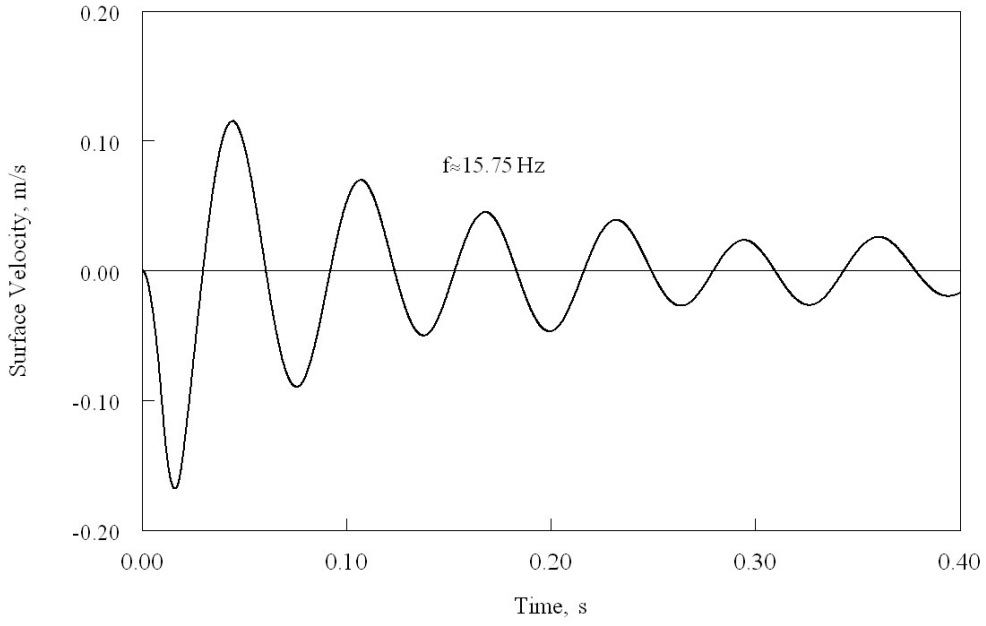

Figure 4.4: Ground Surface Free Vibration (Study Case 1)

The computed and measured ground surface vibrations are compared for stations at 5.5 m and 16.5 m from the pile as shown in Figures 4.5 and 4.6, respectively. The shapes of the computed transient vibration curves in the Figures are in relatively good agreement with the measured curves. The computed peak particle velocity at 5.5 m distance is in good agreement with the measured one as shown in Figure 4.5. At a greater distance (16.5 m), acceptable agreement is noted between the measured and calculated peak particle velocities (Figure 4.6).

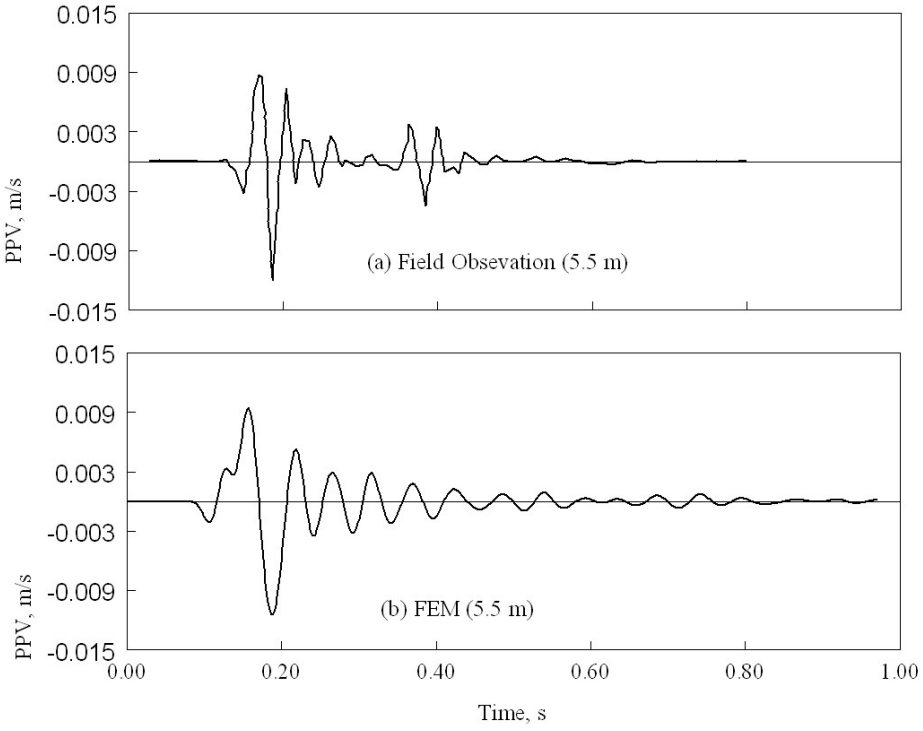

Figure 4.5: Measured Versus Computed Peak Particle Velocities
at station 1 (5.5 m from Pile) (a) Field Observation (b)FEM

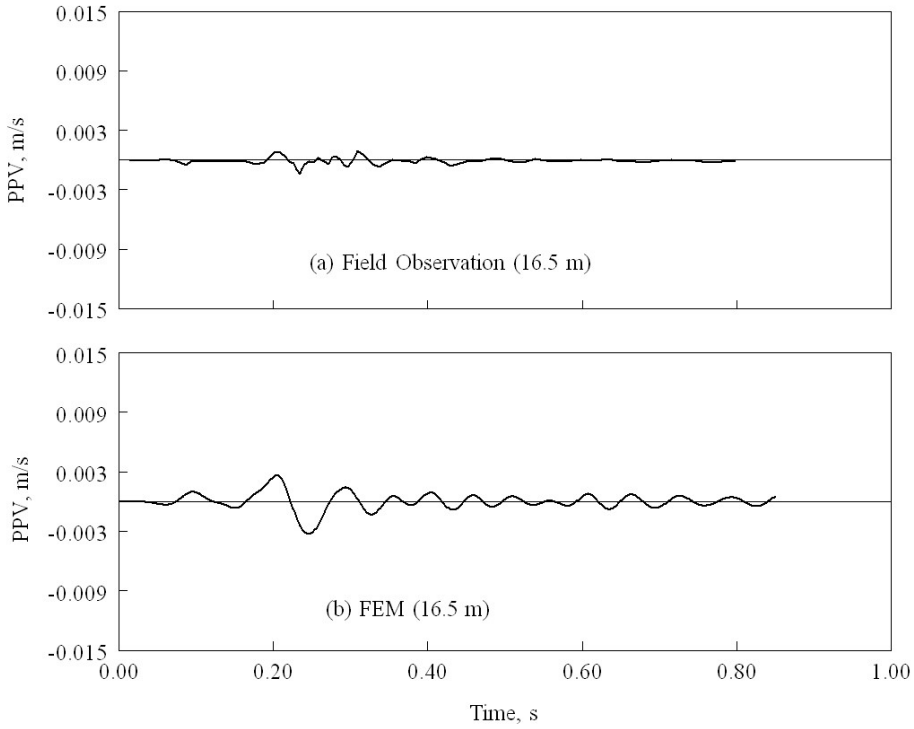

Figure 4.6: Measured Versus Computed Peak Particle Velocities at station 2 (16.5 m from Pile) (a) Field Observation (b)FEM

4.2 FINITE ELEMENT ANALYSIS OF CASE STUDY 2

This case study illustrates the capabilities of the finite element method in simulating the complicated sheet pile-soil interaction problem during driving by vibration. Even though this case does not represent a "driven" pile, it certainly indicates that the method is capable of analyzing driven piles as illustrated in the parametric analysis. Case study 2 (Tawfiq and Abichou, 2003) involves a 13.5-m-long, 900-mm-diameter steel casing that was driven using a vibrator. Measurements of ground surface vibrations, using geophones, and casing velocity records were carried out simultaneously. The testing site was in Boca Raton, Florida, where the soil is predominantly medium to fine sand. The unit weight of the sand is assumed to be 20 kN/m^3, its elastic modulus is 50×10^3 kPa, and

its Poisson's ratio is 0.3. Figure 4.7 shows a schematic presentation of the soil-steel casing system.

In this finite element analysis a dynamic solution is sought for a thick layer of sand loaded by a 13.5-m long steel casing with D=0.9 m. The steel casing is subjected to a sinusoidal vibration with f=20 Hz and a peak particle velocity (amplitude) of 0.254 m/s.

Figure 4.8 shows the two-dimensional axisymmetric finite element mesh used in the analysis. The finite element mesh is 300 m deep and 300 m wide. The model considers only one half of the steel casing taking advantage of symmetry as indicated in the Figure. The steel casing is initially in perfect contact with the soil. The interaction between the steel casing and the soil is simulated using penalty-type interface between the steel casing and the soil with a friction factor of 0.9. This type of interface is capable of describing the frictional interaction between the steel casing surface and the soil in contact.

The element type used in this analysis is a three-node linear axisymmetric triangular element. The element is used for the soil and the steel casing as well. The base of the soil is free in the horizontal direction and fixed in the vertical direction. The vertical boundary on the left side is a symmetry line, and the vertical boundary on the right side is fixed in the horizontal direction but free in the vertical direction. It is noted that the mesh is finer in the vicinity of the pile and near the ground. The dimensions of the finite

element mesh are chosen in a way that the boundary effect on the dynamic pile behavior is minimized within the time domain used for the analysis (0.75 s).

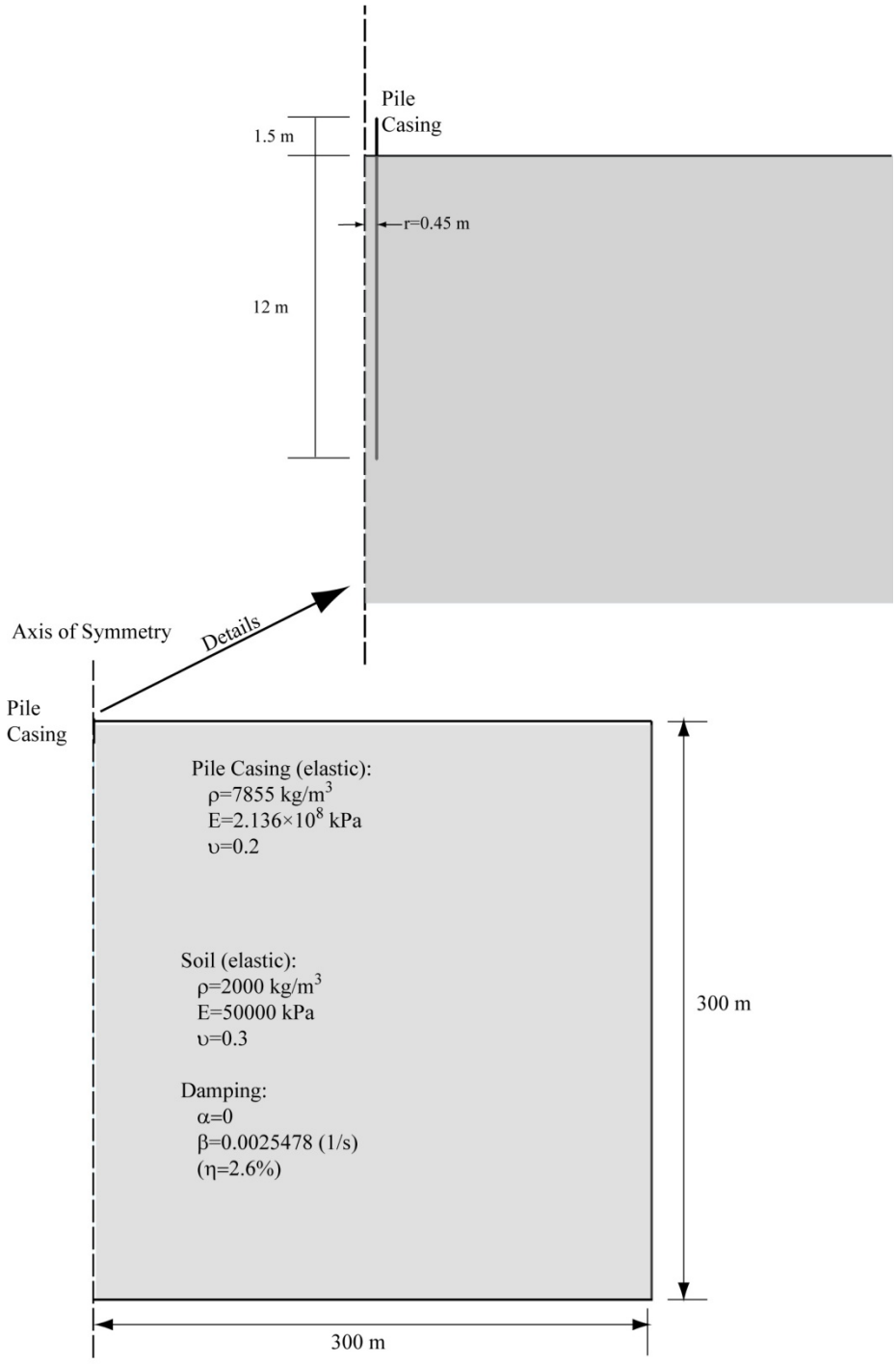

Figure 4.7: Schematic Presentation of Case Study 2

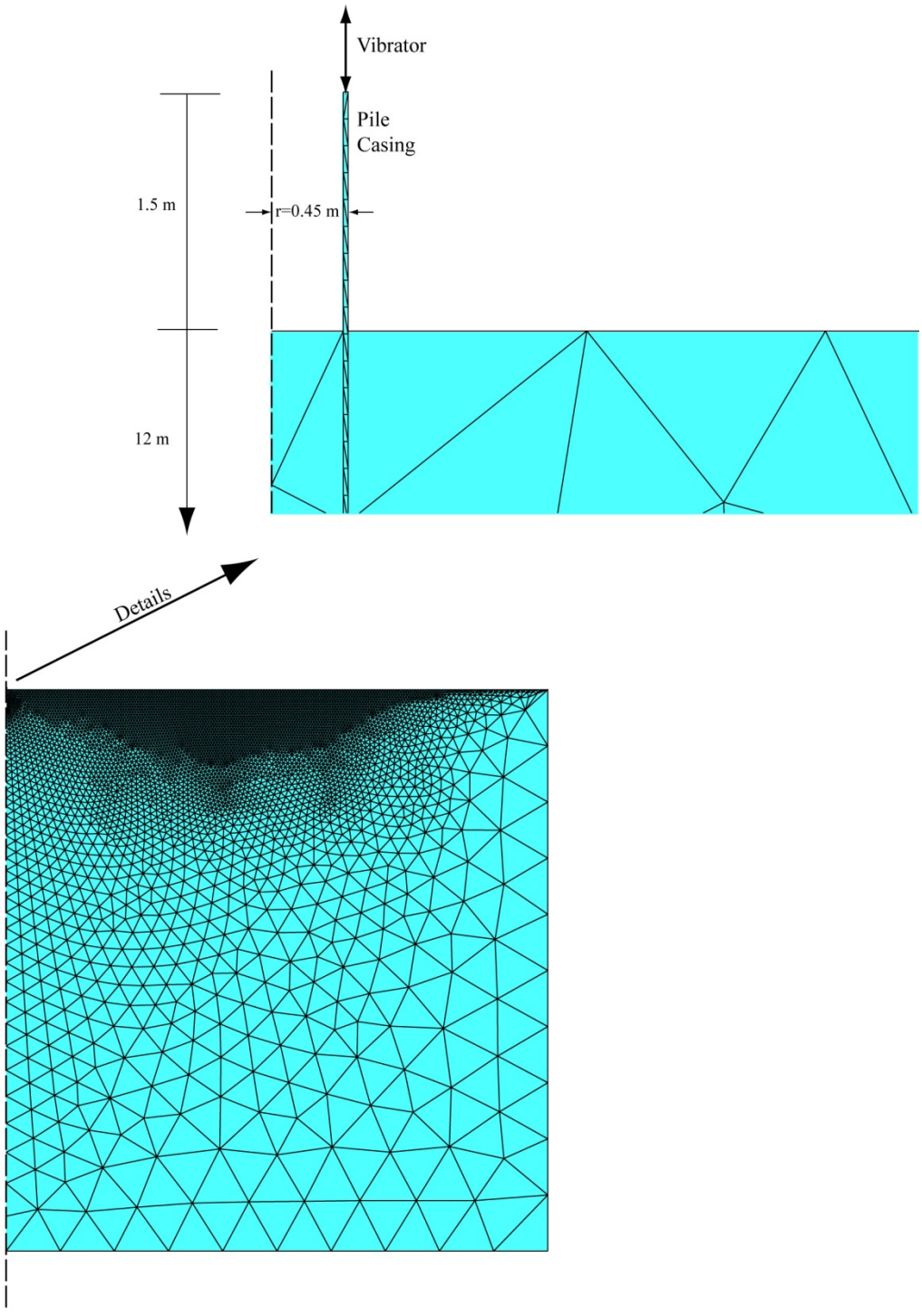

Figure 4.8: Finite Element Discretization of Case Study 2

In this analysis the soil response is assumed to be linear elastic and isotropic. As indicated in the analysis of case study 1, the assumption of linear elasticity is justified since the objective is to predict surface vibrations due to steel casing loading rather than the penetration of the steel casing.

The problem is run in one step with a total duration of 0.75 s. In this step the steel casing is subjected to sinusoidal vibration with f=20 Hz and a peak particle velocity (amplitude) of 0.254 m/s. Figure 4.9a shows the source (steel casing) vibration history. Figure 4.9b shows the vibration history of a point located at the ground surface 1.62 m away from the steel casing. It is noted that the vibration of this point is periodical as expected (not sinusoidal).

Due to source (steel casing) vibration, a stress wave is transmitted to the surrounding soil along the sides of the steel casing generating compression and shear waves in the soil. The compression and shear waves travel through the soil towards the ground surface where Rayleigh wave is formed near the ground surface. Ground surface vibrations, such as the one shown in Figure 4.9b, are produced by these three waves combined.

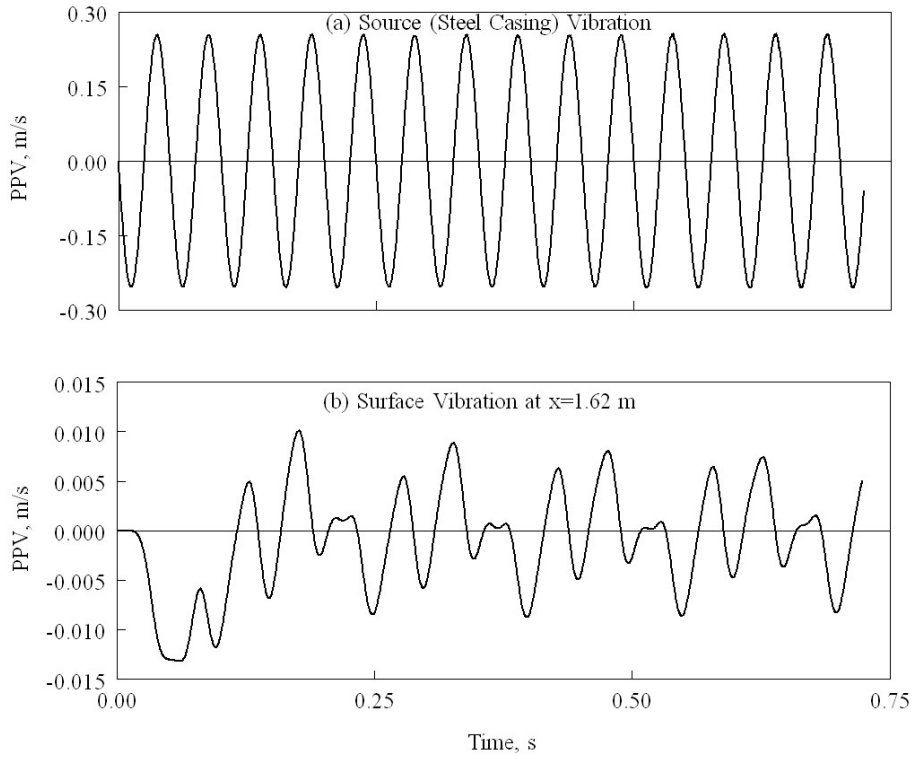

Figure 4.9: Sample Input and Output Vibrations
(a) Source Vibration (b) Ground Surface Vibration 1.62 m from Pile

The material damping properties of the soil are tuned to provide approximately 2.6% fraction of critical damping for the first mode of vibration of the soil system shown in Figure 4.7. Assuming Rayleigh stiffness proportional damping, the factor β required to provide a fraction ζ_1=2.6% of critical damping for the first mode is given as $\beta = 2\xi_1/\omega_1$. The first frequency of the soil system is obtained by a separate analysis in which the system is subjected to a uniform impulse pressure at the ground surface and the resulting system oscillation is observed. Figure 4.10 shows the free vibration of a point at the ground surface. The natural frequency $f_1 \approx 3.25$ Hz is extracted from Figure 4.10. This is used to calculate $\omega_1 = 20.41$ radian/s. Based on this, β is chosen to be 2.5×10^{-3} s.

The computed and measured ground surface vibrations are compared for four stations as shown in Figure 4.11. The computed peak particle velocities in the Figure are in good agreement with the measured ones.

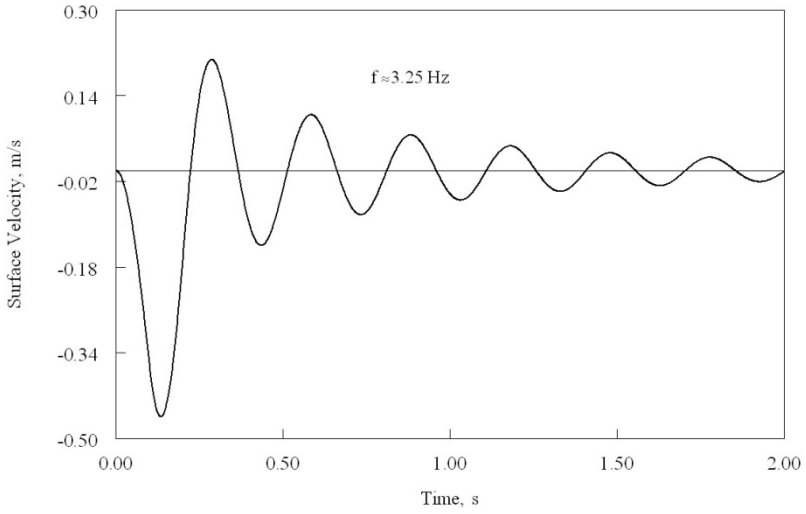

Figure 4.10: Ground Surface Free Vibration (Study Case 2)

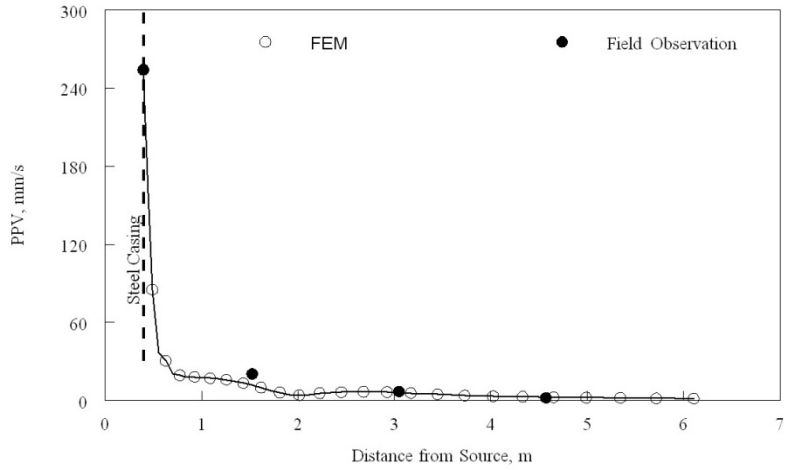

Figure 4.11: Measured Versus Computed Peak Particle Velocities (Case Study 2)

4.3 FINITE ELEMENT PARAMETRIC ANALYSIS

The numerical model has been verified by comparing its results with two case studies as described above. This was done to show that such a numerical model is capable of simulating the complicated dynamic soil-pile-hammer interaction. Also, the analysis has helped to gain more confidence in the numerical model. Next, the numerical model is used to conduct a parametric study to investigate the effects of pile embedded length, soil stiffness, and source energy. The results of this parametric analysis will clarify the effects of the above factors on ground surface vibrations and the propagation and attenuation of stress waves caused by pile driving.

The "Base Case" geometry used in the parametric analysis is shown schematically in Figure 4.12. All parameters of the base case are kept constant in the parametric study except for the parameter that is being investigated. The pile is 1.5-m-long and 0.9 m in diameter. The hammer weighs 27 kN and is raised 0.9 m above the top of the pile (i.e., the falling distance is 0.9 m) as shown in Figure 4.12. Other material parameters for the pile and the hammer are shown in Figure 4.12.

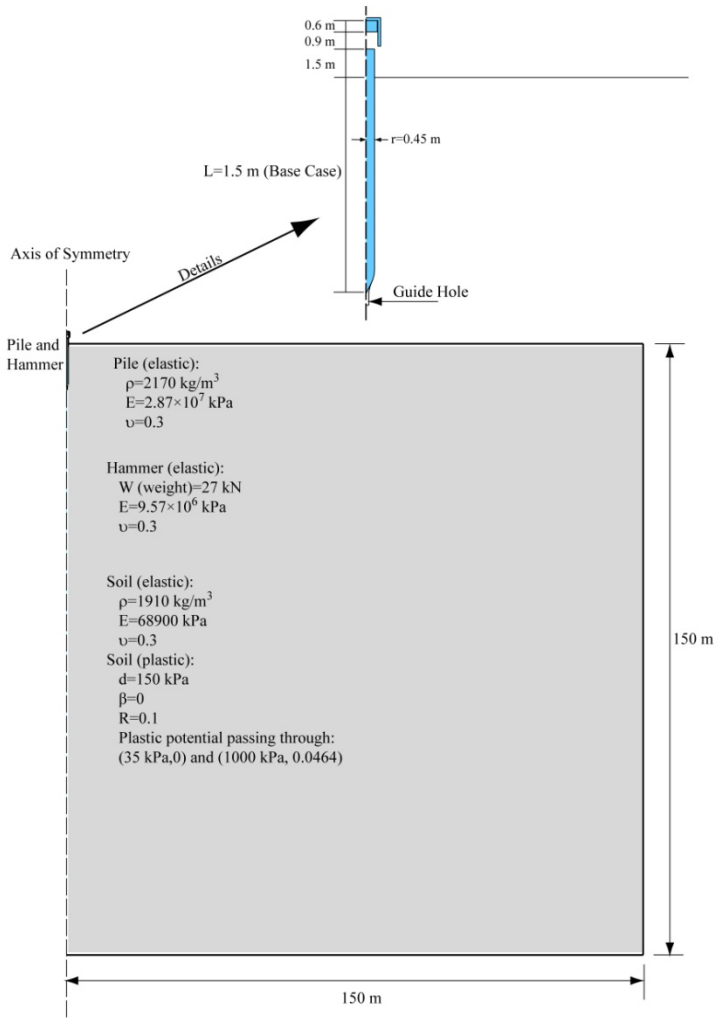

Figure 4.12: Schematic Presentation of "Base Case" for the Parametric Analysis

For a more realistic simulation of the pile driving process, the soil is assumed to be elastoplastic, thus allowing the soil to deform permanently upon pile penetration. To facilitate penetration a guide hole (predrilled hole) with 0.05 m diameter is used as shown in the Figure. The tip of the pile is also made tapered for a smooth penetration. The elastoplastic Drucker Prager model with cap (Abaqus, 2002) is used to simulate the elastoplastic soil behavior.

The soil is assumed to be a silty clay with a unit weight of 19.1 kN/m^3. The elastic response of this silty clay is assumed to be linear and isotropic, with a Young's modulus of 6.89×10^4 kPa and a Poisson's ratio of 0.3. The undrained shear strength parameters of the soil are c_u=86.6 kPa and ϕ_u=0. The cap model parameters d=150 kPa and β=0 are matched to the Mohr-Coulomb failure criterion parameters c_u=86.6 kPa and ϕ_u=0 to simulate the undrained behavior of the silty clay soil layer.

The cap eccentricity parameter is chosen as R= 0.1. The initial cap position (which measures the initial consolidation of the specimen) is taken as $\varepsilon_{vol(0)}^{pl} = 0.0$, and the cap hardening curve is assumed to be a straight line passing through two points (p'=35 kPa, $\varepsilon_{vol}^{pl} = 0.0$) and (p'=1034 kPa, $\varepsilon_{vol}^{pl} = 0.0464$). The transition surface parameter α= 0 is assumed.

Figure 4.13 shows the two-dimensional axisymmetric finite element mesh used in the analysis. The finite element mesh is 150 m deep and 150 m wide. The model considers only one half of the pile taking advantage of symmetry as indicated in the Figure. The embedded part of the pile is initially in perfect contact with the soil. The interaction between the pile and the soil is simulated using penalty-type interface between the pile and the soil with a friction factor of 0.9.

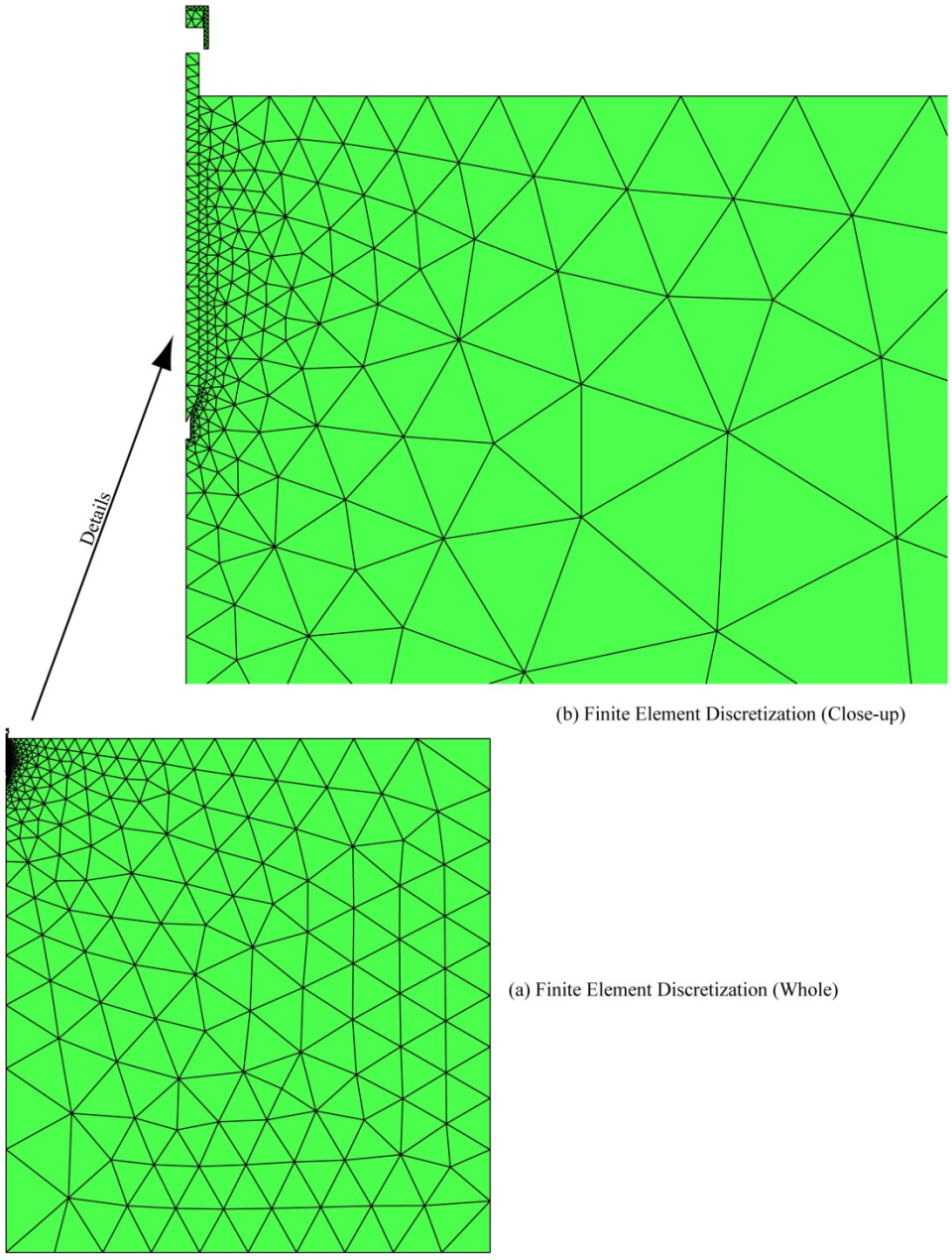

Figure 4.13: Finite Element Discretization of "Base Case" for the Parametric Analysis

The element type used in this analysis is a three-node linear axisymmetric triangular element. This element is used for the soil, the pile, and the hammer as well. The base of

the soil is free in the horizontal direction and fixed in the vertical direction. The vertical boundary on the left side is a symmetry line, and the vertical boundary on the right side is fixed in the horizontal direction but free in the vertical direction. It is noted that the mesh is finer in the vicinity of the pile and near the ground surface.

Figure 4.14 presents the hammer-pile-soil interaction during five hammer blows. The hammer is allowed to fall freely a distance of 0.9 m before impact. At impact, most of the energy is transmitted to the pile then to the soil causing the pile to penetrate the soil about 60 mm (due to the first blow) as shown in the Figure. Next, the hammer is raised 0.9 m above the end of the pile. This is followed by a short resting period of 0.3 s. Then the hammer is allowed to fall again and the same sequence is repeated. Figure 4.15 shows the vibration history of three points located on the ground surface at 4.5 m, 3 m, and 1.5 m from the pile. It is noted that the peak particle velocity decreases as the distance from the pile increases.

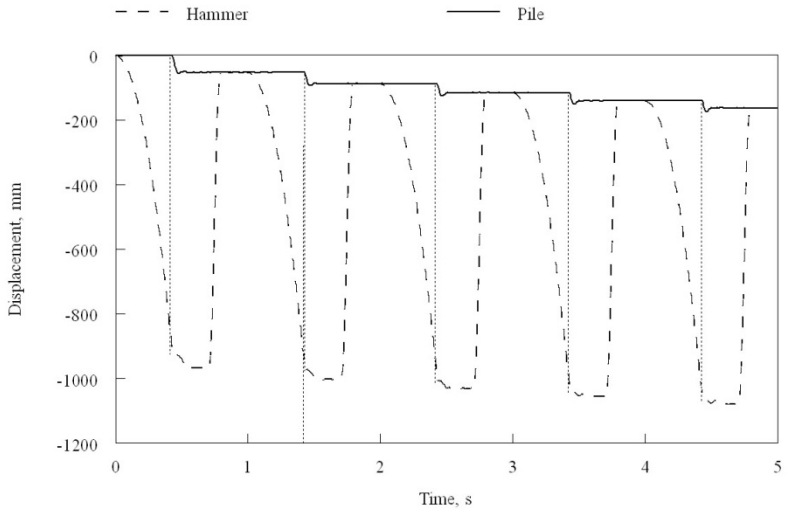

Figure 4.14: Hammer-Pile-Soil Interaction

4.3.1 Effects of Pile Length

To study the effect of the embedded length of the pile on ground vibration, the "base case" with embedded length of L=1.5 m was modified to accommodate embedded pile lengths of L=6.1 m and L=10.7 m. All other parameters of the base case are kept unchanged. Figure 4.16 shows the effects of the embedment length of the pile on the peak particle velocities at the ground surface. The Figure indicates that for this particular hammer-pile-soil system the pile with an embedded length L=1.5 m produced the maximum peak particle velocities.

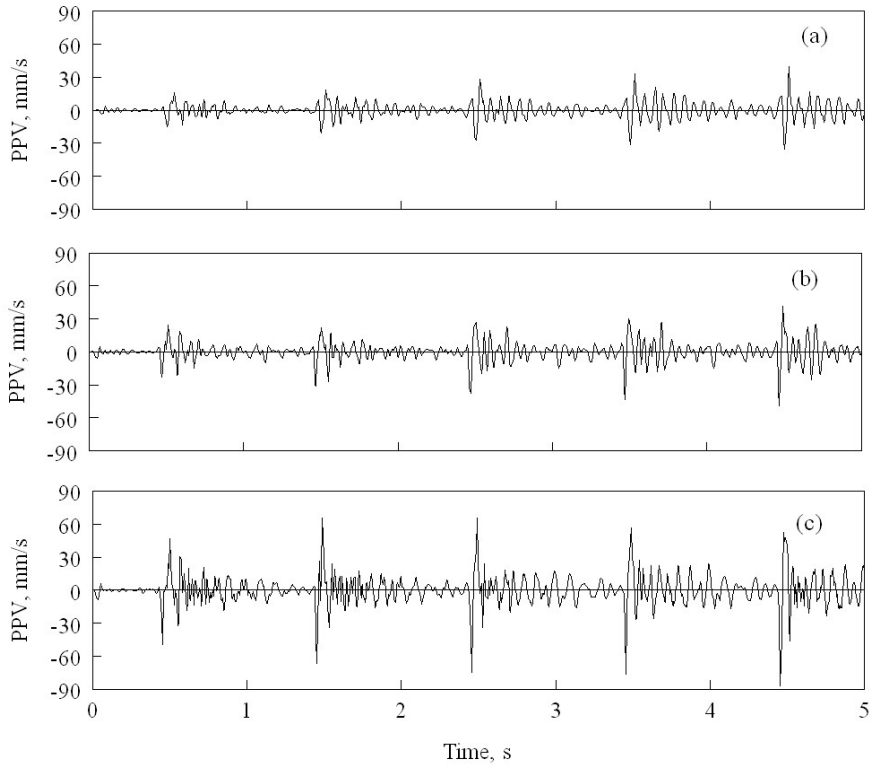

Figure 4.15: Sample Output Ground Surface Vibrations
(a) at 4.5 m from Pile (b) at 3 m from Pile (c) at 1.5 m from Pile

The equation by Wiss (1981): $PPV = K(\sqrt{E_h}/D)$, with K=1.5 (upper bound) and K=0.67 (lower bound), is included in the Figure as a reference. Note that in this equation

the units of the hammer energy E_h is kJ, the units of the distance D from source is meters, and the units of the PPV is millimeters. Also note that in this equation the coefficient K can vary widely (0.67-1.5) as shown in Figure 4.16. The equation by Wiss (1981) has some limitations such as not being able to consider soil stiffness, soil stratification, source frequency, soil-pile interface properties (i.e., friction and cohesion), and not being able to predict the frequency of ground surface vibration at a given distance from the vibration source (pile). Being able to predict the frequency of ground vibration is especially important to avoid resonance in adjacent structures especially those with freshly poured concrete. Fortunately, many of these limitations are effectively considered in a careful finite element analysis.

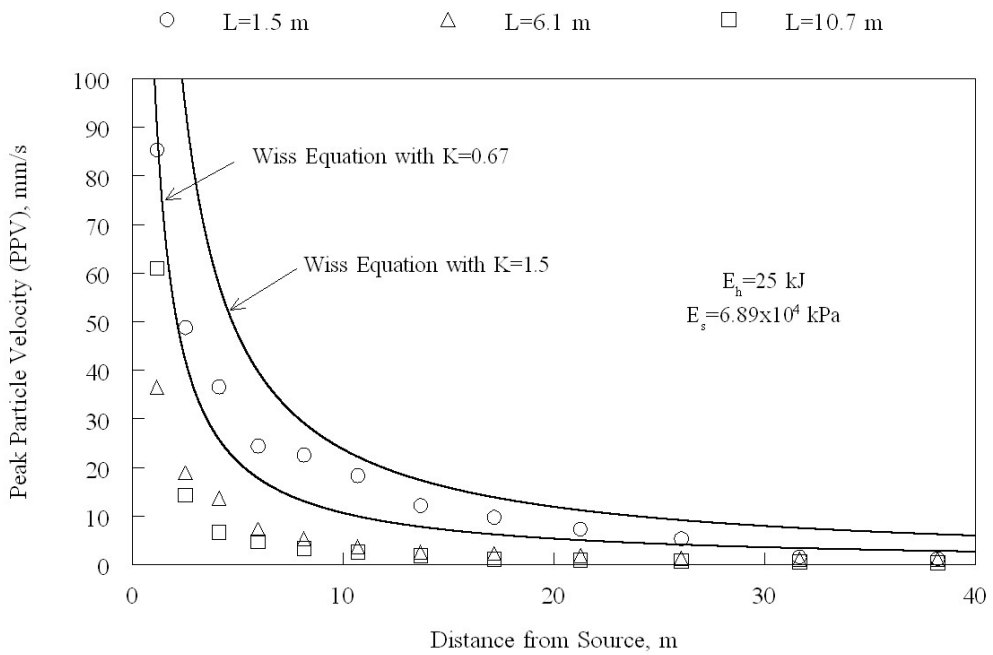

Figure 4.16: Effects of Embedded Pile Length on Ground Surface Vibration

4.3.2 Effects of Soil Stiffness

The elastic modulus E_s of the silty clay soil is varied as follows: $E_s = 13.8\times10^4$ kPa, 6.89×10^4 kPa (Base Case), and 3.45×10^4 kPa. Figure 4.17 shows the effects of the soil stiffness on the peak particle velocities at the ground surface. The Figure indicates that for this particular hammer-pile-soil system the pile with the smallest soil stiffness produced the maximum peak particle velocities. Typically, soil with greater stiffness will produce greater particle velocities. The results shown in the figure are particular to a given geometry and conditions (type of hammer, frequency, etc.) including the embedded length of the pile (1.5 m). However, the soil damping was not increased in this model to show effect. If the soil damping was increased based on lower soil strength, the results would be consistent with observed phenomena. As a reference, the equation by Wiss (1981): $PPV = K(\sqrt{E_h}/D)$ is included in the same Figure with K=1.5 (upper bound) and K=0.67 (lower bound).

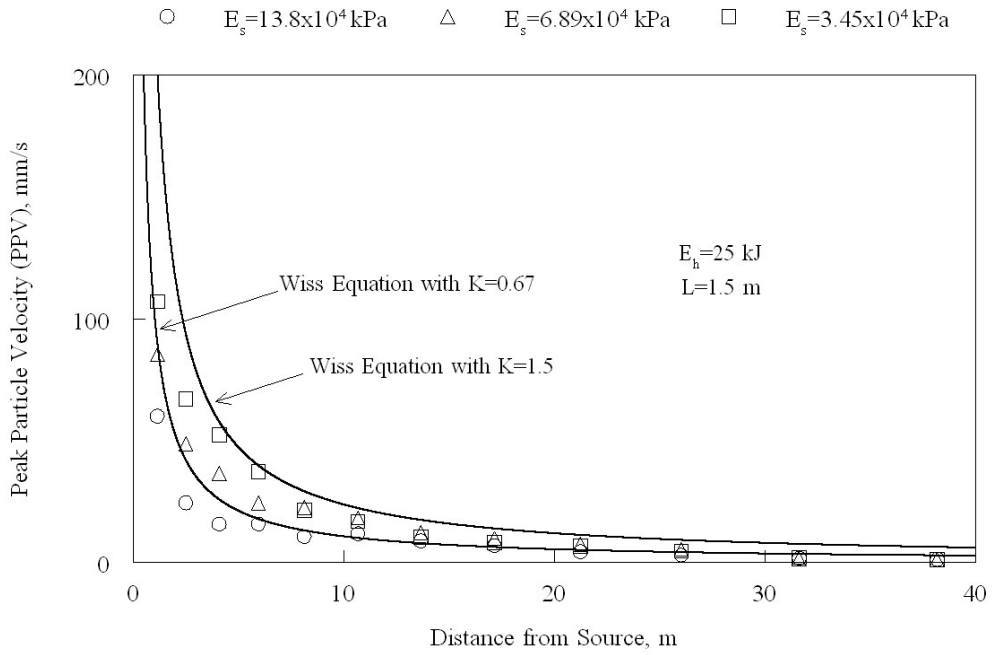

Figure 4.17: Effects of Soil's Stiffness on Ground Surface Vibration

4.3.3 Effects of Hammer Energy

Two hammer energies E_h= 25 kJ (Base Case) and 50 kJ are used. Figure 4.18 shows the effects of hammer energy on the peak particle velocities at the ground surface. The Figure indicates, as expected, that the greater hammer energy produced greater peak particle velocities. Again, the equation by Wiss (1981): $PPV = K(\sqrt{E_h}/D)$ is also included in the Figure with K=1.5 (upper bound) and K=0.67 (lower bound).

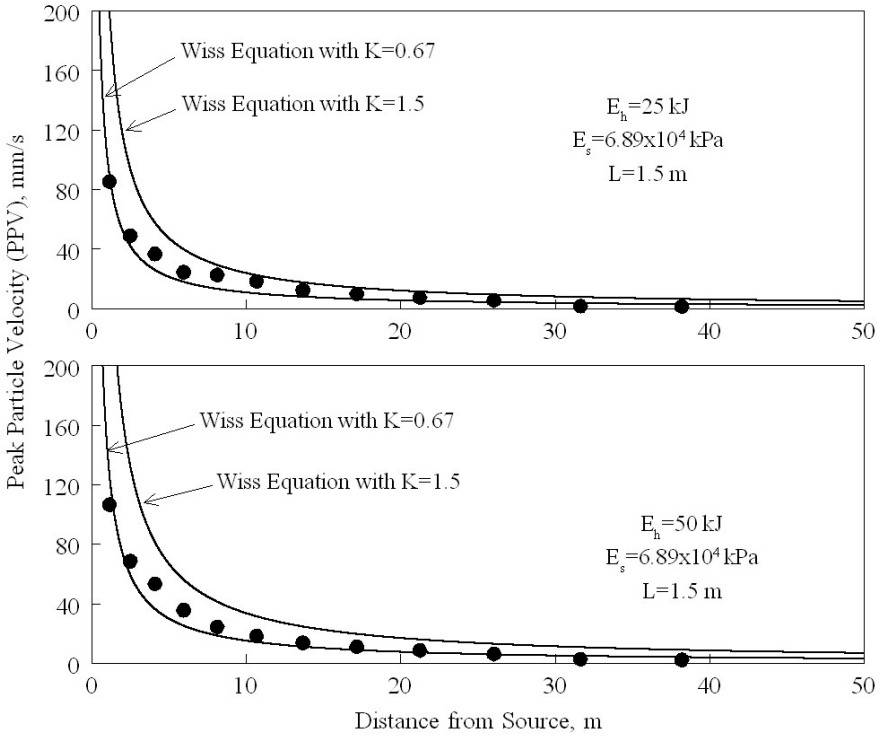

Figure 4.18: Effects of Hammer Energy on Ground Surface Vibrations

4.4 CONCLUSIONS

The finite element method provides a versatile means to calculate ground surface vibrations caused by pile driving. Simple numerical models were used to calculate the ground surface vibrations in a two-layer soil system with a concrete-filled pipe pile (case study I) and a one-layer soil system with a steel casing (case study II). The finite element results of the two case studies were compared with field measurements showing that the finite element method is capable of simulating the complicated soil-pile-hammer interaction. Furthermore, analytical and semi-empirical equations (e.g., Wiss 1981) have many limitations such as not being able to consider soil stiffness, soil stratification, source frequency, soil-pile interface properties (i.e., friction and cohesion), and not being able to predict the frequency of ground surface vibration at a given distance from the

vibration source (pile). Many of these limitations are effectively considered in careful finite element analyses such as those presented above.

CHAPTER 5

5.0 DETERMINING THE QUALITY OF CONCRETE STRENGTH OF LABORATORY SAMPLES WITH VARIABLE CURE TIMES SUBJECTED TO VERTICAL VIBRATIONS

A laboratory testing program is performed to determine the effect of pile-induced vibrations on recently placed concrete. The effect is evaluated by testing the concrete strength of laboratory cast cylindrical and beam specimens.

5.1 LABORATORY TESTING OF CONCRETE CYLINDRICAL SPECIMENS

The procedures for laboratory testing of cylindrical concrete specimens are described in ASTM C-39 and C-138. The laboratory testing program consists of three sets of 30 cylinders each. Within each set, six batches consisting of five cylinders each are made. Each batch is subjected to vibration using a shake table with vertical vibration driven by a double-acting hydraulic actuator. The intent of the laboratory tests was to cover a relatively wide range of peak particle velocities which were measured during vibration monitoring on the Marquette Interchange project. The peak particle velocities were used to determine their effects on concrete strength when the concrete specimens are subjected to vibration at the various curing time. Then the effects of the estimated peak particle velocities can be obtained from the lab test results. Field vibrations are simulated in the laboratory tests using a sinusoidal signal with a frequency of 20 Hz and varying peak particle velocities. As indicated in the Table 5.1, batches A, B, C, D, E and F are subjected to a constant vibration for 15 minutes using PPVs ranging from 0.5 inch/sec to 20 inch/sec. Four cure times prior to shaking are used: 4-6, 12-14, 24-26, and 72-74

hours, as indicated in the same table. Once the cylinders are shaken, they are tested to determine their compressive strength at 3, 7, and 28 days. Thus, the total number of cylinders tested is 90 (5 cylinders × 6 batches × 3 sets).

5.1.1 Test Apparatus

The test apparatus consists of a double-acting hydraulic actuator supported by a rigid frame as shown in Figure 5.1. A container consisting of two thick steel plates and a threaded steel rod is rigidly attached to the actuator as shown in Figure 5.2. The container can accommodate three concrete cylinders as shown in the same Figure. The hydraulic actuator is used to apply the sinusoidal vibrations required for the vibration tests as indicated in Table 5.1. The actuator is driven by the control unit shown in Figure 5.3.

Figure 5.4 Laboratory Vibration Test Apparatus (for Cylindrical Specimens)

Figure 5.5 Close-up: Laboratory Vibration Test Apparatus

5.1.2 Sample Preparation

The ninety cylinders were cast in approximately 1 hr utilizing a ready mix concrete truck that contained 3 cubic yards of concrete. This amount of concrete is at least four times the required amount for the ninety cylinders. This was done to obtain homogeneous, representative, and consistent mix for all the cylinders. The concrete mix is 9488G2 (WisDOT Class A-FA) with a design strength of 4000 psi @ 28 days. The concrete was supplied by a central-mix plant owned by Meyer Materials Company (Meyer Materials) of West Allis, WI. The concrete mix information (per cubic yard) is presented on Table

5.2. The research team is grateful to Meyer Materials for their effort in helping conduct this beneficial research.

Table 5.1: Laboratory Vibration Tests on Young Concrete Cylinders

(Pour all 90 cylinders on **Day 1** by **10:00 AM** and cover cylinders.)

Cure time before vibration	**v=0.5 inch/s**		**v=2 inch/s**		**v=5 inch/s**		**v=10 inch/s**		**v=15 inch/s**		**v=20 inch/s**	
4-6 hrs	**$1A_{3days}$** **$1A_{7days}$** **$1A_{28days}$**	Day 1 2:00PM-6:00PM	**$1B_{3days}$** **$1B_{7days}$** **$1B_{28days}$**	Day 1 2:00PM-6:00PM	**$1C_{3days}$** **$1C_{7days}$** **$1C_{28day}$**	Day 1 2:00PM-6:00PM	**$1D_{3days}$** **$1D_{7days}$** **$1D_{28days}$**	Day 1 2:00PM-6:00PM	**$1E_{3days}$** **$1E_{7days}$** **$1E_{28days}$**	Day 1 2:00PM-6:00PM	**$1F_{3days}$** **$1F_{7days}$** **$1F_{28days}$**	Day 1 2:00PM-6:00PM
12-14 hrs	**$2A_{3days}$** **$2A_{7days}$** **$2A_{28days}$**	Days 1-2 10:00PM-2:00AM	**$2B_{3days}$** **$2B_{7days}$** **$2B_{28days}$**	Days 1-2 10:00PM-2:00AM	**$2C_{3days}$** **$2C_{7days}$** **$2C_{28days}$**	Days 1-2 10:00PM-2:00AM	**$2D_{3days}$** **$2D_{7days}$** **$2D_{28days}$**	Days 1-2 10:00PM-2:00AM	**$2E_{3days}$** **$2E_{7days}$** **$2E_{28days}$**	Days 1-2 10:00PM-2:00AM	**$2F_{3days}$** **$2F_{7days}$** **$2F_{28days}$**	Days 1-2 10:00PM-2:00AM
24-26 hrs	**$3A_{3days}$** **$3A_{7days}$** **$3A_{28days}$**	Day 2 10:00AM -2:00PM	**$3B_{3days}$** **$3B_{7days}$** **$3B_{28days}$**	Day 2 10:00AM -2:00PM	**$3C_{3days}$** **$3C_{7days}$** **$3C_{28days}$**	Day 2 10:00AM -2:00PM	**$3D_{3days}$** **$3D_{7days}$** **$3D_{28days}$**	Day 2 10:00AM -2:00PM	**$3E_{3days}$** **$3E_{7days}$** **$3E_{28days}$**	Day 2 10:00AM -2:00PM	**$3F_{3days}$** **$3F_{7days}$** **$3F_{28days}$**	Day 2 10:00AM -2:00PM
72-74 hrs	**$4A_{3days}$** **$4A_{7days}$** **$4A_{28days}$**	Day 4 10:00AM -2:00PM	**$4B_{3days}$** **$4B_{7days}$** **$4B_{28days}$**	Day 4 10:00AM -2:00PM	**$4C_{3days}$** **$4C_{7days}$** **$4C_{28days}$**	Day 4 10:00AM -2:00PM	**$4D_{3days}$** **$4D_{7days}$** **$4D_{28days}$**	Day 4 10:00AM -2:00PM	**$4E_{3days}$** **$4E_{7days}$** **$4E_{28days}$**	Day 4 10:00AM -2:00PM	**$4F_{3days}$** **$4F_{7days}$** **$4F_{28days}$**	Day 4 10:00AM -2:00PM
No vibration	**$5A_{3days}$** **$5A_{7days}$** **$5A_{28days}$**		**$5B_{3days}$** **$5B_{7days}$** **$5B_{28days}$**		**$5C_{3days}$** **$5C_{7days}$** **$5C_{28days}$**		**$5D_{3days}$** **$5D_{7days}$** **$5D_{28days}$**		**$5E_{3days}$** **$5E_{7days}$** **$5E_{28days}$**		**$5F_{3days}$** **$5F_{7days}$** **$5F_{28days}$**	

All **3-day-specimens** are tested for ultimate strength on **Day 4 at 10:00 AM**
All **7-day-specimens** are tested for ultimate strength on **Day 8 at 10:00 AM**
All **28-day-specimens** are tested for ultimate strength on **Day 29 at 10:00 AM**

Figure 5.6 MTS Control System

Table 5.2 WisDOT A-FA Concrete Mix Information Per Cubic Yard

Component	Quantity
Cement:	480 lb
Fly Ash:	135 lb
Sand:	1188 lb
1½" Gravel:	968 lb
¾" Gravel:	968 lb
Water:	33.2 gal
Water Reducer: (ASTM C494 type A)	18.5-36.9

Upon arrival of the concrete mix the following test results were obtained:

Slump:	4.5 inch
Concrete Temperature:	75° F
Air Temperature:	61º F
Air Entrainment:	7.1%
Unit Weight:	143.56 pcf

5.1.3 Test Results

All test specimens are stored in a moisture room (100% humidity). The specimens were subjected to vibration following the strict time schedule shown in Table 5.1. Each specimen is subject to 15 minutes of vibration with 20-Hz frequency and specific amplitude as specified in Table 5.1. Figure 5.4 shows the displacement amplitude history for the 6 levels of PPV indicated in Table 5.1.

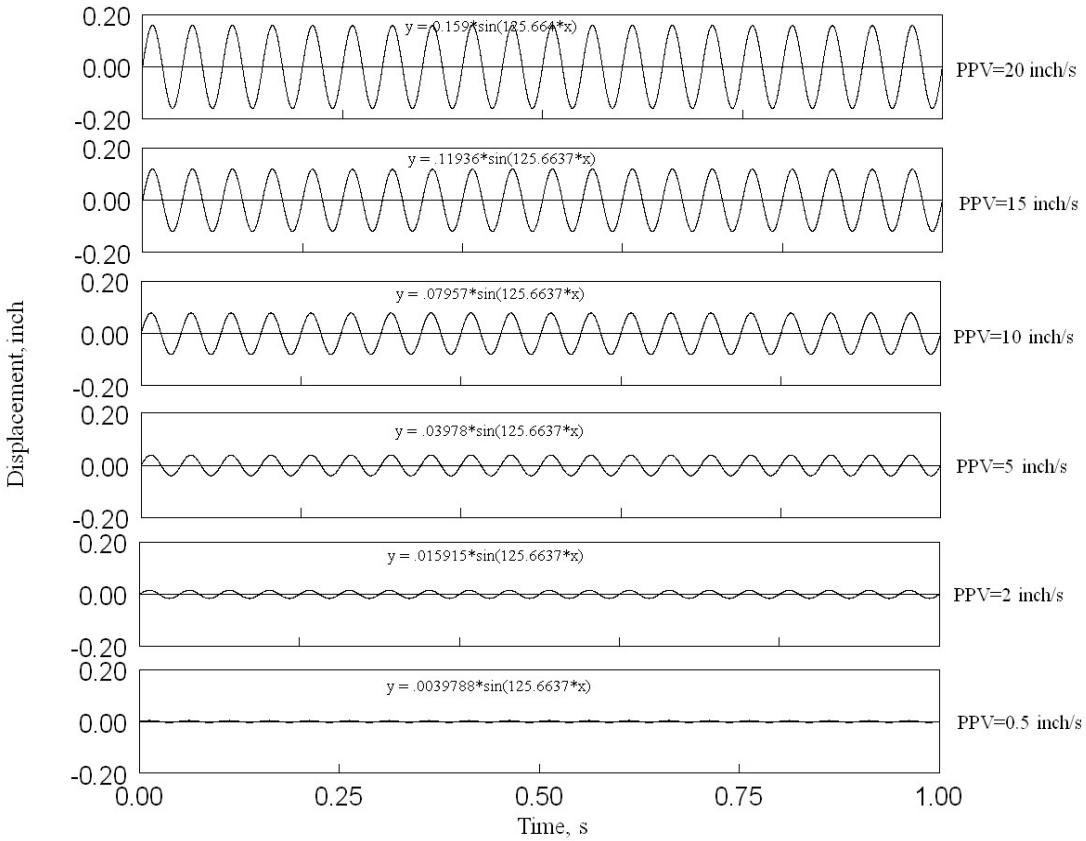

Figure 5.4: Laboratory Test Vibrations

Figure 5.5 shows the 3-day ultimate strength for specimens as function of PPV and cure time during which vibration was applied. The figure shows no specific pattern of strength variation with PPV level.

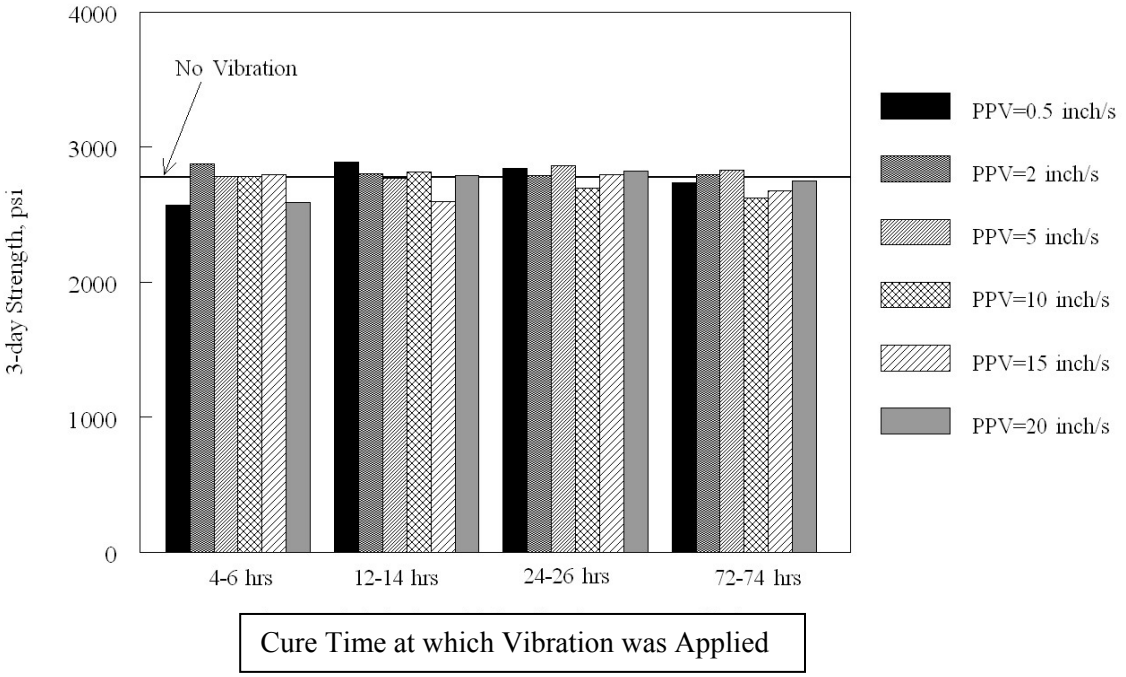

Figure 5.5 Effects of PPV on Cylinder 3-day Strength

Figure 5.6 shows the 3-day stiffness (secant elastic modulus) for specimens as function of PPV and cure time during which vibration was applied. The figure shows some decrease in stiffness due to vibration. No specific pattern is observed for the effects of increasing PPV. It is to be noted that the stiffness considered in this figure is the secant Young's modulus at an axial strain of 0.05%. The strain was measured at the central 6 inches of the 12-inch high cylindrical specimens as shown in Figure 5.7.

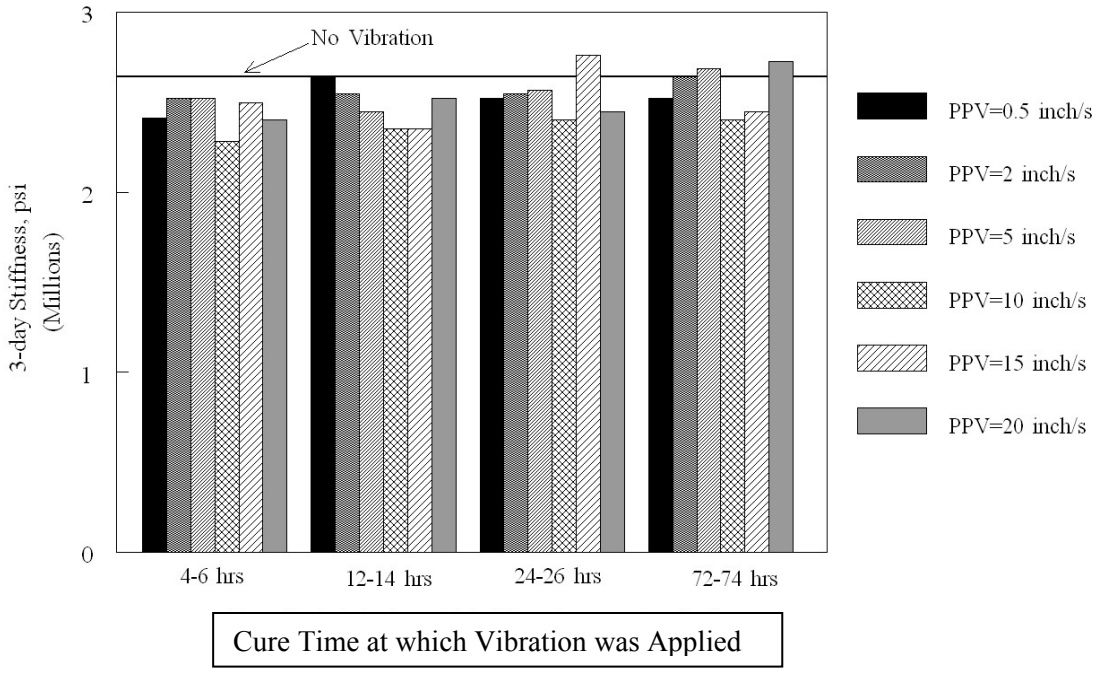

Figure 5.6 Effects of PPV on Cylinder 3-day Stiffness

Figure 5.7 Ultimate Strength/Stiffness Test Apparatus

Figure 5.8 shows the 7-day ultimate strength for specimens as function of PPV and the cure time at which vibration was applied. The figure shows no specific pattern of strength variation with PPV level. Figure 5.9 shows the 7-day stiffness for specimens as function of PPV and the cure time at which vibration was applied. There is some increase in stiffness due to vibration even though there is no specific pattern of stiffness change with PPV level.

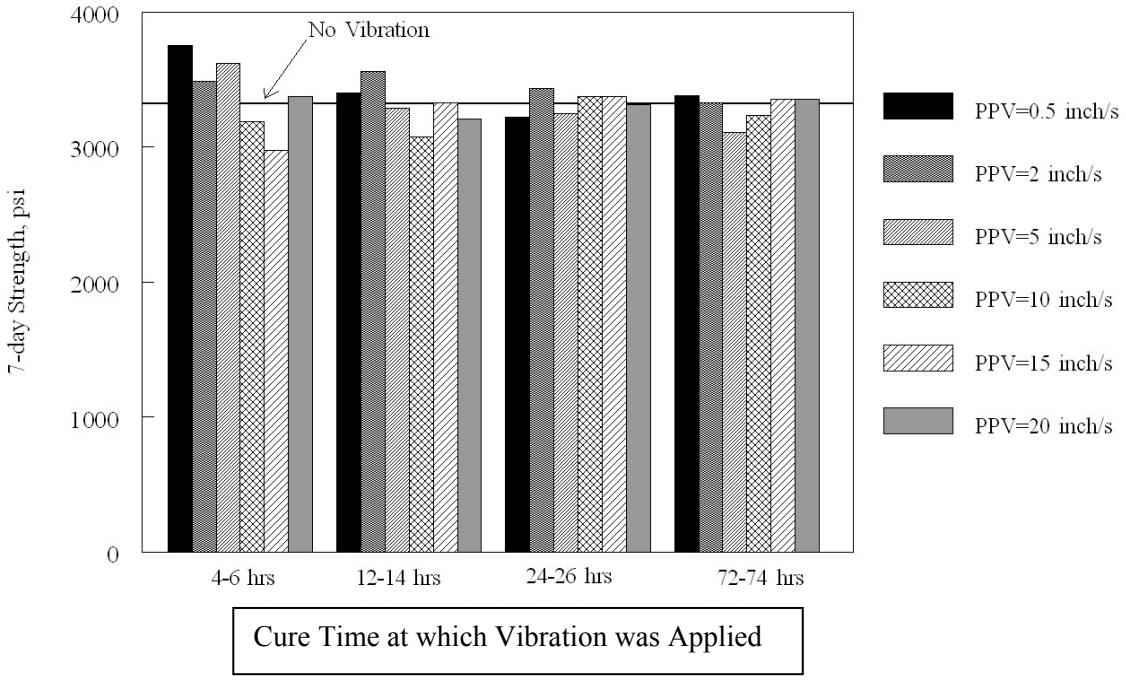

Figure 5.8 Effects of PPV on Cylinder 7-day Strength

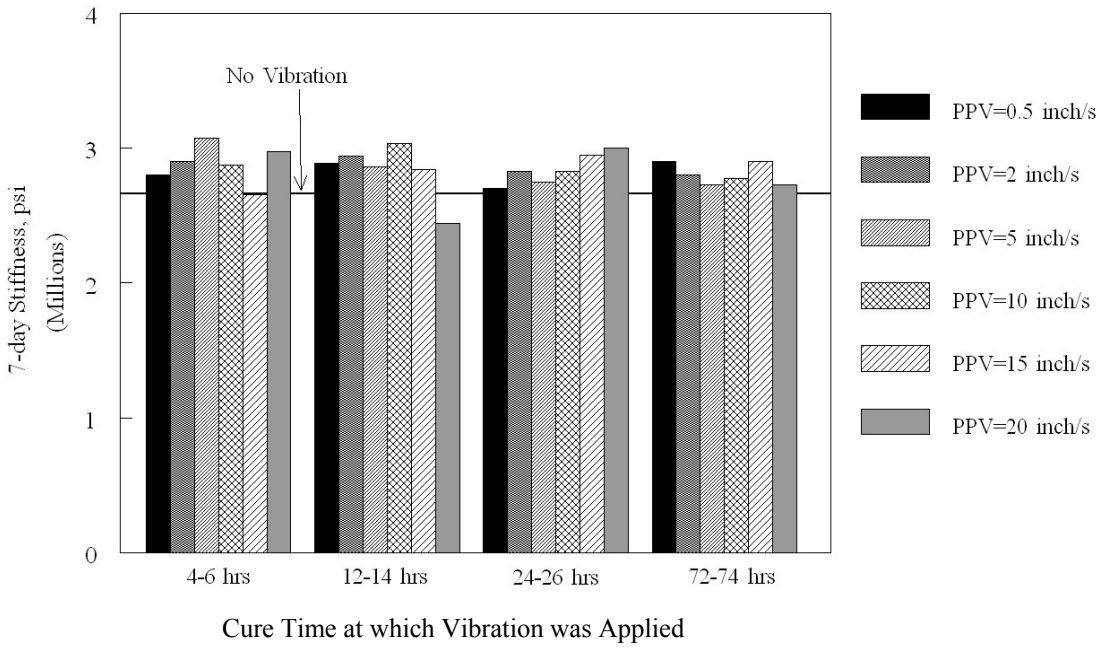

Figure 5.9 Effects of PPV on Cylinder 7-day Stiffness

Figure 5.10 shows the 28-day ultimate strength for specimens as function of PPV and the cure time at which vibration was applied. No specific pattern of strength variation with PPV level is noted from the figure. The figure indicates, however, a slight decrease in 28-days strength due to vibration for nearly all vibration levels. Figure 5.11 shows the 28-day stiffness for concrete specimens as function of PPV and the cure time at which vibration was applied. There is some increase in stiffness due to vibration even though there is no specific pattern of stiffness variation with PPV level. Appendix A includes the measured stress strain curves for all specimens. These curves were used to estimate secant Young's moduli.

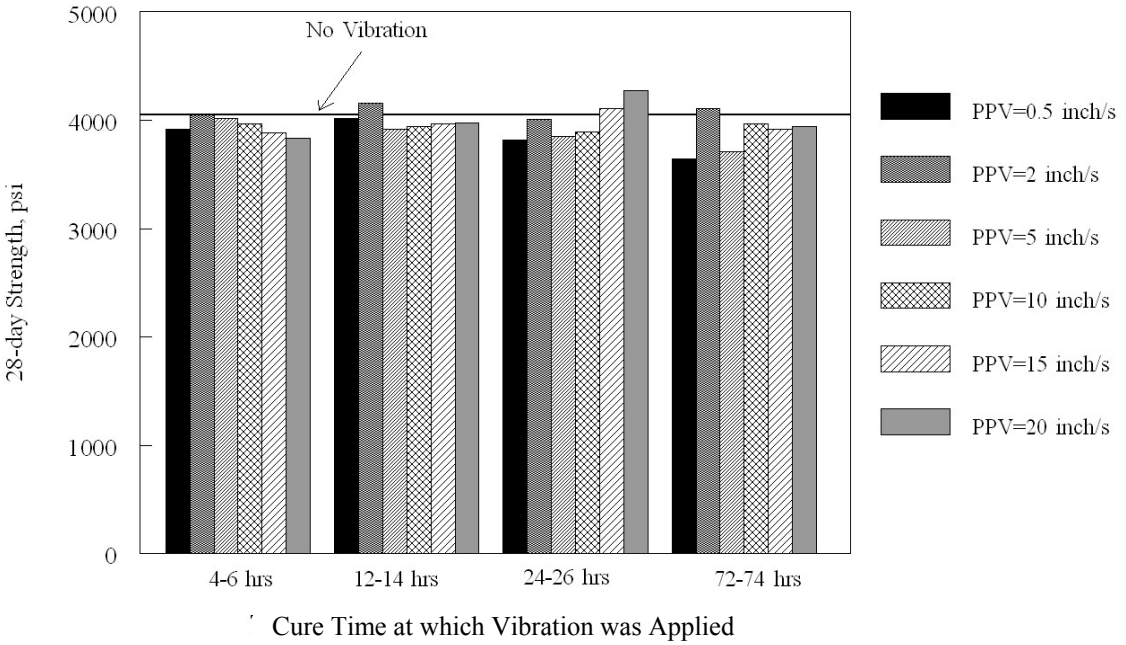

Figure 5.10 Effects of PPV on Cylinder 28-day Strength

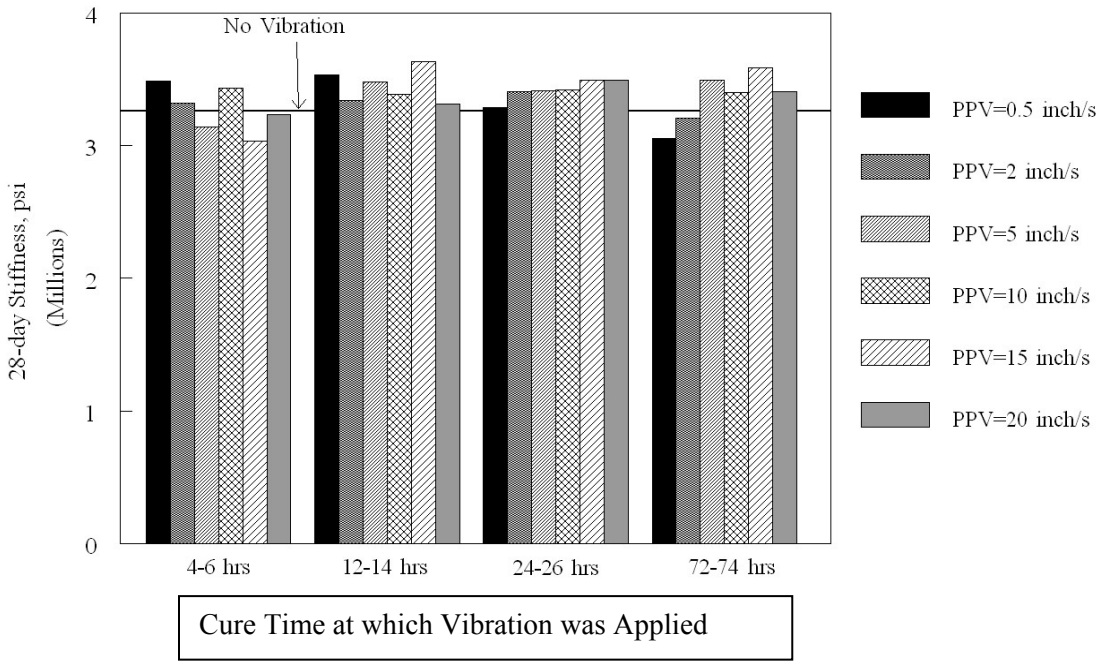

Figure 5.11 Effects of PPV on Cylinder 28-day Stiffness

5.2 LABORATORY TESTING OF CONCRETE BEAM SPECIMENS

To determine the effect of pile-induced vibrations on recently placed concrete, additional laboratory testing was performed. The effect of vibration is evaluated by testing the flexural strength of 36 beam specimens using the standard method of test for flexural strength of concrete (Simple beam with third-point loading: AASHTO Designation: T97-03, ASTM Designation: C78-02). In our tests, the distance (L) between the two roller supports of the simple beam was 18 inches, therefore, the distance between the loading rollers was 6 inches (=L/3).

The laboratory testing program consisted of 36 beams. Each beam measured 6 inch × 6 inch × 24 inch. Of the 36 beams, 32 beams were subjected to different vibration levels at various cure times as described in Table 5.3. Vibration was performed using a shake table with vertical vibration driven by a double-acting hydraulic actuator. Four of the 36 beams were not vibrated to serve as the control case. A sinusoidal signal with a frequency of 20 Hz and varying peak particle velocities was used as indicated in Table 5.2. Batches A, B, C and D were subjected to a constant vibration for 15 minutes using PPVs of 0.5, 5, 10, and 20 inch/sec. Four cure times prior to shaking were used: 4-6, 12-14, 24-26, and 72-74 hours, as indicated in the same table. Once the beams were shaken, they were tested to determine their flexural strength at 3 and 7 days.

Table 5.3: Laboratory Vibration Tests on Young Concrete Beams

(Pour all 36 beams on **Day 1 by 10:00 AM** and cover)

Cure time before vibration	**v=0.5 inch/s**		**v=5 inch/s**		**v=10 inch/s**		**v=20 inch/s**	
4-6 hrs	**$1A_{3days}$** **$1A_{7days}$**	Day 1 2:00PM-6:00PM	**$1B_{3days}$** **$1B_{7days}$**	Day 1 2:00PM-6:00PM	**$1C_{3days}$** **$1C_{7days}$**	Day 1 2:00PM-6:00PM	**$1D_{3days}$** **$1D_{7days}$**	Day 1 2:00PM-6:00PM
12-14 hrs	**$2A_{3days}$** **$2A_{7days}$**	Days 1-2 10:00PM-2:00AM	**$2B_{3days}$** **$2B_{7days}$**	Days 1-2 10:00PM-2:00AM	**$2C_{3days}$** **$2C_{7days}$**	Days 1-2 10:00PM-2:00AM	**$2D_{3days}$** **$2D_{7days}$**	Days 1-2 10:00PM-2:00AM
24-26 hrs	**$3A_{3days}$** **$3A_{7days}$**	Day 2 10:00AM -2:00PM	**$3B_{3days}$** **$3B_{7days}$**	Day 2 10:00AM -2:00PM	**$3C_{3days}$** **$3C_{7days}$**	Day 2 10:00AM -2:00PM	**$3D_{3days}$** **$3D_{7days}$**	Day 2 10:00AM -2:00PM
72-74 hrs	**$4A_{3days}$** **$4A_{7days}$**	Day 4 10:00AM -2:00PM	**$4B_{3days}$** **$4B_{7days}$**	Day 4 10:00AM -2:00PM	**$4C_{3days}$** **$4C_{7days}$**	Day 4 10:00AM -2:00PM	**$4D_{3days}$** **$4D_{7days}$**	Day 4 10:00AM -2:00PM
No vibration	**$5A_{3days}$** **$5A_{7days}$**		**$5B_{3days}$** **$5B_{7days}$**					

All **3-day-specimens** are tested for ultimate strength on **Day 4 at 10:00 AM**
All **7-day-specimens** are tested for ultimate strength on **Day 8 at 10:00 AM**

5.2.1 Test Apparatus

The test apparatus consists of a double-acting hydraulic actuator supported by a rigid frame as shown in Figure 5.12. A container consisting of a thick steel plate and a specially designed fastening system is attached to the actuator as shown in Figure 5.13. The container can accommodate two concrete beams as shown in the same Figure. The hydraulic actuator is used to apply the sinusoidal vibrations required for the vibration tests as indicated in Table 5.3. The actuator is driven by the control unit shown in Figure 5.3.

Figure 5.12: Laboratory Vibration Test Apparatus (for Beam Specimens)

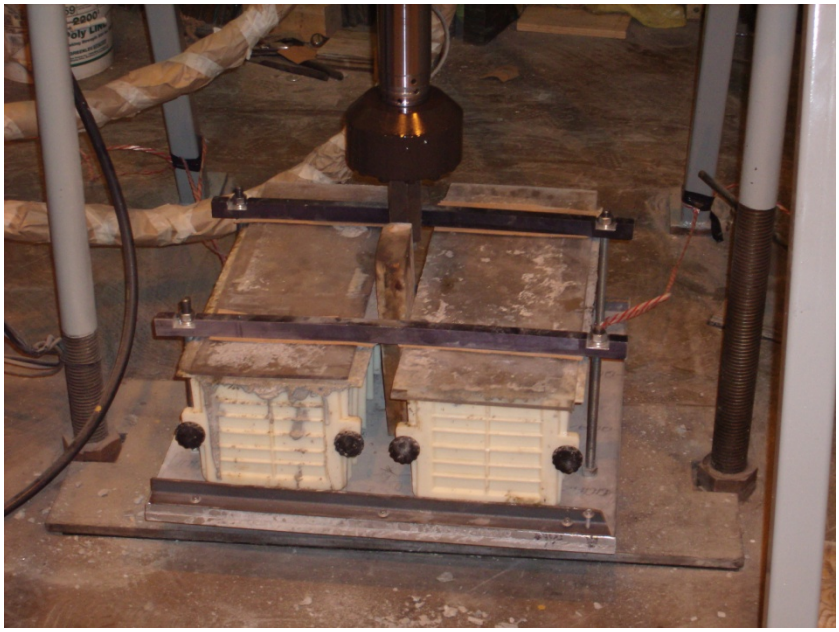

Figure 5.13: Close-up of the Laboratory Vibration Test Apparatus (for Beam Specimens)

5.2.2 Sample Preparation

The thirty six beams were cast in approximately 1 hr utilizing a ready mix concrete truck that contained 3 cubic yards of concrete. This amount of concrete is more than four times the required amount for the thirty six beams. This was done to obtain homogeneous, representative, and consistent mix for all the beams. The concrete mix is 9488G2 (WisDOT Class A-FA) with a design strength of 4000 psi @ 28 days (Meyer Materials). This concrete mix is identical to the mix used for the cylinders as described in the preceding section.

5.2.3 Test Results

All test specimens were stored in a moisture room (100% humidity). The specimens were subjected to vibration following the strict time schedule shown in Table 5.3. Each specimen was subjected to 15 minutes of vibration with 20-Hz frequency and specific amplitude as specified in Table 5.3. Figure 5.4 includes the displacement amplitude history for the four levels of PPV specified in Table 5.3.

Once the beams were shaken, they were tested to determine their flexural strength at 3 and 7 days using the apparatus shown in Figures 5.14 and 5.15. All 36 beam specimens were tested following the standard method of testing for flexural strength of concrete (Simple beam with third-point loading: AASHTO Designation: T97-03, ASTM Designation: C78-02).

Figure 5.14: Simple beam with third-point loading (AASHTO Designation: T97-03, ASTM Designation: C78-02)

Figure 5.15: Simple beam with third-point loading (close-up)

Figure 5.16 shows the 3-day ultimate flexural strength for specimens as function of PPV and the cure time at which vibration was applied. The Figure shows no specific pattern of strength variation with PPV level for specimens vibrated at curing times greater than 12 hours. It is interesting to note, however, that the strength of the specimens vibrated at very early age (4-6 hours cure time) was substantially smaller than the 3-days average strength of the control specimens. Also, the strengths of these specimens were significantly affected by the PPV.

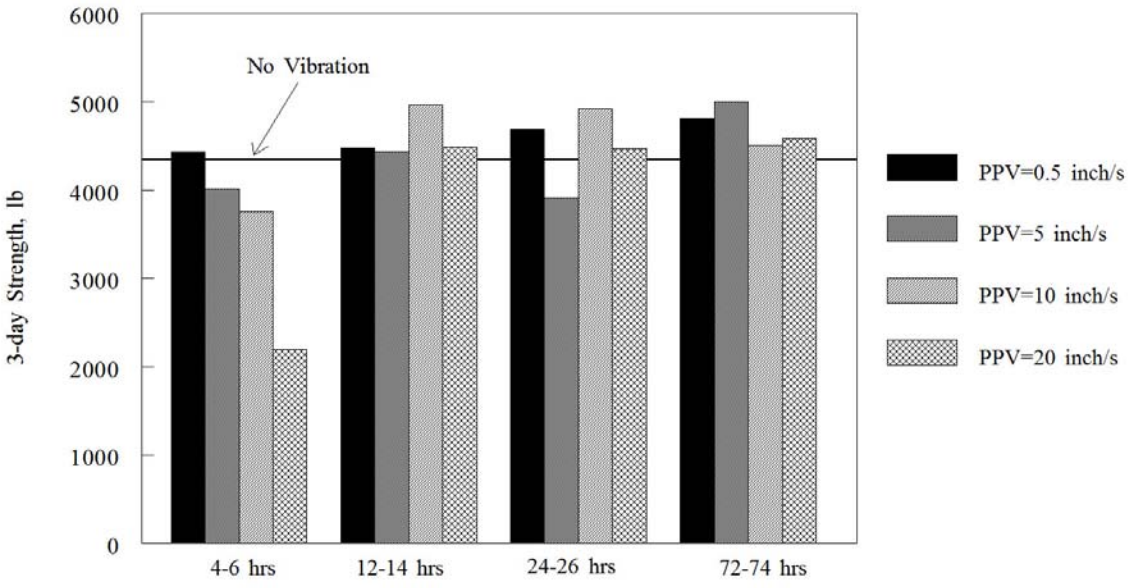

Figure 5.16: Effects of PPV on Beam 3-day flexural strength

Figure 5.17 shows the 7-day ultimate strength for specimens as function of PPV and the cure time at which vibration was applied. The Figure shows no specific pattern of strength variation with PPV level. Appendix B includes the measured load-displacement curves for all specimens.

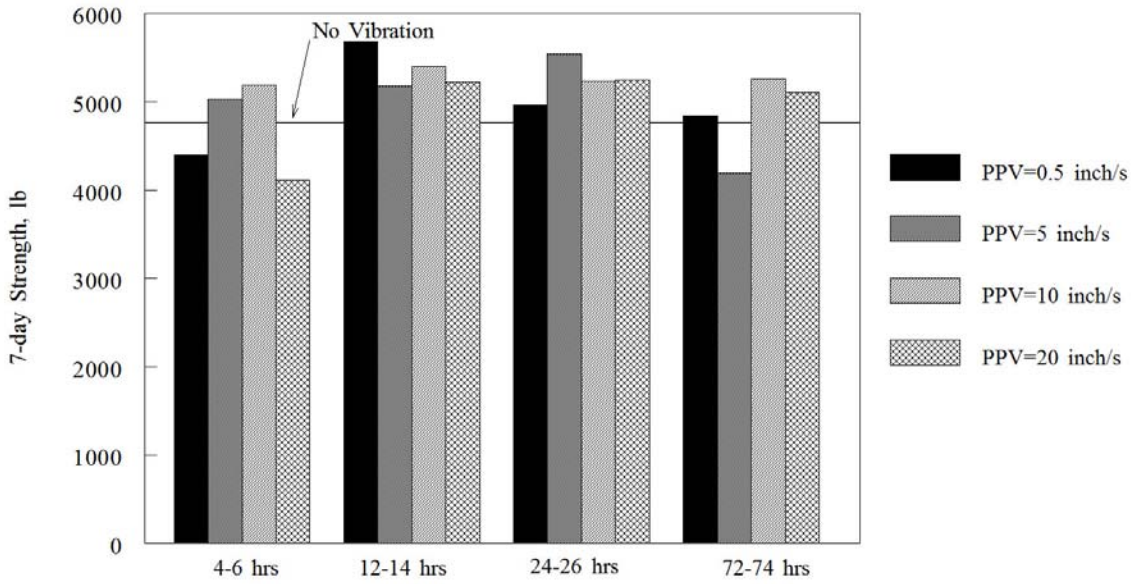

Figure 5.17: Effects of PPV on Beam 7-day flexural strength

CHAPTER 6

6.0 VIBRATION FIELD STUDY

The field study portion of the research was developed to investigate two areas of interest: (1) attenuation of potentially-damaging pile driving vibrations with distance and depth and (2) the effects of distance and age on the quality of concrete exposed to pile driving vibrations. The field study consisted of field vibration monitoring and testing of field concrete samples subjected to pile-driving vibrations. WisDOT also requested that noise data associated with the pile driving be collected and tabulated so it could be evaluated by others.

An objective of the study was to use the supporting data to provide recommendations that would enable WisDOT to better define how pile-induced vibrations from different hammers affect the quality of concrete with distance and depth. These included making recommendations for specifying acceptable ground vibration levels and/or distances for recently-placed concrete based on curing time and/or compressive strength.

6.1 FIELD MONITORING PROGRAM

The Field Monitoring Program, included the tasks of coordinating the program with the Contractors and WisDOT; obtaining subsurface information and installing the field instrumentation; and conducting the vibration and noise field monitoring program. The program incorporated monitoring and evaluating attenuation of pile driving vibrations with distance and at depth at two test sites as well as noise measurements. Full scale

concrete samples of varying age were subjected to pile-driving vibrations at several distances. Emphasis was placed on evaluating early-age concrete. Results for these field samples will be compared with those tested in the laboratory phase.

The field monitoring program consisted of four major tasks:

1. This portion of the program consisted of drilling soil borings on the field test site along with performing laboratory tests on recovered soil samples;

2. The second task consisted of installing and testing full-scale concrete field samples while pile driving induced vibration and noise data was collected during driving of the test piles;

3. The concrete field samples were recovered and conveyed to the laboratory for testing in this phase; and

4. The last task consisted of testing the concrete samples for compressive and flexural strength and comparing the results to the lab study and work of previous investigators. The results of the strength testing are presented in Chapter 7.

6.2 FIELD SITE DETERMINATION

The original plan for this research included collection of field vibration data during production pile driving on the Marquette Interchange project. Access ultimately was not granted for the planned research on the Marquette project, however, and an alternate test site was eventually selected.

A parcel located at the southwest corner of Lincoln Memorial Drive and East Bay Street was selected as the replacement site for this study. Figure 6.1 is a general view of the project location and Figure 6.2 shows an aerial photograph of the site. An additional subsurface exploration program was proposed. WisDOT completed the exploration by drilling two soil borings. The borings were drilled at the two test pile locations. Drilling oversight was done by HNTB personnel. The size of the field study site did not allow driving more than two test piles because of the concern for vibrations from a test location influencing results at an adjacent test location. The field study then developed into the test pile orientation shown in Figure 6.3.

Boring B-1 was drilled at the Test Pile # 1 location and encountered dense sand and gravel fill to about 3 ½ feet underlain by an approximate 1 ½-foot thick layer of hard clay/silt fill. This material was underlain by very loose to loose silty sand fill to 19 feet. The underlying soil consisted of native deposits of medium dense to very dense sand with marine shells to about 25 feet where stiff (CH) clay was encountered that extended to 55 feet. Very stiff to hard silty clay was present to about 75 ½ feet where an approximate 5-foot thick layer of medium dense silty sand was encountered underlain by medium dense gravel to 82 feet. Water was encountered at a depth of approximately 8 feet below the ground surface during drilling.

Boring B-2 was drilled at the Test Pile # 2 location. Dense to loose sand and gravel fill was present in this boring to approximately 14 feet underlain to 18 feet by loose silty sand fill. Slag, nails and foundry sand were present in portions of the silty sand fill. Very

dense sand with gravel and some concrete fragments were present from 18 feet to a depth of 24 feet. Native medium stiff clay (CH) was present below the fill and extended to about 50 feet where a 5-foot thick layer of soft clay was present. Very stiff to hard clay was present below the soft layer and extended to 81 ½ feet. Water was noted at a depth of approximately 71 feet below the ground surface in this boring during drilling.

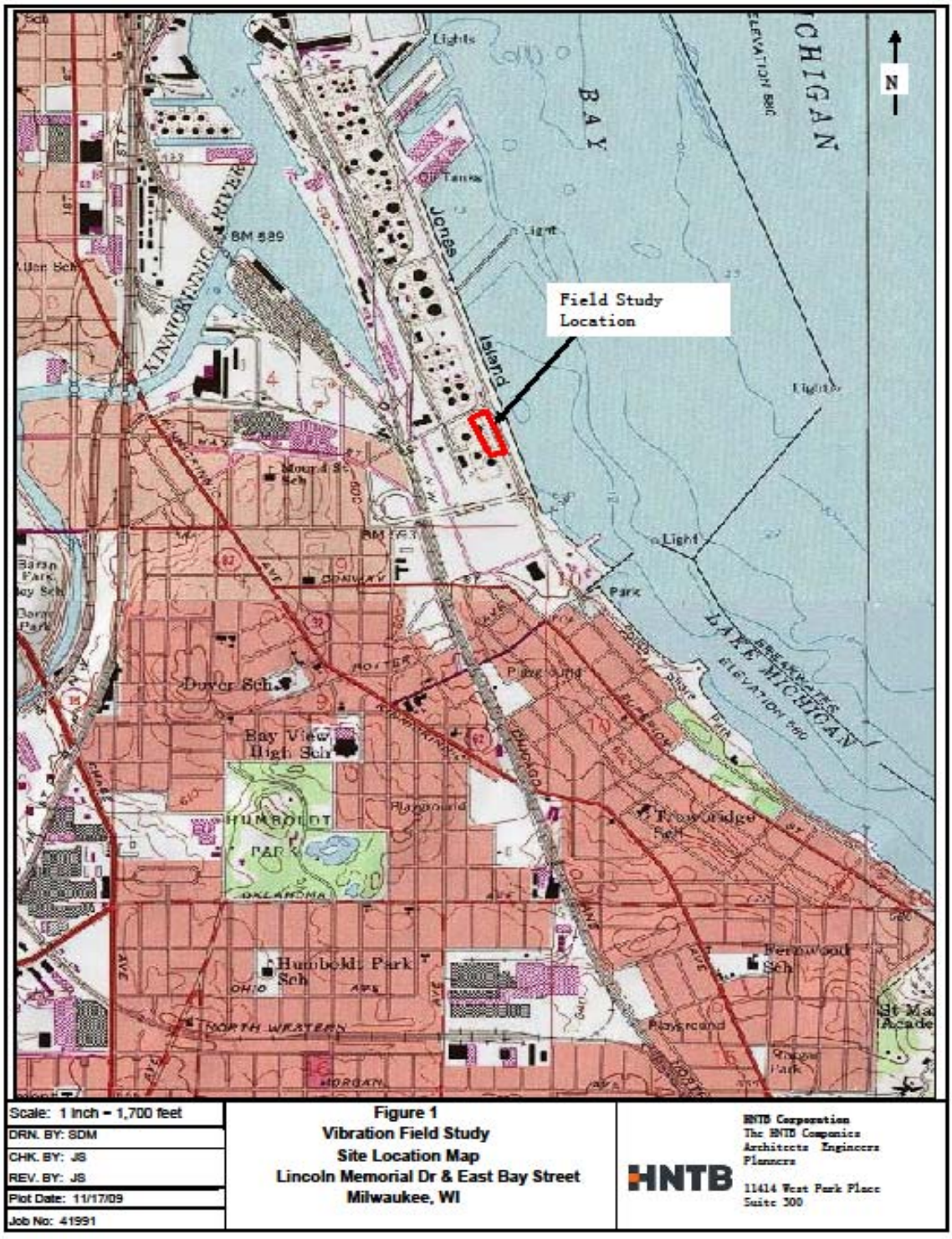

Figure 6.1 Field Study Location

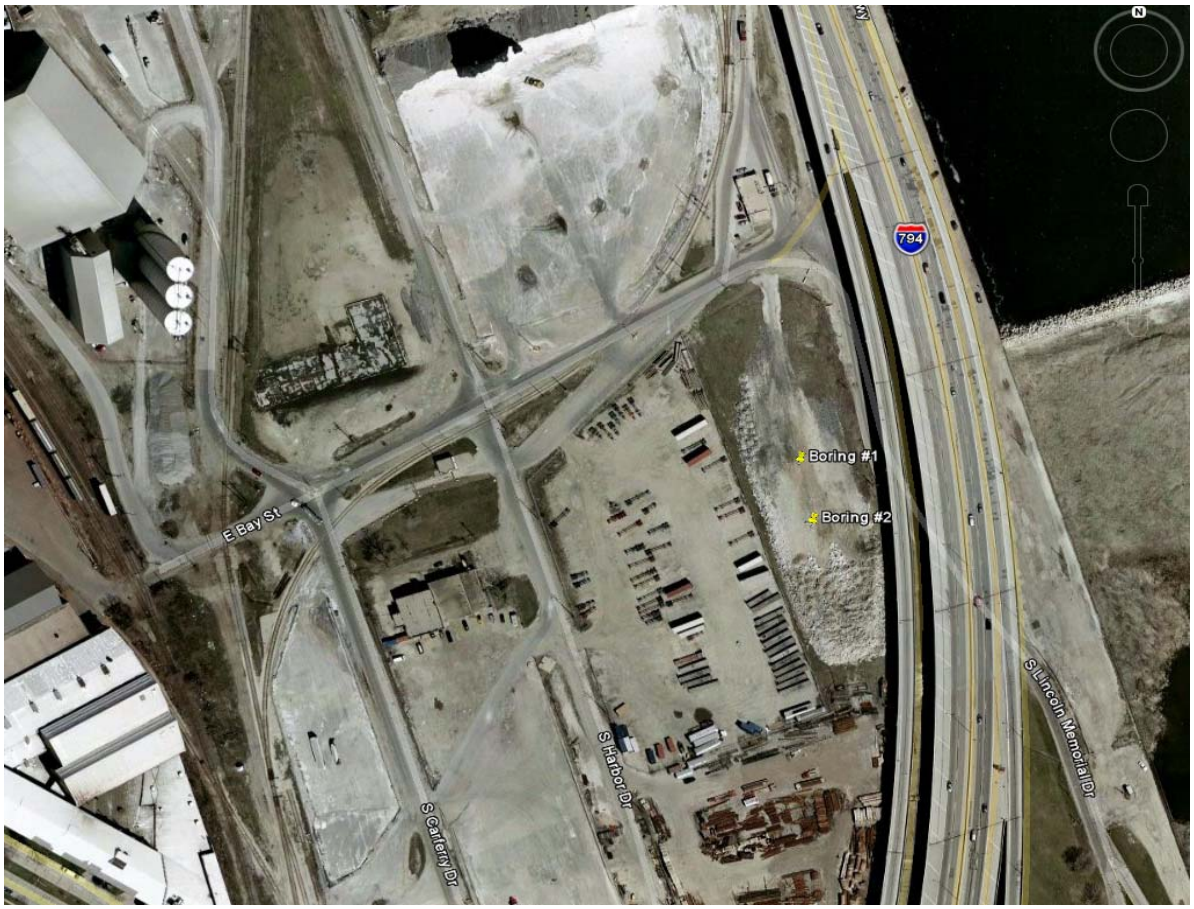

Figure 6.2 Aerial Photograph of Research Site

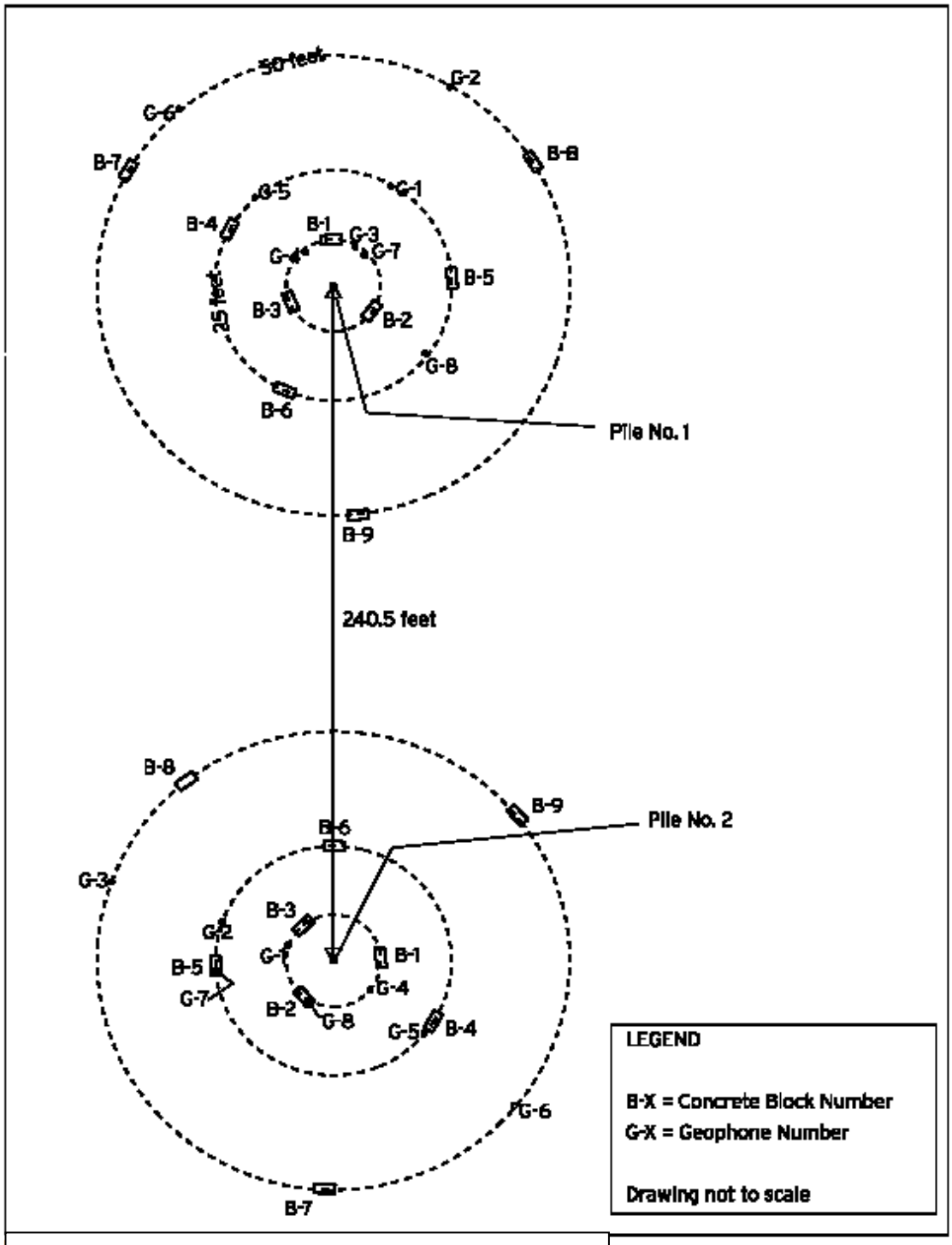

Figure 6.3 Orientation of Field Test Site Piles

6.3 FIELD TESTING PROTOCOL

The original plan to use the pile driving on the Marquette Interchange project had the advantage that no additional cost would be incurred for pile driving. However, the field test site would require a contractor to drive the test piles and incur additional costs. The research team contacted the Edward E. Gillen Company (Gillen) from Milwaukee, Wisconsin and they agreed to drive the piling for the research at a reduced cost which worked within the available budget. The research team is grateful to Gillen for their effort in helping conduct this beneficial research.

The plan for the field study was to place concrete in the ground at locations that allowed vibration and noise data to be collected with instrumentation under controlled conditions during adjacent pile driving. Obtaining concrete samples from the field created a few logistical problems. The issues associated with the field program were:

- Obtaining molds for removable concrete cylinders and developing molds for removable concrete beams;
- Installing instrumentation on and under the ground to monitor the vibrations;
- Placing concrete at variable times prior to pile driving so that the effect of concrete age could be assessed;
- Extraction of concrete cylinder and beam samples from the field concrete blocks and;
- Transporting variable age concrete samples to the lab for strength testing.

The research team was familiar with Cast-In-Place-Punch-Out-Cylncore (CIPPOC) molds that are manufactured by Deslauriers, Inc and are used to obtain concrete samples for testing from field locations. Figure 6.4 shows an exploded view of a CIPPOC. These cylinder molds consist of a 4-inch diameter by 6-inch high PVC mold within a mold that can be removed after initial concrete set. However, an air gap was present between the inner and outer molds that could affect vibration transmission. The team used thin (1/8-inch thick) pieces of High Impact Plastic (HIP) approximately 1-inch wide and 6 inches high placed at eight points around the circumference of the molds to provide direct contact between the inner and outer molds. Two pieces of 1/24-inch diameter wire were set around the top of the inner mold to help with mold removal after casting.

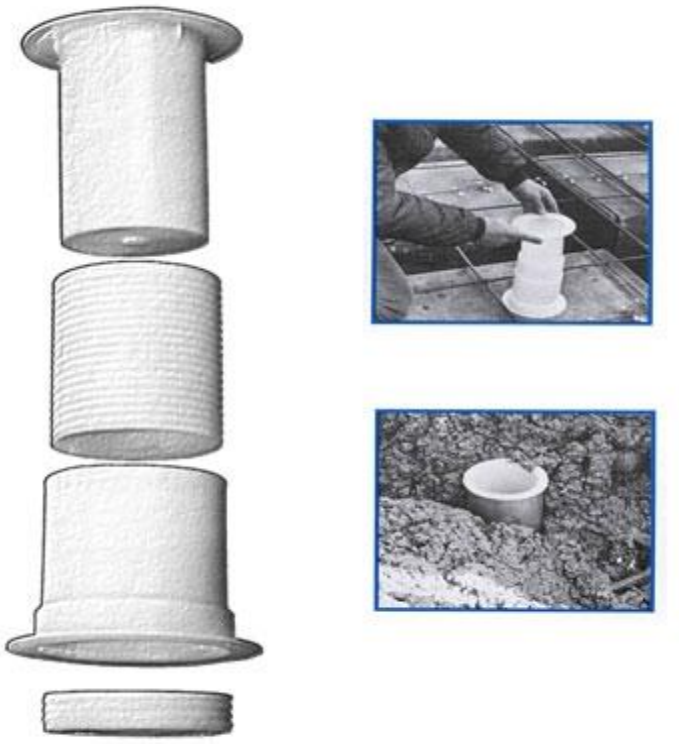

Figure 6.4 CIPPOC Mold

Re-useable beam molds are available for making beam samples but they are expensive. Additionally, these molds require dismantling in order to remove the specimen. The molds could not be dismantled after placement in concrete blocks so another type of mold was required. The research team then developed a cast in place pull out beam mold using

1/8 inch thick HIP sheets from Deslauriers, Inc. The mold consisted of a beam mold within a mold. The inside dimensions of the outer mold were equal to the outside dimensions of the inner mold to avoid an air gap between sections. The inner mold inner dimensions were 6 inches high by 6 inches wide by 20 inches long. This type of pull out mold would work for the research but it was expected that beam removal may be difficult because of the beam weight. Therefore, a thin coat of automotive grease was applied to the outside face of the inner mold to facilitate removal of the mold after concrete placement. Two pieces of 1/24-inch diameter wire were set between the inner and outer mold at one-quarter points from each end of the beam to help with beam removal after casting. The mold material was flexible such that no air gap was present between the inner and outer molds over the majority of the beam length.

It was also desired to collect vibration information at depth. Therefore, a 6-inch diameter PVC closed end pipe was set at a depth of 10 feet below the ground surface at distances of 10 and 25 feet from the Test Pile # 1 location to allow geophones to be placed at the base of the casing to record vibration data. Figure 6.4 is a schematic of the below grade geophone inside of the PVC pipe. Giles Engineering Associates, Inc. drilled the borings for the PVC pipe and grouted it in place with lean mix concrete. An approximate 3-inch thick layer of fine concrete sand was placed in the bottom of the pipe as a base for the

geophone. The surface geophones were all secured to the ground surface using sandbags and those in the PVC pipe were secured using sandbags placed over the geophone

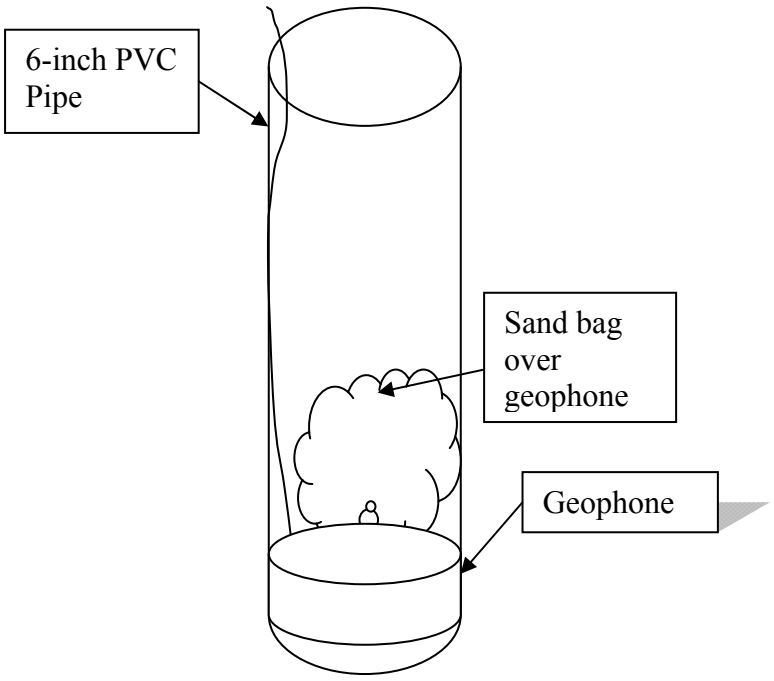

Figure 6.5 Schematic of below Grade Geophone in PVC pipe

Instantel Minimate seismographs were utilized to monitor vibrations using geophones. The seismograph recorded noise using a microphone. In order to determine vibration attenuation with distance, geophones were placed at given radial distances of 10, 25, and 50 feet along 2 radial axes extending away from the test piles that were driven during the Dynamic Testing phase of the project. Figure 6.6 provides a schematic view of a test location and shows the pile, concrete test specimens, and geophones. Two axes of geophones were selected in order to generate enough data to evaluate variability of readings at set distances and to provide a level of redundancy for this phase of the study. Test locations closer to the pile (driving energy) will experience higher levels of vibration and noise compared to locations farther away from the vibration source.

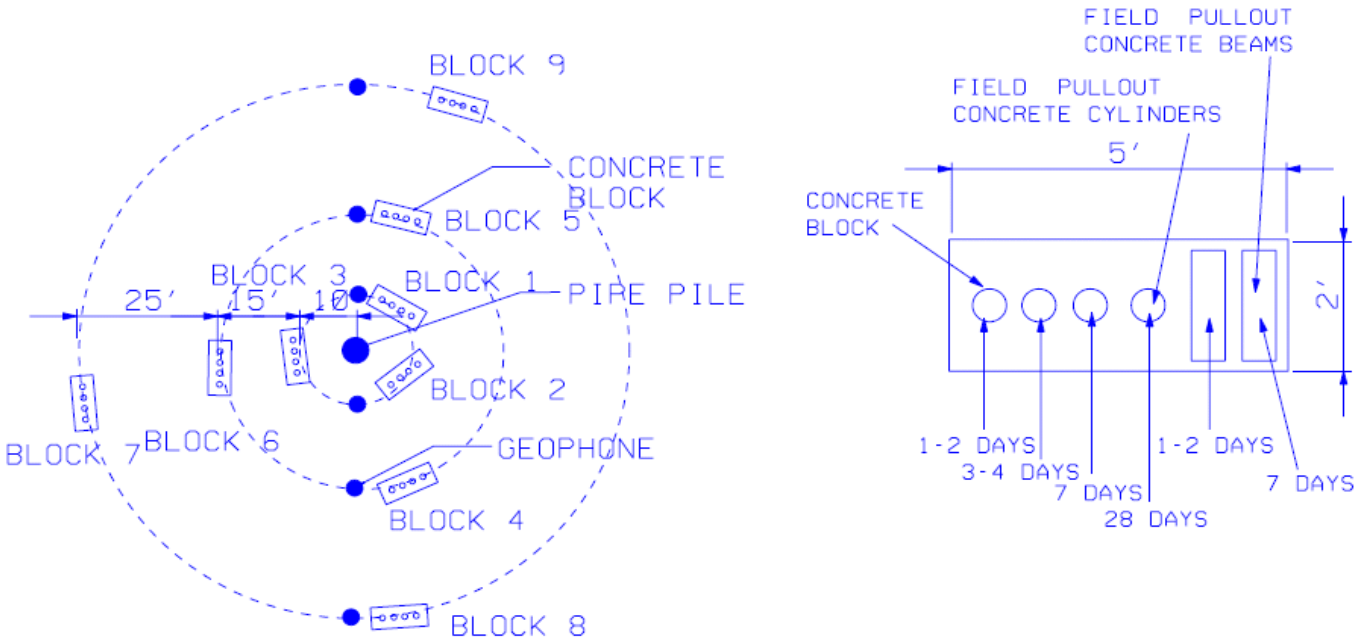

Figure 6.6 – Schematic of Test Pile Location

6.4 FIELD TESTING

Based on previous research by others, it was desired to place concrete in the field at times that allowed for concrete curing times ranging from 4 to 8 hours, 12 to 16 hours and 24 to 36 hours prior to subjecting the samples to pile driving induced vibrations. The concrete was a standard WisDOT A-FA concrete design mix previously approved for use on the project. This was the same mix design that was tested in the lab prior to the field monitoring program. Meyer Materials provided concrete for both the laboratory and field phases of the study. The concrete mix (Meyer Material Mix Number 9488G2 (class A-FA)) was used.

Concrete was placed on Wednesday October 28th, 2009 starting at 10:00 AM, Wednesday afternoon starting at 3:55 PM and Thursday October 29th starting at 9:40 AM. The slump of the concrete was 3.75-inch, 1-inch, and 1.5 inch for the three loads of concrete. The concrete loads were fully discharged from the trucks at times of 1.5, 2.25 and 1.4 hours. Weather data during the field study are presented in Table 6.1

Table 6.1 - Weather Data During Field Study

Date	**Sky Condition**	**Low Temperature, ^{O}F**	**High Temperature, ^{O}F**	**Precipitation, inches**
10/28/09	Cloudy	48	54	0
10/29/09	Cloudy	52	56	0.15
10/30/09	Cloudy	47	68	0.70

The concrete temperature on arrival of the first load was 64 ^{O}F and contained 6.2 percent entrained air. Temperature and air content of the other two loads was not measured. The concrete temperature and air data for first load were consistent with the concrete data from the laboratory study. Concrete blocks with approximate dimensions of 2 feet wide by 5 feet long by 12 inches thick were constructed in trench cast excavations and the CIPPOC and beam molds were incorporated into the blocks during concrete placement.

The pile driving was performed by Gillen using a Vulcan 08 compressed air pile driving hammer with a rated energy of 26,000 ft-lb. The piles were 50 foot sections of closed

end 12 ¾-inch diameter pipe with a 0.25-inch wall thickness. . The vibration levels from various types of pile driving hammers will be different. However, the magnitude of vibration is a function of the hammer energy and not the type of hammer that created the vibration.

Pile driving was done first at Test Pile #1 which was the northern location and then moved to Test Pile #2 at the southern location. Pile driving occurred on Thursday October 29th, 2009 starting at 2:16 PM. Pile driving encountered an obstruction at about 19 feet at the Test Pile # 1 location. Pile driving continued for a period of time on the obstruction but was stopped at about 2:25 PM due to lack of pile advancement into the ground and the rig was moved to the second location. Figure 6.7 shows the pile driving hammer and crane at Test Pile #1 during the vibration monitoring. Figure 6.8 shows Test Pile # 1 after completion of driving and relocation of the hammer/crane.

Figure 6.7 View of Edward E. Gillen Co. Pile driving hammer, crane and compressor during vibration monitoring at Test Pile #1

Figure 6.8 – View of Test Pile # 1 after completion of driving

Pile driving started at the Test Pile # 2 location at approximately 3:23 PM. An obstruction was also encountered at approximately 20 feet at Test Pile # 2 but driving continued until the pile advanced beyond the obstruction. Driving continued at this location until the pile was driven to a depth of about 40 feet which occurred at 3:35 PM. Figure 6.9 is a view of Test Pile # 2 in the leads at completion of driving.

Figure 6.9 – View of Test Pile # 2 after completion of driving, note pile leads/hammer

WisDOT obtained dynamic measurements of the pile driving activities during the research using Pile Driving Analyzer (PDA) equipment. The results are presented in the appendix.

Once the pile driving was finished, the concrete beam and CIPPOC samples were left in the block samples overnight. Figure 6.10 is a view of one of the concrete block samples at the Test Pile 2 location after completion of pile driving. The following day the samples were removed from the concrete blocks. Most samples came out of the blocks with little difficulty. However, the beam samples were more difficult to remove than the CIPPOC samples. This was due to the more flexible beam molds that deformed slightly during concrete placement. The CIPPOC molds did not deform. All samples were able to be extracted from the ground.

Figure 6.10 View of Block 8 at Test Pile #2 Location

Concrete samples were transported via pickup truck from the test site to the UW-Milwaukee Department of Civil Engineering laboratory. Sheets of foam were placed under the samples to cushion the material during transport. A total of 72 CIPPOC samples and 24 beam samples were taken to the lab along with control samples. Three trips were required due to the approximate 2,430 pound weight of the concrete samples. CIPPOC and beam samples were tested on the same equipment using the procedures outlined in Chapter 5.

The maximum recorded vibration levels during pile driving at the two test pile locations are listed in Table 6.2 by seismograph number.

Table 6.2 Maximum Recorded Vibration Levels

Location	**Maximum**	**Location**	**Maximum**
Test pile #1	**Vibration, in/s**	**Test pile #2**	**Vibration, in/s**
Unit 1	0.72	Unit 1	1.41
Unit 2	0.57	Unit 2	0.71
Unit 3	1.79	Unit 3	0.42
Unit 4	2.50	Unit 4	1.55
Unit 5	0.97	Unit 5	0.96
Unit 6	0.52	Unit 6	0.43
Unit 7	1.98	Unit 7	0.89
Unit 8	0.58	Unit 8	1.83

Noise (sound) measurements took place at the test pile locations during pile driving in October 2009. Additional background noise (sound) measurements were obtained using the Instantel Minimate seismographs on December 21, 2009 with the same orientation shown on Figure 6.3 for Test Pile #1. The maximum and minimum recorded sound levels at the 2 ½ feet above the ground surface are listed in Table 6.3. The noise (sound) data are presented in the appendix for future use by WHRP.

Table 6.3 Sound Levels at Test Site

Location	**Maximum Sound Level, pa**	**Minimum Sound Level, pa**	**Date**
Test Pile #1during driving	70.0	6.25	10/29/09
Test Pile #2 during driving	50.8	7.0	10/29/09
Test Pile #1 non-driving event	5.25	1.25	12/21/09

CHAPTER 7

7.0 DETERMINING THE QUALITY OF CONCRETE STRENGTH OF FIELD SAMPLES WITH VARIABLE CURE TIMES SUBJECTED TO PILE DRIVING INDUCED VIBRATIONS

The results of the field study are presented for concrete cylinder and beam strength compared to curing time along with vibration attenuation with distance from the source. The concrete cylinder samples will be discussed first followed by the beam samples.

7.1 CONCRETE CYLINDERS

The CIPPOC field samples (total of 72 cylinders per site = 4 cylinders x 9 blocks x 2 sites) were removed the following day and transported to the UW-Milwaukee lab where the samples in each set were broken at 1-2 days, 3-4 days, 7-8 days, and 26-28 days. Visual inspection of cylinders was documented after testing was completed. An additional 4 concrete cylinders were made from the same batch of concrete as the blocks at a location away from vibration source as a control set. Compressive strength tests were conducted on control samples to compare results, for a total of 76 concrete cylinders that were tested during the field monitoring program (4 cylinders x 9 blocks x 2 sites + 4 control). A matrix showing the number of cylinders per site is shown in Table 7.1.

Table 7.1 Concrete Cylinder Matrix per Site

Block		1	2	3	4	5	6	7	8	9
Distance (feet from pile)		10	25	50	10	25	50	10	25	50
Break Time (days)	Cylinder	Batch A10	Batch A25	Batch A50	Batch B10	Batch B25	Batch B50	Batch C10	Batch C25	Batch C50
1-2	1	1A10	1A25	1A50	1B10	1B25	1B50	1C10	1C25	1C50
3-4	2	2A10	2A25	2A50	2B10	2B25	2B50	2C10	2C25	2C50
7-8	3	3A10	3A25	3A50	3B10	3B25	3B50	3C10	3C25	3C50
28	4	4A10	4A25	4A50	4B10	4B25	4B50	4C10	4C25	4C50

The concrete strength data was determined at different cure times. The field concrete pours occurred at specific times and test samples were made based on the time of the pour. The different cure times of field samples at the time of compressive strength testing did not allow direct comparison to the laboratory compressive strength samples. There was a range in the concrete strength over time that does not appear a function of vibration magnitude or distance from the source of vibrations. The range of strength over time in this study is not expected to be greater than for a "typical" concrete operation because samples were subjected to vibrations that would not be applied to "normal" non-vibrated concrete. The data from this study indicates that the concrete gained strength faster than the strength gain for a typical concrete such as that shown in Figure 7.1. On

average, the strength gain of the CIPPOC samples was approximately 35 percent at 1 day, 55 percent at 4 days and 85 percent at 7 days. One load of concrete had a higher slump than the other two loads. The higher slump could affect results but no trend was observed for the test results from the higher slump load as presented in the next section of the report.

Recognizing that magnitude and rate of strength gain for a given concrete mix is dependent on a number of factors including water:cement ratio, entrained air content and influence of other admixtures, source and quality of aggregate and cement, and curing conditions, Figure 7.1 below is presented as a typical plot of concrete strength gain over time (Wiss, 1981).

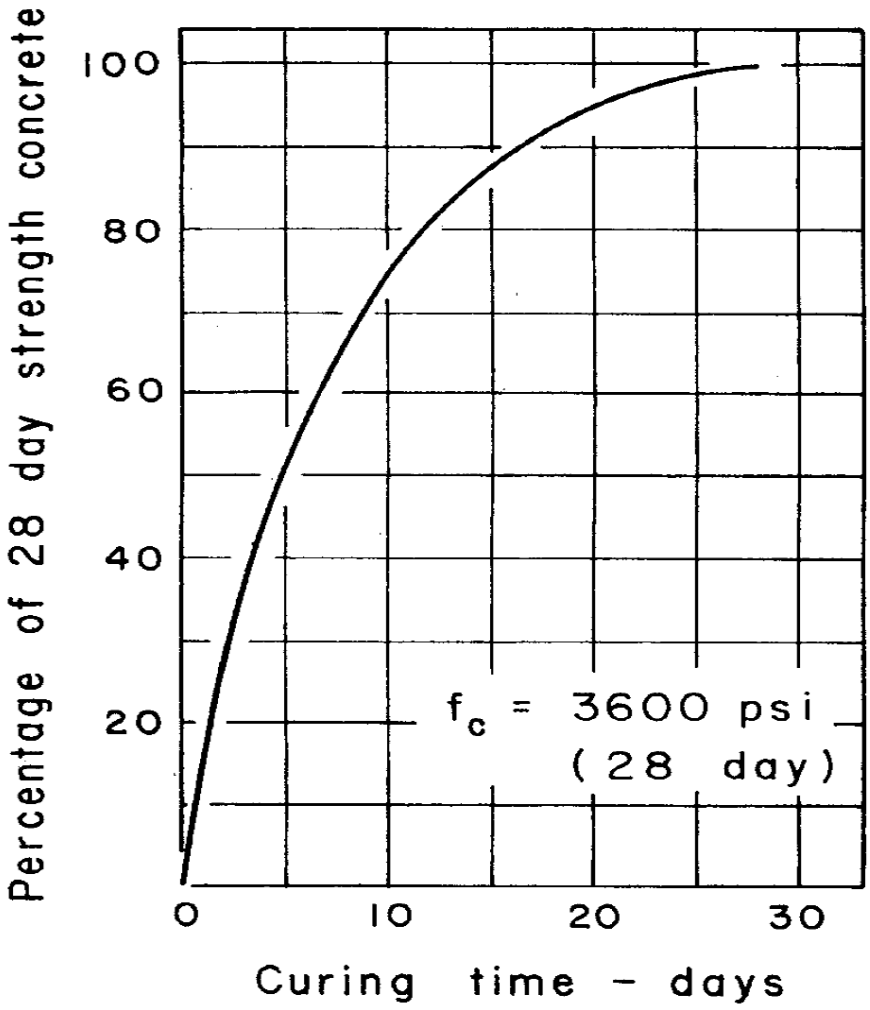

Figure 7.1 Concrete Strength versus Curing Time (Wiss, 1981)

As can be seen in Figure 7.1, approximately 51 percent of the 28-day strength occurs in the first 5 days and 62 percent of the 28-day strength occurs in the first 7 days. The concrete strength gain at early age is greater compared to the strength gain between the 14-day and 28-day cure times. In this example, the increase in strength is approximately 14 percent from 14 to 28 days.

7.0.1 CIPPOC Compressive Strength and Distance to Vibration Source for Test Pile #1

Plots were created of compressive strength compared to cure time for CIPPOC samples based on distance from the vibration source. Figure 7.2 shows CIPPOC strength data for samples based on cure time and distance from the pile driving source for Test Pile # 1.

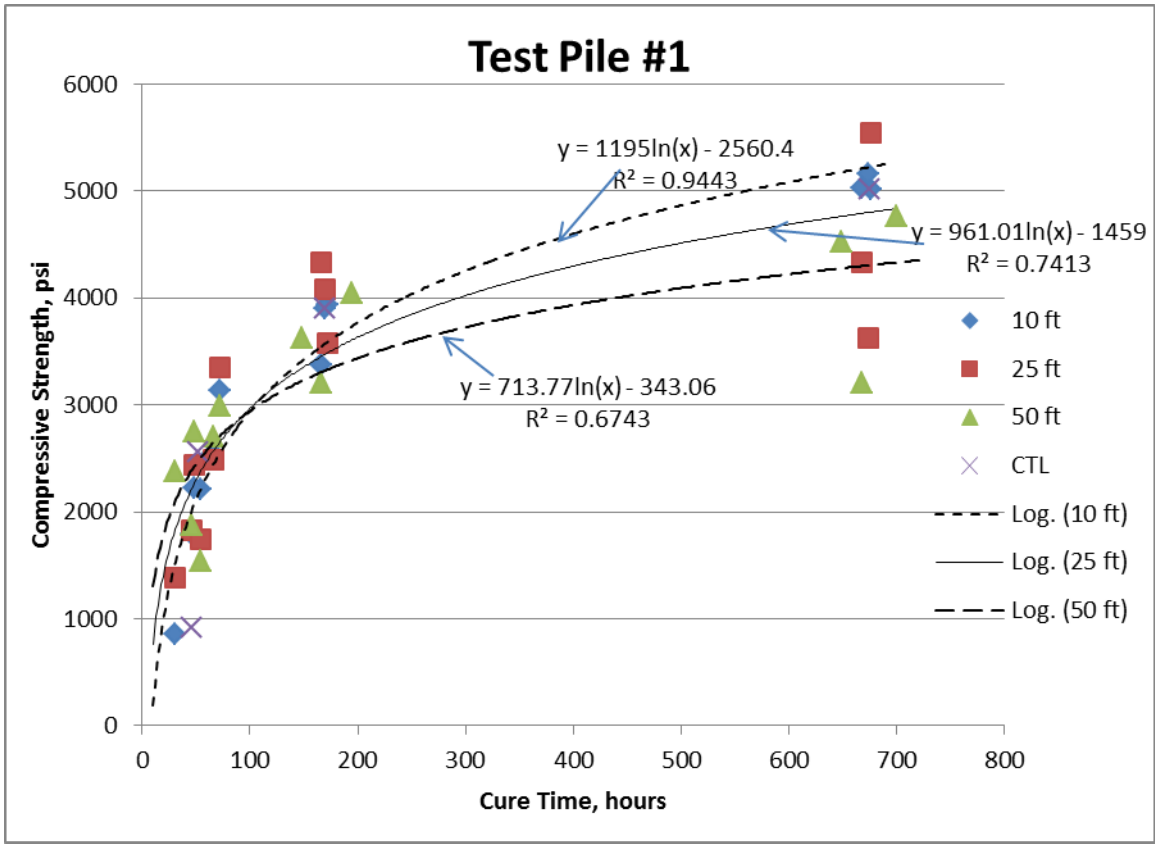

Figure 7.2 Test Pile # 1 Concrete CIPPOC Test Results

The data presented in Figure 7.2 shows that for vibrations induced during pile driving at Test Pile #1 the compressive strength increased for greater cure times, as expected. It is interesting to note that two samples with cure times near 28 days at distances of 25 and 50 feet reported compressive strengths less than the concrete mix design strength of 4,000

psi. The actual strength values of the samples were 3,200 and 3,620 psi. The 3,200 psi value is considered to be an anomaly because the remaining samples near 28-day compressive strength values ranged from 4,330 to 5,540 psi. At a distance of 50 feet where the anomalous strength value occurred, the peak particle velocity was low with a value of 0.5 inches per second (13 mm/s).

Regression equations were used in Figure 7.2. The equations shown on Figure 7.2 generally indicate that the compresive strength is greater for samples exposed to greater magnitudes of vibration, i.e. closer to the source of the vibration. The coeficient of determination (R^2) for the strength equations at distances of 10, 25, and 50 feet are variable ranging from 0.94 to 0.67. The equation for the 10-foot distance has the best R^2 value (0.94). The higher R^2 value for the equation of the compressive strength at the 10-foot distance is due to less strength variability for the different cure times compared to the values at distances of 25 and 50 feet.

7.0.2 Vibration Attenuation for Test Pile #1

Figure 7.3 presents the peak particle velocity vibration attenuation equation with distance along the ground surface for Test Pile # 1 during the pile driving events. The distance is presented in terms of scaled distance related to the pile hammer energy. Scaled distance in this case is equal to the actual distance divided by the square root of the maximum pile hammer energy measured with the PDA equipment. It is important to present the vibration attenuation data in terms of scaled distance because then the energy source is taken into account. If scaled distance was not used, the data from variable energy sources

would not be captured. A larger energy source causes a larger vibration. Historically, vibrations have been plotted against scaled distances to allow attenuation to be determined. The R^2 value for the attenuation equation is 0.94 which is good. The vector sum of the peak particle velocities were variable at the Test Pile # 1 locations ranging from approximately 2.5 to 0.5 inches per second (63.5 to 13 mm/s) for actual distances of 10 to 50 feet (scaled distances of 0.02 to 0.10), respectively as shown in Figure 7.3. Although there is no frequency associated with the Peak Vector Sum, it is always a conservative value compared to using the Peak Particle velocity measured along one of the three recording axes.

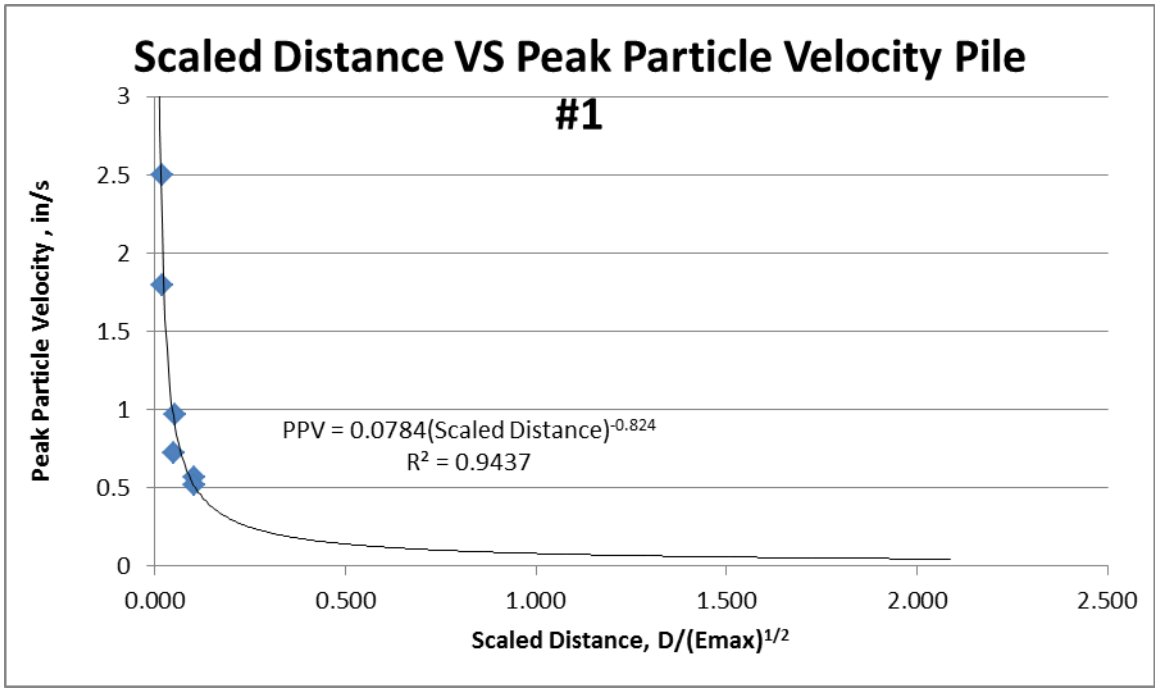

Figure 7.3 Scaled Distance versus Peak Particle Velocity at Surface for Test Pile # 1

Figure 7.4 presents the peak particle velocity vibration attenuation equation with distance for Test Pile # 1 at a depth of 10 feet below the ground surface during the pile driving

events. The distance is presented in terms of scaled distance related to the pile hammer energy. The R^2 value for the attenuation equation is 0.98 which is very good. The vector sum of the peak particle velocities were variable at this depth at the Test Pile # 1 locations ranging from approximately 2.0 to 0.4 inches per second (50 to 10 mm/s) for actual distances of 10 and 25 feet (scaled distances of 0.0 to 0.20), respectively as shown in Figure 7.4. The vibrations measured at a depth of 10 feet were less than those measured at the same distance on the ground surface. The peak particle velocities at 10 feet below grade were approximately 30 to 70 percent of the surface vibration values.

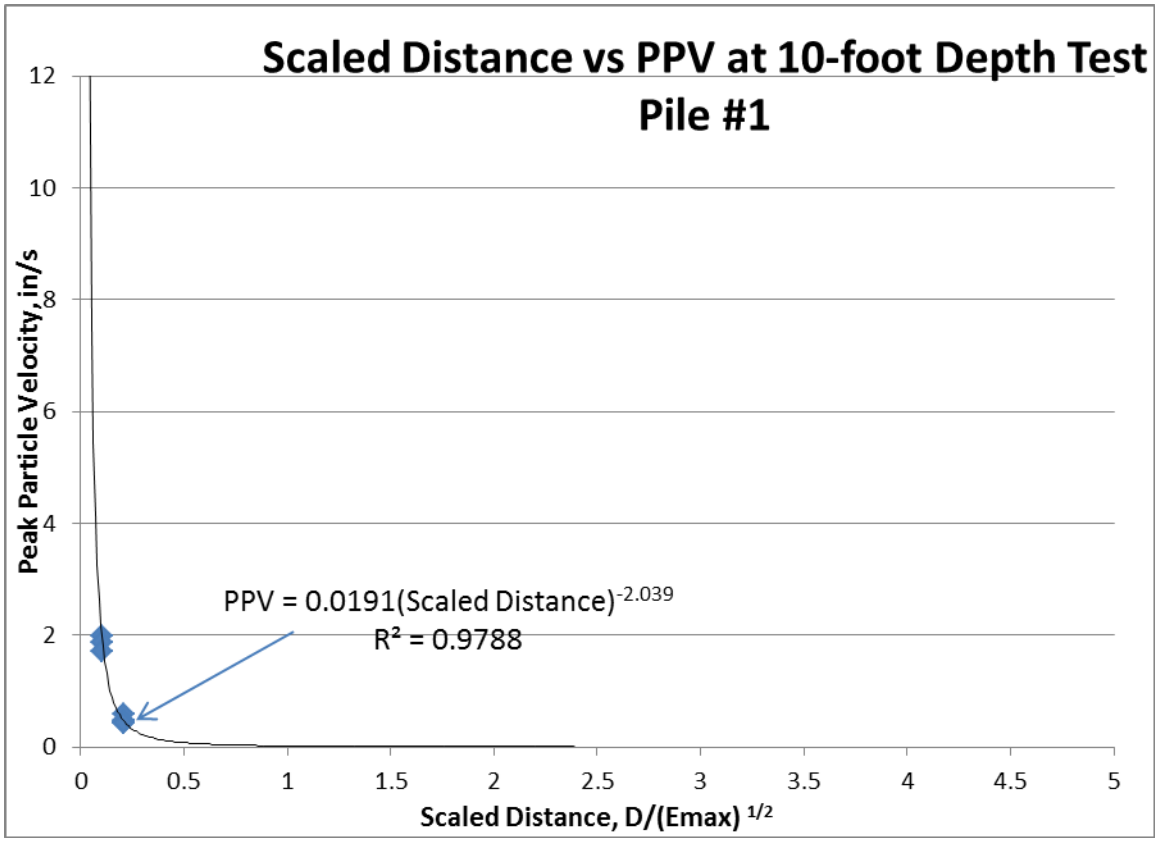

Figure 7.4 Scaled Distance versus Peak Particle Velocity at 10 feet Depth at Test Pile # 1

During pile driving, three main wave types are generated: Rayleigh waves, shear waves and compression waves. Raleigh waves are confined to a zone near the ground surface. Heckman, Richart, and others have stated that approximately 67 percent of the total energy of elastic waves is in the form of Rayleigh waves. Rayleigh waves are more damaging in nature because they attenuate more slowly than the shear and compression waves.

The soil below the ground surface is confined and vibrations are attenuated more quickly due to material damping. Hendron (1977) reported that a shotcrete tunnel liner can take a particle velocity of 36 in/s before the appearance of threshold cracking. As a result of factors such as buried structures having relatively lower vibration levels compared to surface structures, and the damping effect from confinement of buried structures that makes particle displacement more of a concern, the affect of vibration velocity levels below the ground surface on below grade structures are less of a concern than surface vibration levels.

7.0.3 CIPPOC Compressive Strength and Distance to Vibration Source for Test Pile #2

The data presented in Figure 7.5 shows that for vibrations induced during pile driving at Test Pile #2 the compressive strength increased for greater cure times, as expected. Unlike the two samples from the Test Pile # 1 location, the samples with cure times near 28 days all had compressive strengths greater than the concrete mix design strength of 4,000 psi. The sample strength values ranged from 4,160 to 5,170 psi.

Regression equations were used in Figure 7.5. The R^2 values for the equations at distances of 10, 25, and 50 feet in Figure 7.5 are variable ranging from 0.89 to 0.78. The range of R^2 values is less than that noted in Figure 7.2 but the greatest R^2 value (0.89) in Figure 7.5 is less than the greatest R^2 value (0.94) in Figure 7.2. The equation for the 25-foot distance has the best R^2 value.

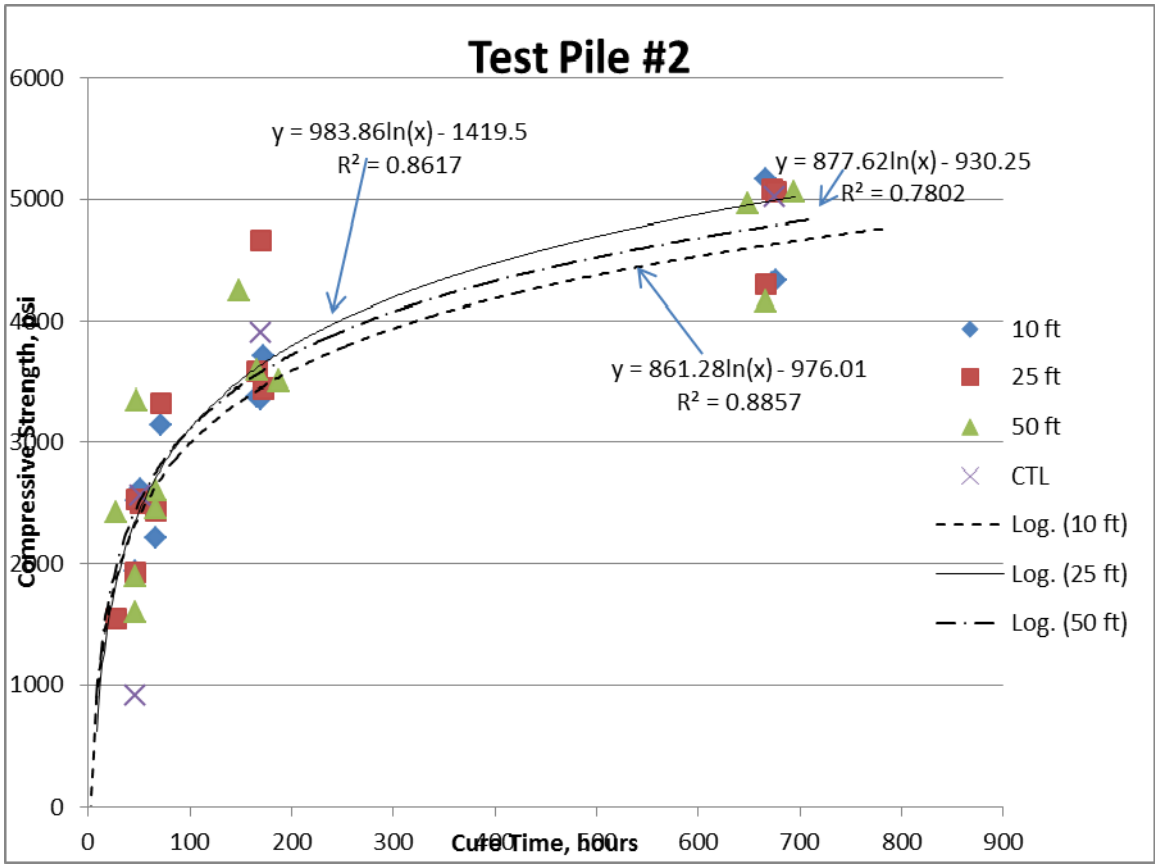

Figure 7.5 Test Pile # 2 Concrete CIPPOC Test Results

The equations for best fit lines presented on Figure 7.5 are not comparable to the equations of Figure 7.2 relative to greater strength with greater magnitude of vibration

because the samples from 25 feet shown on Figure 7.5 had greater strength with cure time than the 50 foot samples which had greater strength than the 10 foot samples. Comparing data from Figure 7.2 and Figure 7.5, there does not appear to be a noticeable correlation between compressive strength and vibration magnitude for the pile hammer utilized at the two test locations.

7.0.4 Vibration Attenuation at Test Pile #2

Figure 7.6 presents the peak particle velocity vibration attenuation equation with distance at the ground surface for Test Pile # 2 during the pile driving events. The distance is presented in terms of scaled distance related to pile hammer energy. The vector sum of the peak particle velocities were variable at Test Pile #2 and ranged from approximately 1.8 to 0.4 inches per second (46 to 10 mm/s) for actual distances of 10 to 50 feet (scaled distances of 0.02 to 0.09), respectively, from the source.

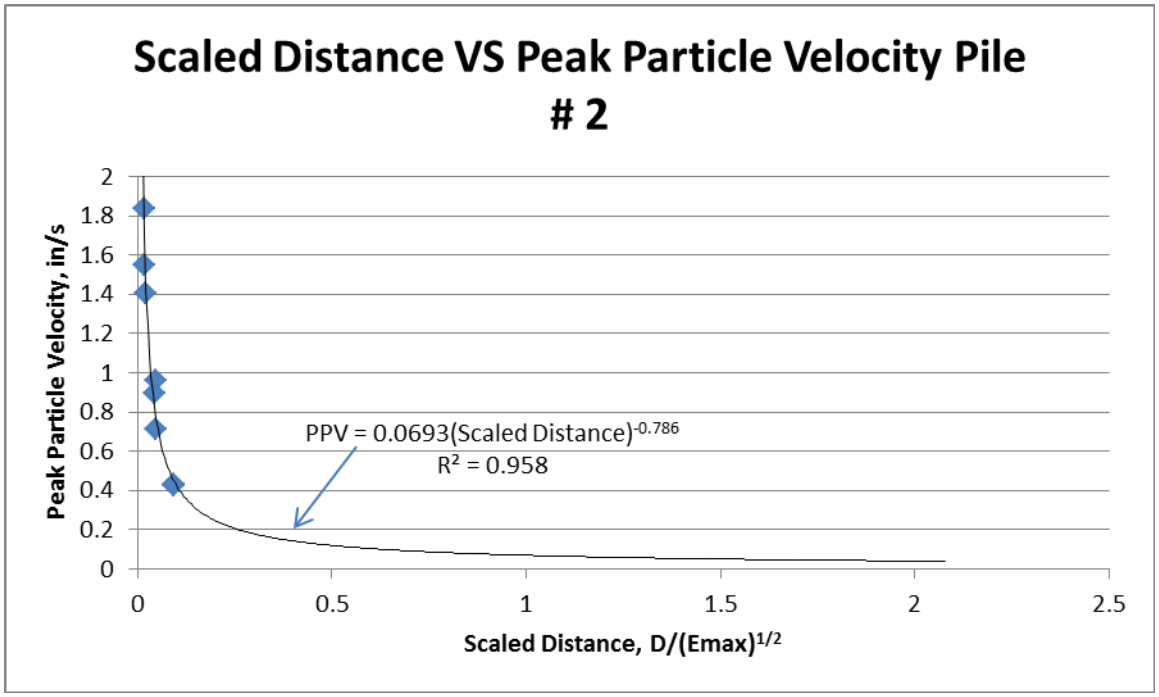

Figure 7.6 Scaled Distance versus Peak Particle Velocity at Surface at Test Pile # 2

The peak particle velocity attenuation equations presented on Figures 7.3 and 7.6 are very similar. The attenuation equation R^2 values are 0.94 and 0.96 for Test Pile # 1 and Test Pile #2, respectively. The correlation between field data and the equations is good in both figures. The equations indicate that the pile driving induced peak vector sum particle velocities range from approximately 10 ins/s to 13 in/s (250 mm/s to 330 mm/s) at a distance of 1 foot from the pile to approximately 0.26 in/s to 0.29 in/s (6.6 mm/s to 7.4 mm/s) at a distance of 100 feet for the pile hammer utilized.

7.2 VIBRATION ATTENUATION AT MARQUETTE INTERCHANGE

Vibration monitoring was performed at part of a design phase load test program during the Marquette Interchange design. The vibration data is presented in terms of distance from the pile driving source in Figure 7.7. Several items need to be discussed relative to the Marquette data. The data was collected at many locations with variable surface materials ranging from soil, concrete and asphalt pavement. Additionally, the vibration monitoring was performed at variable distances during separate pile driving events with differnet hammers using a single seismograph. Therefore, spread of the data is expected to be quite large and this is reflected in the peak particle velocity attenuation equation R^2 value. The R^2 value is 0.25 which does not indicate a good corelation between peak vector sum particle velocity and distance from the vibration source. The vibration attenuation information does indicate relatively rapid decrease in magnitude of peak particle velocity with distance.

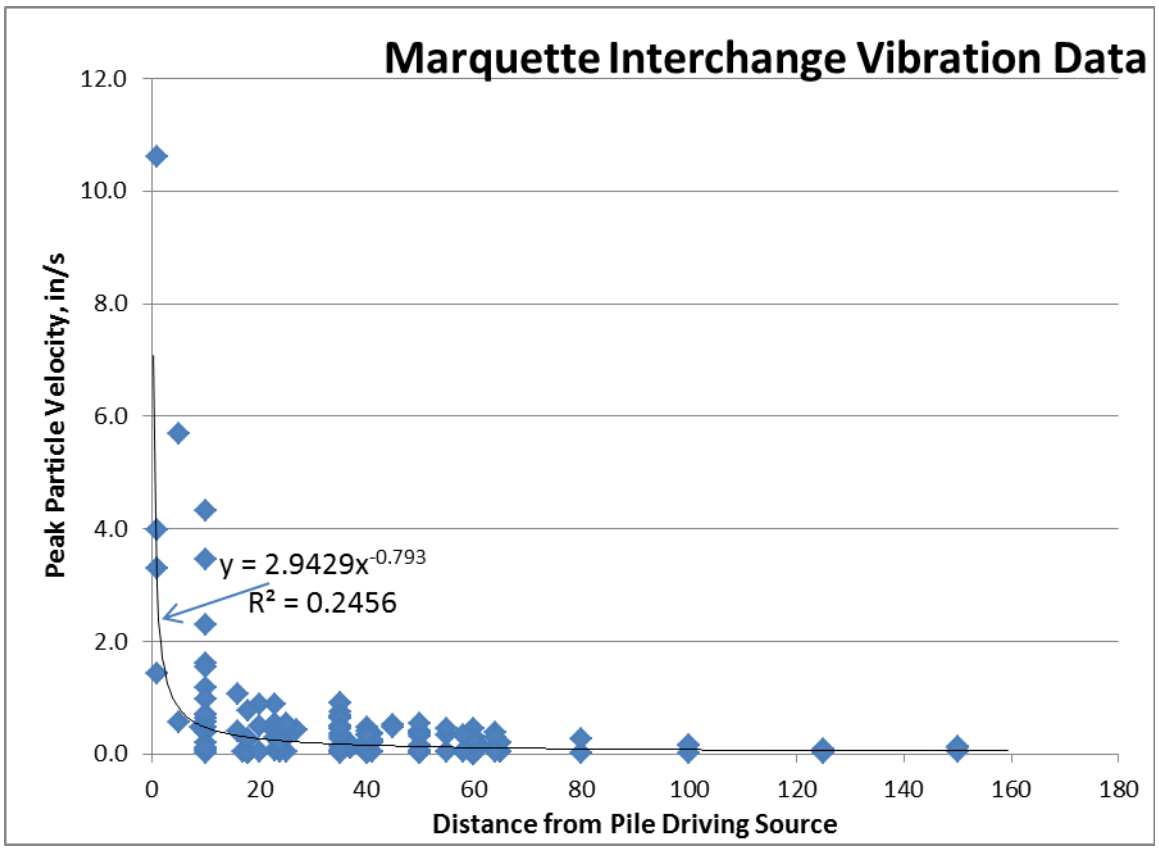

Figure 7.7 Distance versus Peak Particle Velocity From Marquette Interchange

7.3 CONCRETE BEAMS

In addition to the cylinders, two field beams (6"x6"x21") were placed in six of the blocks at the Test Pile # 1 test site and were tested for flexural strength at the UWM concrete lab. Visual inspection of field beams was documented after testing was completed. A matrix showing the number of beams is shown in Table 7.2. A total of 26 beam samples were tested (2 test sites x 6 blocks per site x 2 cure times plus 2 control samples).

Table 7.2 Concrete Beam Matrix per Site

Block		1	4	8	2	5	9
Distance (feet from pile)		10	25	50	10	25	50
Break Time (days)	Beam	Batch A10	Batch BA25	Batch A50	Batch B10	Batch B25	Batch B50
1-3	1	B1A10	B2A25	B1A50	B1B10	B1B25	B1B50
7-8	2	B2A10	B2A25	B2A50	B2B10	B2B25	B2B50

7.3.1 Beam Compressive Strength and Distance to Vibration Source for Test Pile #1

The concrete beam strength data was determined according to ASTM C78-02 at different cure times and is reported in terms of load (pounds) at time of flexural failure and modulus of rupture (psi). The field concrete placement occurred at specific times and test samples were made based on the time of the placement. The range of reported cure time of field beam samples at the time of strength testing did not allow direct comparison to the laboratory compressive strength samples. The time of field beam curing was a function of the concrete placement and included a smaller number of samples compared to the number of laboratory compressive strength samples. The lab beam samples tested were done at cure times that were different from the field cure times. Plots were created of beam strength compared to cure time for samples based on distance from the vibration

source. Figure 7.8 shows beam strength (load) data for samples based on cure time and distance from the pile driving source for Test Pile # 1. The vibration magnitude ranged from approximately 2.5 to 0.5 inches per second (63.5 to 13 mm/s) for actual distances of 10, 25 and 50 feet. The beam test results indicate that the compressive strength varied with cure time.

The R^2 values for the equations at distances of 10, 25, and 50 feet in Figure 7.8 are variable ranging from 0.60 to 0.68. The equation for the 10 foot distance has the best R^2 value (0.68). Some of the beam samples required more effort to remove the molds from the concrete blocks than the CIPPOC samples. Considering the generally lower R^2 values in Figure 7.8 compared to the CIPPOC test results (Figure 7.2), it's possible that sample disturbance may have affected some of the results.

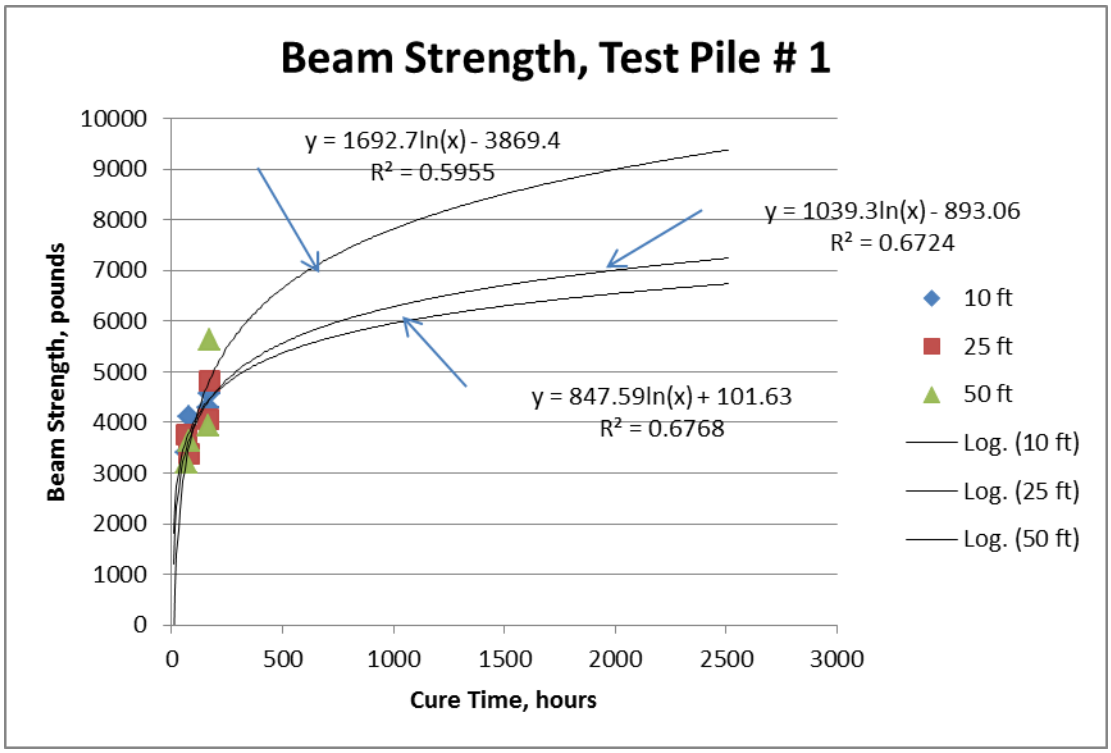

Figure 7.8 Beam Strength Results for Test Pile # 1

7.3.2 Beam Compressive Strength and Distance to Vibration Source for Test Pile #2

Figure 7.9 shows beam strength data for samples based on cure time and distance from the pile driving source for Test Pile # 2. The vibration magnitude ranged from approximately 1.8 inches/second to 0.4 inches per second (46 to 10 mm/s) for actual distances of 10, 25, and 50 feet. The beam test results indicate that the compressive strength was variable ranging from 3,500 to 4650 pounds.

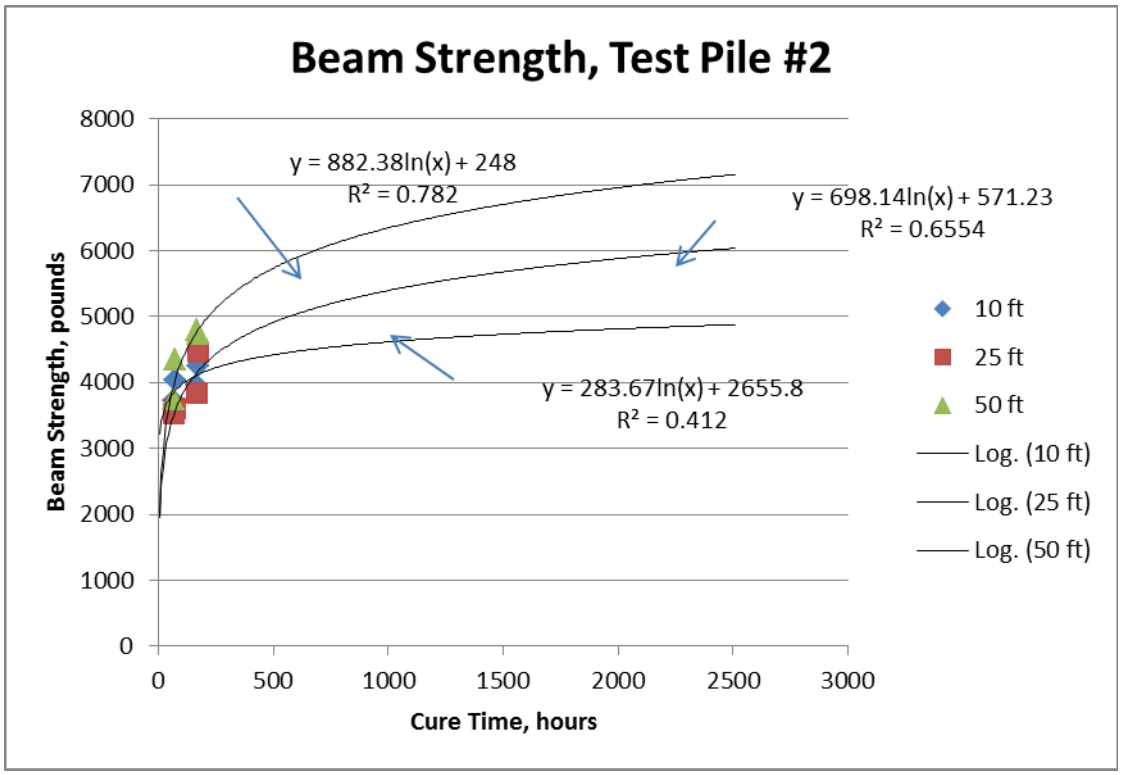

Figure 7.9 Beam Strength Results for Test Pile # 2

The R^2 values for the equations at distances of 10, 25, and 50 feet in Figure 7.9 ranged from 0.78 to 0.41. The range of R^2 values in Figure 7.8 is greater than that noted in Figure 7.7. The equation for the 50 foot distance has the best R^2 value (0.78). Some of

the beam samples required more effort to remove the molds from the concrete blocks than the CIPPOC samples. Considering the generally lower R^2 values in Figure 7.9 compared to the CIPPOC test values (Figure 7.5), it's possible that sample disturbance may have affected some of the results.

7.3.3 Concrete Beam Modulus of Rupture Data

The load values that broke the beam samples were used to calculate modulus of rupture values for the beams. The data are presented in Table 7.3.

Table 7.3 – Concrete Beam Modulus of Rupture Data

Test Pile Location	Concrete Block #	Beam #	Approximate Distance From Vibration Source, ft	Modulus of Rupture, psi	Cure Time, hours
1	1	1	9	470	76
1	2	1	8 ½	380	70
1	4	1	23 ½	440	76
1	5	1	24 ½	400	70
1	8	1	49	350	70
1	9	1	49	410	76
1	1	2	9	500	172
1	2	2	8 ½	470	166
1	4	2	24	510	172
1	5	2	24 ½	420	166

1	8	2	49	420	166
1	9	2	49	590	172
2	1	1	9	470	76
2	2	1	9	390	70
2	4	1	24	410	76
2	5	1	24	370	70
2	8	1	49	390	70
2	9	1	49	470	76
2	1	2	9	470	172
2	2	2	9	400	166
2	4	2	24	490	172
2	5	2	24	400	166
2	8	2	49	530	166
2	9	2	49	550	172

The modulus of rupture data did not indicate consistently higher values with closeness or distance from the vibration source. Also the results indicate modulus values that are similar for the 3 and 7 day cure times.

In Figure 7.10, the load at failure of the concrete beams at Test Pile #1 location were converted to values of compressive strength of concrete cylinders (f'cc) using the following equation and assuming that the compressive strength determined from concrete

beams at the test pile locations were identical to the point load index (I_s) in the equation from Zacoeb and Ishibashi, (2009):

$$f'cc=22.3\ I_s-22.0$$

By converting the compressive strength of concrete beams, the data could be compared directly with those from the CIPPOCS. As expected, the compressive strength of concrete cylinders and beams increase with the cure time. The compressive strength increases at a faster rate up to 8 days for the beams and CIPPOCS. After 8 days to 28 days the strength gain for the CIPPOCS was less than over the first 8 days.

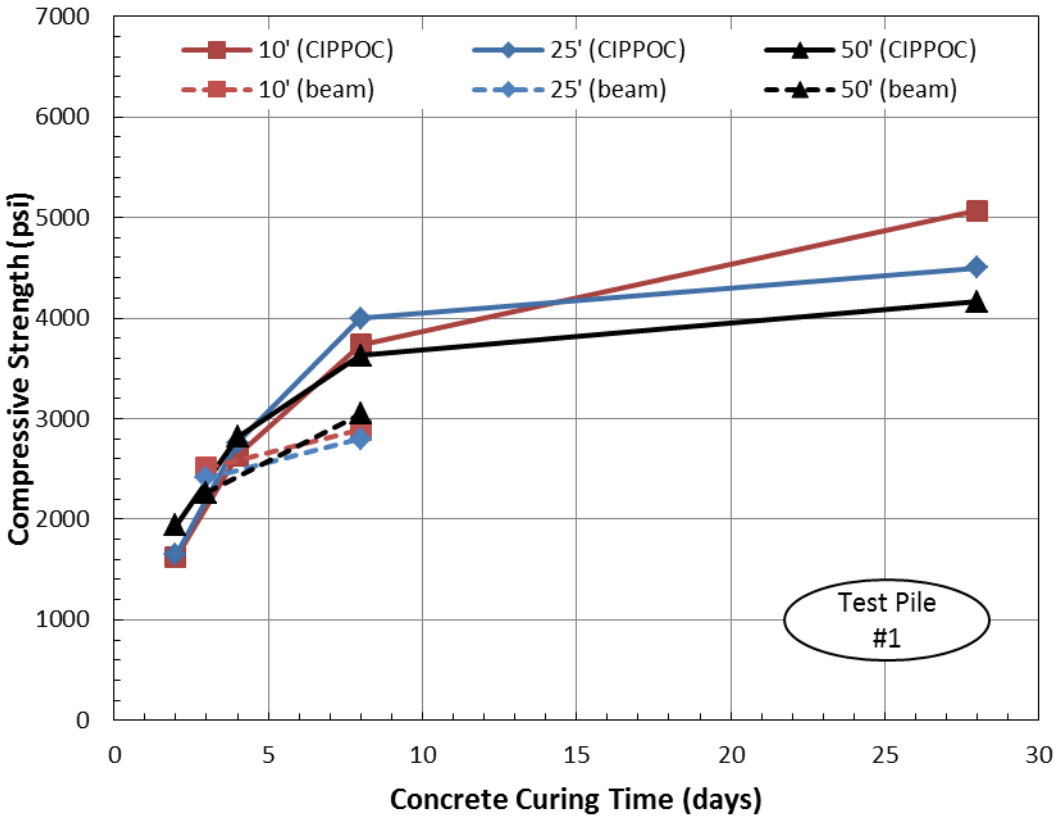

Figure 7.10 Beam and CIPPOC Strength versus Curing Time at Test Pile #1

The data in the figure also indicates that the initial data points less than 5 days old for both beams and CIPPOCS have comparable compressive strength. Beyond that time frame, the beam compressive strength is less than the CIPPOCS. Based on the 28-day CIPPOC data points and assuming a similar trend for beam specimens, it is expected that the beam strength regardless of distance from the vibration source at 28 days would increase to an acceptable value.

In Figure 7.11, the load at failure of the concrete beams at Test Pile # 2 location were converted to values of compressive strength of concrete cylinders (f'_{cc}) with the same equation used for Figure 7.10. By converting the compressive strength of concrete beams, the data could be compared directly with those from the CIPPOCS. As expected, the compressive strength of concrete cylinders and beams increase with the cure time. The compressive strength increases at a faster rate up to 8 days for the beams and CIPPOCS. After 8 days to 28 days the strength gain for the CIPPOCS was less than over the first 8 days.

The data in the figure shows that the initial data points less than 5 days old for both beams and CIPPOCS have comparable compressive strength. Beyond that time frame, the beam compressive strength is less than the CIPPOCS. Based on the 28-day CIPPOC data points and assuming a similar trend for beam specimens, it is expected that the beam strength regardless of distance from the vibration source at 28 days would increase to an acceptable value.

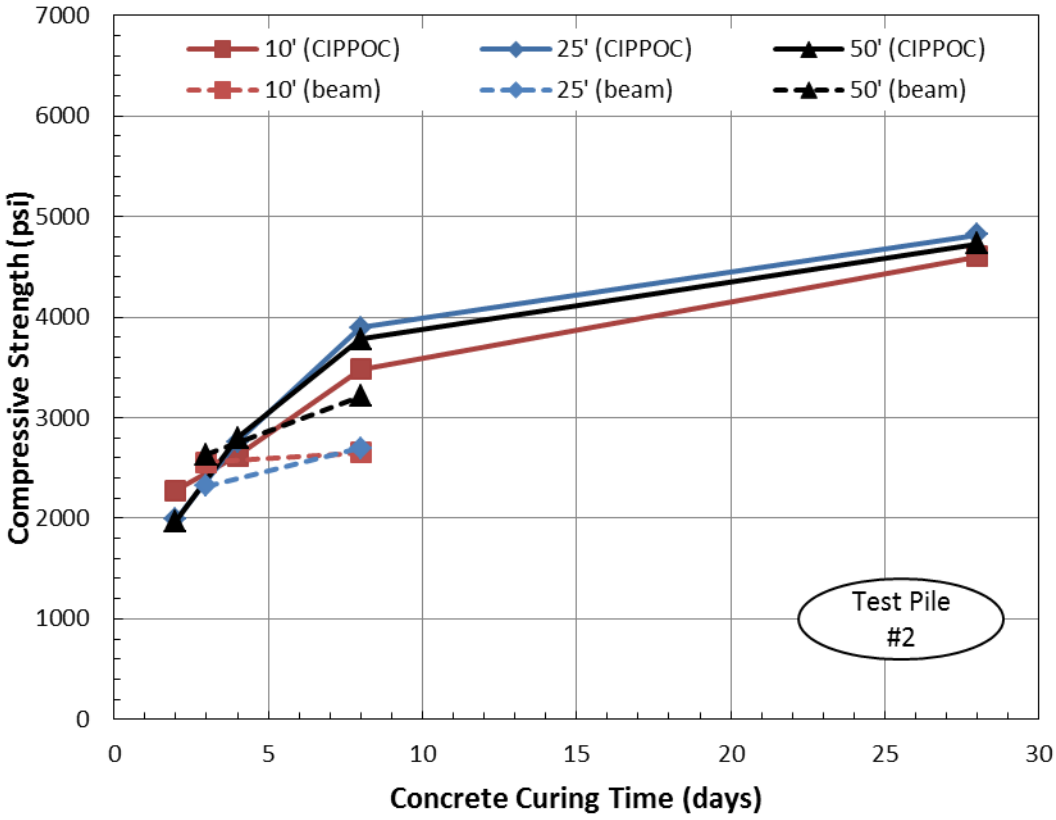

Figure 7.11 Beam and CIPPOC Strength versus Curing Time at Test Pile #2

CHAPTER 8

8.0 SUMMARY AND CONCLUSIONS

This research was carried out to investigate the attenuation of potentially-damaging pile driving vibrations with distance and depth and to investigate the effects of distance and age on the quality (strength) of concrete exposed to pile driving vibrations. Finite element analysis modeling was performed on varying pile sizes, pile types, and hammers. The finite element results were compared with common empirical equations used for vibration predictions and with a limited number of field tests that include vibration measurements. To investigate the effects of distance and age on the quality of concrete exposed to various levels of vibration, a comprehensive laboratory testing program on cylindrical concrete samples subjected to various peak particle velocities was carried out.

The finite element method provides a versatile means to calculate ground surface vibrations caused by pile driving. In Chapter 4, simple numerical models were used to calculate the ground surface vibrations in a two-layer soil system with a concrete-filled pipe pile (case study I) and a one-layer soil system with a steel casing (case study II). The finite element results of the two case studies were compared with field measurements showing that the finite element method is capable of simulating the complicated soil-pile-hammer interaction. Furthermore, analytical and semi-empirical equations (e.g., Wiss 1981) have many limitations such as not being able to consider soil stiffness, soil stratification, source frequency, soil-pile interface properties (i.e., friction and cohesion), and not being able to predict the frequency of ground surface vibration at a given distance

from the vibration source (pile). Many of these limitations are effectively considered in careful finite element analyses such as those presented above.

Ninety 12-inch laboratory concrete cylinders and thirty six laboratory beams were subjected to various levels of vibration at various cure times prior to the excitation. Each specimen was subjected to 15 minutes of vibration with 20-Hz frequency and specific amplitude ranging from 0.5 inch/s to 20 inch/s. In general, vibration level and cure time had negligible effects on stiffness and strength of the concrete specimens that were tested for stiffness and strength at 3 days, 7 days, and 28 days. It was noted that the strength of the beam specimens vibrated at very early age (4-6 hours cure time) was substantially smaller than the 3-days average strength of the control beam specimens. Also, the strengths of these specimens were significantly affected by the PPV.

Seventy two field CIPPOC's and twenty four field beams were subjected to vibrations from a Vulcan #8 pile driving hammer at various cure times prior to the excitation. Two 12 ¾-inch inside diameter test piles were driven into the ground during the field study and encountered hard driving resulting in variable vibration levels at distances from the piles. Vibrations were measured using geophones on the ground surface and at a depth of approximately 10 feet below the surface. The driving occurred over an approximate 15 minute time frame with variable frequencies generally ranging from 10 to 50 Hz with some lower and higher frequencies at times. The peak particle velocities measured were in the range of 0.05 to 2.24 in/s (1.3 to 57.0 mm/s). The peak particle velocities at 10 feet below grade were approximately 30 to 70 percent of the surface vibration values. For

this study, vibration level and cure time generally had negligible effects on the compressive strength of the concrete specimens that were tested at 3 days, 7 days, and 28 days. The field data exhibited more data variability than the laboratory data.

The concrete mix design has a strength value of 4,000 pounds per square inch (psi). The field study test data indicated that all but one of the A-FA concrete samples attained the strength value regardless of the level of vibration and distance from the source.

The WisDOT practice (Standard Specification Section 510.3.4) for cast in place pipe pile driving activities does not allow the contractor to drive pile shells within a 15-foot radius of any concrete filled shell until the concrete cures for at least 7 days (3 days if high early strength concrete). However, for concrete grades A-FA (used in this study), A-S, A-T, A-IS, or A-IP concrete in the work, where field operations are not controlled by cylinder tests, then the curing time is increased to 14 days. If field operations are controlled using concrete cylinder tests, shell driving can proceed with the engineer's approval when cylinder test results show a compressive strength of not less than 2,500 pounds per square inch, as specified under falsework removal in the Wisconsin Department of Transportation Standard Specifications for Highway and Structure Construction, Section 502.3.4.2.

Based on the results of this study and others, the WisDOT cast in place pipe pile driving requirements appear to be too stringent with respect to construction vibration influence on concrete compressive strength. Based on the study, the distance could be reduced to

10 feet and the curing time could be reduced to 5 days, if desired. The specification could be modified to read;

"Cast in place pipe pile driving activities shall not occur within a 10-foot radius of any concrete filled shell until the concrete cures for at least 5 days (1 day for high early strength concrete). However, for concrete grades A-FA, A-S, A-T, A-IS, or A-IP concrete in the work, where field operations are not controlled by cylinder tests, then the curing time is increased to 7 days. If field operations are controlled using concrete cylinder tests, shell driving within a 10 foot distance can proceed with the engineer's approval when cylinder test results show a compressive strength of not less than 2,500 pounds per square inch."

8.1 RECOMMENDATIONS FOR FURTHER STUDY

Pile driving vibrations have the potential to affect early age concrete as well as induce damage to nearby existing structures. The effect on existing structures can be due to vibration caused cracking of construction materials and structure settlement due to vibration induced densification or consolidation of soil supporting the structures. From the WisDOT perspective where the majority of highway structures are pile supported, the immediate concern is potential damage to adjacent offsite construction. The effect can be more pronounced where structures are supported by shallow spread footings. Preconstruction surveys and detailed documentation of pre- and post-pile driving structure condition is beneficial in this regard. However, potential problems are typically a human perception issue. The human body can detect very low levels of

vibration. Vibration levels that would be safe from a structure performance standpoint would be considered unpleasant, annoying, or intolerable by individuals.

This study had relatively narrow focus due to site and budgetary constraints. Several items of additional study should be considered for future research efforts. A more detailed discussion of the items for further study is presented after the list The list of future vibration studies includes:

1. Pile driving vibration related settlement in soil profiles
2 Freeze-thaw effect on early age concrete after pile driving
3. Microstructure inspection of concrete and air voids of concrete
4. Durability, workability and other concrete strength properties for different curing times and vibrations
5. Test other concrete mixes (e.g. different admixtures such as mid-range and high range water reducers, silica fume, corrosion inhibitors, etc) and types of concrete mixes (e.g. high early strength, CLSM, cellular foamed concrete, etc)
6. Determine if a maturity meter application can reliably be used to develop a reliable correlations related to concrete strength subjected to vibrations
7. Shear bond strength for reinforcing steel

The settlement caused by non-steady state pile diving vibrations can be an area of additional study. Loose or soft soils don't typically transmit vibrations as well as dense or stiff soils but are more susceptible to densification or consolidation. This type of study would need to evaluate settlement away from driven piles in different known soil types.

A large transportation project in an urban environment would be well suited to this research. Consideration should be given to also measure displacement in addition to peak particle velocity. Project plans would need to identify the research so contractors are aware and required to accommodate the effort.

Concrete is susceptible to freeze-thaw degradation. Entrained air is typically specified to reduce this effect. Vibration can reduce air voids and aggravate freeze-thaw issues. Additional testing can be performed both in the field and laboratory to determine the effect on freeze-thaw degradation. Simulating rapid freeze-thaw conditions according to ASTM 666-03 should be evaluated.

Microscopic evaluation of concrete structure and air voids is an item of interest. Vibration does affect concrete and this can be studied using a relatively small field and laboratory study. Concrete samples can be cut in horizontal slices to inspect segregation at the top, middle, and bottom of the cylinders to determine if there is an effect. Petrographic analyses of samples should be considered to provide detailed information on the concrete condition.

Concrete durability is needed for structure performance and vibration generally improves concrete durability by increasing density and compressive strength provided air entrainment is adequate. Lightweight cellular foamed concrete has been used as backfill on DOT projects in the past because it results in little to no additional vertical or lateral load on soil after setting in areas where ground surface settlement can cause problems.

However, this material can be negatively affected by vibration resulting in increased weight and corresponding increased settlement of supporting soil. Testing can also be performed on concrete mixes with additives, high early strength concrete, and Controlled Low Strength Material (CLSM). WisDOT likely has already performed much testing on concrete but additional laboratory study of WisDOT concrete mix designs including these suggested mixes/material should be done at variable vibration levels to see if there is an optimum level and time of vibration. This testing could help provide data useful to structure performance and may reduce time of construction.

WisDOT is using maturity meter evaluation of concrete on certain projects and as part of the Quality Management Program. Maturity meter application and correlation could be used to evaluate concrete strength subjected to vibrations. Field and laboratory study could be performed with relatively low cost. This should be considered because it is expected that maturity meter testing will increase over time.

REFERENCES

1. ASCE (1993). *Design of Pile Foundations* (Technical Engineering and Design Guides as adapted from the U.S. Army Corps of Engineers engineering manual, EM 1110-2-2906. American Society of Civil Engineers.
2. ASCE (1984). *Practical Guidelines for the Selection, Design and Installation of Piles.* American Society of Civil Engineers.
3. Ashraf, S., Jayakumaran, S., and Chen, L. (2002). "Case History: Pile Driving and Vibration Monitoring for Avenue P Bridge in Brooklyn, New York", *Proceedings of the International Deep Foundations Congress 2002*, ASCE Geo-Institute, 500-509.
4. Attwell, P.B. and Farmer, I.W. (1973). "Attenuation of Ground Vibrations from Pile Driving", *Ground Engineering*, Vol. 6, 26-29.
5. Bastian, C.E, (1970). "The Effect of Vibrations on Freshly Poured Concrete", Raymond Pile Magazine, Vol. 6, No. 1, 14-17.
6. CTC and Associates (2003). "Construction Vibration and Historic Buildings", WisDOT RD&T Transportation Synthesis Report prepared for Bureau of Environment, Division of Transportation Infrastructure Development.
7. D'Appolonia, (1969). "Effects of Foundation Construction on Nearby Structures", *Proceedings, Third Pan American Soil Mechanics and Foundations Conference*, San Juan, Puerto Rico,
8. Dowding, C. (2000). *Construction Vibrations,* Prentice Hall, Inc. Upper Saddle River New Jersey, 610 pages.

9. Drabkin, S. and Lacy, H. (1998). "Prediction of Settlements of Structures due to Pile Driving." *Geotechnical Earthquake Engineering and Soil Dynamics III, ASCE Special Publication No. 75,* pp 1496-1506.
10. Drabkin, S. and Lacy, H. (1996). Estimating Settlement of Sand Caused by Construction Vibration.
11. Hadjuk et al. (2004). Pile Driving Vibration Energy-Attenuation Relationships in the Charleston, South Carolina Area.
12. Hannigan, P., Goble, G., Likins, G., and Rausche, F., (2006). Design and Construction of Driven Pile Foundations – Volume I and II FHWA - NHI-05-042
13. Heckmand, W.S. and Hagerty, D.J. (1978). "Vibrations Associated with Pile Driving", *Journal of the Construction Division*, ASCE, Vol. 104, No. CO4, Proc Paper 14205, pp 385-394.
14. Hendriks, R. (2002). "Transportation Related Earthborne Vibrations (Caltrans Experiences)", Technical Advisory, Vibration, TAV 02-01-R9601, California Department of Transportation.
15. Hendron, A.J. (1977). "Engineering of Rock Blasting on Civil Projects. Structural and Geotechnical Mechanics (W. J. Hall, Editor), Prentice-Hall.
16. Holloway, D.M et al. (1980). "Field Study of Pile Driving Effects on Nearby Structures." *Special Technical Publication, Minimizing Detrimental Construction Vibrations*, Preprint 80-175, pp. 63-100.
17. Hulshizer, A. J., (1996). "Acceptable Shock and Vibration Limits for Freshly Placed and Maturing Concrete." ACI Materials Journal, 93-M59.
18. Hunaidi (2000). Traffic Vibration in Buildings.

19. Hwang, J., Liang, N., and Chen, C. (2001). "Ground Response during Pile Driving." *Journal of Geotechnical and Geoenvironmental Engineering,* Vol. 127, No. 11, pp. 939-949.

20. Issa (1998). Construction Loads and Vibrations.

21. Klieger, P., and Lamond, J.F. (1994). *ASTM STP 169C, Significance of Tests and Properties of Concrete and concrete-Making Materials,* American Society for Testing and Materials.

22. Konya, C., and Walter, E. (1991). "Rock Blasting and Overbreak Control" FHWA - HI-92-001

23. Kiker, J. (1998). "Blasting a Breach in an Old Concrete Dam to Channel Water into a New Powerplant." *Geotechnical Earthquake Engineering and Soil Dynamics III, ASCE Special Publication No. 75,* pp. 1540-1560.

24. Kim, D. et al. (1994). "Prediction of Low Level Vibration Induced Settlement." *Vertical and Horizontal Deformations of Foundations and Embankments*, *ASCE Geotechnical Special Publication No. 40*, pp. 806-817.

25. Kim, D. and Drabkin, S. (1995). "Investigation of Vibration-Induced Settlement Using Multifactorial Experimental Design." *ASTM Geotechnical Testing Journal*, Vol 18, Issue 4, pp. 463-471.

26. Kim, D. and Lee, J. (1998). "Source and Attenuation Characteristics of Various Ground Vibrations." *Geotechnical Earthquake Engineering and Soil Dynamics III, ASCE Special Publication No. 75,* pp. 1507-1517.

27. Lacy, H.S. and Gould, J.P. (1985). "Settlement from Pile Driving in Sands", *Geotechnical Proceedings – Vibrations Problems in Geotechnical Engineering*, Detroit, Michigan, ASCE pp 152-173.
28. Massarsch, K.R. (2000). "Settlements and Damage Caused By Construction-Induced Vibrations" 1-17.
29. Milwaukee Transportation Partners (2003b). "Core Investigation Report, Marquette Interchange Project, Project ID 1060-05-03."
30. Milwaukee Transportation Partners (2004a). "Geotechnical Exploration Data Report."
31. Milwaukee Transportation Partners (2004d). "Pile Test Program Data Report."
32. Mindness, S., and Young, J.F. (1981). *Concrete,* Prentice-Hall.
33. Nichols, H., Johnson, C., and Duvall, W., (1971). "Blasting Vibration and their Effects on Structures, Bulletin 656", USBM.
34. Oriard, L.L., (1999). *The Effects of Vibrations and Environmental Forces: A Guide for the Investigation of Structures*, International Society of Explosives Engineers.
35. Ramshaw, C. Selby, A., and Bettess, P. (1998). "Computed Ground Waves due to Pile Driving." *Geotechnical Earthquake Engineering and Soil Dynamics III, ASCE Special Publication No. 75,* pp. 1484-1495.
36. Reddy, D.V., Tawfiq, K., and Putcha, S. (2000). "Effects of Vibration and Sound During the Installation of Deep Foundations", Florida Department of Transportation
37. Richart, F.E., Hall, J.R. and Woods, R.D. (1970). *Vibration of Soils and Foundations,* Prentice Hall.

38. Scott, G. and Hinchliff, D. (1998). "Blasting In and Adjacent to Concrete Buffalo Bill Dam." *Geotechnical Earthquake Engineering and Soil Dynamics III, ASCE Special Publication No. 75,* pp. 1530-1539.

39. Siskind, D., Stagg, M., Kopp J., Dowding, C., (1980). "Structure Response and Damage Produced byGround Vibrations from Surface Mine Blasting", Bulletin 8507", USBM.

40. Siwula, J.M., Rudig, D.A., and Powell, B.L. (2005). "A Case Study: Vibrations Recorded During Pile Driving Operations for a Design Phase Pile Load Test Program".

41. Svinkin (2004). Minimizing Construction Vibration Effects.

42. Tawfiq, K., and Abichou, T. (2003). "Effect of Vibration on Concrete Strength During Foundation Construction." Florida Department of Transportation.

43. Winterkorn, H.F., and Fang, H.Y. (1975). *Foundation Engineering Handbook.* Van Nostrand Reinhold Company.

44. WisDOT (2011). *Standard Specifications for Highway and Structure Construction.*

45. WisDOT (2007). *WisDOT Bridge Manual.*

46. WisDOT (2005). *WisDOT Facilities Development Manual.*

47. Wiss, J.F. (1981). "Construction Vibrations: State –of-the-Art." *Journal of the Geotechnical Division*, ASCE Vol. 94 No. 9, 167-181

48. Wiss, J.F. (1974). "Vibrations During Construction Operations", *Journal of the Construction Division*, ASCE, Vol. 100, No. CO3, 239-249

49. Wiss, J.F. (1968). "Effects of Blasting Vibrations on Buildings and People", *Civil Engineering Magazine*, ASCE, July, 46-48.

50. Woods, R.D. (1997). “Dynamic Effects of Pile Installations on Adjacent Structures.” *NCHRP Synthesis of Highway Practice 253.* National Cooperative Highway Research Program.

51. Zacoeb, A., and Ishibashi, K., (2009). “Point Load Test Application for Estimating Compressive Strength of Concrete Structures from Small Core”, *Journal of Engineering and Applied Sciences,* ARPN, Vol. 4 No.7, 46-56

APPENDIX A

Laboratory Concrete Cylinder and Beam Strength Data

1.

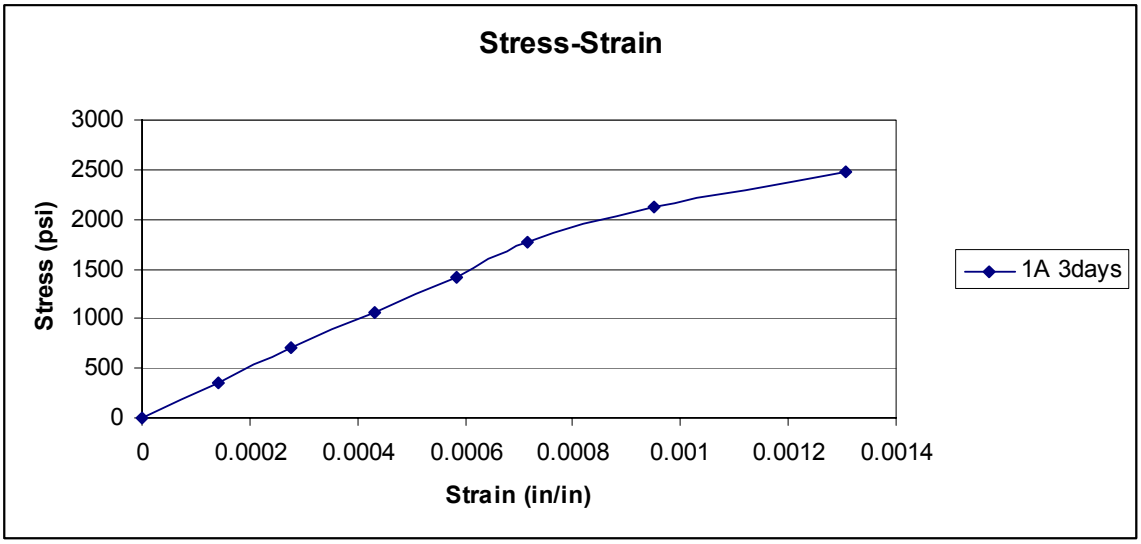

Figure 1 Stress & strain curve- Cylinder 1A at 3 Days

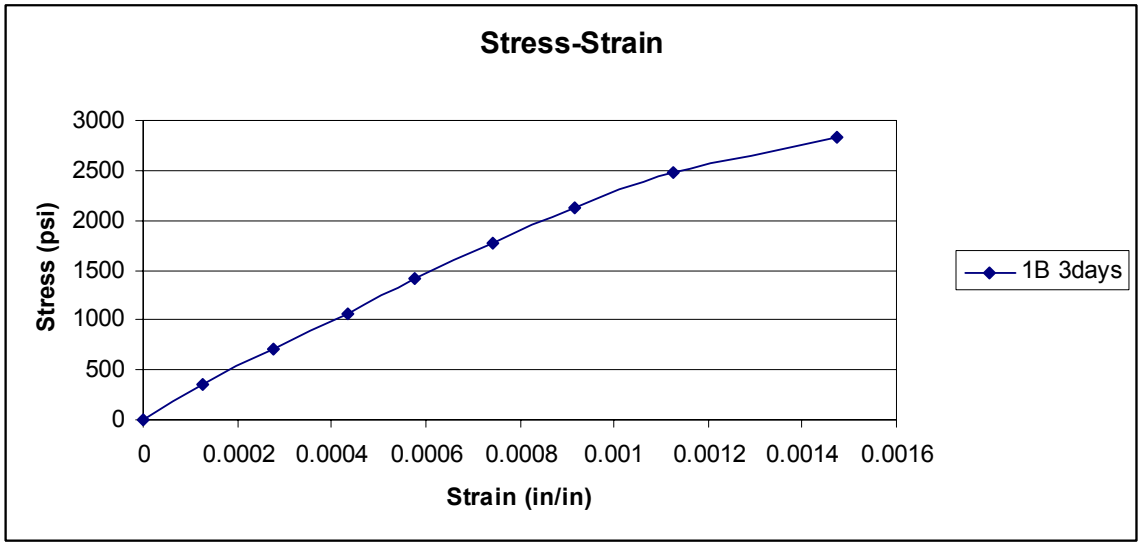

Figure 2 Stress & strain curve-Cylinder 1B at 3Days

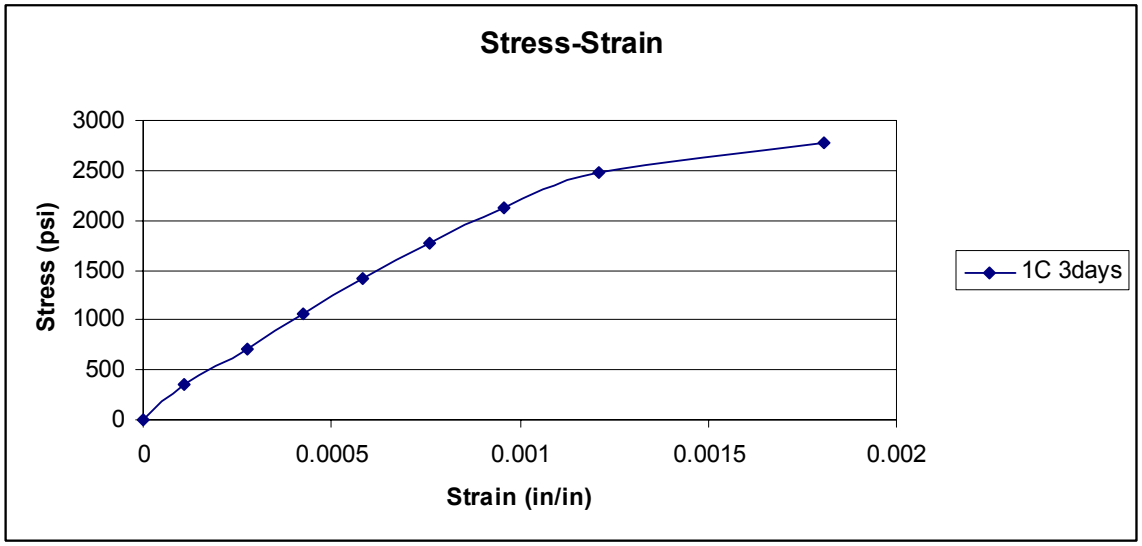

Figure 3 Stress & strain curve- Cylinder 1C at 3 Days

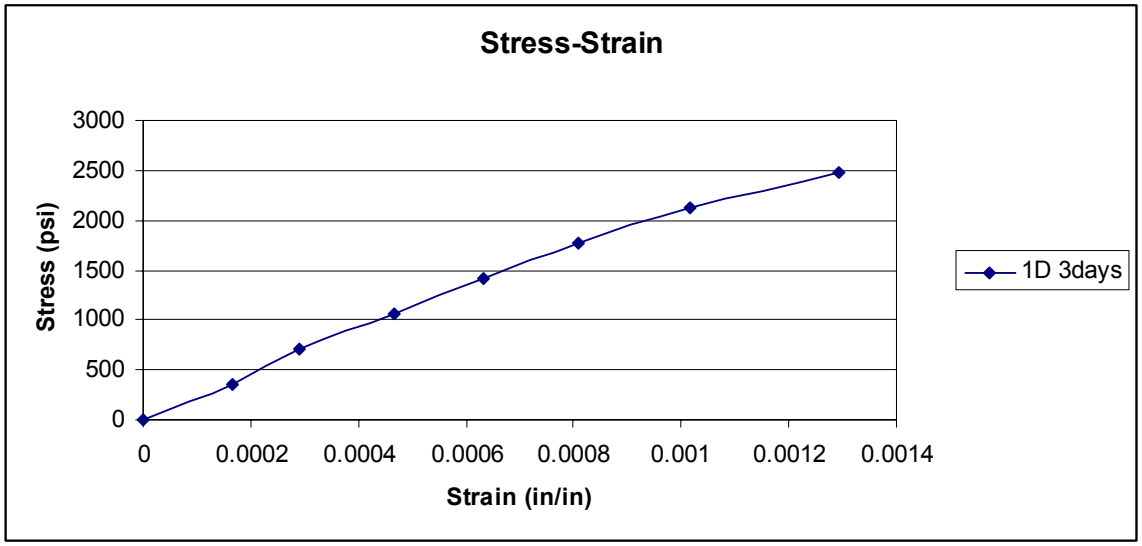

Figure 4 Stress & strain curve- Cylinder 1D at 3 Days

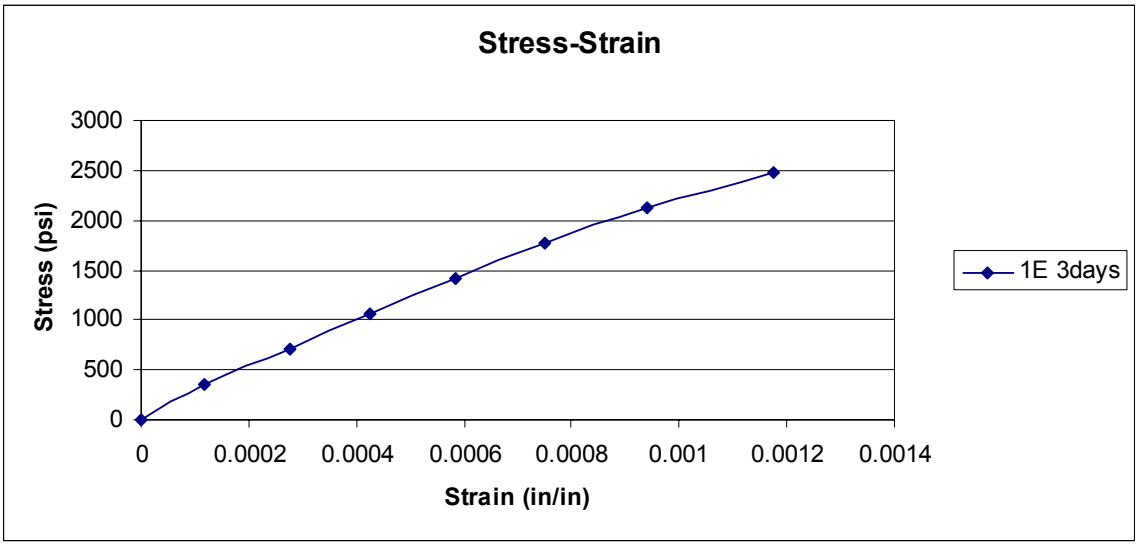

Figure 5 Stress & strain curve- Cylinder 1E at 3 Days

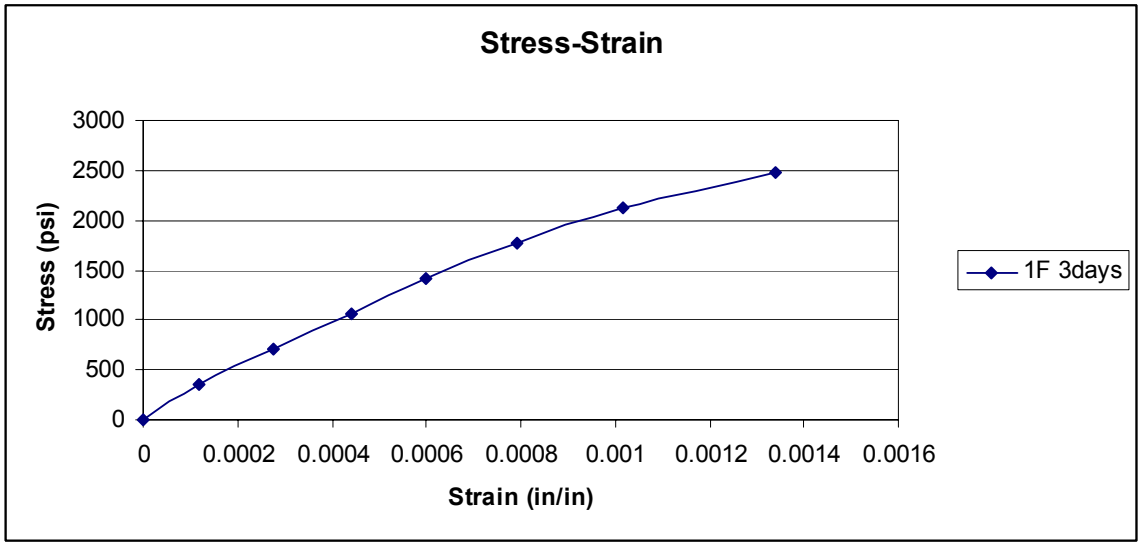

Figure 6 Stress & strain curve- Cylinder 1F at 3 Days

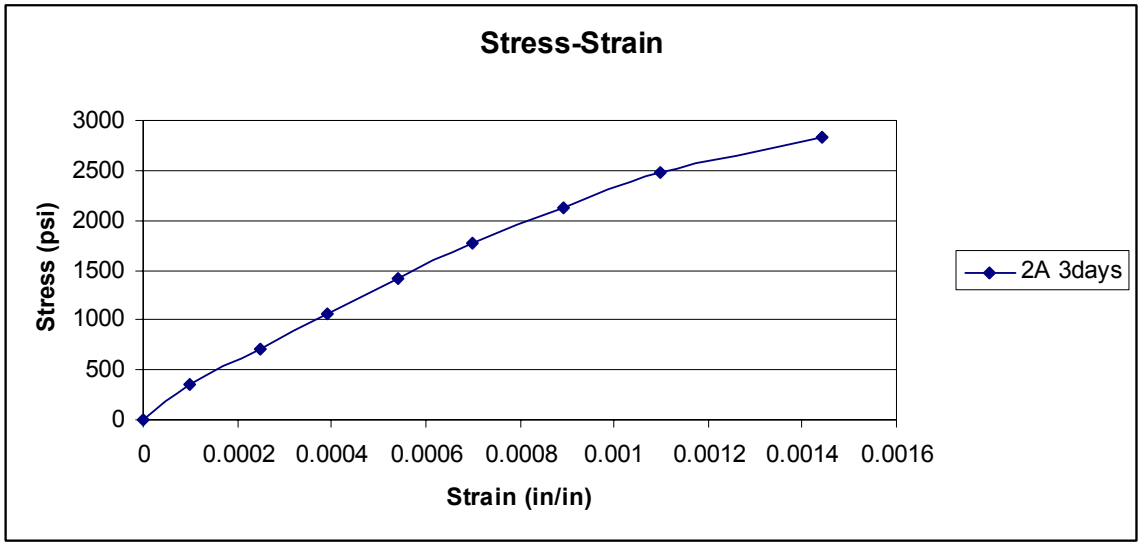

Figure 7 Stress & strain curve- Cylinder 2A at 3 Days

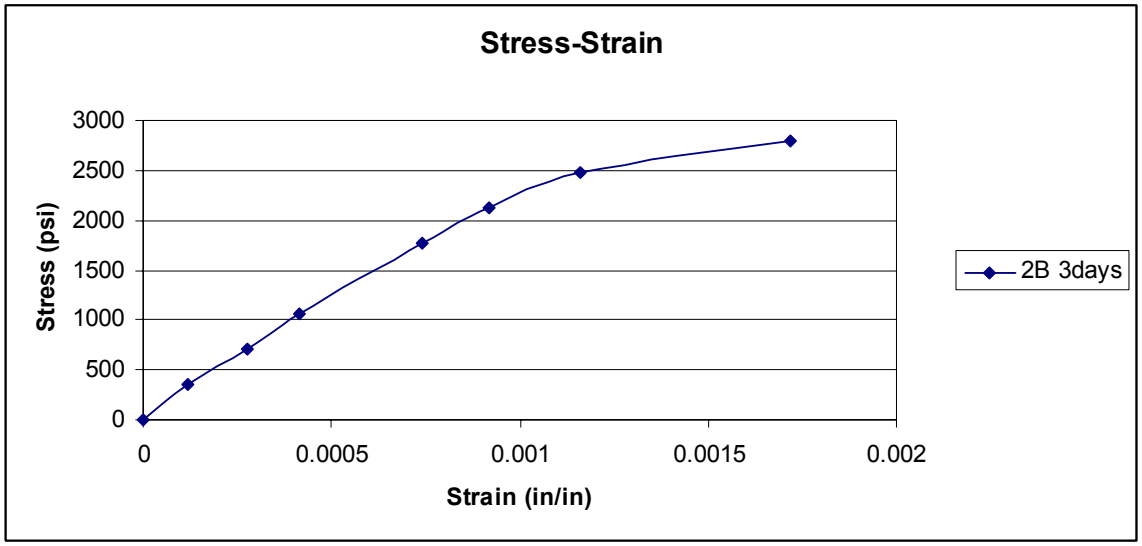

Figure 8 Stress & strain curve - Cylinder 2B at 3 Days

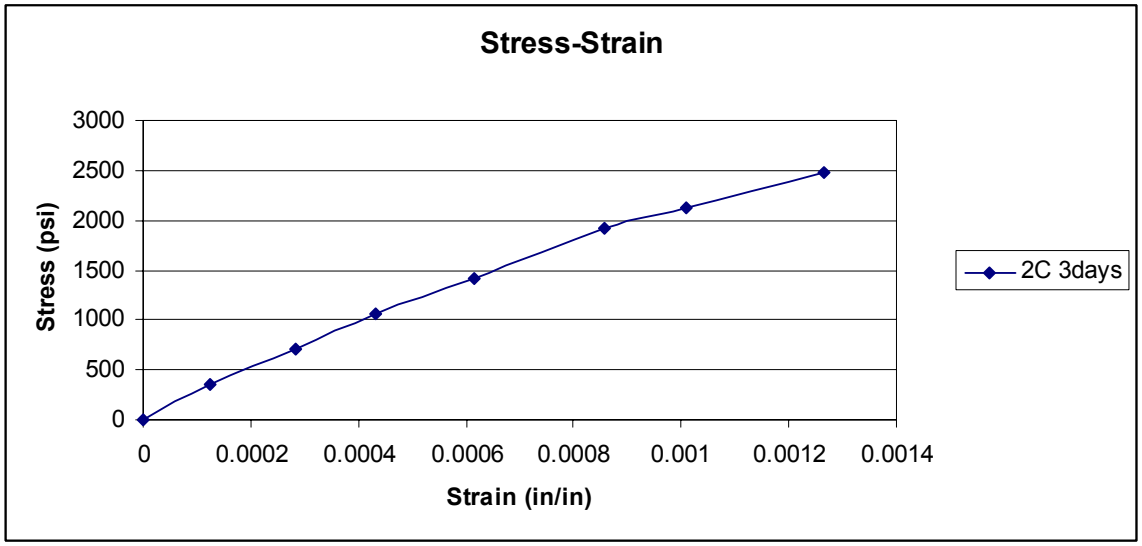

Figure 9 Stress & strain curve- Cylinder 2C at 3 Days

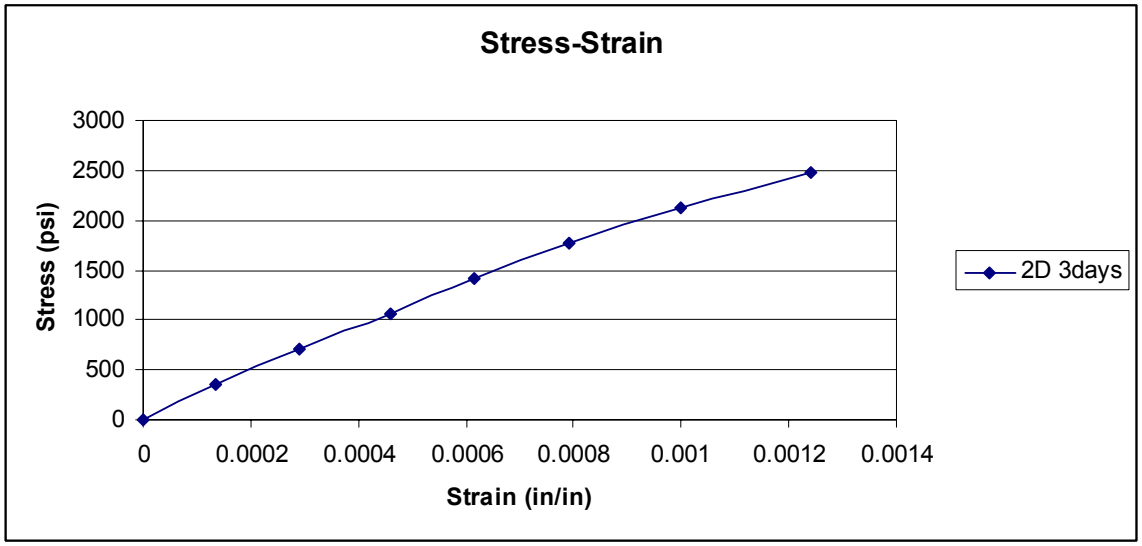

Figure 10 Stress & strain curve- Cylinder 2D at 3 Days

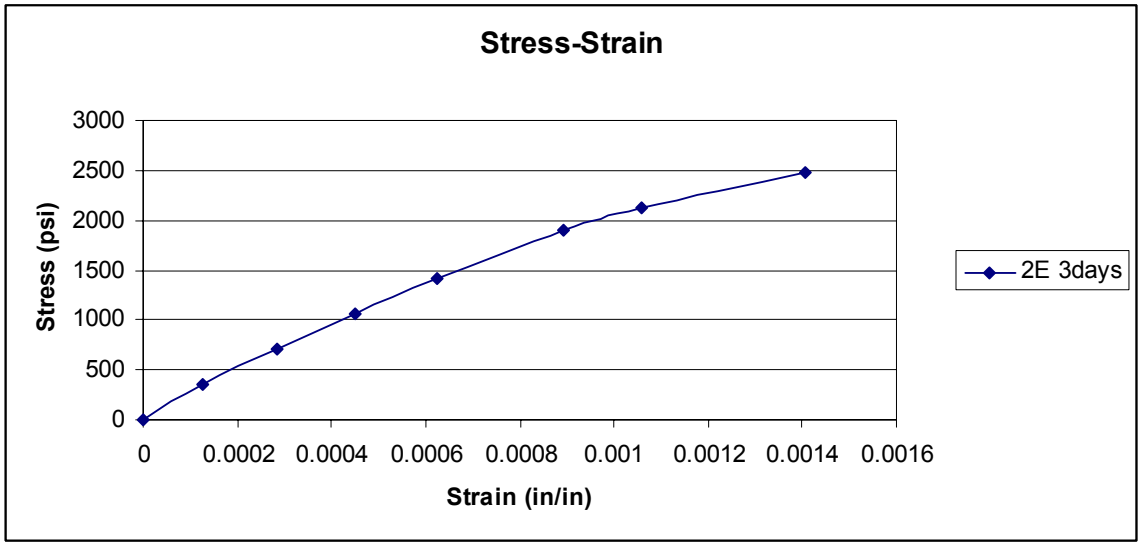

Figure 11 Stress & strain curve- Cylinder 2E at 3 Days

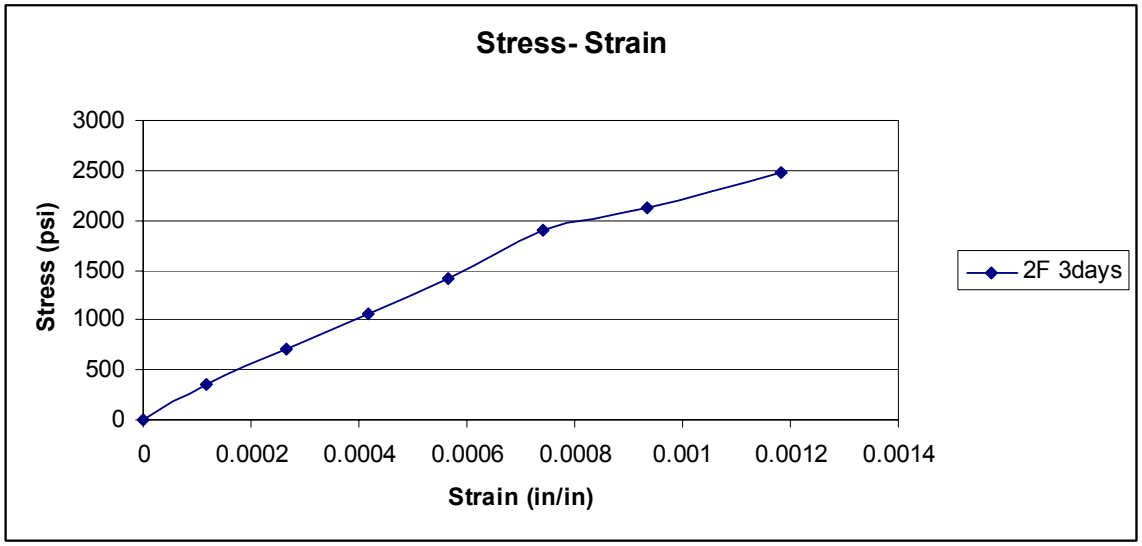

Figure 12 Stress & strain curve- Cylinder 2F at 3 Days

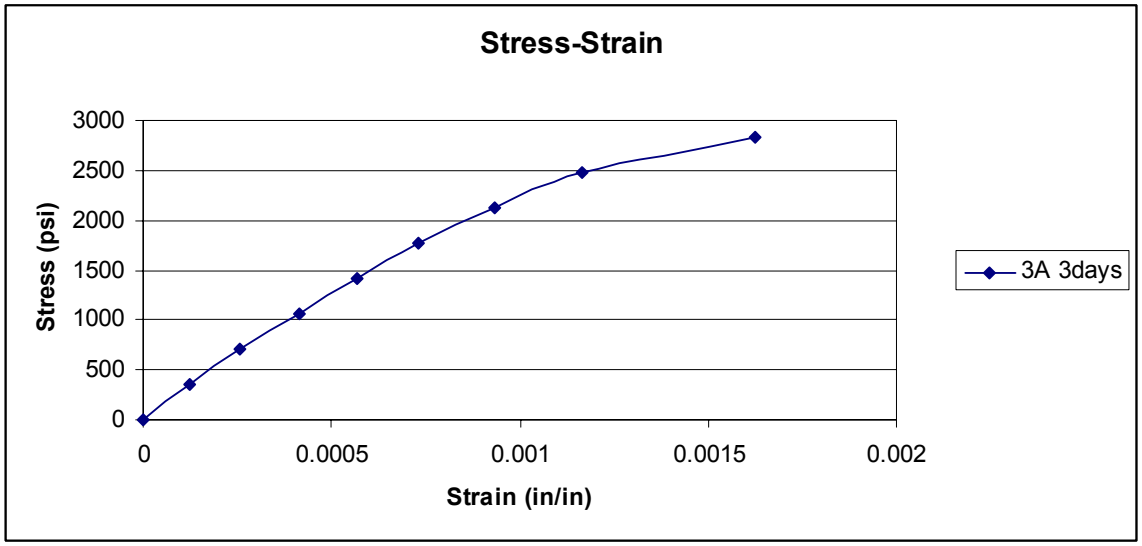

Figure 13 Stress & strain curve- Cylinder 3A at 3 Days

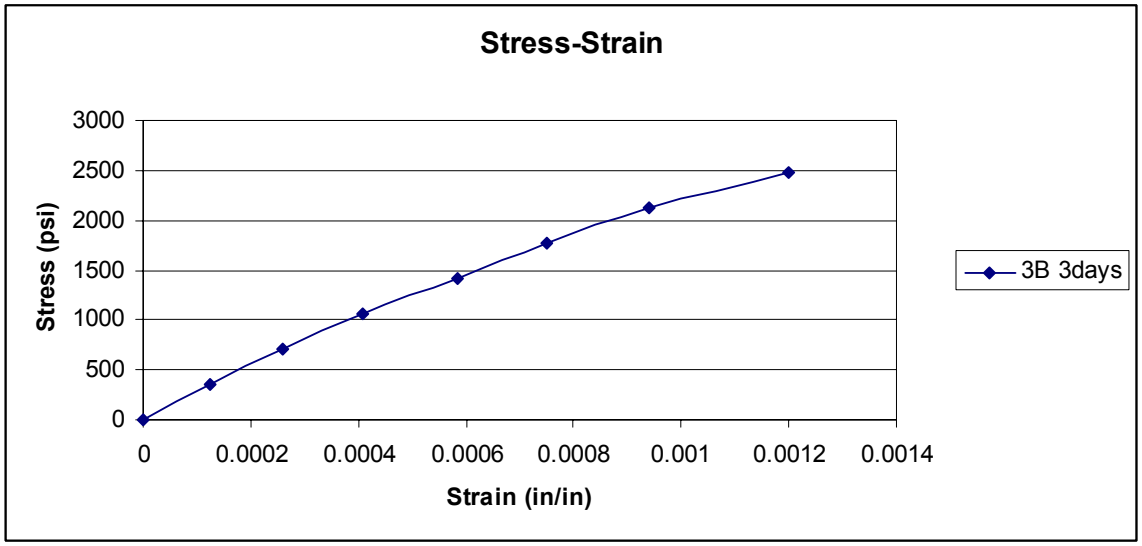

Figure 14 Stress & strain curve- Cylinder 3B at 3 Days

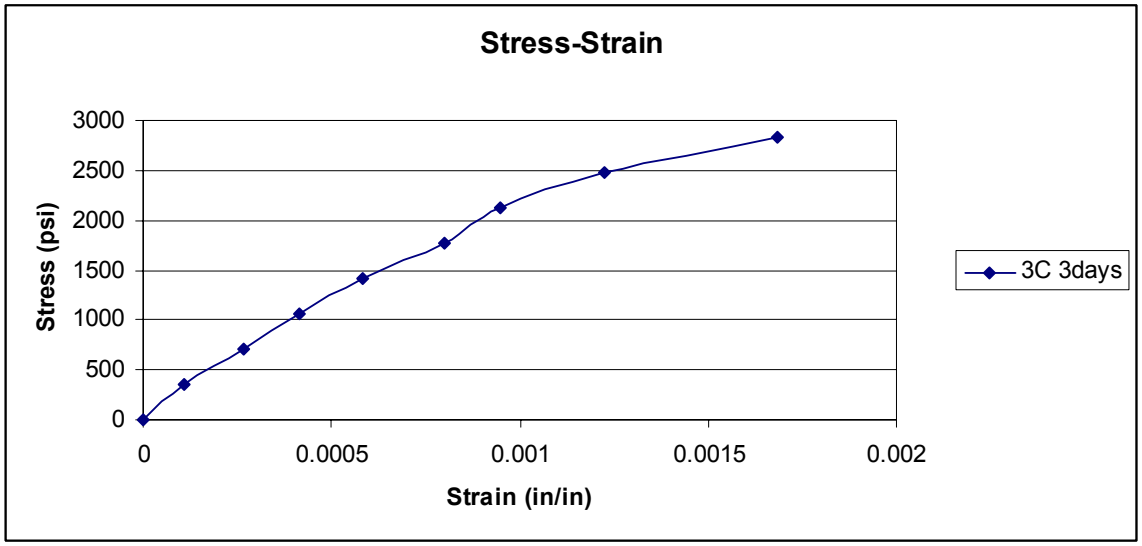

Figure 15 Stress & strain curve- Cylinder 3C at 3 Days

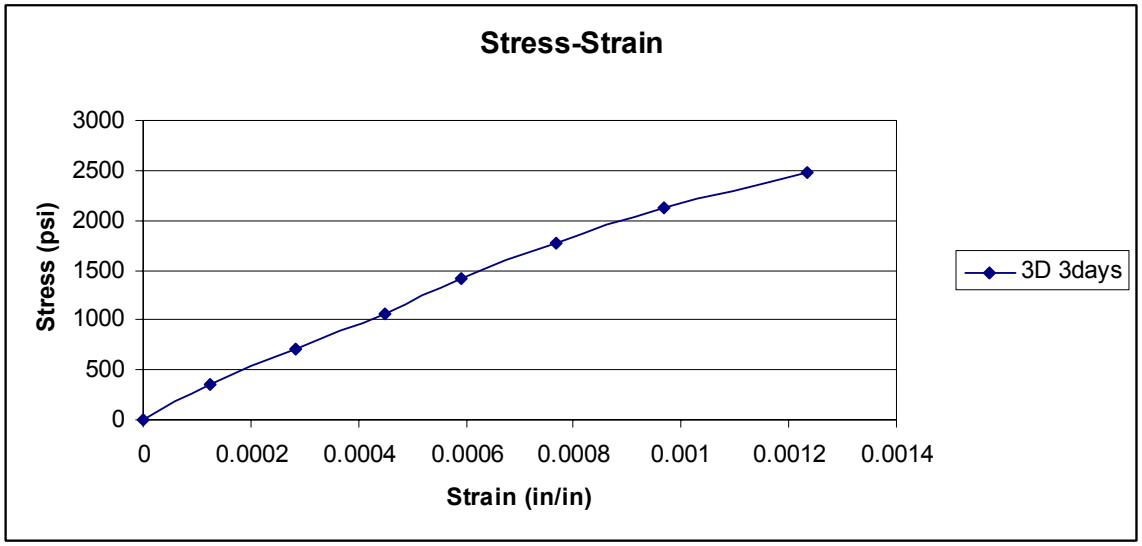

Figure 16 Stress & strain curve- Cylinder 3D at 3 Days

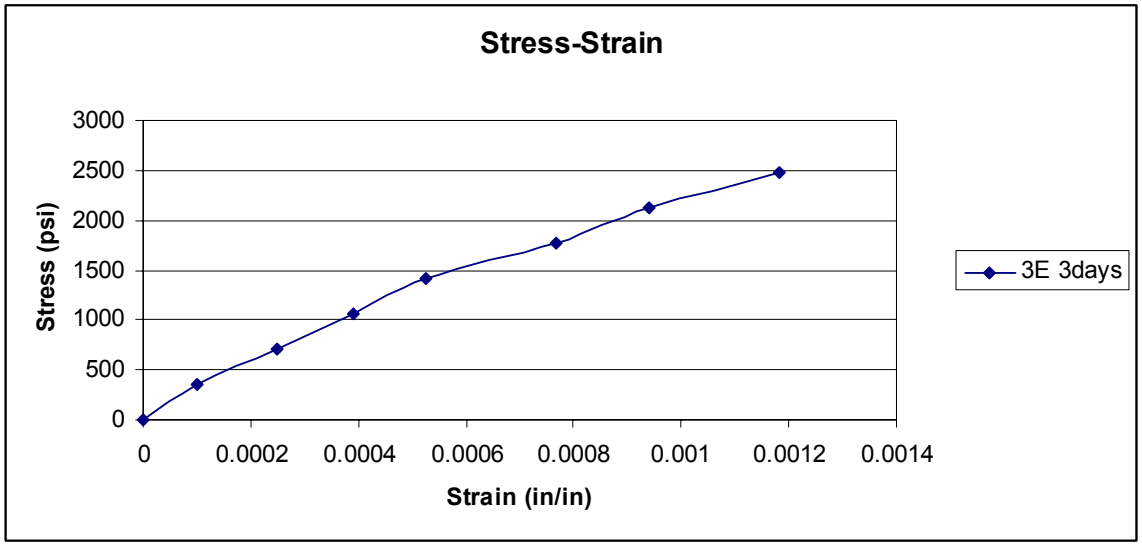

Figure 17 Stress & strain curve- Cylinder 3E at 3 Days

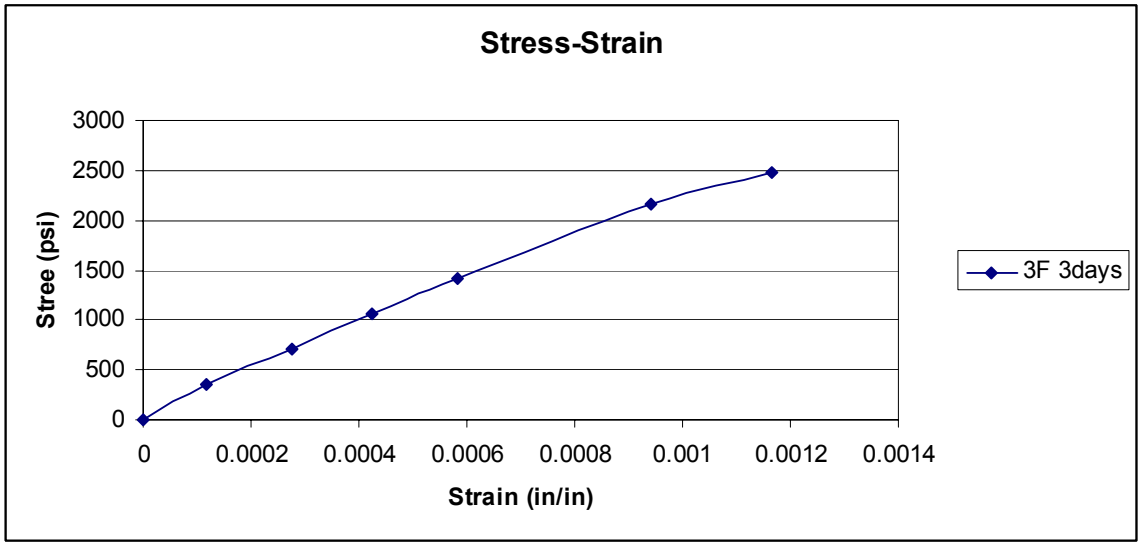

Figure 18 Stress & strain curve- Cylinder 3F at 3 Days

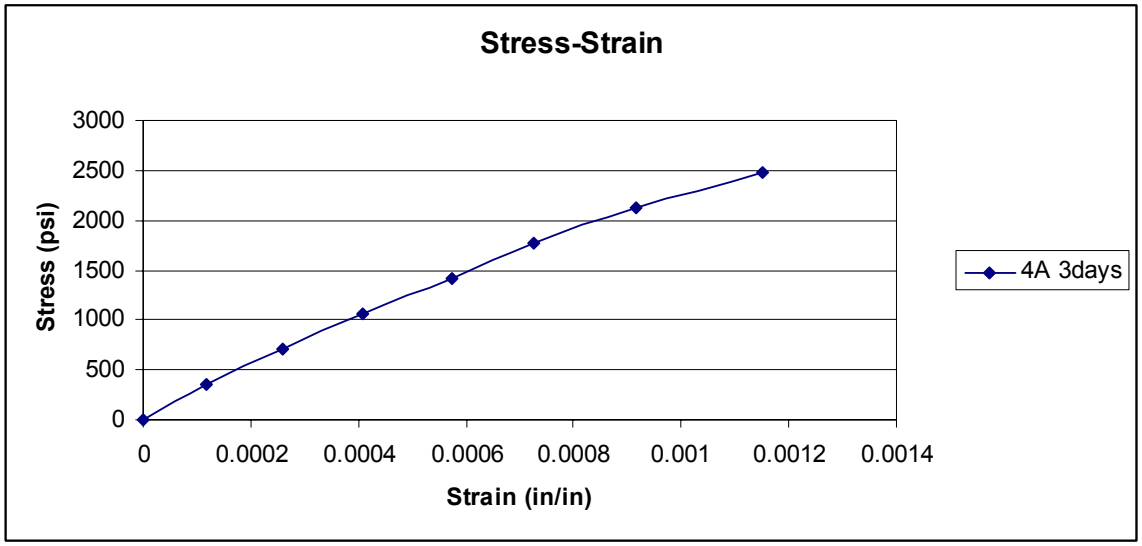

Figure 19 Stress & strain curve- Cylinder 4A at 3 Days

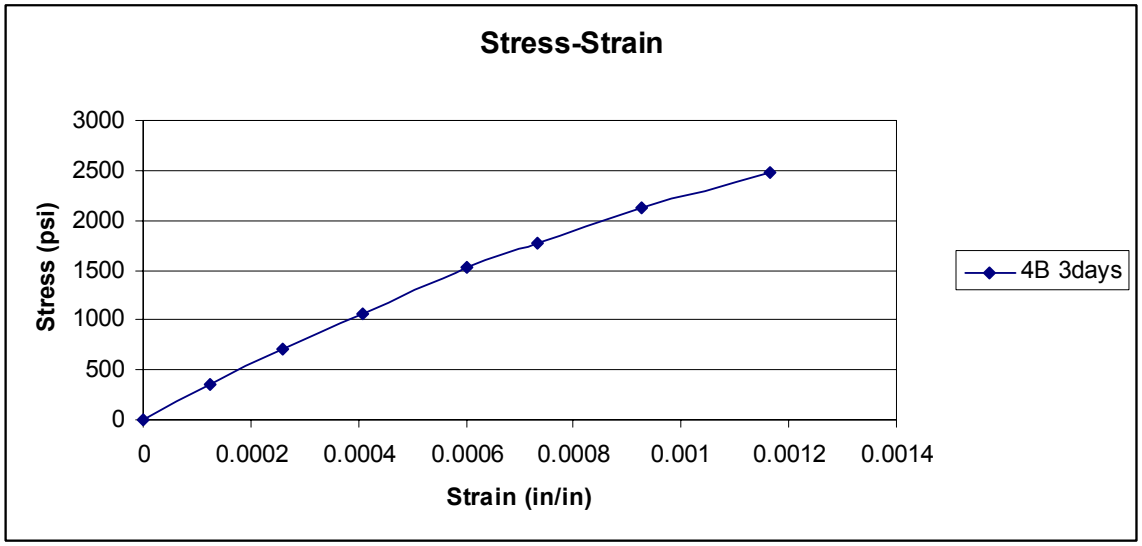

Figure 20 Stress & strain curve- Cylinder 4B at 3 Days

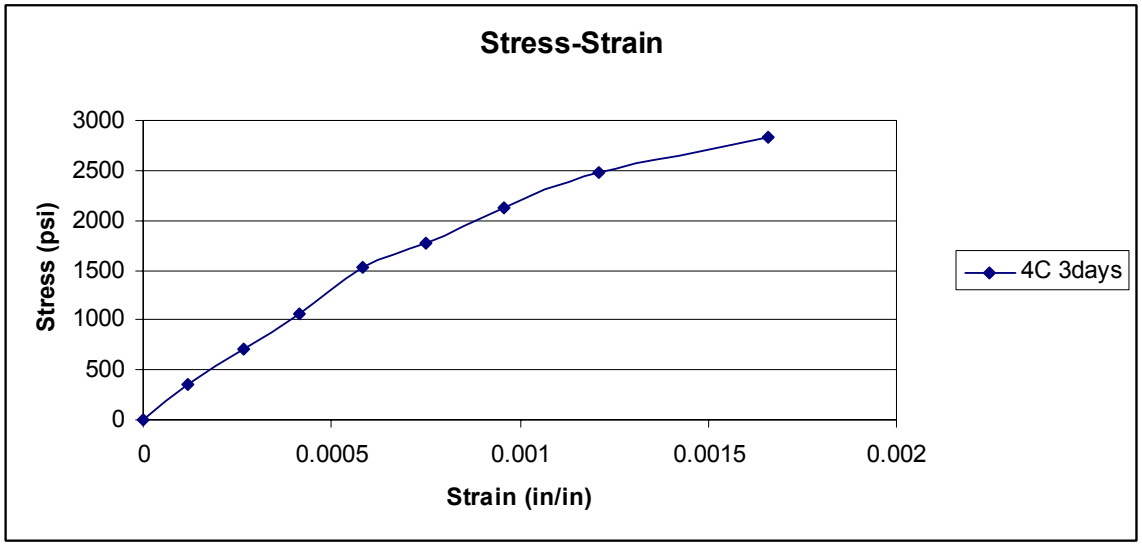

Figure 21 Stress & strain curve- Cylinder 4C at 3 Days

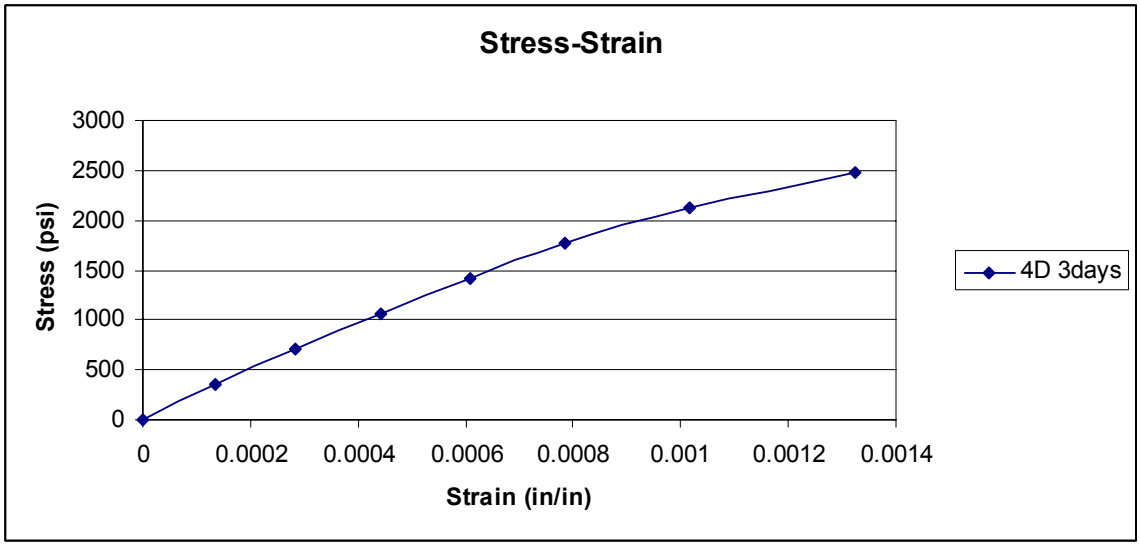

Figure 22 Stress & strain curve- Cylinder 4D at 3 Days

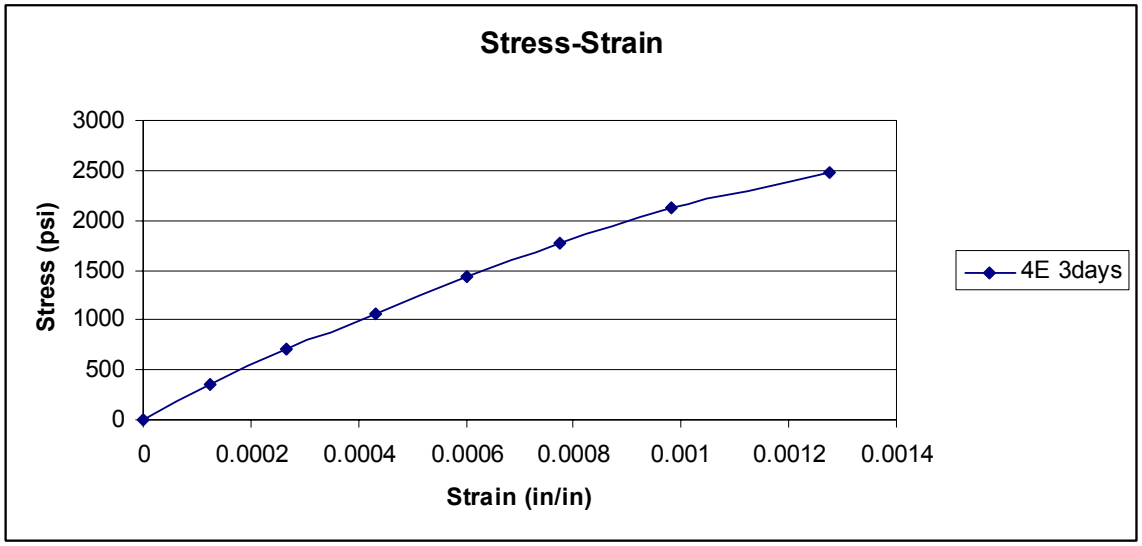

Figure 23 Stress & strain curve- Cylinder 4E at 3 Days

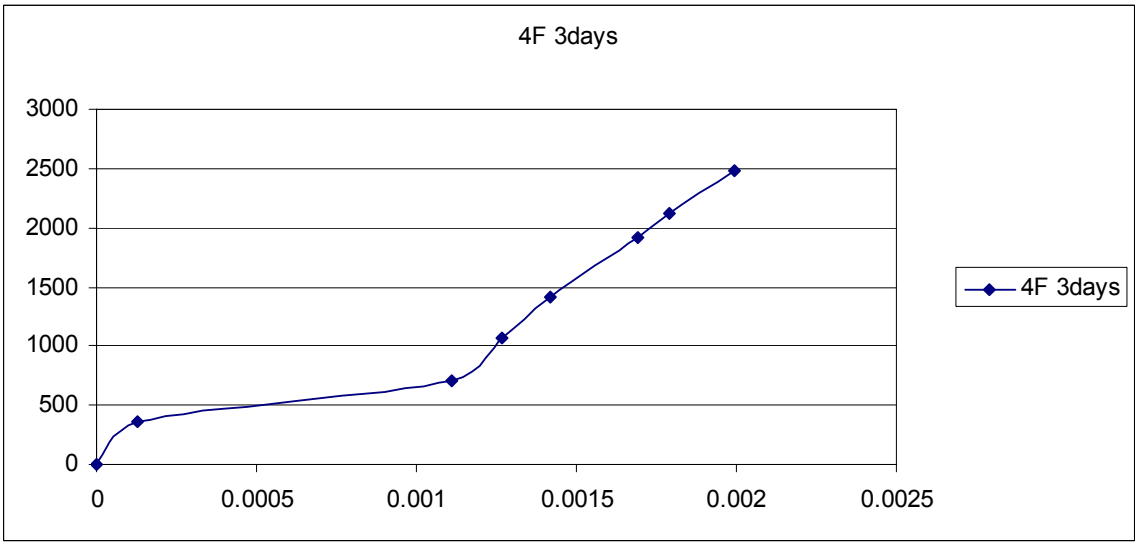

Figure 24 Stress & strain curve- Cylinder 4F at 3 Days

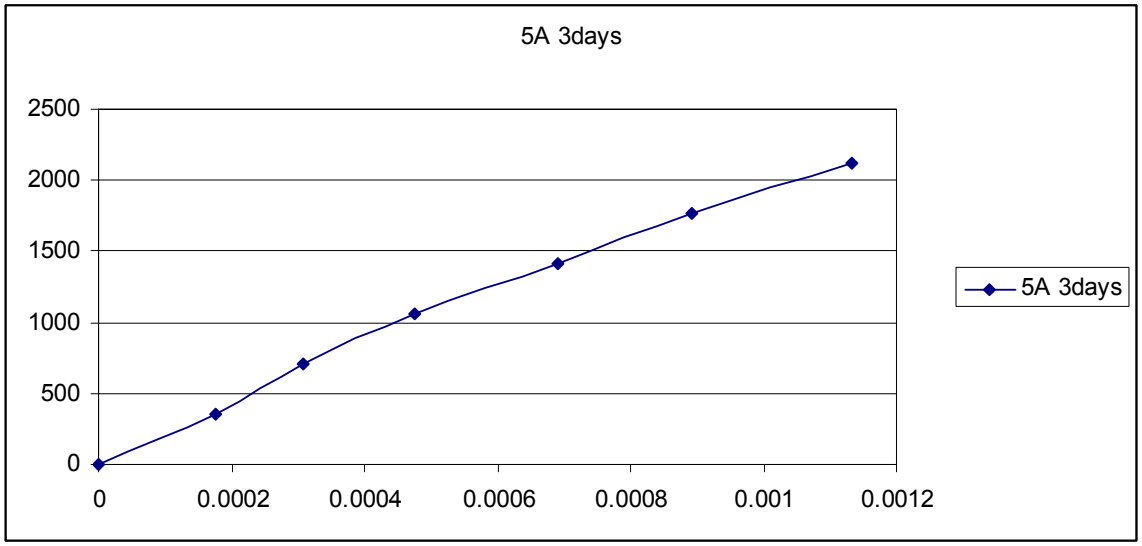

Figure 25 Stress & strain curve- Cylinder 5A at 3 Days

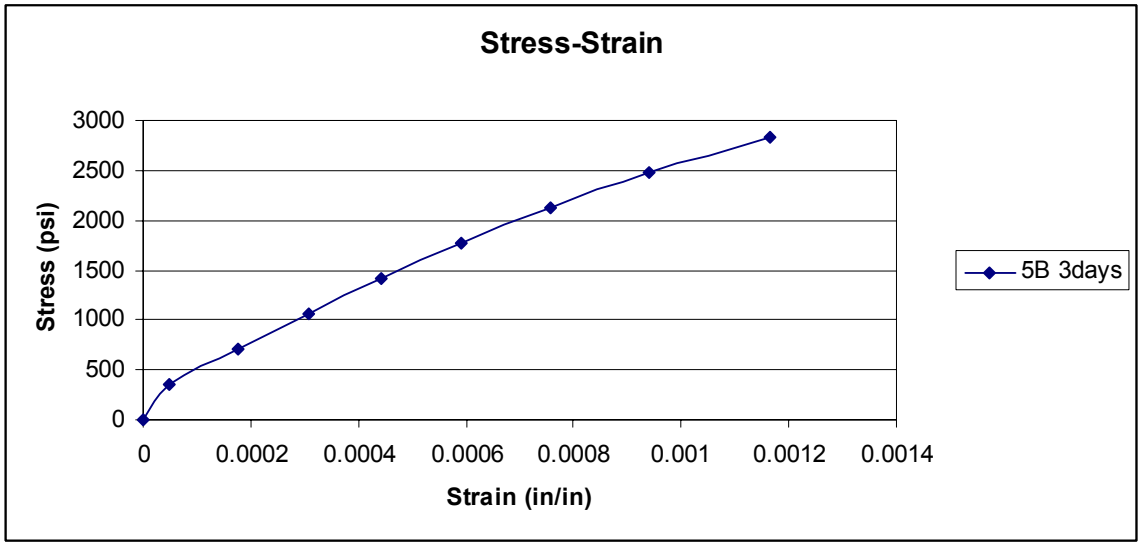

Figure 26 Stress & strain curve- Cylinder 5B at 3 Days

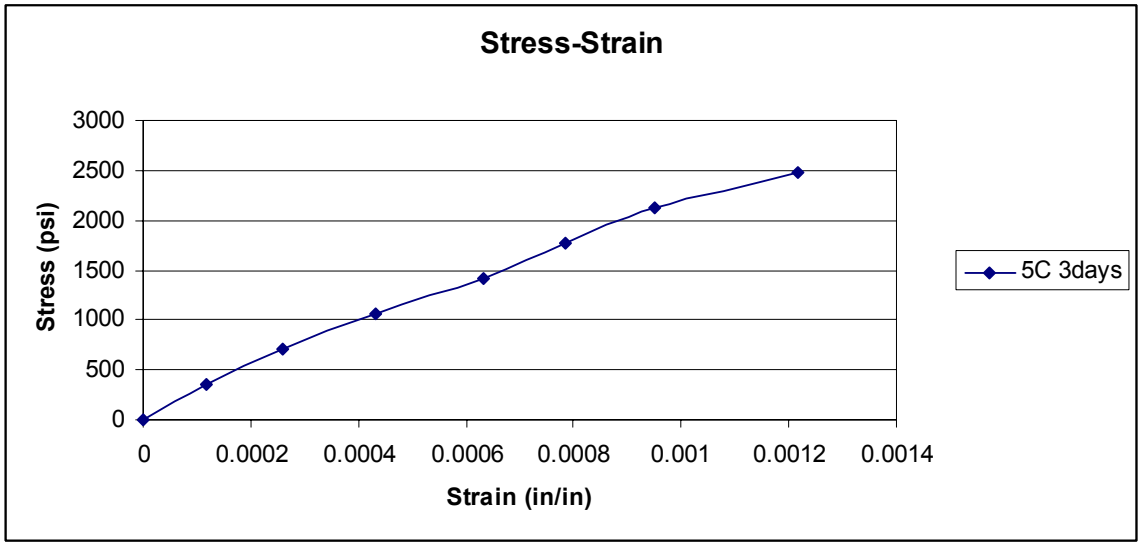

Figure 27 Stress & strain curve- Cylinder 5C at 3 Days

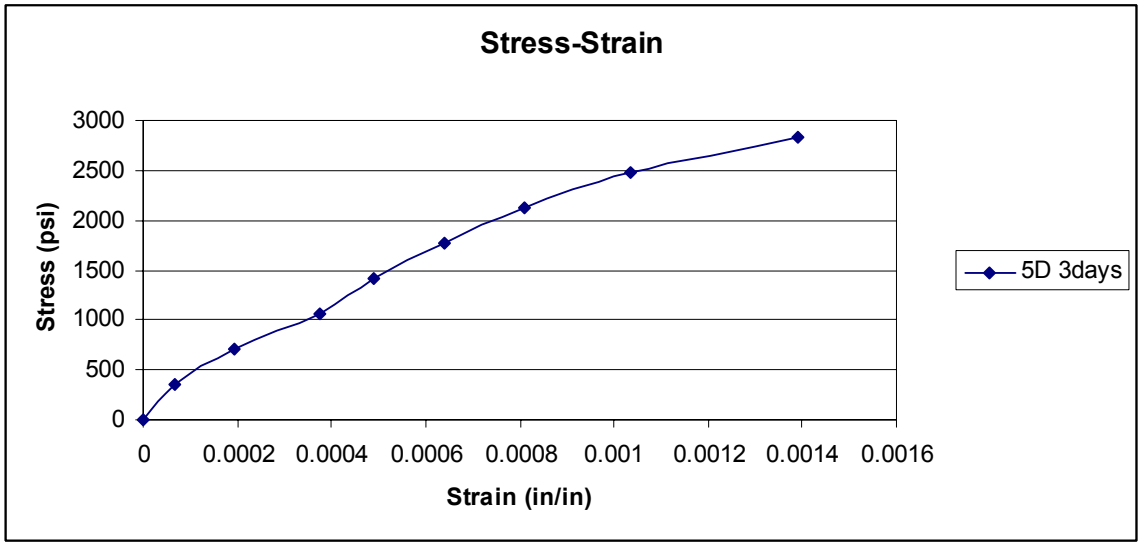

Figure 28 Stress & strain curve- Cylinder 5D at 3 Days

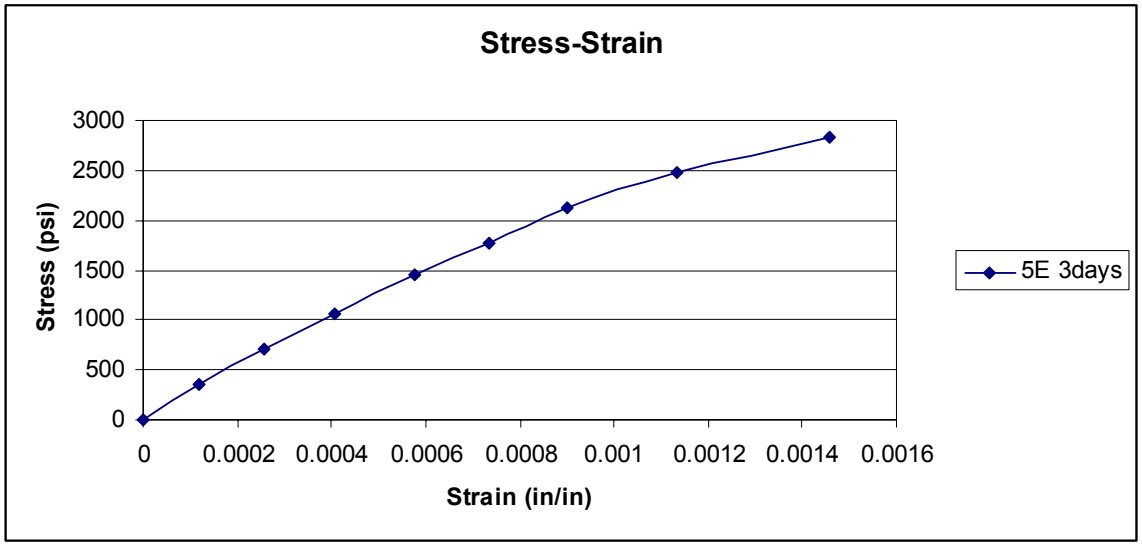

Figure 29 Stress & strain curve- Cylinder 5E at 3 Days

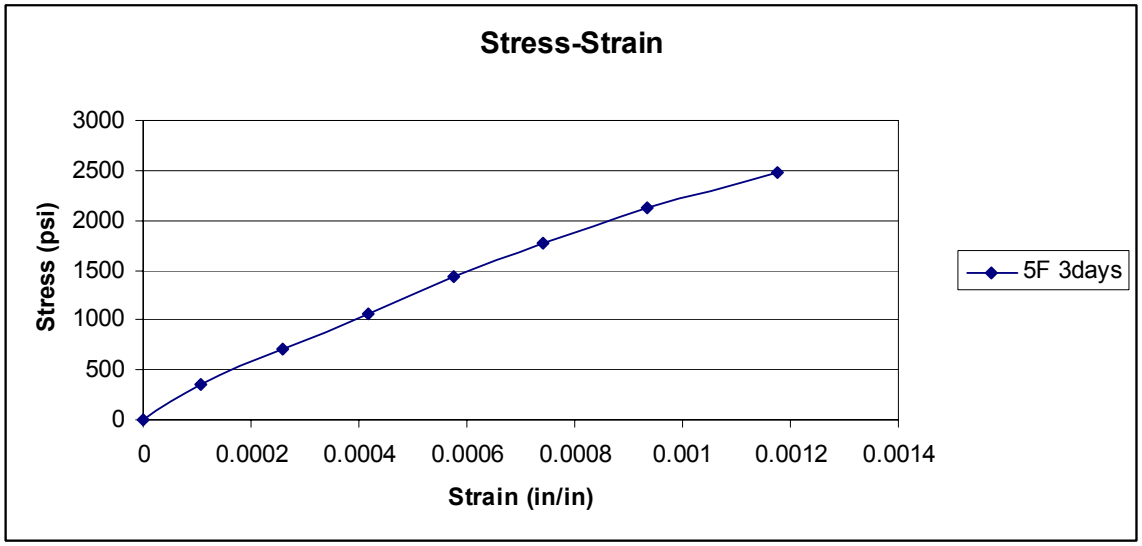

Figure 30 S tress & strain curve- Cylinder 5F at 3 Days

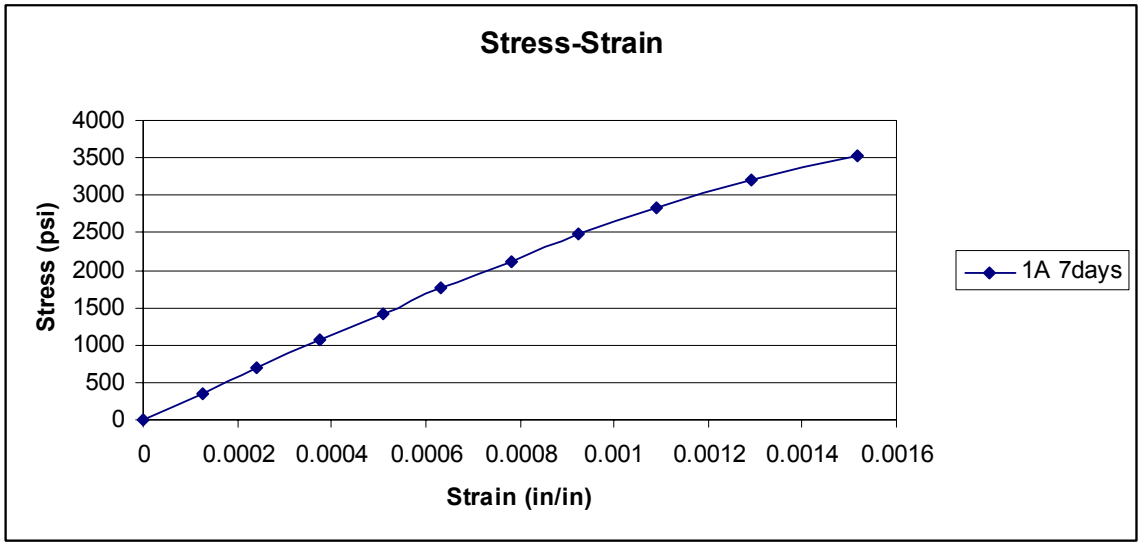

Figure 31 Stress & strain curve- Cylinder 1A at 7 Days

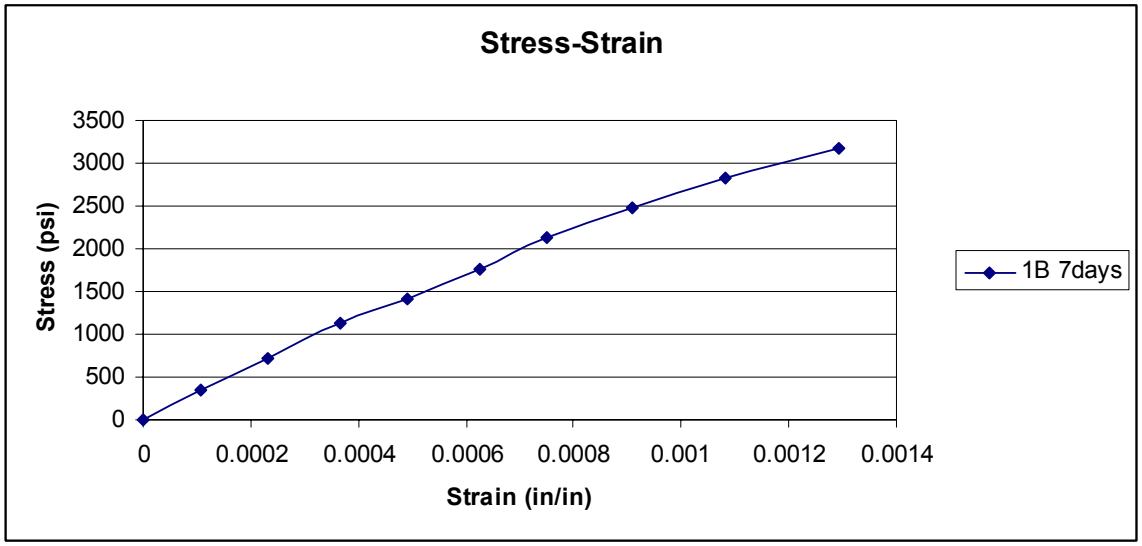

Figure 32 Stress & strain curve- Cylinder 1B at 7 Days

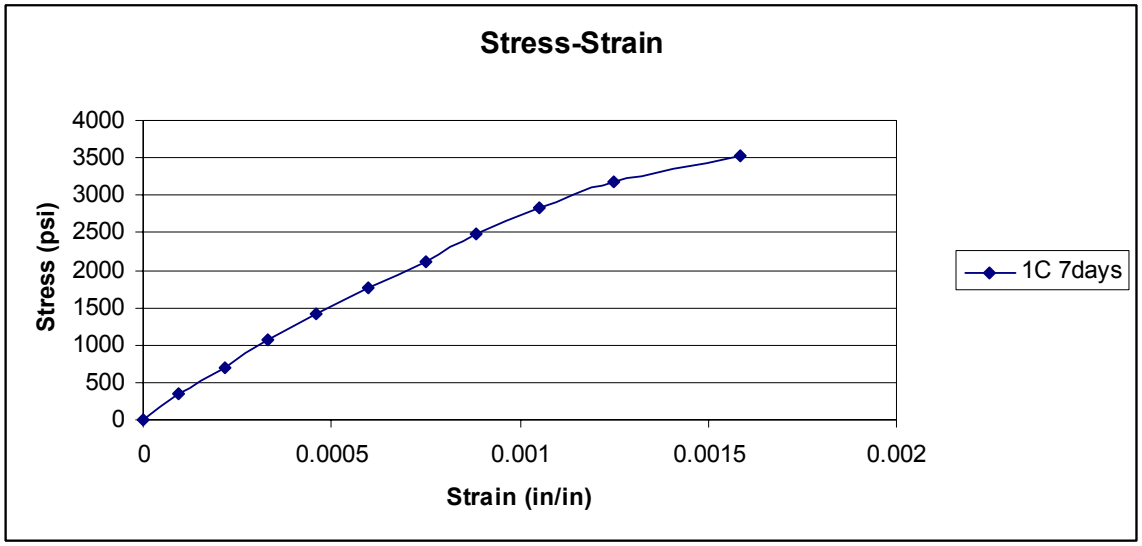

Figure 33 Stress & strain curve- Cylinder 1C at 7 Days

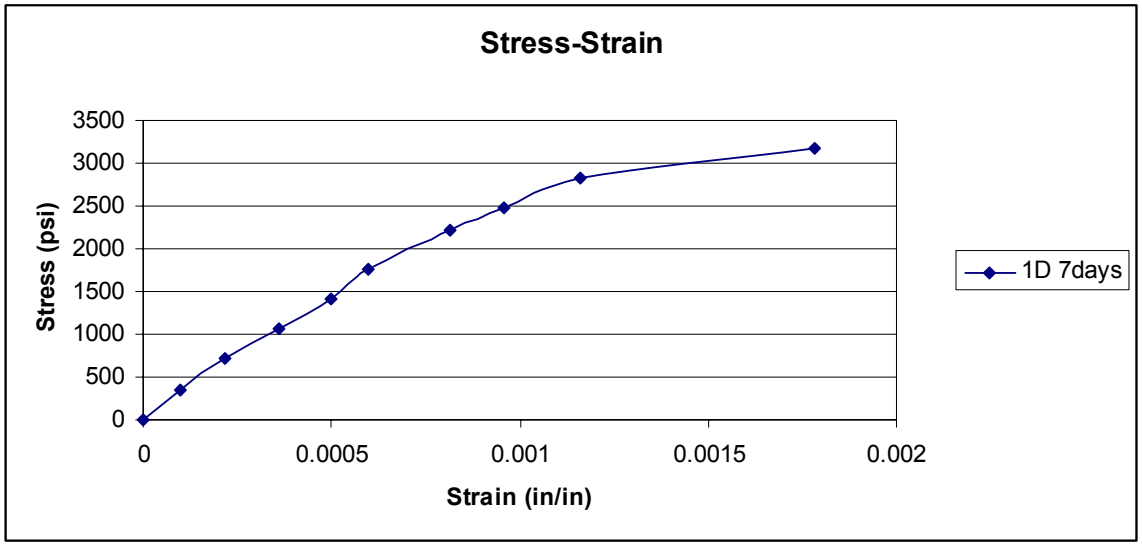

Figure 34 Stress & strain curve- Cylinder 1D at 7 Days

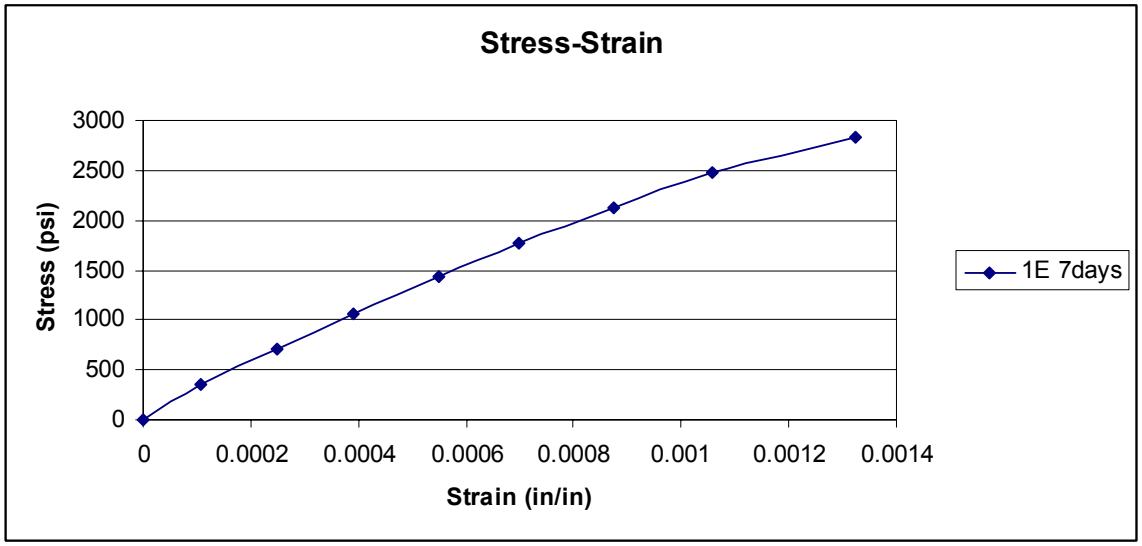

Figure 35 Stress & strain curve- Cylinder 1E at 7 Days

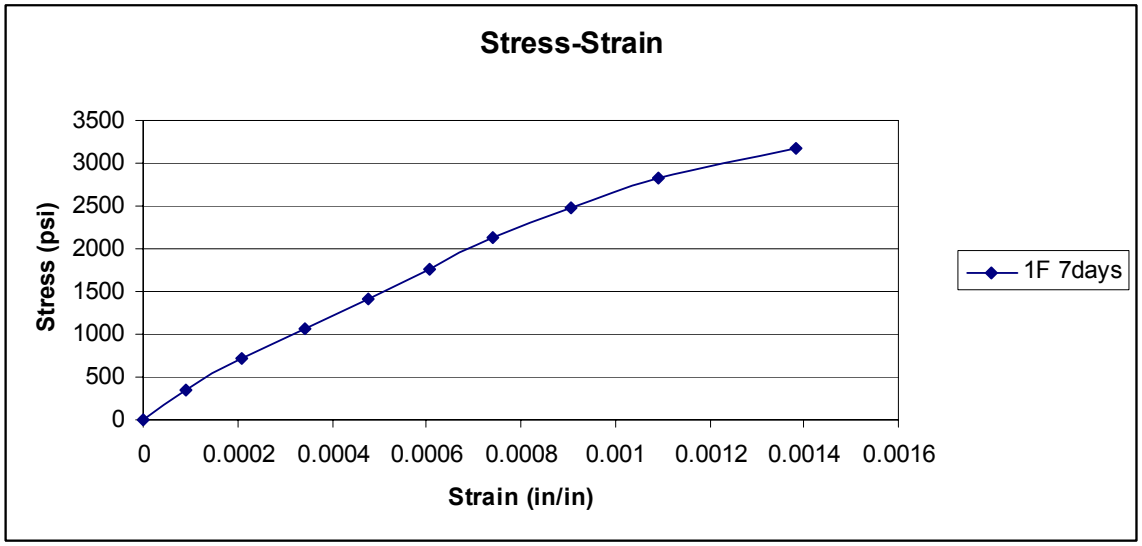

Figure 36 Stress & strain curve- Cylinder 1F at 7 Days

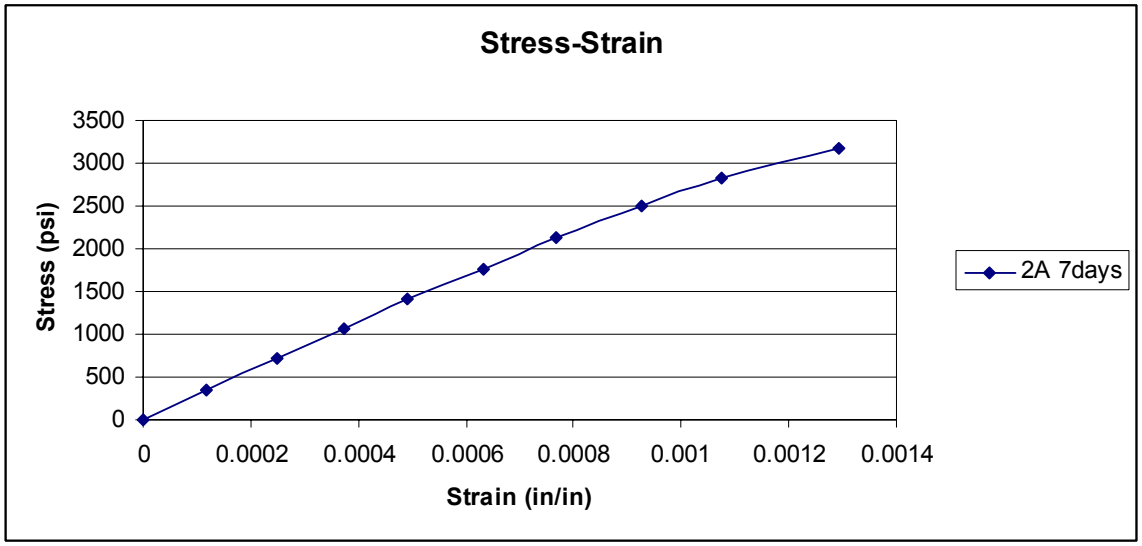

Figure 37 Stress & strain curve- Cylinder 2A at 7 Days

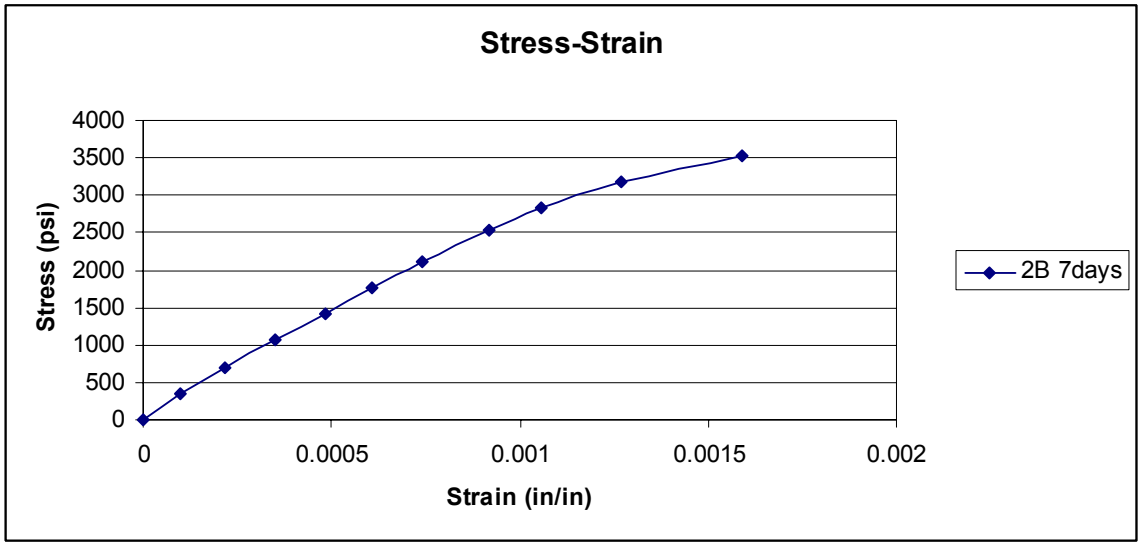

Figure 38 Stress & strain curve- Cylinder 2B at 7 Days

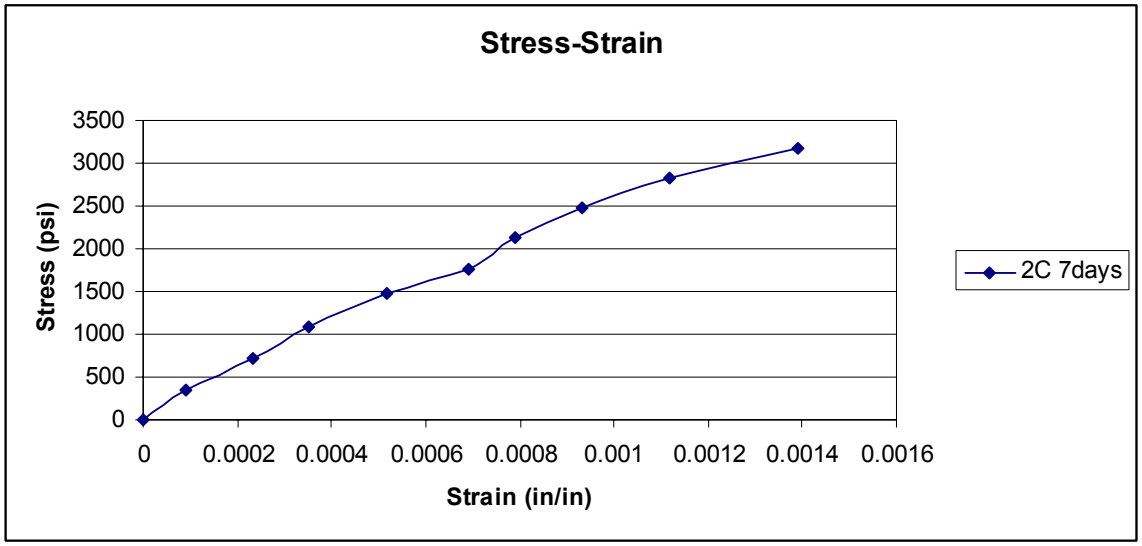

Figure 39 Stress & strain curve- Cylinder 2C at 7 Days

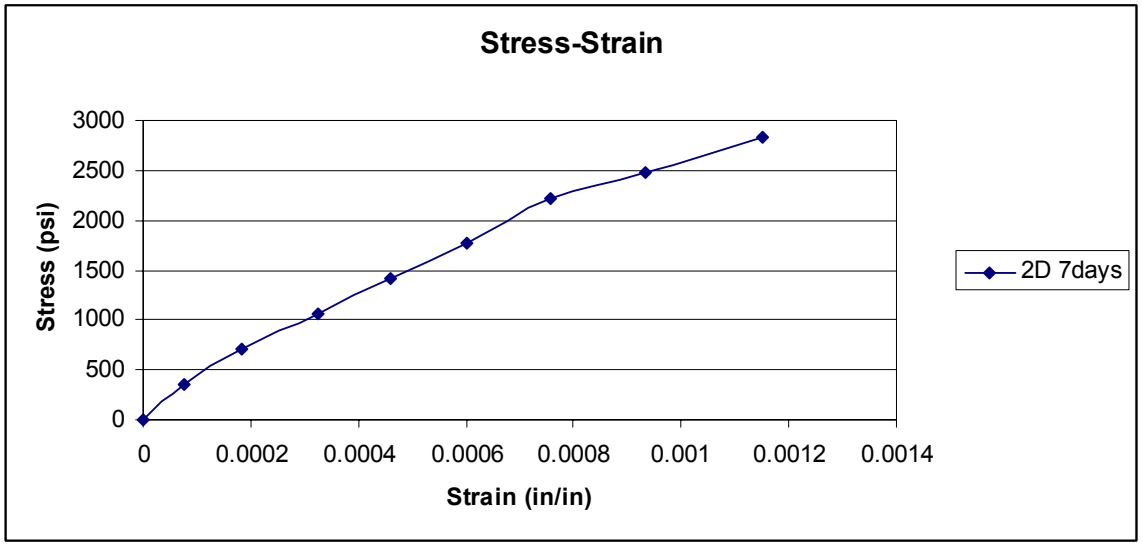

Figure 40 Stress & strain curve- Cylinder 2D at 7 Days

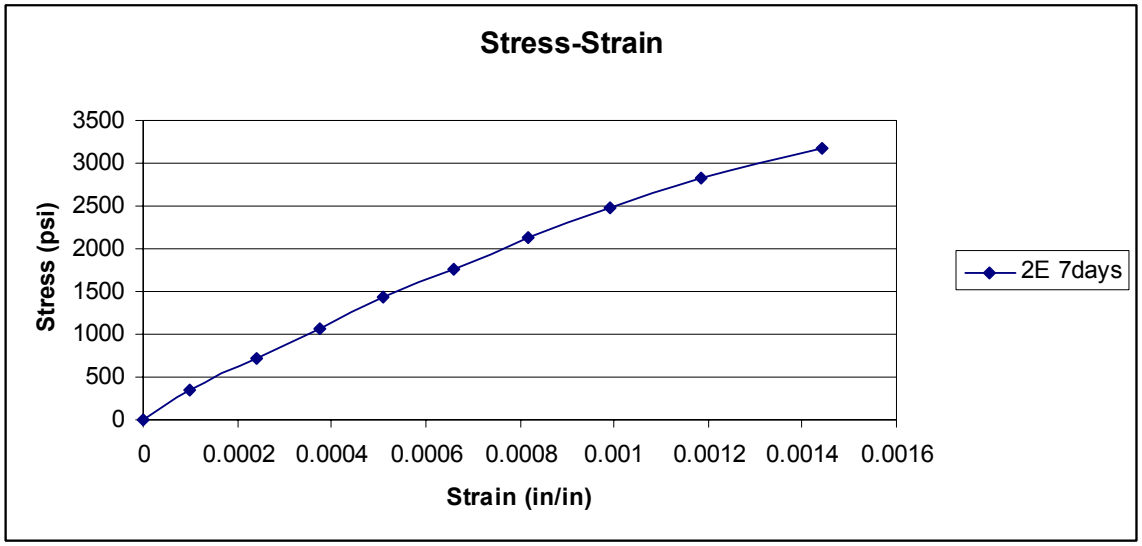

Figure 41 Stress & strain curve- Cylinder 2E at 7 Days

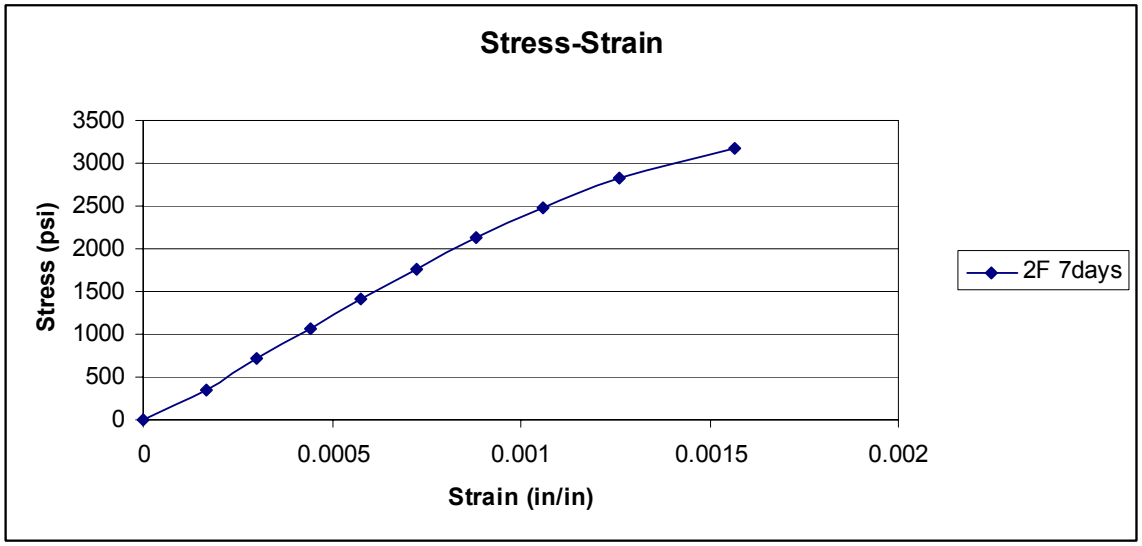

Figure 42 Stress & strain curve- Cylinder 2F at 7 Days

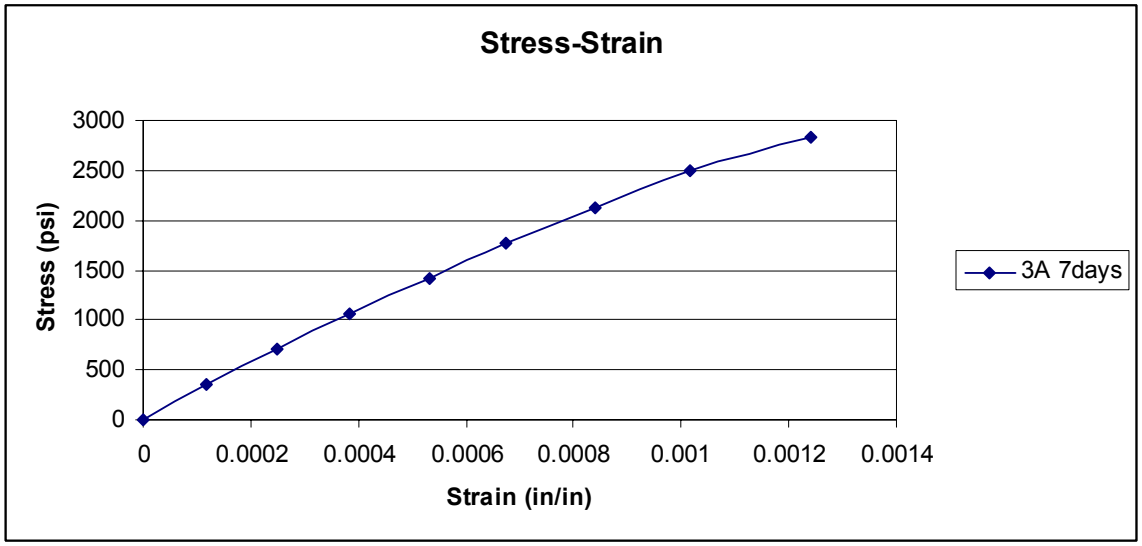

Figure 43 Stress & strain curve- Cylinder 3A at 7 Days

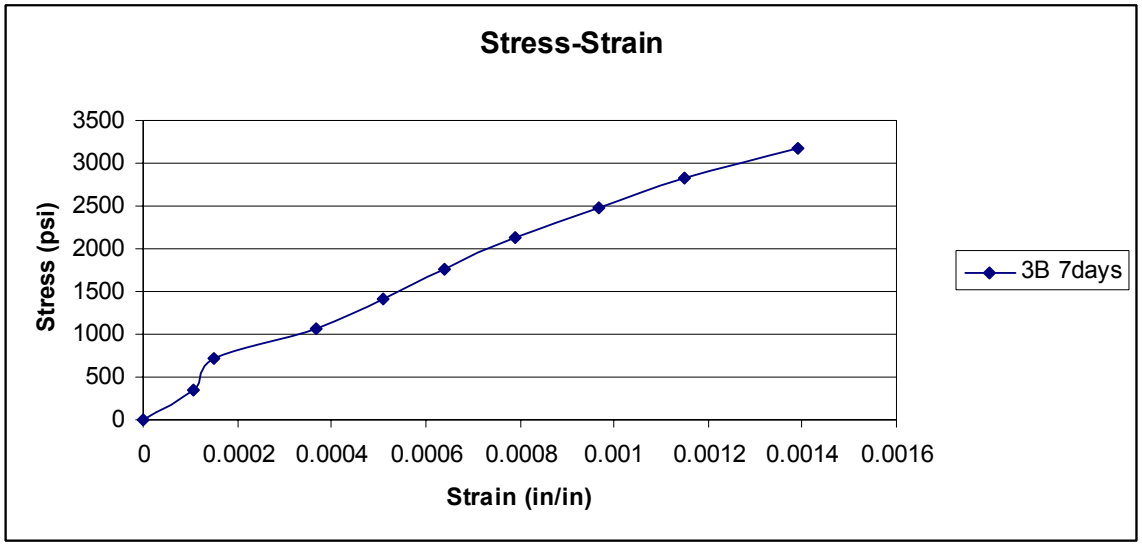

Figure 44 Stress & strain curve- Cylinder 3B at 7 Days

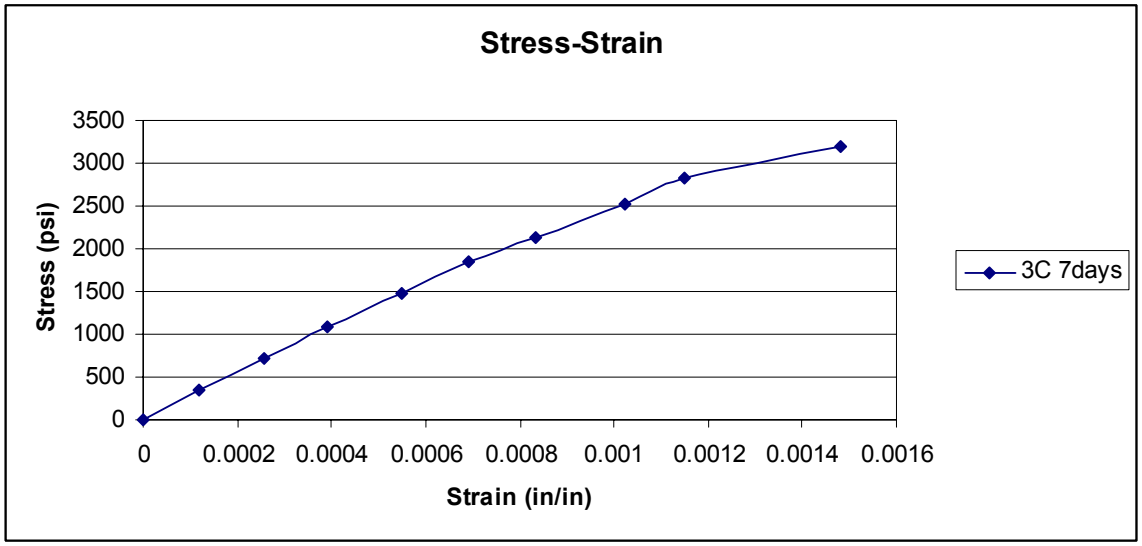

Figure 45 Stress & strain curve- Cylinder 3C at 7 Days

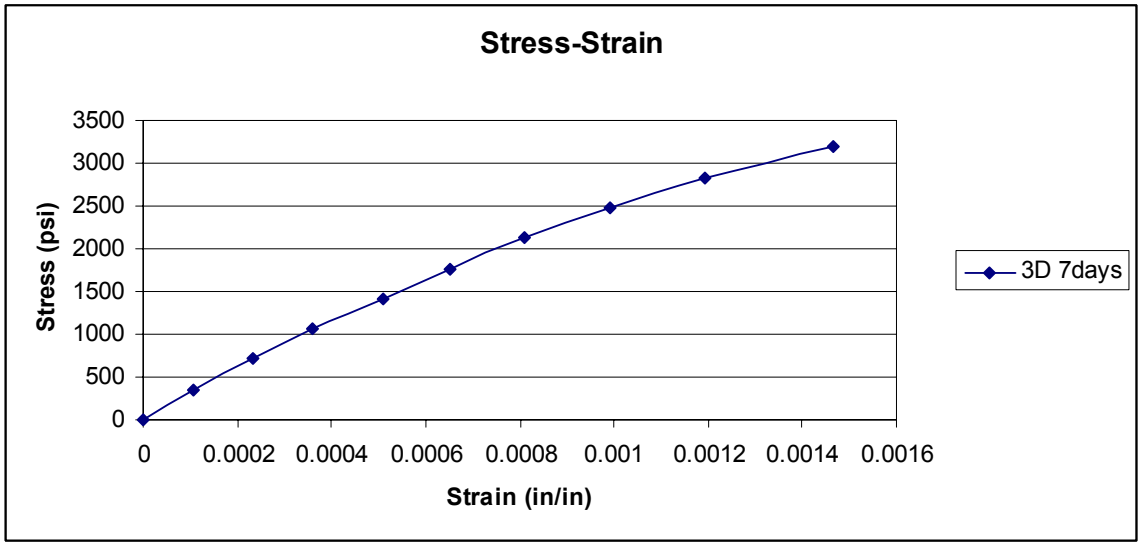

Figure 46 Stress & strain curve- Cylinder 3D at 7 Days

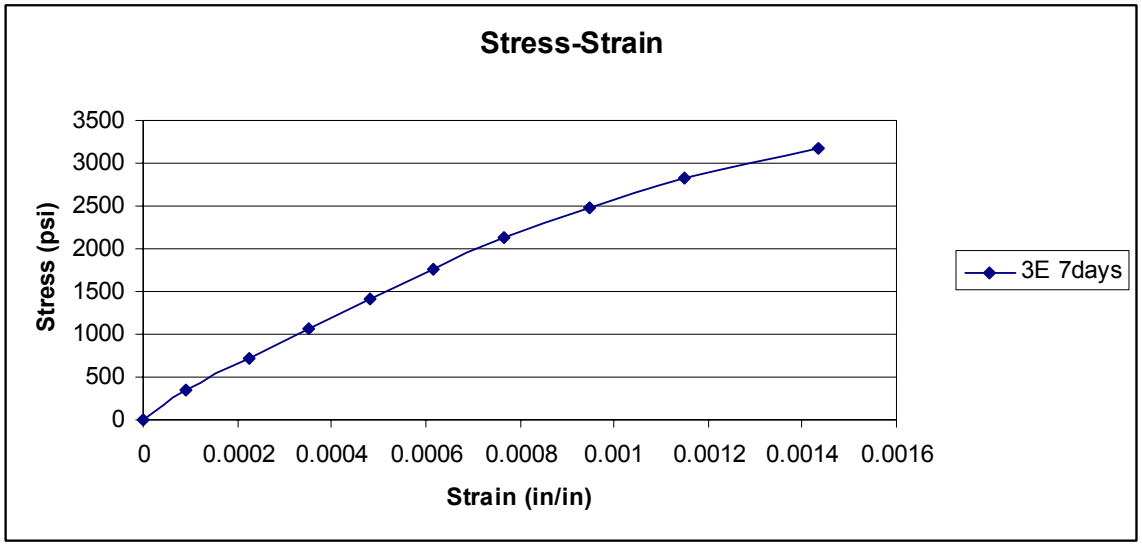

Figure 47 Stress & strain curve- Cylinder 3E at 7 Days

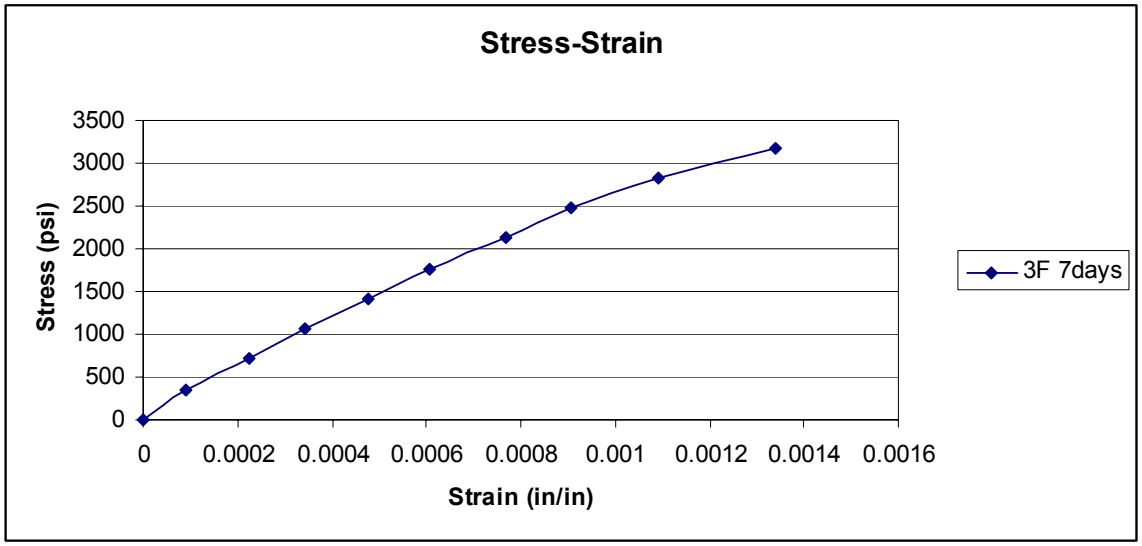

Figure 48 Stress & strain curve- Cylinder 3F at 7 Days

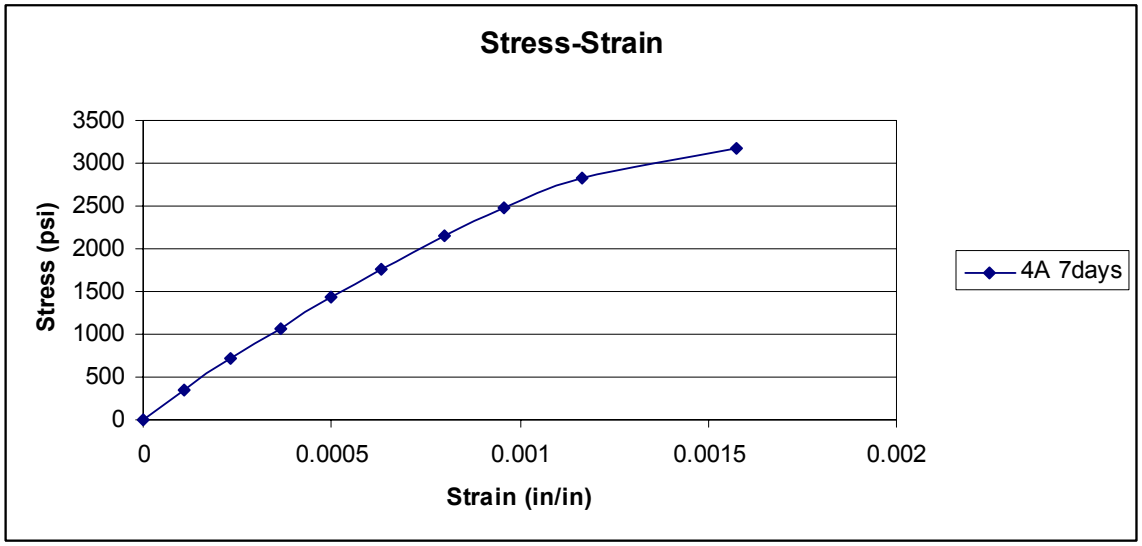

Figure 49 Stress & strain curve- Cylinder 4A at 7 Days

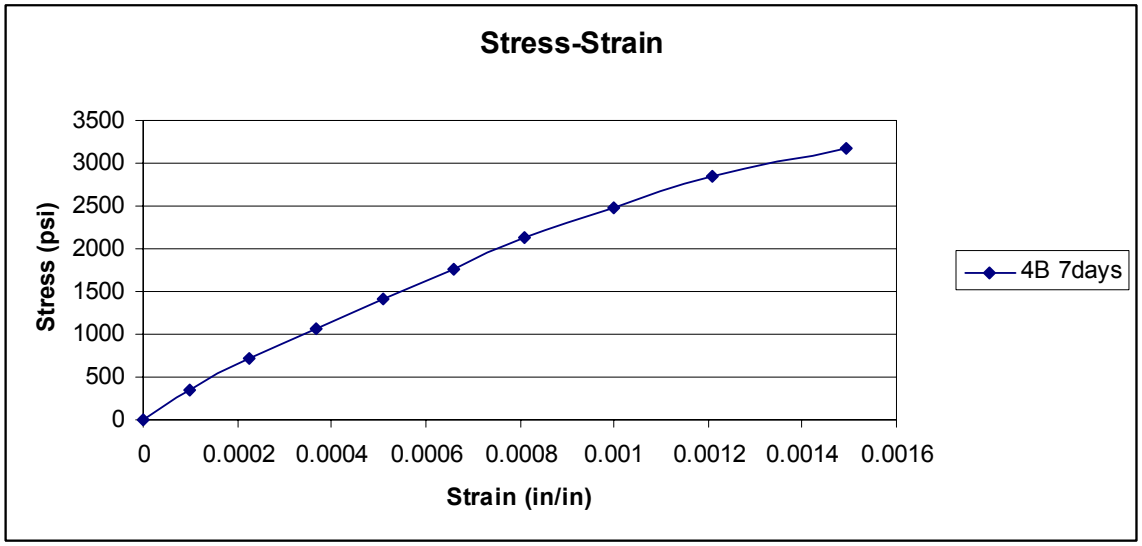

Figure 50 Stress & strain curve- Cylinder 4B at 7 Days

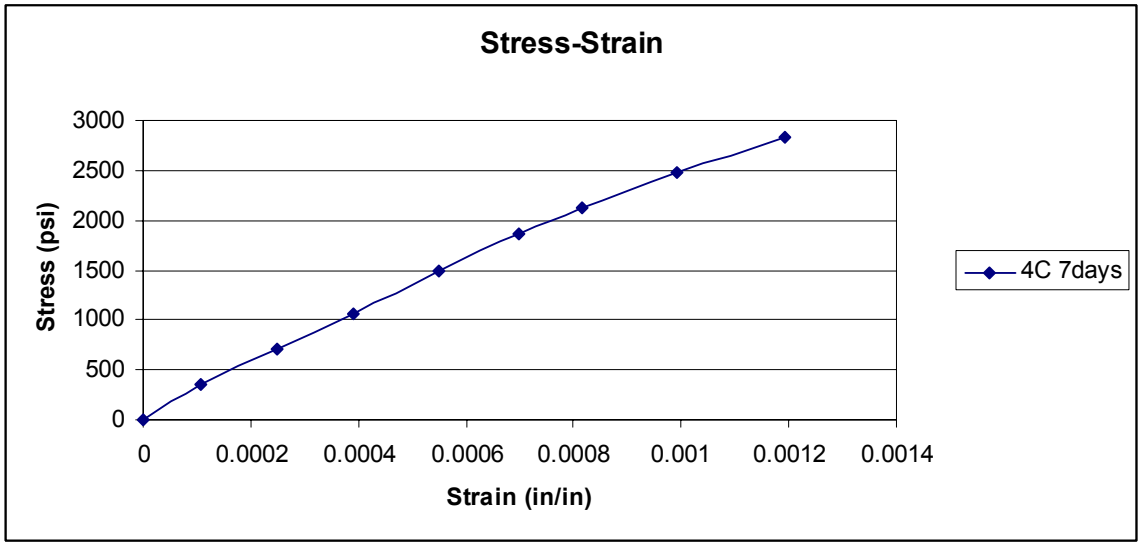

Figure 51 Stress & strain curve- Cylinder 4C at 7 Days

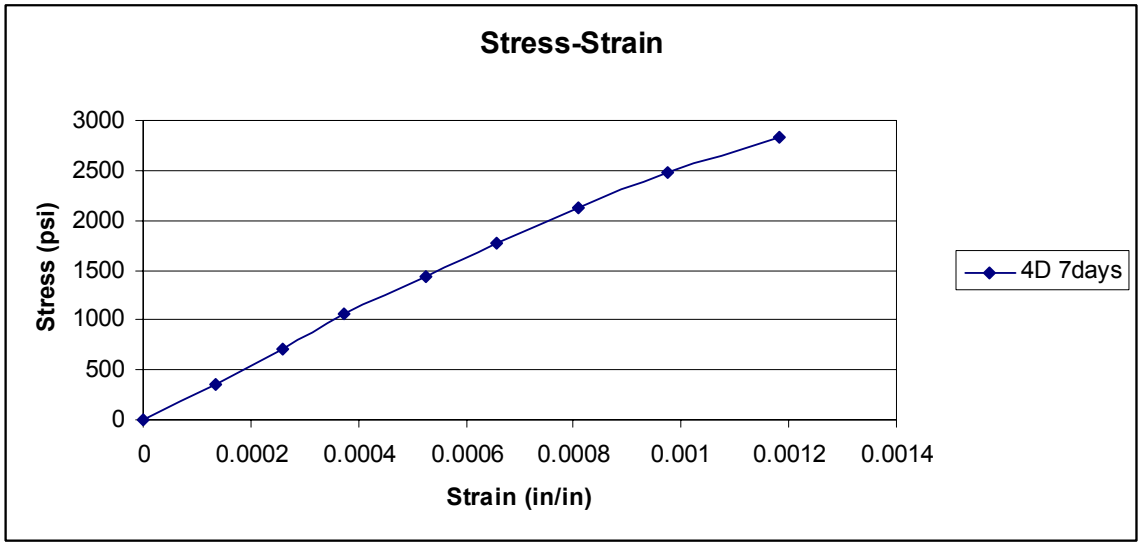

Figure 52 Stress & strain curve- Cylinder 4D at 7 Days

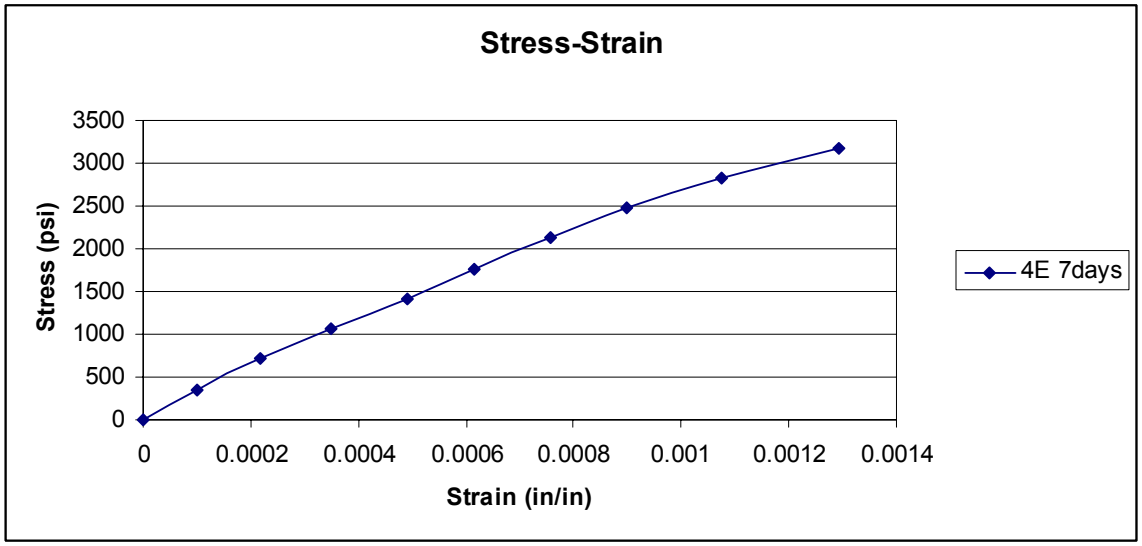

Figure 53 Stress & strain curve- Cylinder 4E at 7 Days

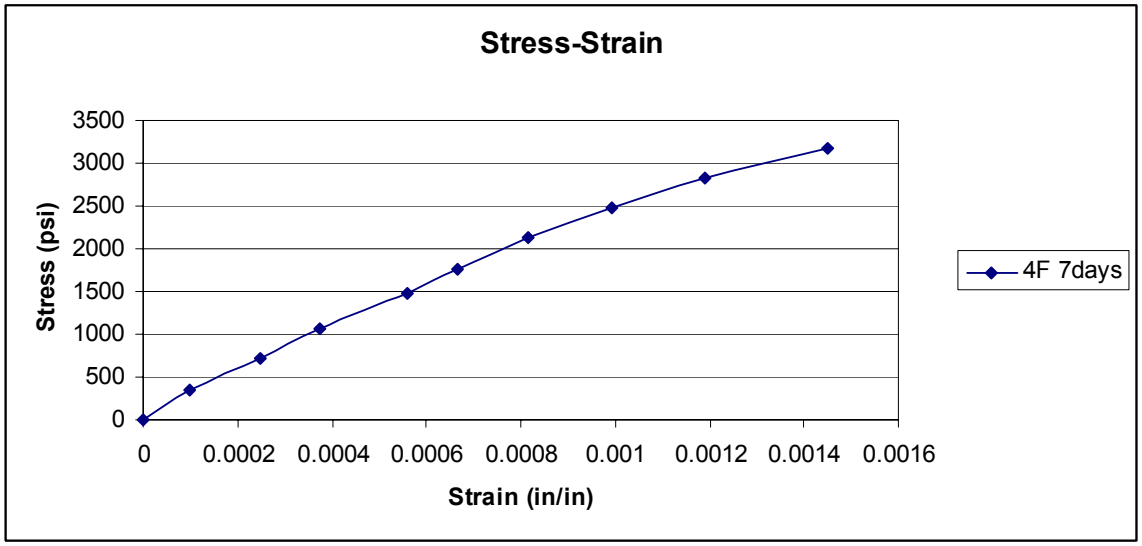

Figure 54 Stress & strain curve- Cylinder 4F at 7 Days

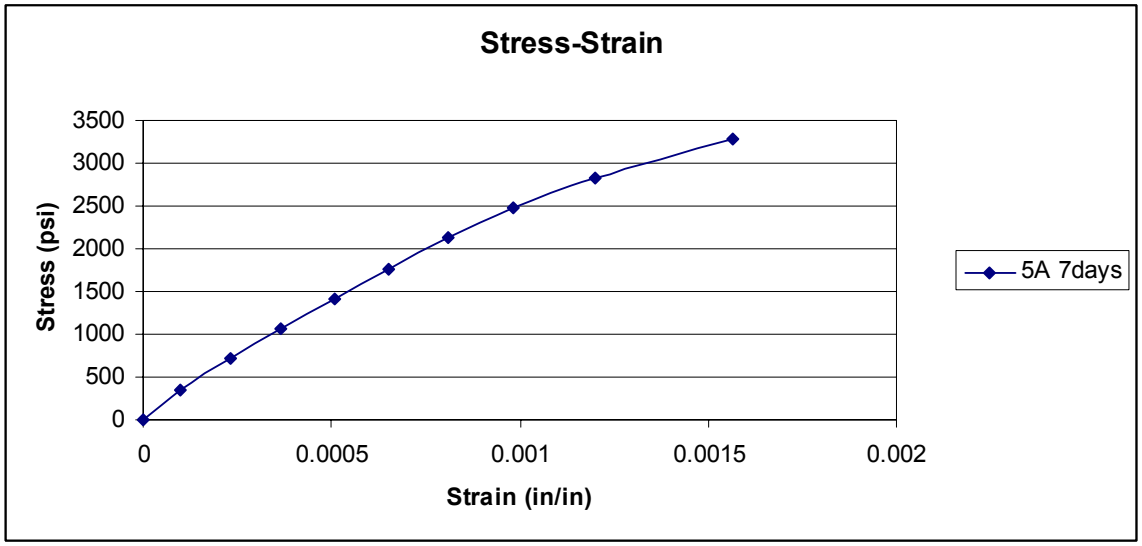

Figure 55 Stress & strain curve- Cylinder 5A at 7 Days

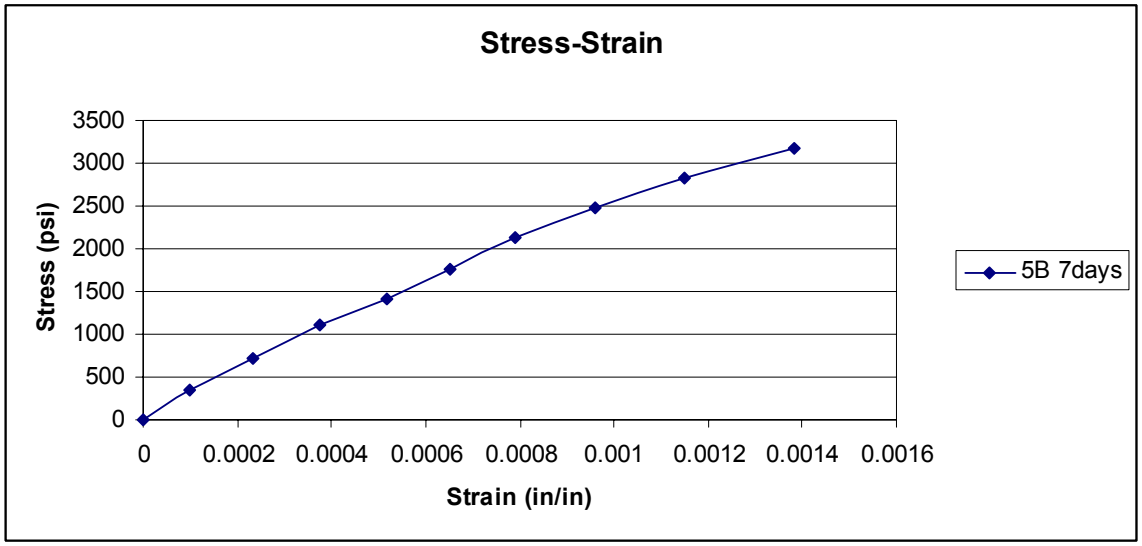

Figure 56 Stress & strain curve- Cylinder 5B at 7 Days

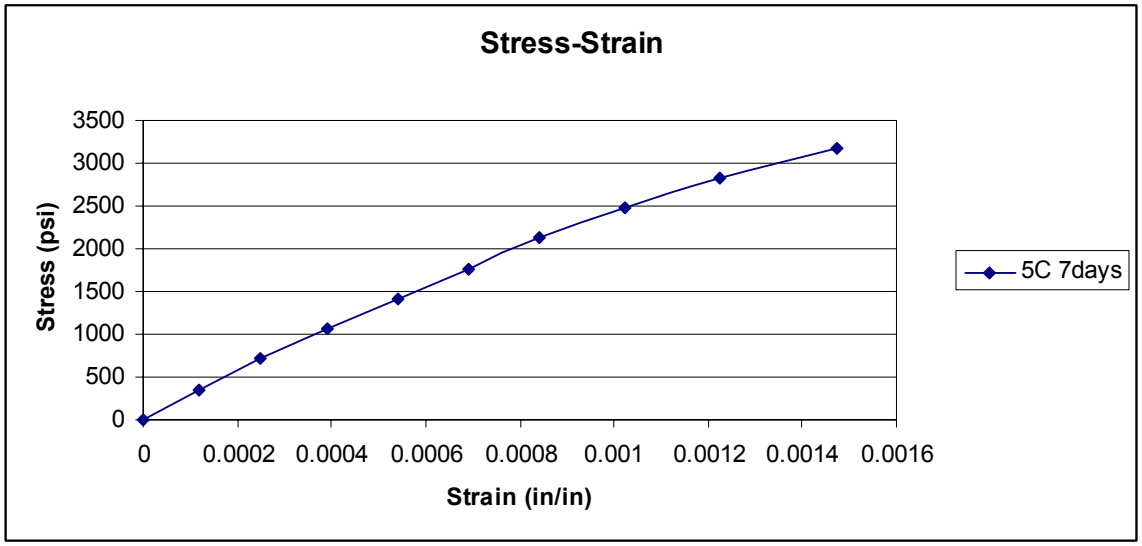

Figure 57 Stress & strain curve- Cylinder 5C at 7 Days

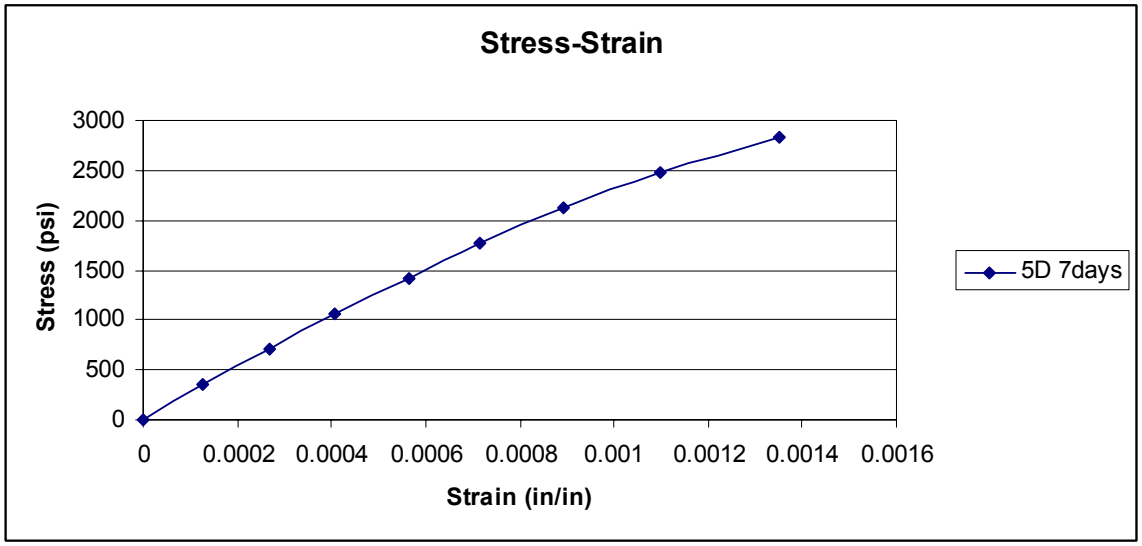

Figure 58 Stress & strain curve- Cylinder 5D at 7 Days

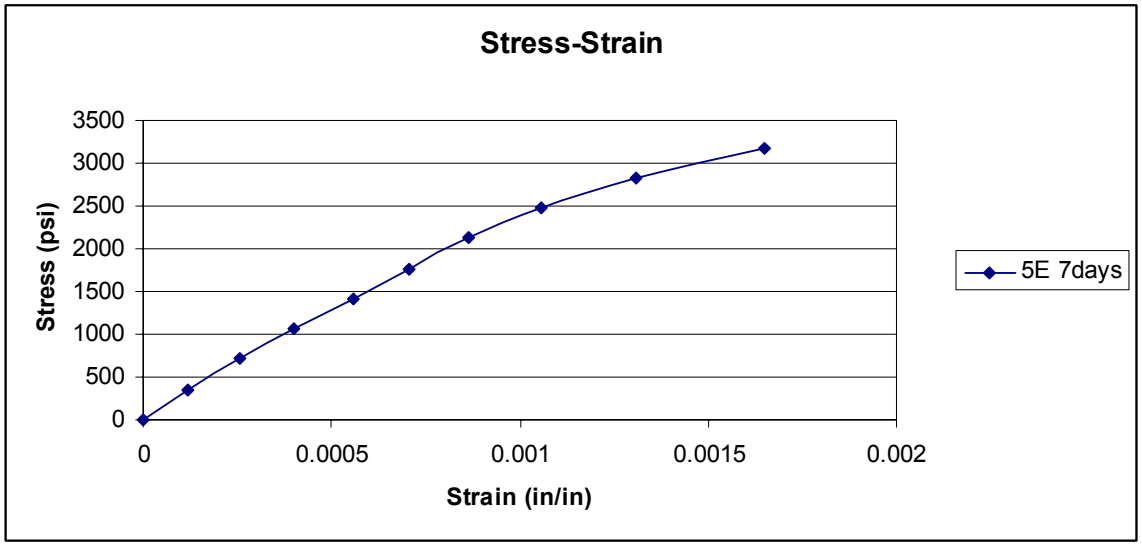

Figure 59 Stress & strain curve- Cylinder 5E at 7 Days

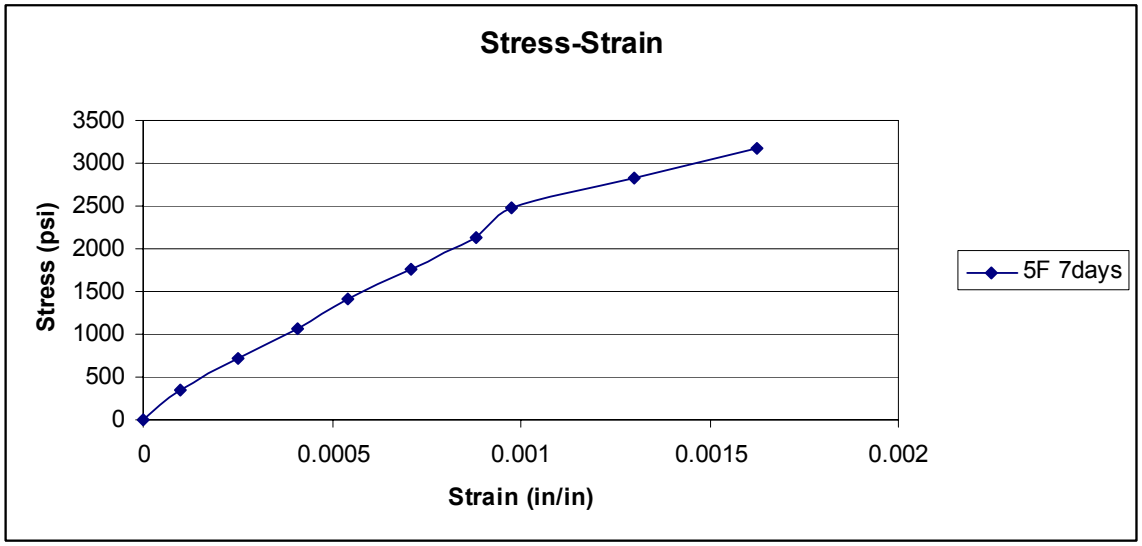

Figure 60 Stress & strain curve- Cylinder 5F at 7 Days

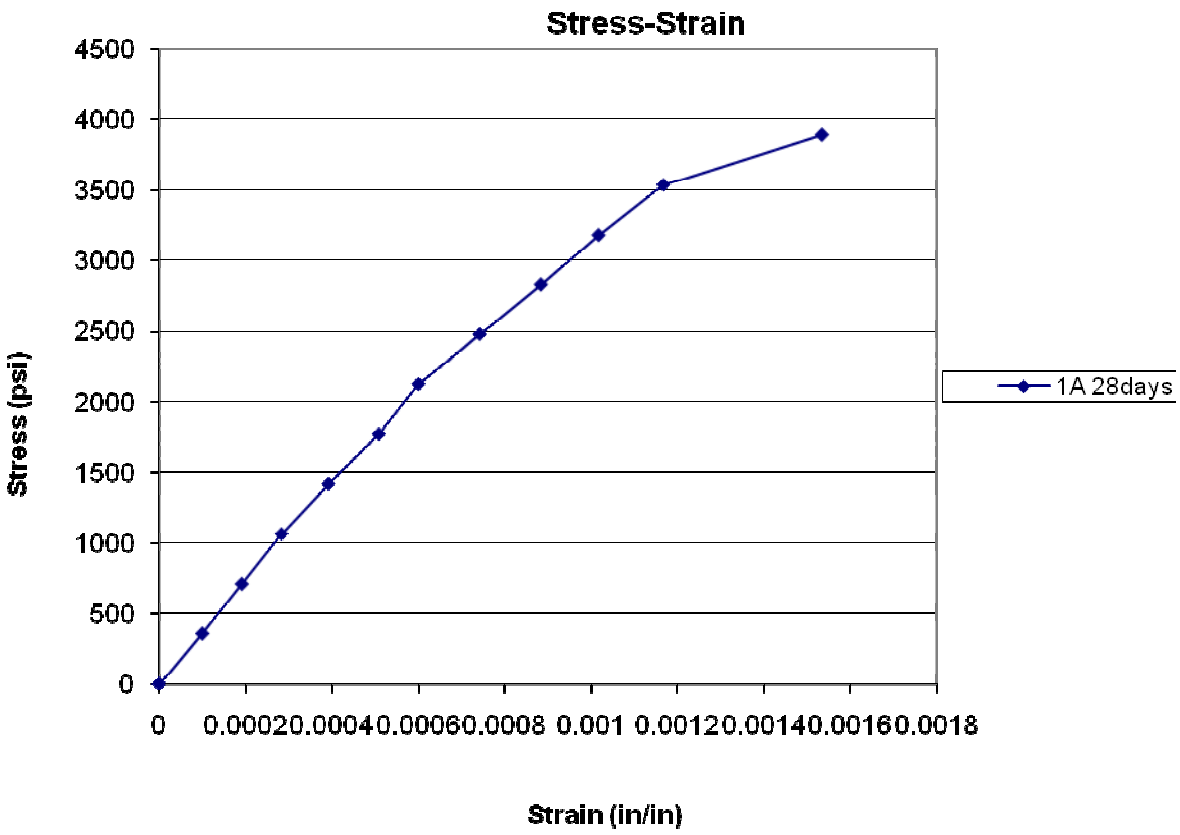

Figure 61 Stress & strain curve- Cylinder 1A at 28 Days

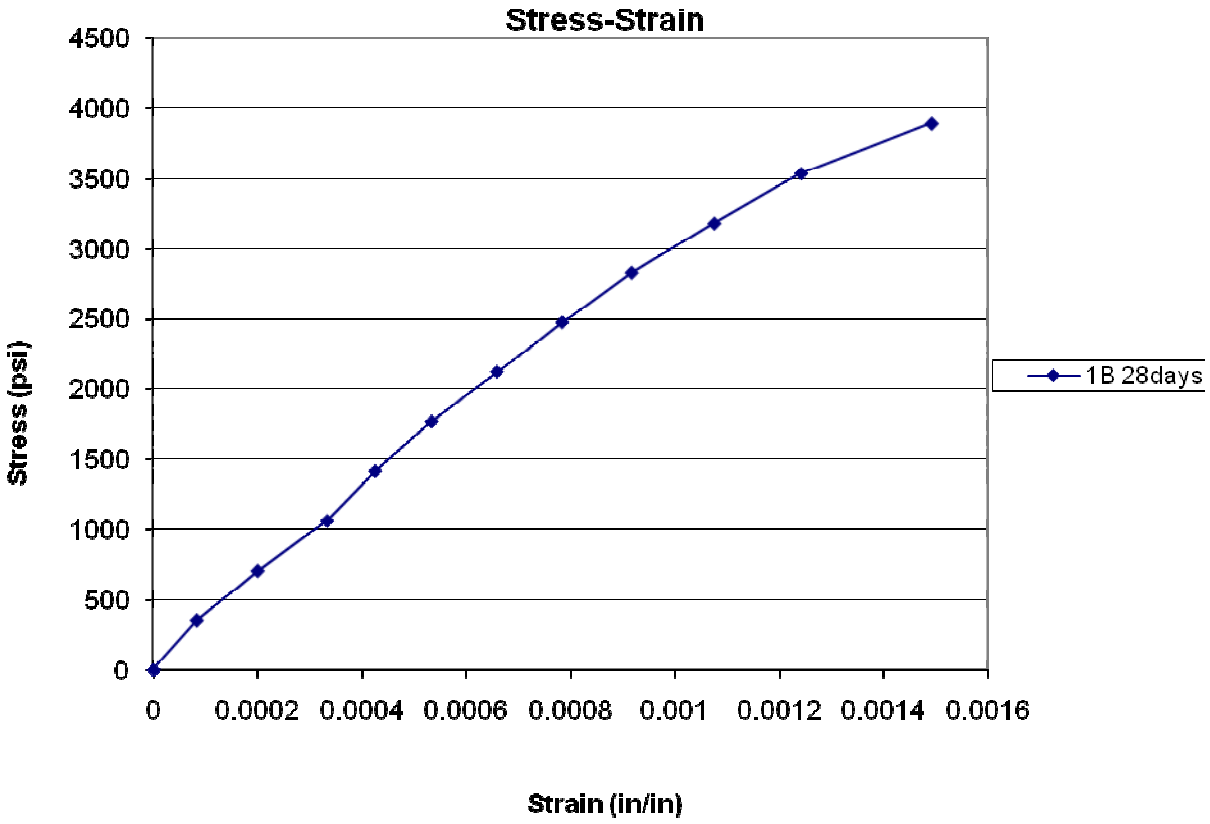

Figure 62 Stress & strain curve- Cylinder 1B at 28 Days

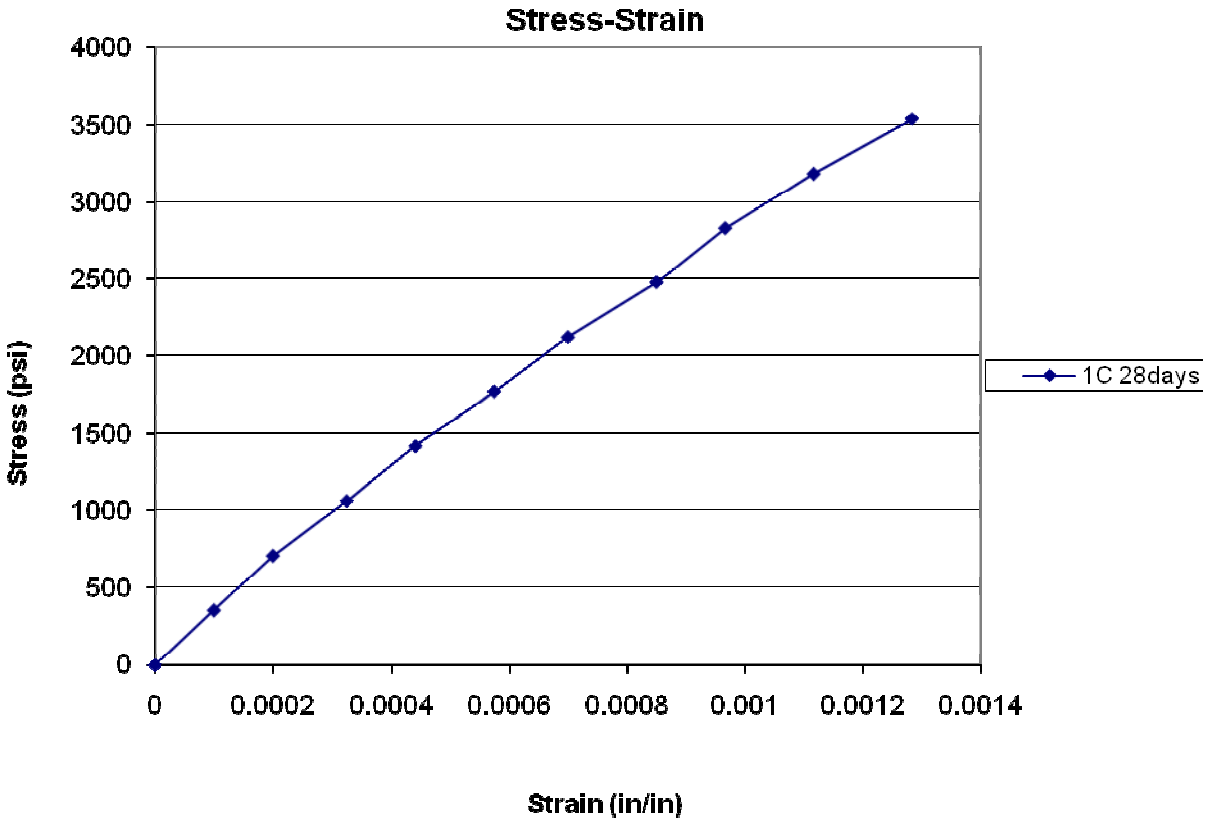

Figure 63 Stress & strain curve- Cylinder 1C at 28 Days

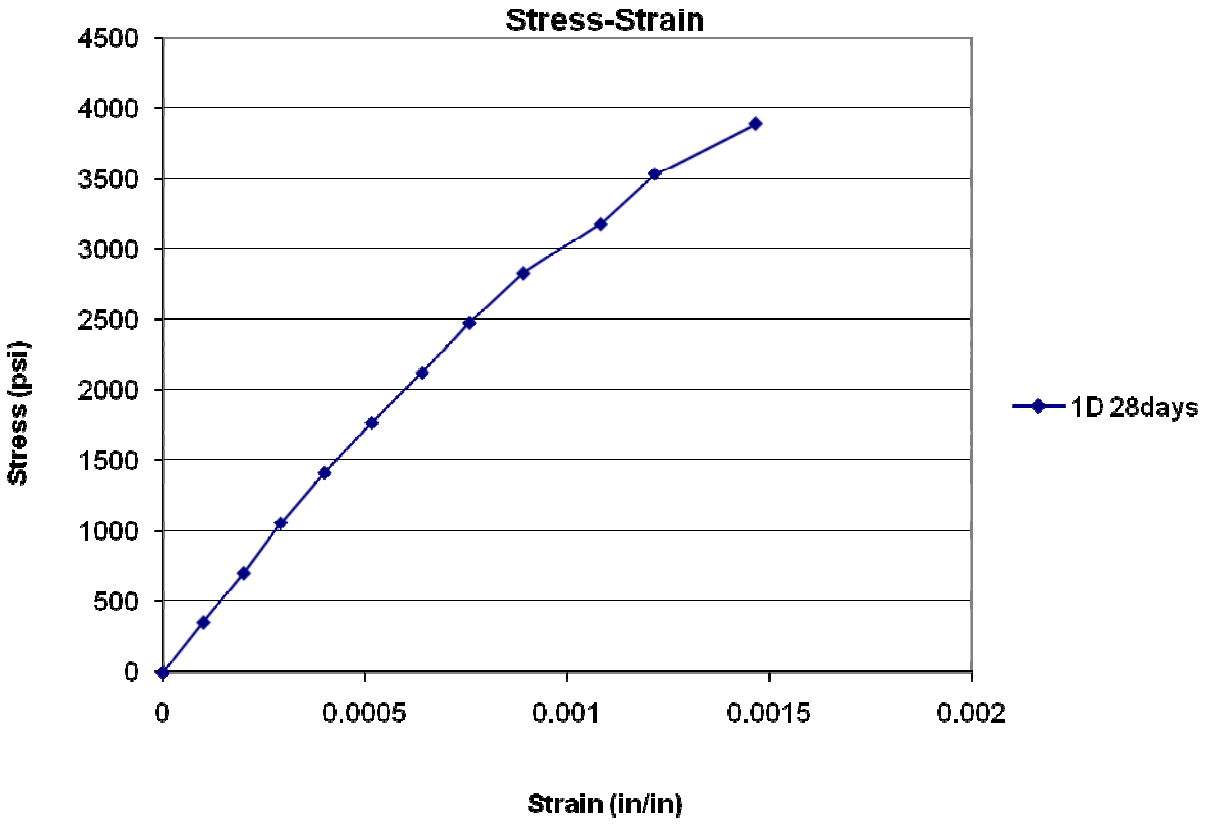

Figure 64 Stress & strain curve- Cylinder 1D at 28 Days

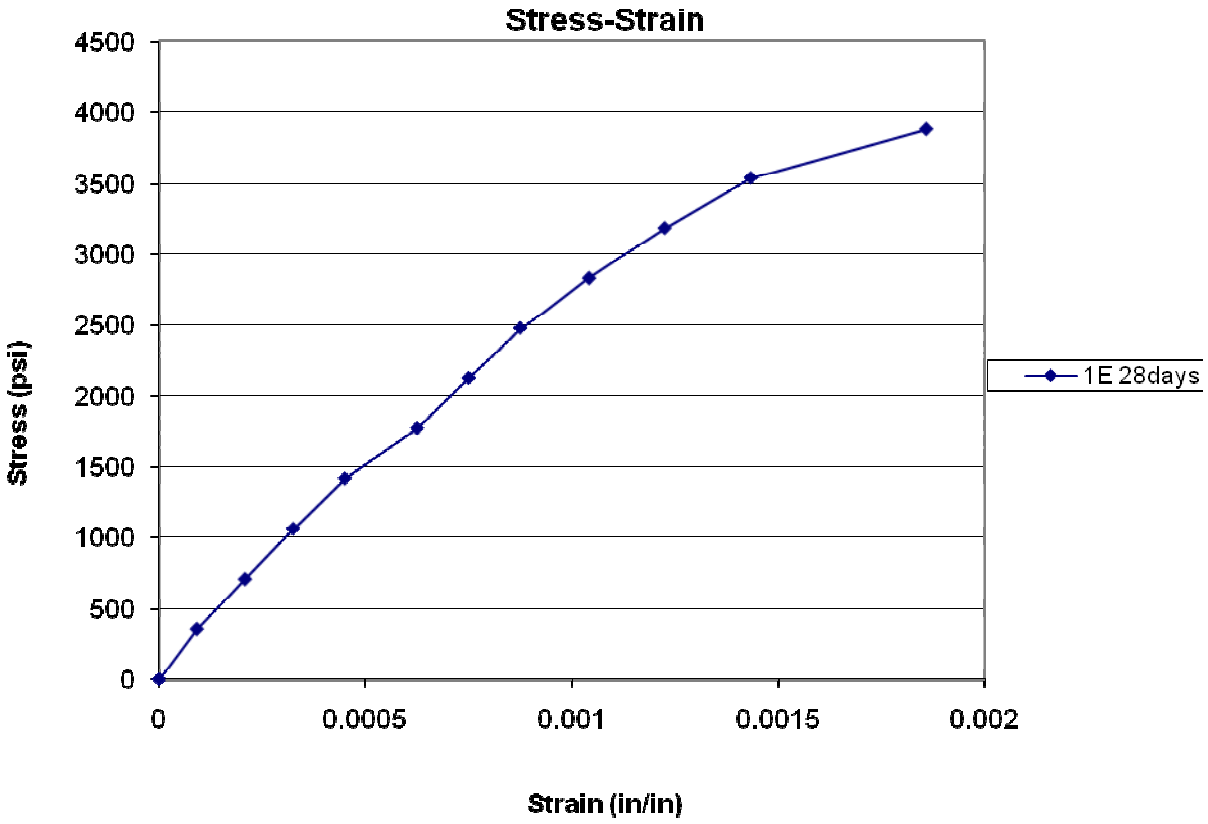

Figure 65 Stress & strain curve- Cylinder 1E at 28 Days

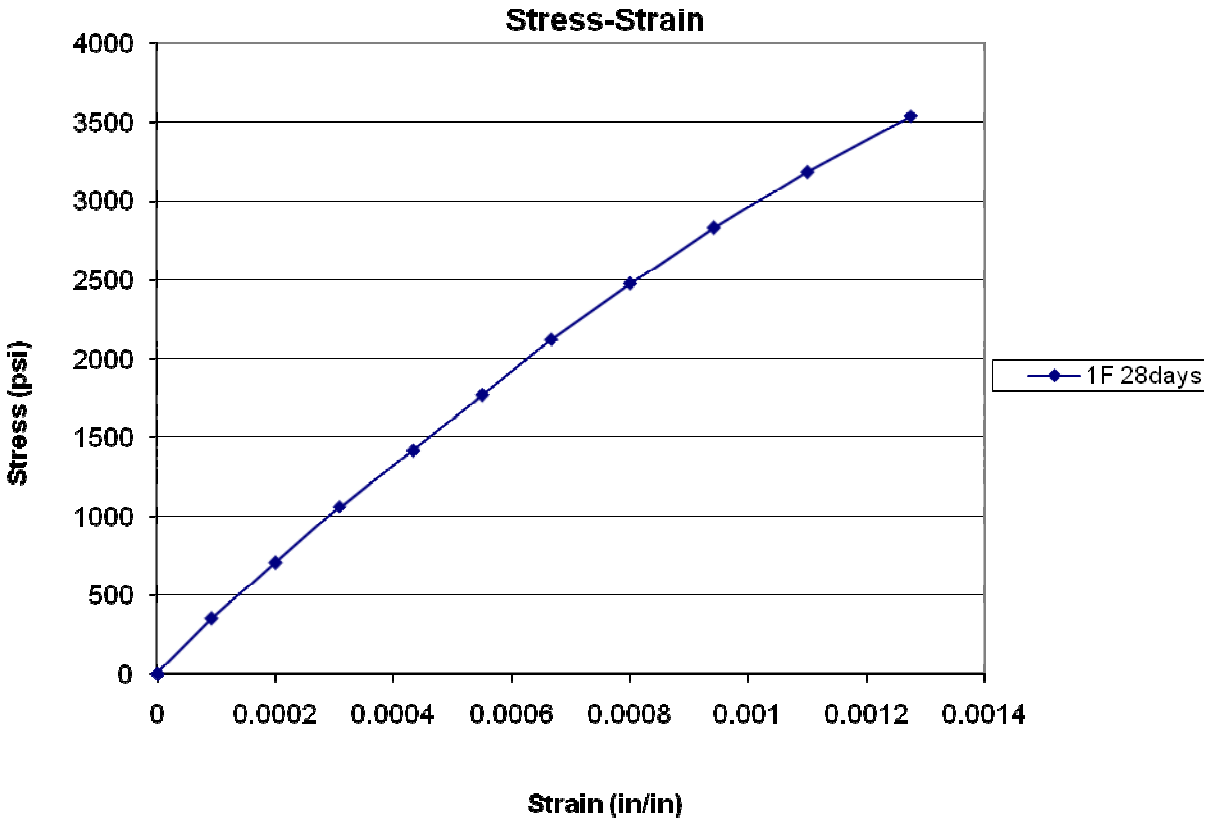

Figure 66 Stress & strain curve- Cylinder 1F at 28 Days

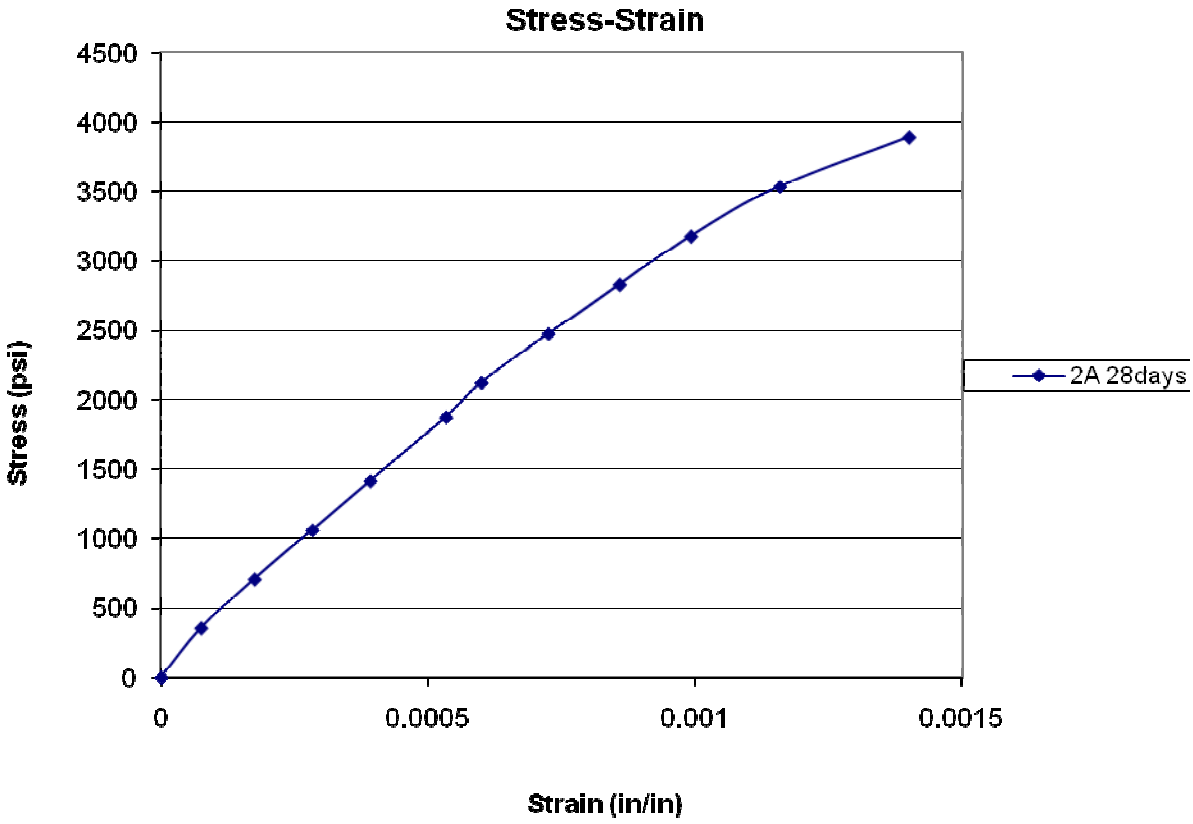

Figure 67 Stress & strain curve- Cylinder 2A at 28 Days

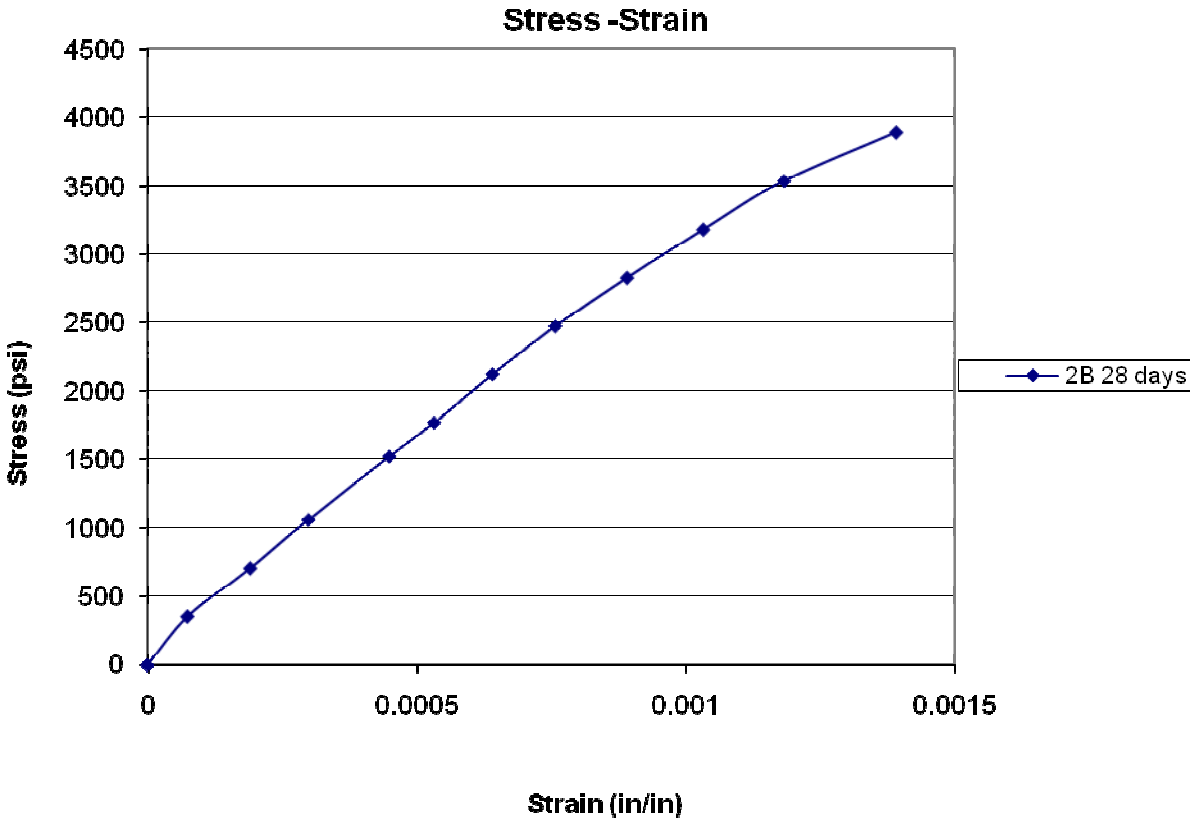

Figure 68 Stress & strain curve- Cylinder 2B at 28 Days

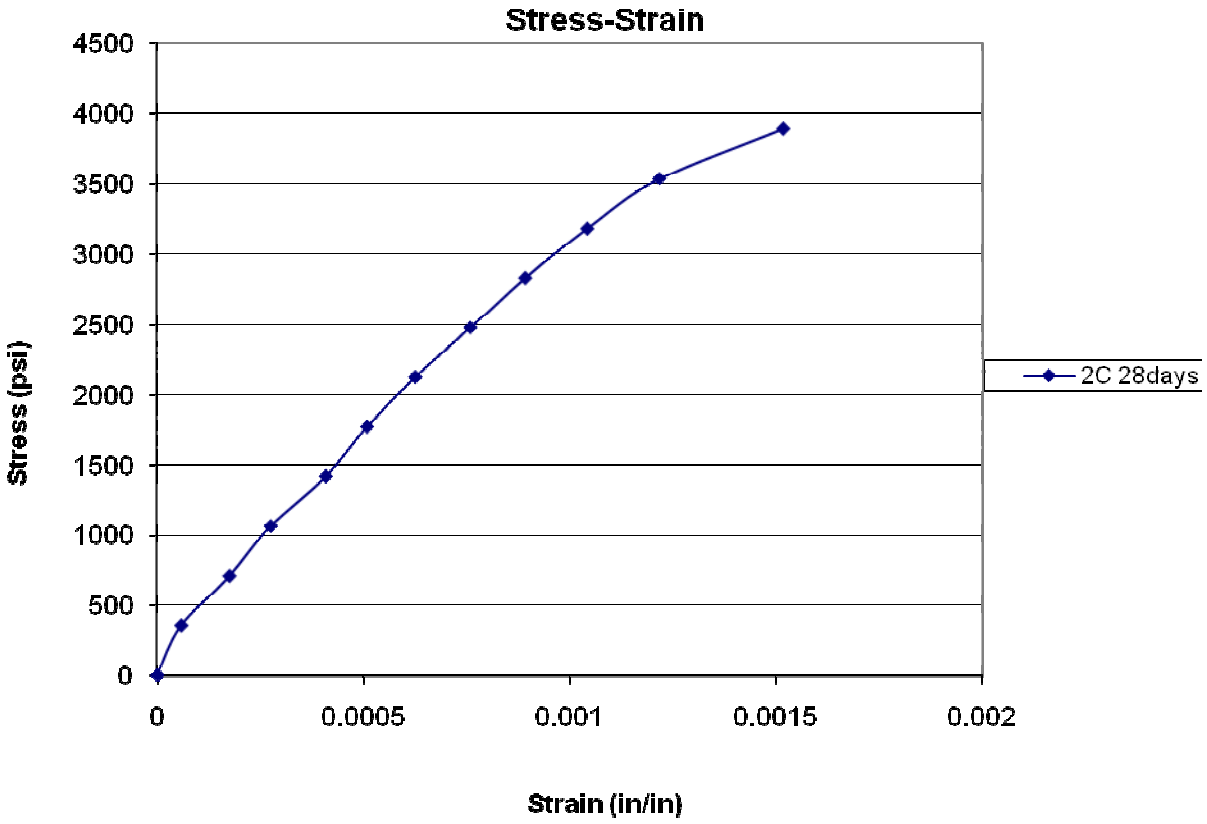

Figure 69 Stress & strain curve- Cylinder 2C at 28 Days

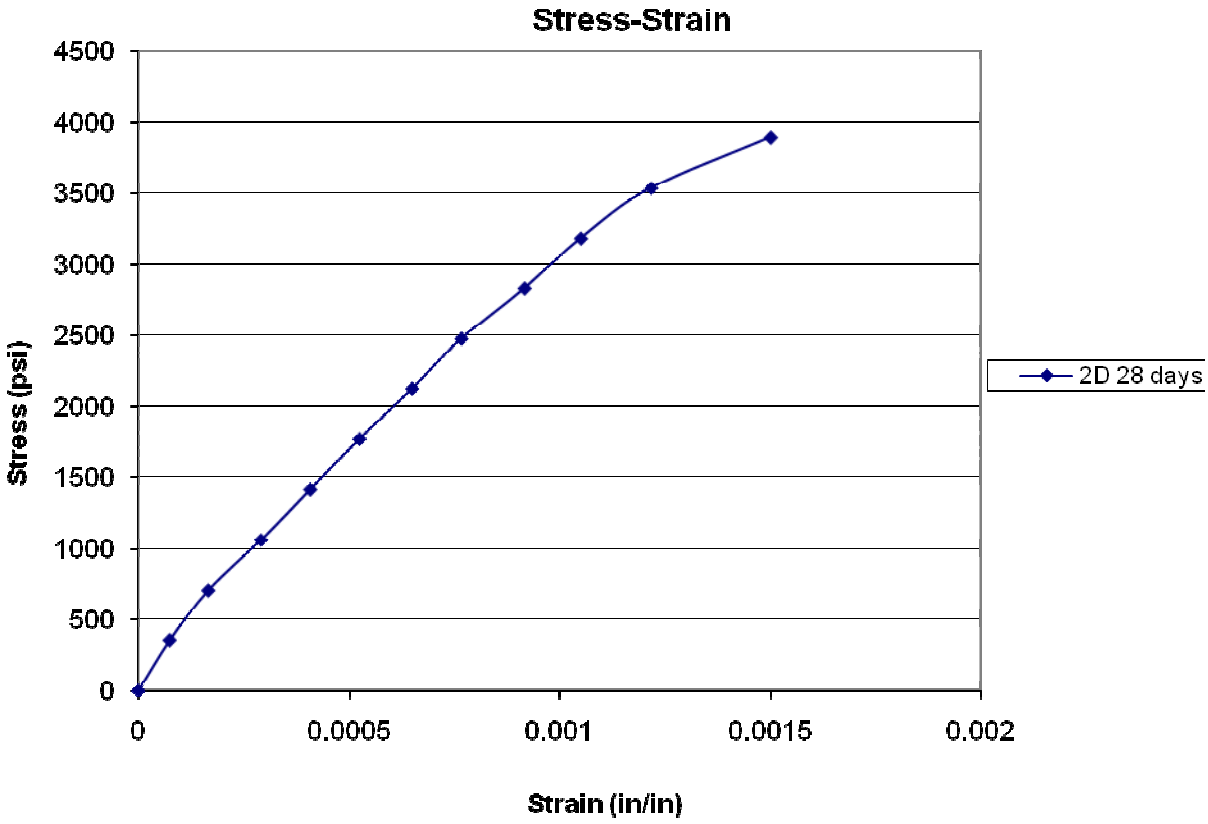

Figure 70 Stress & strain curve- Cylinder 2D at 28 Days

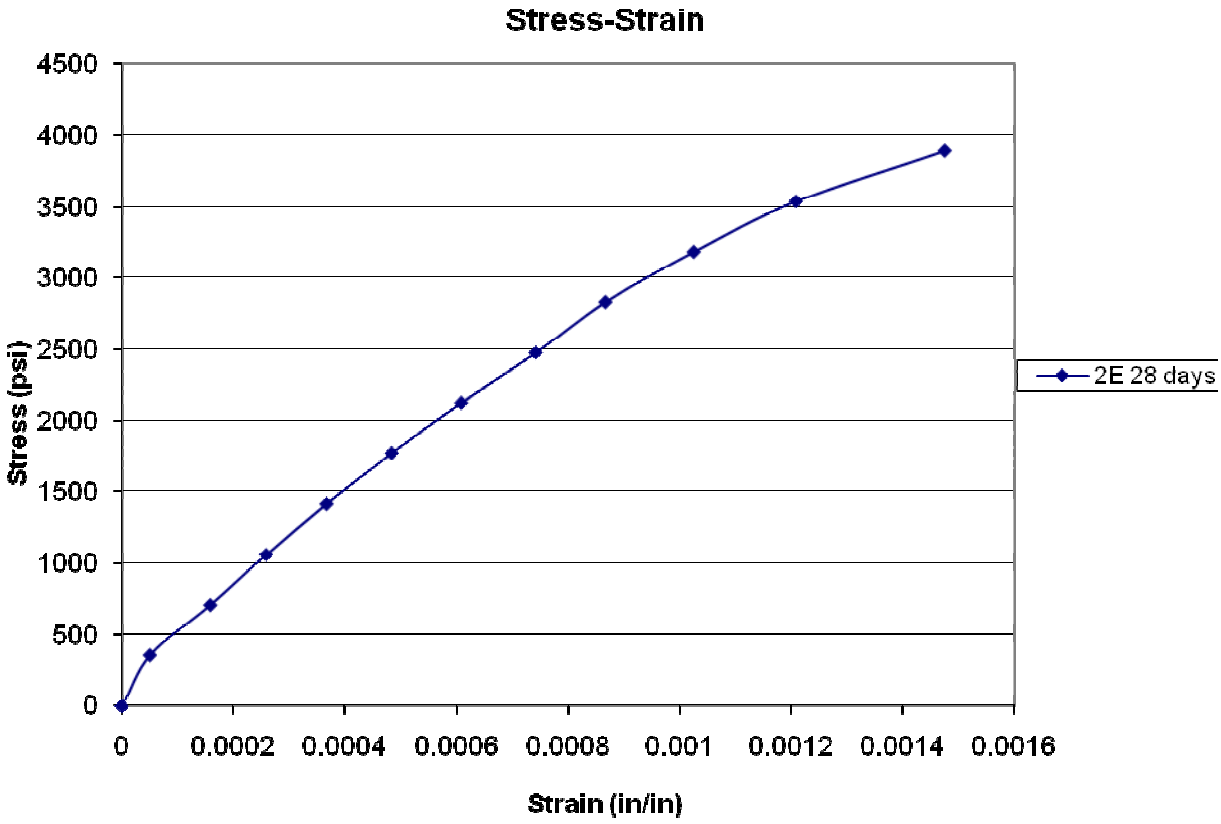

Figure 71 Stress & strain curve- Cylinder 2E at 28 Days

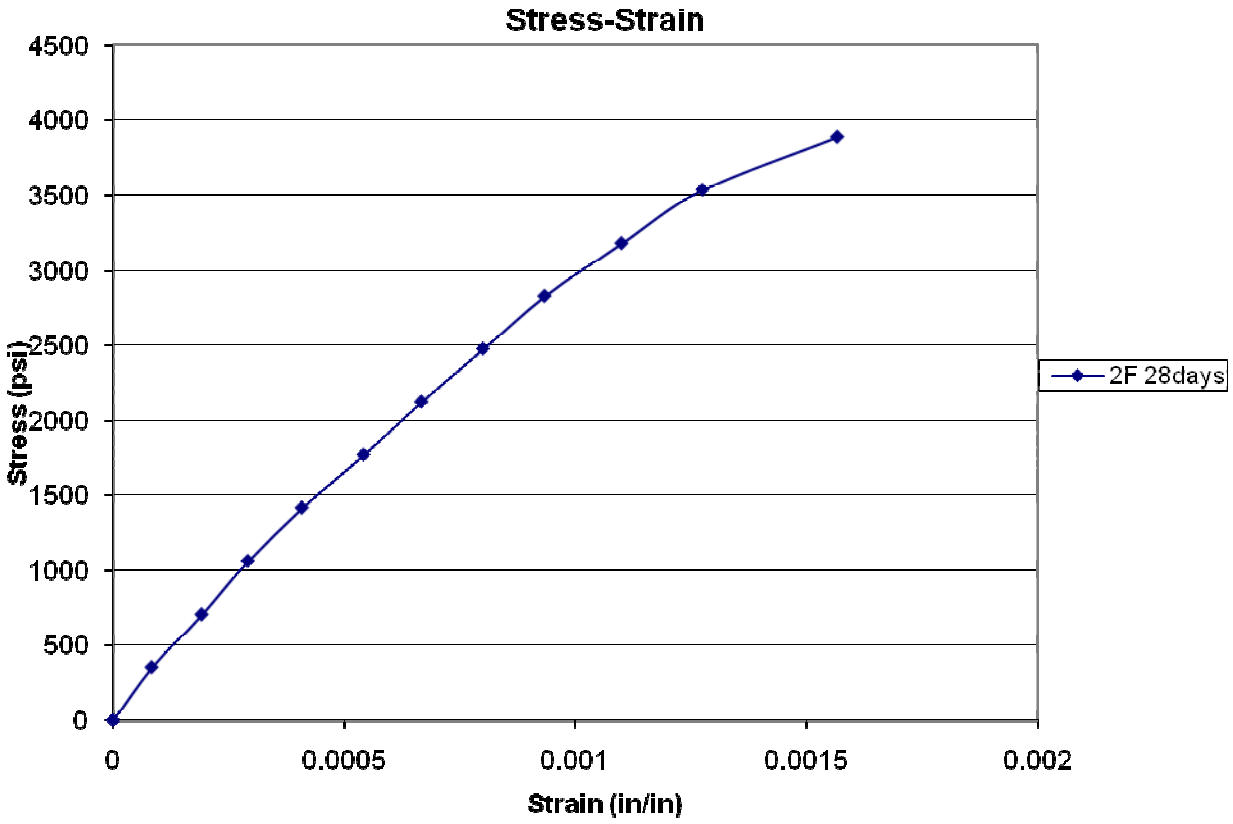

Figure 72 Stress & strain curve- Cylinder 2F at 28 Days

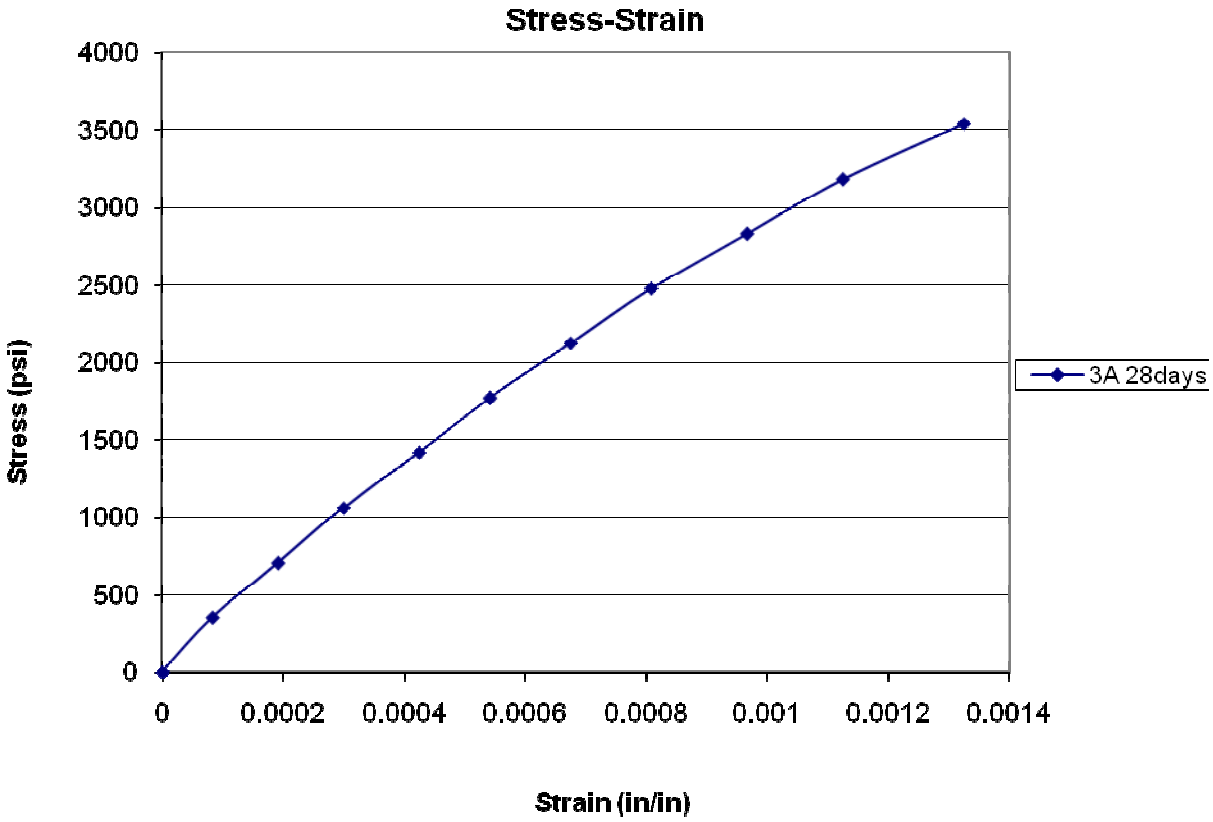

Figure 73 Stress & strain curve- Cylinder 3A at 28 Days

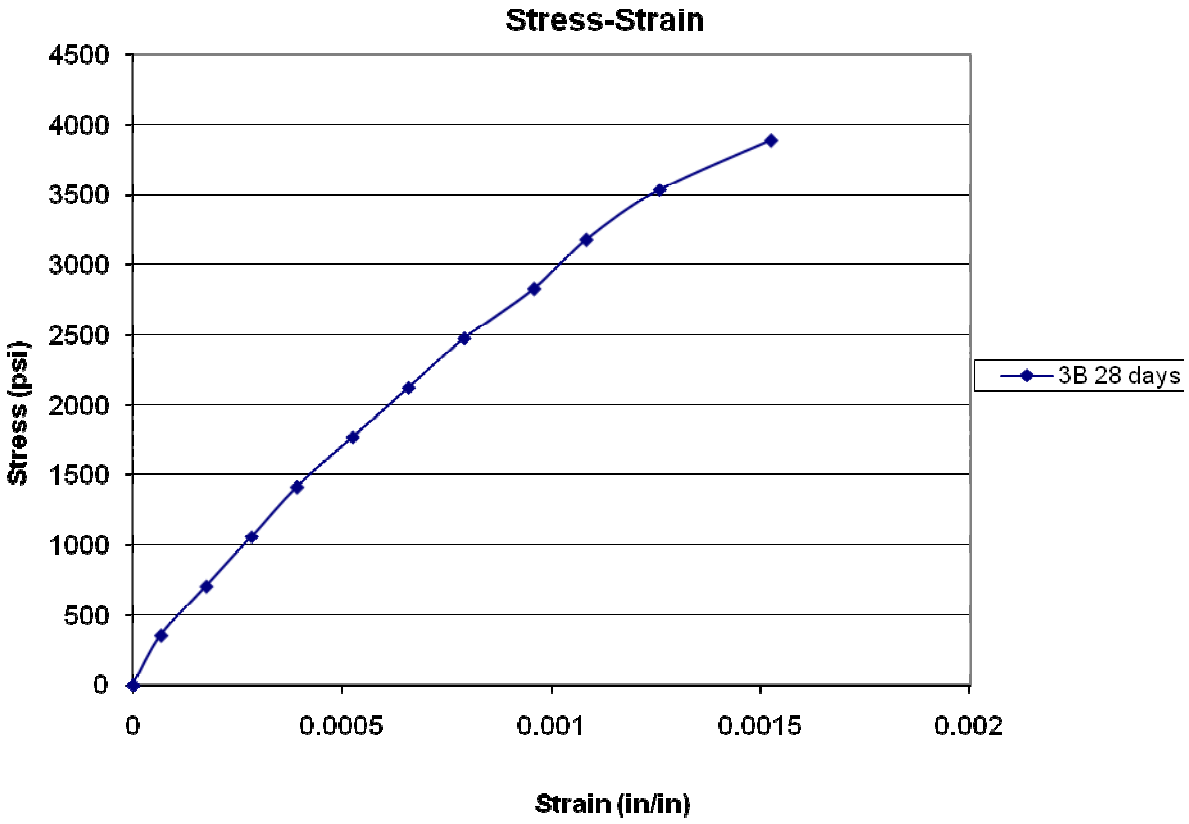

Figure 74 Stress & strain curve- Cylinder 3B at 28 Days

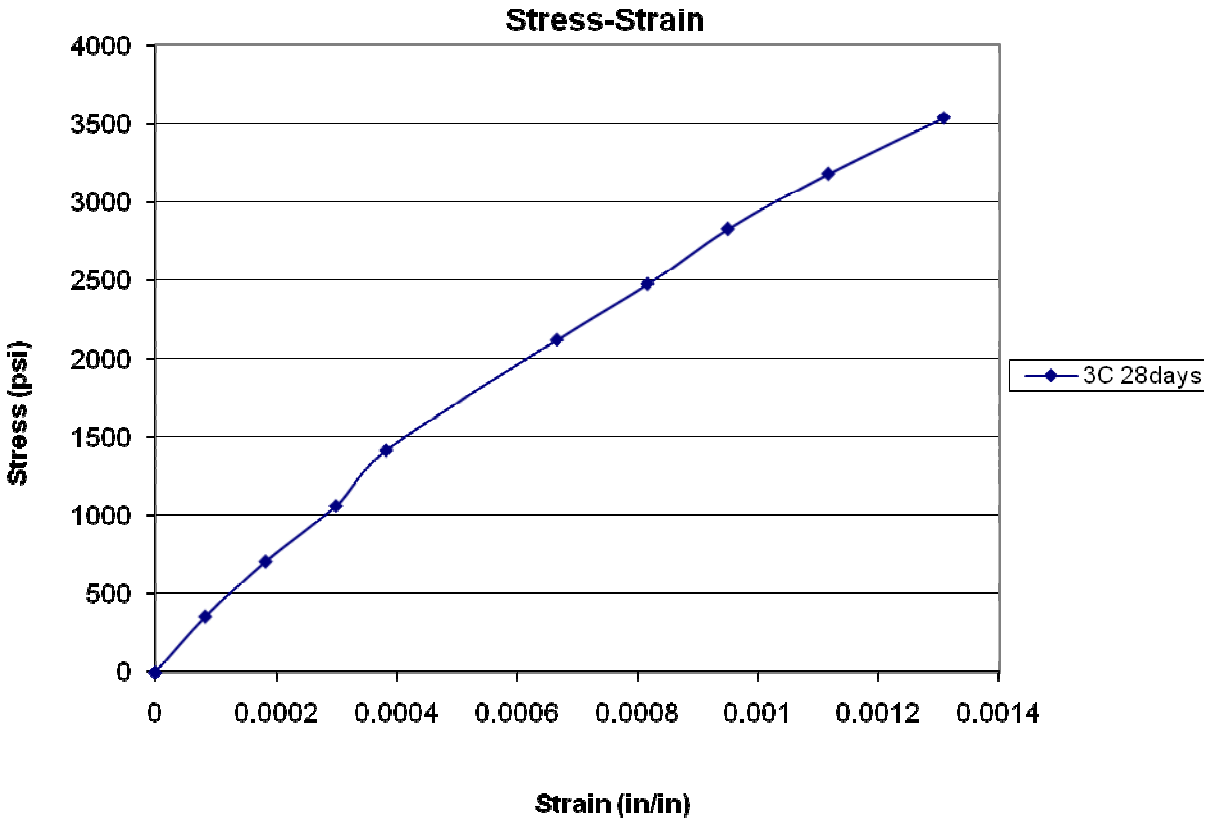

Figure 75 Stress & strain curve- Cylinder 3C at 28 Days

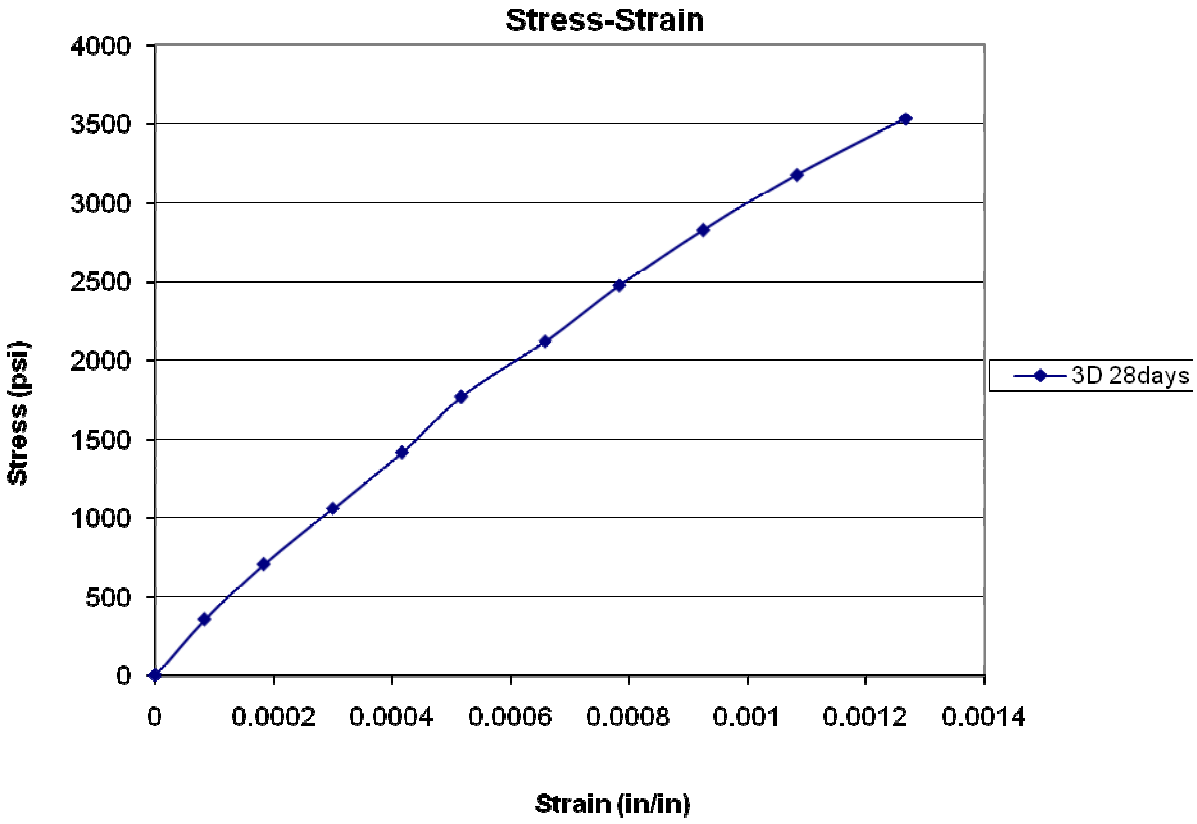

Figure 76 Stress & strain curve- Cylinder 3D at 28 Days

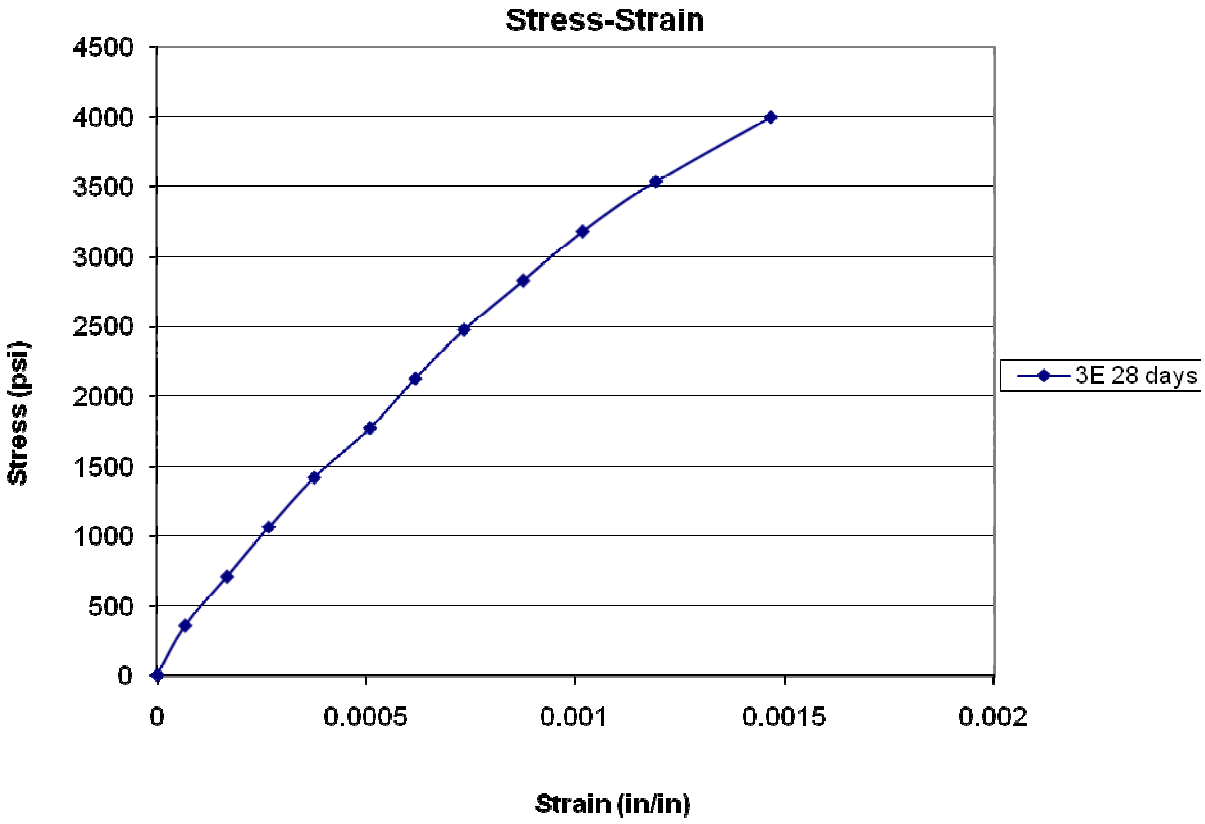

Figure 77 Stress & strain curve- Cylinder 3E at 28 Days

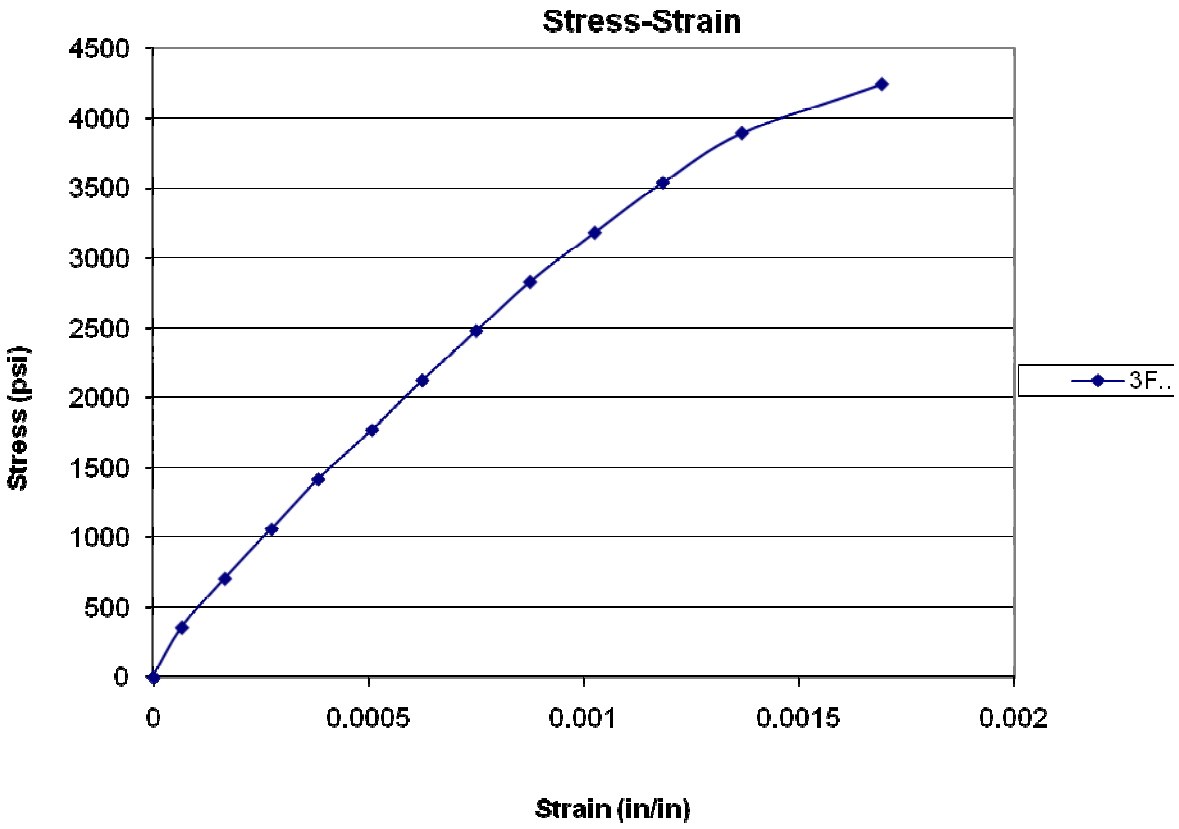

Figure 78 Stress & strain curve- Cylinder 3F at 28 Days

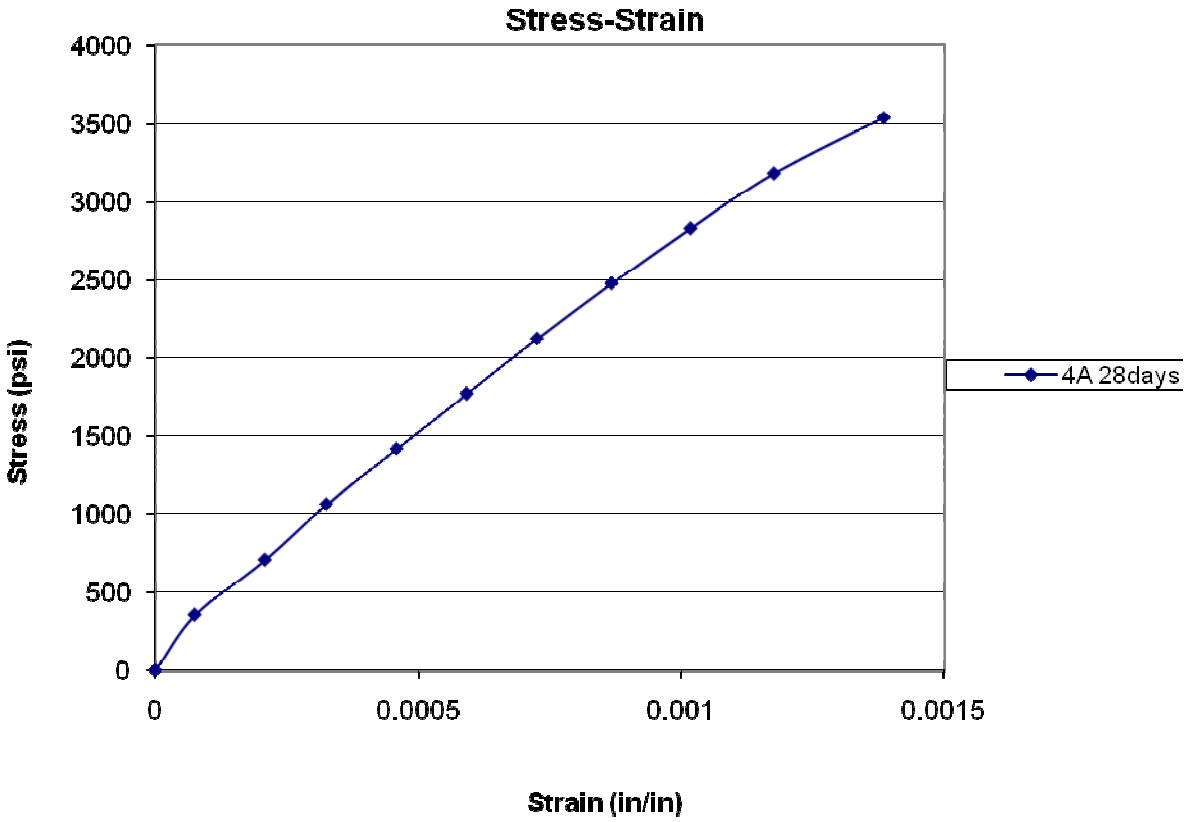

Figure 79 Stress & strain curve - Cylinder 4A at 28 Days

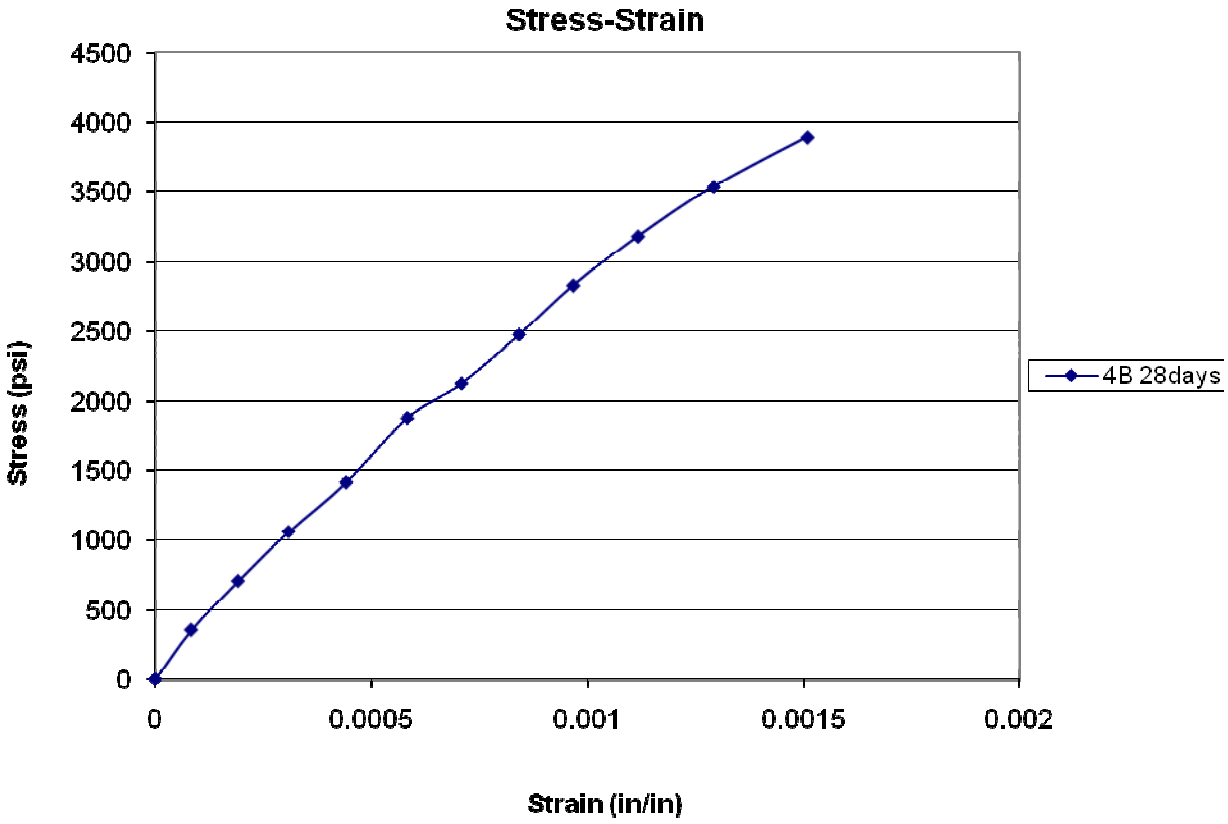

Figure 80 Stress & strain curve - Cylinder 4B at 28 Days

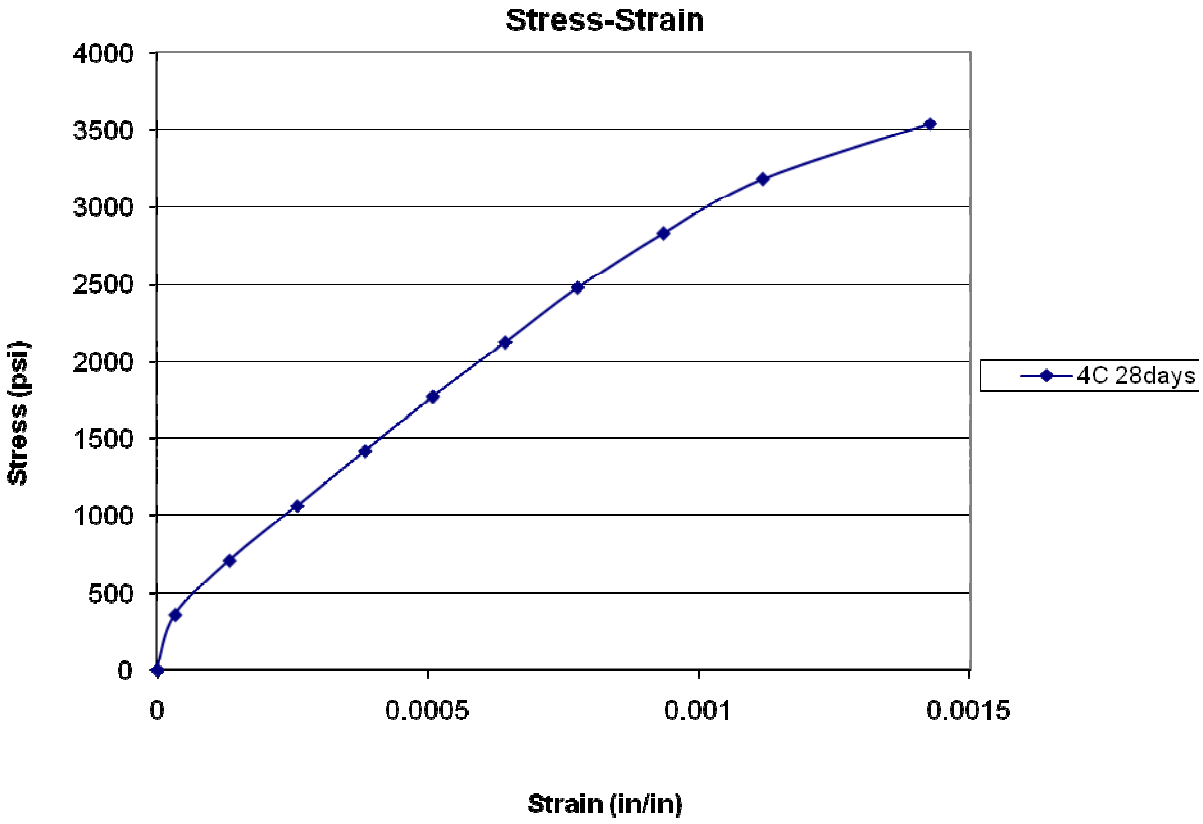

Figure 81 Stress & strain curve - Cylinder 4C at 28 Days

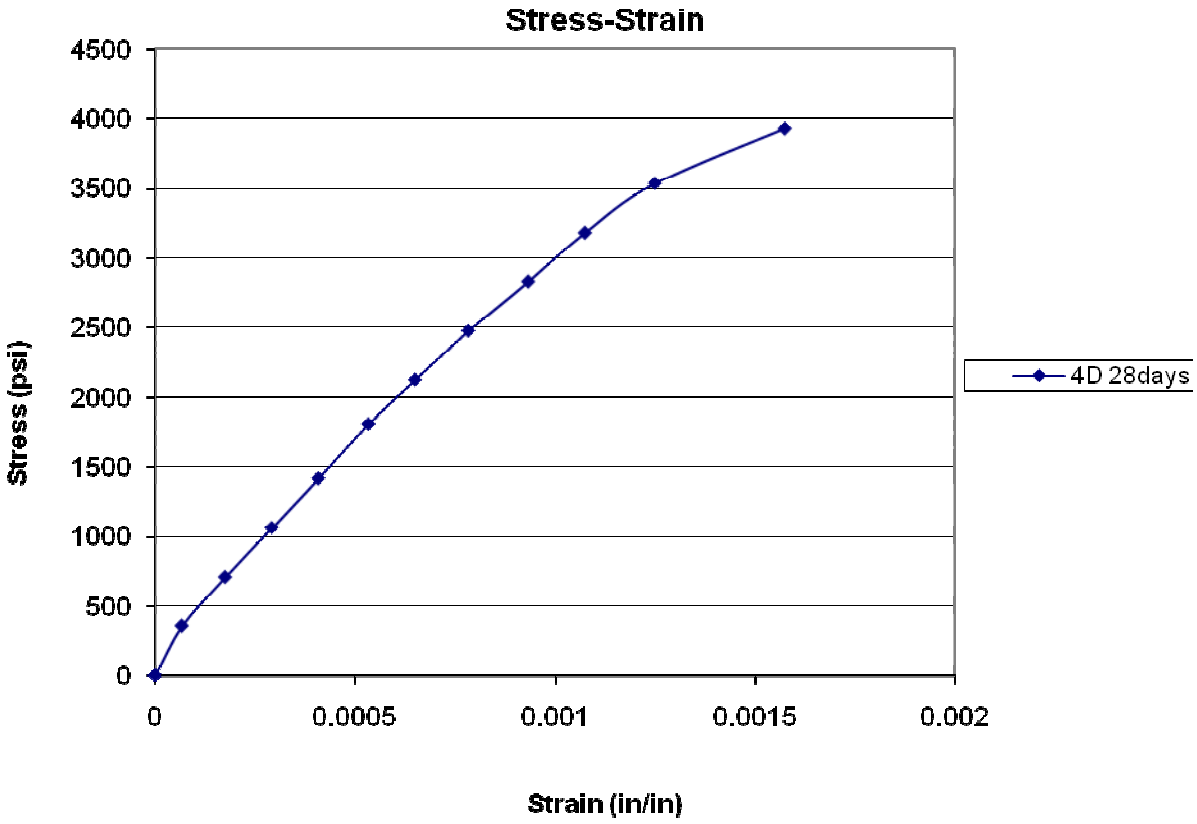

Figure 82 Stress & strain curve - Cylinder 4D at 28 Days

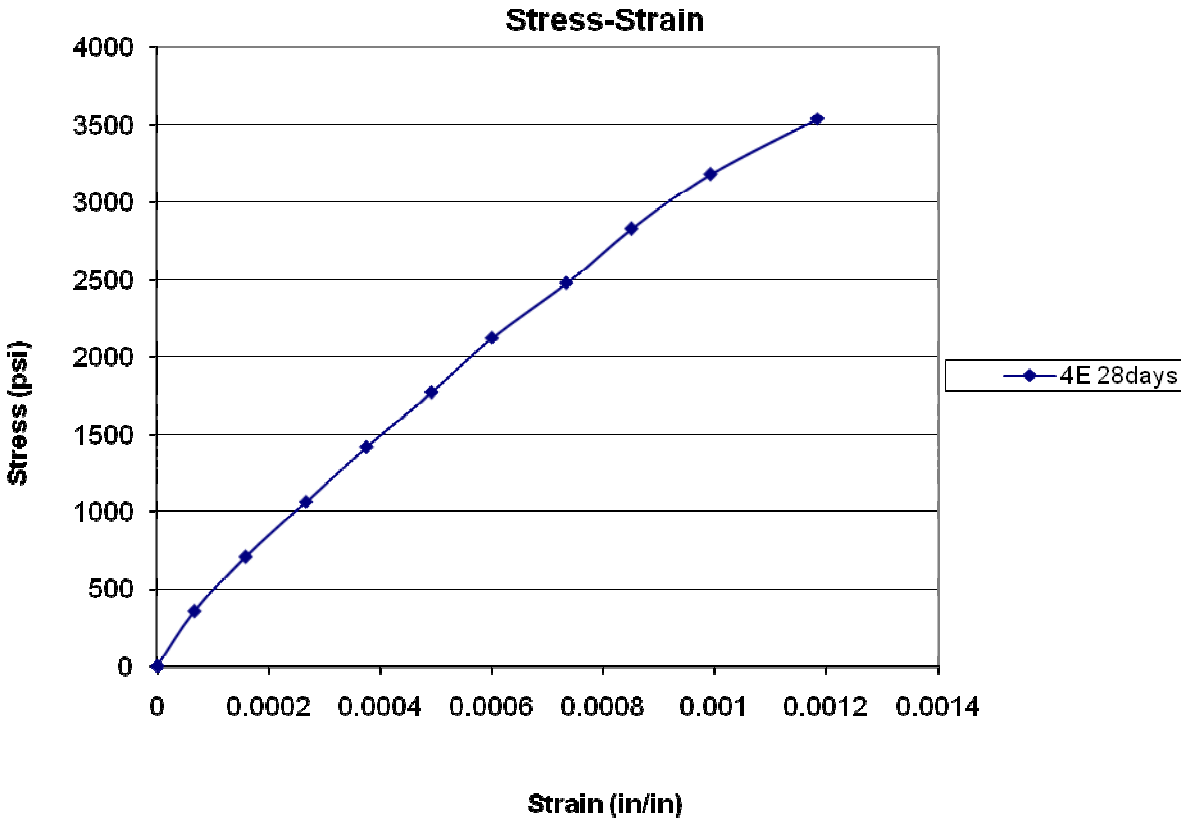

Figure 83 Stress & strain curve - Cylinder 4E at 28 Days

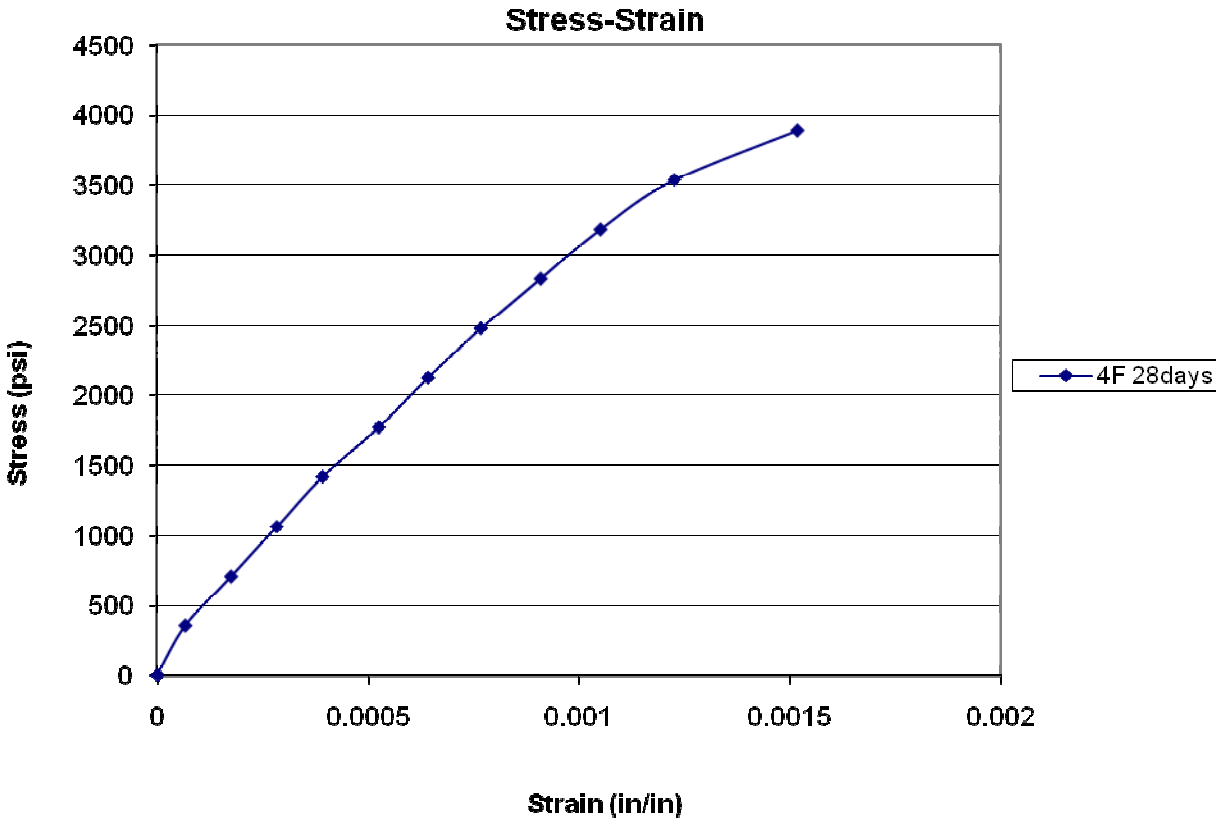

Figure 84 Stress & strain curve - Cylinder 4F at 28 Days

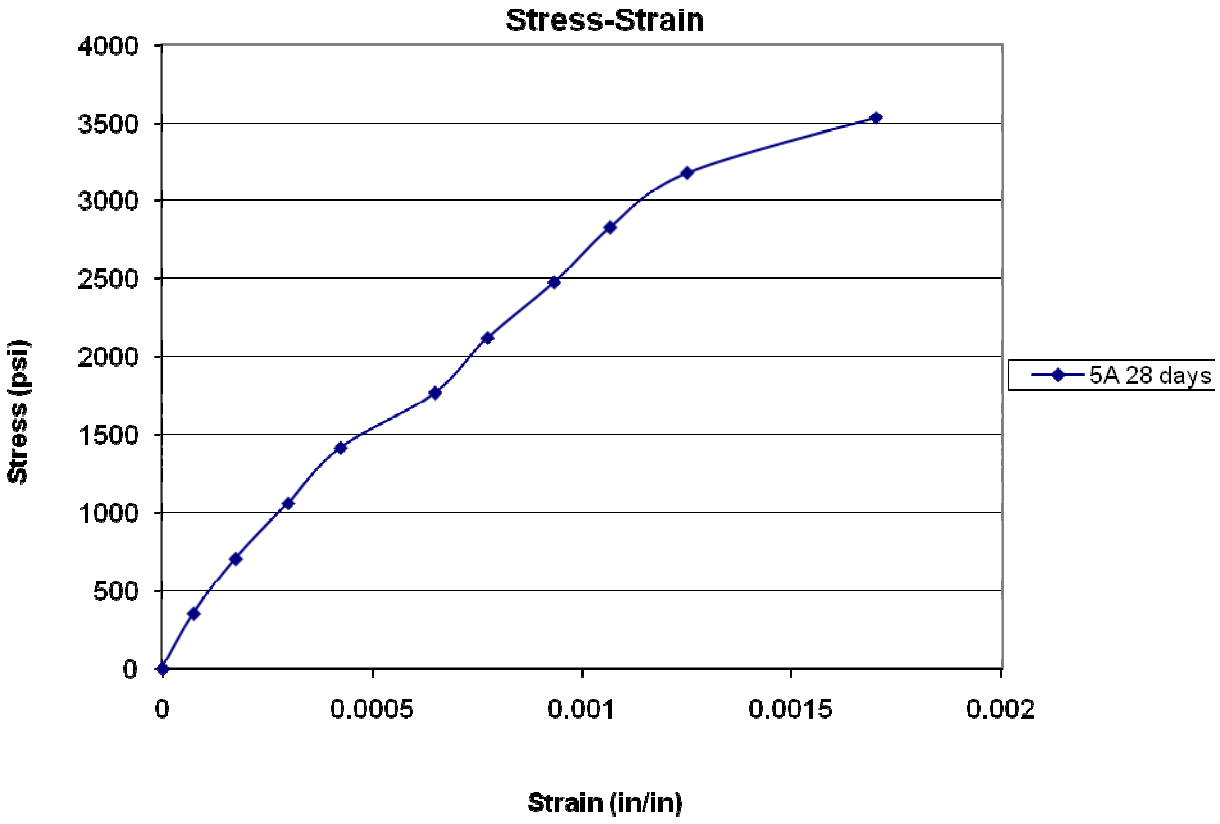

Figure 85 Stress & strain curve - Cylinder 5A at 28 Days

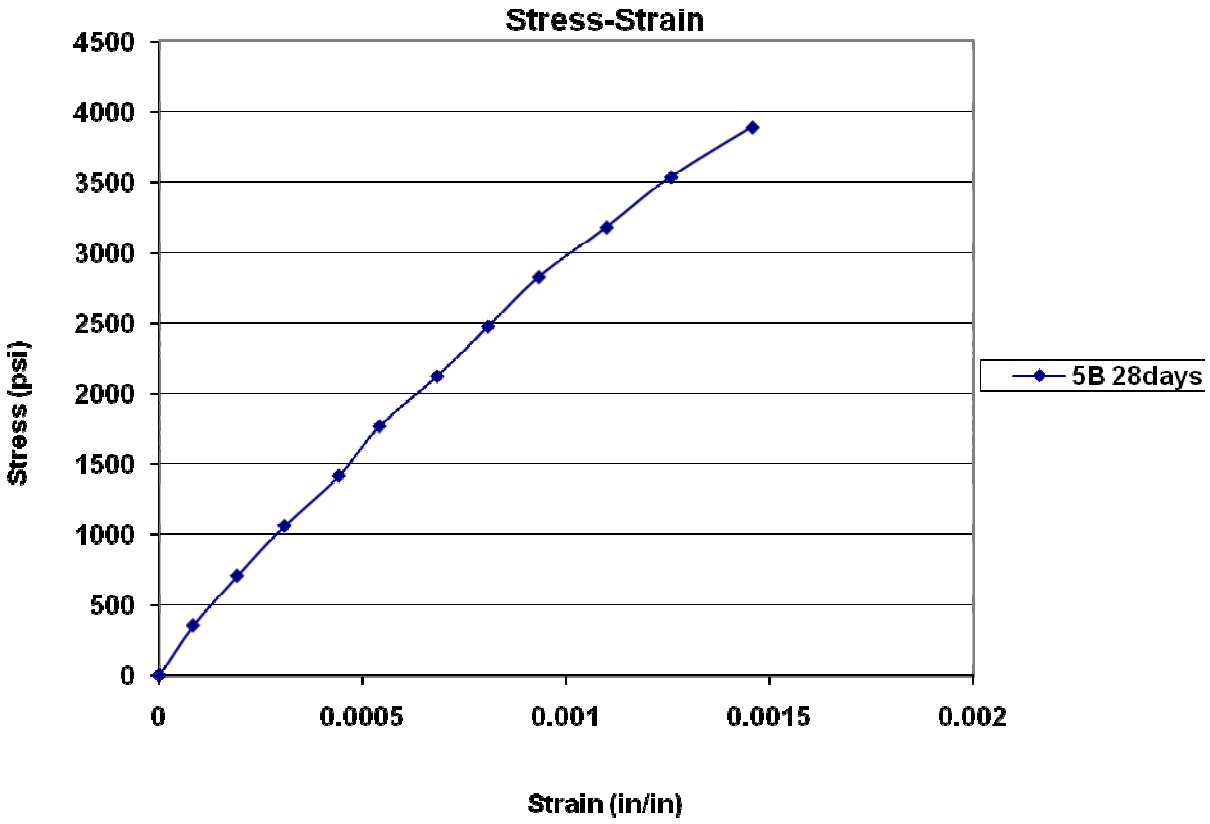

Figure 86 Stress & strain curve - Cylinder 5B at 28 Days

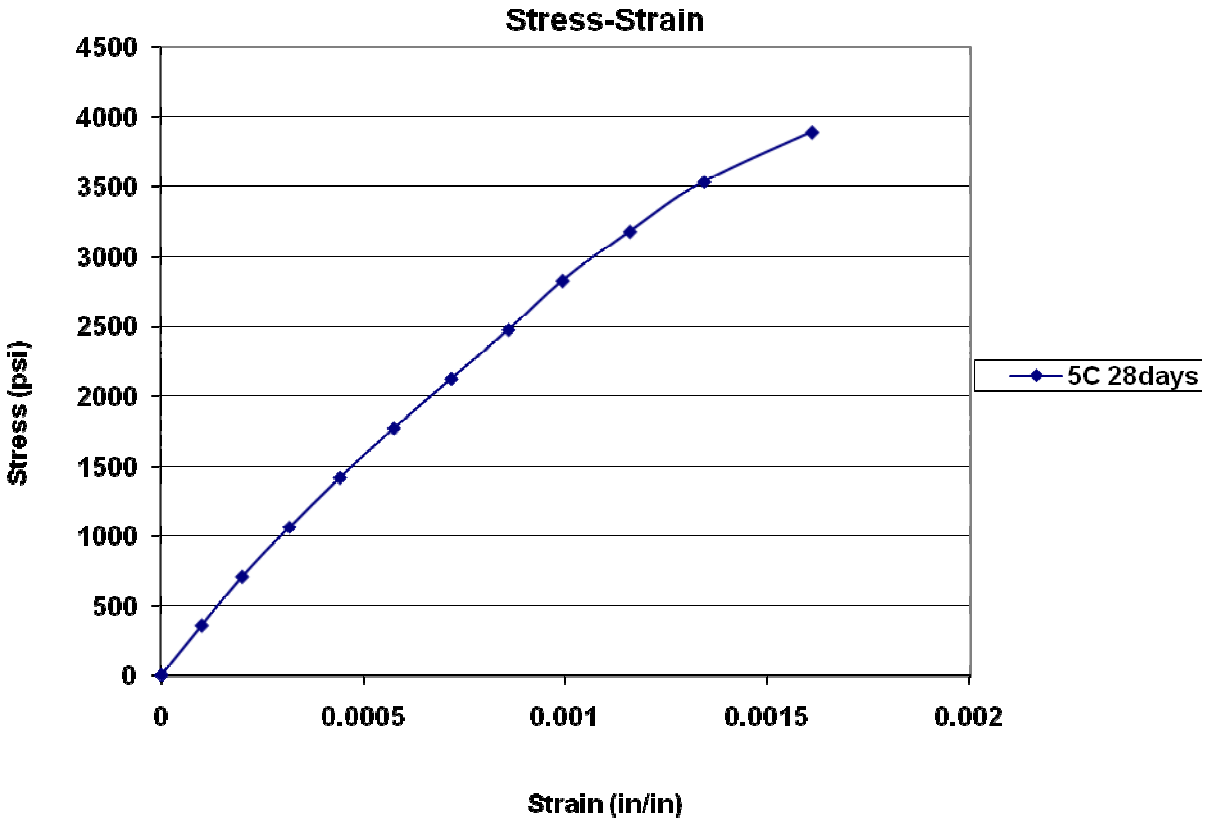

Figure 87 Stress & strain curve - Cylinder 5C at 28 Days

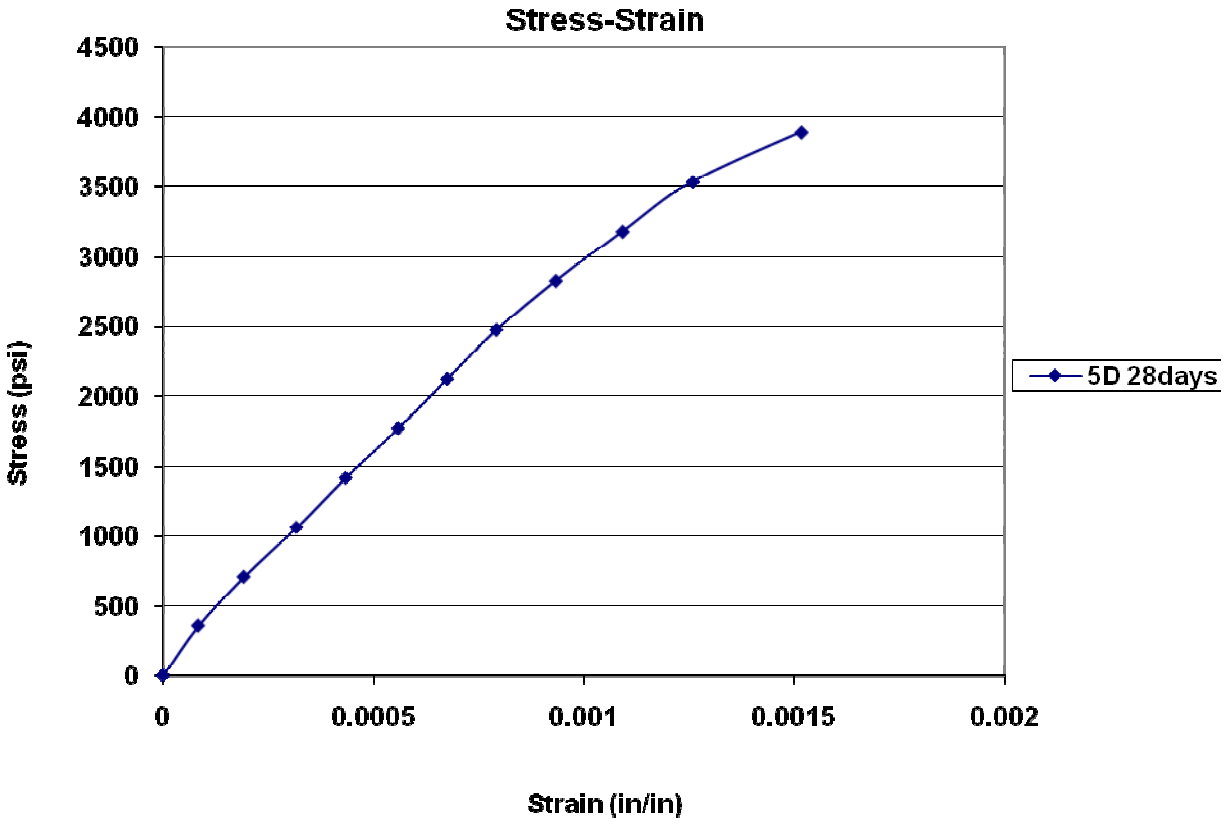

Figure 88 Stress & strain curve - Cylinder 5D at 28 Days

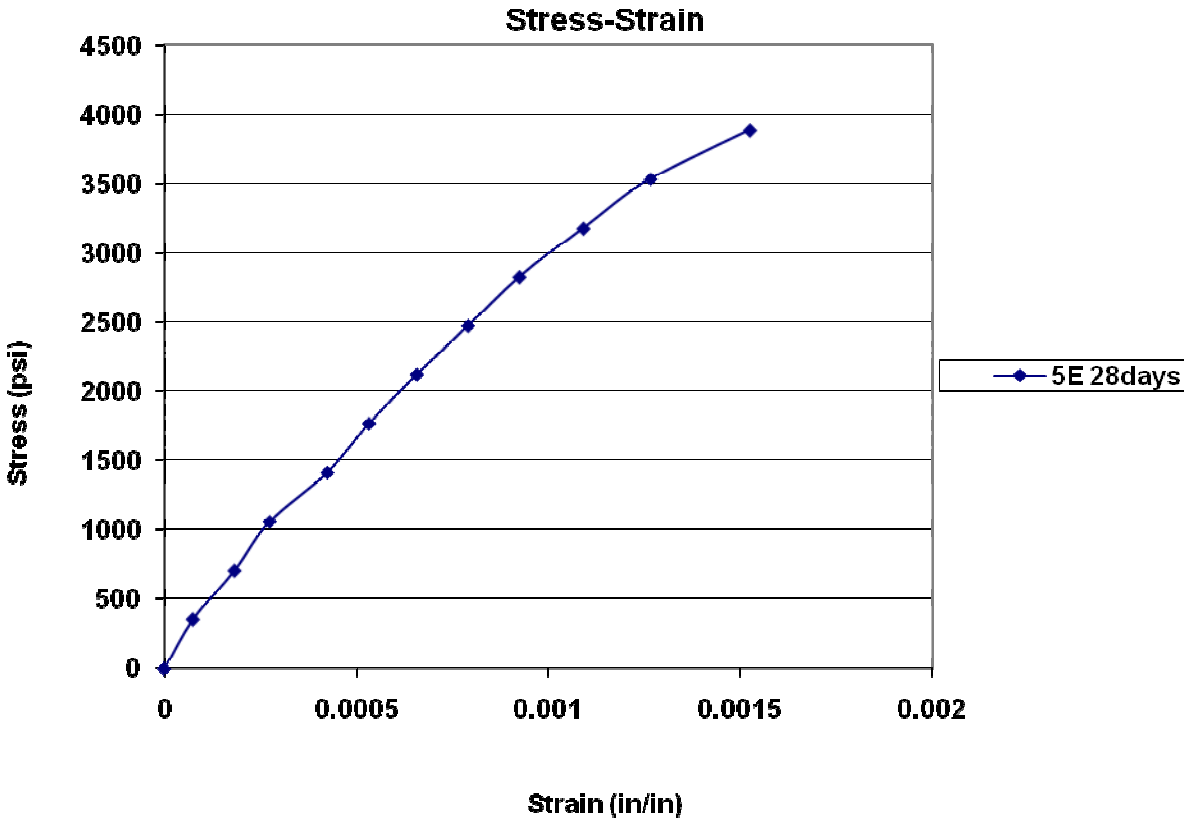

Figure 89 Stress & strain curve - Cylinder 5E at 28 Days

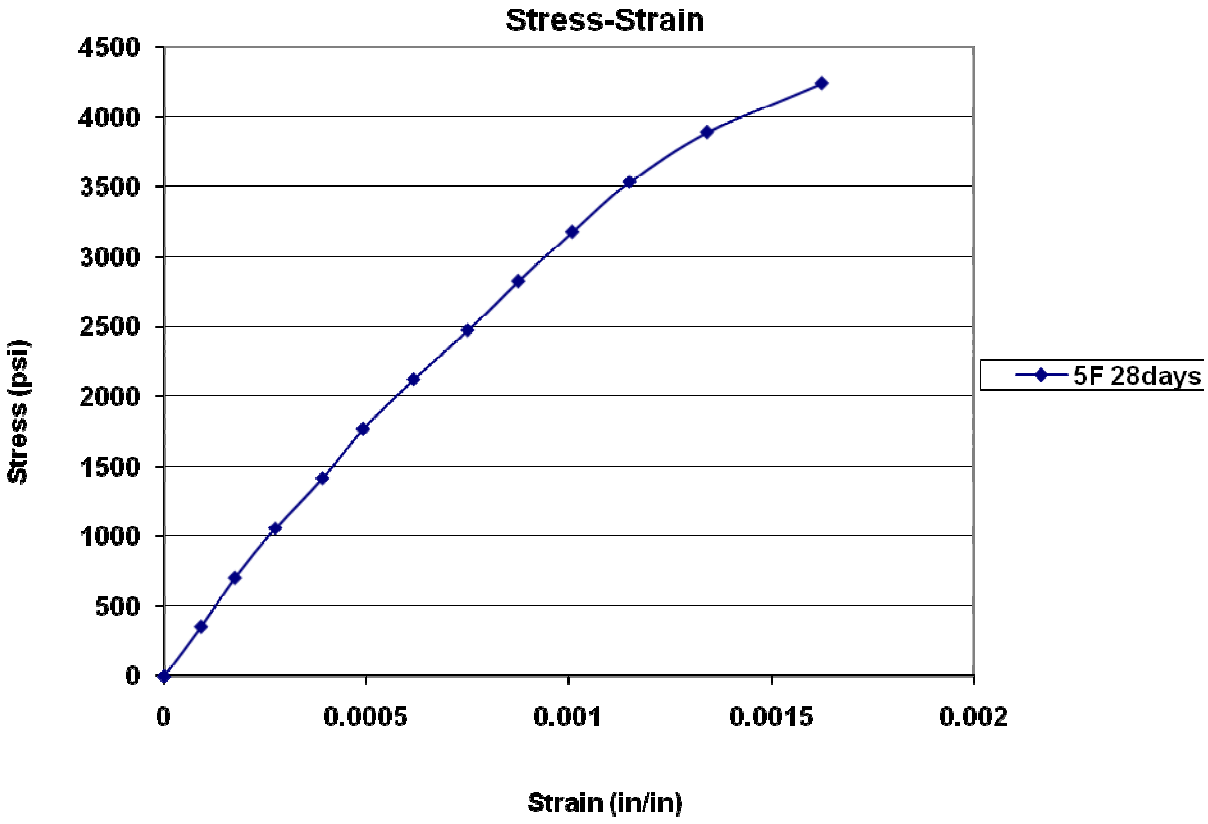

Figure 90 Stress & strain curve - Cylinder 5F at 28 Days

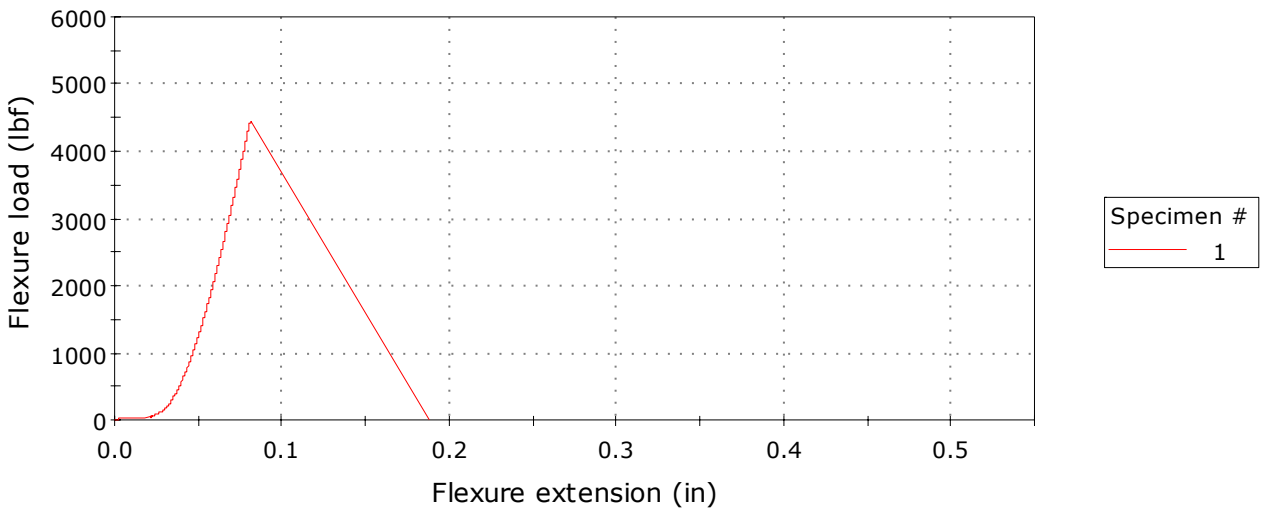

Beam Sample 1 A at 3 Days

	Maximum Flexure load (lbf)	Flexure extension at Maximum Flexure load (in)	Flexure strain at Maximum Flexure load (%)	Flexure stress at Maximum Flexure load (ksi)
1	4433.36564	0.08147	0.11724	26.97654

	Energy at Maximum Flexure load (ft-lbf)	Start Date	Fixture type	Support span (in)
1	8.39893	7/20/2008 10:33:53	4-point	18.00000

	Thickness (in)	Width (in)	Flexure extension at Break (Standard) (in)	Flexure load at Break (Standard) (lbf)
1	0.99300	3.00000	0.59128	-22.66102

	Flexure strain at Break (Standard) (%)	Flexure stress at Break (Standard) (ksi)
1	0.85093	-0.13789

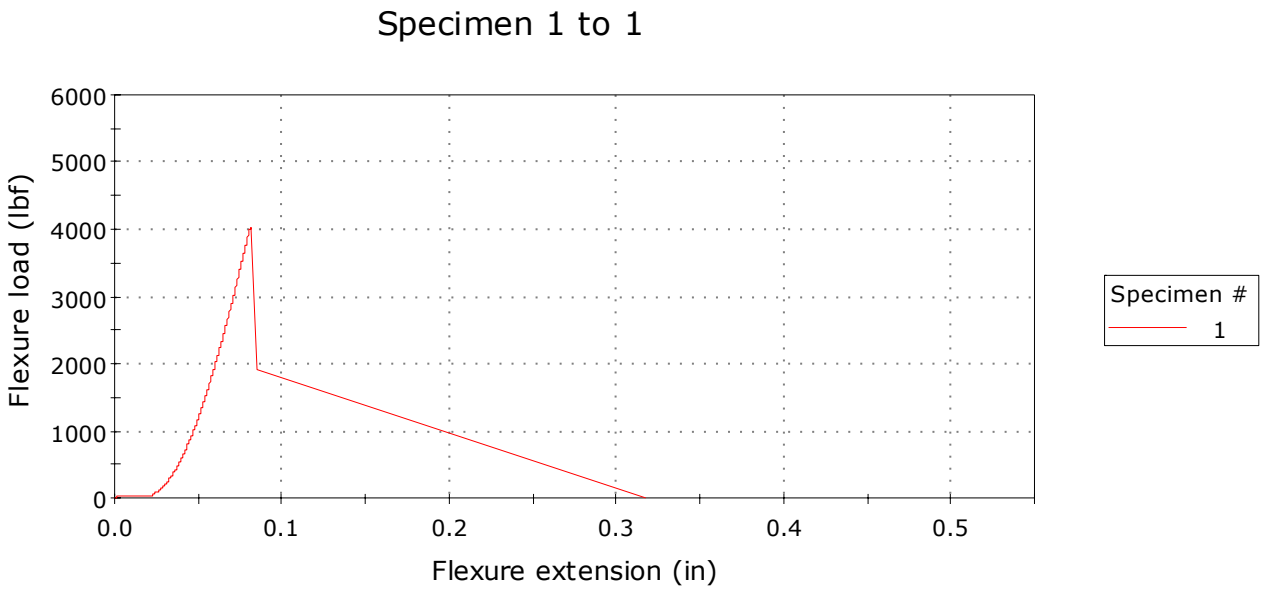

Beam Sample 1B at 3 Days

	Maximum Flexure load (lbf)	Flexure extension at Maximum Flexure load (in)	Flexure strain at Maximum Flexure load (%)	Flexure stress at Maximum Flexure load (ksi)
1	4016.10806	0.08123	0.11689	24.43758

	Energy at Maximum Flexure load (ft-lbf)	Start Date	Fixture type	Support span (in)
1	7.74152	7/20/2008 11:04:07	4-point	18.00000

	Thickness (in)	Width (in)	Flexure extension at Break (Standard) (in)	Flexure load at Break (Standard) (lbf)
1	0.99300	3.00000	0.58346	-28.64414

	Flexure strain at Break (Standard) (%)	Flexure stress at Break (Standard) (ksi)
1	0.83968	-0.17430

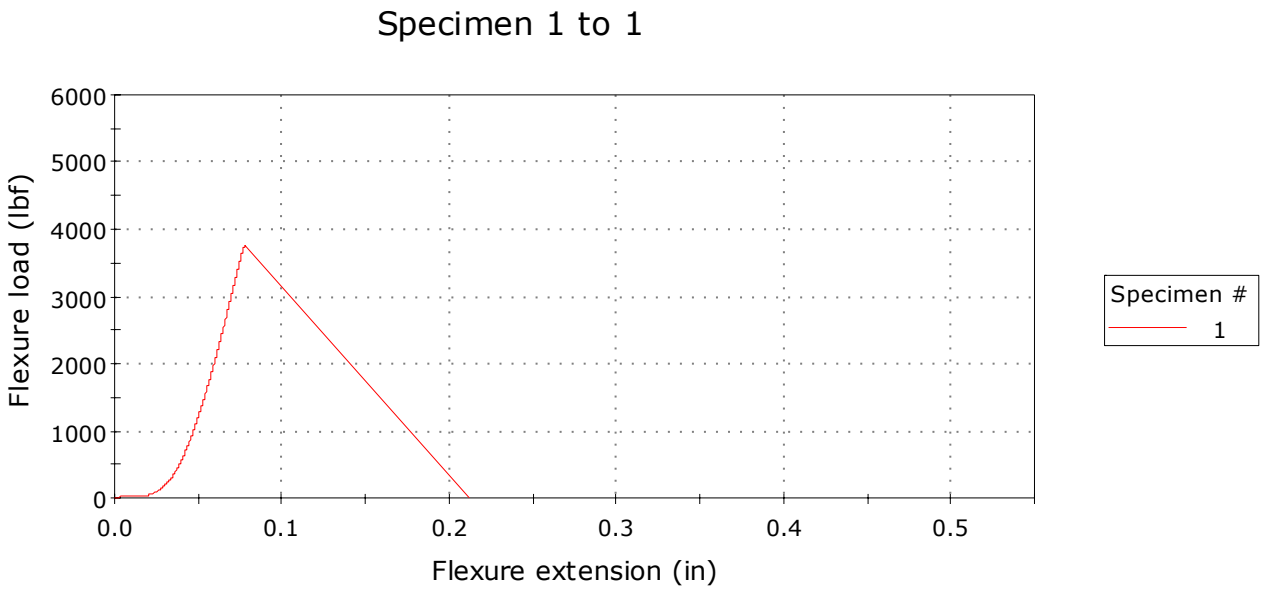

Beam Sample 1C at 3 Days

	Maximum Flexure load (lbf)	Flexure extension at Maximum Flexure load (in)	Flexure strain at Maximum Flexure load (%)	Flexure stress at Maximum Flexure load (ksi)
1	3761.46233	0.07782	0.11199	22.88809

	Energy at Maximum Flexure load (ft-lbf)	Start Date	Fixture type	Support span (in)
1	6.81793	7/20/2008 11:15:58	4-point	18.00000

	Thickness (in)	Width (in)	Flexure extension at Break (Standard) (in)	Flexure load at Break (Standard) (lbf)
1	0.99300	3.00000	0.64418	-45.05323

	Flexure strain at Break (Standard) (%)	Flexure stress at Break (Standard) (ksi)
1	0.92706	-0.27414

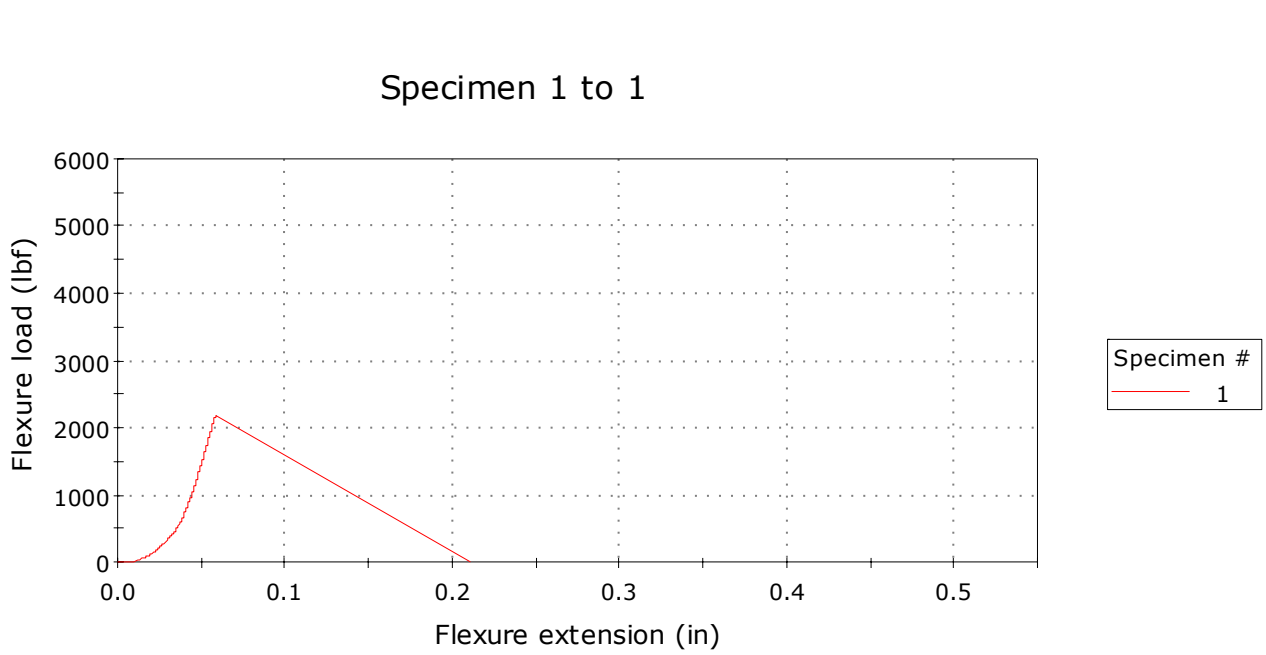

Beam Sample 1D at 3 Days

	Maximum Flexure load (lbf)	Flexure extension at Maximum Flexure load (in)	Flexure strain at Maximum Flexure load (%)	Flexure stress at Maximum Flexure load (ksi)
1	2192.52106	0.05928	0.08531	13.34125

	Energy at Maximum Flexure load (ft-lbf)	Start Date	Fixture type	Support span (in)
1	2.96840	7/20/2008 11:26:16	4-point	18.00000

	Thickness (in)	Width (in)	Flexure extension at Break (Standard) (in)	Flexure load at Break (Standard) (lbf)
1	0.99300	3.00000	0.65154	-58.09806

	Flexure strain at Break (Standard) (%)	Flexure stress at Break (Standard) (ksi)
1	0.93765	-0.35352

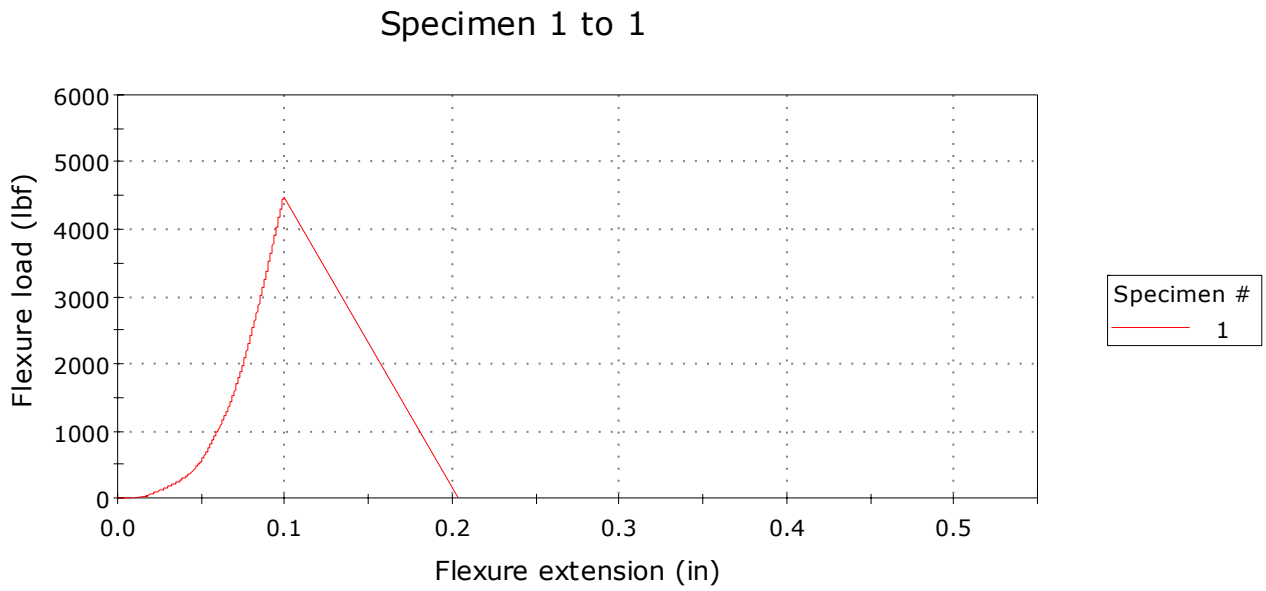

Beam Sample 2A at 3 Days

	Maximum Flexure load (lbf)	Flexure extension at Maximum Flexure load (in)	Flexure strain at Maximum Flexure load (%)	Flexure stress at Maximum Flexure load (ksi)
1	4478.98377	0.09917	0.14272	27.25412

	Energy at Maximum Flexure load (ft-lbf)	Start Date	Fixture type	Support span (in)
1	9.50980	7/20/2008 11:35:33	4-point	18.00000

	Thickness (in)	Width (in)	Flexure extension at Break (Standard) (in)	Flexure load at Break (Standard) (lbf)
1	0.99300	3.00000	0.59508	-61.39101

	Flexure strain at Break (Standard) (%)	Flexure stress at Break (Standard) (ksi)
1	0.85639	-0.37356

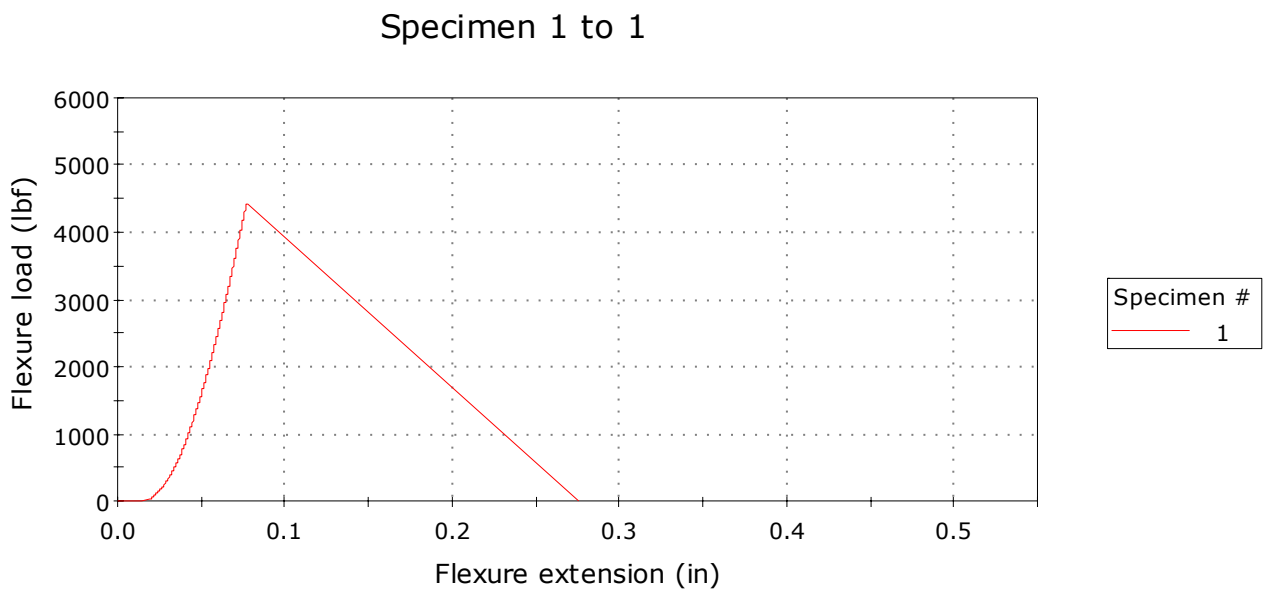

Beam Sample 2B at 3 Days

	Maximum Flexure load (lbf)	Flexure extension at Maximum Flexure load (in)	Flexure strain at Maximum Flexure load (%)	Flexure stress at Maximum Flexure load (ksi)
1	4431.57746	0.07769	0.11181	26.96566

	Energy at Maximum Flexure load (ft-lbf)	Start Date	Fixture type	Support span (in)
1	8.42988	7/20/2008 11:50:30	4-point	18.00000

	Thickness (in)	Width (in)	Flexure extension at Break (Standard) (in)	Flexure load at Break (Standard) (lbf)
1	0.99300	3.00000	0.63689	-57.73457

	Flexure strain at Break (Standard) (%)	Flexure stress at Break (Standard) (ksi)
1	0.91656	-0.35131

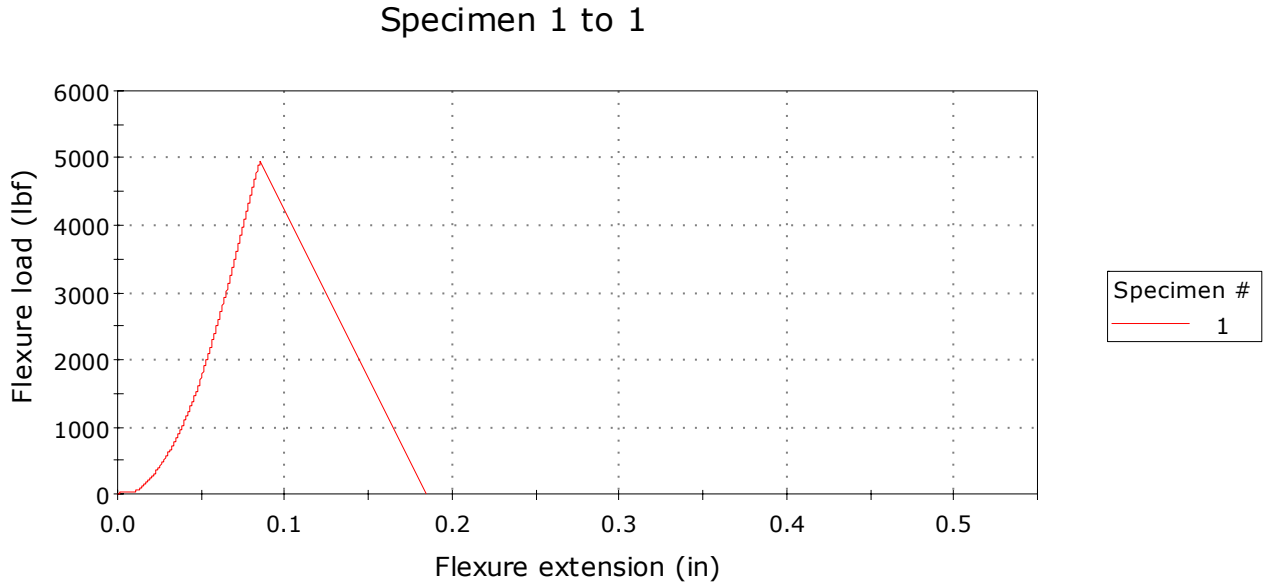

Beam Sample 2C at 3 Days

	Maximum Flexure load (lbf)	**Flexure extension at Maximum Flexure load (in)**	**Flexure strain at Maximum Flexure load (%)**	**Flexure stress at Maximum Flexure load (ksi)**
1	4969.77732	0.08530	0.12275	30.24055

	Energy at Maximum Flexure load (ft-lbf)	Start Date	Fixture type	Support span (in)
1	12.00575	7/20/2008 12:03:29	4-point	18.00000

	Thickness (in)	Width (in)	Flexure extension at Break (Standard) (in)	Flexure load at Break (Standard) (lbf)
1	0.99300	3.00000	0.67966	-55.66087

	Flexure strain at Break (Standard) (%)	Flexure stress at Break (Standard) (ksi)
1	0.97812	-0.33869

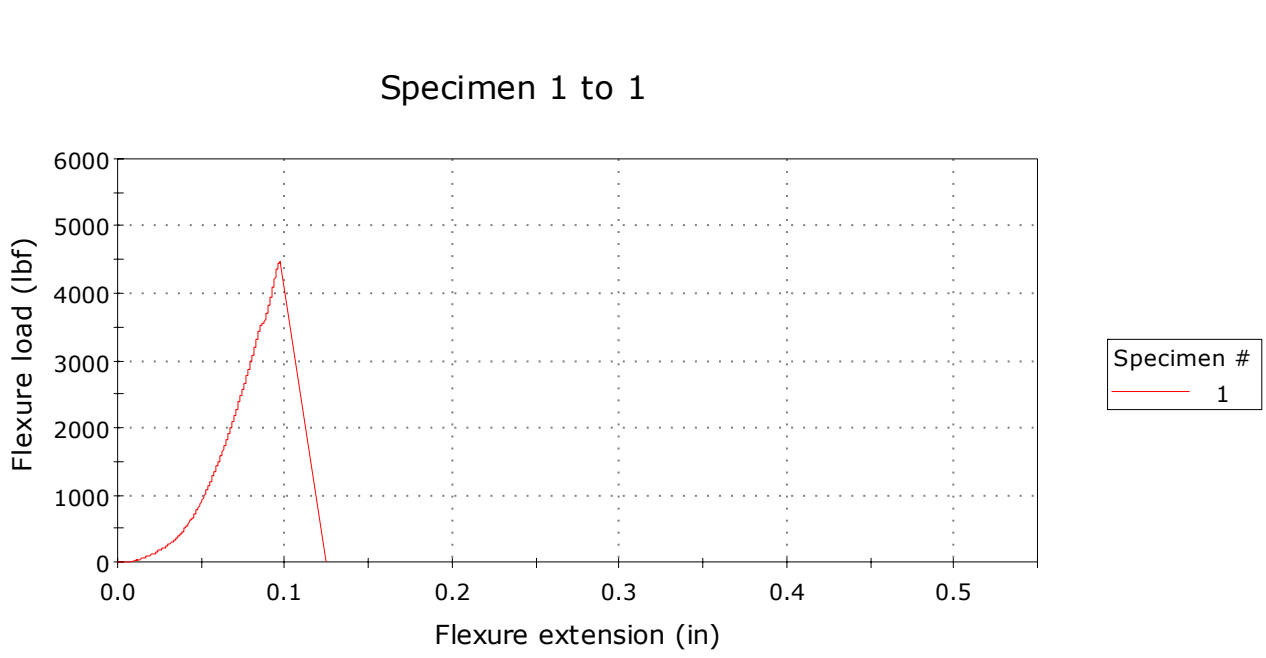

Beam Sample 2D at 3 Days

	Maximum Flexure load (lbf)	Flexure extension at Maximum Flexure load (in)	Flexure strain at Maximum Flexure load (%)	Flexure stress at Maximum Flexure load (ksi)
1	4491.02403	0.09702	0.13962	27.32739

	Energy at Maximum Flexure load (ft-lbf)	Start Date	Fixture type	Support span (in)
1	10.97438	7/20/2008 12:16:15	4-point	18.00000

	Thickness (in)	Width (in)	Flexure extension at Break (Standard) (in)	Flexure load at Break (Standard) (lbf)
1	0.99300	3.00000	0.63995	-58.08928

	Flexure strain at Break (Standard) (%)	Flexure stress at Break (Standard) (ksi)
1	0.92097	-0.35347

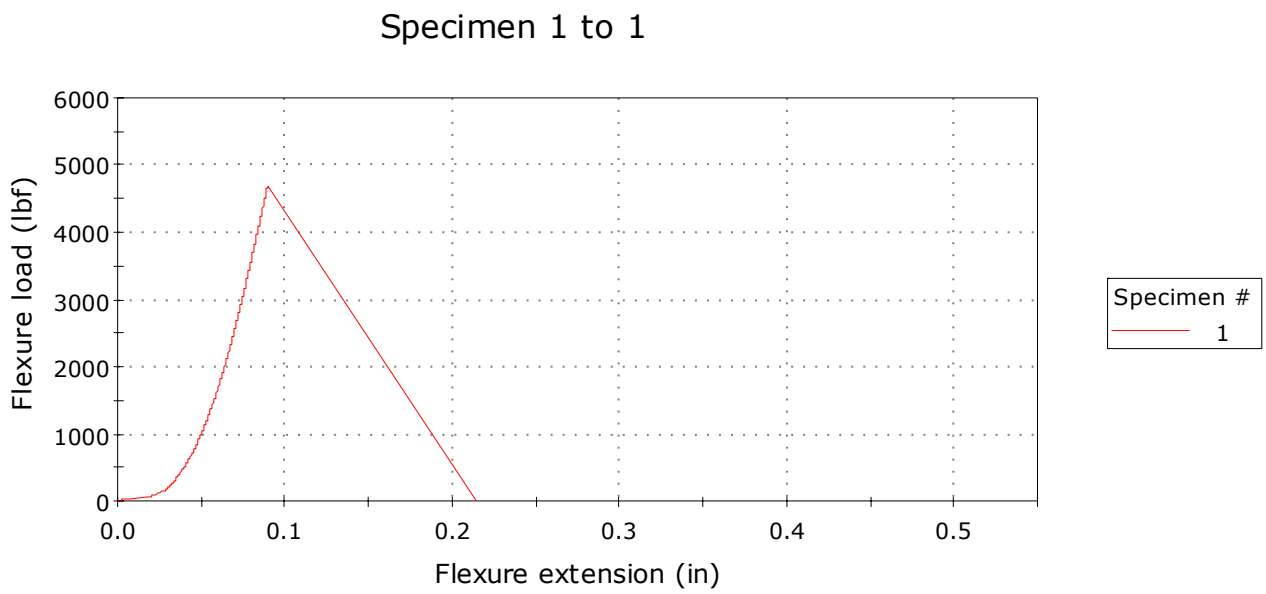

Beam Sample 3A at 3 Days

	Maximum Flexure load (lbf)	Flexure extension at Maximum Flexure load (in)	Flexure strain at Maximum Flexure load (%)	Flexure stress at Maximum Flexure load (ksi)
1	4688.40465	0.08994	0.12944	28.52843

	Energy at Maximum Flexure load (ft-lbf)	Start Date	Fixture type	Support span (in)
1	9.91581	7/20/2008 12:28:02	4-point	18.00000

	Thickness (in)	Width (in)	Flexure extension at Break (Standard) (in)	Flexure load at Break (Standard) (lbf)
1	0.99300	3.00000	0.54782	-36.01215

	Flexure strain at Break (Standard) (%)	Flexure stress at Break (Standard) (ksi)
1	0.78839	-0.21913

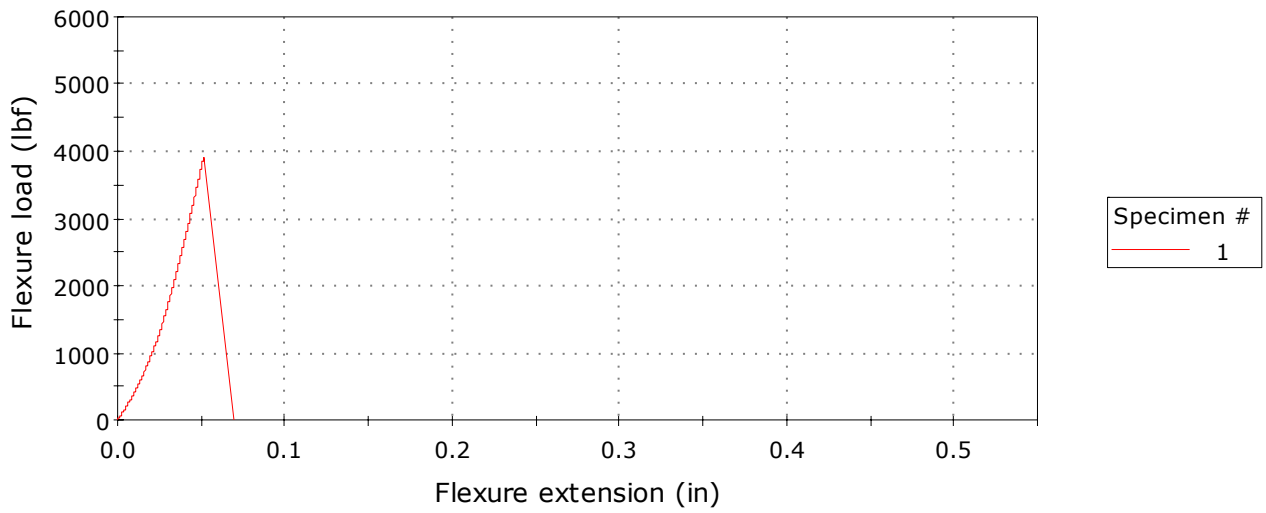

Beam Sample 3B at 3 Days

	Maximum Flexure load (lbf)	Flexure extension at Maximum Flexure load (in)	Flexure strain at Maximum Flexure load (%)	Flexure stress at Maximum Flexure load (ksi)
1	3908.50782	0.05193	0.07473	23.78284

	Energy at Maximum Flexure load (ft-lbf)	Start Date	Fixture type	Support span (in)
1	6.91567	7/20/2008 12:50:19	4-point	18.00000

	Thickness (in)	Width (in)	Flexure extension at Break (Standard) (in)	Flexure load at Break (Standard) (lbf)
1	0.99300	3.00000	0.51477	-202.07276

	Flexure strain at Break (Standard) (%)	Flexure stress at Break (Standard) (ksi)
1	0.74082	-1.22959

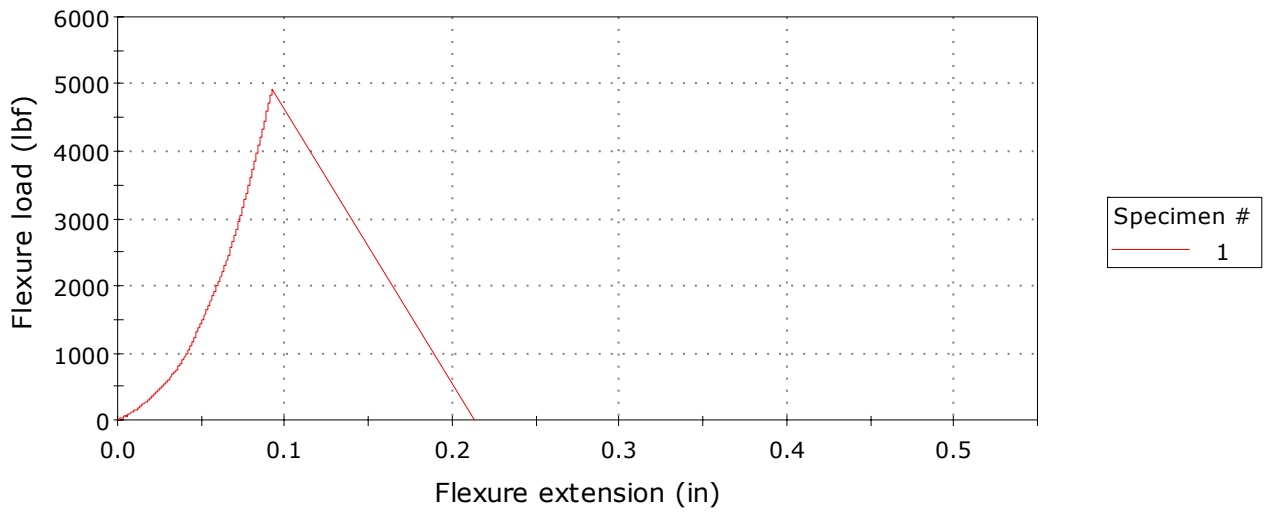

Beam Sample 3C at 3 Days

	Maximum Flexure load (lbf)	Flexure extension at Maximum Flexure load (in)	Flexure strain at Maximum Flexure load (%)	Flexure stress at Maximum Flexure load (ksi)
1	4924.37024	0.09267	0.13337	29.96425

	Energy at Maximum Flexure load (ft-lbf)	Start Date	Fixture type	Support span (in)
1	12.82864	7/20/2008 13:01:43	4-point	18.00000

	Thickness (in)	Width (in)	Flexure extension at Break (Standard) (in)	Flexure load at Break (Standard) (lbf)
1	0.99300	3.00000	0.55188	-154.61156

	Flexure strain at Break (Standard) (%)	Flexure stress at Break (Standard) (ksi)
1	0.79422	-0.94079

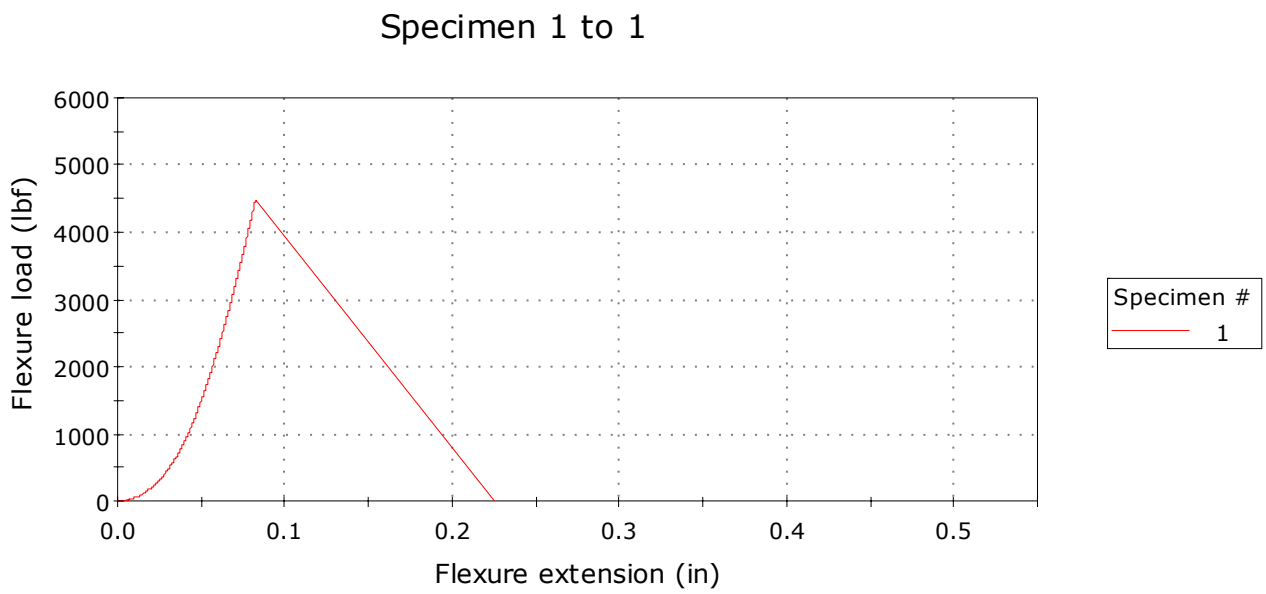

Beam Sample 3D at 3 Days

	Maximum Flexure load (lbf)	Flexure extension at Maximum Flexure load (in)	Flexure strain at Maximum Flexure load (%)	Flexure stress at Maximum Flexure load (ksi)
1	4466.24873	0.08274	0.11908	27.17663

	Energy at Maximum Flexure load (ft-lbf)	Start Date	Fixture type	Support span (in)
1	9.78610	7/20/2008 13:13:30	4-point	18.00000

	Thickness (in)	Width (in)	Flexure extension at Break (Standard) (in)	Flexure load at Break (Standard) (lbf)
1	0.99300	3.00000	0.64605	-60.53999

	Flexure strain at Break (Standard) (%)	Flexure stress at Break (Standard) (ksi)
1	0.92975	-0.36838

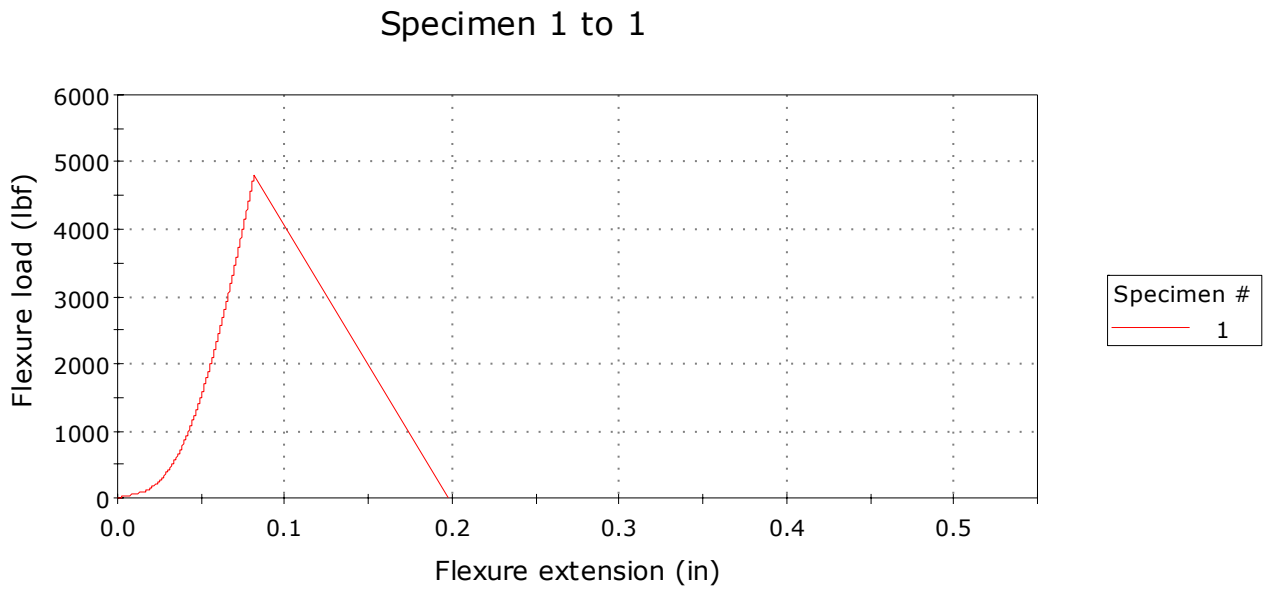

Beam Sample 4A at 3 Days

	Maximum Flexure load (lbf)	Flexure extension at Maximum Flexure load (in)	Flexure strain at Maximum Flexure load (%)	Flexure stress at Maximum Flexure load (ksi)
1	4811.73039	0.08195	0.11794	29.27885

	Energy at Maximum Flexure load (ft-lbf)	Start Date	Fixture type	Support span (in)
1	9.95737	7/20/2008 13:25:19	4-point	18.00000

	Thickness (in)	Width (in)	Flexure extension at Break (Standard) (in)	Flexure load at Break (Standard) (lbf)
1	0.99300	3.00000	0.58617	-62.04341

	Flexure strain at Break (Standard) (%)	Flexure stress at Break (Standard) (ksi)
1	0.84357	-0.37753

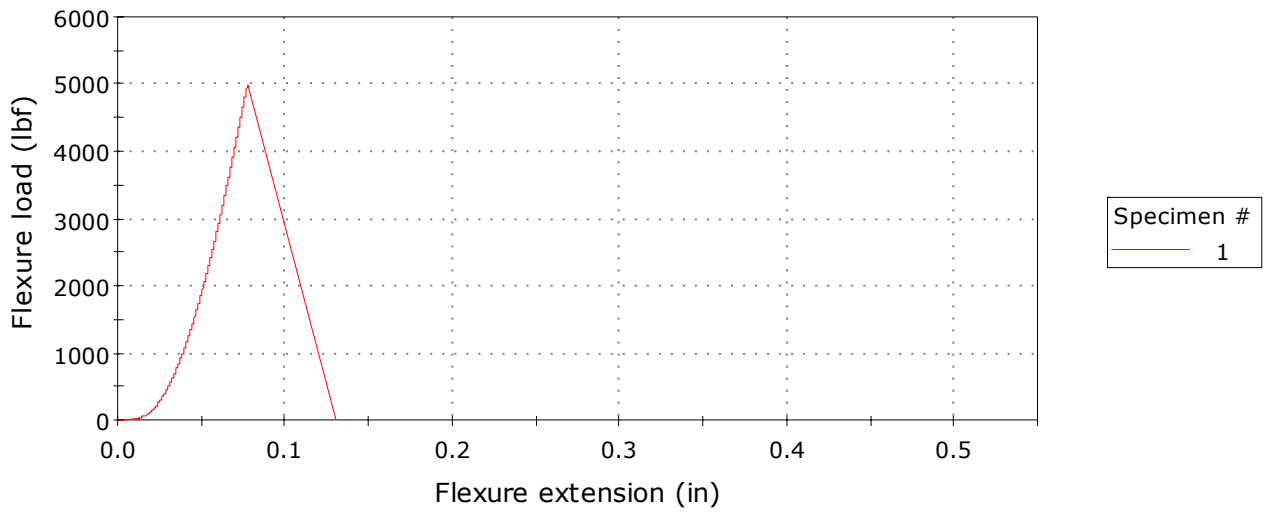

Beam Sample 4B at 3 Days

	Maximum Flexure load (lbf)	Flexure extension at Maximum Flexure load (in)	Flexure strain at Maximum Flexure load (%)	Flexure stress at Maximum Flexure load (ksi)
1	4999.49743	0.07791	0.11213	30.42139

	Energy at Maximum Flexure load (ft-lbf)	Start Date	Fixture type	Support span (in)
1	9.95708	7/20/2008 13:44:26	4-point	18.00000

	Thickness (in)	Width (in)	Flexure extension at Break (Standard) (in)	Flexure load at Break (Standard) (lbf)
1	0.99300	3.00000	0.65053	-61.47754

	Flexure strain at Break (Standard) (%)	Flexure stress at Break (Standard) (ksi)
1	0.93620	-0.37408

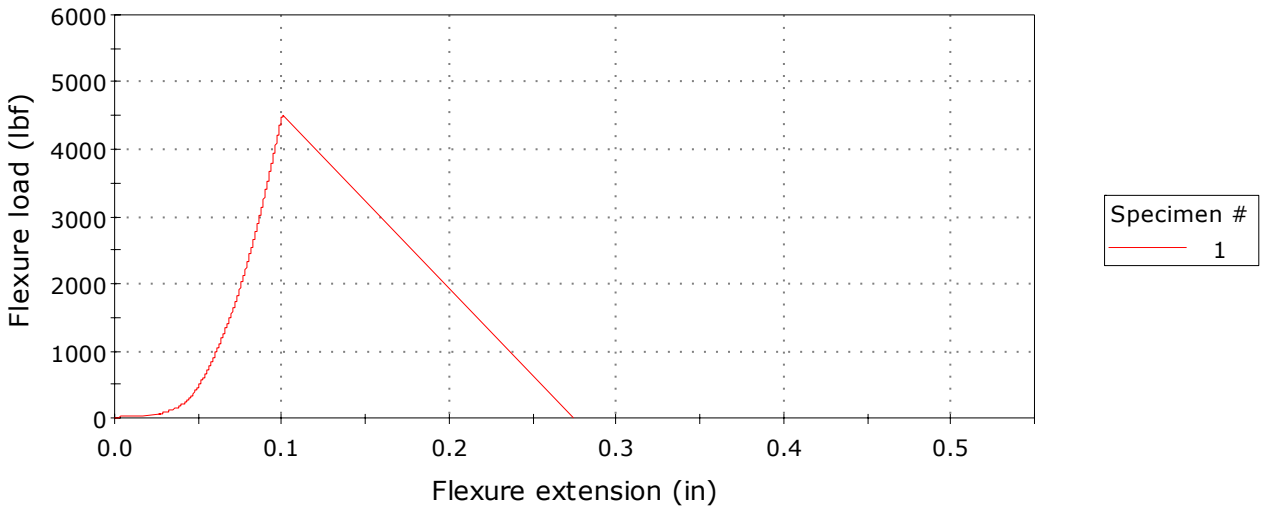

Beam Sample 4C at 3 Days

	Maximum Flexure load (lbf)	Flexure extension at Maximum Flexure load (in)	Flexure strain at Maximum Flexure load (%)	Flexure stress at Maximum Flexure load (ksi)
1	4500.45638	0.10081	0.14509	27.38478

	Energy at Maximum Flexure load (ft-lbf)	Start Date	Fixture type	Support span (in)
1	9.62783	7/20/2008 13:56:29	4-point	18.00000

	Thickness (in)	Width (in)	Flexure extension at Break (Standard) (in)	Flexure load at Break (Standard) (lbf)
1	0.99300	3.00000	0.52451	-28.55529

	Flexure strain at Break (Standard) (%)	Flexure stress at Break (Standard) (ksi)
1	0.75484	-0.17376

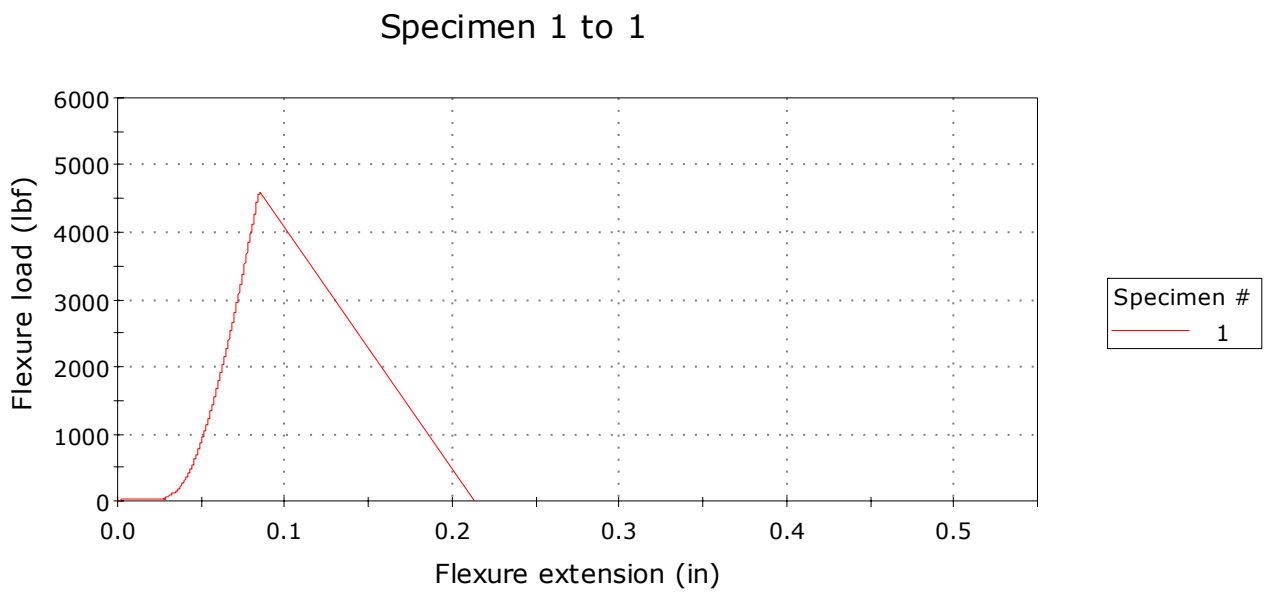

Beam Sample 4D at 3 Days

	Maximum Flexure load (lbf)	Flexure extension at Maximum Flexure load (in)	Flexure strain at Maximum Flexure load (%)	Flexure stress at Maximum Flexure load (ksi)
1	4587.35248	0.08476	0.12198	27.91354

	Energy at Maximum Flexure load (ft-lbf)	Start Date	Fixture type	Support span (in)
1	8.16426	7/20/2008 14:10:27	4-point	18.00000

	Thickness (in)	Width (in)	Flexure extension at Break (Standard) (in)	Flexure load at Break (Standard) (lbf)
1	0.99300	3.00000	0.67337	-38.51441

	Flexure strain at Break (Standard) (%)	Flexure stress at Break (Standard) (ksi)
1	0.96907	-0.23436

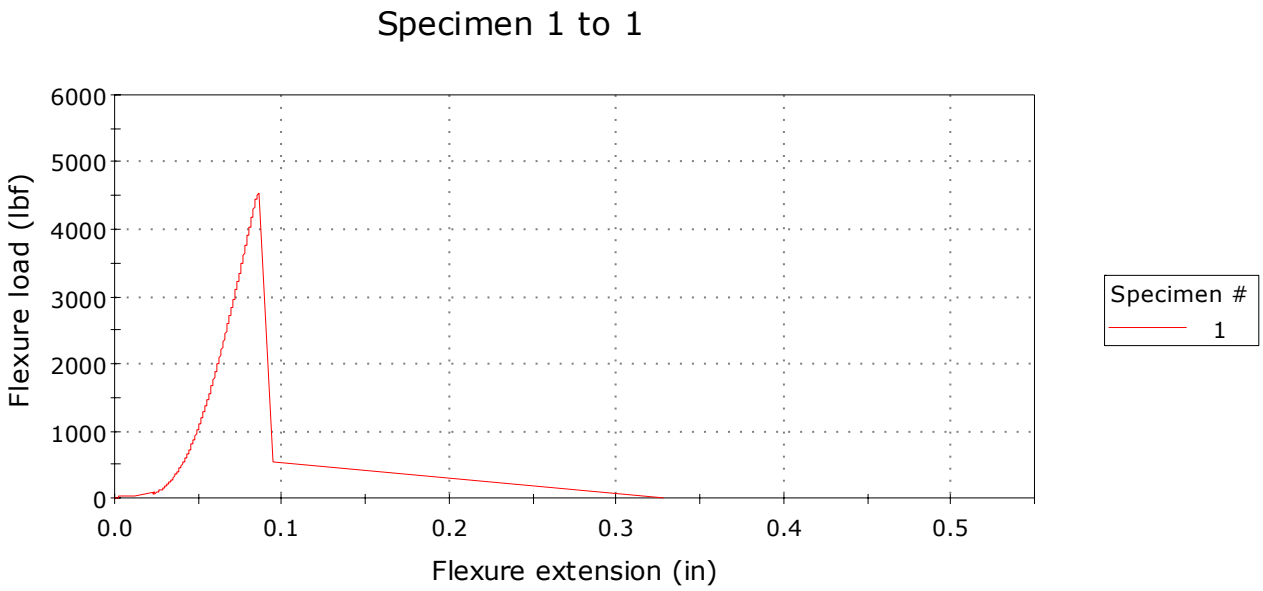

Beam Sample 5A at 3 Days

	Maximum Flexure load (lbf)	Flexure extension at Maximum Flexure load (in)	Flexure strain at Maximum Flexure load (%)	Flexure stress at Maximum Flexure load (ksi)
1	4524.71110	0.08572	0.12336	27.53237

	Energy at Maximum Flexure load (ft-lbf)	Start Date	Fixture type	Support span (in)
1	8.97816	7/20/2008 14:21:34	4-point	18.00000

	Thickness (in)	Width (in)	Flexure extension at Break (Standard) (in)	Flexure load at Break (Standard) (lbf)
1	0.99300	3.00000	0.62115	-22.99663

	Flexure strain at Break (Standard) (%)	Flexure stress at Break (Standard) (ksi)
1	0.89391	-0.13993

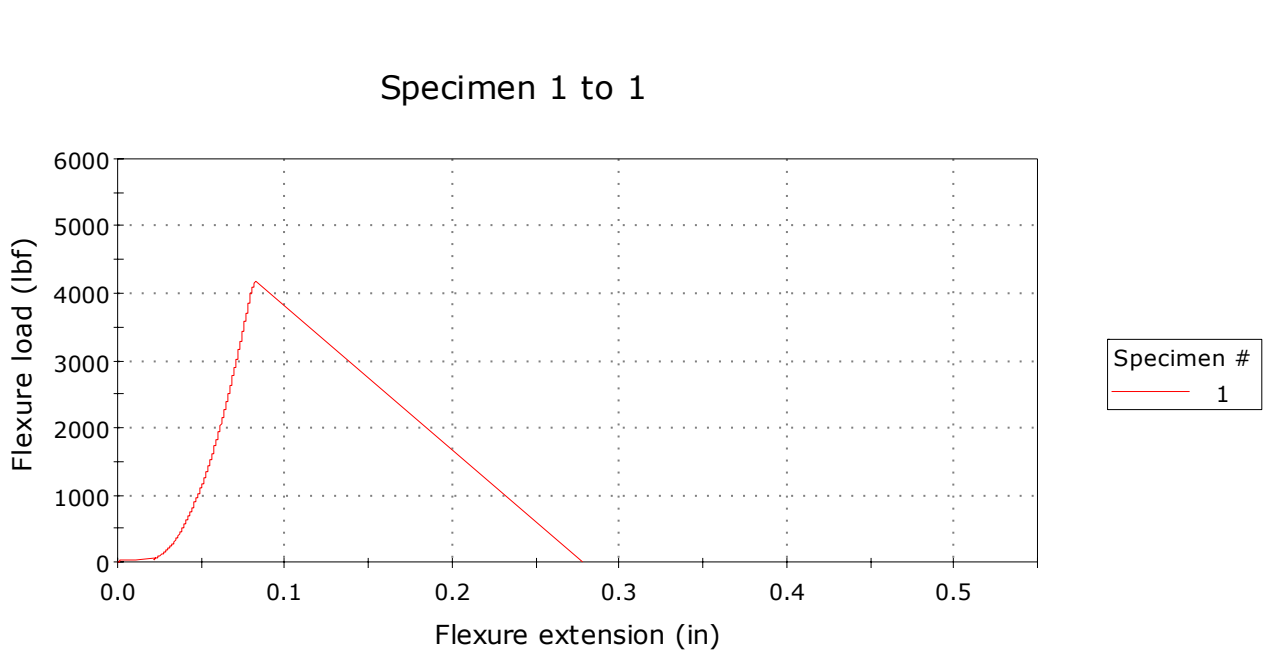

Beam Sample 5B at 3 Days

	Maximum Flexure load (lbf)	Flexure extension at Maximum Flexure load (in)	Flexure strain at Maximum Flexure load (%)	Flexure stress at Maximum Flexure load (ksi)
1	4164.20441	0.08253	0.11877	25.33873

	Energy at Maximum Flexure load (ft-lbf)	Start Date	Fixture type	Support span (in)
1	8.07110	7/20/2008 14:32:56	4-point	18.00000

	Thickness (in)	Width (in)	Flexure extension at Break (Standard) (in)	Flexure load at Break (Standard) (lbf)
1	0.99300	3.00000	0.51969	-68.14701

	Flexure strain at Break (Standard) (%)	Flexure stress at Break (Standard) (ksi)
1	0.74791	-0.41467

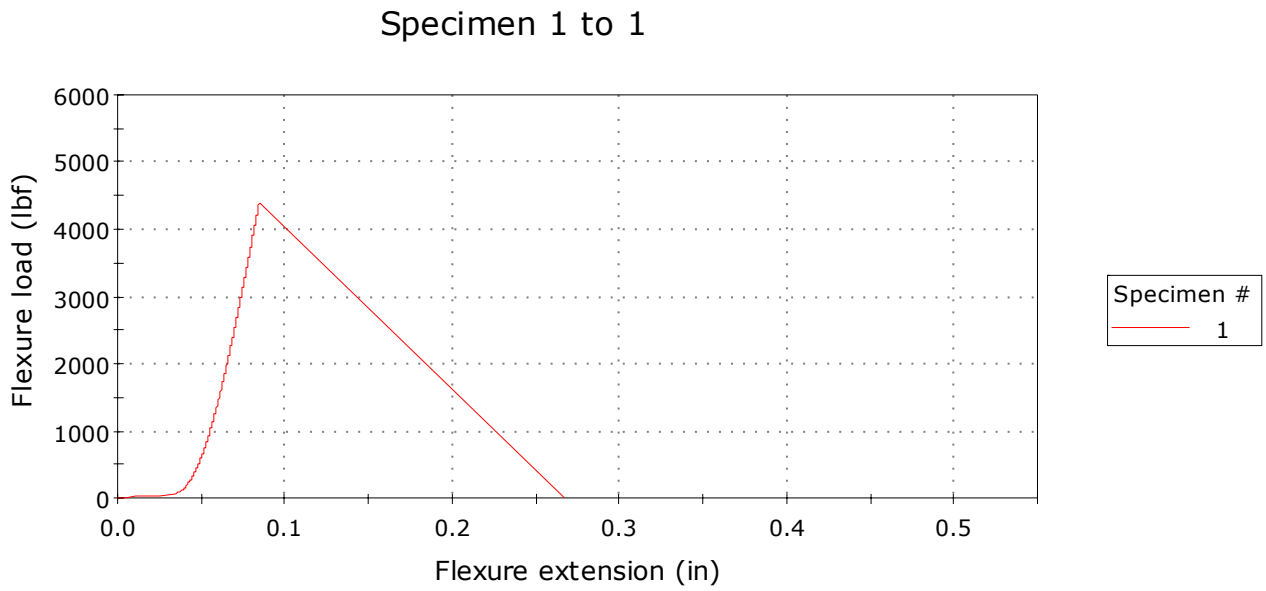

Beam Sample 1A at 7 Days

	Maximum Flexure load (lbf)	Flexure extension at Maximum Flexure load (in)	Flexure strain at Maximum Flexure load (%)	Flexure stress at Maximum Flexure load (ksi)
1	4402.68043	0.08505	0.12240	26.78983

	Energy at Maximum Flexure load (ft-lbf)	Start Date	Fixture type	Support span (in)
1	7.23825	7/24/2008 08:57:24	4-point	18.00000

	Thickness (in)	Width (in)	Flexure extension at Break (Standard) (in)	Flexure load at Break (Standard) (lbf)
1	0.99300	3.00000	0.68061	-18.89275

	Flexure strain at Break (Standard) (%)	Flexure stress at Break (Standard) (ksi)
1	0.97948	-0.11496

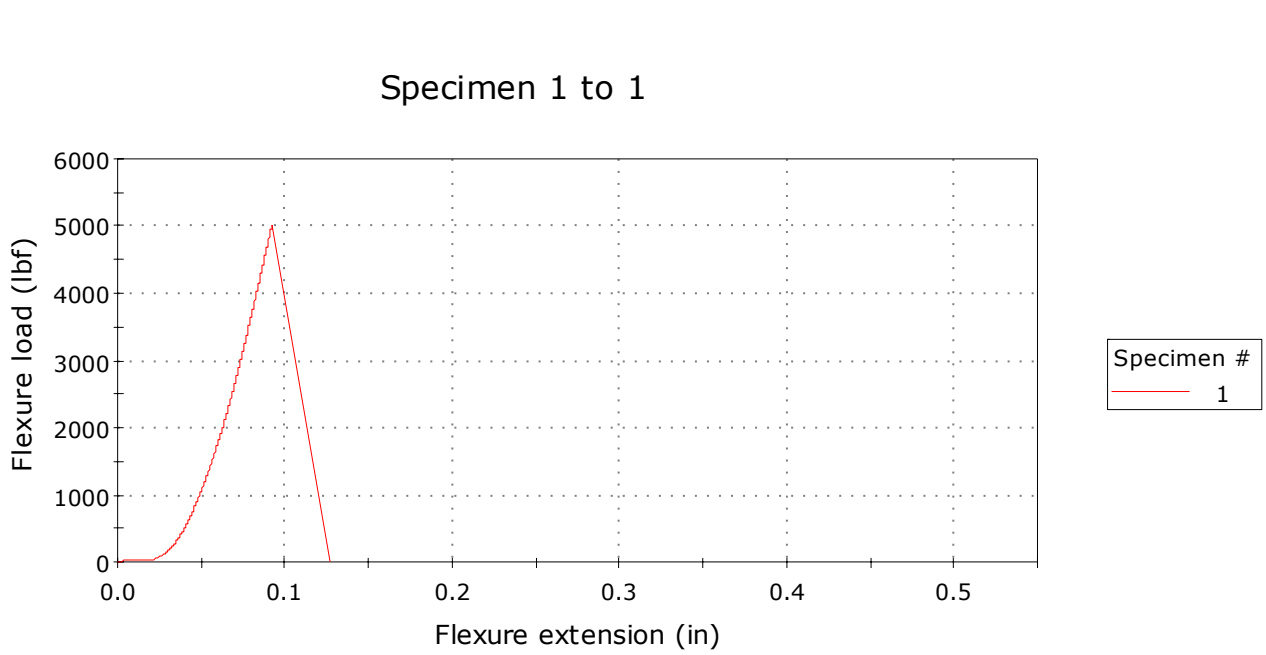

Beam Sample 1B at 7 Days

	Maximum Flexure load (lbf)	Flexure extension at Maximum Flexure load (in)	Flexure strain at Maximum Flexure load (%)	Flexure stress at Maximum Flexure load (ksi)
1	5029.41886	0.09248	0.13309	30.60346

	Energy at Maximum Flexure load (ft-lbf)	Start Date	Fixture type	Support span (in)
1	11.16010	7/24/2008 09:08:53	4-point	18.00000

	Thickness (in)	Width (in)	Flexure extension at Break (Standard) (in)	Flexure load at Break (Standard) (lbf)
1	0.99300	3.00000	0.66039	-41.81139

	Flexure strain at Break (Standard) (%)	Flexure stress at Break (Standard) (ksi)
1	0.95039	-0.25442

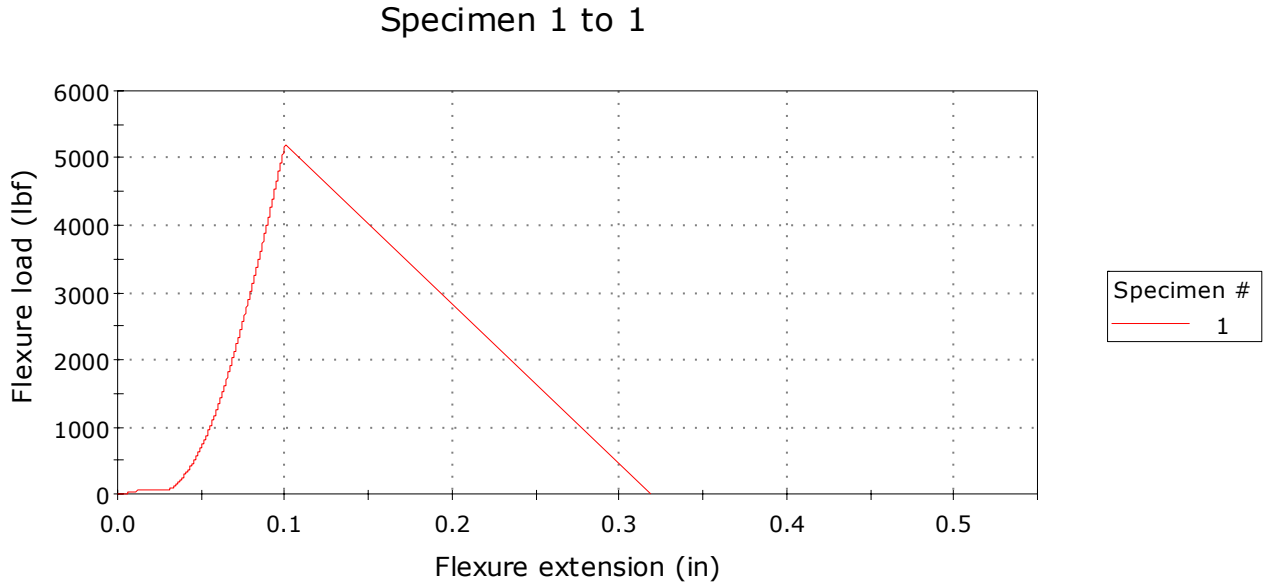

Beam Sample 1C at 7 Days

	Maximum Flexure load (lbf)	Flexure extension at Maximum Flexure load (in)	Flexure strain at Maximum Flexure load (%)	Flexure stress at Maximum Flexure load (ksi)
1	5187.24068	0.10018	0.14417	31.56379

	Energy at Maximum Flexure load (ft-lbf)	Start Date	Fixture type	Support span (in)
1	11.90421	7/24/2008 09:21:12	4-point	18.00000

	Thickness (in)	Width (in)	Flexure extension at Break (Standard) (in)	Flexure load at Break (Standard) (lbf)
1	0.99300	3.00000	0.54656	-28.77016

	Flexure strain at Break (Standard) (%)	Flexure stress at Break (Standard) (ksi)
1	0.78658	-0.17506

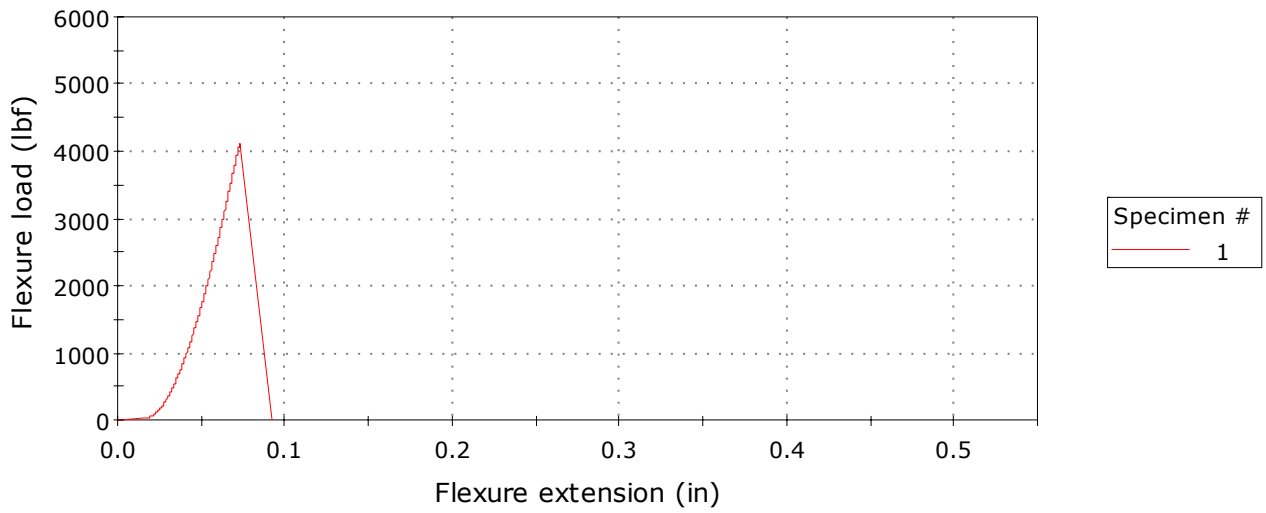

Beam Sample 1D at 7 Days

	Maximum Flexure load (lbf)	Flexure extension at Maximum Flexure load (in)	Flexure strain at Maximum Flexure load (%)	Flexure stress at Maximum Flexure load (ksi)
1	4116.46780	0.07328	0.10547	25.04825

	Energy at Maximum Flexure load (ft-lbf)	Start Date	Fixture type	Support span (in)
1	7.31108	7/24/2008 09:34:51	4-point	18.00000

	Thickness (in)	Width (in)	Flexure extension at Break (Standard) (in)	Flexure load at Break (Standard) (lbf)
1	0.99300	3.00000	0.68279	-59.66611

	Flexure strain at Break (Standard) (%)	Flexure stress at Break (Standard) (ksi)
1	0.98262	-0.36306

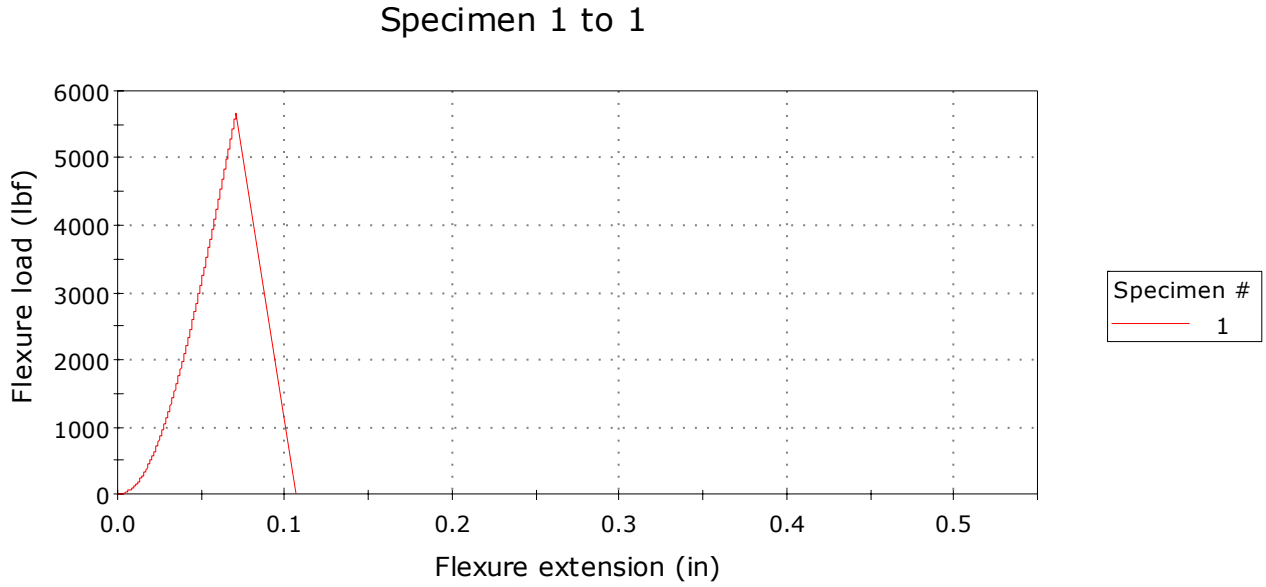

Beam Sample 2A at 7 Days

	Maximum Flexure load (lbf)	Flexure extension at Maximum Flexure load (in)	Flexure strain at Maximum Flexure load (%)	Flexure stress at Maximum Flexure load (ksi)
1	5683.29996	0.07125	0.10254	34.58226

	Energy at Maximum Flexure load (ft-lbf)	Start Date	Fixture type	Support span (in)
1	12.28927	7/24/2008 09:45:55	4-point	18.00000

	Thickness (in)	Width (in)	Flexure extension at Break (Standard) (in)	Flexure load at Break (Standard) (lbf)
1	0.99300	3.00000	0.71285	-68.79190

	Flexure strain at Break (Standard) (%)	Flexure stress at Break (Standard) (ksi)
1	1.02589	-0.41859

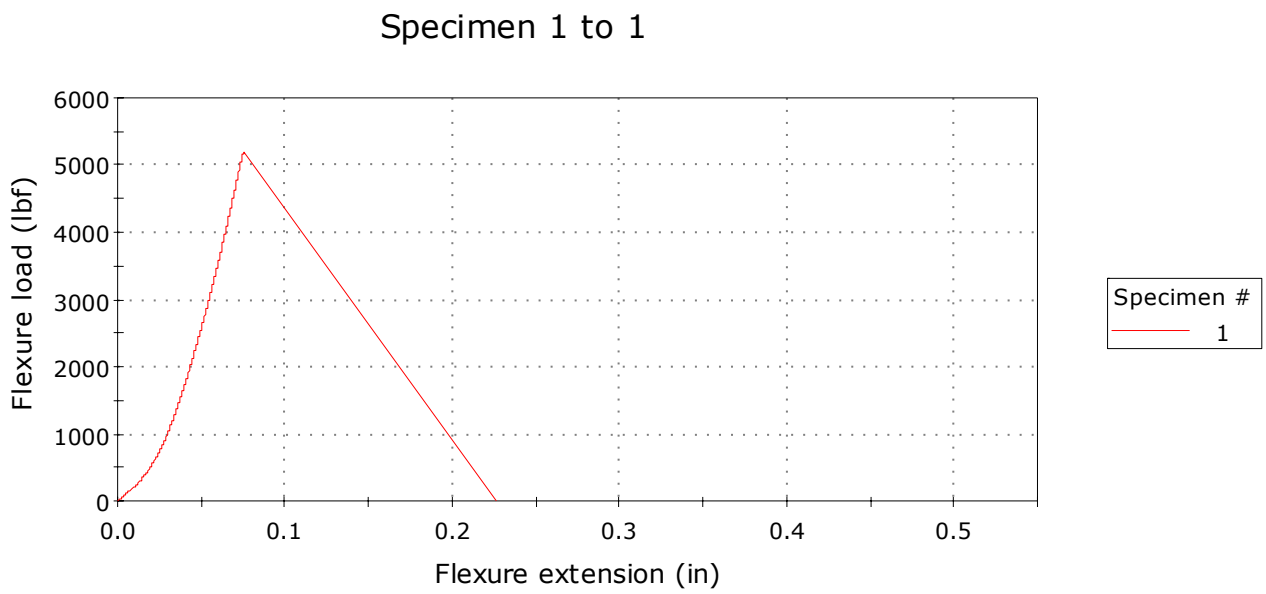

Beam Sample 2B at 7 Days

	Maximum Flexure load (lbf)	Flexure extension at Maximum Flexure load (in)	Flexure strain at Maximum Flexure load (%)	Flexure stress at Maximum Flexure load (ksi)
1	5181.79171	0.07582	0.10912	31.53063

	Energy at Maximum Flexure load (ft-lbf)	Start Date	Fixture type	Support span (in)
1	12.23334	7/24/2008 09:59:32	4-point	18.00000

	Thickness (in)	Width (in)	Flexure extension at Break (Standard) (in)	Flexure load at Break (Standard) (lbf)
1	0.99300	3.00000	0.56732	-80.09662

	Flexure strain at Break (Standard) (%)	Flexure stress at Break (Standard) (ksi)
1	0.81644	-0.48738

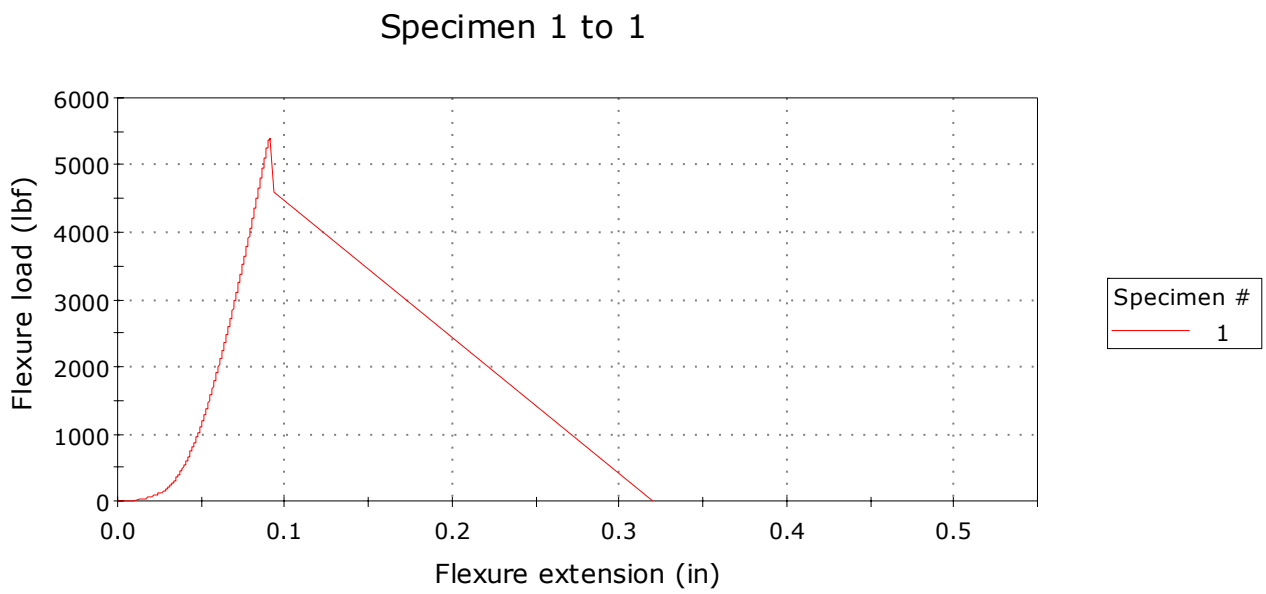

Beam Sample 2C at 7 Days

	Maximum Flexure load (lbf)	Flexure extension at Maximum Flexure load (in)	Flexure strain at Maximum Flexure load (%)	Flexure stress at Maximum Flexure load (ksi)
1	5403.94494	0.09095	0.13090	32.88241

	Energy at Maximum Flexure load (ft-lbf)	Start Date	Fixture type	Support span (in)
1	11.72202	7/24/2008 10:11:58	4-point	18.00000

	Thickness (in)	Width (in)	Flexure extension at Break (Standard) (in)	Flexure load at Break (Standard) (lbf)
1	0.99300	3.00000	0.51832	-57.85641

	Flexure strain at Break (Standard) (%)	Flexure stress at Break (Standard) (ksi)
1	0.74593	-0.35205

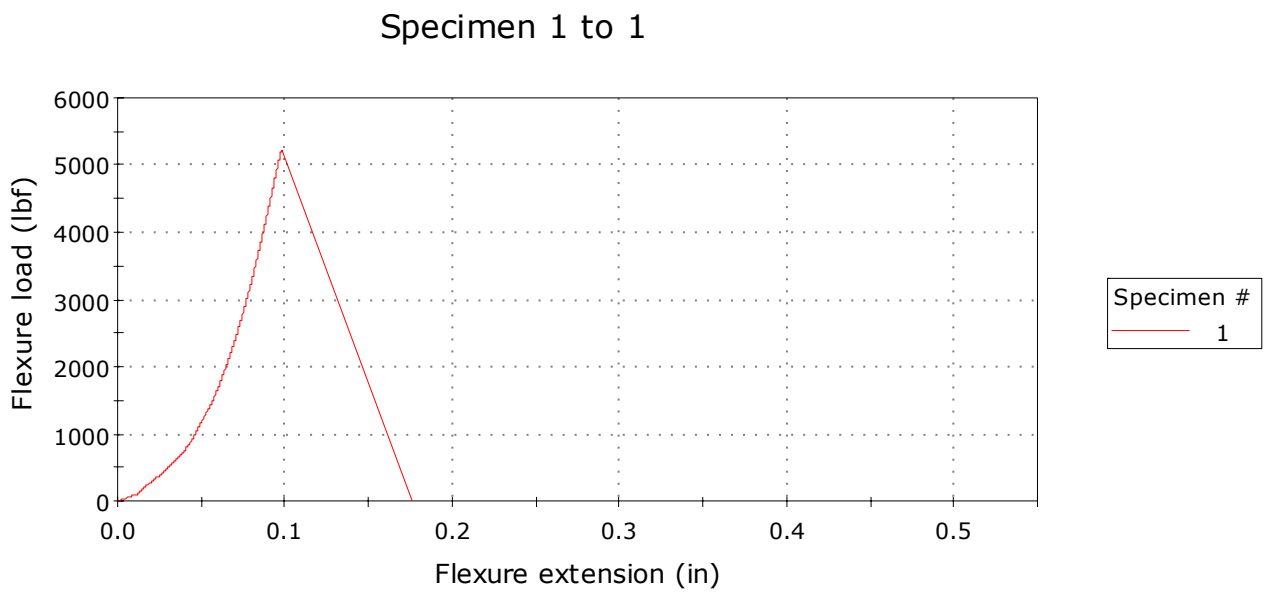

Beam Sample 2D at 7 Days

	Maximum Flexure load (lbf)	Flexure extension at Maximum Flexure load (in)	Flexure strain at Maximum Flexure load (%)	Flexure stress at Maximum Flexure load (ksi)
1	5224.45052	0.09824	0.14138	31.79021

	Energy at Maximum Flexure load (ft-lbf)	Start Date	Fixture type	Support span (in)
1	13.45704	7/24/2008 10:24:53	4-point	18.00000

	Thickness (in)	Width (in)	Flexure extension at Break (Standard) (in)	Flexure load at Break (Standard) (lbf)
1	0.99300	3.00000	0.61970	-61.85229

	Flexure strain at Break (Standard) (%)	Flexure stress at Break (Standard) (ksi)
1	0.89183	-0.37636

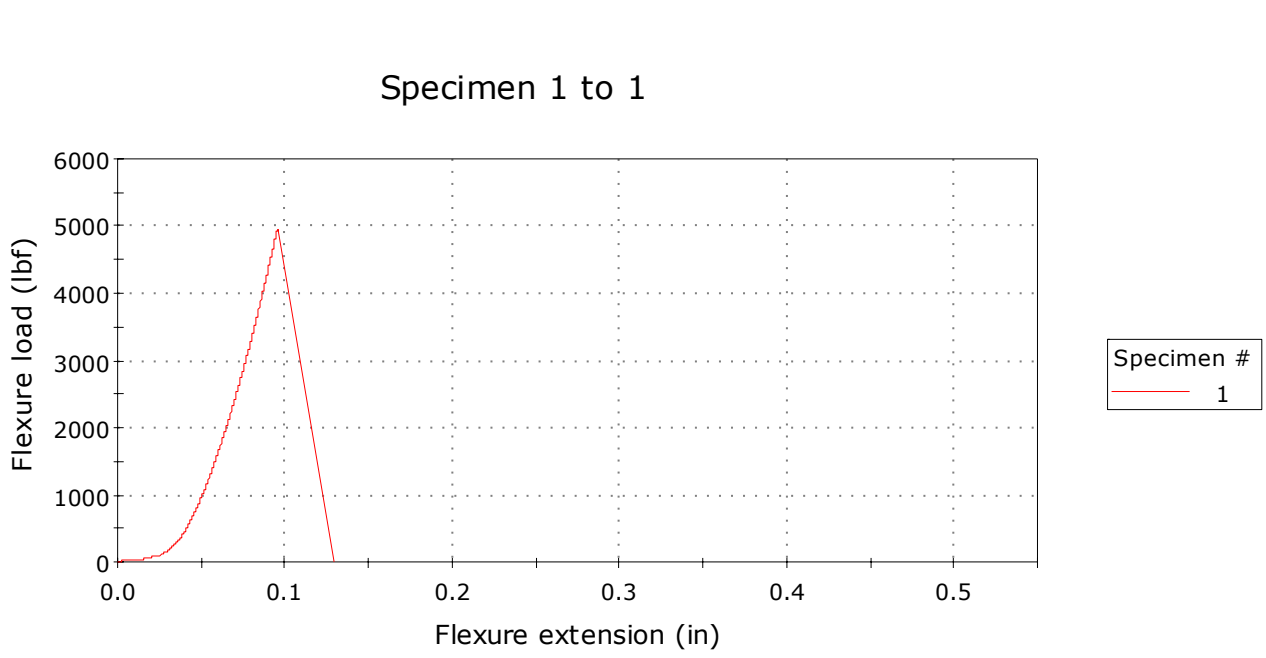

Beam Sample 3A at 7 Days

	Maximum Flexure load (lbf)	Flexure extension at Maximum Flexure load (in)	Flexure strain at Maximum Flexure load (%)	Flexure stress at Maximum Flexure load (ksi)
1	4966.99488	0.09609	0.13829	30.22362

	Energy at Maximum Flexure load (ft-lbf)	Start Date	Fixture type	Support span (in)
1	11.65755	7/24/2008 10:37:19	4-point	18.00000

	Thickness (in)	Width (in)	Flexure extension at Break (Standard) (in)	Flexure load at Break (Standard) (lbf)
1	0.99300	3.00000	0.53571	-39.17144

	Flexure strain at Break (Standard) (%)	Flexure stress at Break (Standard) (ksi)
1	0.77095	-0.23835

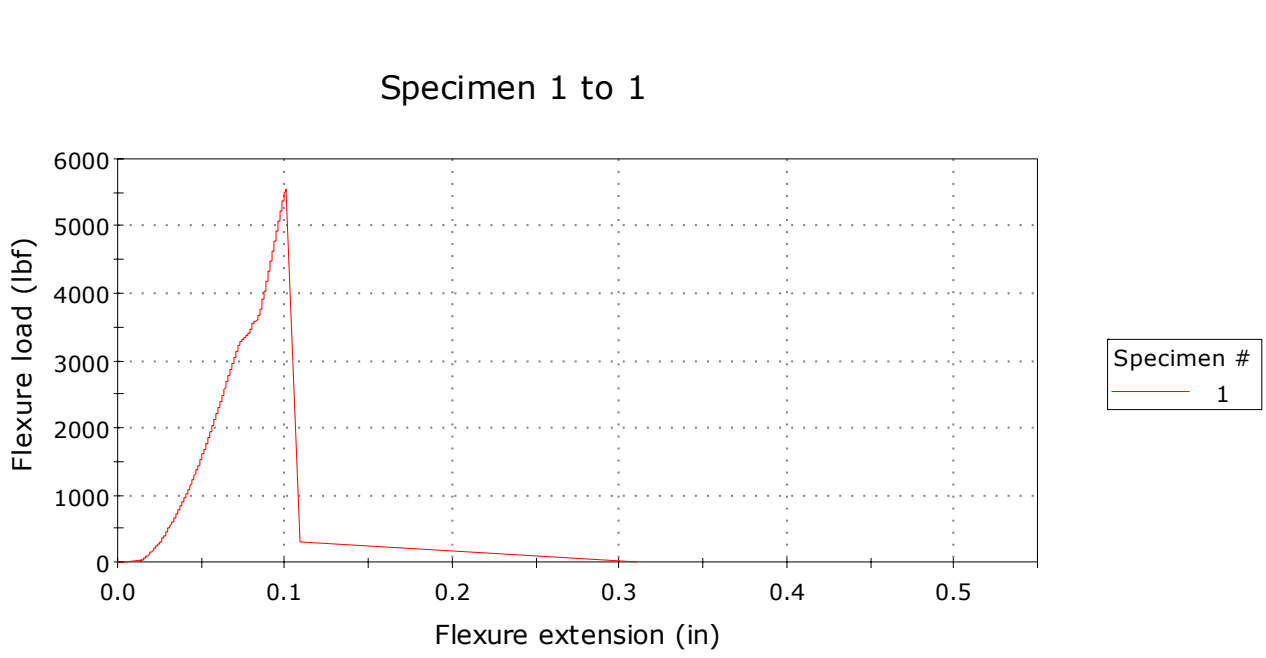

Beam Sample 3B at 7 Days

	Maximum Flexure load (lbf)	Flexure extension at Maximum Flexure load (in)	Flexure strain at Maximum Flexure load (%)	Flexure stress at Maximum Flexure load (ksi)
1	5541.58687	0.10078	0.14503	33.71995

	Energy at Maximum Flexure load (ft-lbf)	Start Date	Fixture type	Support span (in)
1	16.01295	7/24/2008 10:49:48	4-point	18.00000

	Thickness (in)	Width (in)	Flexure extension at Break (Standard) (in)	Flexure load at Break (Standard) (lbf)
1	0.99300	3.00000	0.60440	-62.17966

	Flexure strain at Break (Standard) (%)	Flexure stress at Break (Standard) (ksi)
1	0.86981	-0.37836

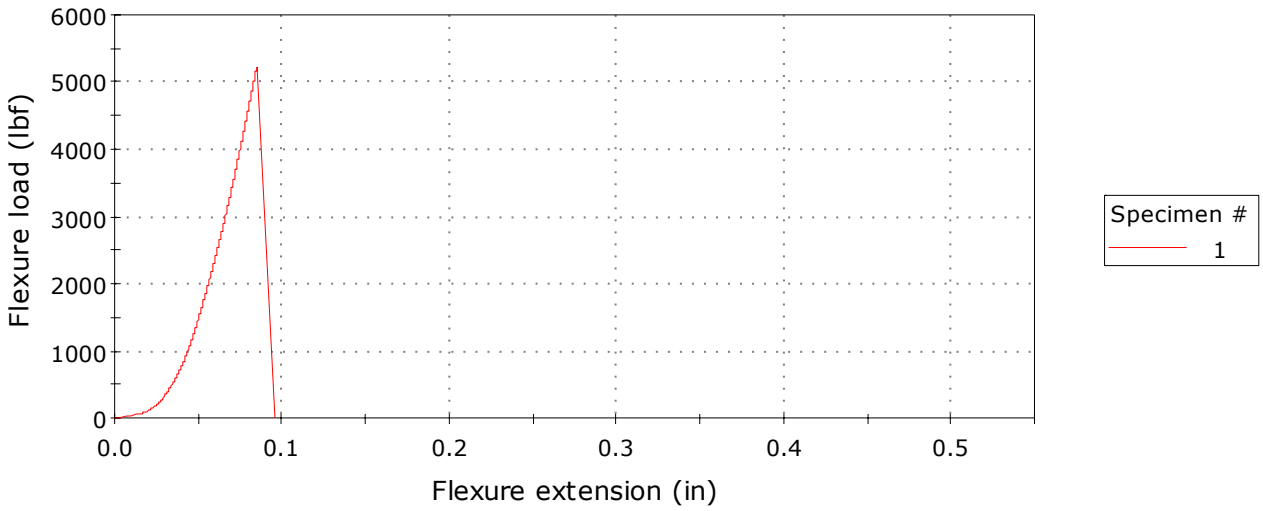

Beam Sample 3C at 7 Days

	Maximum Flexure load (lbf)	Flexure extension at Maximum Flexure load (in)	Flexure strain at Maximum Flexure load (%)	Flexure stress at Maximum Flexure load (ksi)
1	5228.34312	0.08522	0.12264	31.81389

	Energy at Maximum Flexure load (ft-lbf)	Start Date	Fixture type	Support span (in)
1	11.06786	7/24/2008 11:02:54	4-point	18.00000

	Thickness (in)	Width (in)	Flexure extension at Break (Standard) (in)	Flexure load at Break (Standard) (lbf)
1	0.99300	3.00000	0.59087	-58.95938

	Flexure strain at Break (Standard) (%)	Flexure stress at Break (Standard) (ksi)
1	0.85034	-0.35876

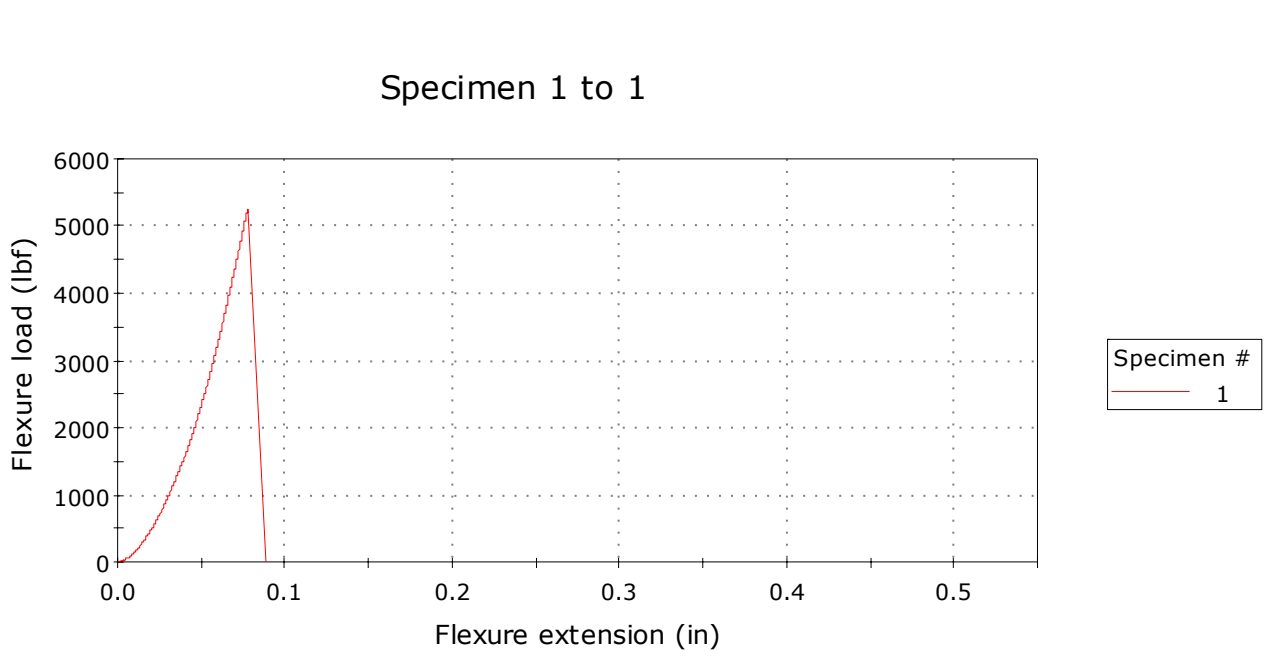

Beam Sample 3D at 7 Days

	Maximum Flexure load (lbf)	Flexure extension at Maximum Flexure load (in)	Flexure strain at Maximum Flexure load (%)	Flexure stress at Maximum Flexure load (ksi)
1	5245.64743	0.07799	0.11224	31.91919

	Energy at Maximum Flexure load (ft-lbf)	Start Date	Fixture type	Support span (in)
1	12.22258	7/24/2008 11:15:22	4-point	18.00000

	Thickness (in)	Width (in)	Flexure extension at Break (Standard) (in)	Flexure load at Break (Standard) (lbf)
1	0.99300	3.00000	0.59891	-61.86889

	Flexure strain at Break (Standard) (%)	Flexure stress at Break (Standard) (ksi)
1	0.86191	-0.37647

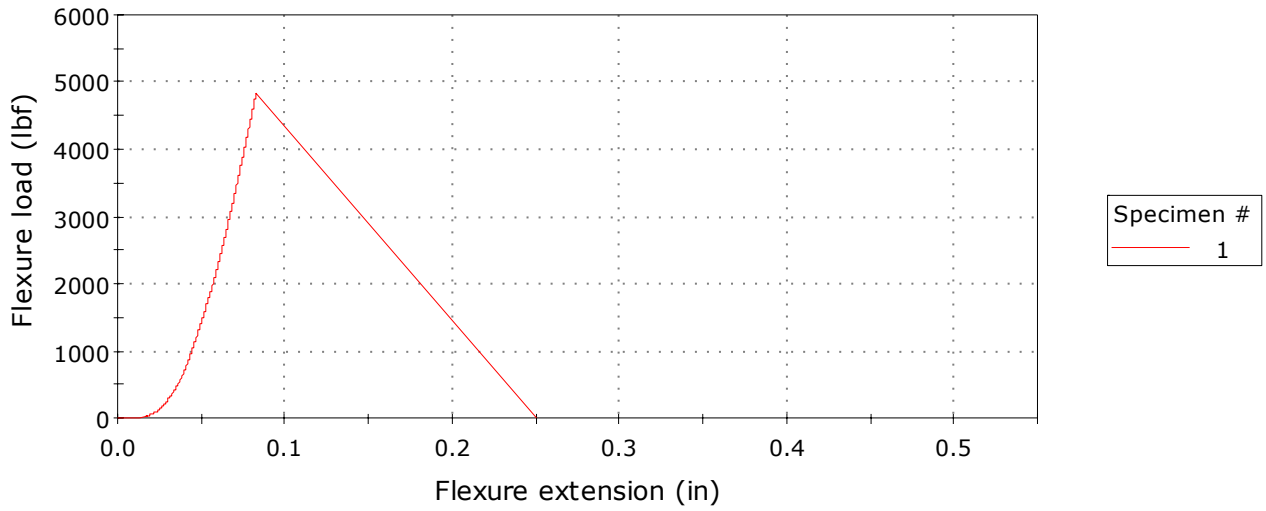

Beam Sample 4A at 7 Days

	Maximum Flexure load (lbf)	Flexure extension at Maximum Flexure load (in)	Flexure strain at Maximum Flexure load (%)	Flexure stress at Maximum Flexure load (ksi)
1	4844.41349	0.08322	0.11977	29.47772

	Energy at Maximum Flexure load (ft-lbf)	Start Date	Fixture type	Support span (in)
1	9.75770	7/24/2008 11:28:16	4-point	18.00000

	Thickness (in)	Width (in)	Flexure extension at Break (Standard) (in)	Flexure load at Break (Standard) (lbf)
1	0.99300	3.00000	0.54895	-59.56107

	Flexure strain at Break (Standard) (%)	Flexure stress at Break (Standard) (ksi)
1	0.79001	-0.36242

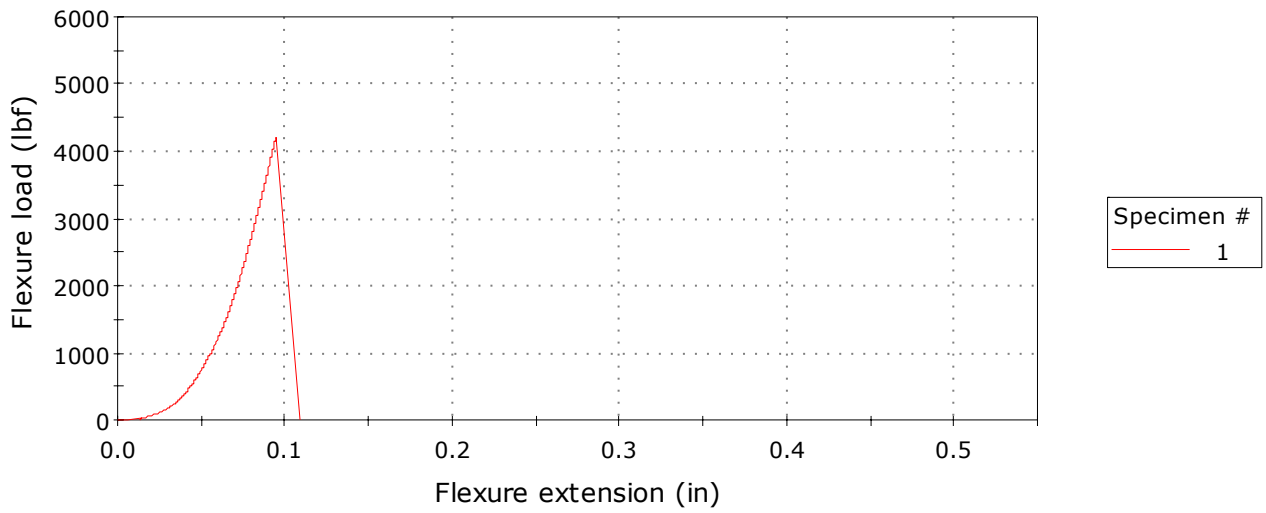

Beam Sample 4B at 7 Days

	Maximum Flexure load (lbf)	Flexure extension at Maximum Flexure load (in)	Flexure strain at Maximum Flexure load (%)	Flexure stress at Maximum Flexure load (ksi)
1	4195.67149	0.09464	0.13620	25.53020

	Energy at Maximum Flexure load (ft-lbf)	Start Date	Fixture type	Support span (in)
1	9.00931	7/24/2008 11:40:48	4-point	18.00000

	Thickness (in)	Width (in)	Flexure extension at Break (Standard) (in)	Flexure load at Break (Standard) (lbf)
1	0.99300	3.00000	0.59001	-59.62962

	Flexure strain at Break (Standard) (%)	Flexure stress at Break (Standard) (ksi)
1	0.84911	-0.36284

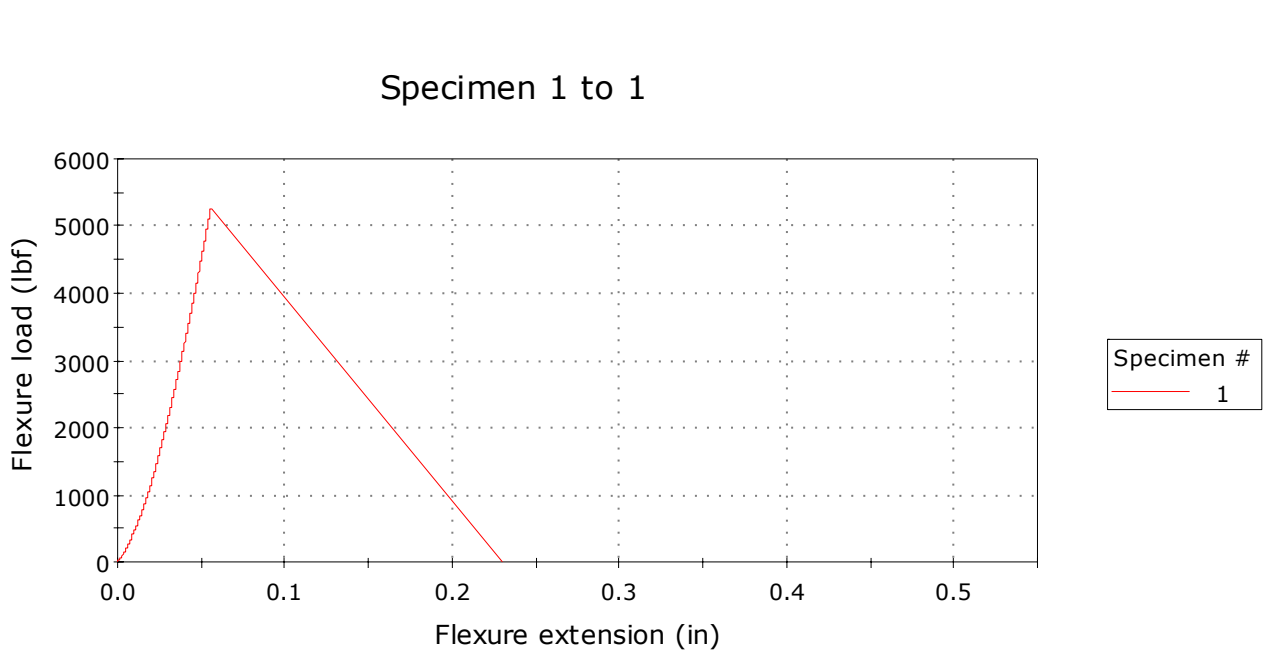

Beam Sample 4C at 7 Days

	Maximum Flexure load (lbf)	Flexure extension at Maximum Flexure load (in)	Flexure strain at Maximum Flexure load (%)	Flexure stress at Maximum Flexure load (ksi)
1	5263.27769	0.05603	0.08064	32.02647

	Energy at Maximum Flexure load (ft-lbf)	Start Date	Fixture type	Support span (in)
1	10.09932	7/24/2008 11:51:57	4-point	18.00000

	Thickness (in)	Width (in)	Flexure extension at Break (Standard) (in)	Flexure load at Break (Standard) (lbf)
1	0.99300	3.00000	0.64240	-151.35689

	Flexure strain at Break (Standard) (%)	Flexure stress at Break (Standard) (ksi)
1	0.92450	-0.92099

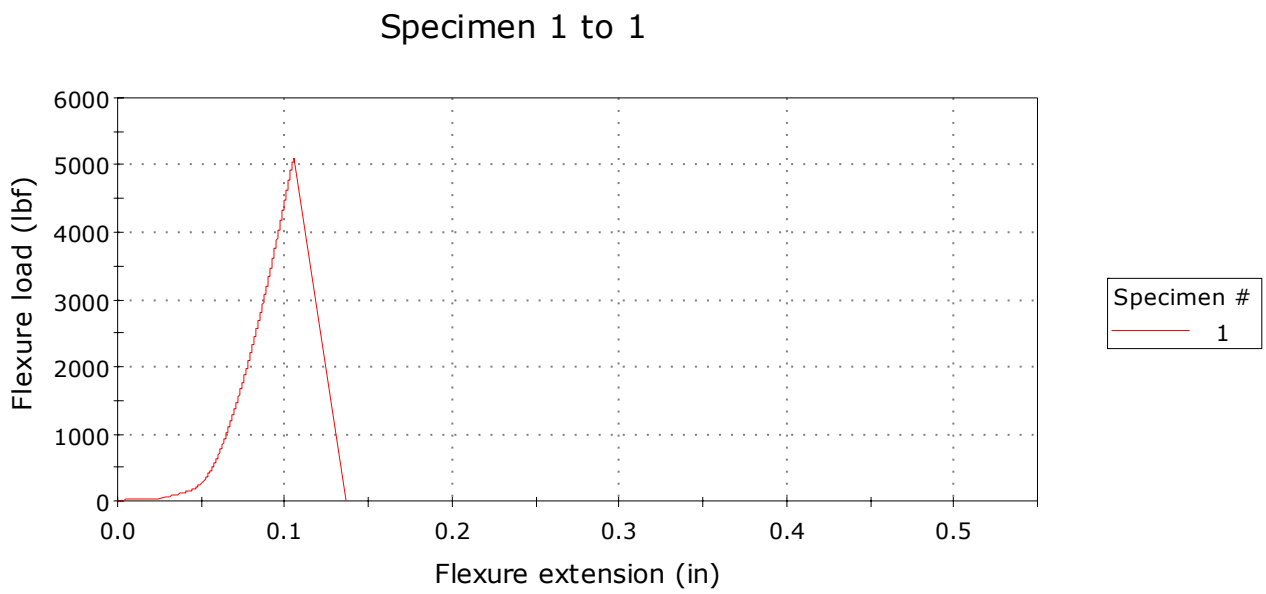

Beam Sample 4D at 7 Days

	Maximum Flexure load (lbf)	Flexure extension at Maximum Flexure load (in)	Flexure strain at Maximum Flexure load (%)	Flexure stress at Maximum Flexure load (ksi)
1	5108.77598	0.10585	0.15233	31.08634

	Energy at Maximum Flexure load (ft-lbf)	Start Date	Fixture type	Support span (in)
1	10.86242	7/24/2008 12:04:04	4-point	18.00000

	Thickness (in)	Width (in)	Flexure extension at Break (Standard) (in)	Flexure load at Break (Standard) (lbf)
1	0.99300	3.00000	0.56861	-31.20122

	Flexure strain at Break (Standard) (%)	Flexure stress at Break (Standard) (ksi)
1	0.81830	-0.18986

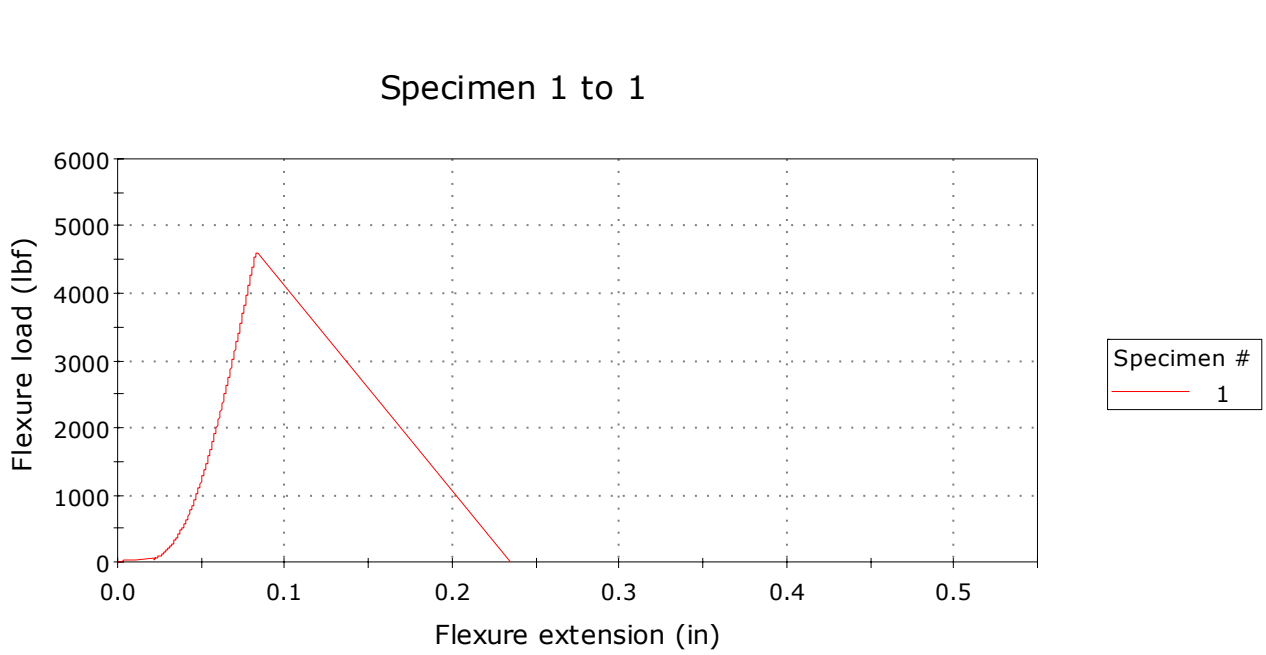

Beam Sample 5A at 7 Days

	Maximum Flexure load (lbf)	Flexure extension at Maximum Flexure load (in)	Flexure strain at Maximum Flexure load (%)	Flexure stress at Maximum Flexure load (ksi)
1	4596.54531	0.08328	0.11985	27.96947

	Energy at Maximum Flexure load (ft-lbf)	Start Date	Fixture type	Support span (in)
1	8.97015	7/24/2008 12:16:41	4-point	18.00000

	Thickness (in)	Width (in)	Flexure extension at Break (Standard) (in)	Flexure load at Break (Standard) (lbf)
1	0.99300	3.00000	0.66388	-46.26361

	Flexure strain at Break (Standard) (%)	Flexure stress at Break (Standard) (ksi)
1	0.95541	-0.28151

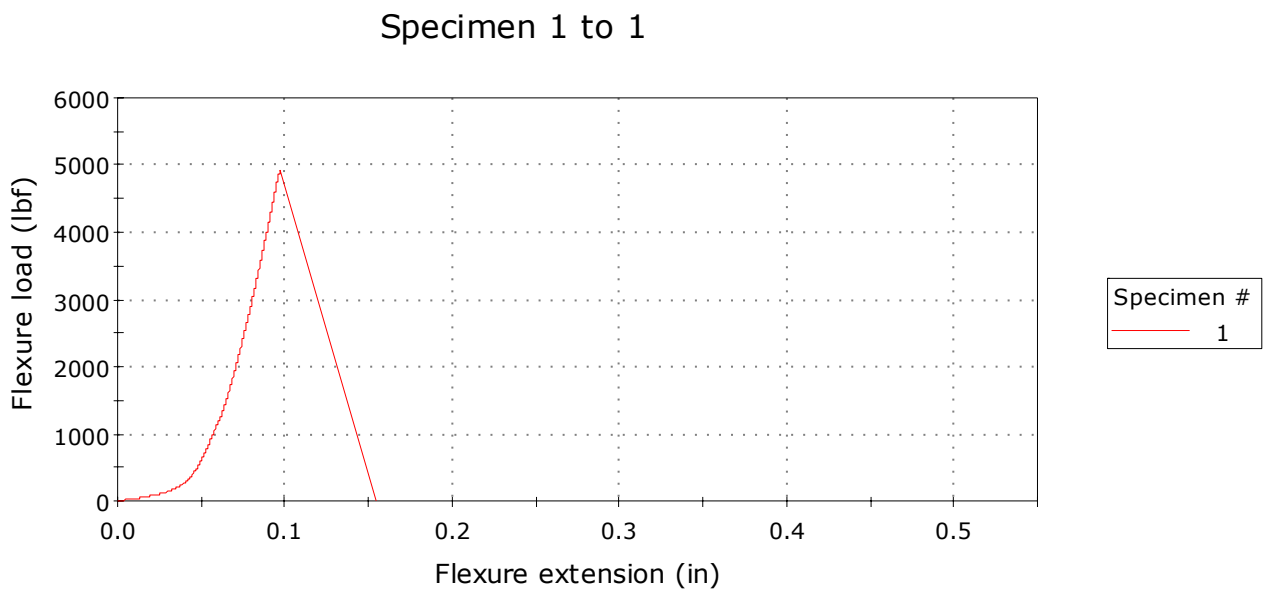

Beam Sample 5B at 7 Days

	Maximum Flexure load (lbf)	Flexure extension at Maximum Flexure load (in)	Flexure strain at Maximum Flexure load (%)	Flexure stress at Maximum Flexure load (ksi)
1	4920.29809	0.09710	0.13974	29.93947

	Energy at Maximum Flexure load (ft-lbf)	Start Date	Fixture type	Support span (in)
1	10.27072	7/24/2008 12:29:17	4-point	18.00000

	Thickness (in)	Width (in)	Flexure extension at Break (Standard) (in)	Flexure load at Break (Standard) (lbf)
1	0.99300	3.00000	0.62377	-68.23554

	Flexure strain at Break (Standard) (%)	Flexure stress at Break (Standard) (ksi)
1	0.89769	-0.41521

Appendix B

Soil Boring Logs

HNTB
ENGINEERS ARCHITECTS PLANNERS
11414 West Park Place, Ste. 300, Milwaukee, WI 53224
Phone (414) 359-2300 Fax (414) 359-2310

SOIL BORING LOG

BORING NUMBER: **B-1**

PROJECT NAME: Wisconsin Highway Research Project		DATE DRILLING STARTED: 4/6/2009	DRILLING METHOD: wash boring
PROJECT NUMBER: 41991		DATE DRILLING ENDED: 4/7/2009	DRILL RIG:
BORING DRILLED BY: FIRM: WisDOT CREW CHIEF: Skolos	FIELD LOG: Skolos LAB LOG / QC: SDM/DAJ	NORTHING: EASTING:	BOREHOLE DIAMETER: 4 in. SURFACE ELEVATION: Feet

Number and Type	Recovery (in)	Blow Counts	N - Value	Depth (ft) / Elevation	Soil Description and Geological Origin for Each Major Unit	USCS	Graphic	Well Diagram	Unconfined Compressive Strength (Qu or **Qp**) (tsf)	Liquid Limit	Plasticity Index	Moisture Content (%)	Comments
SPT - 1	24		32		Dense, gray to brown GRANULAR FILL, fine to coarse sand and gravel, moist								
SPT - 2	24		11										
					Hard, brown CLAY/SILT FILL, little fine gravel, moist								
SPT - 3	24		11	**5**	Very loose to loose, dark brown to black silty SAND, little to some fine to coarse gravel, trace organics, moist to wet (Possible Fill)								
SPT - 4	12		7	▽									
SPT - 5	24		1										
				10									
SPT - 6	0		6										No recovery @ 10-12 feet sample interval
SPT - 7	24		9		- with trace fine gravel	SM							
SH - 8	0			**15**									No recovery in Shelby Tube
SPT - 9	24		2										
SPT - 10	24		19										
				20	Medium dense to very dense well-graded SAND with silt, trace organics (marine shells), moist	SW-SM							

WATER OBSERVATION DATA

▽	WATER ENCOUNTERED DURING DRILLING: 8 ft.		CAVE DEPTH AT COMPLETION: ft.	WET ☐ DRY ☐
▼	WATER LEVEL AT COMPLETION: ft.	■	CAVE DEPTH AFTER HOURS: ft., hrs.	WET ☐ DRY ☐
▼	WATER LEVEL AFTER HOURS: ft., hrs.		NOTE: Bolded Unconfined Compressive Strength values denote a Qp test.	

NOTE: Stratification lines between soil types represent the approximate boundary; gradual transition between in-situ soil layers should be expected.

HNTB GEOTECH SBL WHRP 2009 BORINGS.GPJ HNTB-WIDNR.GDT 5/20/09

HNTB
ENGINEERS ARCHITECTS PLANNERS
11414 West Park Place, Ste. 300, Milwaukee, WI 53224
Phone (414) 359-2300 Fax (414) 359-2310

SOIL BORING LOG

PROJECT NAME: Wisconsin Highway Research Project		DATE DRILLING STARTED: 4/6/2009	BORING NUMBER: B-1
PROJECT NUMBER: 41991		DATE DRILLING ENDED: 4/7/2009	DRILLING METHOD: wash boring
BORING DRILLED BY: FIRM: WisDOT CREW CHIEF: Skolos	FIELD LOG: Skolos LAB LOG / QC: SDM/DAJ	NORTHING EASTING	DRILL RIG BOREHOLE DIAMETER: 4 in. SURFACE ELEVATION: Feet

Number and Type	Recovery (in)	Blow Counts	N - Value	Depth (ft) / Elevation	Soil Description and Geological Origin for Each Major Unit	USCS	Graphic	Well Diagram	Unconfined Compressive Strength (Qu or Qp) (tsf)	Liquid Limit	Plasticity Index	Moisture Content (%)	Comments
SPT - 11	18		56		Medium dense to very dense well-graded SAND with silt, trace organics (marine shells), moist - with little coarse gravel and less silt	SW-SM							
				25									
SPT - 12	18		12		Stiff, brown CLAY, trace fine to coarse gravel, little fine sand, moist				**1.75**				
				30									
SPT - 13	18		15			CH			**1.75**				
				35									
SPT - 14	18		11		- with little to some silt - Shelby Tube collected @ 36.5-39 feet				**1.5**				
				40									

WATER OBSERVATION DATA

WATER ENCOUNTERED DURING DRILLING: 8 ft.		CAVE DEPTH AT COMPLETION: ft.	WET ☐ DRY ☐
WATER LEVEL AT COMPLETION: ft.		CAVE DEPTH AFTER HOURS: ft., hrs.	WET ☐ DRY ☐
WATER LEVEL AFTER HOURS: ft., hrs.		NOTE: Bolded Unconfined Compressive Strength values denote a Qp test.	

NOTE: Stratification lines between soil types represent the approximate boundary; gradual transition between in-situ soil layers should be expected.

HNTB GEOTECH SBL WHRP 2009 BORINGS.GPJ HNTB-WIDNR.GDT 5/20/09

HNTB
ENGINEERS ARCHITECTS PLANNERS
11414 West Park Place, Ste. 300, Milwaukee, WI 53224
Phone (414) 359-2300 Fax (414) 359-2310

SOIL BORING LOG

BORING NUMBER: B-1

PROJECT NAME: Wisconsin Highway Research Project
PROJECT NUMBER: 41991
DATE DRILLING STARTED: 4/6/2009
DATE DRILLING ENDED: 4/7/2009
DRILLING METHOD: wash boring
DRILL RIG:

BORING DRILLED BY: FIRM: WisDOT; CREW CHIEF: Skolos
FIELD LOG: Skolos
LAB LOG / QC: SDM/DAJ
NORTHING:
EASTING:
BOREHOLE DIAMETER: 4 in.
SURFACE ELEVATION: Feet

Number and Type	Recovery (in)	Blow Counts	N - Value	Depth (ft) / Elevation	Soil Description and Geological Origin for Each Major Unit	USCS	Graphic	Well Diagram	Unconfined Compressive Strength (Qu or Qp) (tsf)	Liquid Limit	Plasticity Index	Moisture Content (%)	Comments
					Stiff, brown CLAY, trace fine to coarse gravel, little fine sand, moist								
SPT - 15	18		10						1				
				45									
SPT - 16	18		1.25						1.25				
						CH							
				50									
SPT - 17	18		14						1.5				
				55									
SPT - 18	18		19		Very stiff to hard, brownish gray silty CLAY, little fine sand, moist				2.5				
						CL							
				60									

WATER OBSERVATION DATA

▽	WATER ENCOUNTERED DURING DRILLING: 8 ft.		CAVE DEPTH AT COMPLETION: ft.	WET ☐ DRY ☐
▼	WATER LEVEL AT COMPLETION: ft.		CAVE DEPTH AFTER HOURS: ft., hrs.	WET ☐ DRY ☐
▼	WATER LEVEL AFTER HOURS: ft., hrs.		NOTE: Bolded Unconfined Compressive Strength values denote a Qp test.	

NOTE: Stratification lines between soil types represent the approximate boundary; gradual transition between in-situ soil layers should be expected.

HNTB GEOTECH SBL WHRP 2009 BORINGS.GPJ HNTB-WIDNR.GDT 5/20/09

HNTB
ENGINEERS ARCHITECTS PLANNERS
11414 West Park Place, Ste. 300, Milwaukee, WI 53224
Phone (414) 359-2300 Fax (414) 359-2310

SOIL BORING LOG

BORING NUMBER: **B-1**

PROJECT NAME: Wisconsin Highway Research Project		DATE DRILLING STARTED: 4/6/2009	DRILLING METHOD: wash boring
PROJECT NUMBER: 41991		DATE DRILLING ENDED: 4/7/2009	DRILL RIG:
BORING DRILLED BY: FIRM: WisDOT CREW CHIEF: Skolos	FIELD LOG: Skolos LAB LOG / QC: SDM/DAJ	NORTHING: EASTING:	BOREHOLE DIAMETER: 4 in. SURFACE ELEVATION: Feet

Number and Type	Recovery (in)	Blow Counts	N - Value	Depth (ft) / Elevation	Soil Description and Geological Origin for Each Major Unit	USCS	Graphic	Well Diagram	Unconfined Compressive Strength (Qu or **Qp**) (tsf)	Liquid Limit	Plasticity Index	Moisture Content (%)	Comments
					Very stiff to hard, brownish gray silty CLAY, little fine sand, moist								
SPT - 19	18		24		- with wet silt seam				**0.5**				
				65									
SPT - 20	18		28						**3.5**				
						CL							
				70									
SPT - 21	18		40						**4.5**				
				75									
SPT - 22	18		27		Medium dense, gray silty SAND with clay, wet				**0.5**				
						SM							
				80									

WATER OBSERVATION DATA

▽	WATER ENCOUNTERED DURING DRILLING: 8 ft.	CAVE DEPTH AT COMPLETION: ft.	WET ☐ DRY ☐
▼	WATER LEVEL AT COMPLETION: ft.	CAVE DEPTH AFTER HOURS: ft., hrs.	WET ☐ DRY ☐
▼	WATER LEVEL AFTER HOURS: ft., hrs.	NOTE: Bolded Unconfined Compressive Strength values denote a Qp test.	

NOTE: Stratification lines between soil types represent the approximate boundary; gradual transition between in-situ soil layers should be expected.

HNTB GEOTECH SBL WHRP 2009 BORINGS.GPJ HNTB-WIDNR.GDT 5/20/09

HNTB
ENGINEERS ARCHITECTS PLANNERS
11414 West Park Place, Ste. 300, Milwaukee, WI 53224
Phone (414) 359-2300 Fax (414) 359-2310

SOIL BORING LOG

BORING NUMBER: **B-1**

PROJECT NAME: Wisconsin Highway Research Project		DATE DRILLING STARTED: 4/6/2009	DRILLING METHOD: wash boring
PROJECT NUMBER: 41991		DATE DRILLING ENDED: 4/7/2009	DRILL RIG:
BORING DRILLED BY: FIRM: WisDOT CREW CHIEF: Skolos	FIELD LOG: Skolos LAB LOG / QC: SDM/DAJ	NORTHING: EASTING:	BOREHOLE DIAMETER: 4 in. SURFACE ELEVATION: Feet

Number and Type	Recovery (in)	Blow Counts	N - Value	Depth (ft) / Elevation	Soil Description and Geological Origin for Each Major Unit	USCS	Graphic	Well Diagram	Unconfined Compressive Strength (Qu or **Qp**) (tsf)	Liquid Limit	Plasticity Index	Moisture Content (%)	Comments
					Medium dense, gray silty SAND with clay, wet	SM							
SPT - 23	18		27		Medium dense, gray well-graded GRAVEL with sand, little to some silt, wet	GW-GM							
					End of Boring @ 82 feet								
				85									
				90									
				95									
				100									

WATER OBSERVATION DATA

▽	WATER ENCOUNTERED DURING DRILLING: 8 ft.		CAVE DEPTH AT COMPLETION: ft.	WET ☐ DRY ☐
▼	WATER LEVEL AT COMPLETION: ft.	■	CAVE DEPTH AFTER HOURS: ft., hrs.	WET ☐ DRY ☐
▼	WATER LEVEL AFTER HOURS: ft., hrs.		NOTE: Bolded Unconfined Compressive Strength values denote a Qp test.	

NOTE: Stratification lines between soil types represent the approximate boundary; gradual transition between in-situ soil layers should be expected.

HNTB GEOTECH SBL WHRP 2009 BORINGS.GPJ HNTB-WIDNR.GDT 5/20/09

HNTB
ENGINEERS ARCHITECTS PLANNERS
11414 West Park Place, Ste. 300, Milwaukee, WI 53224
Phone (414) 359-2300 Fax (414) 359-2310

SOIL BORING LOG

BORING NUMBER: **B-2**

PROJECT NAME: Wisconsin Highway Research Project		DATE DRILLING STARTED: 4/7/2009	DRILLING METHOD: wash boring
PROJECT NUMBER: 41991		DATE DRILLING ENDED: 4/8/2009	DRILL RIG:
BORING DRILLED BY: FIRM: WisDOT CREW CHIEF: Skolos	FIELD LOG: Skolos LAB LOG / QC: SDM/DAJ	NORTHING: EASTING:	BOREHOLE DIAMETER: 4 in. SURFACE ELEVATION: Feet

Number and Type	Recovery (in)	Blow Counts	N - Value	Depth (ft) / Elevation	Soil Description and Geological Origin for Each Major Unit	USCS	Graphic	Well Diagram	Unconfined Compressive Strength (Qu or **Qp**) (tsf)	Liquid Limit	Plasticity Index	Moisture Content (%)	Comments
SPT - 1	24		37		Dense to loose, light brown to black GRANULAR FILL, fine to coarse sand and gravel, dry to moist								
SPT - 2	24		19		- with black foundry sand and glass fragments								
SPT - 3	24		65	**5**	- with nails and foundry sand								
SPT - 4	24		16		- with slag and foundry sand								
SPT - 5	24		7	**10**									
SPT - 6	12		8		- with petroleum odor								
SPT - 7	6		9										
SPT - 8	6		8	**15**	Loose, black to gray silty SAND, moist to wet (Fill)	SM							Petroleum odor noted @ 14-20 feet
SPT - 9	24		4										
SPT - 10	2		100	**20**	Very dense, light to dark gray SAND with gravel, fine to coarse sand and gravel, some silt, cemented concrete fragments, wet (Fill)	SW-SM							

WATER OBSERVATION DATA

▽	WATER ENCOUNTERED DURING DRILLING: ft.	▨	CAVE DEPTH AT COMPLETION: ft. WET ☐ DRY ☐
▼	WATER LEVEL AT COMPLETION: ft.	■	CAVE DEPTH AFTER HOURS: ft., hrs. WET ☐ DRY ☐
▼	WATER LEVEL AFTER HOURS: ft., hrs.		NOTE: Bolded Unconfined Compressive Strength values denote a Qp test.

NOTE: Stratification lines between soil types represent the approximate boundary; gradual transition between in-situ soil layers should be expected.

HNTB GEOTECH SBL WHRP 2009 BORINGS.GPJ HNTB-WIDNR.GDT 5/20/09

HNTB
ENGINEERS ARCHITECTS PLANNERS
11414 West Park Place, Ste. 300, Milwaukee, WI 53224
Phone (414) 359-2300 Fax (414) 359-2310

SOIL BORING LOG

PROJECT NAME: Wisconsin Highway Research Project		DATE DRILLING STARTED: 4/7/2009	BORING NUMBER: B-2
PROJECT NUMBER: 41991		DATE DRILLING ENDED: 4/8/2009	DRILLING METHOD: wash boring
BORING DRILLED BY: FIRM: WisDOT CREW CHIEF: Skolos	FIELD LOG: Skolos LAB LOG / QC: SDM/DAJ	NORTHING EASTING	DRILL RIG BOREHOLE DIAMETER: 4 in. SURFACE ELEVATION: Feet

Number and Type	Recovery (in)	Blow Counts	N - Value	Depth (ft) / Elevation	Soil Description and Geological Origin for Each Major Unit	USCS	Graphic	Well Diagram	Unconfined Compressive Strength (Qu or Qp) (tsf)	Liquid Limit	Plasticity Index	Moisture Content (%)	Comments
SPT - 11	24		65		Very dense, light to dark gray SAND with gravel, fine to coarse sand and gravel, some silt, cemented concrete fragments, wet (Fill)	SW-SM							
SPT - 12	24		101										
SPT - 13	24		14	25	Medium, grayish brown CLAY, some fine sand, little fine gravel, moist								
				30									
SPT - 14	18		15		- with trace fine gravel	CH							
				35									
SPT - 15	18		15										
				40									

WATER OBSERVATION DATA

▽	WATER ENCOUNTERED DURING DRILLING: ft.	▨	CAVE DEPTH AT COMPLETION: ft. WET ☐ DRY ☐
▼	WATER LEVEL AT COMPLETION: ft.	■	CAVE DEPTH AFTER HOURS: ft., hrs. WET ☐ DRY ☐
▼	WATER LEVEL AFTER HOURS: ft., hrs.		NOTE: Bolded Unconfined Compressive Strength values denote a Qp test.

NOTE: Stratification lines between soil types represent the approximate boundary; gradual transition between in-situ soil layers should be expected.

HNTB GEOTECH SBL WHRP 2009 BORINGS.GPJ HNTB-WIDNR.GDT 5/20/09

HNTB
ENGINEERS ARCHITECTS PLANNERS
11414 West Park Place, Ste. 300, Milwaukee, WI 53224
Phone (414) 359-2300 Fax (414) 359-2310

SOIL BORING LOG

PROJECT NAME: Wisconsin Highway Research Project		DATE DRILLING STARTED: 4/7/2009	BORING NUMBER: B-2
PROJECT NUMBER: 41991		DATE DRILLING ENDED: 4/8/2009	DRILLING METHOD: wash boring
BORING DRILLED BY: FIRM: WisDOT CREW CHIEF: Skolos	FIELD LOG: Skolos LAB LOG / QC: SDM/DAJ	NORTHING EASTING	DRILL RIG BOREHOLE DIAMETER: 4 in. SURFACE ELEVATION: Feet

Number and Type	Recovery (in)	Blow Counts	N - Value	Depth (ft) / Elevation	Soil Description and Geological Origin for Each Major Unit	USCS	Graphic	Well Diagram	Unconfined Compressive Strength (Qu or Qp) (tsf)	Liquid Limit	Plasticity Index	Moisture Content (%)	Comments
					Medium, grayish brown CLAY, some fine sand, little fine gravel, moist								
SPT - 16	18		12										
				45		CH							
SPT - 17	18		12						0.5				
				50									
SPT - 18	18		18		Soft, gray silty CLAY, little to some fine sand, moist				0.25				
						CL							
				55									
SPT - 19	18		22		Very stiff to hard, gray silty CLAY, litte to some fine sand, moist to wet				2.5				
						CL							
				60									

WATER OBSERVATION DATA

▽	WATER ENCOUNTERED DURING DRILLING: ft.	▨	CAVE DEPTH AT COMPLETION: ft. WET ☐ DRY ☐
▼	WATER LEVEL AT COMPLETION: ft.	■	CAVE DEPTH AFTER HOURS: ft., hrs. WET ☐ DRY ☐
▼	WATER LEVEL AFTER HOURS: ft., hrs.		NOTE: Bolded Unconfined Compressive Strength values denote a Qp test.

NOTE: Stratification lines between soil types represent the approximate boundary; gradual transition between in-situ soil layers should be expected.

HNTB GEOTECH SBL WHRP 2009 BORINGS.GPJ HNTB-WIDNR.GDT 5/20/09

HNTB
ENGINEERS ARCHITECTS PLANNERS
11414 West Park Place, Ste. 300, Milwaukee, WI 53224
Phone (414) 359-2300 Fax (414) 359-2310

SOIL BORING LOG

PROJECT NAME: Wisconsin Highway Research Project		DATE DRILLING STARTED: 4/7/2009	BORING NUMBER: B-2
PROJECT NUMBER: 41991		DATE DRILLING ENDED: 4/8/2009	DRILLING METHOD: wash boring
BORING DRILLED BY: FIRM: WisDOT CREW CHIEF: Skolos	FIELD LOG: Skolos LAB LOG / QC: SDM/DAJ	NORTHING EASTING	DRILL RIG BOREHOLE DIAMETER: 4 in. SURFACE ELEVATION: Feet

Number and Type	Recovery (in)	Blow Counts	N - Value	Depth (ft) / Elevation	Soil Description and Geological Origin for Each Major Unit	USCS	Graphic	Well Diagram	Unconfined Compressive Strength (Qu or Qp) (tsf)	Liquid Limit	Plasticity Index	Moisture Content (%)	Comments
SPT - 20	18		19		Very stiff to hard, gray silty CLAY, litte to some fine sand, moist to wet	CL			**1.75**				
				65									
SPT - 21	18		17						**2.25**				
				70									
SPT - 22	18		20		- wet @ 71 feet				**2.5**				
				75									
SPT - 23	18		32		- with trace fine gravel				**4**				
				80									

WATER OBSERVATION DATA

▽	WATER ENCOUNTERED DURING DRILLING: ft.	▨	CAVE DEPTH AT COMPLETION: ft. WET ☐ DRY ☐
▼	WATER LEVEL AT COMPLETION: ft.	■	CAVE DEPTH AFTER HOURS: ft., hrs. WET ☐ DRY ☐
▼	WATER LEVEL AFTER HOURS: ft., hrs.		NOTE: Bolded Unconfined Compressive Strength values denote a Qp test.

NOTE: Stratification lines between soil types represent the approximate boundary; gradual transition between in-situ soil layers should be expected.

HNTB GEOTECH SBL WHRP 2009 BORINGS.GPJ HNTB-WIDNR.GDT 5/20/09

HNTB
ENGINEERS ARCHITECTS PLANNERS
11414 West Park Place, Ste. 300, Milwaukee, WI 53224
Phone (414) 359-2300 Fax (414) 359-2310

SOIL BORING LOG

BORING NUMBER: **B-2**

PROJECT NAME: Wisconsin Highway Research Project		DATE DRILLING STARTED: 4/7/2009	DRILLING METHOD: wash boring
PROJECT NUMBER: 41991		DATE DRILLING ENDED: 4/8/2009	DRILL RIG:
BORING DRILLED BY: FIRM: WisDOT CREW CHIEF: Skolos	FIELD LOG: Skolos LAB LOG / QC: SDM/DAJ	NORTHING: EASTING:	BOREHOLE DIAMETER: 4 in. SURFACE ELEVATION: Feet

Number and Type	Recovery (in)	Blow Counts	N - Value	Depth (ft) / Elevation	Soil Description and Geological Origin for Each Major Unit	USCS	Graphic	Well Diagram	Unconfined Compressive Strength (Qu or **Qp**) (tsf)	Liquid Limit	Plasticity Index	Moisture Content (%)	Comments
SPT - 24	18		43		Very stiff to hard, gray silty CLAY, litte to some fine sand, moist to wet	CL			**4.5**				
					End of Boring @ 81.5 feet								
				85									
				90									
				95									
				100									

WATER OBSERVATION DATA

▽	WATER ENCOUNTERED DURING DRILLING: ft.		CAVE DEPTH AT COMPLETION: ft.	WET ☐ DRY ☐
▼	WATER LEVEL AT COMPLETION: ft.	■	CAVE DEPTH AFTER HOURS: ft., hrs.	WET ☐ DRY ☐
▼	WATER LEVEL AFTER HOURS: ft., hrs.		NOTE: Bolded Unconfined Compressive Strength values denote a Qp test.	

NOTE: Stratification lines between soil types represent the approximate boundary; gradual transition between in-situ soil layers should be expected.

HNTB GEOTECH SBL WHRP 2009 BORINGS.GPJ HNTB-WIDNR.GDT 5/20/09

Appendix C

Field Concrete Strength Data

WHRP
Summary of Concrete Breaks
Cylinders and Beams

Pile No.	Sample No.	Distance from Center of Pile (feet)	Block No.	Cylinder/Beam No.	Pour Date/Time	Planned Break Interval	Lab Break Day/Time	Break Value (pounds)	Compressive Strength or Modulus of Rupture (psi)
1	1A10	9'-8 7/8"	1	Cylinder 1	10-28/1000 hrs	1-2 days	10-30/1400 hrs	27800	2213
1	1B10	9'-10 3/8"	2	Cylinder 1	10-28/1600 hrs	1-2 days	10-30/1400 hrs	22500	1791
1	1C10	9'-10"	3	Cylinder 1	10-29/1000 hrs	1-2 days	10-30/1400 hrs	10700	852
1	1A25	24'-4"	4	Cylinder 1	10-28/1000 hrs	1-2 days	10-30/1400 hrs	21900	1744
1	1B25	25'-2 3/8"	5	Cylinder 1	10-28/1600 hrs	1-2 days	10-30/1400 hrs	22900	1823
1	1C25	24'-11 1/4"	6	Cylinder 1	10-29/1000 hrs	1-2 days	10-30/1400 hrs	17300	1377
1	1A50	49'-7 3/4"	7	Cylinder 1	10-29/1000 hrs	1-2 days	10-30/1400 hrs	29900	2381
1	1B50	49'-10 1/4"	8	Cylinder 1	10-28/1600 hrs	1-2 days	10-30/1400 hrs	23600	1879
1	1C50	49'-11 3/4"	9	Cylinder 1	10-28/1000 hrs	1-2 days	10-30/1400 hrs	19400	1545
	Control 1-2				10-28/1600 hrs	46	10-30/1400 hrs	25800	913
	Control 3-4				10-28/1000 hrs	52	10-30/1400 hrs	72300	2558
2	1A10	9'-10"	1	Cylinder 1	10-28/1000 hrs	1-2 days	10-30/1400 hrs	32800	2611
2	1B10	9'-6 3/4"	2	Cylinder 1	10-28/1600 hrs	1-2 days	10-30/1400 hrs	24400	1943
2	1C10	10'-1/2"	3	Cylinder 1	10-29/1000 hrs	1-2 days	10-30/1400 hrs	Broken cylinder	
2	1A25	24'-6 1/4"	4	Cylinder 1	10-28/1000 hrs	1-2 days	10-30/1400 hrs	31400	2500
2	1B25	24'-7 1/2"	5	Cylinder 1	10-28/1600 hrs	1-2 days	10-30/1400 hrs	24200	1927
2	1C25	25'-2"	6	Cylinder 1	10-29/1000 hrs	1-2 days	10-30/1400 hrs	19400	1545
2	1A50	49'-8 3/8"	7	Cylinder 1	10-29/1000 hrs	1-2 days	10-30/1400 hrs	30400	2420
2	1B50	50'-3/4"	8	Cylinder 1	10-28/1600 hrs	1-2 days	10-30/1400 hrs	23800	1895
2	1C50	50'-1/8"	9	Cylinder 1	10/28/1600 hrs	1-2 days	10-30/1400 hrs	20000	1592
1	2A10	9'-7 1/8"	1	Cylinder 2	10-28/1000 hrs	3-4 days	10-31/1000 hrs	39300	3129
1	2B10	9'-8 3/8"	2	Cylinder 2	10-28/1600 hrs	3-4 days	10-31/1000 hrs	32000	2548
1	2C10	9'8 1/2"	3	Cylinder 2	10-29/1000 hrs	3-4 days	10-31/1000 hrs	27900	2221
1	2A25	24'-4"	4	Cylinder 2	10-28/1000 hrs	3-4 days	10-31/1000 hrs	42100	3352
1	2B25	25'-1 3/8"	5	Cylinder 2	10-28/1600 hrs	3-4 days	10-31/1000 hrs	31200	2484
1	2C25	24'-11"	6	Cylinder 2	10-29/1000 hrs	3-4 days	10-31/1000 hrs	30600	2436
1	2A50	49'-7 1/2"	7	Cylinder 2	10-29/1000 hrs	3-4 days	10-31/1000 hrs	37600	2994
1	2B50	49'-10 1/2"	8	Cylinder 2	10-28/1600 hrs	3-4 days	10-31/1000 hrs	34000	2707
1	2C50	49'-11 1/4"	9	Cylinder 2	10-28/1000 hrs	3-4 days	10-31/1000 hrs	34500	2747
	Control 1633				10-28/1600 hrs	46	10-31/1000 hrs	114000	4034
	Control 1634				10-28/1000 hrs	52	10-31/1000 hrs	120200	4253
2	2A10	9'-7 1/2"	1	Cylinder 2	10-28/1000 hrs	3-4 days	10-31/1000 hrs	39400	3137
2	2B10	9'-6 1/8"	2	Cylinder 2	10-28/1600 hrs	3-4 days	10-31/1000 hrs	27700	2205
2	2C10	10'-0"	3	Cylinder 2	10-29/1000 hrs	3-4 days	10-31/1000 hrs	31600	2516
2	2A25	24'-7"	4	Cylinder 2	10-28/1000 hrs	3-4 days	10-31/1000 hrs	41700	3320
2	2B25	24'7"	5	Cylinder 2	10-28/1600 hrs	3-4 days	10-31/1000 hrs	30600	2436
2	2C25	25'-3/4"	6	Cylinder 2	10-29/1000 hrs	3-4 days	10-31/1000 hrs	31800	2532
2	2A50	49'-8 1/4"	7	Cylinder 2	10-29/1000 hrs	3-4 days	10-31/1000 hrs	42000	3344
2	2B50	49'-11 3/4"	8	Cylinder 2	10-28/1600 hrs	3-4 days	10-31/1000 hrs	30800	2452
2	2C50	49'-11 5/8"	9	Cylinder 2	10/28/1600 hrs	3-4 days	10-31/1000 hrs	32700	2604
1	3A10	9'-7 1/8"	1	Cylinder 3	10-28/1000 hrs	7-8 days	11-04/1400 hrs	49500	3941
1	3B10	9'-7 7/8"	2	Cylinder 3	10-28/1600 hrs	7-8 days	11-04/1400 hrs	42300	3368
1	3A25	24'-3 1/2"	4	Cylinder 3	10-28/1000 hrs	7-8 days	11-04/1400 hrs	44900	3575
1	3B25	25'-1 7/8"	5	Cylinder 3	10-28/1600 hrs	7-8 days	11-04/1400 hrs	54400	4331
1	3A50	49'-6 3/4"	7	Cylinder 3	10-29/1000 hrs	7-8 days	11-04/1400 hrs	45600	3631
1	3B50	49'-11"	8	Cylinder 3	10-28/1600 hrs	7-8 days	11-04/1400 hrs	40200	3201
2	3A10	9'-6 1/8"	1	Cylinder 3	10-28/1000 hrs	7-8 days	11-04/1400 hrs	46600	3710
2	3B10	9'-5 3/4"	2	Cylinder 3	10-28/1600 hrs	7-8 days	11-04/1400 hrs	42400	3376
2	3A25	24'-7 5/8"	4	Cylinder 3	10-28/1000 hrs	7-8 days	11-04/1400 hrs	43200	3439
2	3B25	24'-7 1/8"	5	Cylinder 3	10-28/1600 hrs	7-8 days	11-04/1400 hrs	45000	3583
2	3A50	49'-7 7/8"	7	Cylinder 3	10-29/1000 hrs	7-8 days	11-04/1400 hrs	53300	4244
2	3B50	49'-11 1/8"	8	Cylinder 3	10-28/1600 hrs	7-8 days	11-04/1400 hrs	45100	3591
1	3C10	9'-7 1/2"	3	Cylinder 3	10-29/1000 hrs	7-8 days	11-05/1200 hrs	49000	3901
1	3C25	24'-10 3/4"	6	Cylinder 3	10-29/1000 hrs	7-8 days	11-05/1200 hrs	51200	4076
1	3C50	49'-11"	9	Cylinder 3	10-28/1000 hrs	7-8 days	11-05/1200 hrs	50800	4045
2	3C10	10'-1/2"	3	Cylinder 3	10-29/1000 hrs	7-8 days	11-05/1200 hrs	42200	3360
2	3C25	24'-11 3/4"	6	Cylinder 3	10-29/1000 hrs	7-8 days	11-05/1200 hrs	58600	4666
2	3C50	49'-11 1/2"	9	Cylinder 3	10/28/1600 hrs	7-8 days	11-05/1200 hrs	44000	3503
1	B1A10	9'-5/8"	1	Beam 1	10-28/1000 hrs	1-3 days	10-31/1400 hrs	4114	471
1	B1B10	8'-7 3/8"	2	Beam 1	10-28/1600 hrs	1-3 days	10-31/1400 hrs	3398	384
1	B1A25	23'-7"	4	Beam 1	10-28/1000 hrs	1-3 days	10-31/1400 hrs	3367	438
1	B1B25	24'-5 3/8"	5	Beam 1	10-28/1600 hrs	1-3 days	10-31/1400 hrs	3755	396
1	B1A50	49'-2 3/4"	9	Beam 1	10-28/1000 hrs	1-3 days	10-31/1400 hrs	3634	405
1	B1B50	49'-2 7/8"	8	Beam 1	10-28/1600 hrs	1-3 days	10-31/1400 hrs	3198	350
	Control Beam				10-28/1600 hrs	1-3 days	10-31/1400 hrs	4877	463
	Control Beam				10-28/1400 hrs	7-8 days	11-04/1400 hrs	5436	516
2	B1A10	8'-9 1/2"	1	Beam 1	10-28/1000 hrs	1-3 days	10-31/1400 hrs	4034	466
2	B1B10	8'-10 3/4"	2	Beam 1	10-28/1600 hrs	1-3 days	10-31/1400 hrs	3731	388
2	B1A25	24'-2 3/8"	4	Beam 1	10-28/1000 hrs	1-3 days	10-31/1400 hrs	3615	411
2	B1B25	23'-10"	5	Beam 1	10-28/1600 hrs	1-3 days	10-31/1400 hrs	3531	367
2	B1A50	49'-2 3/8"	9	Beam 1	10-28/1000 hrs	1-3 days	10-31/1400 hrs	4355	469
2	B1B50	49'-2 1/2"	8	Beam 1	10-28/1600 hrs	1-3 days	10-31/1400 hrs	3736	391
1	B2A10	8'-10 3/8"	1	Beam 2	10-28/1000 hrs	7-8 days	11-04/1400 hrs	4575	497
1	B2B10	8'-8 3/8"	2	Beam 2	10-28/1600 hrs	7-8 days	11-04/1400 hrs	4287	465
1	B2A25	23'-8"	4	Beam 2	10-28/1000 hrs	7-8 days	11-04/1400 hrs	4822	511
1	B2B25	24'-5 3/8"	5	Beam 2	10-28/1600 hrs	7-8 days	11-04/1400 hrs	4062	419
1	B2A50	49'/2"	9	Beam 2	10-28/1000 hrs	7-8 days	11-04/1400 hrs	5636	591
1	B2B50	49'-2 1/2"	8	Beam 2	10-28/1600 hrs	7-8 days	11-04/1400 hrs	3942	417
2	B2A10	8'-8 1/2"	1	Beam 2	10-28/1000 hrs	7-8 days	11-04/1400 hrs	4251	466
2	B2B10	8'-9"	2	Beam 2	10-28/1600 hrs	7-8 days	11-04/1400 hrs	3951	402
2	B2A25	23'-11 3/8"	4	Beam 2	10-28/1000 hrs	7-8 days	11-04/1400 hrs	4459	491
2	B2B25	23'-9 3/4"	5	Beam 2	10-28/1600 hrs	7-8 days	11-04/1400 hrs	3832	404
2	B2A50	49'-2 3/8"	9	Beam 2	10-28/1000 hrs	7-8 days	11-04/1400 hrs	4732	548
2	B2B50	49'-2 3/8"	8	Beam 2	10-28/1600 hrs	7-8 days	11-04/1400 hrs	4792	530
1	4A10	9'-7 3/8"	1	Cylinder 4	10-28/1000 hrs	28 days	11-25/1100 hrs	63000	5016
1	4B10	9'-6 3/8"	2	Cylinder 4	10-28/1600 hrs	28 days	11-25/1100 hrs	64800	5159
1	4A25	24'-4"	4	Cylinder 4	10-28/1000 hrs	28 days	11-25/1100 hrs	45500	3623
1	4B25	25'-1 7/8"	5	Cylinder 4	10-28/1600 hrs	28 days	11-25/1100 hrs	54400	4331
1	4A50	49'-7"	7	Cylinder 4	10-29/1000 hrs	28 days	11-25/1100 hrs	56800	4522
1	4B50	49'-11 1/2"	8	Cylinder 4	10-28/1600 hrs	28 days	11-25/1100 hrs	40200	3201
	Control 1635					28 days	11-25/1100 hrs	155100	5488
	Control 1636					28 days	11-25/1100 hrs	155000	5485
2	4A10	9'-5 1/2"	1	Cylinder 4	10-28/1000 hrs	28 days	11-25/1100 hrs	54200	4315
2	4B10	9'-6 1/2"	2	Cylinder 4	10-28/1600 hrs	28 days	11-25/1100 hrs	64900	5167
2	4A25	24'-9 1/8"	4	Cylinder 4	10-28/1000 hrs	28 days	11-25/1100 hrs	63900	5088
2	4B25	24'-7 3/4"	5	Cylinder 4	10-28/1600 hrs	28 days	11-25/1100 hrs	54000	4299
2	4A50	49'-8 3/8"	7	Cylinder 4	10-29/1000 hrs	28 days	11-25/1100 hrs	62400	4968
2	4B50	49'-10 1/2"	8	Cylinder 4	10-28/1600 hrs	28 days	11-25/1100 hrs	52200	4156
1	4C10	9'-7 3/8"	3	Cylinder 4	10-29/1000 hrs	28 days	11-26/1400 hrs	63100	5024
1	4C25	24'-10 1/2"	6	Cylinder 4	10-29/1000 hrs	28 days	11-26/1400 hrs	69600	5541
1	4C50	49'-10 3/4"	9	Cylinder 4	10-28/1000 hrs	28 days	11-26/1400 hrs	59800	4761
2	4C10	10'-2"	3	Cylinder 4	10-29/1000 hrs	28 days	11-26/1400 hrs	54400	4331
2	4C25	24'-10 7/8"	6	Cylinder 4	10-29/1000 hrs	28 days	11-26/1400 hrs	63600	5064
2	4C50	50'-0"	9	Cylinder 4	10/28/1600 hrs	28 days	11-26/1400 hrs	63600	5064

Appendix D

WisDOT PDA Information for Test Piles

Wisconsin Department of Transportation - Case Method Results

PDIPLOT Ver. 2009.1 - Printed: 22-Mar-2010

Test date: 29-Oct-2009

RESEARCH - 1P

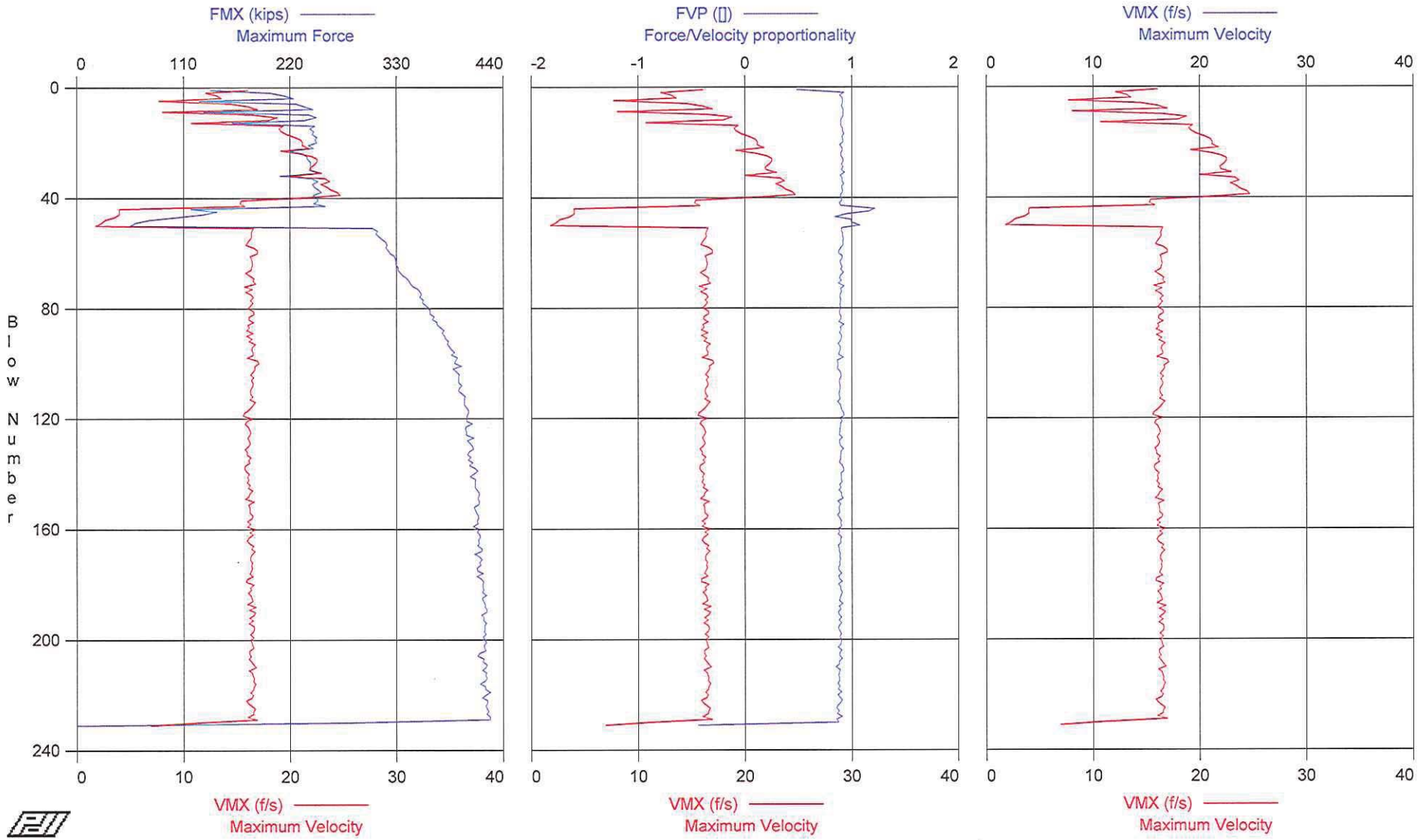

RESEARCH - 1P
OP: SGM

PILE DESCRIPTION
Test date: 29-Oct-2009

AR: 9.82 in^2
LE: 47.00 ft
WS: 16,807.9 f/s

SP: 0.492 k/ft3
EM: 30,000 ksi
JC: 0.90

FMX: Maximum Force
VMX: Maximum Velocity
FVP: Force/Velocity proportionality
VMX: Maximum Velocity
VMX: Maximum Velocity

VMX: Maximum Velocity
VMX: Maximum Velocity
VMX: Maximum Velocity
VMX: Maximum Velocity

Statistics for entire file (230 blows)

	FMX	VMX	FVP	VMX	VMX	VMX	VMX	VMX	VMX
	kips	f/s	[]	f/s	f/s	f/s	f/s	f/s	f/s
Average	356	16.4	0.9	16.4	16.4	16.4	16.4	16.4	16.4
Std. Dev.	85	3.2	0.0	3.2	3.2	3.2	3.2	3.2	3.2
Maximum	427	24.7	1.2	24.7	24.7	24.7	24.7	24.7	24.7
@ Blow#	219	39	44	39	39	39	39	39	39

Time Summary

Drive		12:47:35 PM - 12:47:35 PM (10/29/2009) BN 1 - 1
Stop	30 minutes 28 seconds	12:47:35 PM - 1:18:03 PM
Drive	5 minutes 59 seconds	1:18:03 PM - 1:24:02 PM BN 2 - 231

Total time [0:36:27] = (Driving [0:05:59] + Stop [0:30:28])

Wisconsin Department of Transportation - Case Method Results

PDIPLOT Ver. 2009.1 - Printed: 22-Mar-2010

Test date: 29-Oct-2009

RESEARCH - 2P

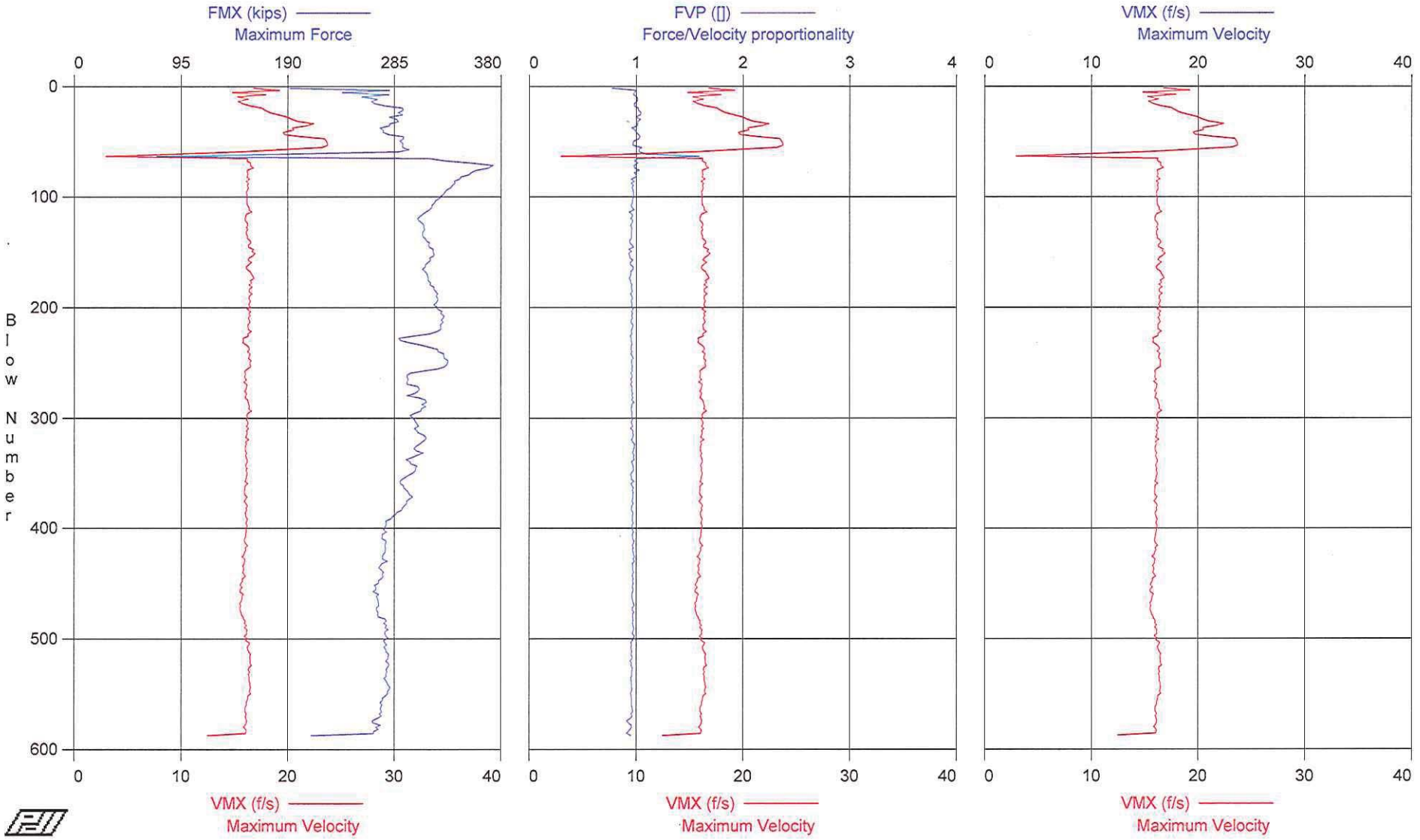

RESEARCH - 2P
OP: SGM

PILE DESCRIPTION
Test date: 29-Oct-2009

AR: 9.82 in^2
LE: 47.00 ft
WS: 16,807.9 f/s

SP: 0.492 k/ft3
EM: 30,000 ksi
JC: 0.90

FMX: Maximum Force
VMX: Maximum Velocity
FVP: Force/Velocity proportionality
VMX: Maximum Velocity
VMX: Maximum Velocity

VMX: Maximum Velocity
VMX: Maximum Velocity
VMX: Maximum Velocity
VMX: Maximum Velocity

Statistics for entire file (588 blows)

	FMX	VMX	FVP	VMX	VMX	VMX	VMX	VMX	VMX
	kips	f/s	[]	f/s	f/s	f/s	f/s	f/s	f/s
Average	296	16.4	1.0	16.4	16.4	16.4	16.4	16.4	16.4
Std. Dev.	29	1.7	0.1	1.7	1.7	1.7	1.7	1.7	1.7
Maximum	374	23.9	2.0	23.9	23.9	23.9	23.9	23.9	23.9
@ Blow#	72	51	63	51	51	51	51	51	51

Time Summary

Drive 17 minutes 7 seconds 2:19:54 PM - 2:37:01 PM (10/29/2009) BN 1 - 588

Appendix E

Field Vibration Data

Field Vibration Data

Seismograph Unit # 1

at 24.8 feet from Test Pile #1

Event Report

Date/Time Long at 14:18:11 October 29, 2009
Trigger Source Geo: 1.27 mm/s
Range Geo :254 mm/s
Record Time 8.0 sec at 1024 sps
Job Number: 1

Serial Number BE13074 V 8.12-8.0 MiniMate Plus
Battery Level 6.2 Volts
Calibration December 7, 2007 by Instantel Inc.
File Name O074CYFU.EB0

Notes
Location:
Client:
User Name:
General:

Extended Notes
Combo Mode October 29, 2009 14:17:35

Post Event Notes

Microphone Linear Weighting
PSPL 13.0 pa.(L) at 1.136 sec
ZC Freq >100 Hz
Channel Test Passed (Freq = 20.5 Hz Amp = 587 mv)

	Tran	Vert	Long	
PPV	4.44	7.11	16.3	mm/s
ZC Freq	39	16	18	Hz
Time (Rel. to Trig)	2.324	0.084	0.056	sec
Peak Acceleration	0.119	0.212	0.384	g
Peak Displacement	0.0231	0.0658	0.139	mm
Sensorcheck	Passed	Passed	Passed	
Frequency	7.3	7.3	7.4	Hz
Overswing Ratio	4.1	4.0	3.9	

Peak Vector Sum 16.8 mm/s at 0.054 sec

USBM RI8507 And OSMRE

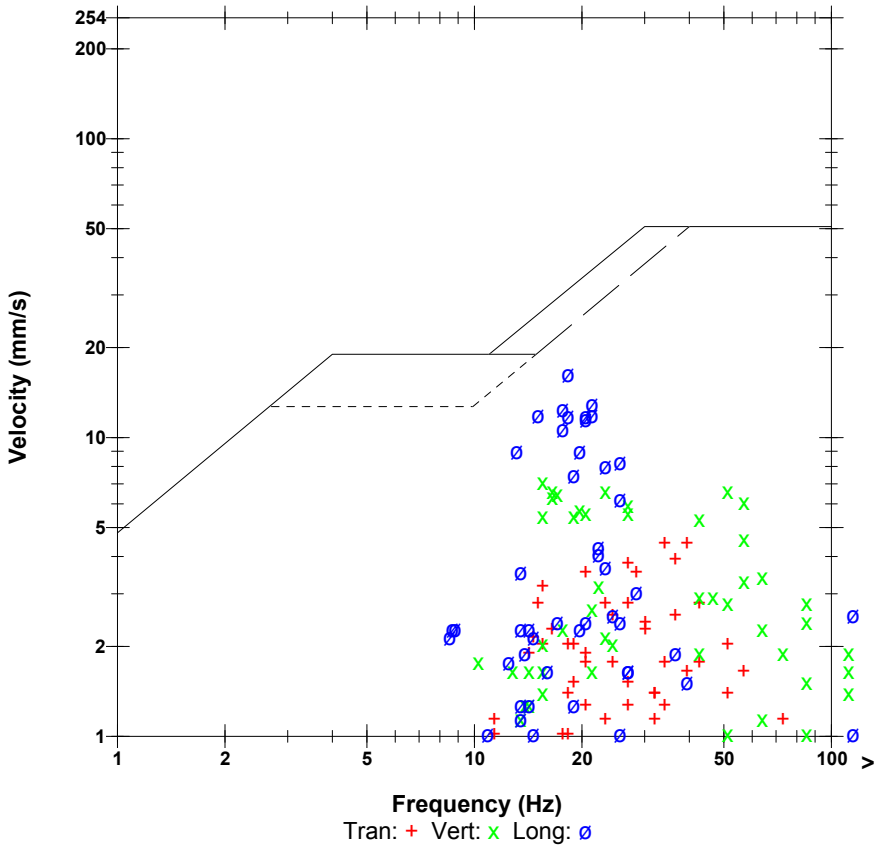

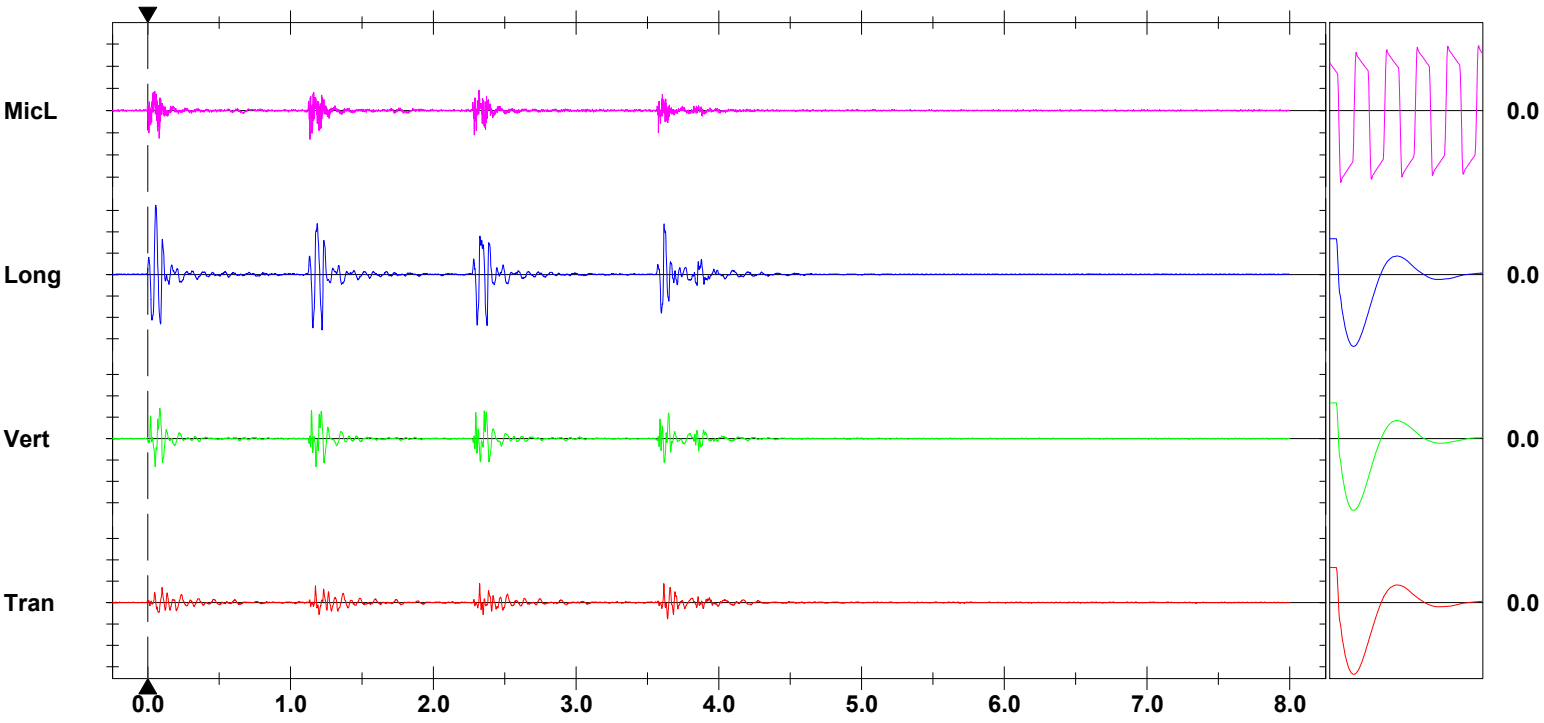

Time Scale: 0.50 sec/div **Amplitude Scale:** Geo: 5.00 mm/s/div Mic: 10.00 pa.(L)/div Sensorcheck
Trigger =

Event Report

Date/Time	Long at 14:18:51 October 29, 2009	**Serial Number**	BE13074 V 8.12-8.0 MiniMate Plus
Trigger Source	Geo: 1.27 mm/s	**Battery Level**	6.3 Volts
Range	Geo :254 mm/s	**Calibration**	December 7, 2007 by Instantel Inc.
Record Time	8.0 sec at 1024 sps	**File Name**	O074CYFU.FF0
Job Number:	1		

Notes
Location:
Client:
User Name:
General:

Extended Notes
Combo Mode October 29, 2009 14:17:35

Post Event Notes

Microphone Linear Weighting
PSPL 16.3 pa.(L) at 0.078 sec
ZC Freq >100 Hz
Channel Test Passed (Freq = 20.5 Hz Amp = 587 mv)

	Tran	Vert	Long	
PPV	4.57	6.86	11.2	mm/s
ZC Freq	39	18	19	Hz
Time (Rel. to Trig)	1.188	1.223	1.170	sec
Peak Acceleration	0.106	0.239	0.305	g
Peak Displacement	0.0246	0.0591	0.117	mm
Sensorcheck	Passed	Passed	Passed	
Frequency	7.3	7.3	7.4	Hz
Overswing Ratio	4.1	4.0	3.9	

Peak Vector Sum 12.1 mm/s at 0.098 sec

USBM RI8507 And OSMRE

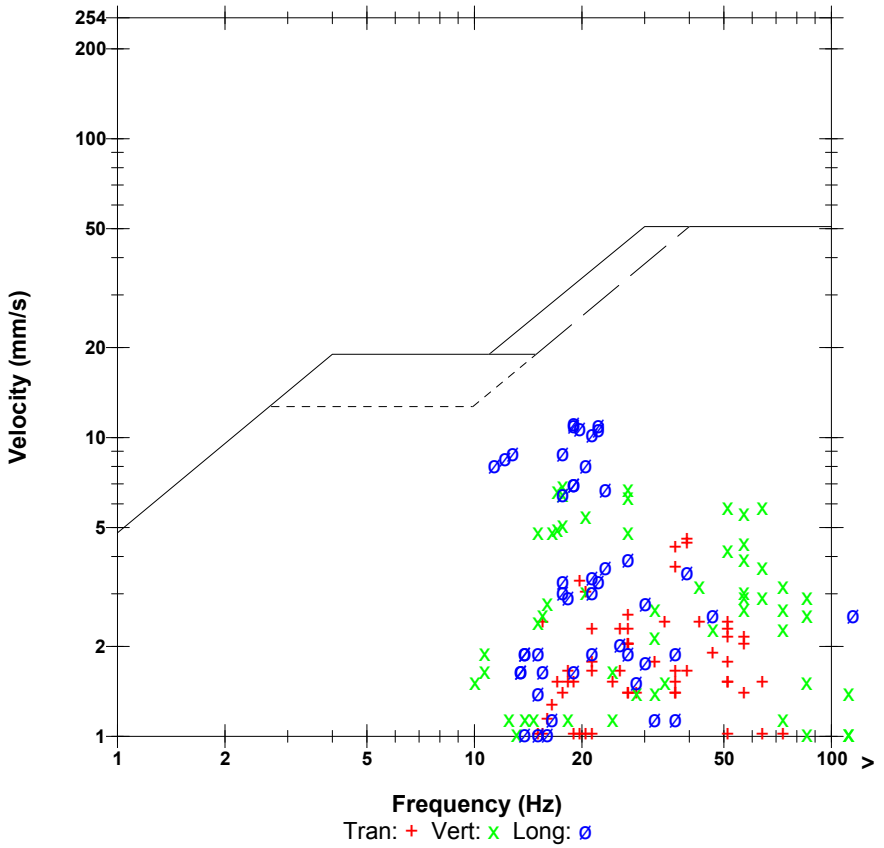

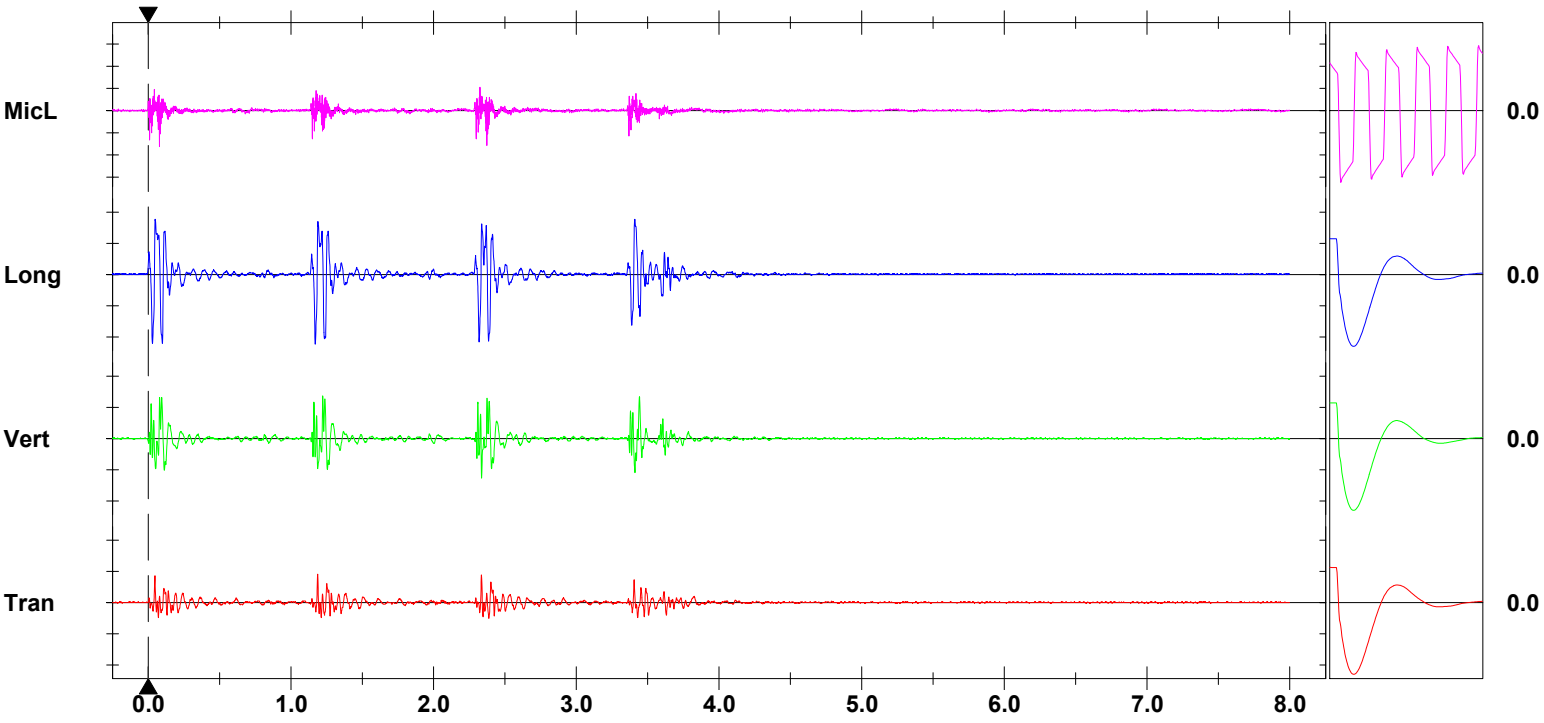

Time Scale: 0.50 sec/div **Amplitude Scale:** Geo: 5.00 mm/s/div Mic: 10.00 pa.(L)/div Sensorcheck
Trigger =

Event Report

Date/Time Long at 14:19:39 October 29, 2009
Trigger Source Geo: 1.27 mm/s
Range Geo :254 mm/s
Record Time 7.601 sec at 1024 sps
Job Number: 1

Serial Number BE13074 V 8.12-8.0 MiniMate Plus
Battery Level 6.2 Volts
Calibration December 7, 2007 by Instantel Inc.
File Name O074CYFU.GR0

Notes
Location:
Client:
User Name:
General:

Extended Notes
Combo Mode October 29, 2009 14:17:35

Post Event Notes

Microphone Linear Weighting
PSPL 13.5 pa.(L) at 0.075 sec
ZC Freq >100 Hz
Channel Test Passed (Freq = 20.5 Hz Amp = 587 mv)

	Tran	Vert	Long	
PPV	4.57	7.49	10.3	mm/s
ZC Freq	39	51	22	Hz
Time (Rel. to Trig)	1.186	1.188	0.095	sec
Peak Acceleration	0.119	0.278	0.358	g
Peak Displacement	0.0226	0.0527	0.102	mm
Sensorcheck	Passed	Passed	Passed	
Frequency	7.3	7.3	7.4	Hz
Overswing Ratio	4.1	4.0	3.9	

Peak Vector Sum 11.9 mm/s at 1.188 sec

USBM RI8507 And OSMRE

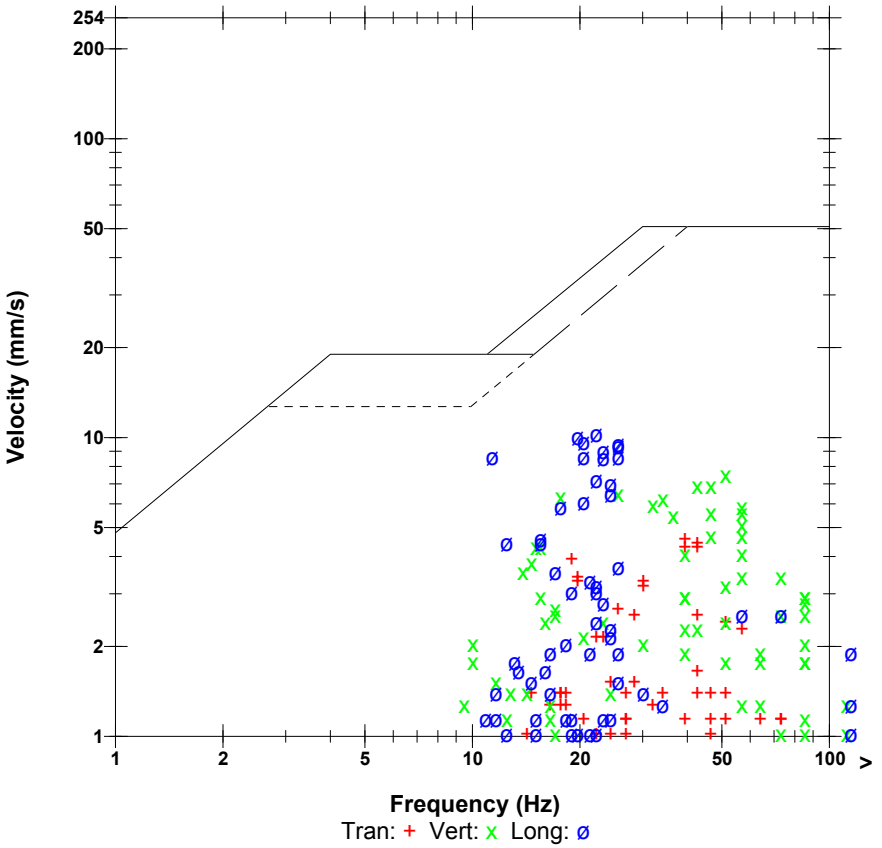

Monitor Log
Oct 29 /09 14:19:39 Oct 29 /09 14:19:47 Event recorded. (Memory Full Exit)

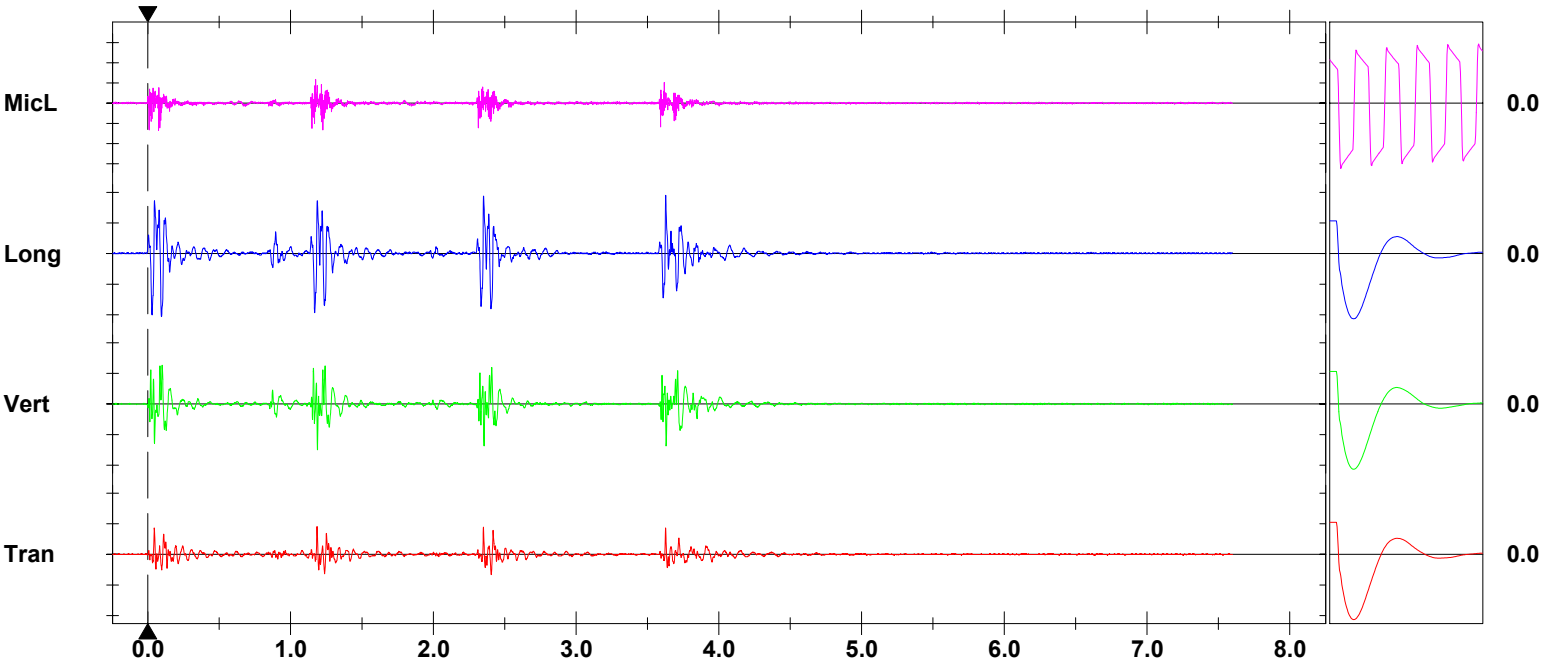

Time Scale: 0.50 sec/div **Amplitude Scale:** Geo: 5.00 mm/s/div Mic: 10.00 pa.(L)/div Sensorcheck
Trigger =

Field Vibration Data

Seismograph Unit # 1

at 10.0 feet from Test Pile #2

Event Report

Histogram Start Time	15:23:54 October 29, 2009	**Serial Number**	BE13074 V 8.12-8.0 MiniMate Plus
Histogram Finish Time	15:38:05 October 29, 2009	**Battery Level**	6.3 Volts
Number of Intervals	425 at 2 seconds	**Calibration**	December 7, 2007 by Instantel Inc.
Range	Geo :254 mm/s	**File Name**	O074CYFX.FU0
Sample Rate	1024sps		
Job Number:	1		

Notes
Location:
Client:
User Name:
General:

Extended Notes

Post Event Notes

Microphone Linear Weighting
PSPL 41.5 pa.(L) on October 29, 2009 at 15:35:42
ZC Freq >100 Hz
Channel Test Passed (Freq = 20.5 Hz Amp = 575 mv)

	Tran	Vert	Long	
PPV	6.86	31.9	14.5	mm/s
ZC Freq	32	21	18	Hz
Date	Oct 29 /09	Oct 29 /09	Oct 29 /09	
Time	15:25:30	15:27:02	15:26:46	
Sensorcheck	Passed	Passed	Passed	
Frequency	7.2	7.2	7.4	Hz
Overswing Ratio	4.1	4.1	3.8	

Peak Vector Sum 33.4 mm/s on October 29, 2009 at 15:27:02

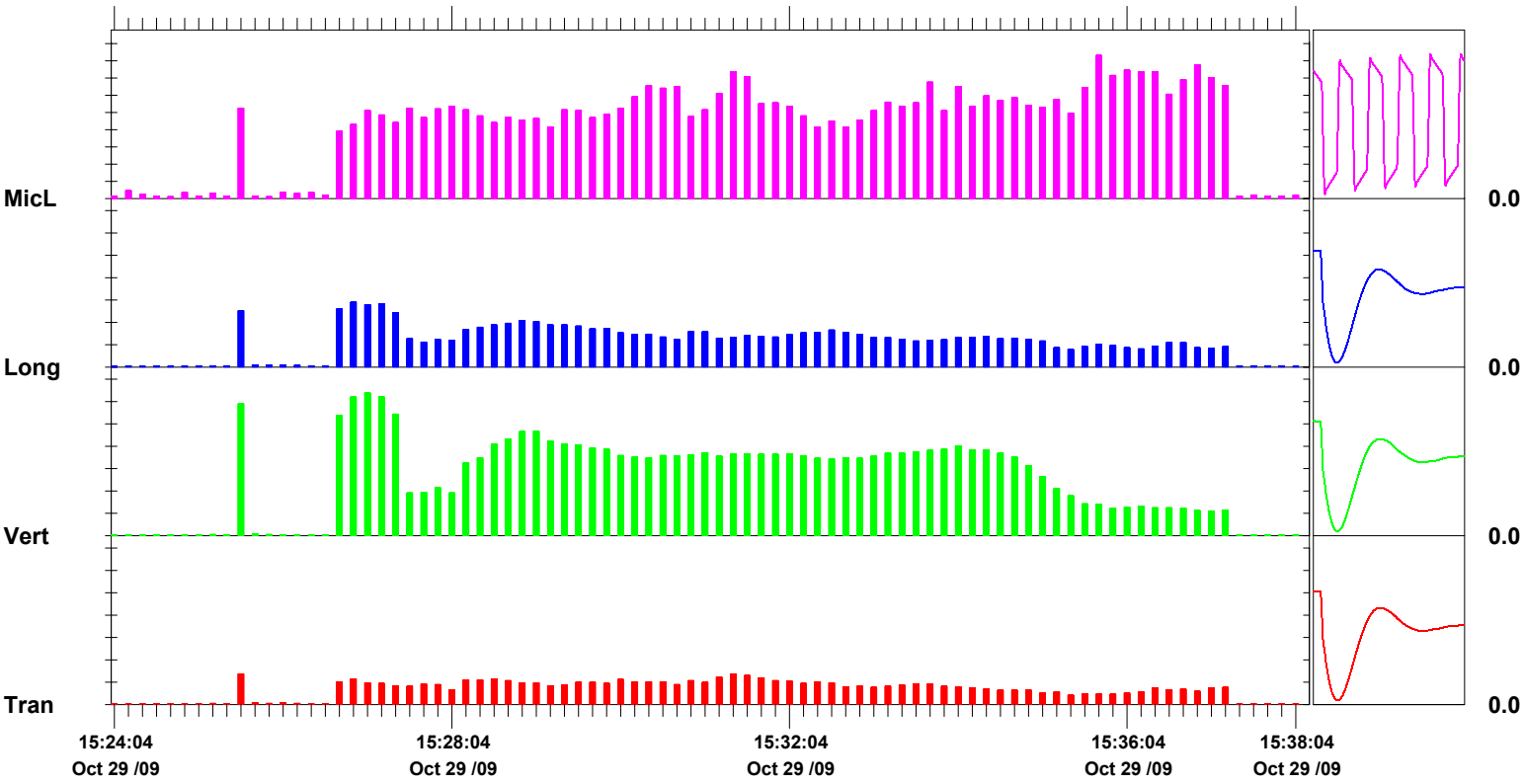

Time Scale: 10 seconds /div **Amplitude Scale:** Geo: 5.00 mm/s/div Mic: 5.00 pa.(L)/div Sensorcheck

Event Report

Date/Time	Long at 15:25:29 October 29, 2009	**Serial Number**	BE13074 V 8.12-8.0 MiniMate Plus
Trigger Source	Geo: 1.27 mm/s	**Battery Level**	6.2 Volts
Range	Geo :254 mm/s	**Calibration**	December 7, 2007 by Instantel Inc.
Record Time	8.0 sec at 1024 sps	**File Name**	O074CYFX.IH0
Job Number:	1		

Notes
Location:
Client:
User Name:
General:

Extended Notes
Combo Mode October 29, 2009 15:23:54

Post Event Notes

Microphone Linear Weighting
PSPL 26.3 pa.(L) at 1.312 sec
ZC Freq 43 Hz
Channel Test Passed (Freq = 20.5 Hz Amp = 575 mv)

	Tran	Vert	Long	
PPV	6.86	29.5	12.6	mm/s
ZC Freq	32	20	17	Hz
Time (Rel. to Trig)	0.031	2.501	2.525	sec
Peak Acceleration	0.318	0.782	0.504	g
Peak Displacement	0.0313	0.181	0.104	mm
Sensorcheck	Passed	Passed	Passed	
Frequency	7.2	7.2	7.4	Hz
Overswing Ratio	4.1	4.1	3.8	

Peak Vector Sum 30.2 mm/s at 2.501 sec

USBM RI8507 And OSMRE

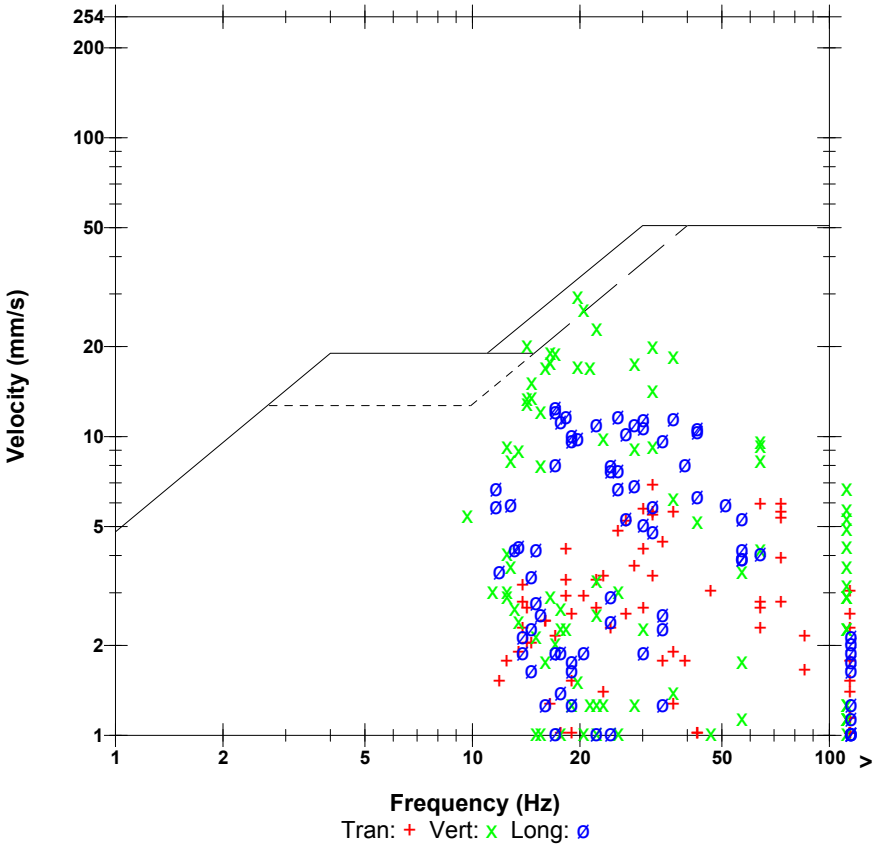

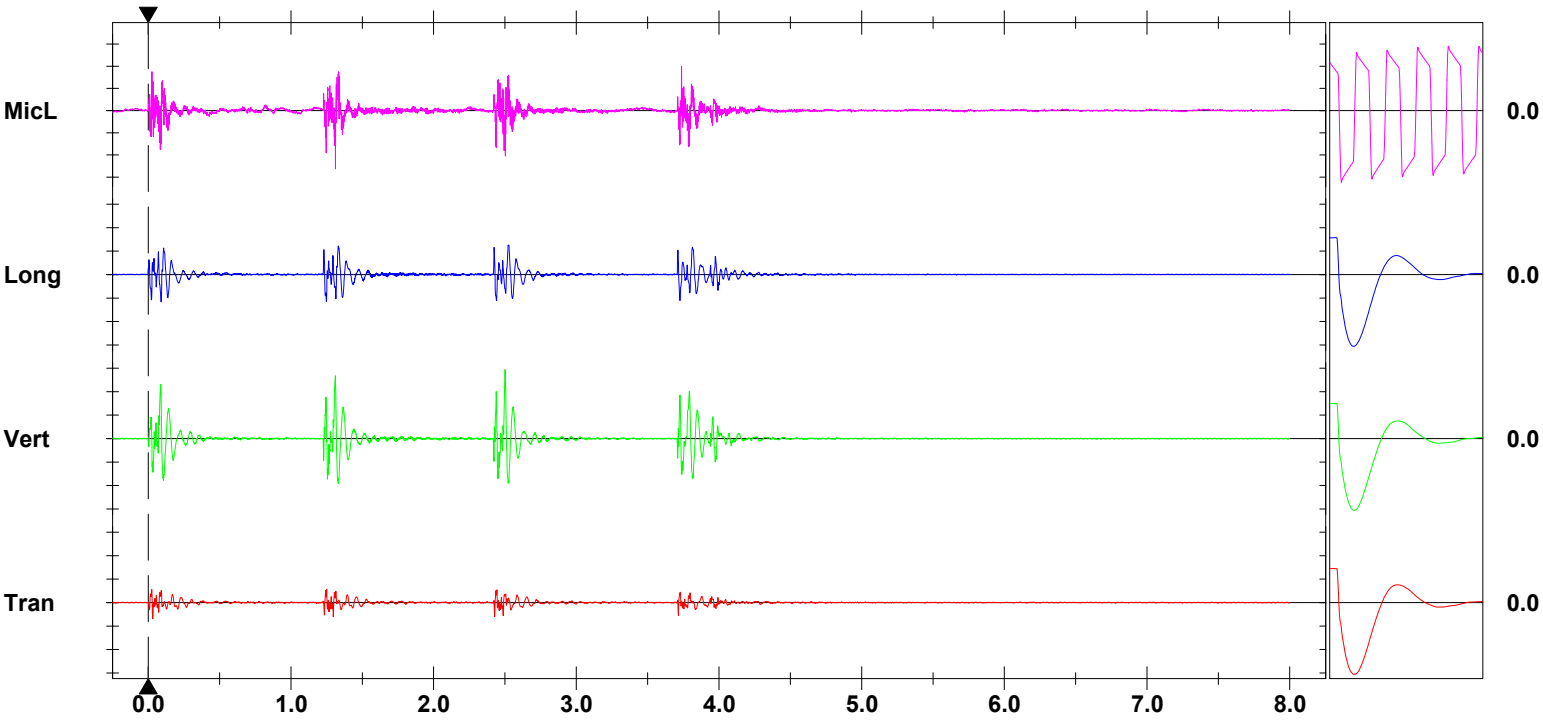

Time Scale: 0.50 sec/div **Amplitude Scale:** Geo: 10.00 mm/s/div Mic: 10.00 pa.(L)/div Sensorcheck
Trigger =

Event Report

Date/Time	Vert at 15:26:43 October 29, 2009	**Serial Number**	BE13074 V 8.12-8.0 MiniMate Plus
Trigger Source	Geo: 1.27 mm/s	**Battery Level**	6.2 Volts
Range	Geo :254 mm/s	**Calibration**	December 7, 2007 by Instantel Inc.
Record Time	8.0 sec at 1024 sps	**File Name**	O074CYFX.KJ0
Job Number:	1		

Notes
Location:
Client:
User Name:
General:

Extended Notes
Combo Mode October 29, 2009 15:23:54

Post Event Notes

Microphone Linear Weighting
PSPL 21.5 pa.(L) at 1.373 sec
ZC Freq 27 Hz
Channel Test Passed (Freq = 20.5 Hz Amp = 575 mv)

	Tran	Vert	Long	
PPV	5.71	31.0	14.5	mm/s
ZC Freq	85	19	18	Hz
Time (Rel. to Trig)	1.281	2.629	2.651	sec
Peak Acceleration	0.265	0.835	0.371	g
Peak Displacement	0.0320	0.188	0.112	mm
Sensorcheck	Passed	Passed	Passed	
Frequency	7.2	7.2	7.4	Hz
Overswing Ratio	4.1	4.1	3.8	

Peak Vector Sum 32.3 mm/s at 2.629 sec

USBM RI8507 And OSMRE

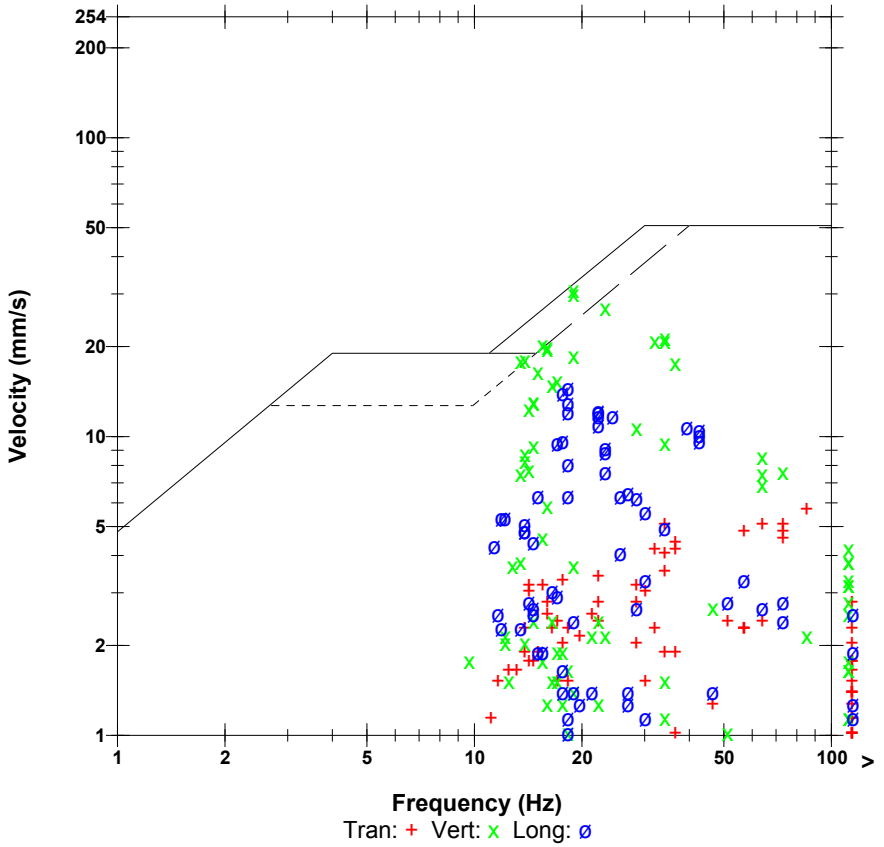

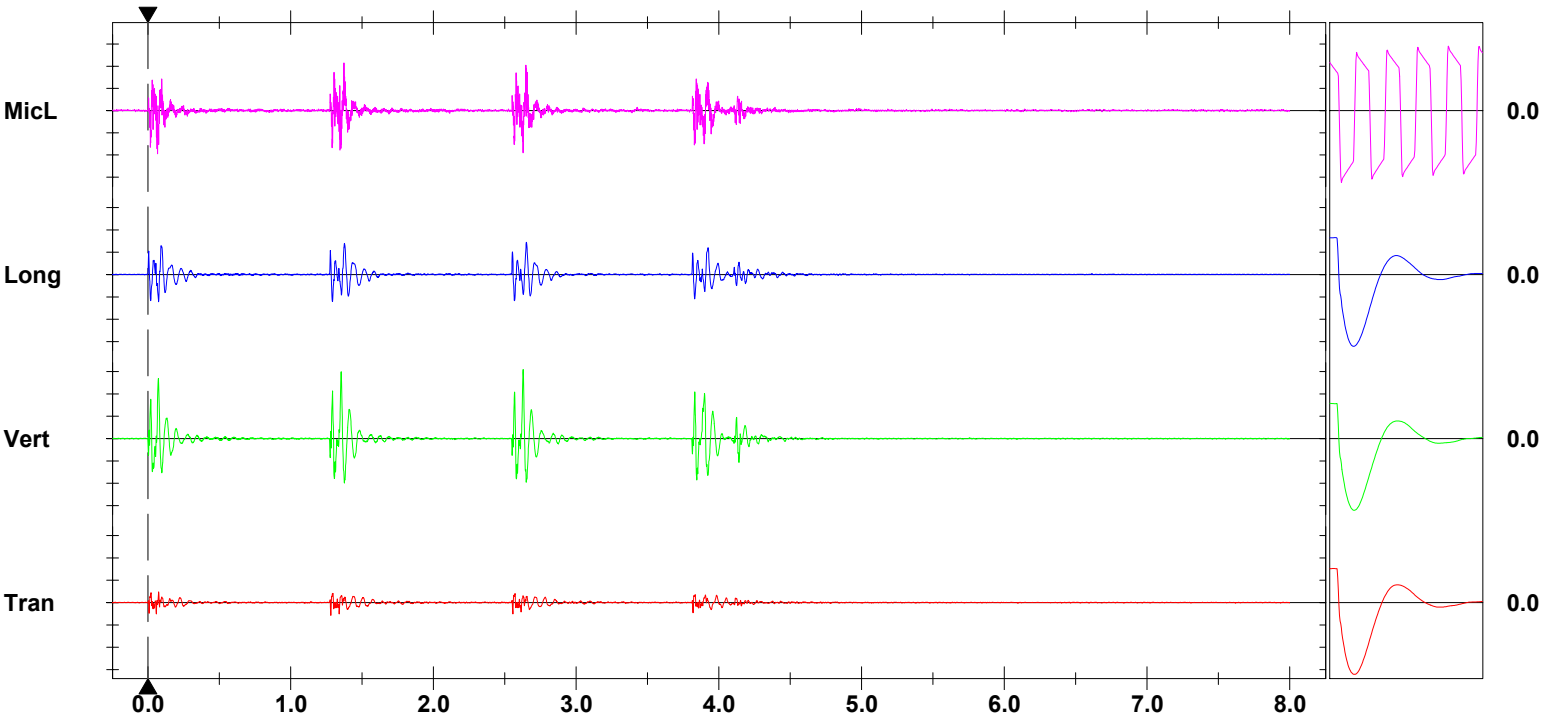

Time Scale: 0.50 sec/div **Amplitude Scale:** Geo: 10.00 mm/s/div Mic: 10.00 pa.(L)/div Sensorcheck
Trigger =

Event Report

Date/Time	Vert at 15:26:59 October 29, 2009	**Serial Number**	BE13074 V 8.12-8.0 MiniMate Plus
Trigger Source	Geo: 1.27 mm/s	**Battery Level**	6.3 Volts
Range	Geo :254 mm/s	**Calibration**	December 7, 2007 by Instantel Inc.
Record Time	5.263 sec at 1024 sps	**File Name**	O074CYFX.KZ0
Job Number:	1		

Notes
Location:
Client:
User Name:
General:

Extended Notes
Combo Mode October 29, 2009 15:23:54

Post Event Notes

Microphone Linear Weighting
PSPL 25.5 pa.(L) at 4.095 sec
ZC Freq >100 Hz
Channel Test Passed (Freq = 20.5 Hz Amp = 575 mv)

	Tran	Vert	Long	
PPV	4.83	31.9	14.0	mm/s
ZC Freq	22	21	18	Hz
Time (Rel. to Trig)	4.126	1.360	2.733	sec
Peak Acceleration	0.159	0.650	0.358	g
Peak Displacement	0.0337	0.198	0.104	mm
Sensorcheck	Passed	Passed	Passed	
Frequency	7.2	7.2	7.4	Hz
Overswing Ratio	4.1	4.1	3.8	

Peak Vector Sum 33.4 mm/s at 1.360 sec

USBM RI8507 And OSMRE

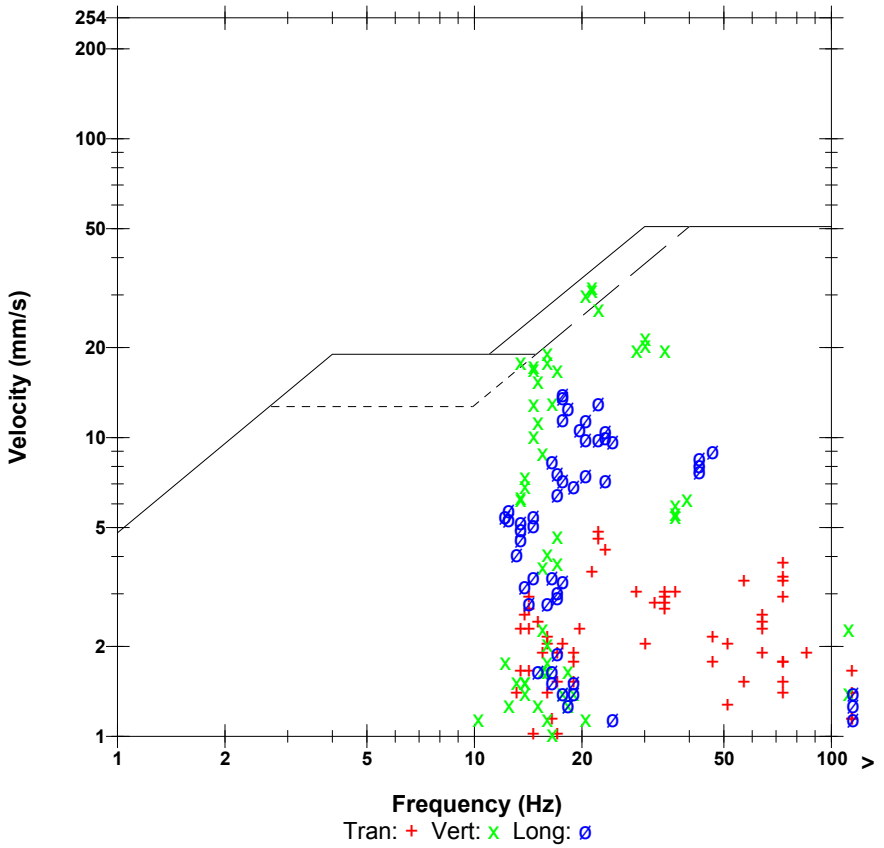

Monitor Log
Oct 29 /09 15:26:59 Oct 29 /09 15:27:05 Event recorded. (Memory Full Exit)

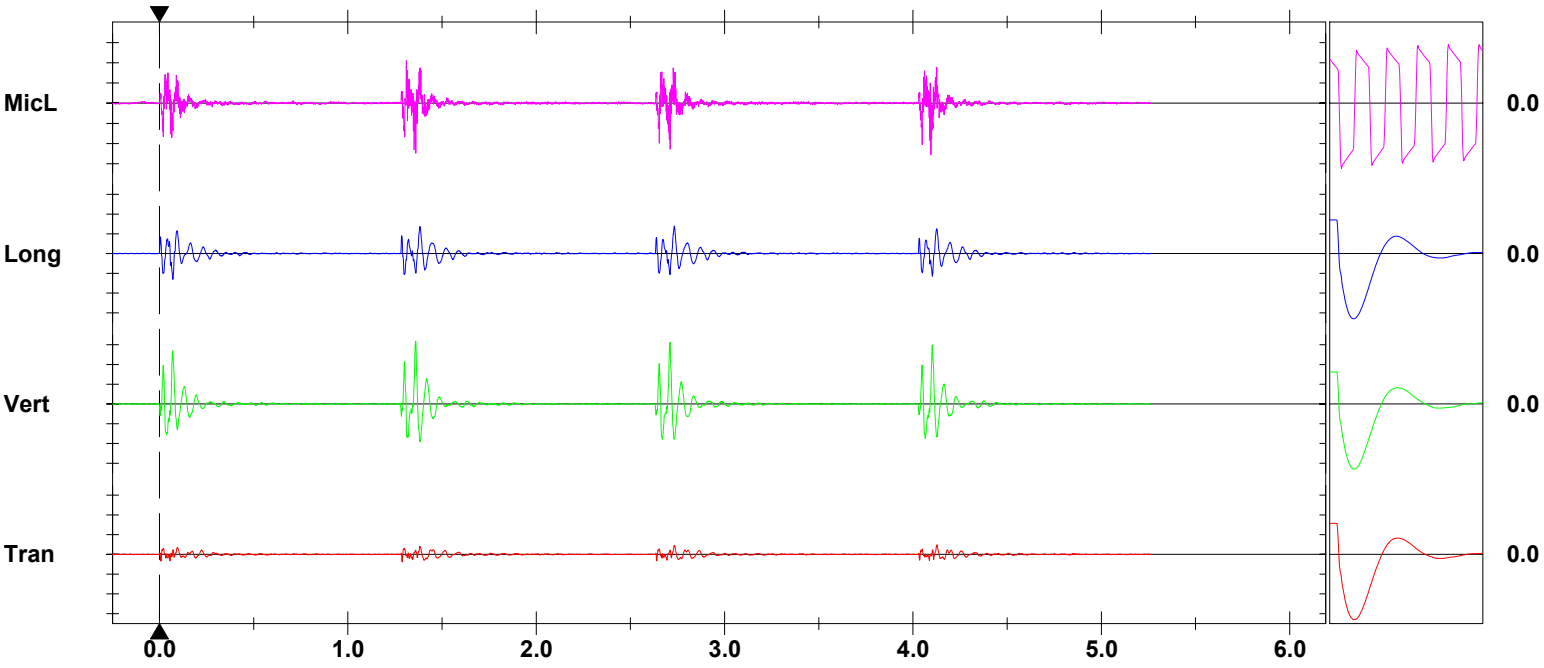

Time Scale: 0.50 sec/div **Amplitude Scale:** Geo: 10.00 mm/s/div Mic: 10.00 pa.(L)/div Sensorcheck
Trigger =

Field Vibration Data

Seismograph Unit # 1

at 24.8 feet from Test Pile #1

Non Driving Event

Event Report

Date/Time Manual at 10:30:26 December 21, 2009
Range Geo :254 mm/s
Record Time 8.0 sec at 1024 sps
Job Number: 1

Serial Number BE13074 V 8.12-8.0 MiniMate Plus
Battery Level 6.3 Volts
Calibration December 7, 2007 by Instantel Inc.
File Name O074D15P.6Q0

Notes
Location:
Client:
User Name:
General:

Extended Notes

Post Event Notes

Microphone Linear Weighting
PSPL 1.75 pa.(L) at 0.315 sec
ZC Freq 9.8 Hz
Channel Test Passed (Freq = 19.7 Hz Amp = 698 mv)

	Tran	Vert	Long	
PPV	0.127	0.127	0.127	mm/s
ZC Freq	>100	>100	>100	Hz
Time (Rel. to Trig)	0.230	0.035	0.001	sec
Peak Acceleration	0.0133	0.0133	0.0133	g
Peak Displacement	0.0	0.0	0.0	mm
Sensorcheck	Check	Check	Check	
Frequency	1024.0	60.2	1024.0	Hz
Overswing Ratio	0.0	1.0	0.0	

Peak Vector Sum 0.220 mm/s at 0.266 sec

USBM RI8507 And OSMRE

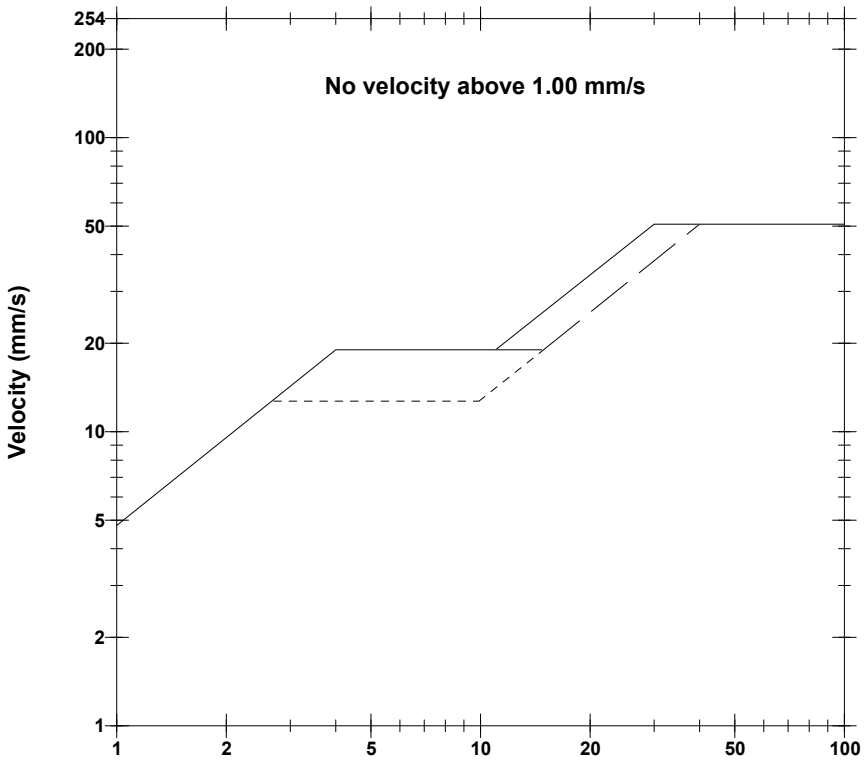

Tran: + Vert: x Long: ø

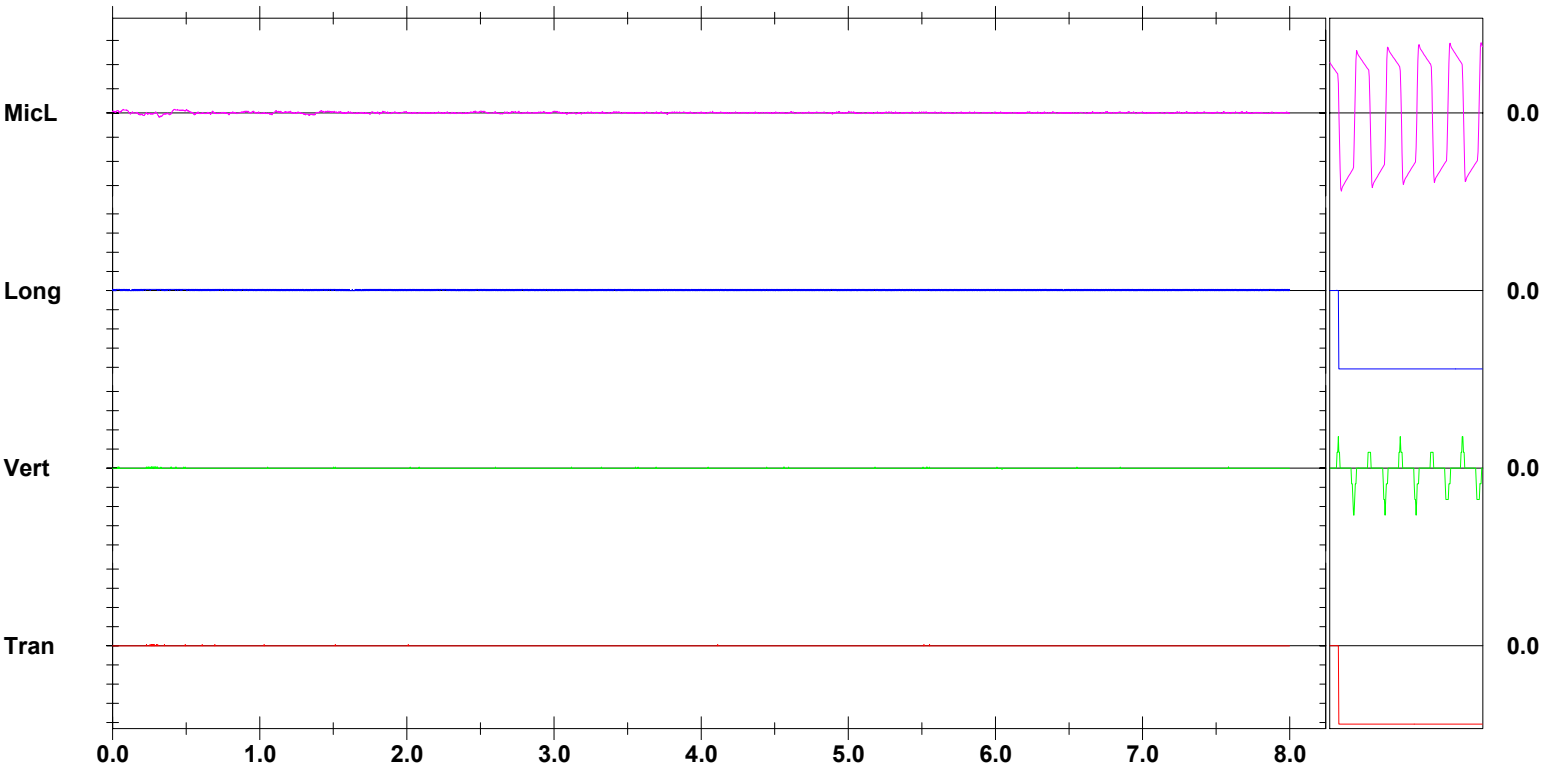

Time Scale: 0.50 sec/div **Amplitude Scale:** Geo: 2.00 mm/s/div Mic: 10.00 pa.(L)/div Sensorcheck

Event Report

Date/Time Manual at 10:34:25 December 21, 2009
Range Geo :254 mm/s
Record Time 8.0 sec at 1024 sps
Job Number: 1

Serial Number BE13074 V 8.12-8.0 MiniMate Plus
Battery Level 6.3 Volts
Calibration December 7, 2007 by Instantel Inc.
File Name O074D15P.DD0

Notes
Location:
Client:
User Name:
General:

Extended Notes

Post Event Notes

Microphone Linear Weighting
PSPL 1.25 pa.(L) at 7.630 sec
ZC Freq 37 Hz
Channel Test Passed (Freq = 20.1 Hz Amp = 659 mv)

	Tran	Vert	Long	
PPV	0.254	0.254	0.254	mm/s
ZC Freq	>100	34	>100	Hz
Time (Rel. to Trig)	0.242	0.237	0.230	sec
Peak Acceleration	0.0133	0.0133	0.0133	g
Peak Displacement	0.00025	0.00174	0.00248	mm
Sensorcheck	Check	Check	Check	
Frequency	1024.0	60.2	1024.0	Hz
Overswing Ratio	0.0	1.5	0.0	

Peak Vector Sum 0.440 mm/s at 0.242 sec

USBM RI8507 And OSMRE

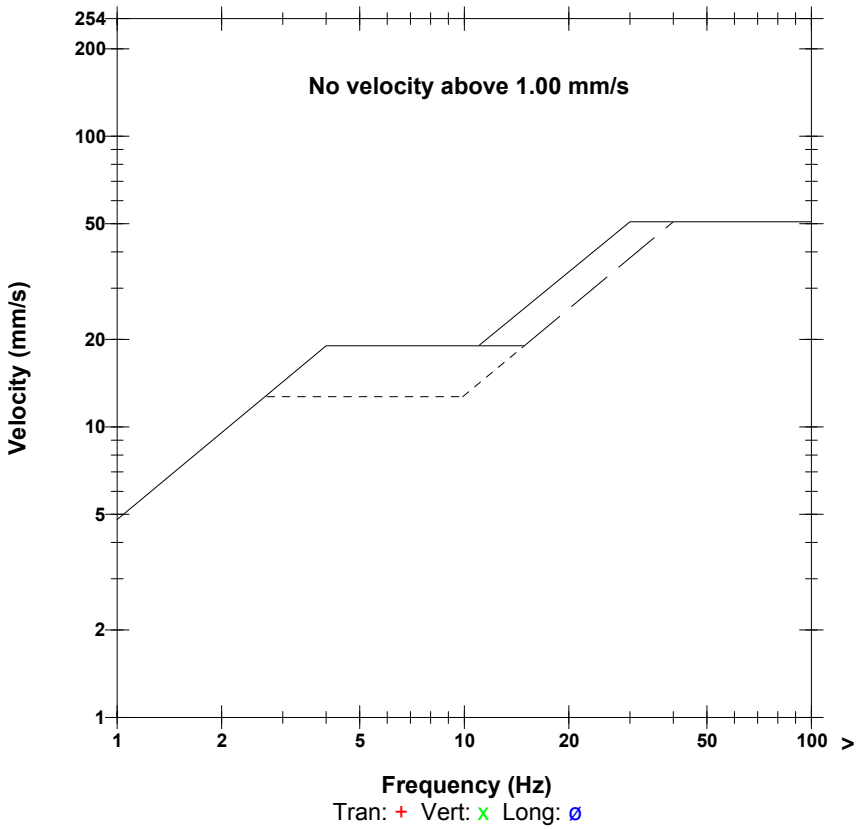

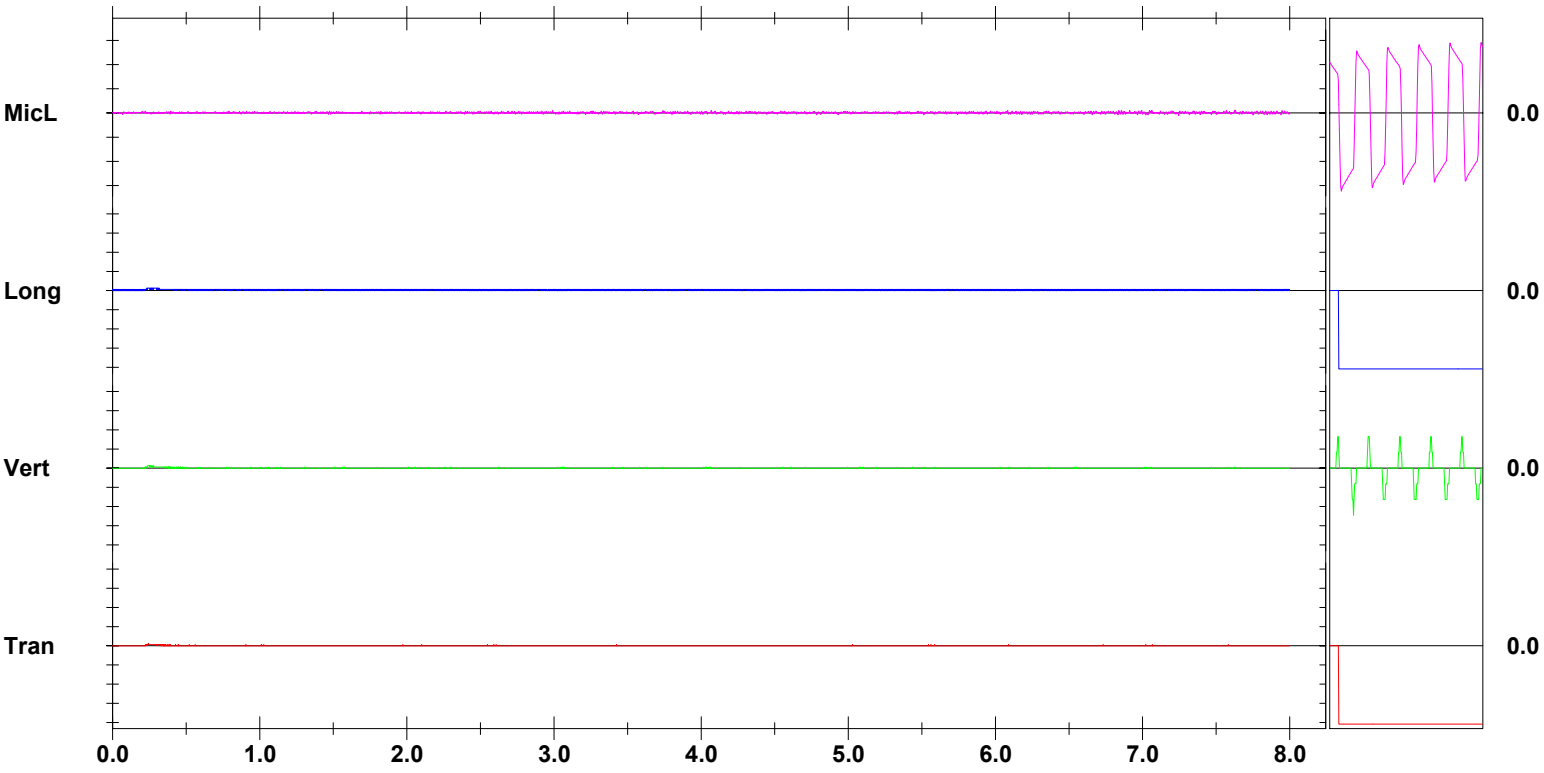

Time Scale: 0.50 sec/div **Amplitude Scale:** Geo: 2.00 mm/s/div Mic: 10.00 pa.(L)/div Sensorcheck

Event Report

Histogram Start Time	11:30:22 December 21, 2009	**Serial Number**	BE13074 V 8.12-8.0 MiniMate Plus
Histogram Finish Time	11:54:41 December 21, 2009	**Battery Level**	6.2 Volts
Number of Intervals	729 at 2 seconds	**Calibration**	December 7, 2007 by Instantel Inc.
Range	Geo :254 mm/s	**File Name**	O074D15R.YM0
Sample Rate	1024sps		
Job Number:	1		

Notes
Location:
Client:
User Name:
General:

Extended Notes

Post Event Notes

Microphone Linear Weighting
PSPL 3.75 pa.(L) on December 21, 2009 at 11:38:00
ZC Freq 9.7 Hz
Channel Test Passed (Freq = 20.1 Hz Amp = 643 mv)

	Tran	Vert	Long	
PPV	0.127	0.127	0.254	mm/s
ZC Freq	>100	>100	>100	Hz
Date	Dec 21 /09	Dec 21 /09	Dec 21 /09	
Time	11:30:24	11:30:24	11:49:10	
Sensorcheck	Check	Check	Check	
Frequency	1024.0	60.2	78.8	Hz
Overswing Ratio	0.0	1.0	1.0	

Peak Vector Sum 0.311 mm/s on December 21, 2009 at 11:54:40

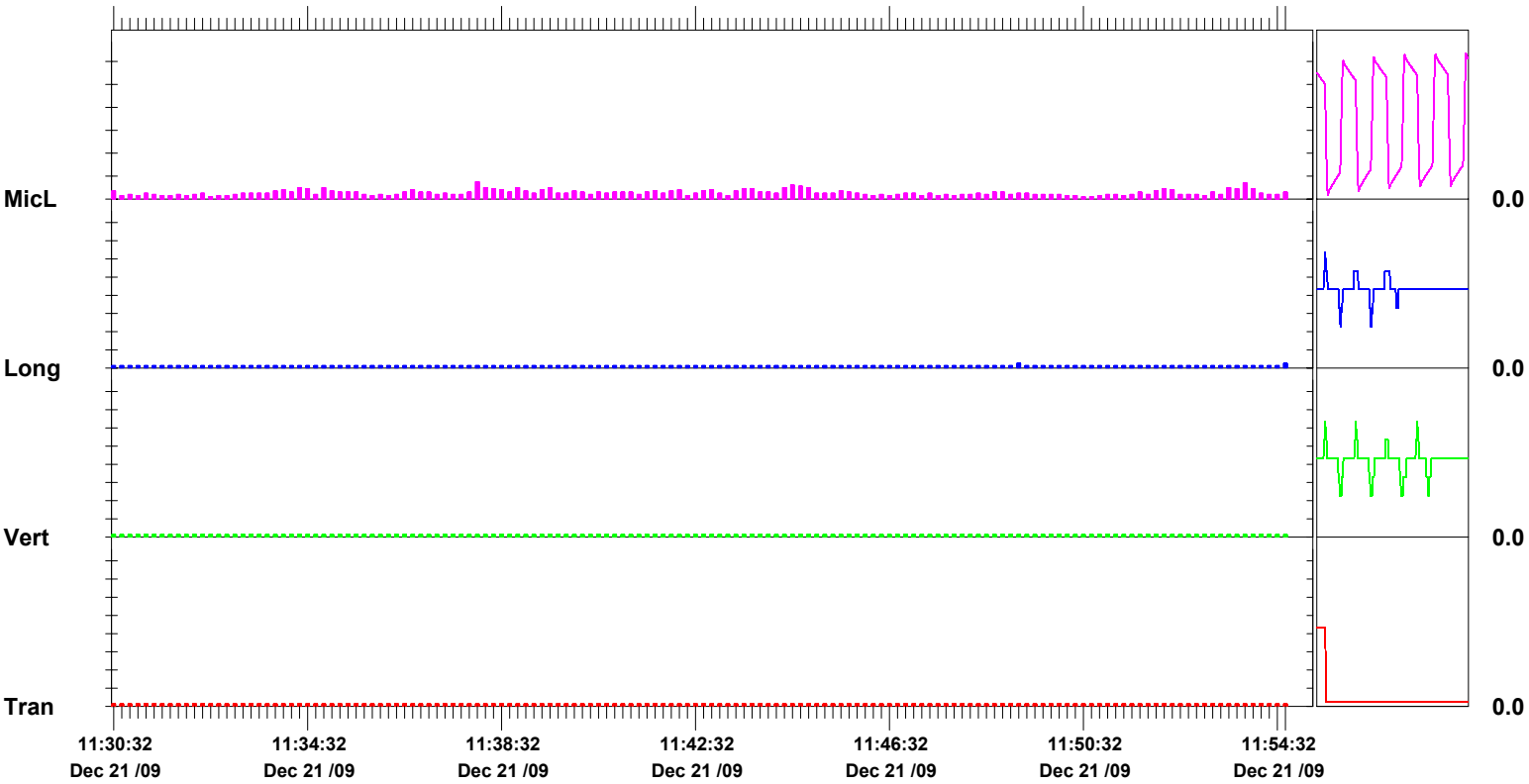

Time Scale: 10 seconds /div **Amplitude Scale:** Geo: 1.000 mm/s/div Mic: 5.00 pa.(L)/div Sensorcheck

Field Vibration Data

Seismograph Unit # 2

at 49.8 feet from Test Pile #1

Event Report

Histogram Start Time	14:17:25 October 29, 2009	**Serial Number**	BE13055 V 8.12-8.0 MiniMate Plus
Histogram Finish Time	14:25:43 October 29, 2009	**Battery Level**	6.3 Volts
Number of Intervals	249 at 2 seconds	**Calibration**	December 7, 2007 by Instantel Inc.
Range	Geo :254 mm/s	**File Name**	O055CYFU.D10
Sample Rate	1024sps		
Job Number:	1		

Notes
Location:
Client:
User Name:
General:

Extended Notes

Post Event Notes

Microphone Linear Weighting
PSPL 14.3 pa.(L) on October 29, 2009 at 14:23:45
ZC Freq >100 Hz
Channel Test Passed (Freq = 20.5 Hz Amp = 605 mv)

	Tran	Vert	Long	
PPV	4.19	4.57	13.0	mm/s
ZC Freq	37	28	27	Hz
Date	Oct 29 /09	Oct 29 /09	Oct 29 /09	
Time	14:24:15	14:18:17	14:24:13	
Sensorcheck	Passed	Passed	Passed	
Frequency	7.3	7.6	7.2	Hz
Overswing Ratio	4.0	3.6	4.2	

Peak Vector Sum 13.3 mm/s on October 29, 2009 at 14:24:13

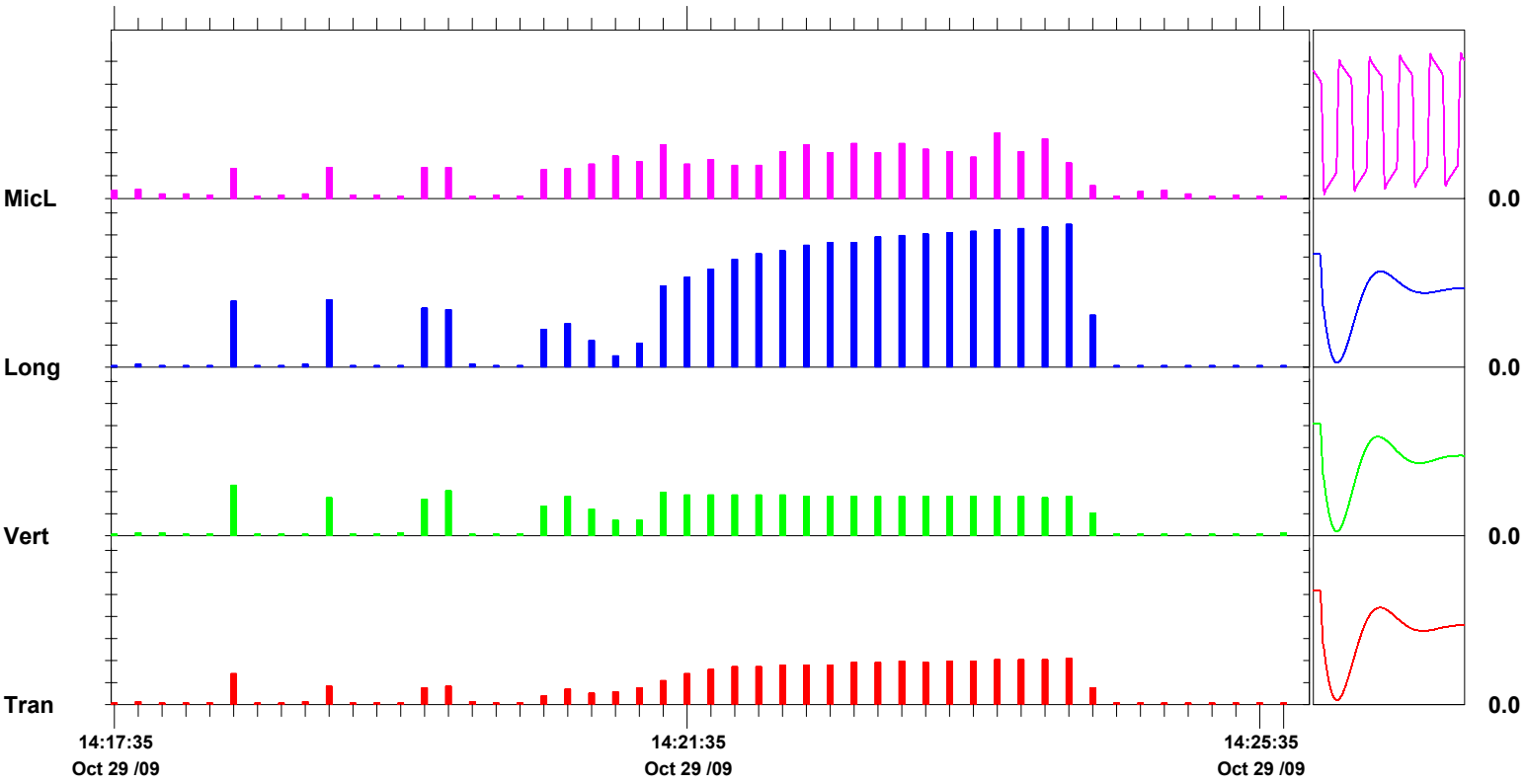

Time Scale: 10 seconds /div **Amplitude Scale:** Geo: 2.00 mm/s/div Mic: 5.00 pa.(L)/div Sensorcheck

Event Report

Date/Time Long at 14:18:16 October 29, 2009
Trigger Source Geo: 1.27 mm/s
Range Geo :254 mm/s
Record Time 8.0 sec at 1024 sps
Job Number: 1

Serial Number BE13055 V 8.12-8.0 MiniMate Plus
Battery Level 6.3 Volts
Calibration December 7, 2007 by Instantel Inc.
File Name O055CYFU.EG0

Notes
Location:
Client:
User Name:
General:

Extended Notes
Combo Mode October 29, 2009 14:17:24

Post Event Notes

Microphone Linear Weighting
PSPL 6.50 pa.(L) at 0.066 sec
ZC Freq 73 Hz
Channel Test Passed (Freq = 20.5 Hz Amp = 605 mv)

	Tran	Vert	Long	
PPV	2.79	4.57	5.97	mm/s
ZC Freq	18	28	17	Hz
Time (Rel. to Trig)	0.058	0.065	2.345	sec
Peak Acceleration	0.0398	0.0928	0.0928	g
Peak Displacement	0.0195	0.0278	0.0588	mm
Sensorcheck	Passed	Passed	Passed	
Frequency	7.3	7.6	7.2	Hz
Overswing Ratio	4.0	3.6	4.2	

Peak Vector Sum 6.63 mm/s at 1.192 sec

USBM RI8507 And OSMRE

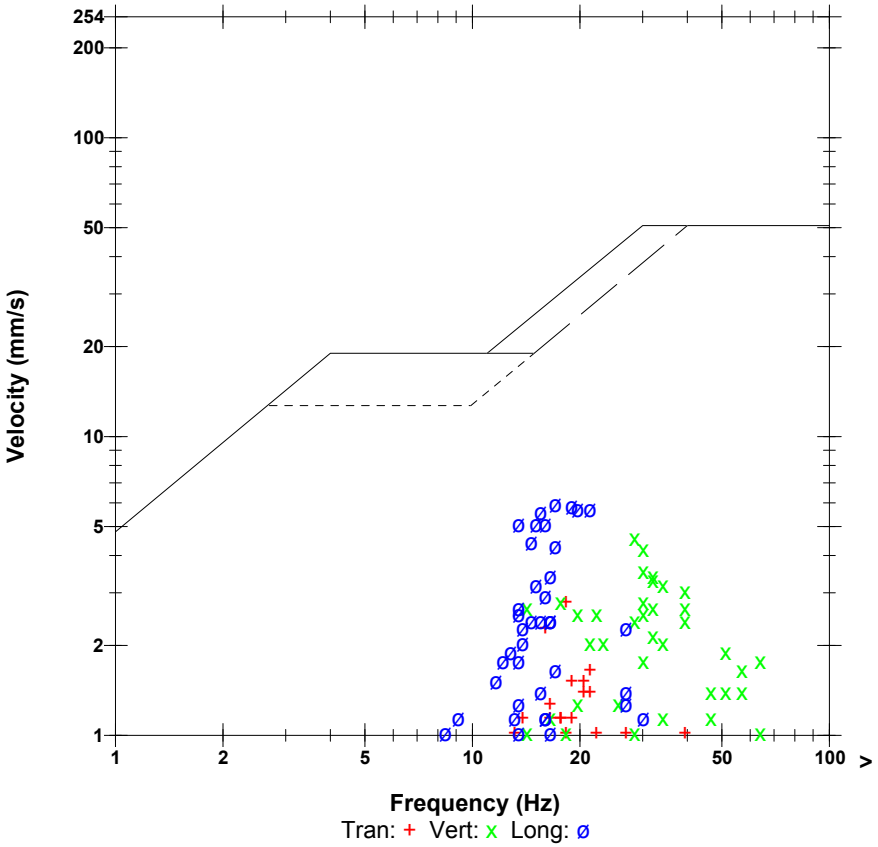

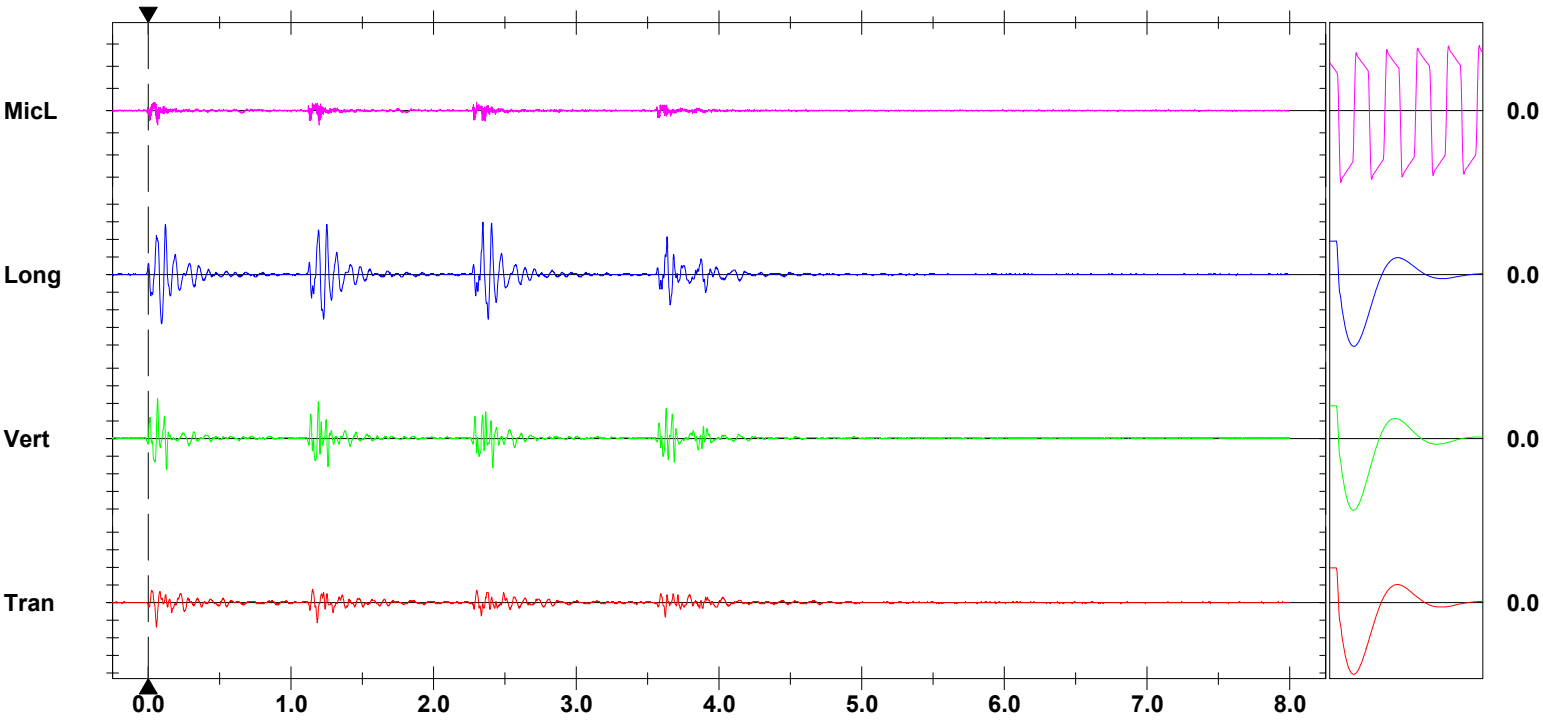

Time Scale: 0.50 sec/div **Amplitude Scale:** Geo: 2.00 mm/s/div Mic: 10.00 pa.(L)/div Sensorcheck
Trigger =

FFT Report

Date/Time	Long at 14:18:16 October 29, 2009	**Serial Number**	BE13055 V 8.12-8.0 MiniMate Plus
Trigger Source	Geo: 1.27 mm/s	**Battery Level**	6.3 Volts
Range	Geo :254 mm/s	**Calibration**	December 7, 2007 by Instantel Inc.
Record Time	8.0 sec at 1024 sps	**File Name**	O055CYFU.EG0
Job Number:	1		

Notes
Location:
Client:
User Name:
General:

Extended Notes
Combo Mode October 29, 2009 14:17:24

Post Event Notes

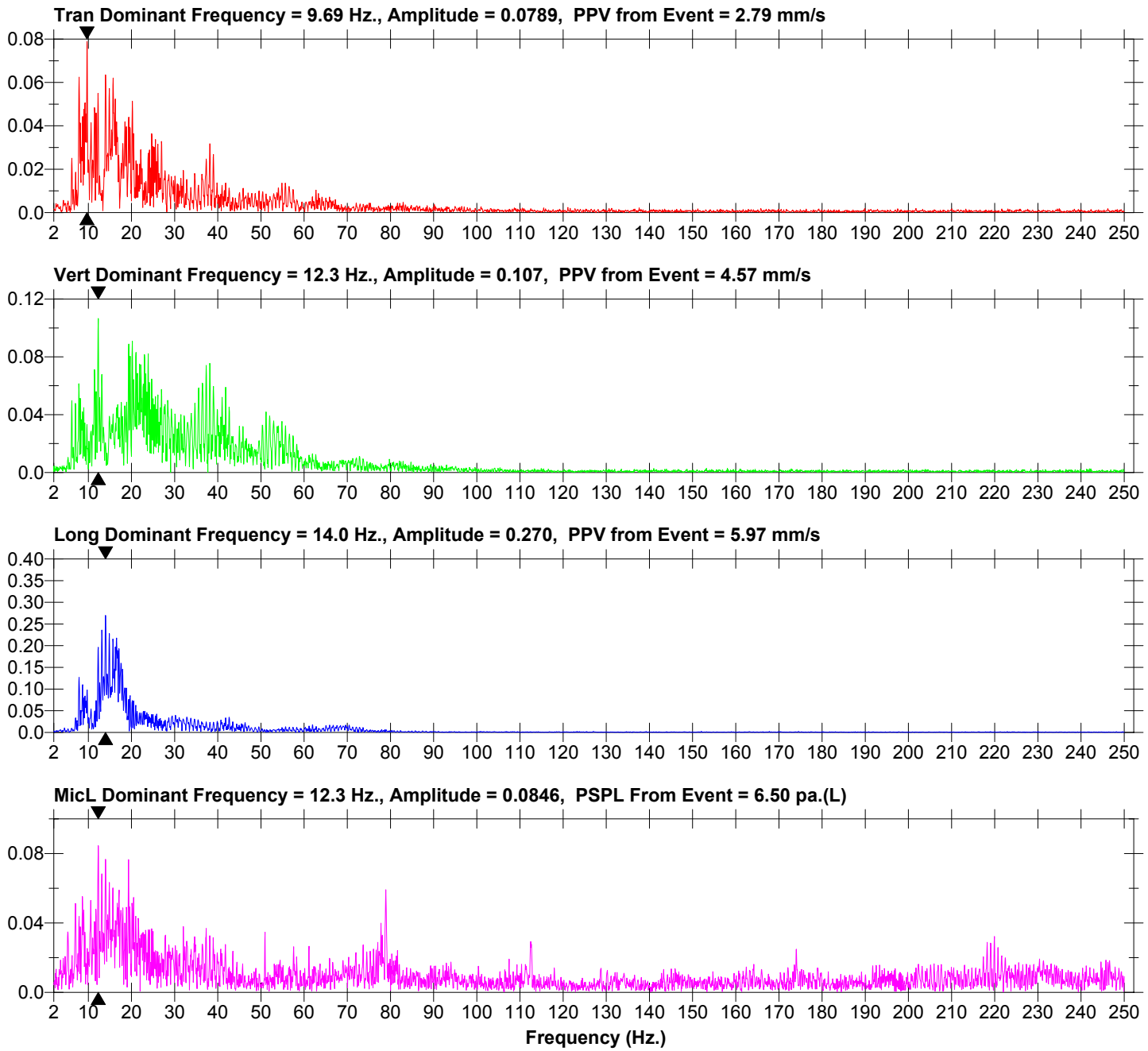

Event Report

Date/Time	Vert at 14:18:56 October 29, 2009	**Serial Number**	BE13055 V 8.12-8.0 MiniMate Plus
Trigger Source	Geo: 1.27 mm/s	**Battery Level**	6.3 Volts
Range	Geo :254 mm/s	**Calibration**	December 7, 2007 by Instantel Inc.
Record Time	8.0 sec at 1024 sps	**File Name**	O055CYFU.FK0
Job Number:	1		

Notes
Location:
Client:
User Name:
General:

Extended Notes
Combo Mode October 29, 2009 14:17:24

Post Event Notes

Microphone Linear Weighting
PSPL 6.75 pa.(L) at 0.004 sec
ZC Freq 47 Hz
Channel Test Passed (Freq = 20.5 Hz Amp = 605 mv)

	Tran	Vert	Long	
PPV	1.65	3.43	6.10	mm/s
ZC Freq	21	32	18	Hz
Time (Rel. to Trig)	2.380	2.423	0.121	sec
Peak Acceleration	0.0398	0.0795	0.106	g
Peak Displacement	0.0106	0.0165	0.0517	mm
Sensorcheck	Passed	Passed	Passed	
Frequency	7.3	7.6	7.2	Hz
Overswing Ratio	4.0	3.6	4.2	

Peak Vector Sum 6.21 mm/s at 0.121 sec

USBM RI8507 And OSMRE

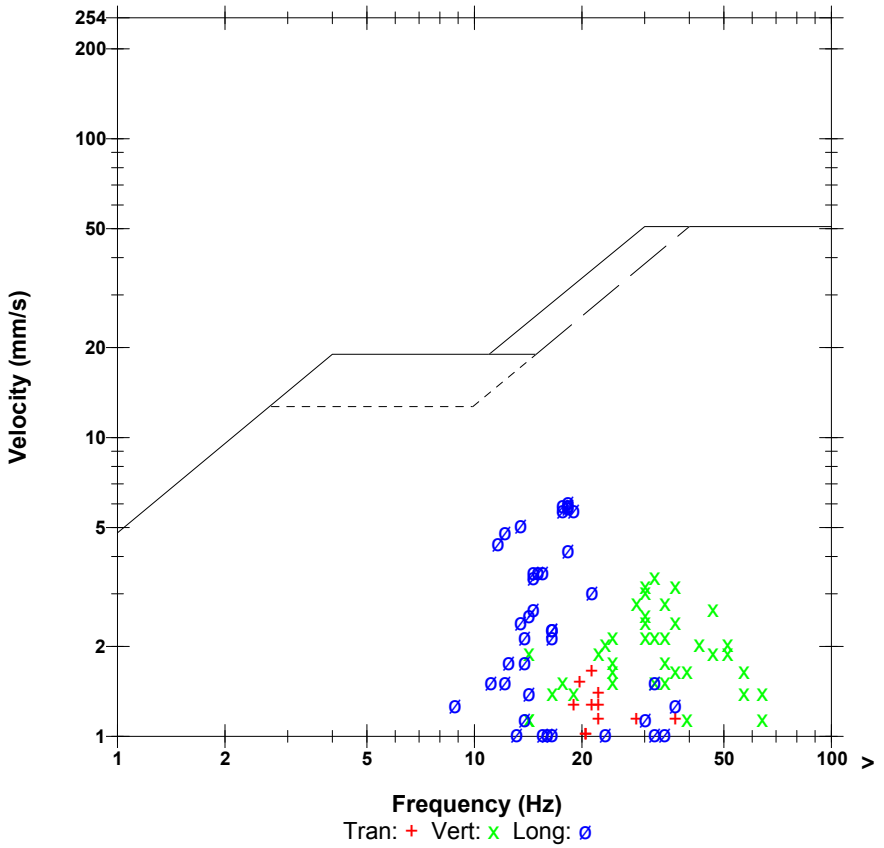

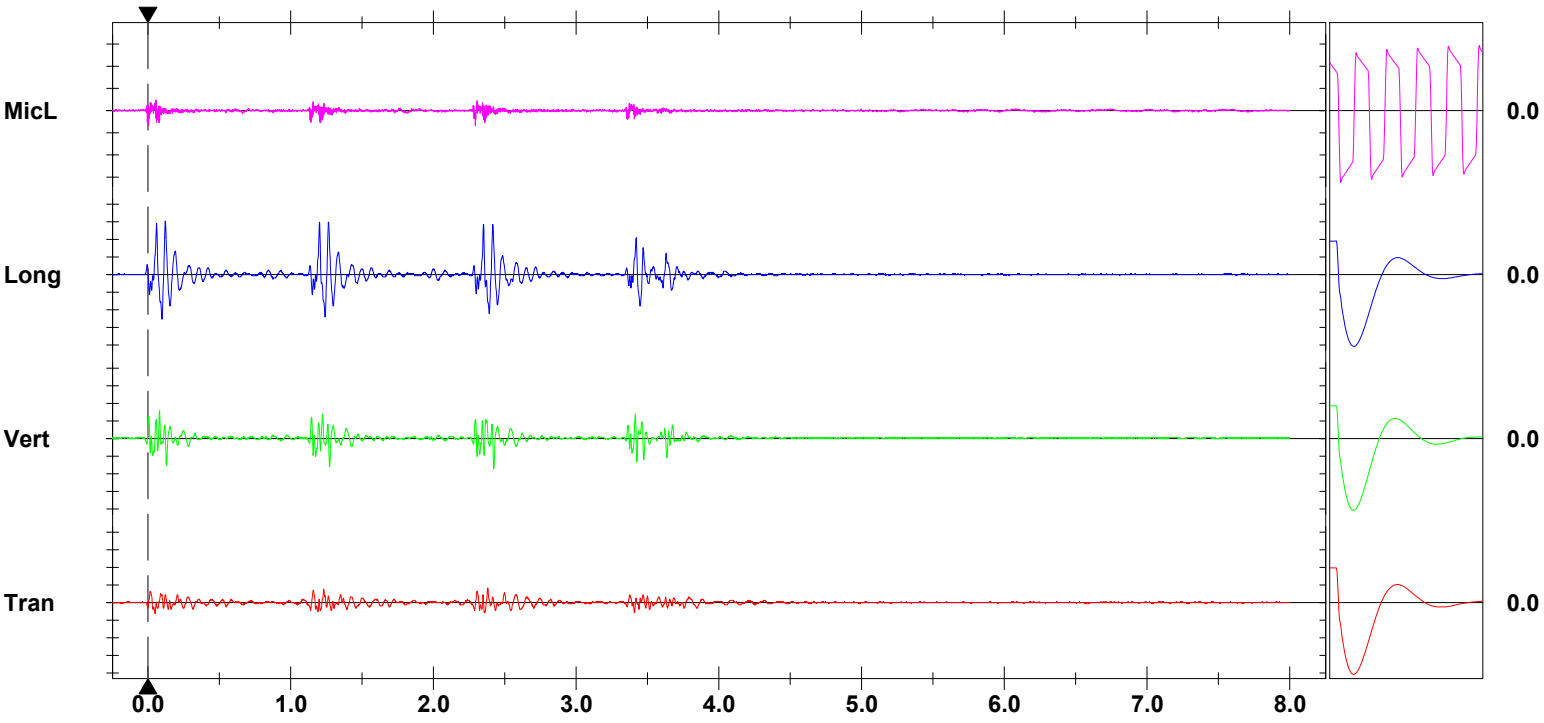

Time Scale: 0.50 sec/div **Amplitude Scale:** Geo: 2.00 mm/s/div Mic: 10.00 pa.(L)/div Sensorcheck
Trigger =

FFT Report

Date/Time	Vert at 14:18:56 October 29, 2009	**Serial Number**	BE13055 V 8.12-8.0 MiniMate Plus
Trigger Source	Geo: 1.27 mm/s	**Battery Level**	6.3 Volts
Range	Geo :254 mm/s	**Calibration**	December 7, 2007 by Instantel Inc.
Record Time	8.0 sec at 1024 sps	**File Name**	O055CYFU.FK0
Job Number:	1		

Notes
Location:
Client:
User Name:
General:

Extended Notes
Combo Mode October 29, 2009 14:17:24

Post Event Notes

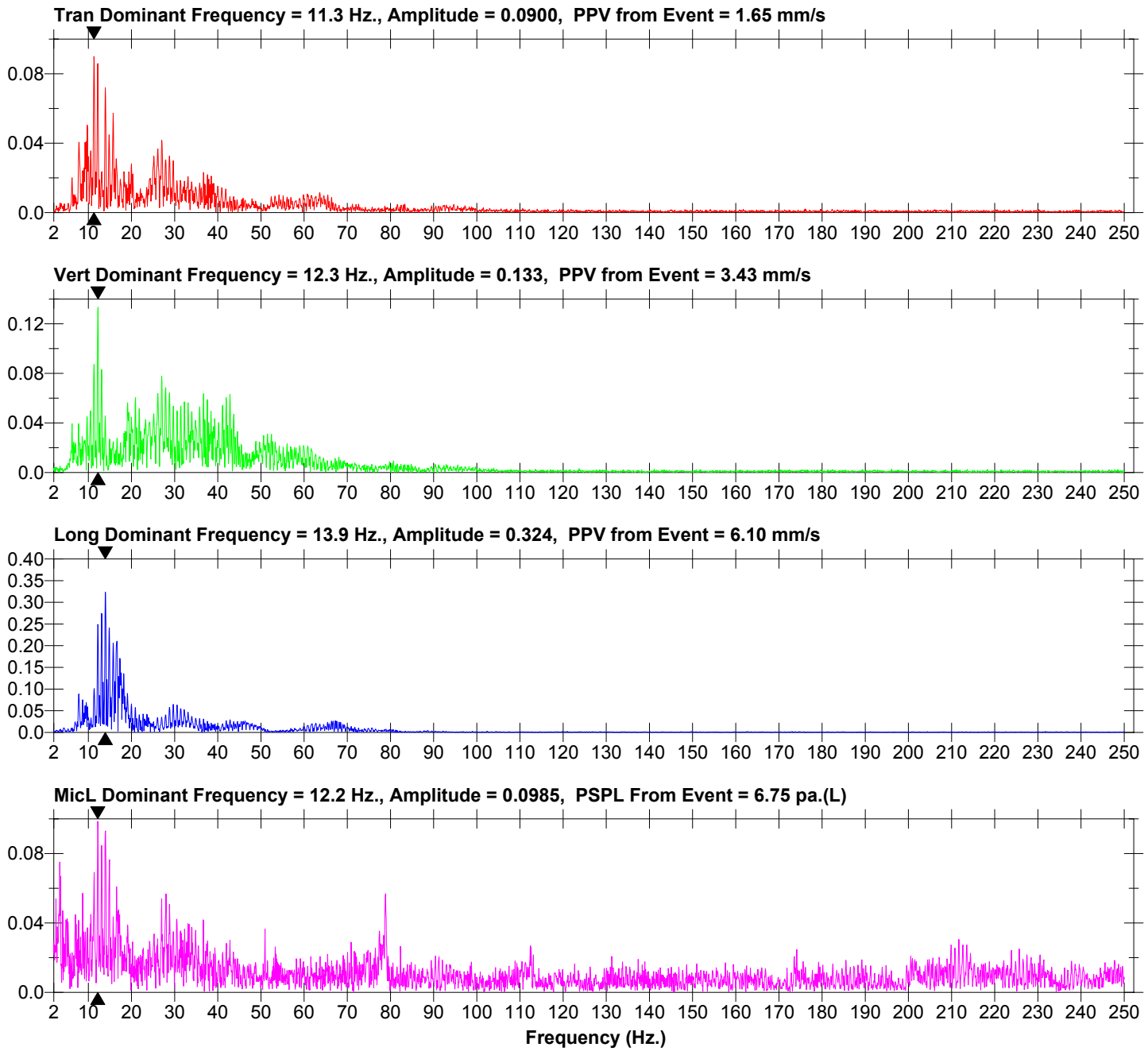

Event Report

Date/Time	Vert at 14:19:44 October 29, 2009	**Serial Number**	BE13055 V 8.12-8.0 MiniMate Plus
Trigger Source	Geo: 1.27 mm/s	**Battery Level**	6.3 Volts
Range	Geo :254 mm/s	**Calibration**	December 7, 2007 by Instantel Inc.
Record Time	8.0 sec at 1024 sps	**File Name**	O055CYFU.GW0
Job Number:	1		

Notes
Location:
Client:
User Name:
General:

Extended Notes
Combo Mode October 29, 2009 14:17:24

Post Event Notes

Microphone Linear Weighting
PSPL 6.75 pa.(L) at 0.005 sec
ZC Freq >100 Hz
Channel Test Passed (Freq = 20.5 Hz Amp = 605 mv)

	Tran	Vert	Long	
PPV	1.65	4.06	5.33	mm/s
ZC Freq	28	39	19	Hz
Time (Rel. to Trig)	1.231	3.648	0.062	sec
Peak Acceleration	0.0398	0.0928	0.106	g
Peak Displacement	0.0144	0.0201	0.0394	mm
Sensorcheck	Passed	Passed	Passed	
Frequency	7.3	7.6	7.2	Hz
Overswing Ratio	4.0	3.6	4.2	

Peak Vector Sum 5.44 mm/s at 1.204 sec

USBM RI8507 And OSMRE

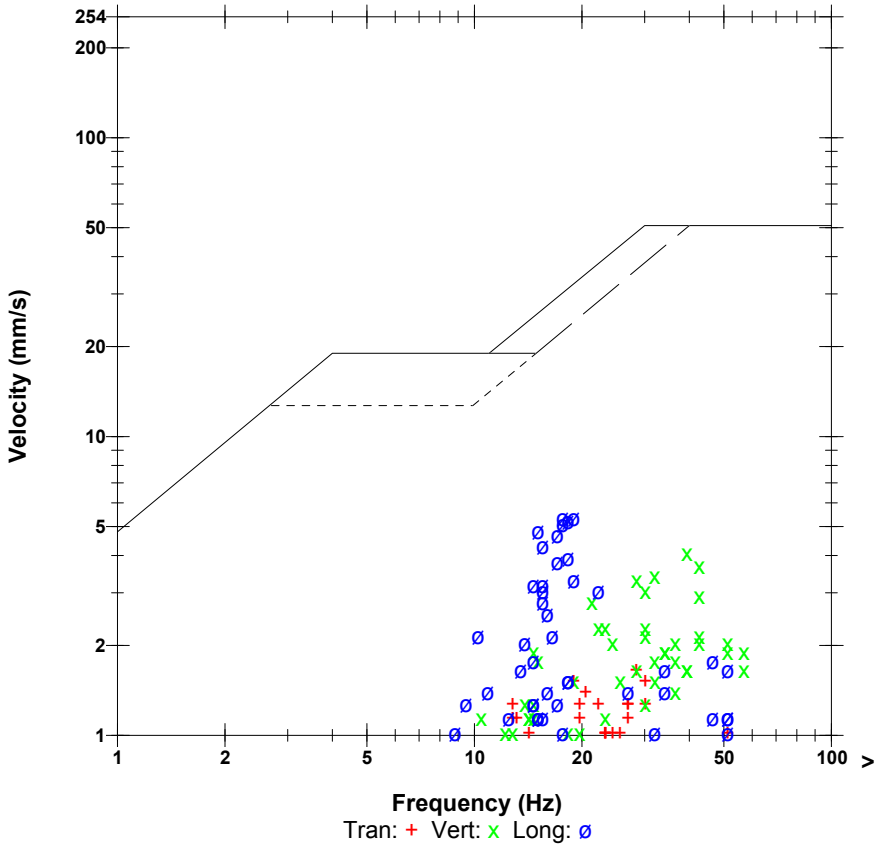

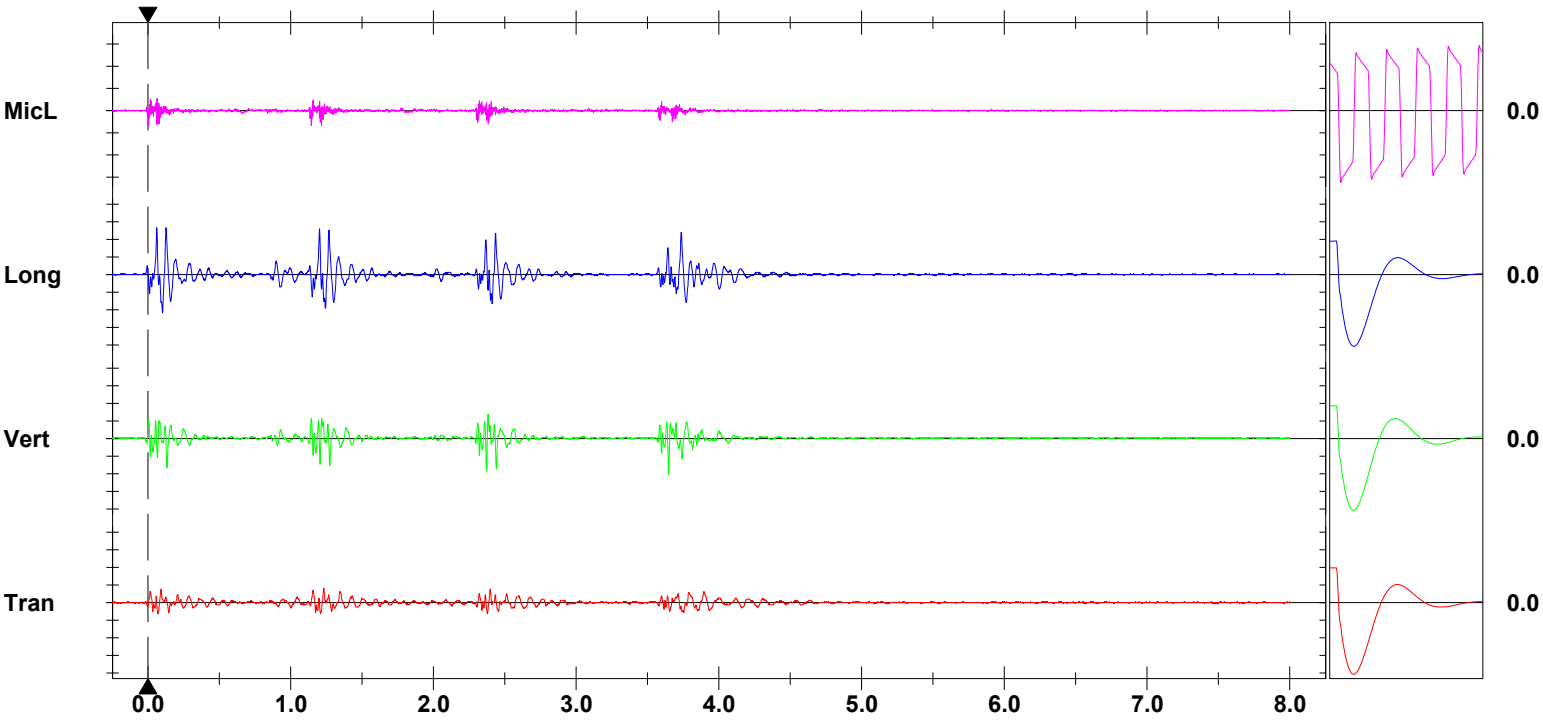

Time Scale: 0.50 sec/div **Amplitude Scale:** Geo: 2.00 mm/s/div Mic: 10.00 pa.(L)/div Sensorcheck
Trigger =

FFT Report

Date/Time	Vert at 14:19:44 October 29, 2009	**Serial Number**	BE13055 V 8.12-8.0 MiniMate Plus
Trigger Source	Geo: 1.27 mm/s	**Battery Level**	6.3 Volts
Range	Geo :254 mm/s	**Calibration**	December 7, 2007 by Instantel Inc.
Record Time	8.0 sec at 1024 sps	**File Name**	O055CYFU.GW0
Job Number:	1		

Notes
Location:
Client:
User Name:
General:

Extended Notes
Combo Mode October 29, 2009 14:17:24

Post Event Notes

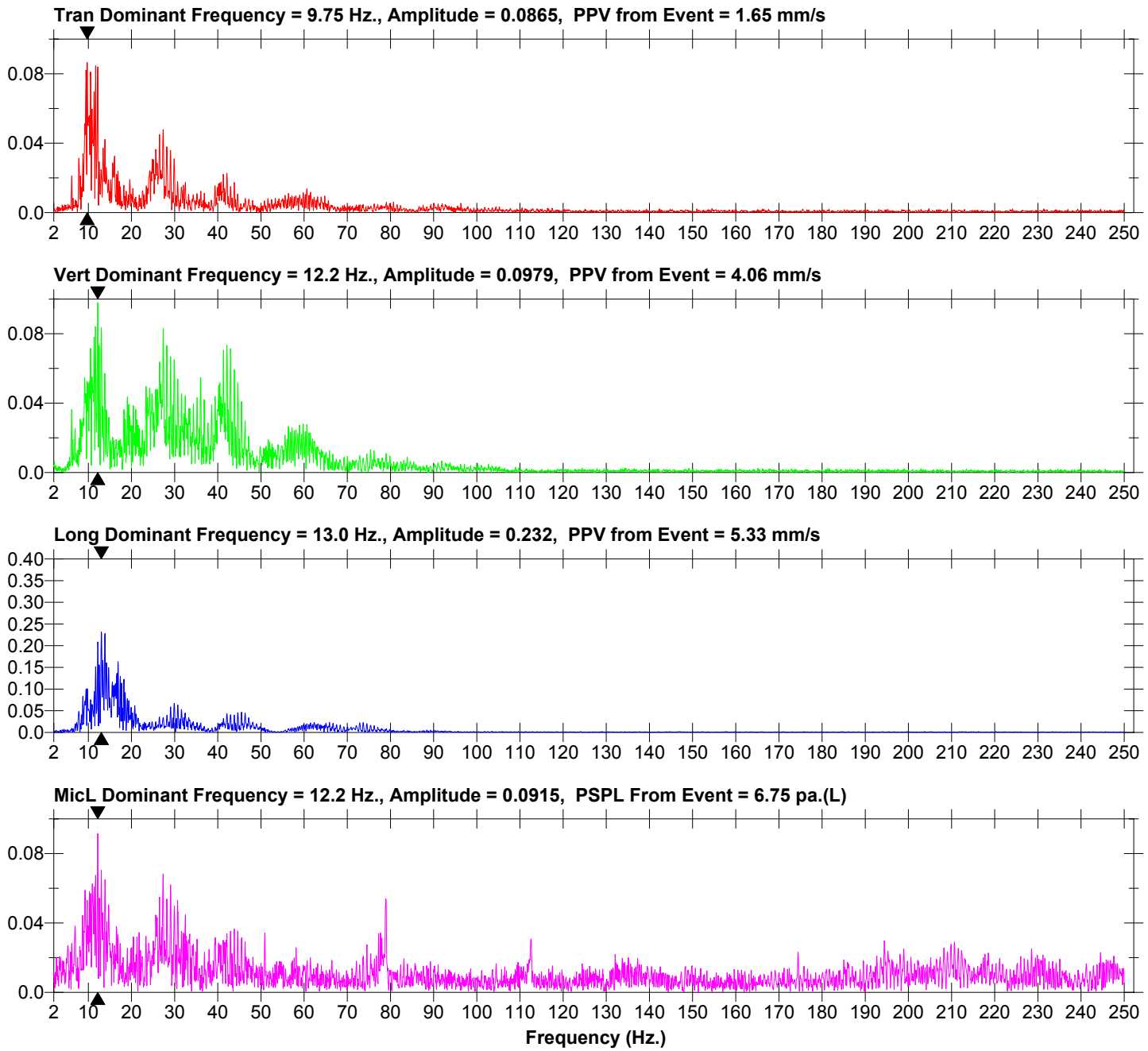

Field Vibration Data

Seismograph Unit # 2

at 25.0 feet from Test Pile #2

Event Report

Histogram Start Time	15:24:15 October 29, 2009	**Serial Number**	BE13055 V 8.12-8.0 MiniMate Plus
Histogram Finish Time	15:38:21 October 29, 2009	**Battery Level**	6.3 Volts
Number of Intervals	423 at 2 seconds	**Calibration**	December 7, 2007 by Instantel Inc.
Range	Geo :254 mm/s	**File Name**	O055CYFX.GF0
Sample Rate	1024sps		
Job Number:	1		

Notes
Location:
Client:
User Name:
General:

Extended Notes

Post Event Notes

Microphone Linear Weighting
PSPL 27.3 pa.(L) on October 29, 2009 at 15:36:41
ZC Freq >100 Hz
Channel Test Passed (Freq = 20.1 Hz Amp = 574 mv)

	Tran	Vert	Long	
PPV	5.71	12.6	11.7	mm/s
ZC Freq	30	16	22	Hz
Date	Oct 29 /09	Oct 29 /09	Oct 29 /09	
Time	15:31:17	15:27:09	15:33:57	
Sensorcheck	Passed	Passed	Passed	
Frequency	7.4	7.5	7.2	Hz
Overswing Ratio	3.9	3.6	4.2	

Peak Vector Sum 13.4 mm/s on October 29, 2009 at 15:27:09

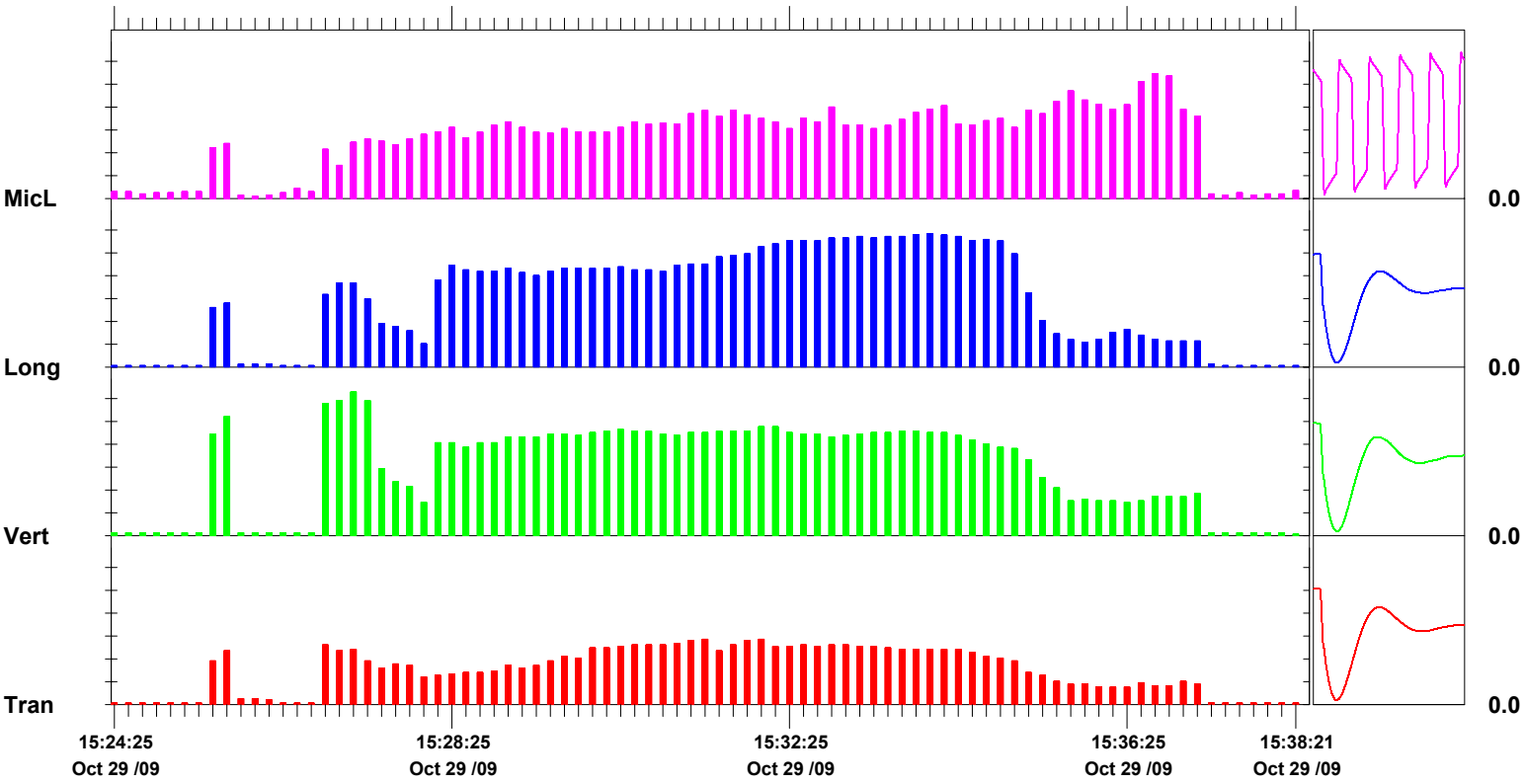

Time Scale: 10 seconds /div **Amplitude Scale:** Geo: 2.00 mm/s/div Mic: 5.00 pa.(L)/div Sensorcheck

Event Report

Date/Time	Long at 15:25:35 October 29, 2009	**Serial Number**	BE13055 V 8.12-8.0 MiniMate Plus
Trigger Source	Geo: 1.27 mm/s	**Battery Level**	6.3 Volts
Range	Geo :254 mm/s	**Calibration**	December 7, 2007 by Instantel Inc.
Record Time	8.0 sec at 1024 sps	**File Name**	O055CYFX.IN0
Job Number:	1		

Notes
Location:
Client:
User Name:
General:

Extended Notes
Combo Mode October 29, 2009 15:24:15

Post Event Notes

Microphone Linear Weighting
PSPL 12.0 pa.(L) at 2.506 sec
ZC Freq 57 Hz
Channel Test Passed (Freq = 20.1 Hz Amp = 574 mv)

	Tran	Vert	Long	
PPV	4.70	10.4	5.59	mm/s
ZC Freq	24	19	17	Hz
Time (Rel. to Trig)	2.482	2.542	2.446	sec
Peak Acceleration	0.0795	0.199	0.106	g
Peak Displacement	0.0308	0.0894	0.0407	mm
Sensorcheck	Passed	Passed	Passed	
Frequency	7.4	7.5	7.2	Hz
Overswing Ratio	3.9	3.6	4.2	

Peak Vector Sum 11.2 mm/s at 2.542 sec

USBM RI8507 And OSMRE

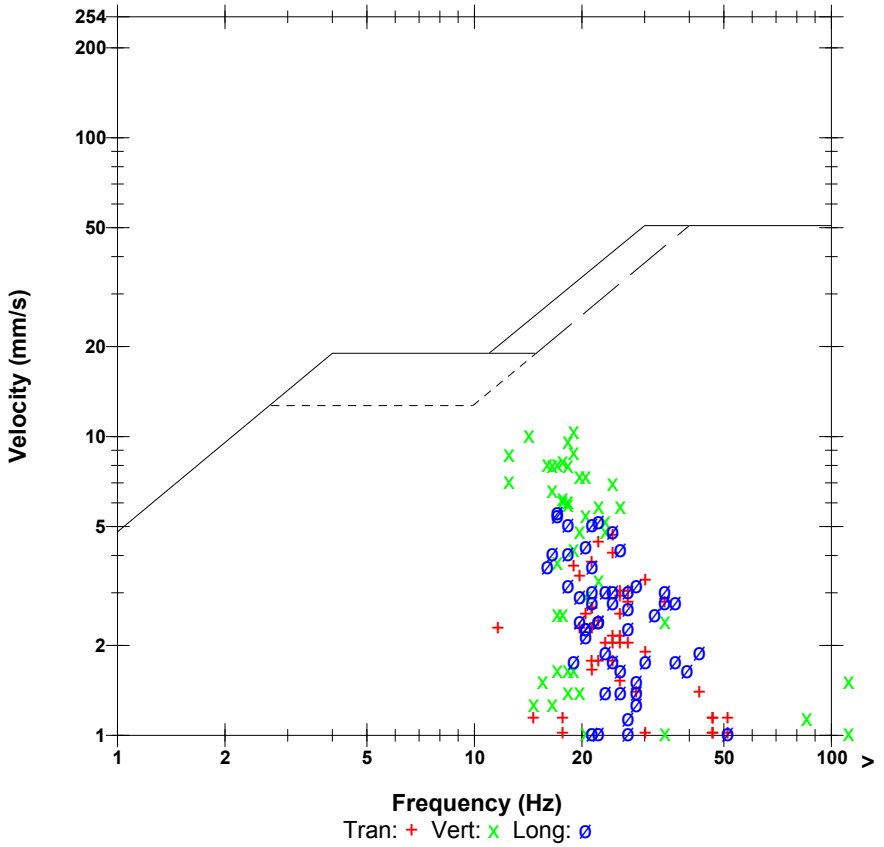

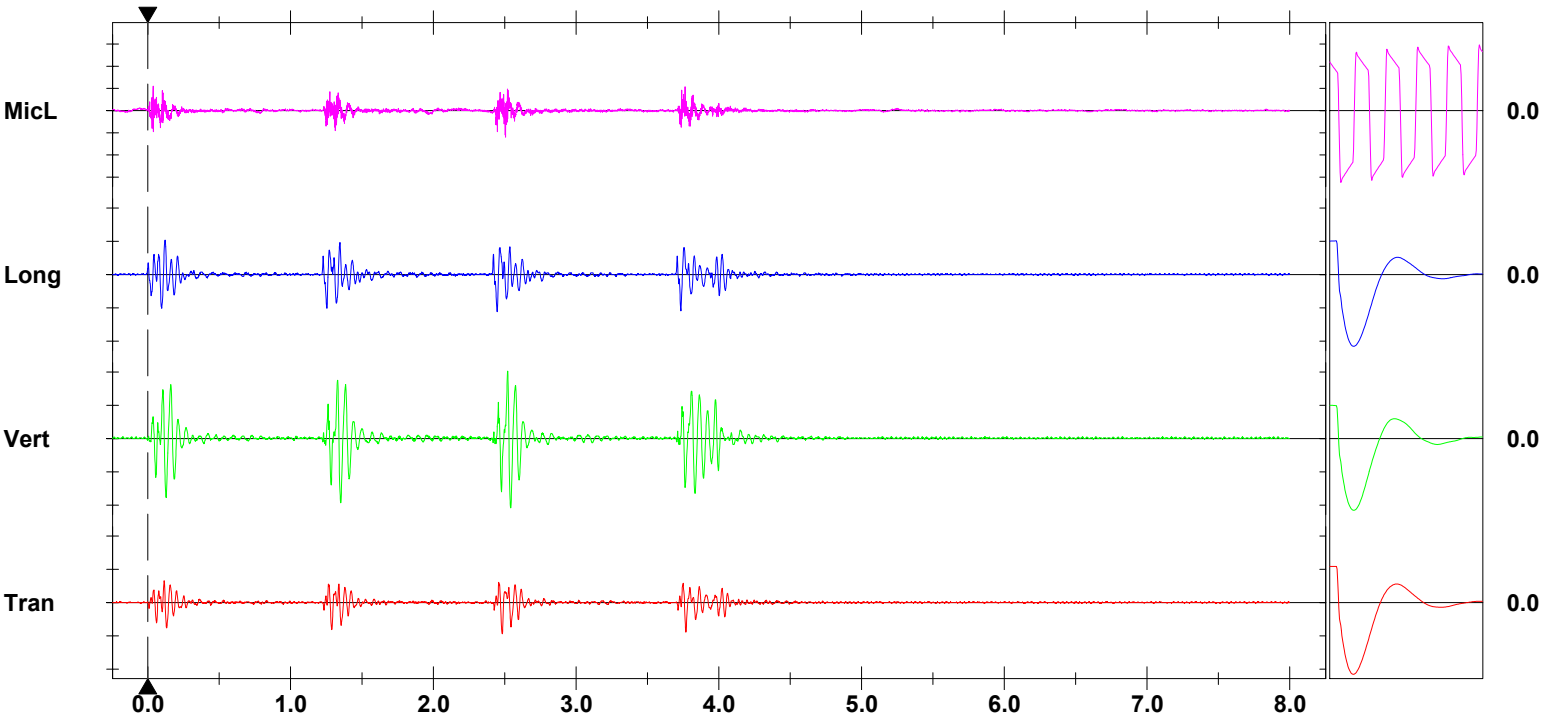

Time Scale: 0.50 sec/div **Amplitude Scale:** Geo: 5.00 mm/s/div Mic: 10.00 pa.(L)/div Sensorcheck
Trigger =

FFT Report

Date/Time	Long at 15:25:35 October 29, 2009	**Serial Number**	BE13055 V 8.12-8.0 MiniMate Plus
Trigger Source	Geo: 1.27 mm/s	**Battery Level**	6.3 Volts
Range	Geo :254 mm/s	**Calibration**	December 7, 2007 by Instantel Inc.
Record Time	8.0 sec at 1024 sps	**File Name**	O055CYFX.IN0
Job Number:	1		

Notes
Location:
Client:
User Name:
General:

Extended Notes
Combo Mode October 29, 2009 15:24:15

Post Event Notes

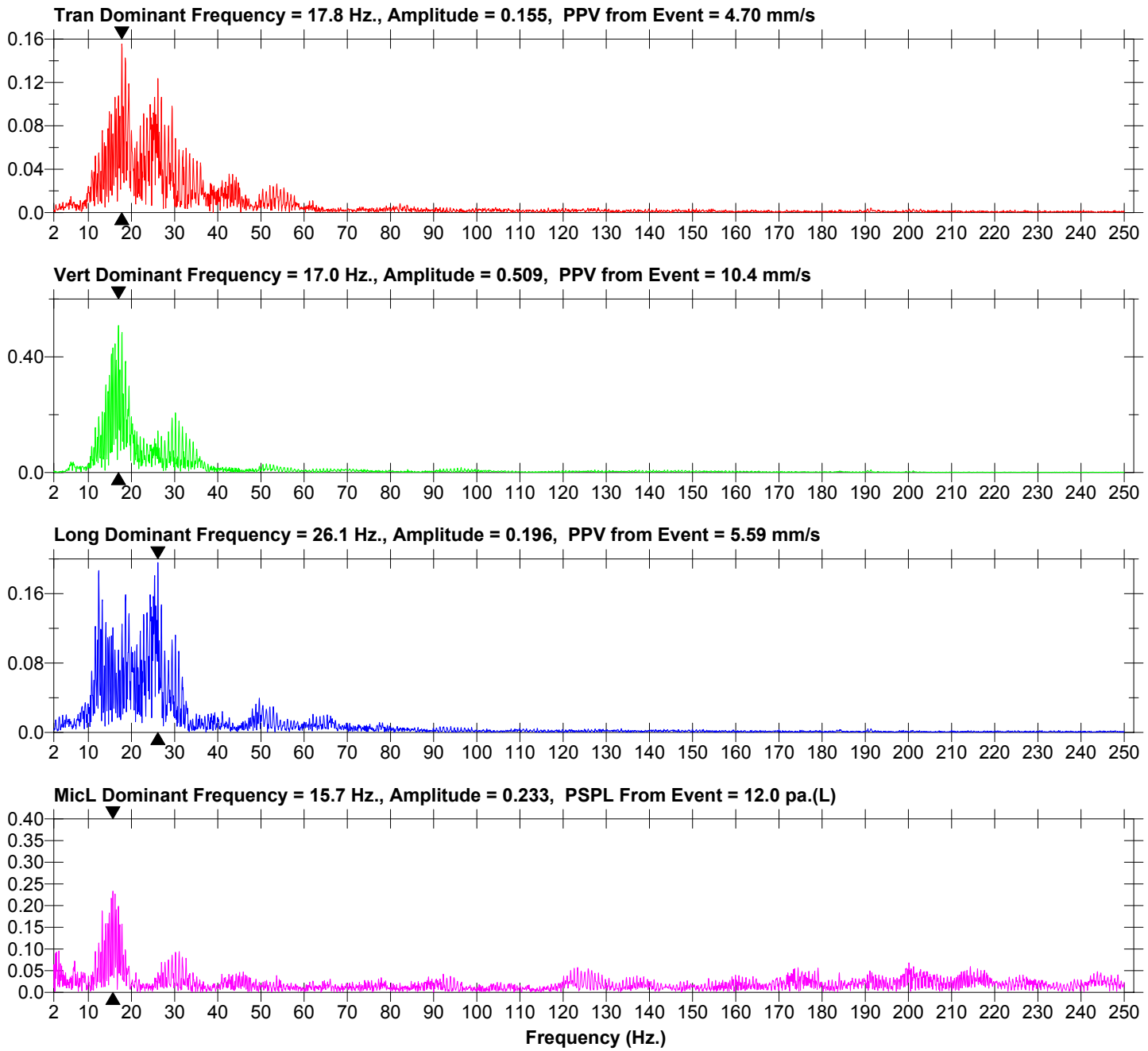

Event Report

Date/Time Long at 15:26:48 October 29, 2009
Trigger Source Geo: 1.27 mm/s
Range Geo :254 mm/s
Record Time 8.0 sec at 1024 sps
Job Number: 1

Serial Number BE13055 V 8.12-8.0 MiniMate Plus
Battery Level 6.3 Volts
Calibration December 7, 2007 by Instantel Inc.
File Name O055CYFX.KO0

Notes
Location:
Client:
User Name:
General:

Extended Notes
Combo Mode October 29, 2009 15:24:15

Post Event Notes

Microphone Linear Weighting
PSPL 10.8 pa.(L) at 3.925 sec
ZC Freq 73 Hz
Channel Test Passed (Freq = 20.1 Hz Amp = 574 mv)

	Tran	Vert	Long	
PPV	5.21	11.6	6.35	mm/s
ZC Freq	22	17	20	Hz
Time (Rel. to Trig)	2.614	0.096	0.053	sec
Peak Acceleration	0.0795	0.225	0.0928	g
Peak Displacement	0.0334	0.0967	0.0441	mm
Sensorcheck	Passed	Passed	Passed	
Frequency	7.4	7.5	7.2	Hz
Overswing Ratio	3.9	3.6	4.2	

Peak Vector Sum 12.4 mm/s at 0.117 sec

USBM RI8507 And OSMRE

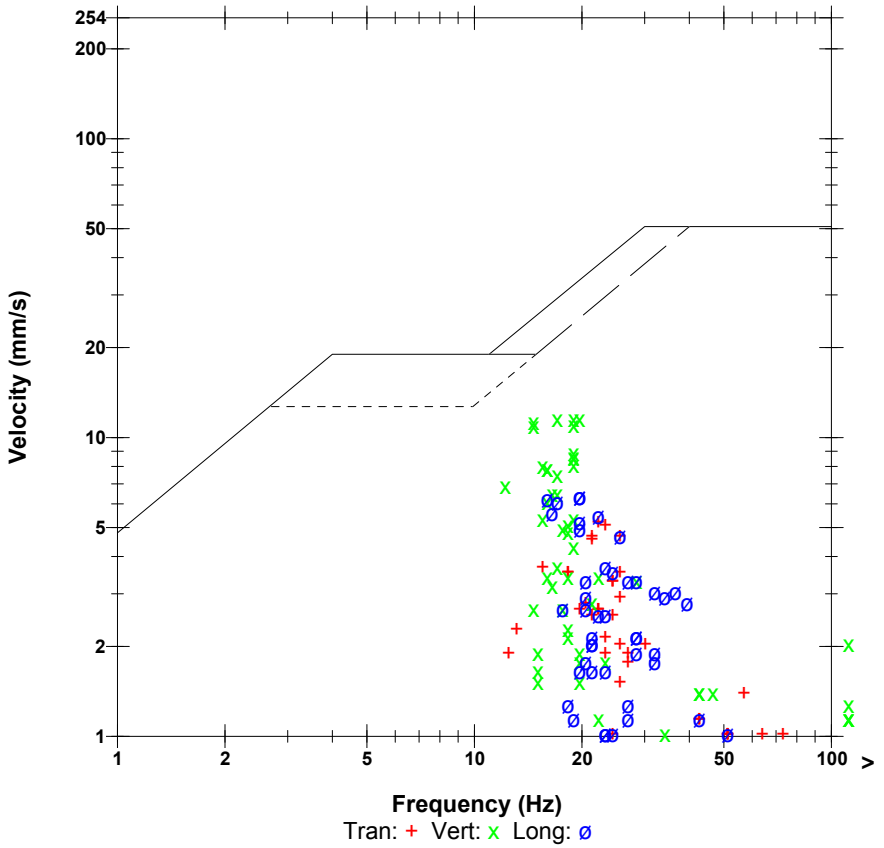

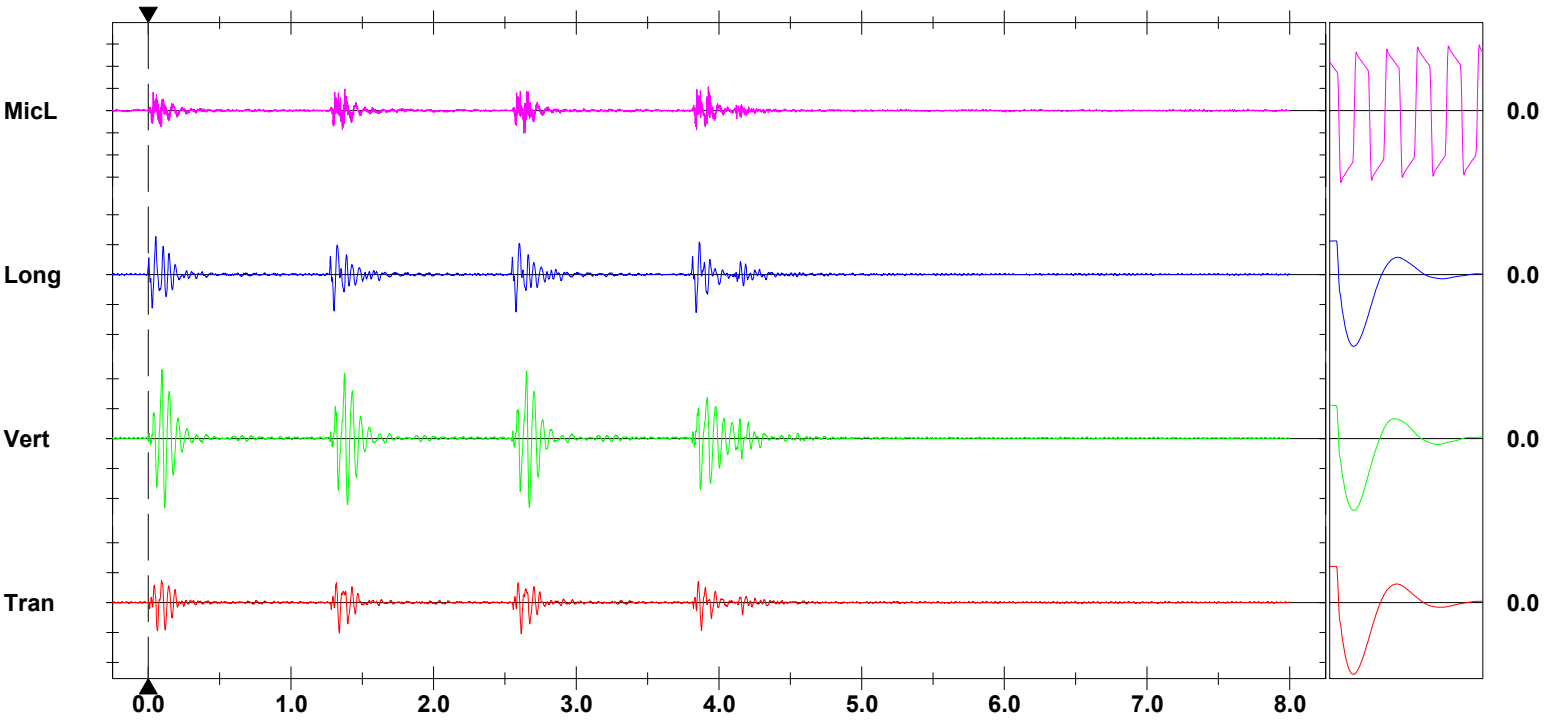

Time Scale: 0.50 sec/div **Amplitude Scale:** Geo: 5.00 mm/s/div Mic: 10.00 pa.(L)/div Sensorcheck
Trigger =

FFT Report

Date/Time	Long at 15:26:48 October 29, 2009	**Serial Number**	BE13055 V 8.12-8.0 MiniMate Plus
Trigger Source	Geo: 1.27 mm/s	**Battery Level**	6.3 Volts
Range	Geo :254 mm/s	**Calibration**	December 7, 2007 by Instantel Inc.
Record Time	8.0 sec at 1024 sps	**File Name**	O055CYFX.KO0
Job Number:	1		

Notes
Location:
Client:
User Name:
General:

Extended Notes
Combo Mode October 29, 2009 15:24:15

Post Event Notes

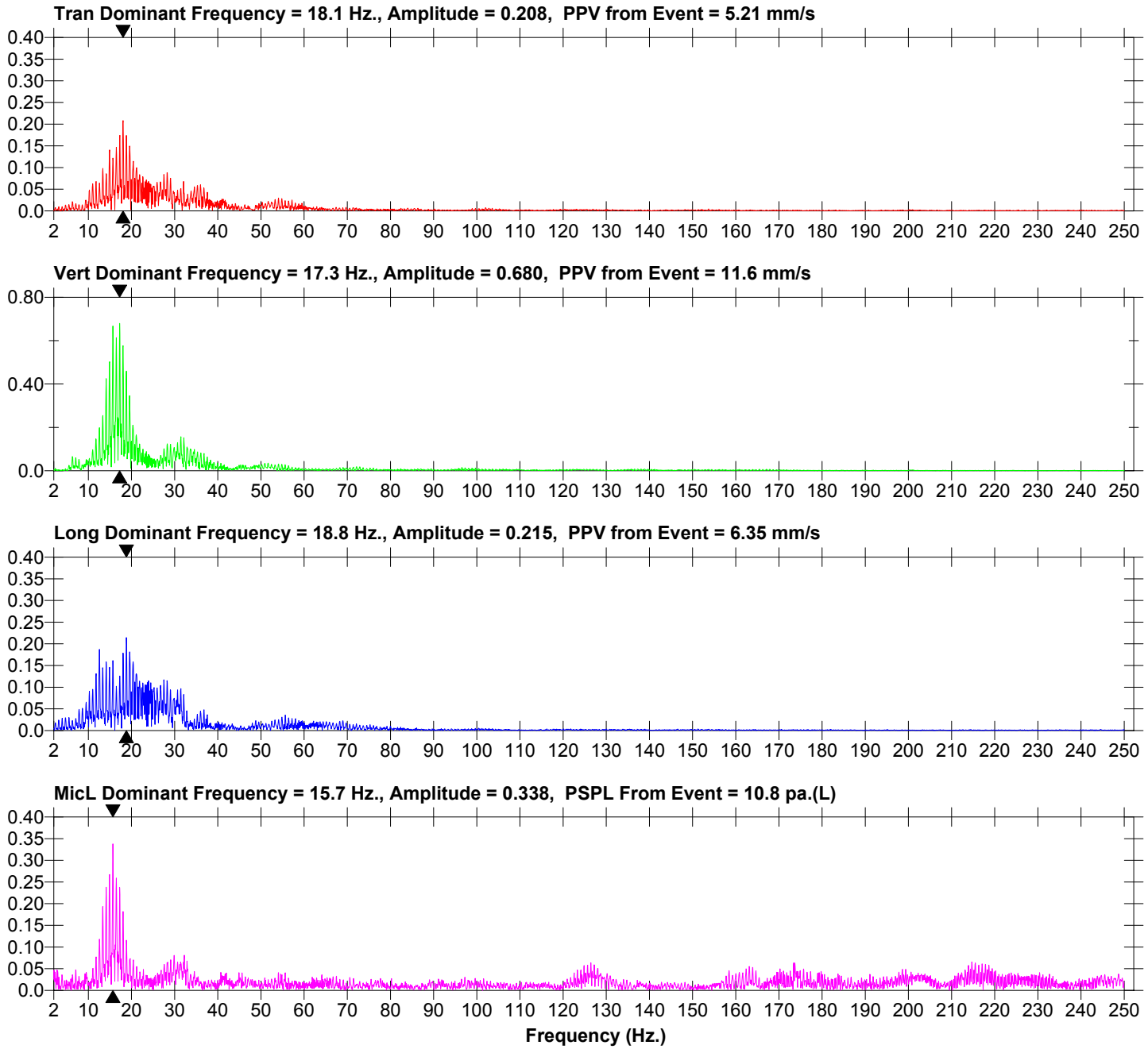

Event Report

Date/Time	Long at 15:27:04 October 29, 2009	**Serial Number**	BE13055 V 8.12-8.0 MiniMate Plus
Trigger Source	Geo: 1.27 mm/s	**Battery Level**	6.3 Volts
Range	Geo :254 mm/s	**Calibration**	December 7, 2007 by Instantel Inc.
Record Time	6.565 sec at 1024 sps	**File Name**	O055CYFX.L40
Job Number:	1		

Notes
Location:
Client:
User Name:
General:

Extended Notes
Combo Mode October 29, 2009 15:24:15

Post Event Notes

Microphone Linear Weighting
PSPL 12.3 pa.(L) at 2.726 sec
ZC Freq 30 Hz
Channel Test Passed (Freq = 20.1 Hz Amp = 574 mv)

	Tran	Vert	Long	
PPV	4.83	12.6	7.37	mm/s
ZC Freq	21	16	20	Hz
Time (Rel. to Trig)	1.346	4.126	0.052	sec
Peak Acceleration	0.0928	0.239	0.106	g
Peak Displacement	0.0376	0.104	0.0513	mm
Sensorcheck	Passed	Passed	Passed	
Frequency	7.4	7.5	7.2	Hz
Overswing Ratio	3.9	3.6	4.2	

Peak Vector Sum 13.4 mm/s at 4.126 sec

USBM RI8507 And OSMRE

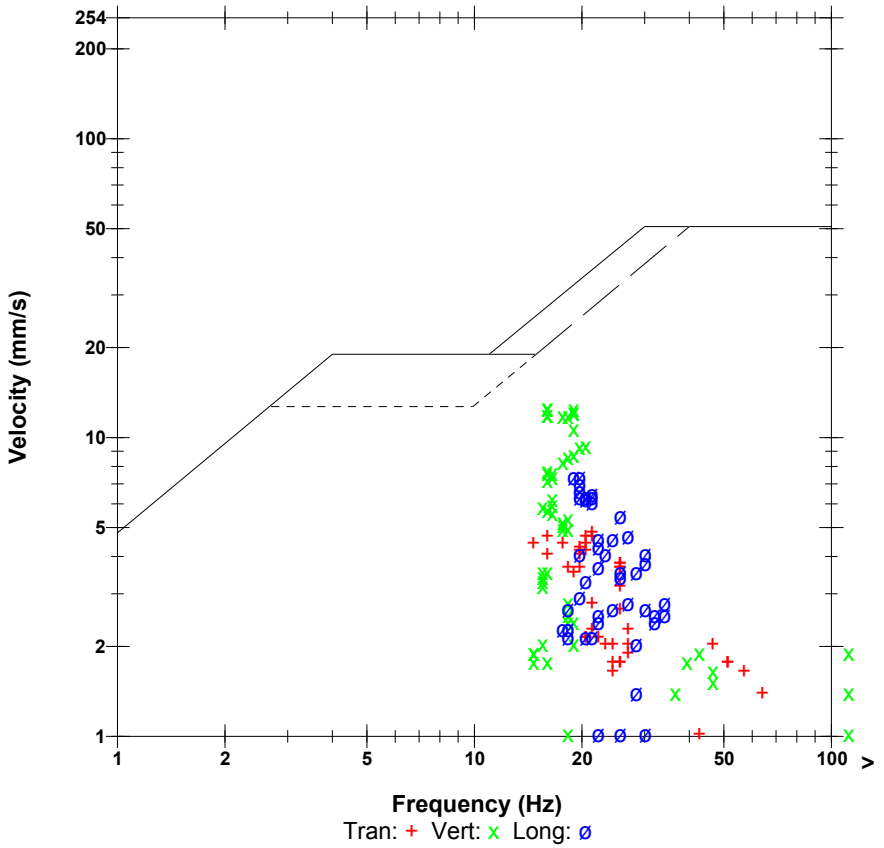

Monitor Log
Oct 29 /09 15:27:04 Oct 29 /09 15:27:11 Event recorded. (Memory Full Exit)

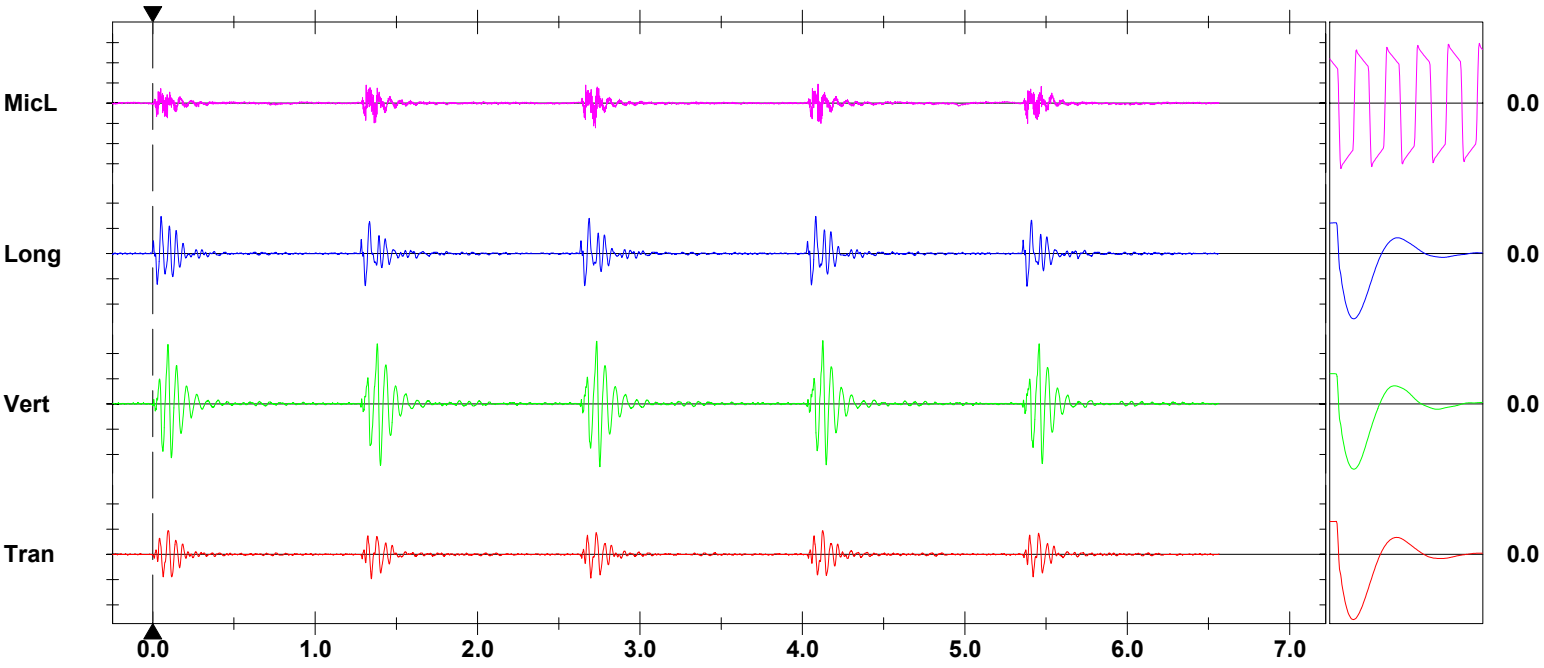

Time Scale: 0.50 sec/div **Amplitude Scale:** Geo: 5.00 mm/s/div Mic: 10.00 pa.(L)/div Sensorcheck
Trigger =

FFT Report

Date/Time	Long at 15:27:04 October 29, 2009	**Serial Number**	BE13055 V 8.12-8.0 MiniMate Plus
Trigger Source	Geo: 1.27 mm/s	**Battery Level**	6.3 Volts
Range	Geo :254 mm/s	**Calibration**	December 7, 2007 by Instantel Inc.
Record Time	6.565 sec at 1024 sps	**File Name**	O055CYFX.L40
Job Number:	1		

Notes
Location:
Client:
User Name:
General:

Extended Notes
Combo Mode October 29, 2009 15:24:15

Post Event Notes

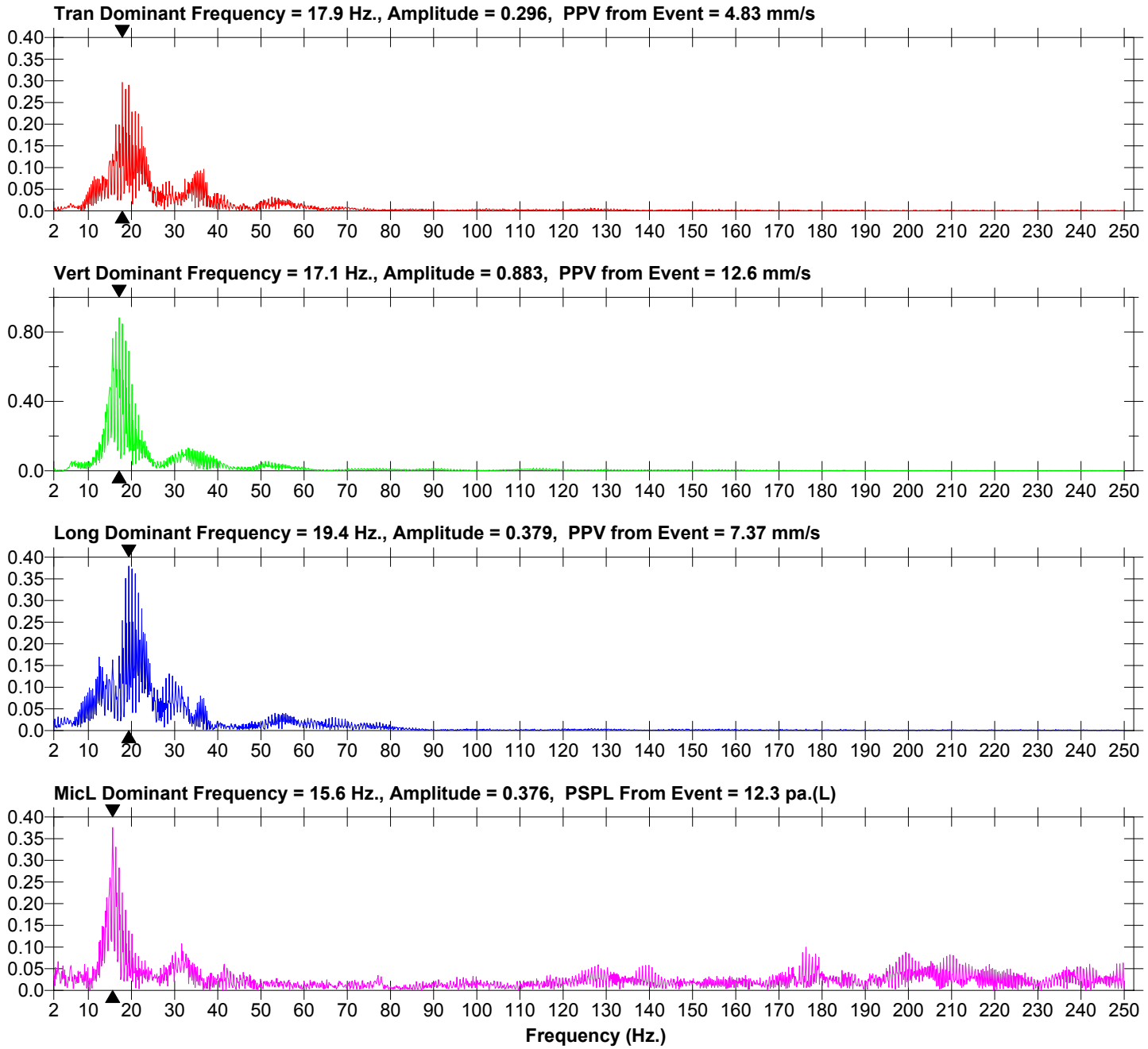

Field Vibration Data

Seismograph Unit # 2

at 49.8 feet from Test Pile #1

Non Driving Event

Event Report

Histogram Start Time	10:31:04 December 21, 2009	**Serial Number**	BE13055 V 8.12-8.0 MiniMate Plus
Histogram Finish Time	11:04:39 December 21, 2009	**Battery Level**	6.2 Volts
Number of Intervals	1007 at 2 seconds	**Calibration**	December 7, 2007 by Instantel Inc.
Range	Geo :254 mm/s	**File Name**	O055D15P.7S0
Sample Rate	1024sps		
Job Number:	1		

Notes
Location:
Client:
User Name:
General:

Extended Notes

Post Event Notes

Microphone Linear Weighting
PSPL 2.75 pa.(L) on December 21, 2009 at 10:58:04
ZC Freq 5.4 Hz
Channel Test Passed (Freq = 20.5 Hz Amp = 705 mv)

	Tran	Vert	Long	
PPV	0.127	0.127	0.127	mm/s
ZC Freq	>100	>100	>100	Hz
Date	Dec 21 /09	Dec 21 /09	Dec 21 /09	
Time	10:31:06	10:31:06	10:31:06	
Sensorcheck	Check	Check	Check	
Frequency	1024.0	53.9	1024.0	Hz
Overswing Ratio	0.0	1.0	0.0	

Peak Vector Sum 0.220 mm/s on December 21, 2009 at 10:36:24

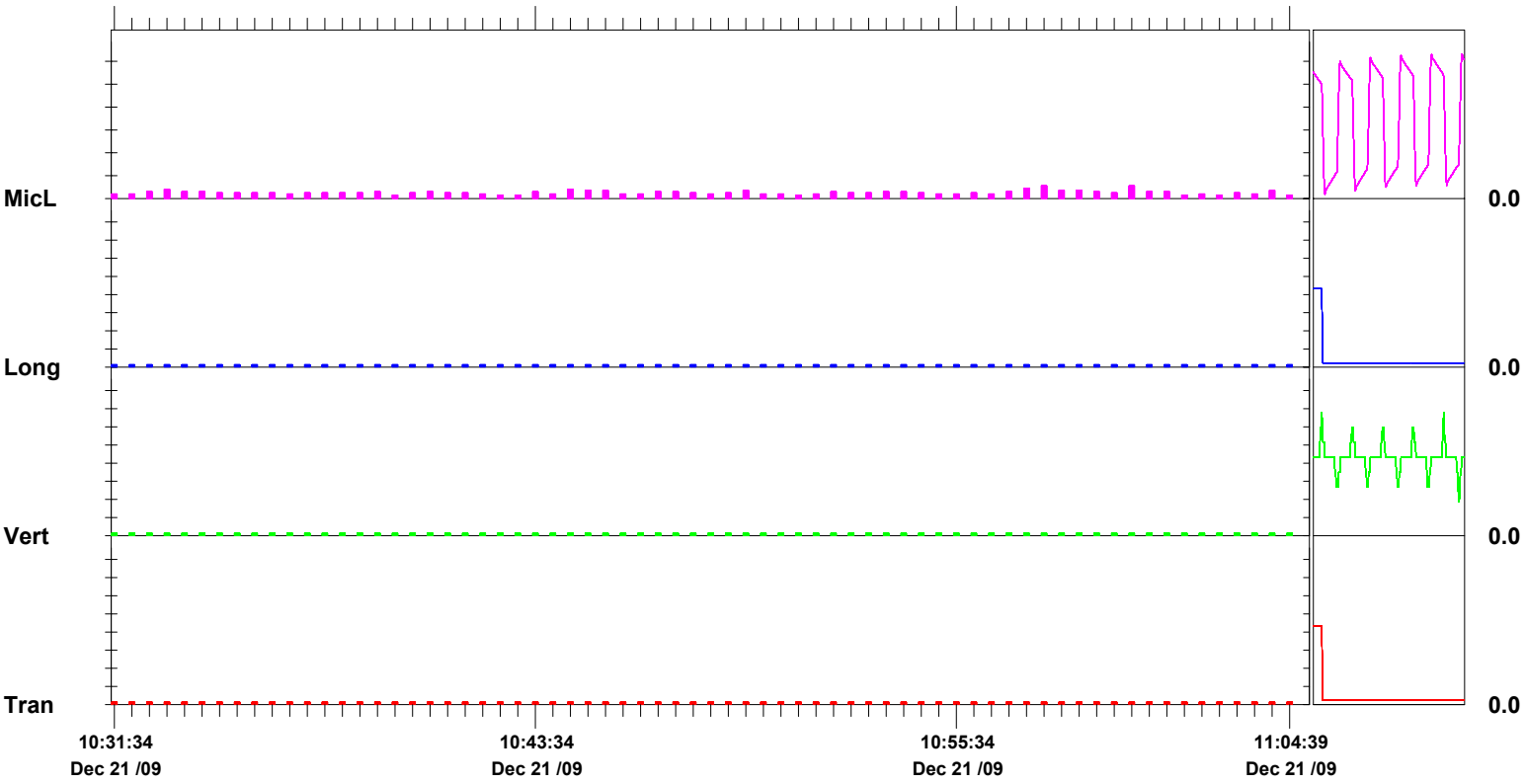

Time Scale: 30 seconds /div **Amplitude Scale:** Geo: 1.000 mm/s/div Mic: 5.00 pa.(L)/div Sensorcheck

Event Report

Histogram Start Time	11:30:58 December 21, 2009	**Serial Number**	BE13055 V 8.12-8.0 MiniMate Plus
Histogram Finish Time	11:55:42 December 21, 2009	**Battery Level**	6.2 Volts
Number of Intervals	742 at 2 seconds	**Calibration**	December 7, 2007 by Instantel Inc.
Range	Geo :254 mm/s	**File Name**	O055D15R.ZM0
Sample Rate	1024sps		
Job Number:	1		

Notes
Location:
Client:
User Name:
General:

Extended Notes

Post Event Notes

Microphone Linear Weighting
PSPL 3.00 pa.(L) on December 21, 2009 at 11:35:56
ZC Freq 8.1 Hz
Channel Test Passed (Freq = 20.1 Hz Amp = 695 mv)

	Tran	Vert	Long	
PPV	0.127	0.127	0.127	mm/s
ZC Freq	>100	>100	>100	Hz
Date	Dec 21 /09	Dec 21 /09	Dec 21 /09	
Time	11:31:00	11:31:00	11:31:00	
Sensorcheck	Check	Check	Check	
Frequency	1024.0	60.2	1024.0	Hz
Overswing Ratio	0.0	1.0	0.0	

Peak Vector Sum 0.220 mm/s on December 21, 2009 at 11:39:02

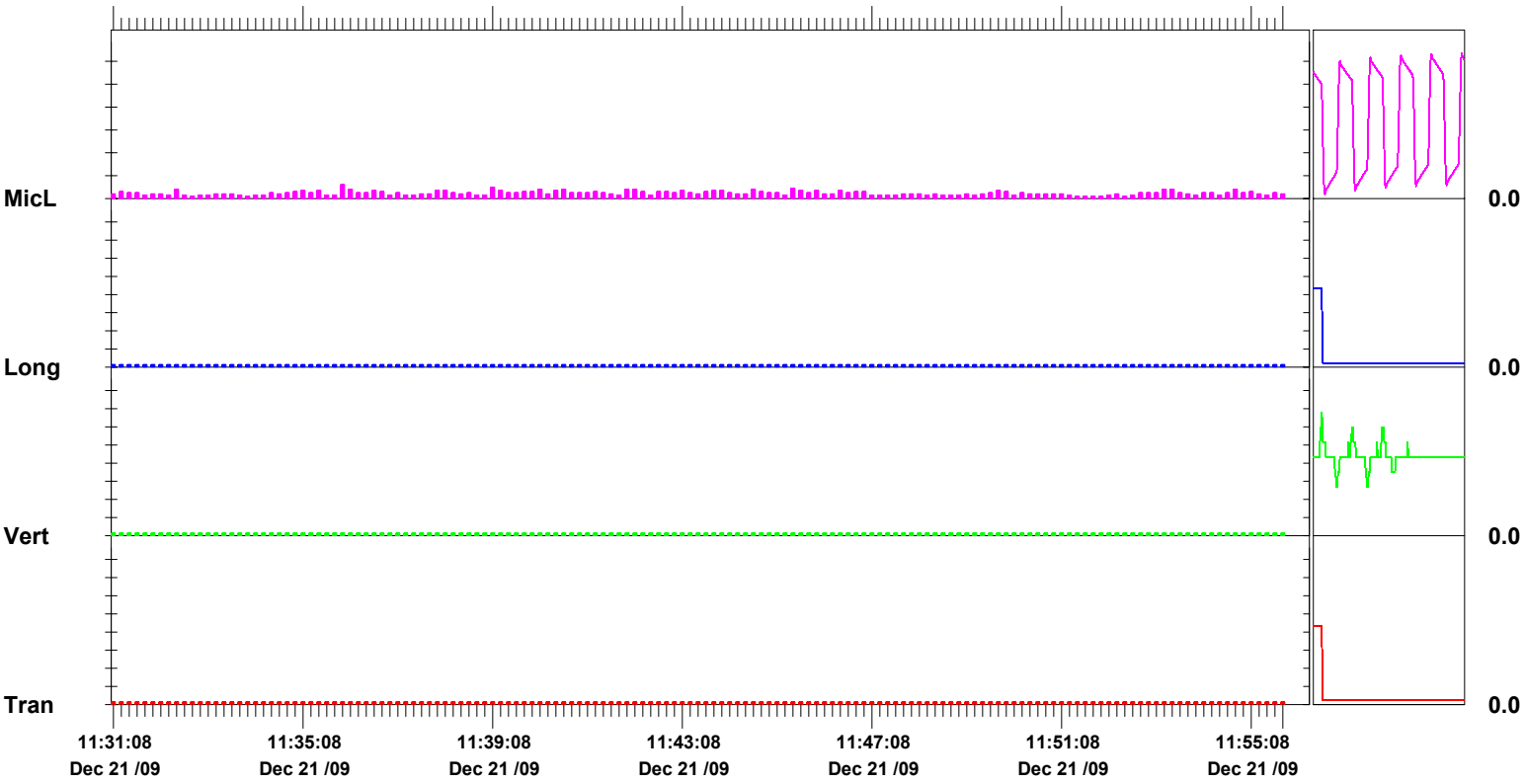

Time Scale: 10 seconds /div **Amplitude Scale:** Geo: 1.000 mm/s/div Mic: 5.00 pa.(L)/div Sensorcheck

Field Vibration Data

Seismograph Unit # 3

at 9.7 feet from Test Pile #1

Event Report

Histogram Start Time	14:17:10 October 29, 2009	**Serial Number**	BE13073 V 8.12-8.0 MiniMate Plus
Histogram Finish Time	14:25:49 October 29, 2009	**Battery Level**	6.3 Volts
Number of Intervals	259 at 2 seconds	**Calibration**	December 7, 2007 by Instantel Inc.
Range	Geo :254 mm/s	**File Name**	O073CYFU.CM0
Sample Rate	1024sps		
Job Number:	1		

Notes
Location:
Client:
User Name:
General:

Extended Notes

Post Event Notes

Microphone Linear Weighting
PSPL 70.0 pa.(L) on October 29, 2009 at 14:21:14
ZC Freq >100 Hz
Channel Test Passed (Freq = 20.1 Hz Amp = 603 mv)

	Tran	Vert	Long	
PPV	9.65	38.1	23.0	mm/s
ZC Freq	32	22	18	Hz
Date	Oct 29 /09	Oct 29 /09	Oct 29 /09	
Time	14:22:36	14:18:10	14:18:10	
Sensorcheck	Passed	Passed	Passed	
Frequency	7.5	7.4	7.1	Hz
Overswing Ratio	3.9	3.7	4.1	

Peak Vector Sum 40.9 mm/s on October 29, 2009 at 14:18:10

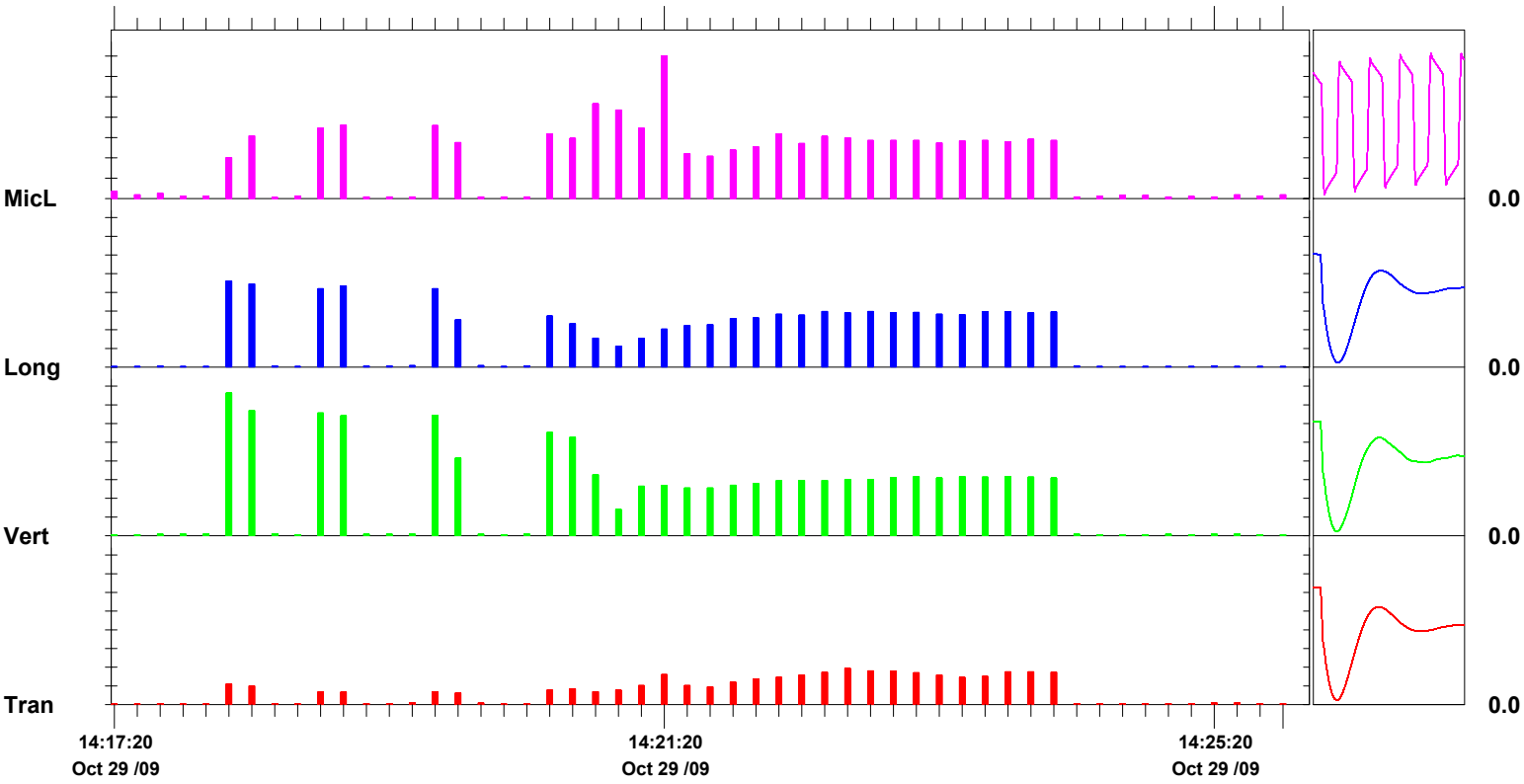

Time Scale: 10 seconds /div **Amplitude Scale:** Geo: 5.00 mm/s/div Mic: 10.00 pa.(L)/div Sensorcheck

Event Report

Date/Time	Vert at 14:18:10 October 29, 2009	**Serial Number**	BE13073 V 8.12-8.0 MiniMate Plus
Trigger Source	Geo: 1.27 mm/s	**Battery Level**	6.3 Volts
Range	Geo :254 mm/s	**Calibration**	December 7, 2007 by Instantel Inc.
Record Time	8.0 sec at 1024 sps	**File Name**	O073CYFU.EA0
Job Number:	1		

Notes
Location:
Client:
User Name:
General:

Extended Notes
Combo Mode October 29, 2009 14:17:09

Post Event Notes

Microphone Linear Weighting
PSPL 30.8 pa.(L) at 2.291 sec
ZC Freq 73 Hz
Channel Test Passed (Freq = 20.1 Hz Amp = 603 mv)

	Tran	Vert	Long	
PPV	5.46	38.1	23.0	mm/s
ZC Freq	24	22	18	Hz
Time (Rel. to Trig)	0.087	0.077	0.024	sec
Peak Acceleration	0.172	0.610	0.451	g
Peak Displacement	0.0336	0.257	0.171	mm
Sensorcheck	Passed	Passed	Passed	
Frequency	7.5	7.4	7.1	Hz
Overswing Ratio	3.9	3.7	4.1	

Peak Vector Sum 40.9 mm/s at 0.077 sec

USBM RI8507 And OSMRE

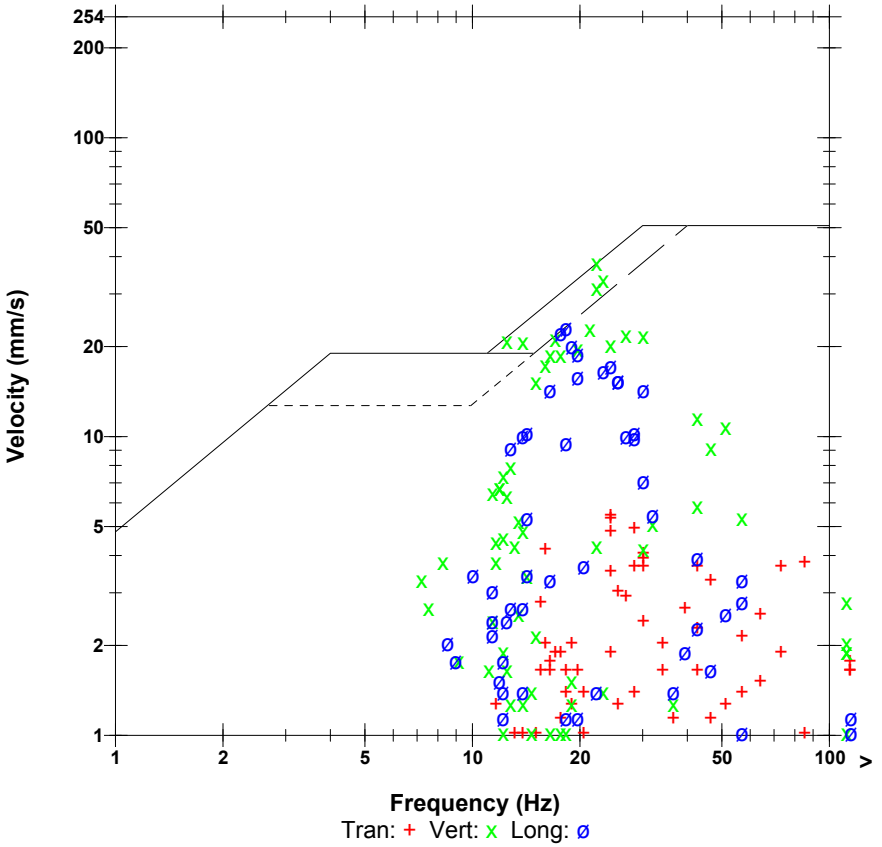

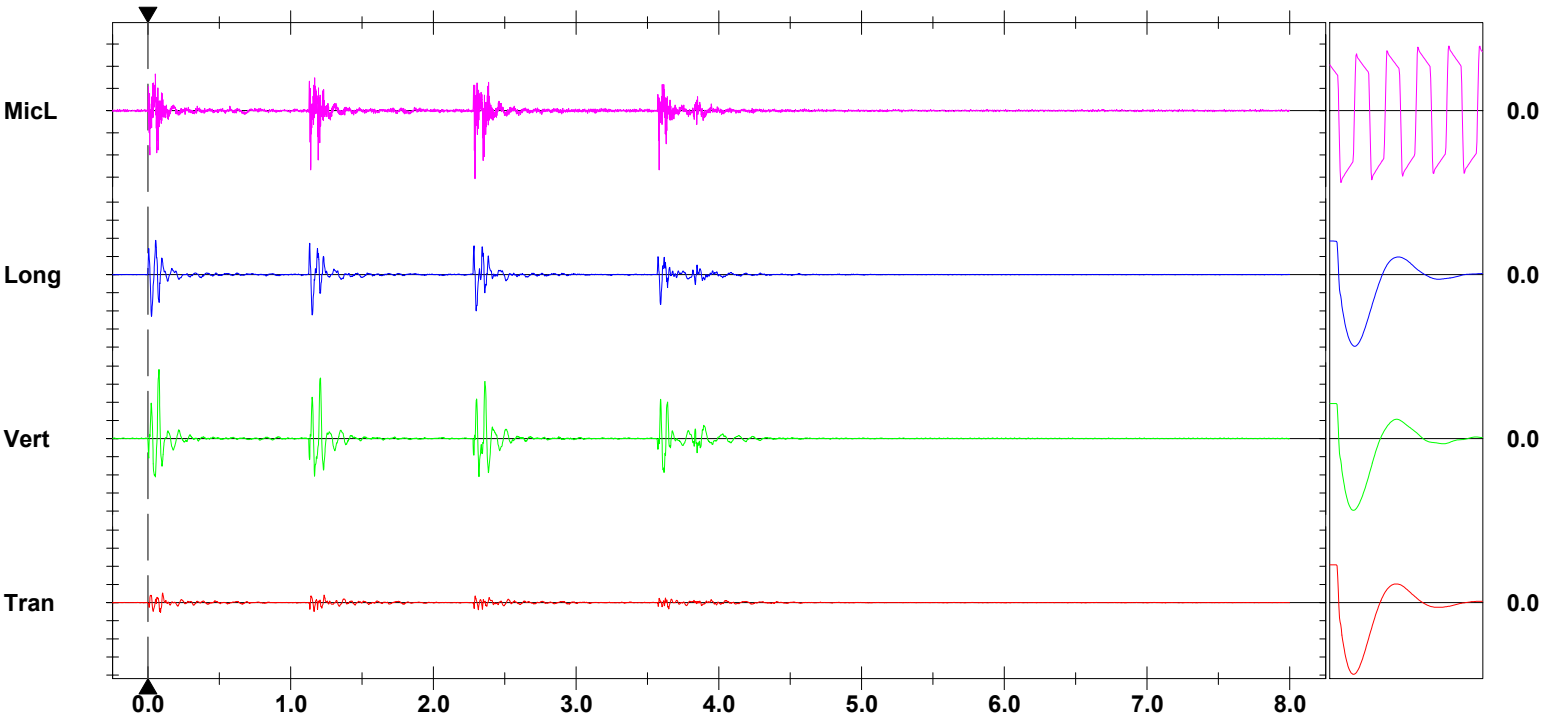

Time Scale: 0.50 sec/div **Amplitude Scale:** Geo: 10.00 mm/s/div Mic: 10.00 pa.(L)/div Sensorcheck
Trigger =

FFT Report

Date/Time	Vert at 14:18:10 October 29, 2009	**Serial Number**	BE13073 V 8.12-8.0 MiniMate Plus
Trigger Source	Geo: 1.27 mm/s	**Battery Level**	6.3 Volts
Range	Geo :254 mm/s	**Calibration**	December 7, 2007 by Instantel Inc.
Record Time	8.0 sec at 1024 sps	**File Name**	O073CYFU.EA0
Job Number:	1		

Notes
Location:
Client:
User Name:
General:

Extended Notes
Combo Mode October 29, 2009 14:17:09

Post Event Notes

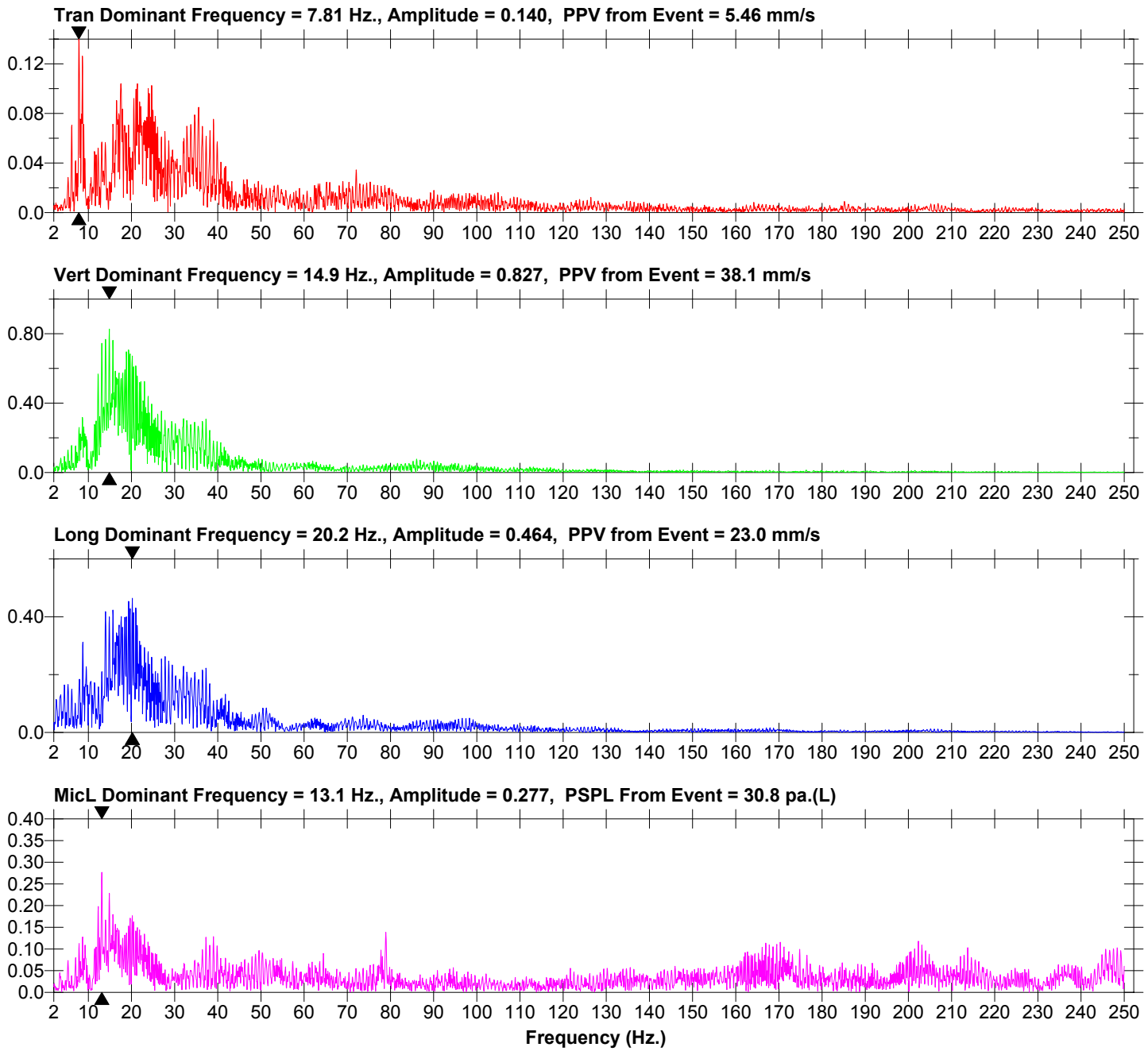

Event Report

Date/Time	Vert at 14:18:49 October 29, 2009	**Serial Number**	BE13073 V 8.12-8.0 MiniMate Plus
Trigger Source	Geo: 1.27 mm/s	**Battery Level**	6.3 Volts
Range	Geo :254 mm/s	**Calibration**	December 7, 2007 by Instantel Inc.
Record Time	8.0 sec at 1024 sps	**File Name**	O073CYFU.FD0
Job Number:	1		

Notes
Location:
Client:
User Name:
General:

Extended Notes
Combo Mode October 29, 2009 14:17:09

Post Event Notes

Microphone Linear Weighting
PSPL 36.0 pa.(L) at 1.153 sec
ZC Freq 64 Hz
Channel Test Passed (Freq = 20.1 Hz Amp = 603 mv)

	Tran	Vert	Long	
PPV	3.30	32.8	21.7	mm/s
ZC Freq	28	22	21	Hz
Time (Rel. to Trig)	0.013	0.082	1.161	sec
Peak Acceleration	0.159	0.517	0.504	g
Peak Displacement	0.0190	0.214	0.132	mm
Sensorcheck	Passed	Passed	Passed	
Frequency	7.5	7.4	7.1	Hz
Overswing Ratio	3.9	3.7	4.1	

Peak Vector Sum 34.6 mm/s at 0.082 sec

USBM RI8507 And OSMRE

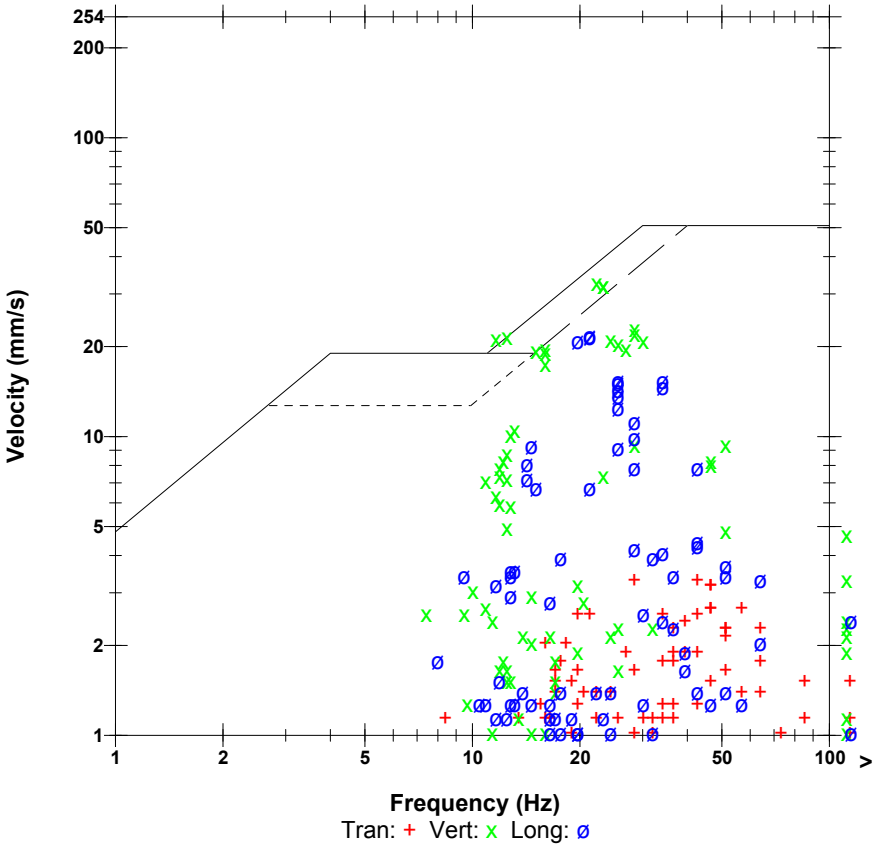

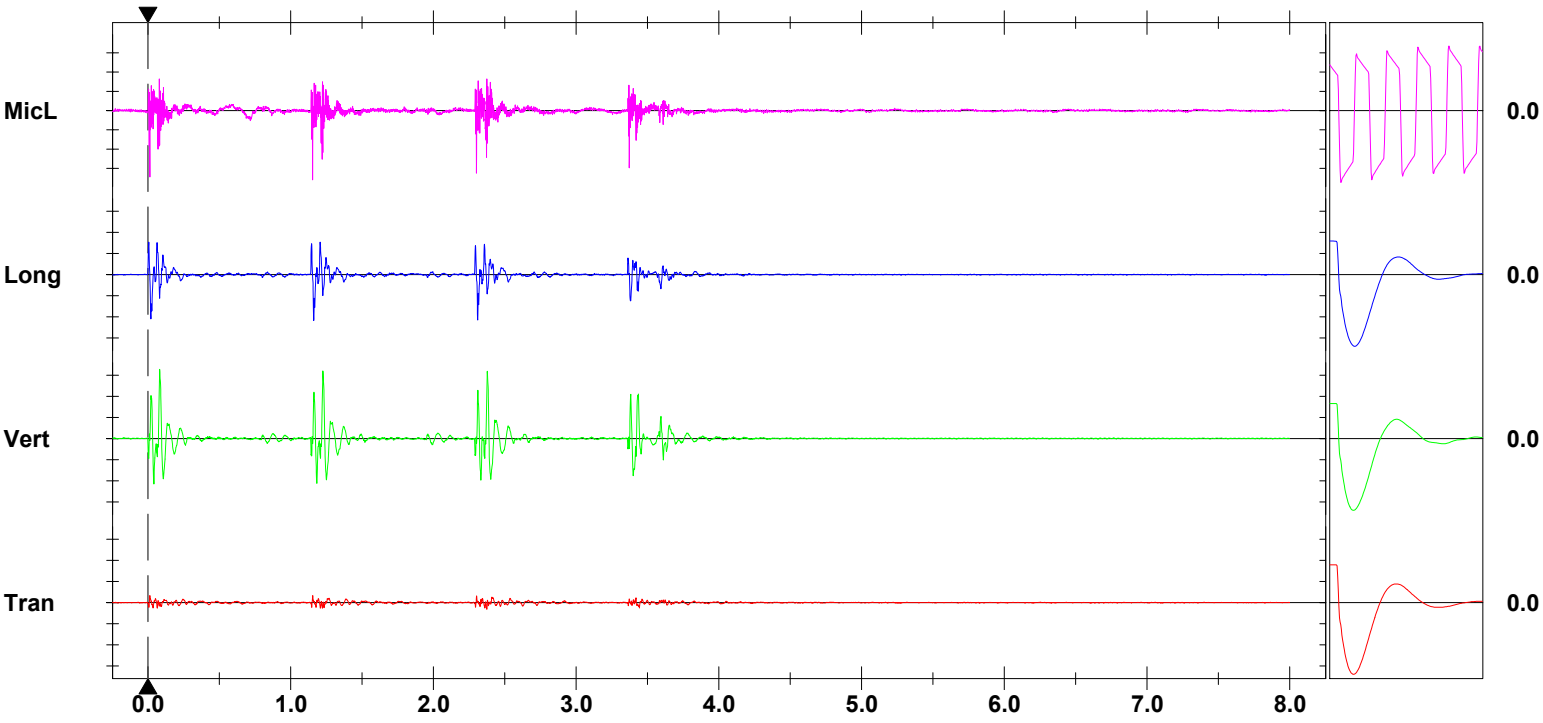

Time Scale: 0.50 sec/div **Amplitude Scale:** Geo: 10.00 mm/s/div Mic: 10.00 pa.(L)/div Sensorcheck
Trigger =

FFT Report

Date/Time	Vert at 14:18:49 October 29, 2009	**Serial Number**	BE13073 V 8.12-8.0 MiniMate Plus
Trigger Source	Geo: 1.27 mm/s	**Battery Level**	6.3 Volts
Range	Geo :254 mm/s	**Calibration**	December 7, 2007 by Instantel Inc.
Record Time	8.0 sec at 1024 sps	**File Name**	O073CYFU.FD0
Job Number:	1		

Notes
Location:
Client:
User Name:
General:

Extended Notes
Combo Mode October 29, 2009 14:17:09

Post Event Notes

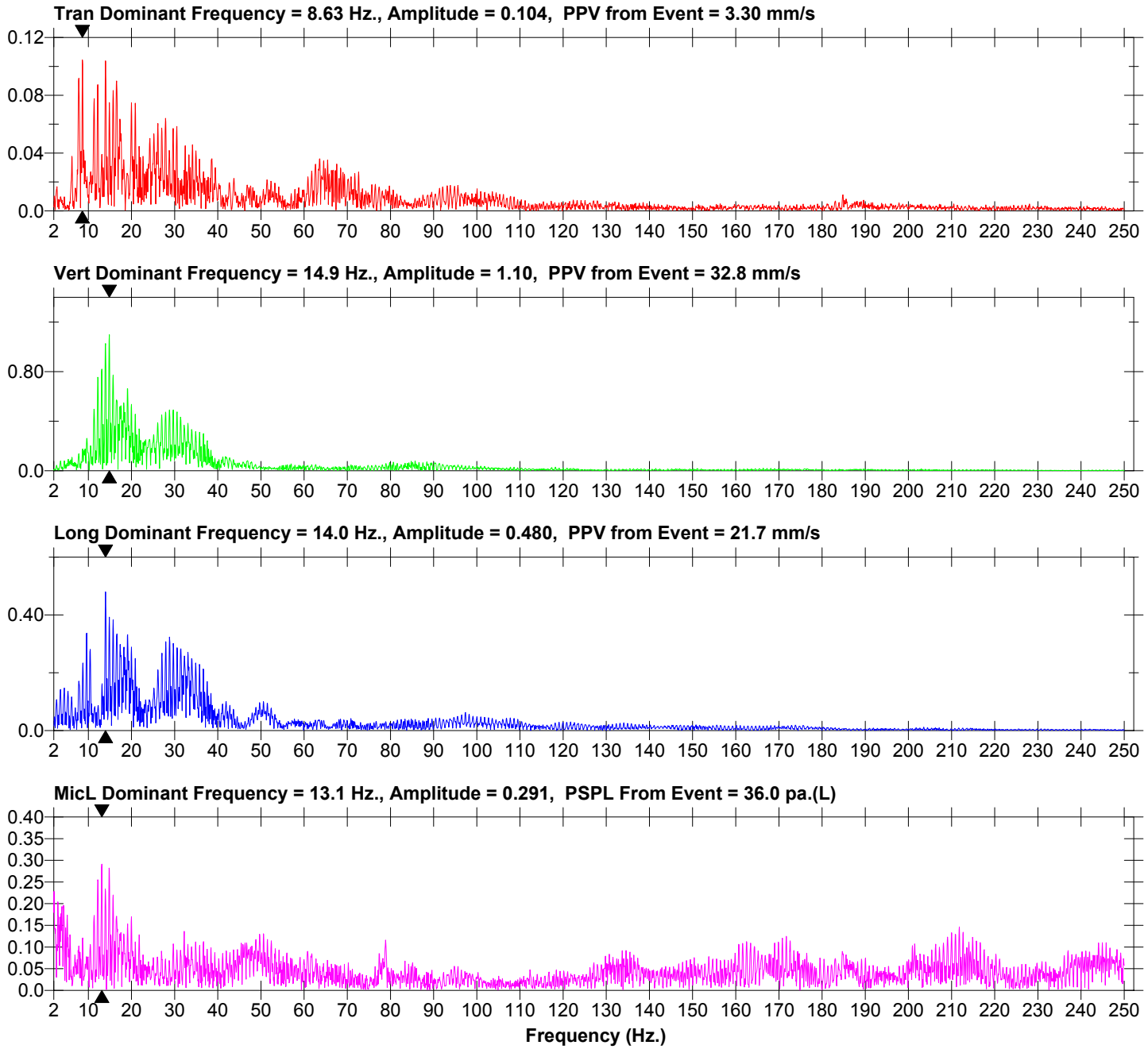

Event Report

Date/Time	Vert at 14:19:37 October 29, 2009	**Serial Number**	BE13073 V 8.12-8.0 MiniMate Plus
Trigger Source	Geo: 1.27 mm/s	**Battery Level**	6.3 Volts
Range	Geo :254 mm/s	**Calibration**	December 7, 2007 by Instantel Inc.
Record Time	5.513 sec at 1024 sps	**File Name**	O073CYFU.GP0
Job Number:	1		

Notes
Location:
Client:
User Name:
General:

Extended Notes
Combo Mode October 29, 2009 14:17:09

Post Event Notes

Microphone	Linear Weighting
PSPL	35.8 pa.(L) at 0.013 sec
ZC Freq	>100 Hz
Channel Test	Passed (Freq = 20.1 Hz Amp = 603 mv)

	Tran	Vert	Long	
PPV	3.43	32.1	21.0	mm/s
ZC Freq	23	21	23	Hz
Time (Rel. to Trig)	1.225	0.087	0.021	sec
Peak Acceleration	0.212	0.583	0.570	g
Peak Displacement	0.0198	0.197	0.100	mm
Sensorcheck	Passed	Passed	Passed	
Frequency	7.5	7.4	7.1	Hz
Overswing Ratio	3.9	3.7	4.1	

Peak Vector Sum 33.7 mm/s at 0.087 sec

USBM RI8507 And OSMRE

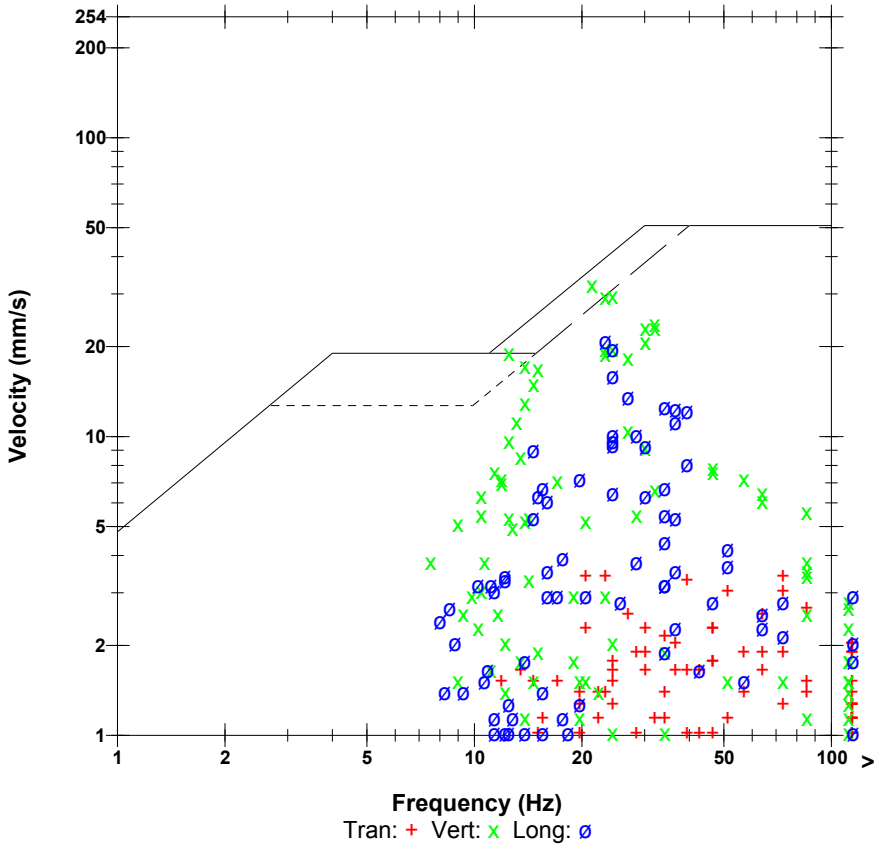

Monitor Log
Oct 29 /09 14:19:37 Oct 29 /09 14:19:43 Event recorded. (Memory Full Exit)

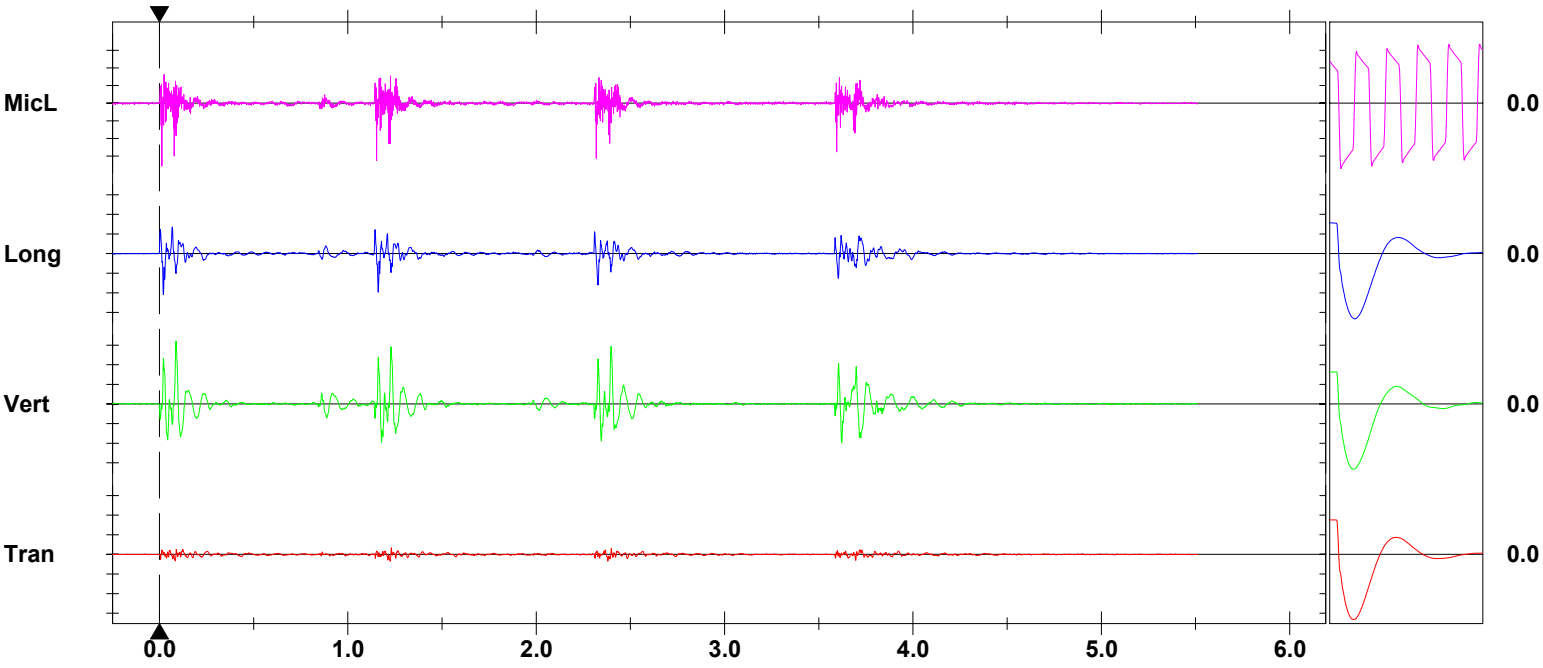

Time Scale: 0.50 sec/div **Amplitude Scale:** Geo: 10.00 mm/s/div Mic: 10.00 pa.(L)/div Sensorcheck
Trigger =

FFT Report

Date/Time	Vert at 14:19:37 October 29, 2009	**Serial Number**	BE13073 V 8.12-8.0 MiniMate Plus
Trigger Source	Geo: 1.27 mm/s	**Battery Level**	6.3 Volts
Range	Geo :254 mm/s	**Calibration**	December 7, 2007 by Instantel Inc.
Record Time	5.513 sec at 1024 sps	**File Name**	O073CYFU.GP0
Job Number:	1		

Notes
Location:
Client:
User Name:
General:

Extended Notes
Combo Mode October 29, 2009 14:17:09

Post Event Notes

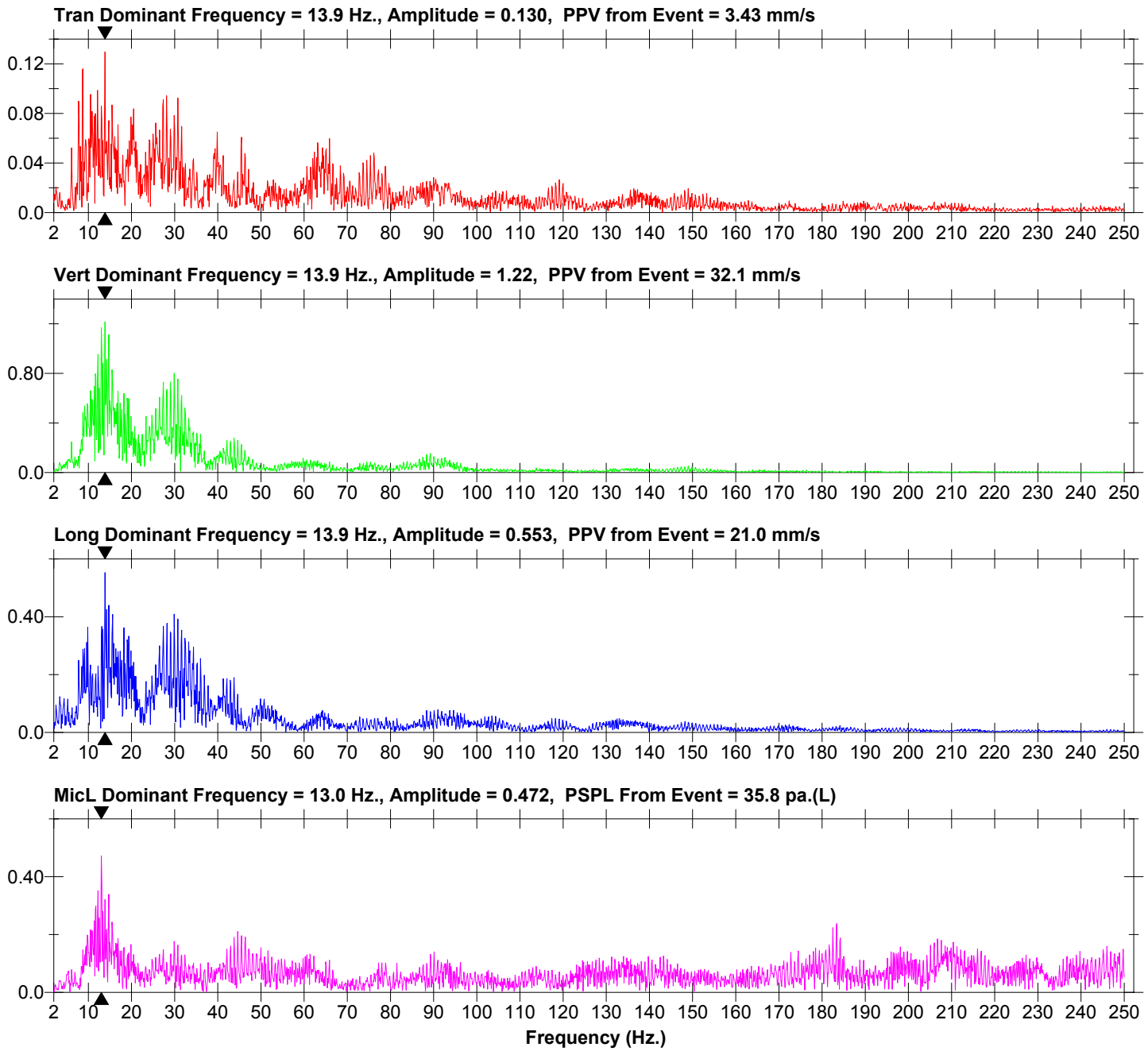

Field Vibration Data

Seismograph Unit # 3

at 50.0 feet from Test Pile #2

Event Report

Histogram Start Time	15:24:01 October 29, 2009	**Serial Number**	BE13073 V 8.12-8.0 MiniMate Plus
Histogram Finish Time	15:38:28 October 29, 2009	**Battery Level**	6.3 Volts
Number of Intervals	433 at 2 seconds	**Calibration**	December 7, 2007 by Instantel Inc.
Range	Geo :254 mm/s	**File Name**	O073CYFX.G10
Sample Rate	1024sps		
Job Number:	1		

Notes
Location:
Client:
User Name:
General:

Extended Notes

Post Event Notes

Microphone Linear Weighting
PSPL 12.0 pa.(L) on October 29, 2009 at 15:33:13
ZC Freq >100 Hz
Channel Test Passed (Freq = 20.1 Hz Amp = 638 mv)

	Tran	Vert	Long	
PPV	5.08	4.06	8.51	mm/s
ZC Freq	27	43	23	Hz
Date	Oct 29 /09	Oct 29 /09	Oct 29 /09	
Time	15:31:51	15:31:49	15:33:13	
Sensorcheck	Passed	Passed	Passed	
Frequency	7.4	7.4	7.2	Hz
Overswing Ratio	4.0	3.8	4.0	

Peak Vector Sum 9.44 mm/s on October 29, 2009 at 15:33:23

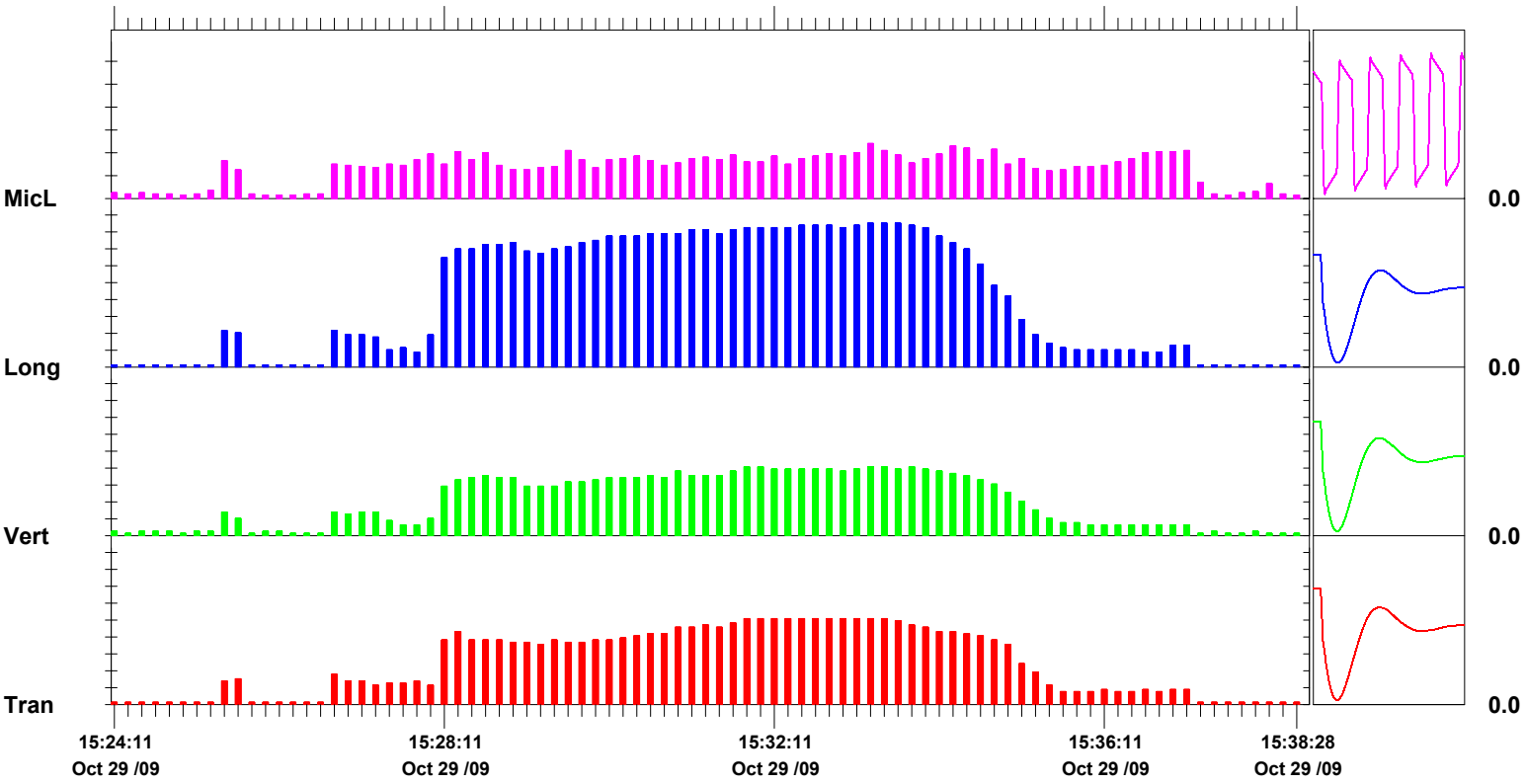

Time Scale: 10 seconds /div **Amplitude Scale:** Geo: 1.000 mm/s/div Mic: 5.00 pa.(L)/div Sensorcheck

Event Report

Date/Time	Tran at 15:25:28 October 29, 2009	**Serial Number**	BE13073 V 8.12-8.0 MiniMate Plus
Trigger Source	Geo: 1.27 mm/s	**Battery Level**	6.3 Volts
Range	Geo :254 mm/s	**Calibration**	December 7, 2007 by Instantel Inc.
Record Time	8.0 sec at 1024 sps	**File Name**	O073CYFX.IG0
Job Number:	1		

Notes
Location:
Client:
User Name:
General:

Extended Notes
Combo Mode October 29, 2009 15:24:01

Post Event Notes

Microphone Linear Weighting
PSPL 8.25 pa.(L) at 2.406 sec
ZC Freq 47 Hz
Channel Test Passed (Freq = 20.1 Hz Amp = 638 mv)

	Tran	Vert	Long	
PPV	1.52	1.40	2.16	mm/s
ZC Freq	57	18	19	Hz
Time (Rel. to Trig)	3.737	2.479	1.272	sec
Peak Acceleration	0.0530	0.0398	0.0530	g
Peak Displacement	0.00955	0.0101	0.0159	mm
Sensorcheck	Passed	Passed	Passed	
Frequency	7.4	7.4	7.2	Hz
Overswing Ratio	4.0	3.8	4.0	

Peak Vector Sum 2.23 mm/s at 1.272 sec

USBM RI8507 And OSMRE

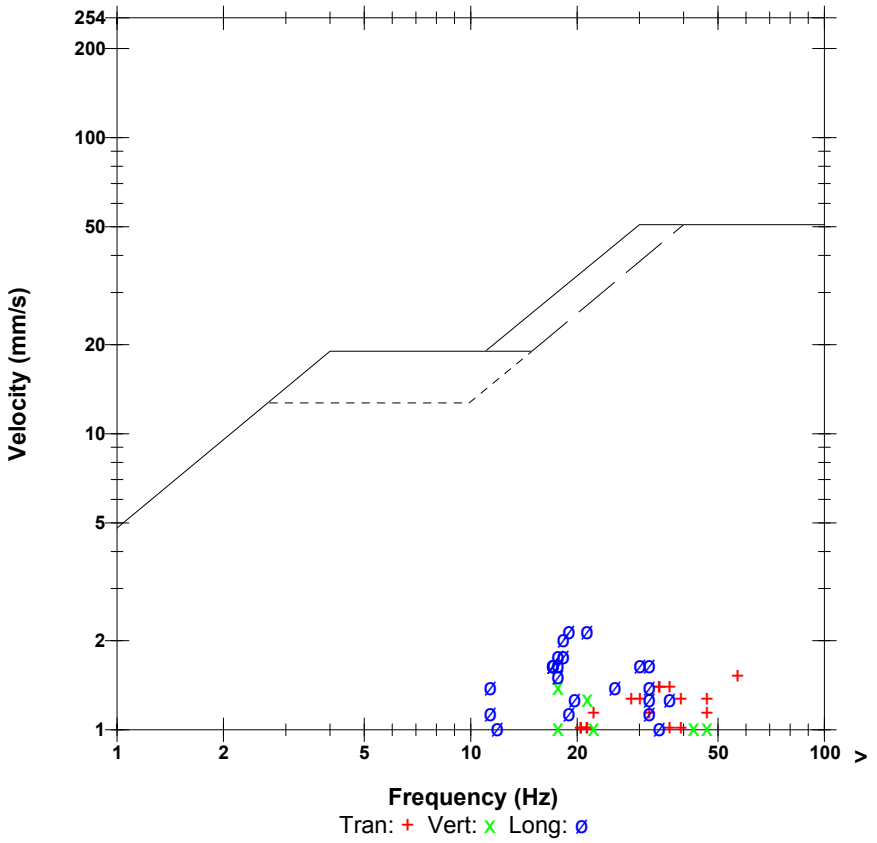

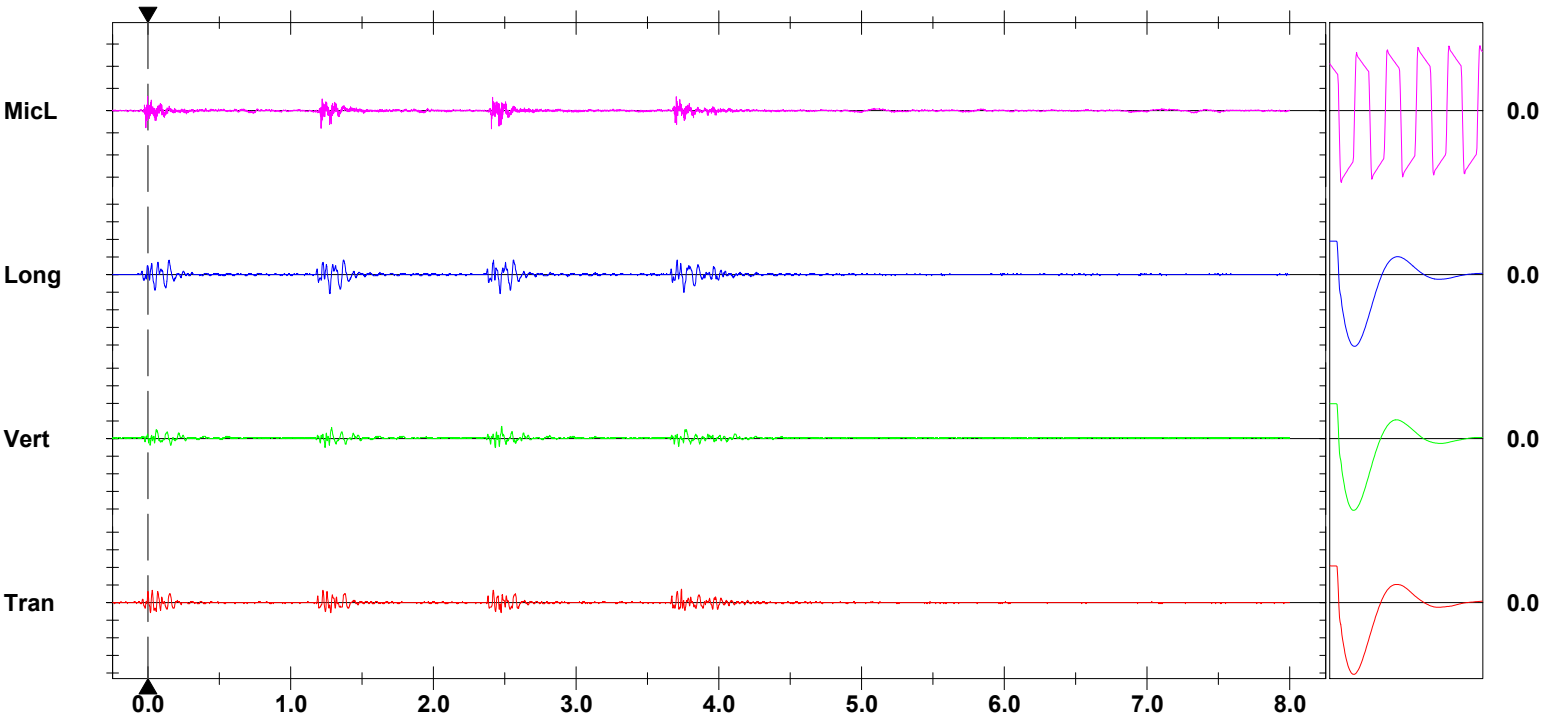

Time Scale: 0.50 sec/div **Amplitude Scale:** Geo: 2.00 mm/s/div Mic: 10.00 pa.(L)/div Sensorcheck
Trigger =

FFT Report

Date/Time	Tran at 15:25:28 October 29, 2009	**Serial Number**	BE13073 V 8.12-8.0 MiniMate Plus
Trigger Source	Geo: 1.27 mm/s	**Battery Level**	6.3 Volts
Range	Geo :254 mm/s	**Calibration**	December 7, 2007 by Instantel Inc.
Record Time	8.0 sec at 1024 sps	**File Name**	O073CYFX.IG0
Job Number:	1		

Notes
Location:
Client:
User Name:
General:

Extended Notes
Combo Mode October 29, 2009 15:24:01

Post Event Notes

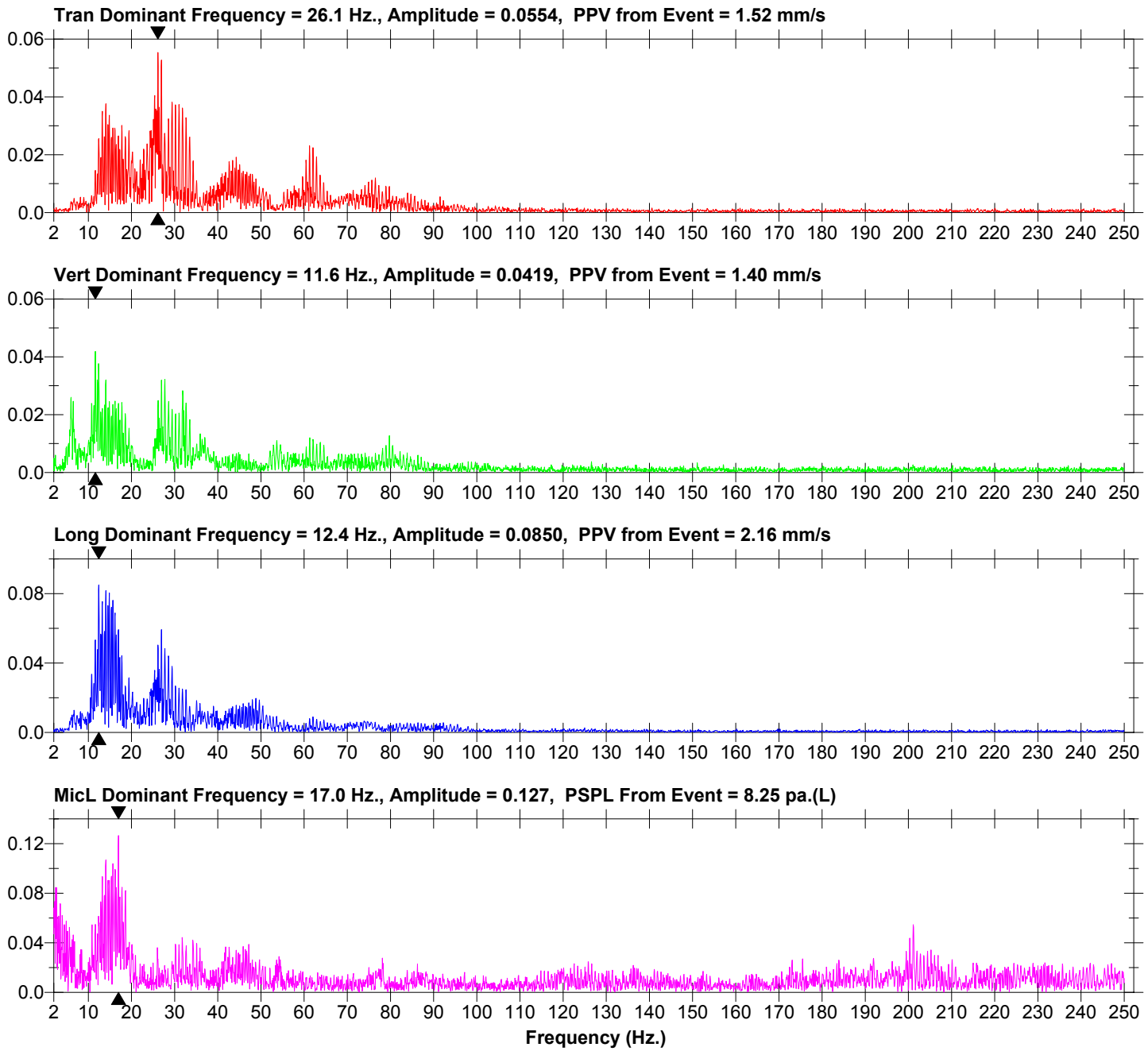

Event Report

Date/Time	Long at 15:26:42 October 29, 2009	**Serial Number**	BE13073 V 8.12-8.0 MiniMate Plus
Trigger Source	Geo: 1.27 mm/s	**Battery Level**	6.3 Volts
Range	Geo :254 mm/s	**Calibration**	December 7, 2007 by Instantel Inc.
Record Time	8.0 sec at 1024 sps	**File Name**	O073CYFX.KI0
Job Number:	1		

Notes
Location:
Client:
User Name:
General:

Extended Notes
Combo Mode October 29, 2009 15:24:01

Post Event Notes

Microphone Linear Weighting
PSPL 7.50 pa.(L) at 2.607 sec
ZC Freq >100 Hz
Channel Test Passed (Freq = 20.1 Hz Amp = 638 mv)

	Tran	Vert	Long	
PPV	1.78	1.40	2.16	mm/s
ZC Freq	51	16	24	Hz
Time (Rel. to Trig)	3.847	1.335	1.324	sec
Peak Acceleration	0.0530	0.0398	0.0398	g
Peak Displacement	0.00881	0.0111	0.0163	mm
Sensorcheck	Passed	Passed	Passed	
Frequency	7.4	7.4	7.2	Hz
Overswing Ratio	4.0	3.8	4.0	

Peak Vector Sum 2.35 mm/s at 3.817 sec

USBM RI8507 And OSMRE

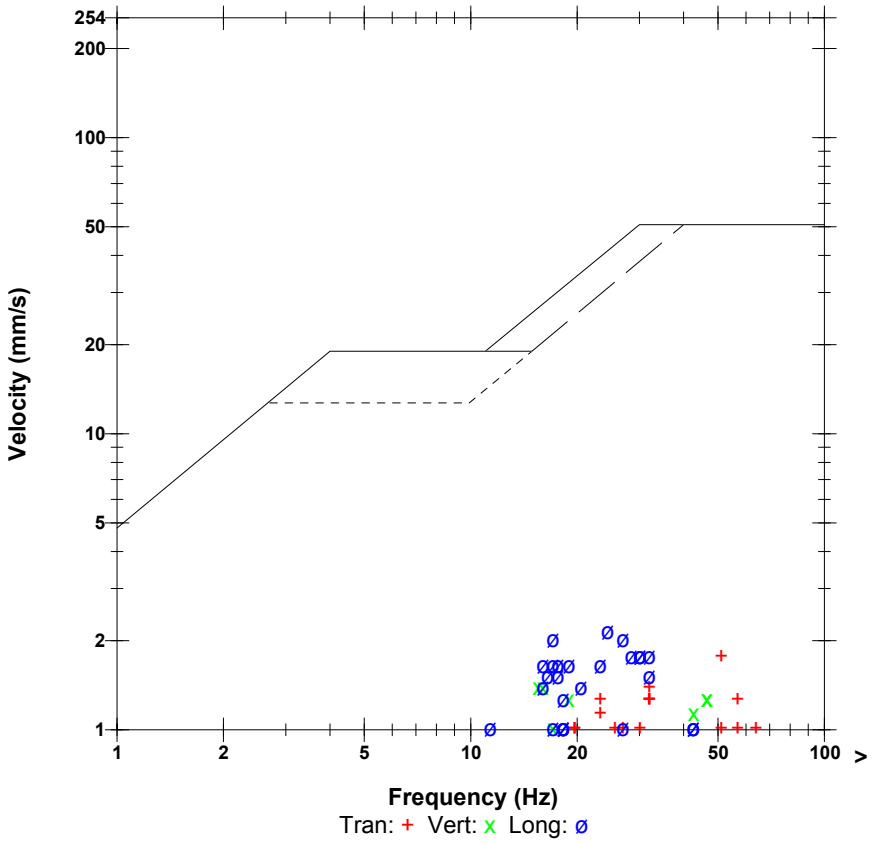

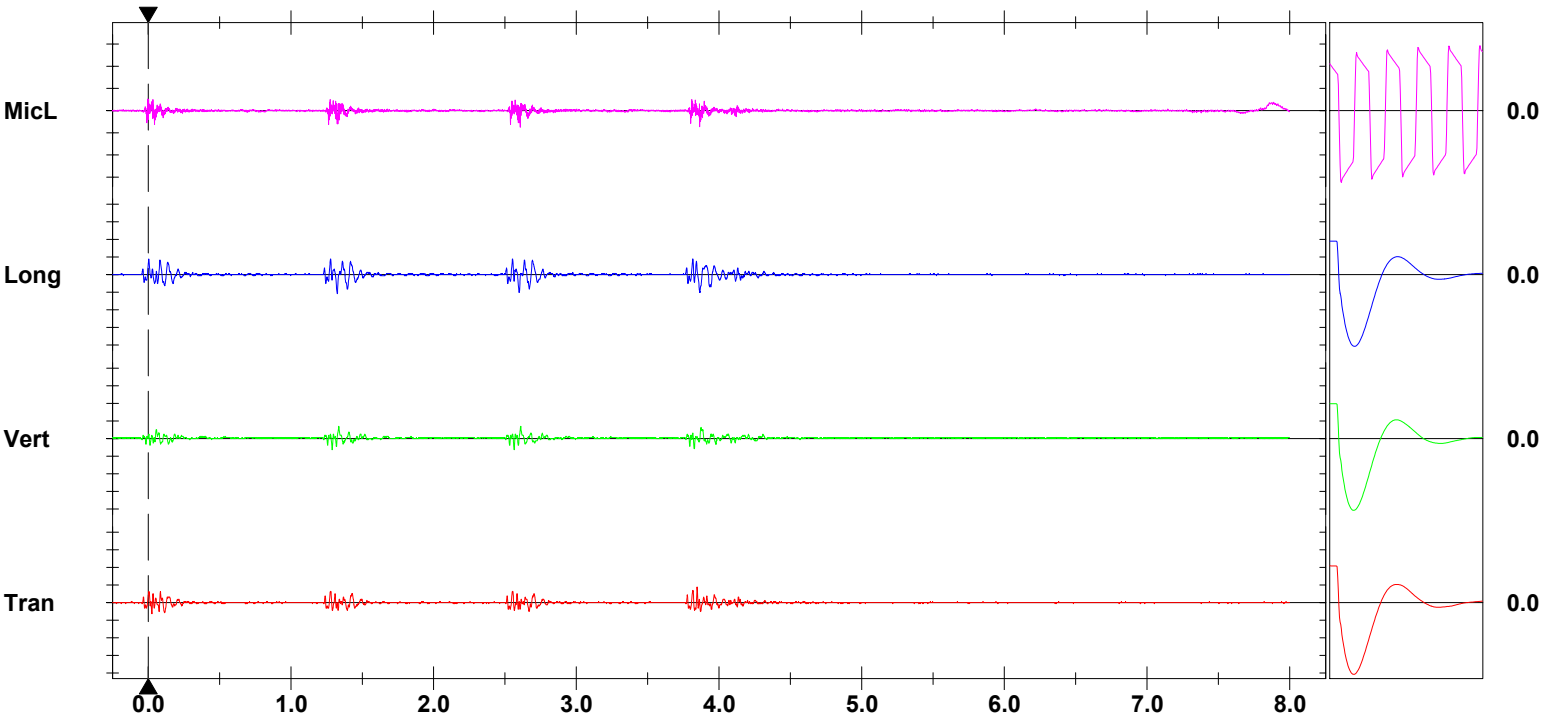

Time Scale: 0.50 sec/div **Amplitude Scale:** Geo: 2.00 mm/s/div Mic: 10.00 pa.(L)/div Sensorcheck
Trigger =

FFT Report

Date/Time	Long at 15:26:42 October 29, 2009	**Serial Number**	BE13073 V 8.12-8.0 MiniMate Plus
Trigger Source	Geo: 1.27 mm/s	**Battery Level**	6.3 Volts
Range	Geo :254 mm/s	**Calibration**	December 7, 2007 by Instantel Inc.
Record Time	8.0 sec at 1024 sps	**File Name**	O073CYFX.KI0
Job Number:	1		

Notes
Location:
Client:
User Name:
General:

Extended Notes
Combo Mode October 29, 2009 15:24:01

Post Event Notes

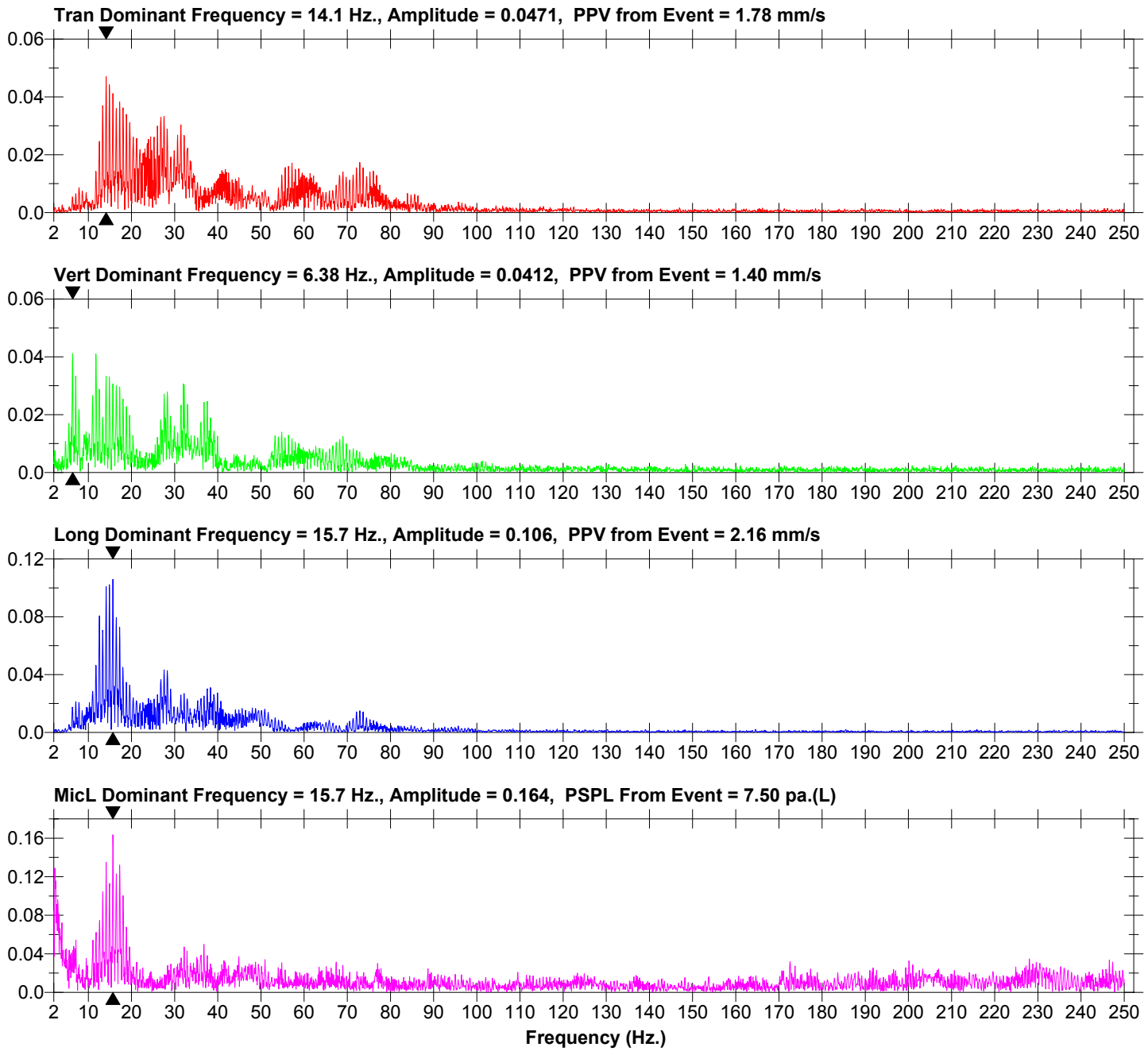

Event Report

Date/Time	Long at 15:26:58 October 29, 2009	**Serial Number**	BE13073 V 8.12-8.0 MiniMate Plus
Trigger Source	Geo: 1.27 mm/s	**Battery Level**	6.3 Volts
Range	Geo :254 mm/s	**Calibration**	December 7, 2007 by Instantel Inc.
Record Time	8.0 sec at 1024 sps	**File Name**	O073CYFX.KY0
Job Number:	1		

Notes
Location:
Client:
User Name:
General:

Extended Notes
Combo Mode October 29, 2009 15:24:01

Post Event Notes

Microphone Linear Weighting
PSPL 7.25 pa.(L) at 1.329 sec
ZC Freq 73 Hz
Channel Test Passed (Freq = 20.1 Hz Amp = 638 mv)

	Tran	Vert	Long	
PPV	1.40	1.27	1.90	mm/s
ZC Freq	32	47	30	Hz
Time (Rel. to Trig)	1.284	1.293	0.005	sec
Peak Acceleration	0.0530	0.0398	0.0398	g
Peak Displacement	0.00893	0.0105	0.0136	mm
Sensorcheck	Passed	Passed	Passed	
Frequency	7.4	7.4	7.2	Hz
Overswing Ratio	4.0	3.8	4.0	

Peak Vector Sum 2.39 mm/s at 1.284 sec

USBM RI8507 And OSMRE

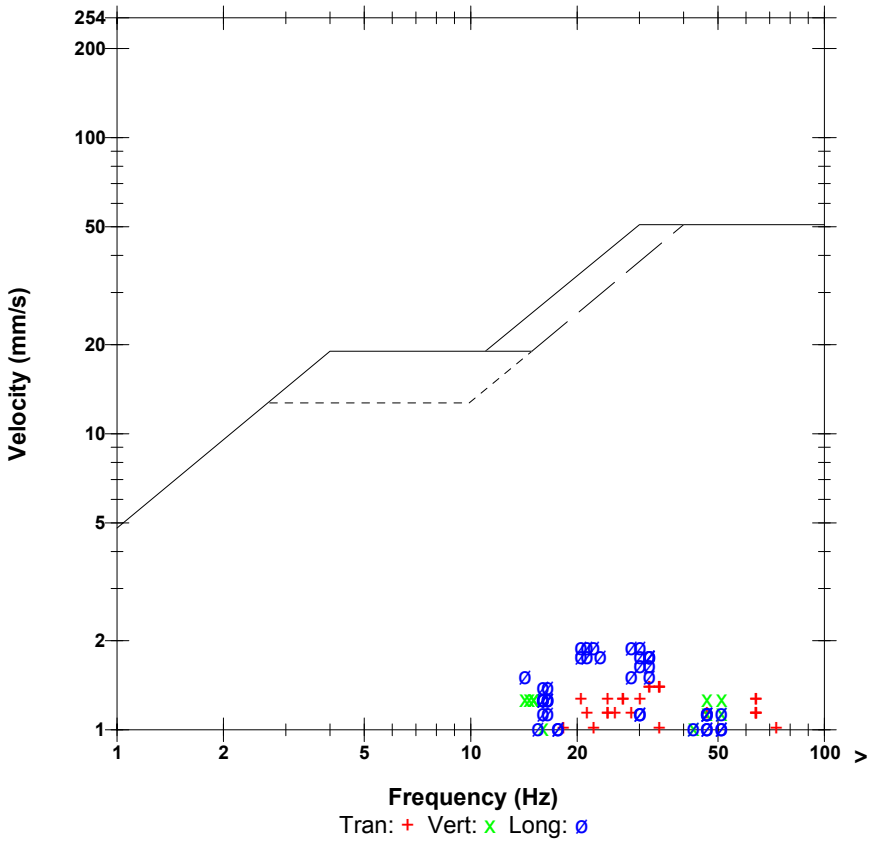

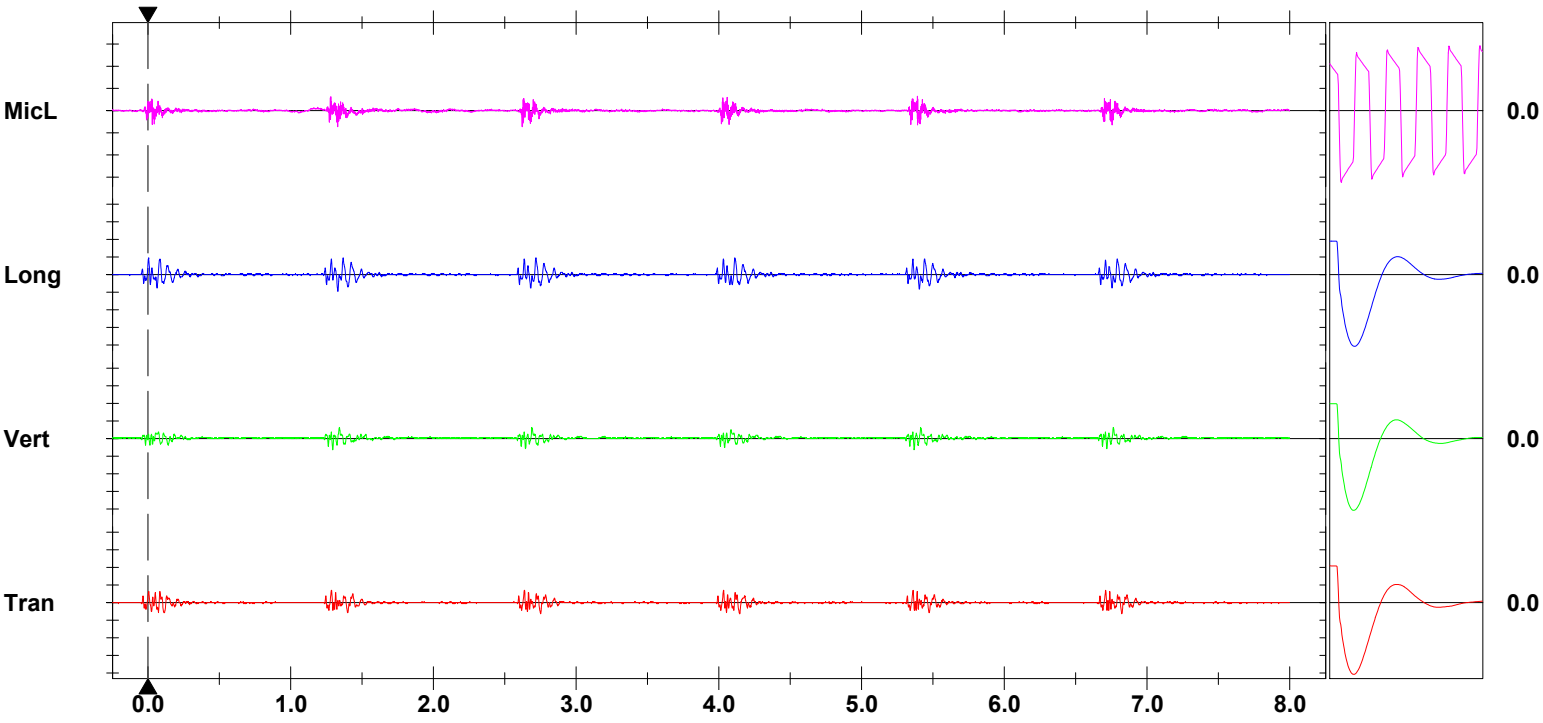

Time Scale: 0.50 sec/div **Amplitude Scale:** Geo: 2.00 mm/s/div Mic: 10.00 pa.(L)/div Sensorcheck
Trigger =

FFT Report

Date/Time	Long at 15:26:58 October 29, 2009	**Serial Number**	BE13073 V 8.12-8.0 MiniMate Plus
Trigger Source	Geo: 1.27 mm/s	**Battery Level**	6.3 Volts
Range	Geo :254 mm/s	**Calibration**	December 7, 2007 by Instantel Inc.
Record Time	8.0 sec at 1024 sps	**File Name**	O073CYFX.KY0
Job Number:	1		

Notes
Location:
Client:
User Name:
General:

Extended Notes
Combo Mode October 29, 2009 15:24:01

Post Event Notes

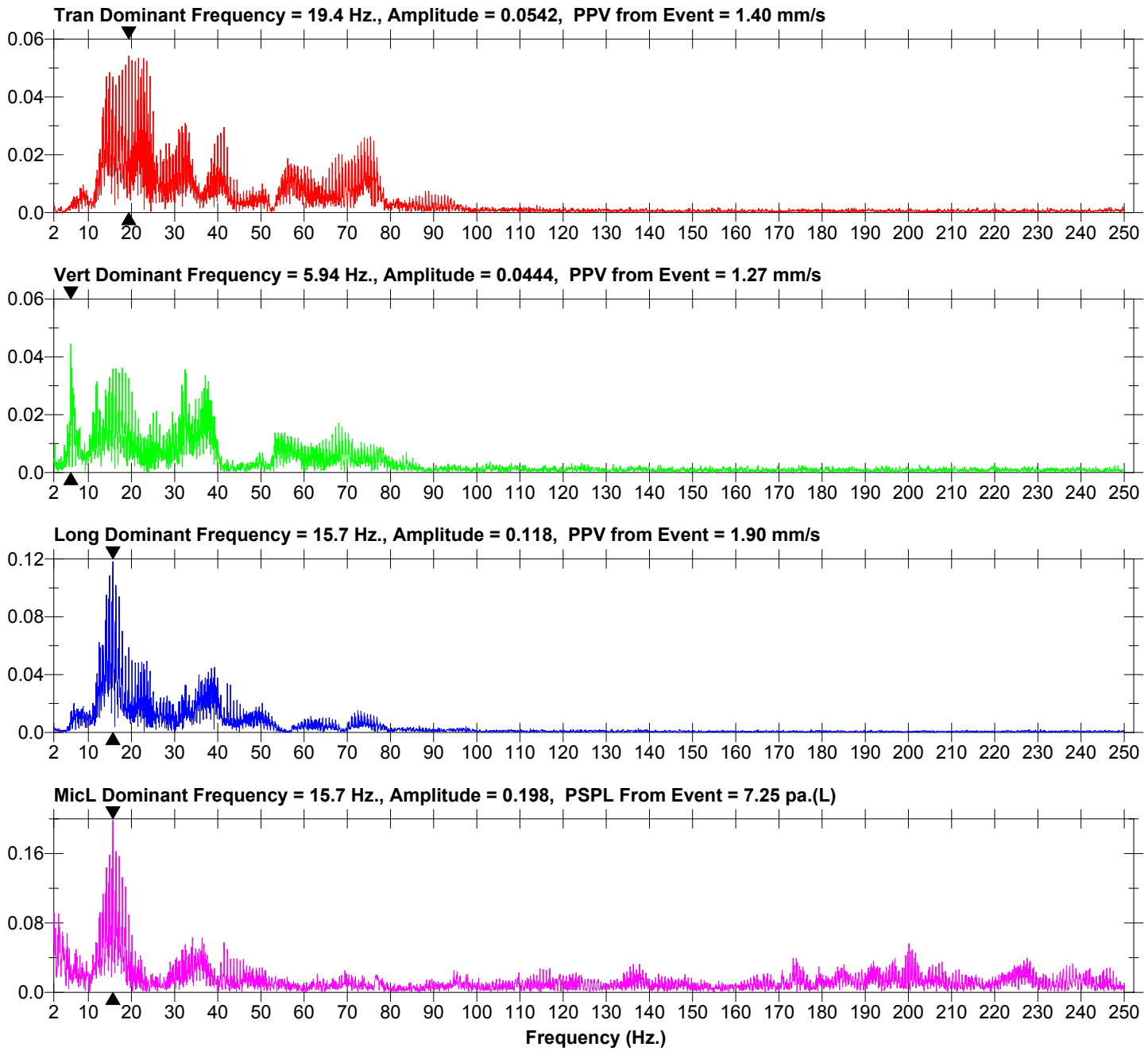

Event Report

Date/Time	Long at 15:27:07 October 29, 2009	**Serial Number**	BE13073 V 8.12-8.0 MiniMate Plus
Trigger Source	Geo: 1.27 mm/s	**Battery Level**	6.3 Volts
Range	Geo :254 mm/s	**Calibration**	December 7, 2007 by Instantel Inc.
Record Time	2.697 sec at 1024 sps	**File Name**	O073CYFX.L70
Job Number:	1		

Notes
Location:
Client:
User Name:
General:

Extended Notes
Combo Mode October 29, 2009 15:24:01

Post Event Notes

Microphone Linear Weighting
PSPL 7.00 pa.(L) at 1.322 sec
ZC Freq >100 Hz
Channel Test Passed (Freq = 20.1 Hz Amp = 638 mv)

	Tran	Vert	Long	
PPV	1.27	1.40	1.78	mm/s
ZC Freq	32	43	21	Hz
Time (Rel. to Trig)	0.003	1.285	0.084	sec
Peak Acceleration	0.0530	0.0530	0.0398	g
Peak Displacement	0.00800	0.00961	0.0133	mm
Sensorcheck	Passed	Passed	Passed	
Frequency	7.4	7.4	7.2	Hz
Overswing Ratio	4.0	3.8	4.0	

Peak Vector Sum 2.22 mm/s at 0.003 sec

USBM RI8507 And OSMRE

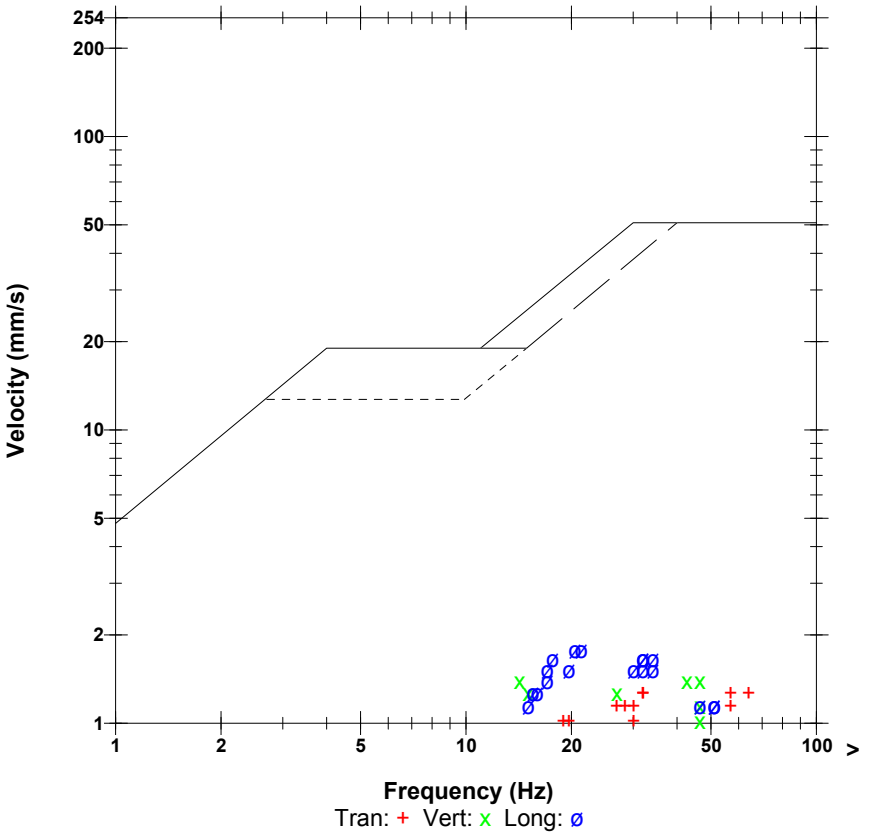

Monitor Log
Oct 29 /09 15:27:07 Oct 29 /09 15:27:10 Event recorded. (Memory Full Exit)

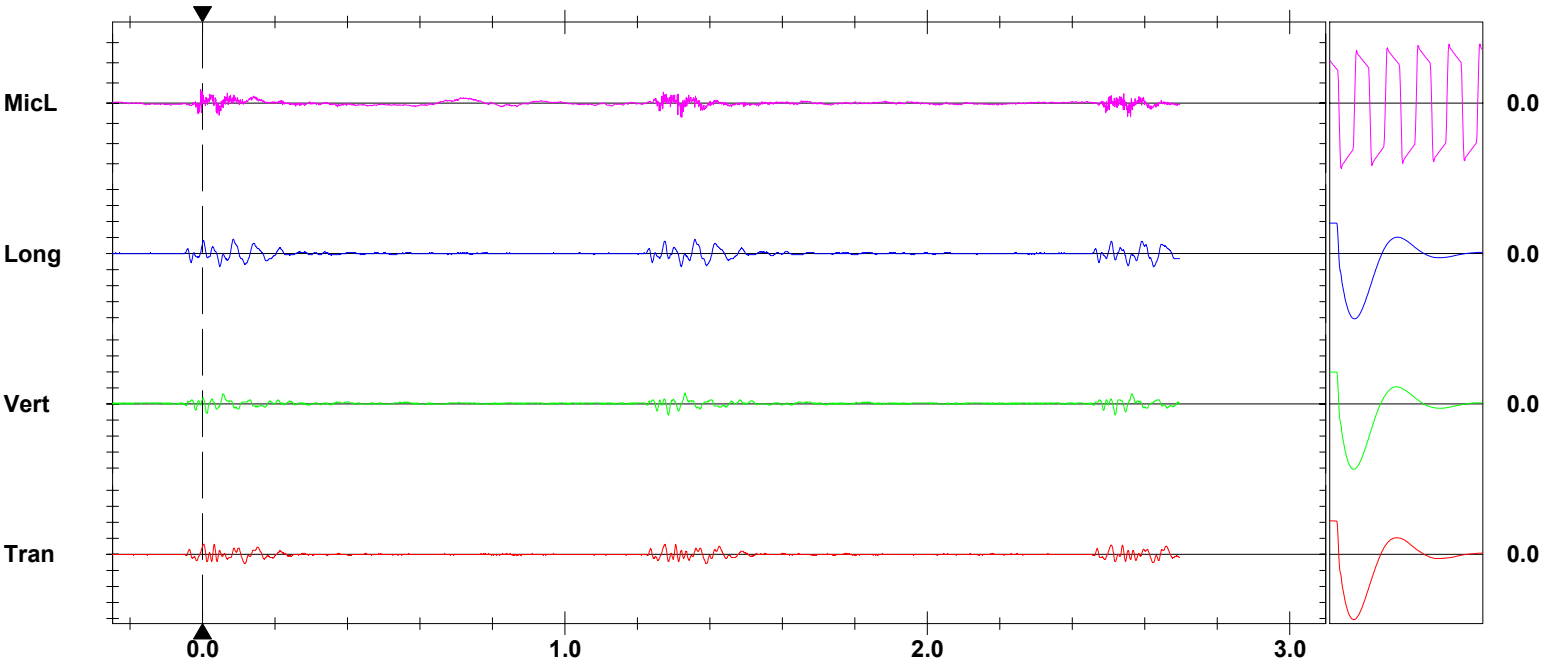

Time Scale: 0.20 sec/div **Amplitude Scale:** Geo: 2.00 mm/s/div Mic: 10.00 pa.(L)/div Sensorcheck
Trigger =

FFT Report

Date/Time	Long at 15:27:07 October 29, 2009	**Serial Number**	BE13073 V 8.12-8.0 MiniMate Plus
Trigger Source	Geo: 1.27 mm/s	**Battery Level**	6.3 Volts
Range	Geo :254 mm/s	**Calibration**	December 7, 2007 by Instantel Inc.
Record Time	2.697 sec at 1024 sps	**File Name**	O073CYFX.L70
Job Number:	1		

Notes
Location:
Client:
User Name:
General:

Extended Notes
Combo Mode October 29, 2009 15:24:01

Post Event Notes

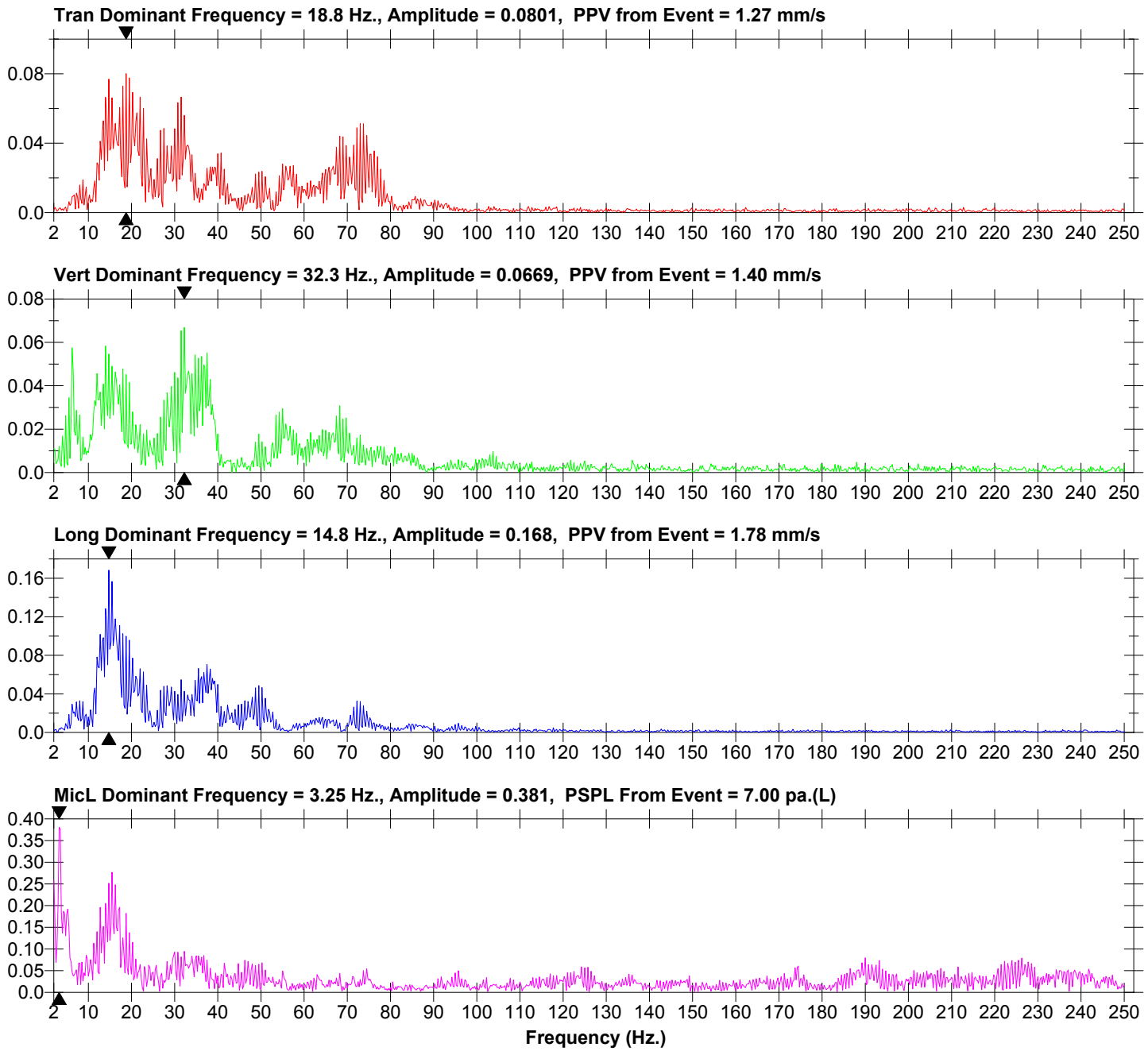

Field Vibration Data

Seismograph Unit # 3

at 9.7 feet from Test Pile #1

Non Driving Event

Event Report

Histogram Start Time	10:31:13 December 21, 2009	**Serial Number**	BE13073 V 8.12-8.0 MiniMate Plus
Histogram Finish Time	11:03:44 December 21, 2009	**Battery Level**	6.2 Volts
Number of Intervals	975 at 2 seconds	**Calibration**	December 7, 2007 by Instantel Inc.
Range	Geo :254 mm/s	**File Name**	O073D15P.810
Sample Rate	1024sps		
Job Number:	1		

Notes
Location:
Client:
User Name:
General:

Extended Notes

Post Event Notes

Microphone Linear Weighting
PSPL 5.25 pa.(L) on December 21, 2009 at 10:56:55
ZC Freq 2.9 Hz
Channel Test Passed (Freq = 20.1 Hz Amp = 690 mv)

	Tran	Vert	Long	
PPV	0.127	0.254	0.127	mm/s
ZC Freq	>100	>100	>100	Hz
Date	Dec 21 /09	Dec 21 /09	Dec 21 /09	
Time	10:31:15	10:31:17	10:31:15	
Sensorcheck	Check	Check	Check	
Frequency	1024.0	1024.0	1024.0	Hz
Overswing Ratio	0.0	0.0	0.0	

Peak Vector Sum 0.284 mm/s on December 21, 2009 at 10:36:39

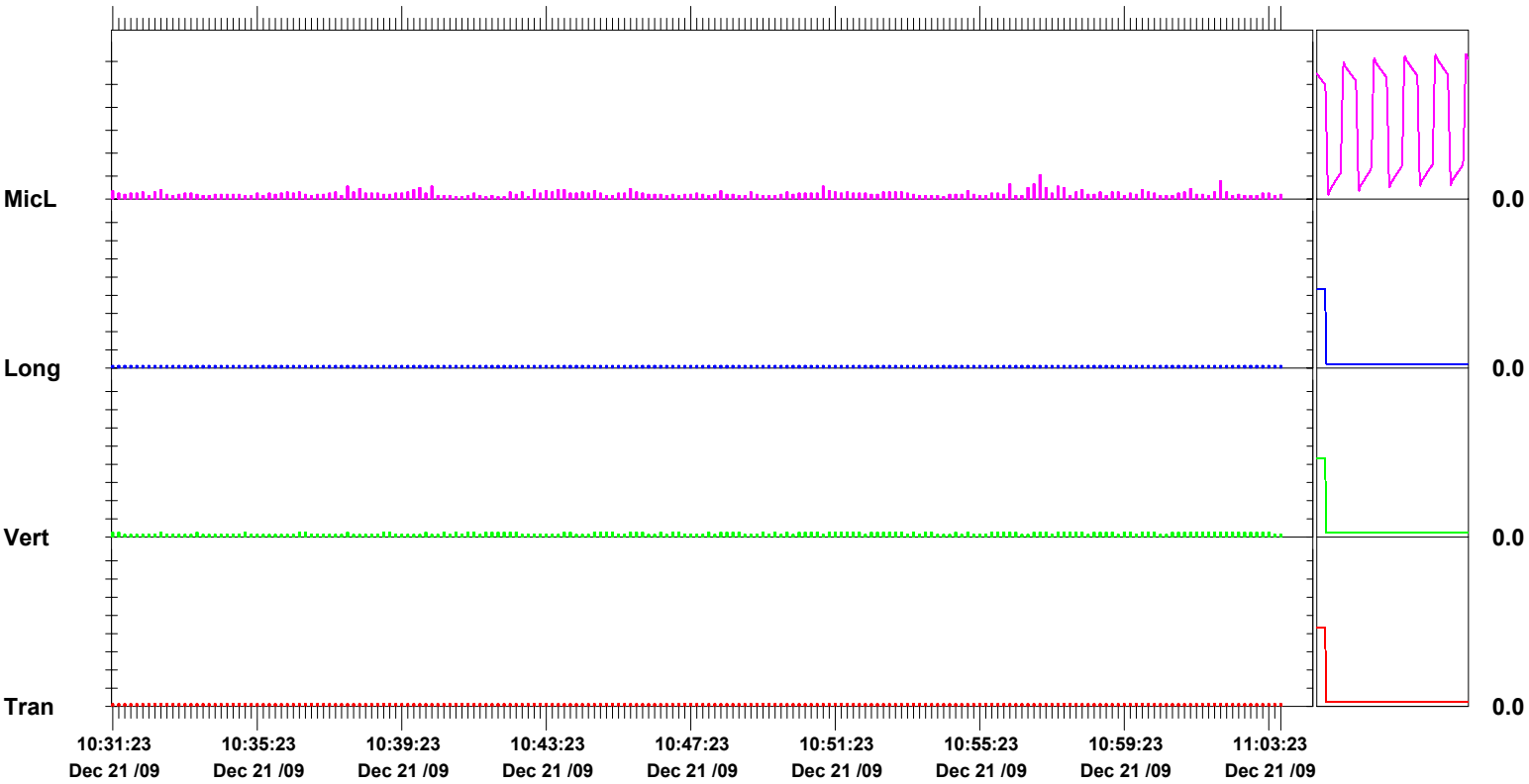

Time Scale: 10 seconds /div **Amplitude Scale:** Geo: 1.000 mm/s/div Mic: 5.00 pa.(L)/div Sensorcheck

Event Report

Histogram Start Time	11:29:08 December 21, 2009	**Serial Number**	BE13073 V 8.12-8.0 MiniMate Plus
Histogram Finish Time	11:54:14 December 21, 2009	**Battery Level**	6.2 Volts
Number of Intervals	753 at 2 seconds	**Calibration**	December 7, 2007 by Instantel Inc.
Range	Geo :254 mm/s	**File Name**	O073D15R.WK0
Sample Rate	1024sps		
Job Number:	1		

Notes
Location:
Client:
User Name:
General:

Extended Notes

Post Event Notes

Microphone Linear Weighting
PSPL 2.75 pa.(L) on December 21, 2009 at 11:34:12
ZC Freq 2.7 Hz
Channel Test Passed (Freq = 20.1 Hz Amp = 762 mv)

	Tran	Vert	Long	
PPV	0.127	0.254	0.127	mm/s
ZC Freq	>100	>100	>100	Hz
Date	Dec 21 /09	Dec 21 /09	Dec 21 /09	
Time	11:29:10	11:29:10	11:29:10	
Sensorcheck	Check	Check	Check	
Frequency	1024.0	1024.0	1024.0	Hz
Overswing Ratio	0.0	0.0	0.0	

Peak Vector Sum 0.311 mm/s on December 21, 2009 at 11:29:50

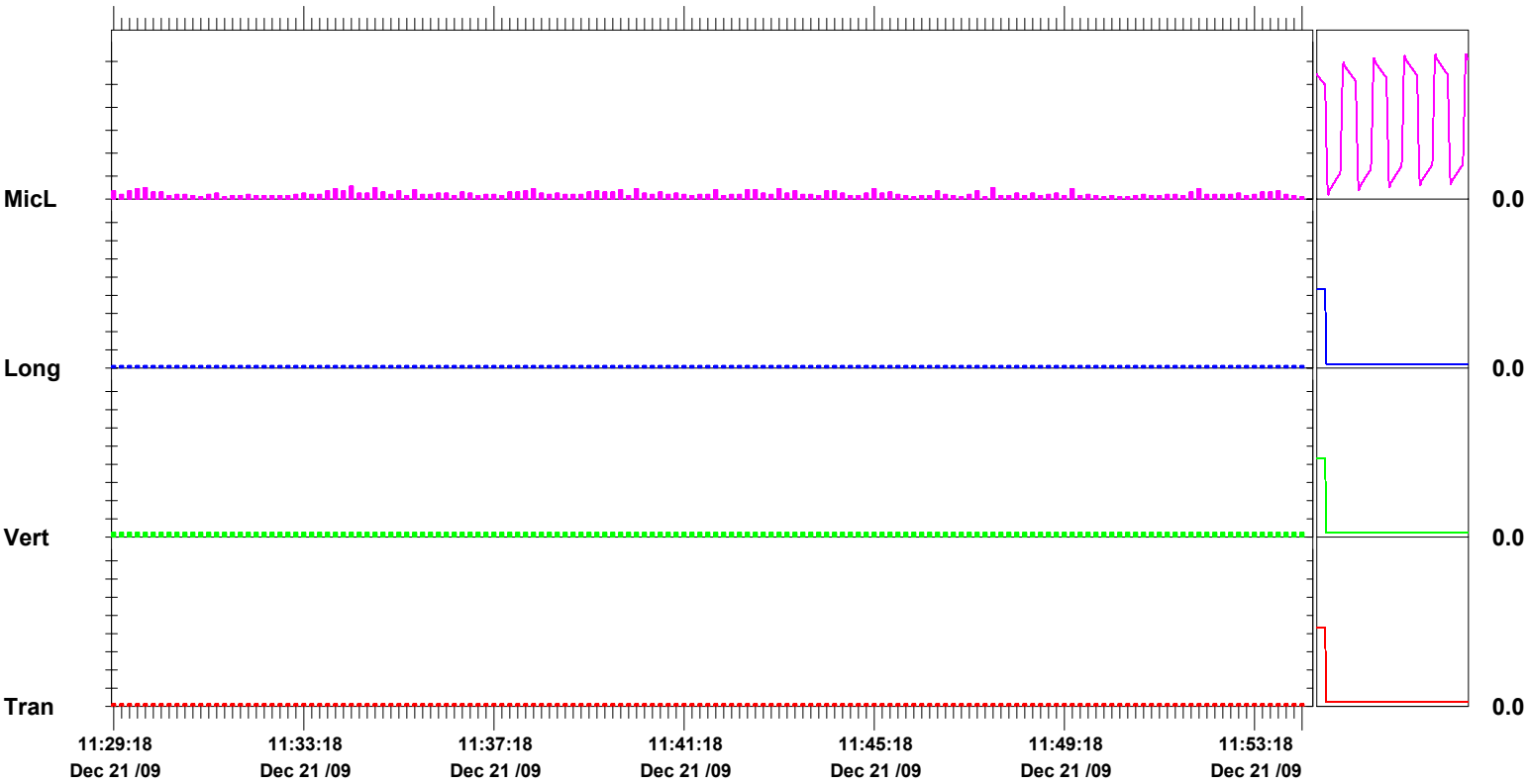

Time Scale: 10 seconds /div **Amplitude Scale:** Geo: 1.000 mm/s/div Mic: 5.00 pa.(L)/div Sensorcheck

Field Vibration Data

Seismograph Unit # 4

at 9.1 feet from Test Pile #1

Event Report

Histogram Start Time	14:17:31 October 29, 2009	**Serial Number**	BE13056 V 8.12-8.0 MiniMate Plus
Histogram Finish Time	14:26:06 October 29, 2009	**Battery Level**	6.3 Volts
Number of Intervals	257 at 2 seconds	**Calibration**	December 7, 2007 by Instantel Inc.
Range	Geo :254 mm/s	**File Name**	O056CYFU.D70
Sample Rate	1024sps		
Job Number:	1		

Notes
Location:
Client:
User Name:
General:

Extended Notes

Post Event Notes

Microphone Linear Weighting
PSPL 39.0 pa.(L) on October 29, 2009 at 14:22:47
ZC Freq >100 Hz
Channel Test Passed (Freq = 20.1 Hz Amp = 591 mv)

	Tran	Vert	Long	
PPV	12.6	57.0	24.8	mm/s
ZC Freq	12	20	16	Hz
Date	Oct 29 /09	Oct 29 /09	Oct 29 /09	
Time	14:18:09	14:18:09	14:18:09	
Sensorcheck	Passed	Passed	Passed	
Frequency	7.4	7.4	7.4	Hz
Overswing Ratio	3.7	3.7	4.2	

Peak Vector Sum 59.1 mm/s on October 29, 2009 at 14:18:09

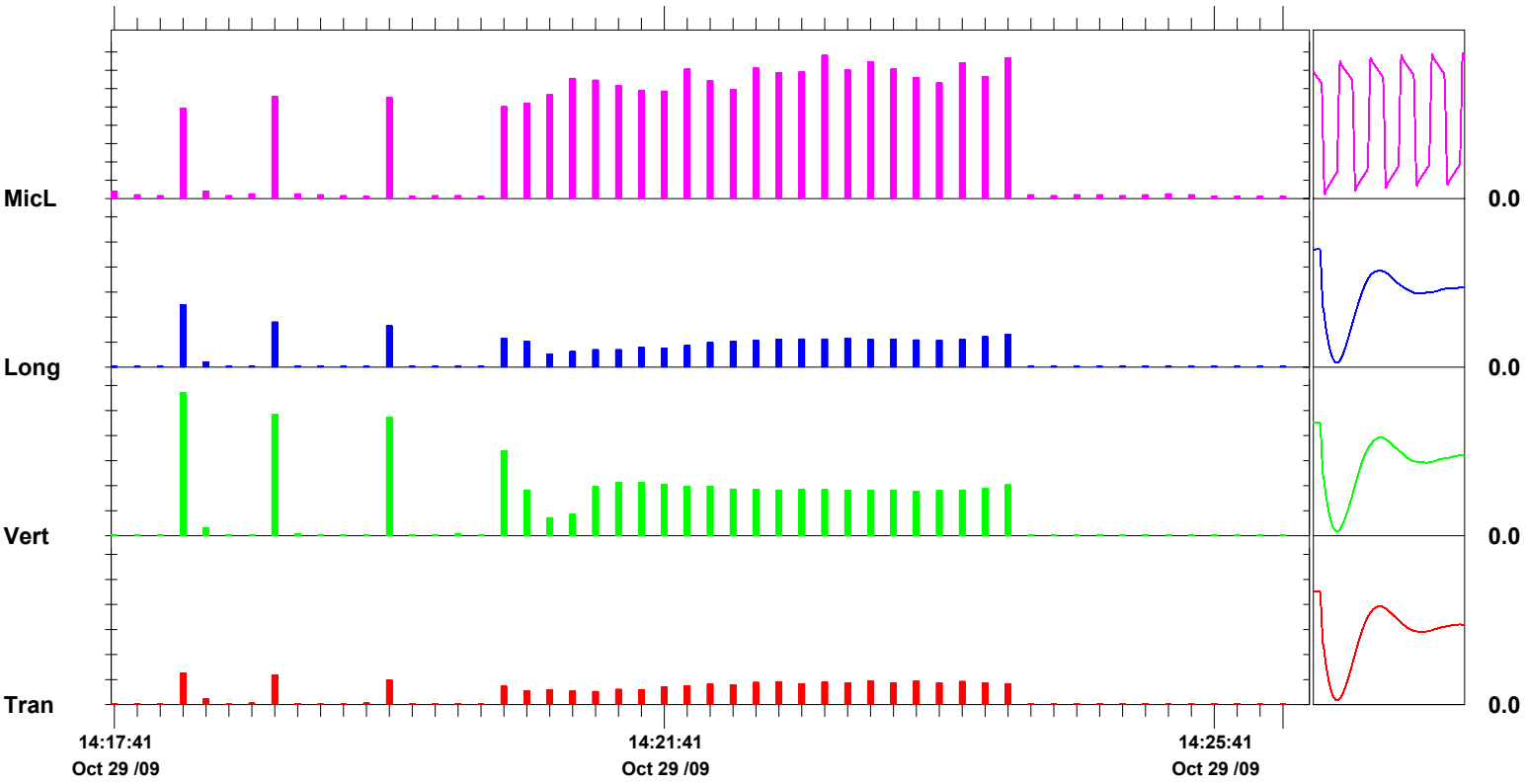

Time Scale: 10 seconds /div **Amplitude Scale:** Geo: 10.00 mm/s/div Mic: 5.00 pa.(L)/div Sensorcheck

Event Report

Date/Time Long at 14:18:07 October 29, 2009
Trigger Source Geo: 1.27 mm/s
Range Geo :254 mm/s
Record Time 8.0 sec at 1024 sps
Job Number: 1

Serial Number BE13056 V 8.12-8.0 MiniMate Plus
Battery Level 6.3 Volts
Calibration December 7, 2007 by Instantel Inc.
File Name O056CYFU.E70

Notes
Location:
Client:
User Name:
General:

Extended Notes
Combo Mode October 29, 2009 14:17:30

Post Event Notes

Microphone Linear Weighting
PSPL 24.5 pa.(L) at 0.010 sec
ZC Freq >100 Hz
Channel Test Passed (Freq = 20.1 Hz Amp = 591 mv)

	Tran	Vert	Long	
PPV	12.6	57.0	24.8	mm/s
ZC Freq	12	20	16	Hz
Time (Rel. to Trig)	0.094	0.078	1.152	sec
Peak Acceleration	0.305	0.676	0.477	g
Peak Displacement	0.114	0.443	0.195	mm
Sensorcheck	Passed	Passed	Passed	
Frequency	7.4	7.4	7.4	Hz
Overswing Ratio	3.7	3.7	4.2	

Peak Vector Sum 59.1 mm/s at 0.078 sec

USBM RI8507 And OSMRE

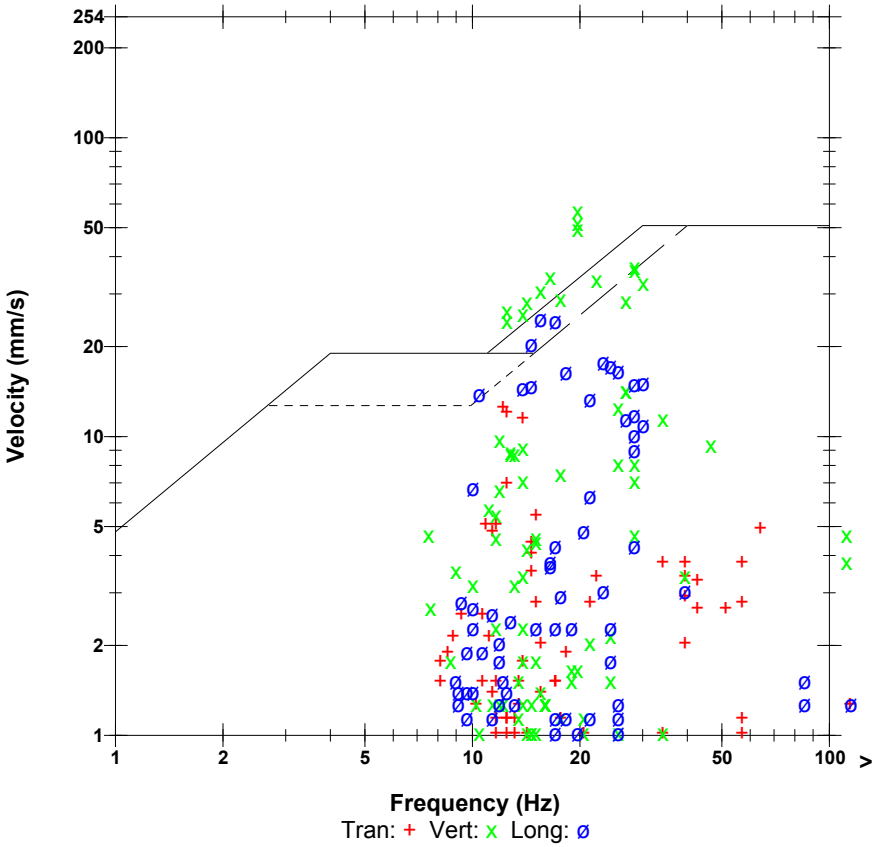

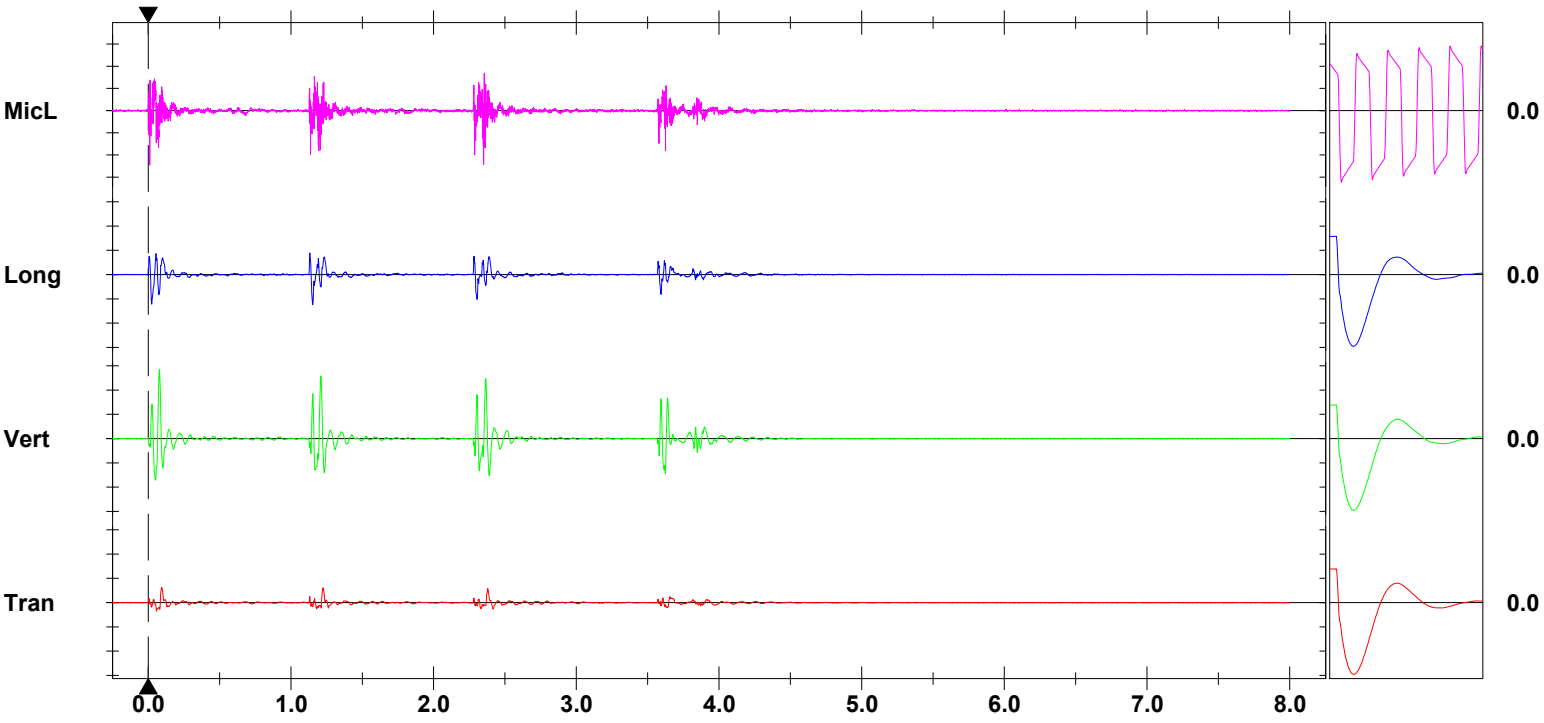

Time Scale: 0.50 sec/div **Amplitude Scale:** Geo: 20.0 mm/s/div Mic: 10.00 pa.(L)/div Sensorcheck
Trigger =

Event Report

Date/Time	Vert at 14:18:47 October 29, 2009	**Serial Number**	BE13056 V 8.12-8.0 MiniMate Plus
Trigger Source	Geo: 1.27 mm/s	**Battery Level**	6.3 Volts
Range	Geo :254 mm/s	**Calibration**	December 7, 2007 by Instantel Inc.
Record Time	8.0 sec at 1024 sps	**File Name**	O056CYFU.FB0
Job Number:	1		

Notes
Location:
Client:
User Name:
General:

Extended Notes
Combo Mode October 29, 2009 14:17:30

Post Event Notes

Microphone Linear Weighting
PSPL 27.8 pa.(L) at 1.216 sec
ZC Freq 85 Hz
Channel Test Passed (Freq = 20.1 Hz Amp = 591 mv)

	Tran	Vert	Long	
PPV	11.8	48.4	17.9	mm/s
ZC Freq	14	20	18	Hz
Time (Rel. to Trig)	0.102	1.229	0.026	sec
Peak Acceleration	0.252	0.716	0.451	g
Peak Displacement	0.0969	0.368	0.140	mm
Sensorcheck	Passed	Passed	Passed	
Frequency	7.4	7.4	7.4	Hz
Overswing Ratio	3.7	3.7	4.2	

Peak Vector Sum 49.3 mm/s at 1.229 sec

USBM RI8507 And OSMRE

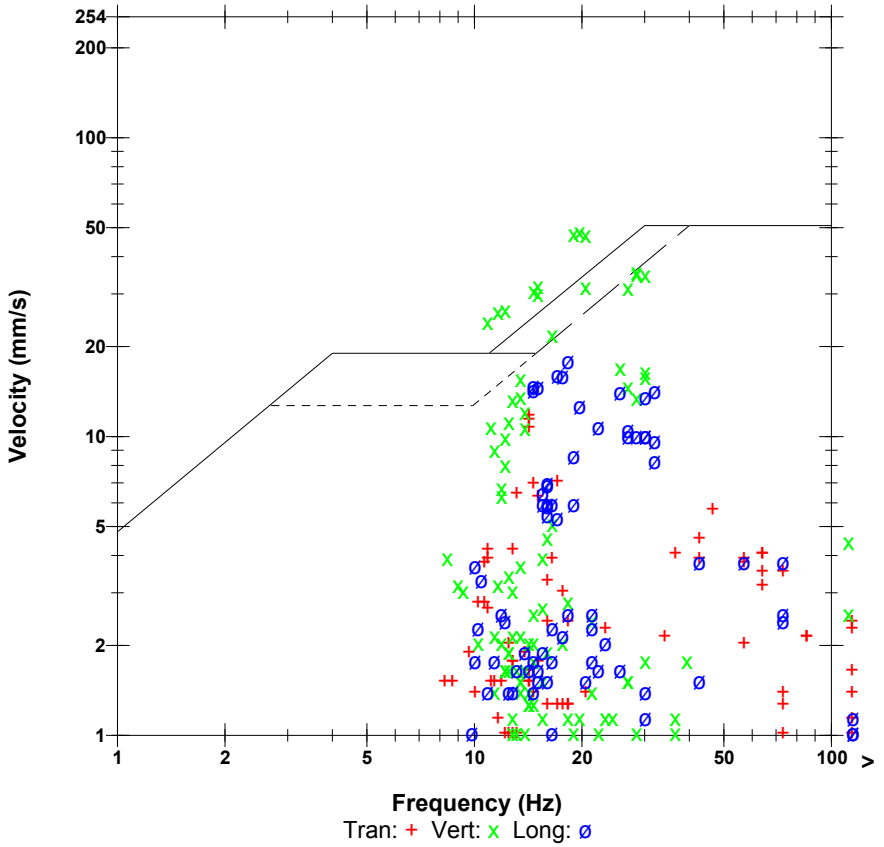

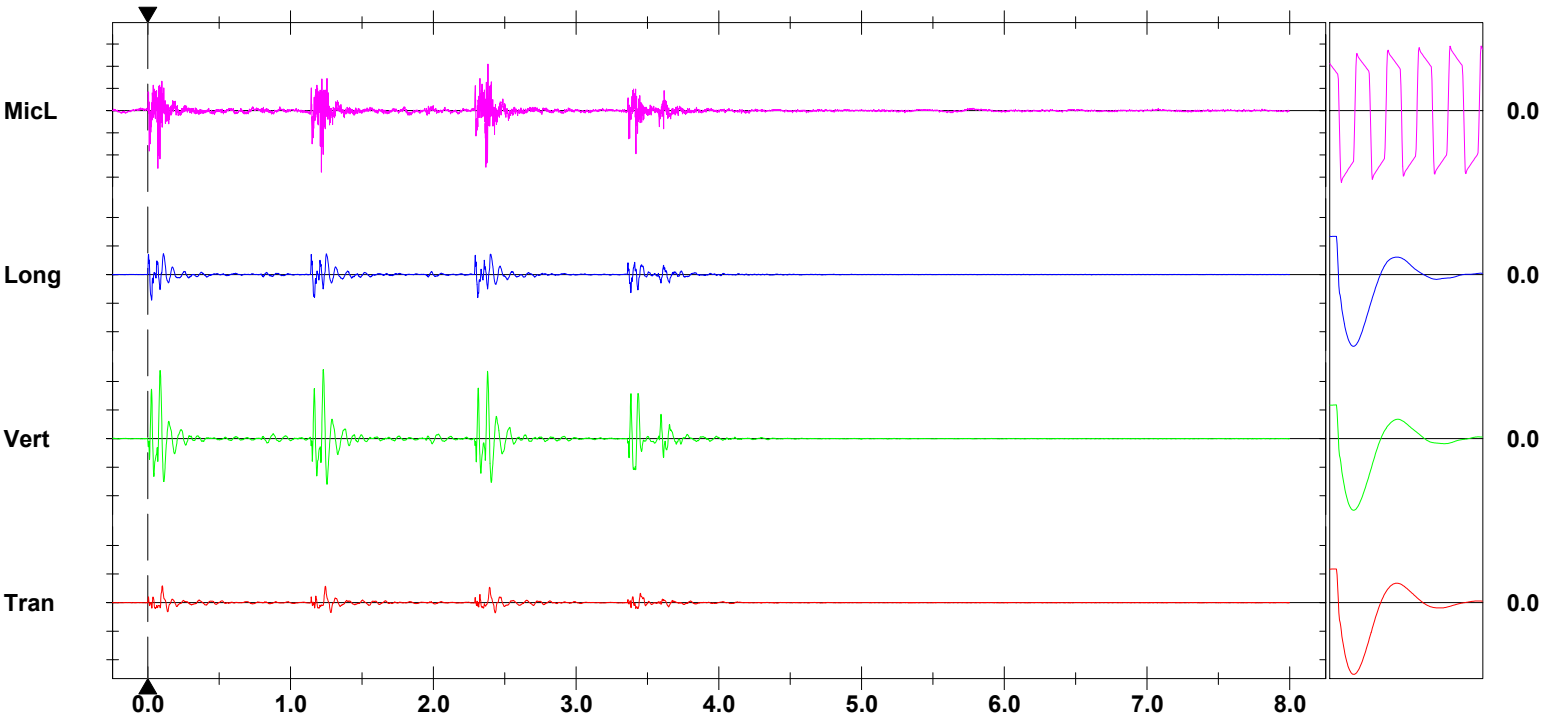

Time Scale: 0.50 sec/div **Amplitude Scale:** Geo: 20.0 mm/s/div Mic: 10.00 pa.(L)/div Sensorcheck
Trigger =

Event Report

Date/Time	Vert at 14:19:35 October 29, 2009	**Serial Number**	BE13056 V 8.12-8.0 MiniMate Plus
Trigger Source	Geo: 1.27 mm/s	**Battery Level**	6.3 Volts
Range	Geo :254 mm/s	**Calibration**	December 7, 2007 by Instantel Inc.
Record Time	5.063 sec at 1024 sps	**File Name**	O056CYFU.GN0
Job Number:	1		

Notes
Location:
Client:
User Name:
General:

Extended Notes
Combo Mode October 29, 2009 14:17:30

Post Event Notes

Microphone Linear Weighting
PSPL 27.5 pa.(L) at 0.075 sec
ZC Freq 85 Hz
Channel Test Passed (Freq = 20.1 Hz Amp = 591 mv)

	Tran	Vert	Long	
PPV	9.65	47.2	16.4	mm/s
ZC Freq	15	20	19	Hz
Time (Rel. to Trig)	0.103	0.090	1.163	sec
Peak Acceleration	0.225	0.623	0.464	g
Peak Displacement	0.0920	0.323	0.135	mm
Sensorcheck	Passed	Passed	Passed	
Frequency	7.4	7.4	7.4	Hz
Overswing Ratio	3.7	3.7	4.2	

Peak Vector Sum 48.4 mm/s at 0.090 sec

USBM RI8507 And OSMRE

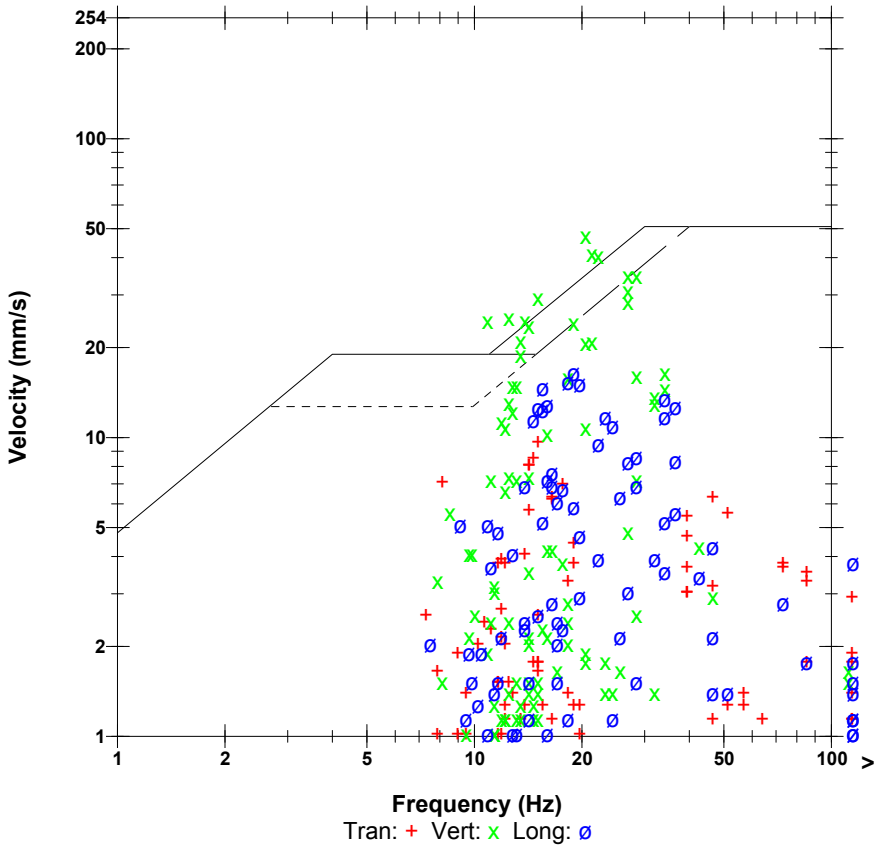

Monitor Log
Oct 29 /09 14:19:35 Oct 29 /09 14:19:40 Event recorded. (Memory Full Exit)

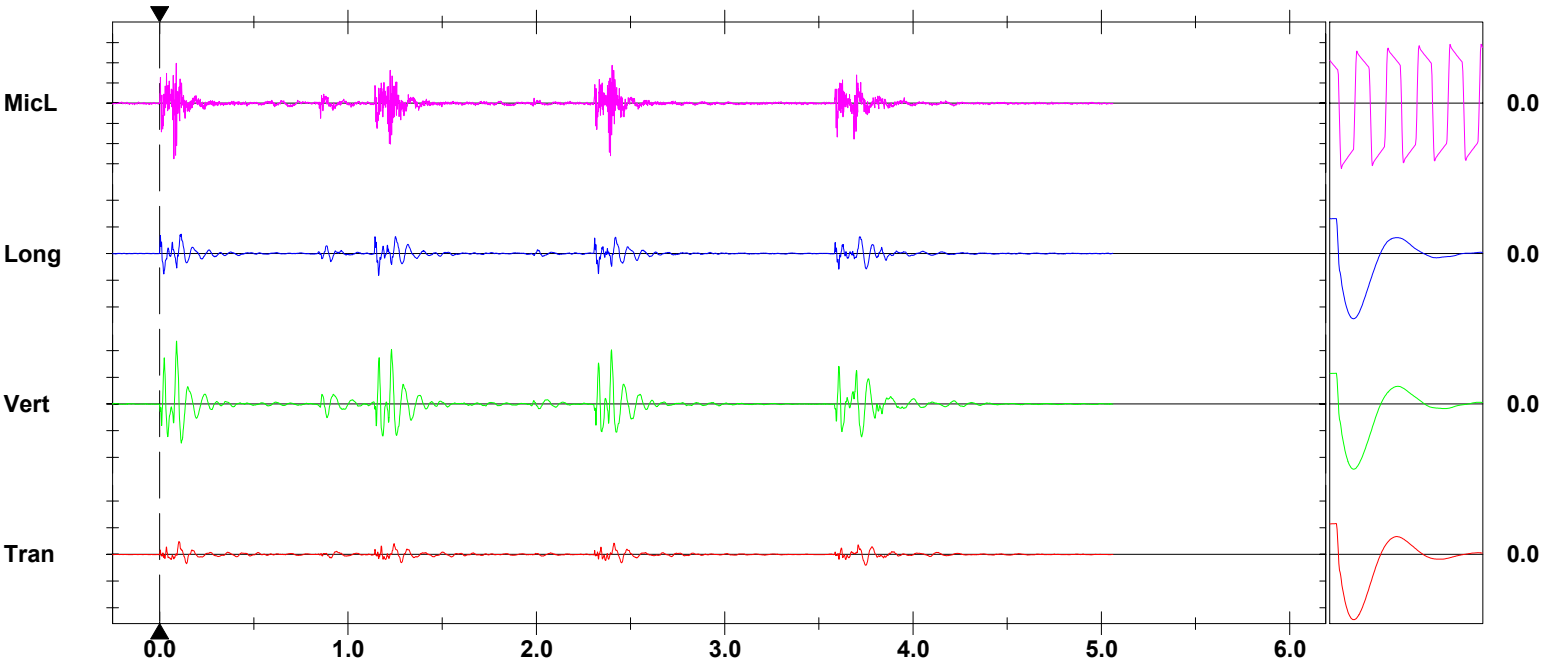

Time Scale: 0.50 sec/div **Amplitude Scale:** Geo: 20.0 mm/s/div Mic: 10.00 pa.(L)/div Sensorcheck
Trigger =

Field Vibration Data

Seismograph Unit # 4

at 9.9 feet from Test Pile #2

Event Report

Histogram Start Time	15:24:51 October 29, 2009	**Serial Number**	BE13056 V 8.12-8.0 MiniMate Plus
Histogram Finish Time	15:38:04 October 29, 2009	**Battery Level**	6.3 Volts
Number of Intervals	396 at 2 seconds	**Calibration**	December 7, 2007 by Instantel Inc.
Range	Geo :254 mm/s	**File Name**	O056CYFX.HF0
Sample Rate	1024sps		
Job Number:	1		

Notes
Location:
Client:
User Name:
General:

Extended Notes

Post Event Notes

Microphone	Linear Weighting
PSPL	50.8 pa.(L) on October 29, 2009 at 15:31:21
ZC Freq	>100 Hz
Channel Test	Passed (Freq = 19.7 Hz Amp = 611 mv)

	Tran	Vert	Long	
PPV	16.9	29.2	20.1	mm/s
ZC Freq	43	21	27	Hz
Date	Oct 29 /09	Oct 29 /09	Oct 29 /09	
Time	15:31:13	15:27:09	15:31:01	
Sensorcheck	Passed	Passed	Passed	
Frequency	7.4	7.3	7.4	Hz
Overswing Ratio	3.7	3.9	4.0	

Peak Vector Sum 35.3 mm/s on October 29, 2009 at 15:31:49

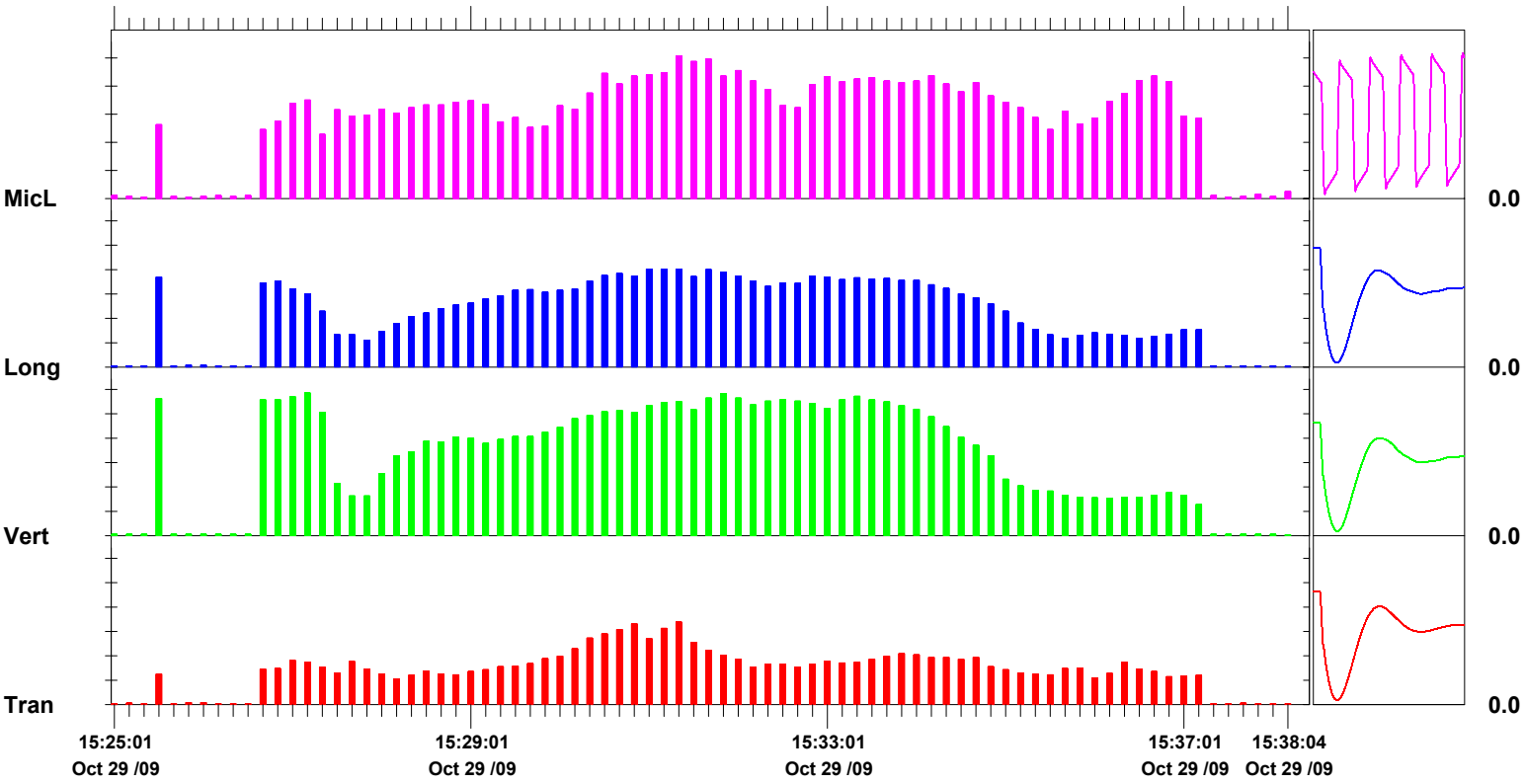

Time Scale: 10 seconds /div **Amplitude Scale:** Geo: 5.00 mm/s/div Mic: 10.00 pa.(L)/div Sensorcheck

Event Report

Date/Time	Long at 15:25:25 October 29, 2009	**Serial Number**	BE13056 V 8.12-8.0 MiniMate Plus
Trigger Source	Geo: 1.27 mm/s	**Battery Level**	6.2 Volts
Range	Geo :254 mm/s	**Calibration**	December 7, 2007 by Instantel Inc.
Record Time	8.0 sec at 1024 sps	**File Name**	O056CYFX.ID0
Job Number:	1		

Notes
Location:
Client:
User Name:
General:

Extended Notes
Combo Mode October 29, 2009 15:24:51

Post Event Notes

Microphone Linear Weighting
PSPL 26.3 pa.(L) at 3.787 sec
ZC Freq 57 Hz
Channel Test Passed (Freq = 19.7 Hz Amp = 611 mv)

	Tran	Vert	Long	
PPV	6.22	28.1	18.4	mm/s
ZC Freq	20	24	20	Hz
Time (Rel. to Trig)	1.329	2.505	1.295	sec
Peak Acceleration	0.186	0.517	0.769	g
Peak Displacement	0.0633	0.190	0.136	mm
Sensorcheck	Passed	Passed	Passed	
Frequency	7.4	7.3	7.4	Hz
Overswing Ratio	3.7	3.9	4.0	

Peak Vector Sum 28.6 mm/s at 1.314 sec

USBM RI8507 And OSMRE

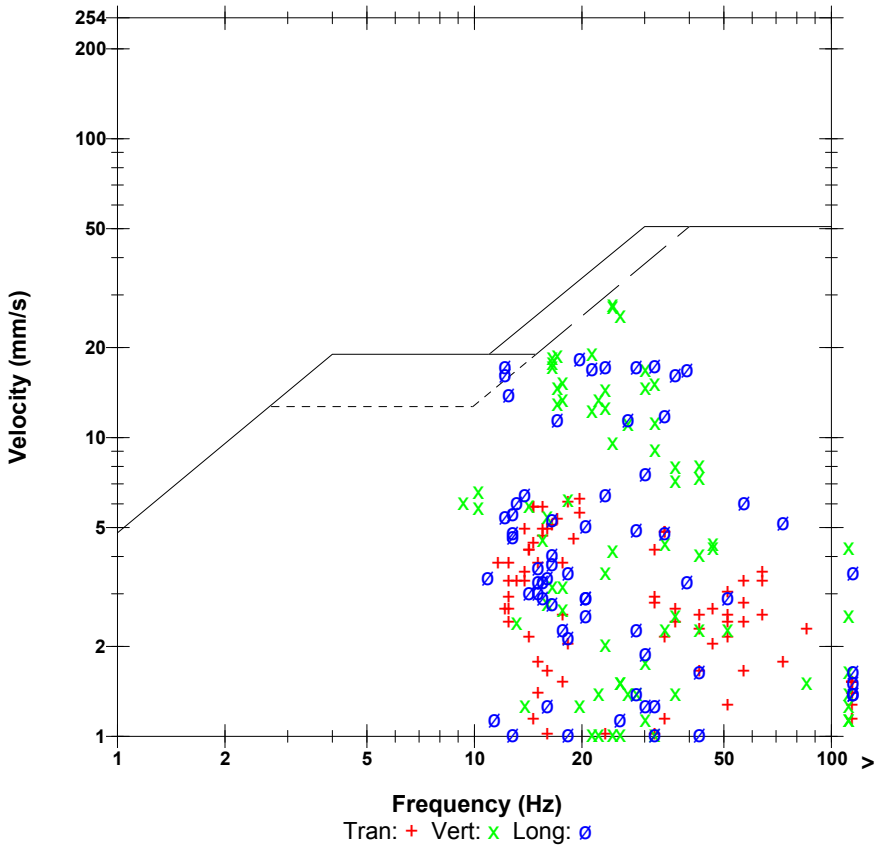

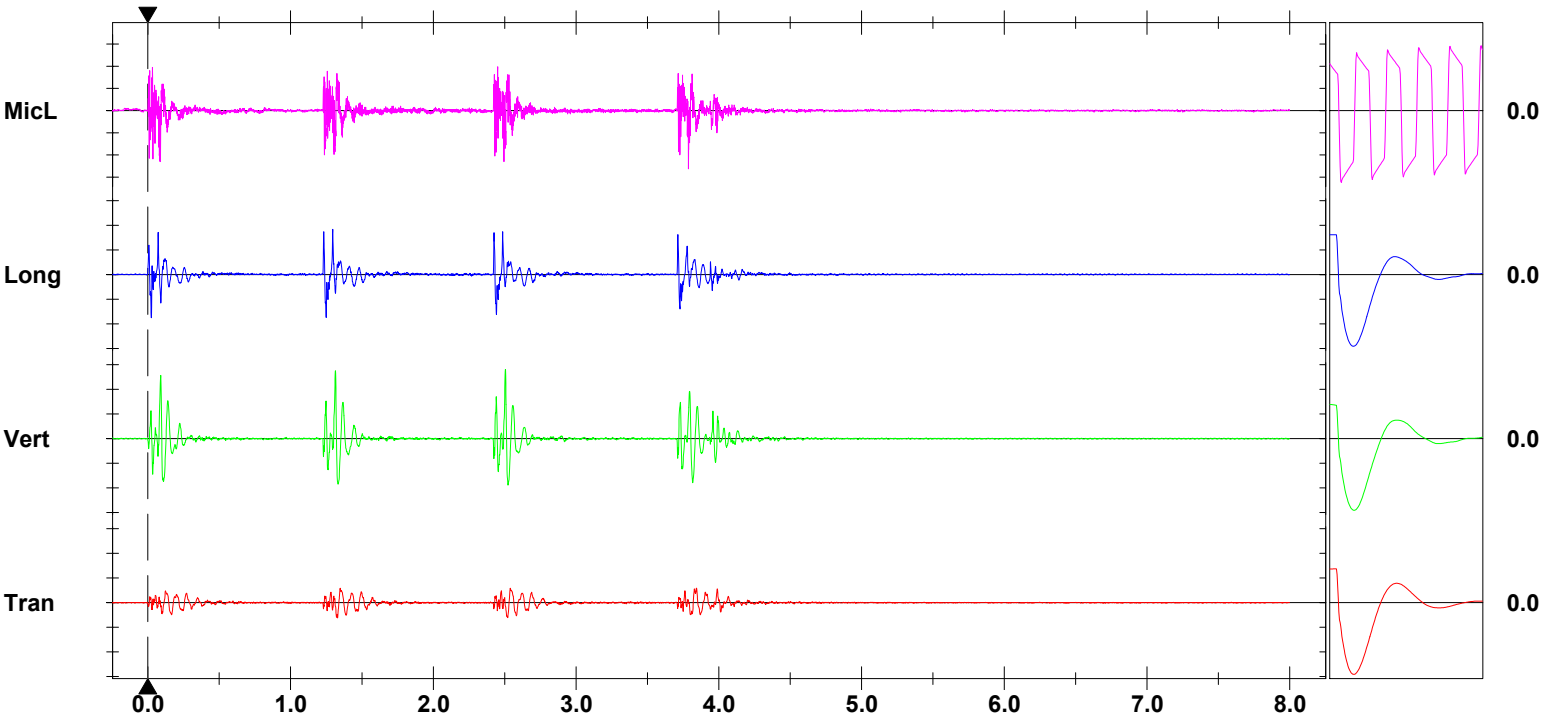

Time Scale: 0.50 sec/div **Amplitude Scale:** Geo: 10.00 mm/s/div Mic: 10.00 pa.(L)/div Sensorcheck
Trigger =

Event Report

Date/Time	Vert at 15:26:39 October 29, 2009	**Serial Number**	BE13056 V 8.12-8.0 MiniMate Plus
Trigger Source	Geo: 1.27 mm/s	**Battery Level**	6.3 Volts
Range	Geo :254 mm/s	**Calibration**	December 7, 2007 by Instantel Inc.
Record Time	8.0 sec at 1024 sps	**File Name**	O056CYFX.KF0
Job Number:	1		

Notes
Location:
Client:
User Name:
General:

Extended Notes
Combo Mode October 29, 2009 15:24:51

Post Event Notes

Microphone Linear Weighting
PSPL 27.5 pa.(L) at 3.830 sec
ZC Freq 64 Hz
Channel Test Passed (Freq = 19.7 Hz Amp = 611 mv)

	Tran	Vert	Long	
PPV	7.37	27.8	17.7	mm/s
ZC Freq	17	23	37	Hz
Time (Rel. to Trig)	2.648	1.356	2.553	sec
Peak Acceleration	0.172	0.610	0.623	g
Peak Displacement	0.0668	0.187	0.134	mm
Sensorcheck	Passed	Passed	Passed	
Frequency	7.4	7.3	7.4	Hz
Overswing Ratio	3.7	3.9	4.0	

Peak Vector Sum 27.9 mm/s at 1.356 sec

USBM RI8507 And OSMRE

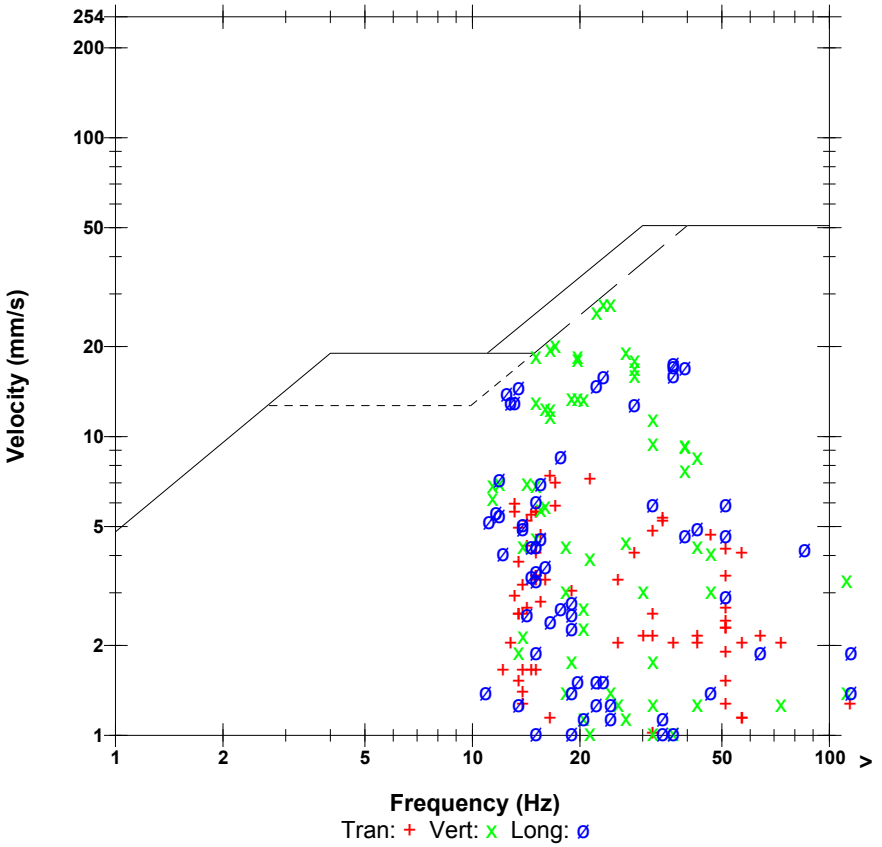

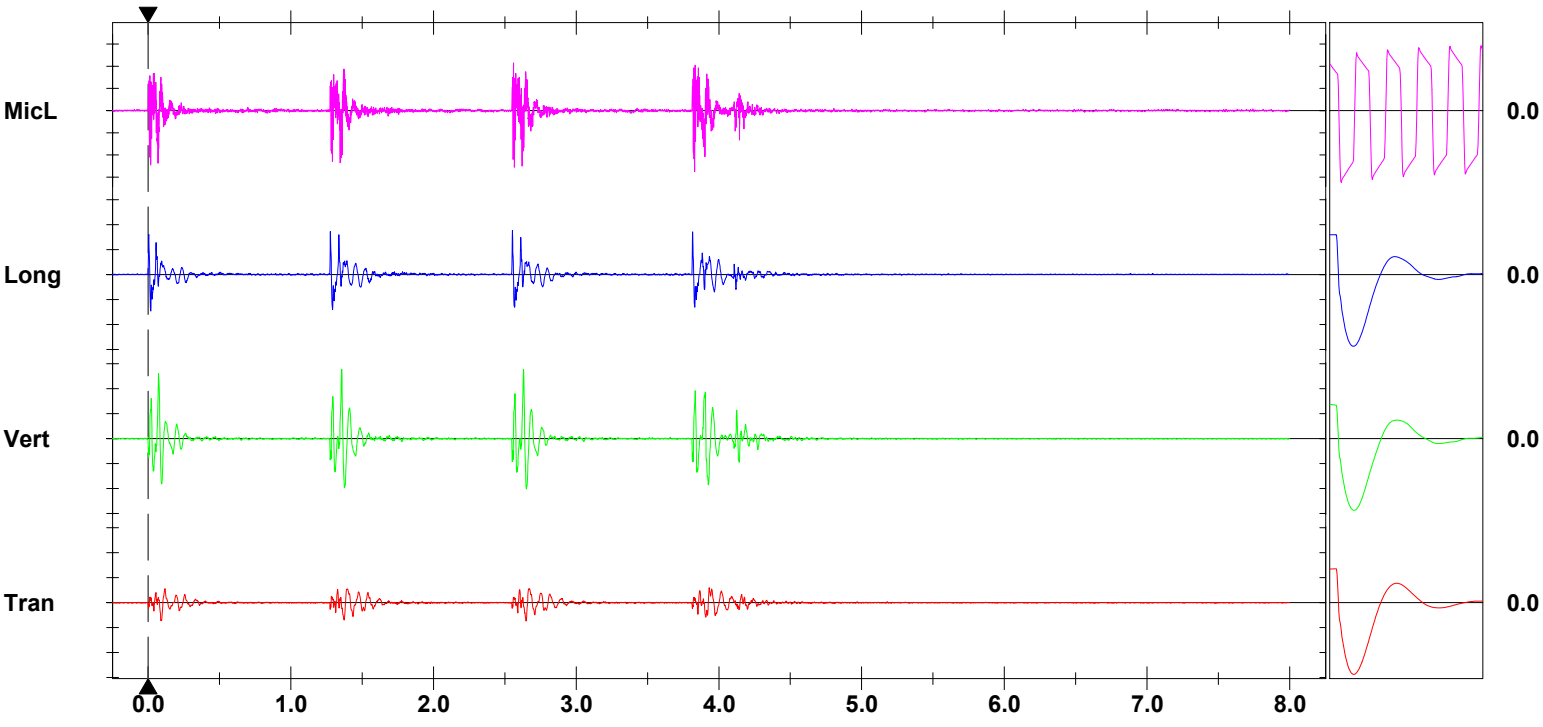

Time Scale: 0.50 sec/div **Amplitude Scale:** Geo: 10.00 mm/s/div Mic: 10.00 pa.(L)/div Sensorcheck
Trigger =

Event Report

Date/Time	Vert at 15:26:55 October 29, 2009	**Serial Number**	BE13056 V 8.12-8.0 MiniMate Plus
Trigger Source	Geo: 1.27 mm/s	**Battery Level**	6.2 Volts
Range	Geo :254 mm/s	**Calibration**	December 7, 2007 by Instantel Inc.
Record Time	4.765 sec at 1024 sps	**File Name**	O056CYFX.KV0
Job Number:	1		

Notes
Location:
Client:
User Name:
General:

Extended Notes
Combo Mode October 29, 2009 15:24:51

Post Event Notes

Microphone Linear Weighting
PSPL 30.5 pa.(L) at 2.706 sec
ZC Freq 47 Hz
Channel Test Passed (Freq = 19.7 Hz Amp = 611 mv)

	Tran	Vert	Long	
PPV	8.64	28.3	16.0	mm/s
ZC Freq	18	21	39	Hz
Time (Rel. to Trig)	1.380	2.711	1.284	sec
Peak Acceleration	0.186	0.583	0.583	g
Peak Displacement	0.0634	0.188	0.114	mm
Sensorcheck	Passed	Passed	Passed	
Frequency	7.4	7.3	7.4	Hz
Overswing Ratio	3.7	3.9	4.0	

Peak Vector Sum 28.4 mm/s at 2.711 sec

USBM RI8507 And OSMRE

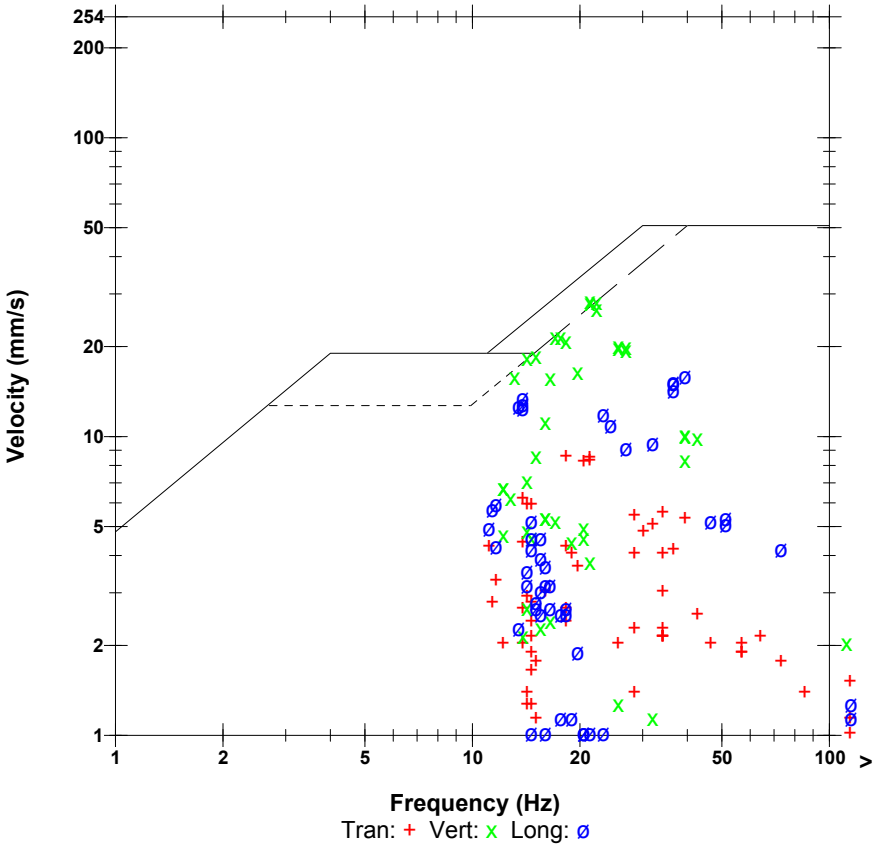

Monitor Log
Oct 29 /09 15:26:55 Oct 29 /09 15:27:00 Event recorded. (Memory Full Exit)

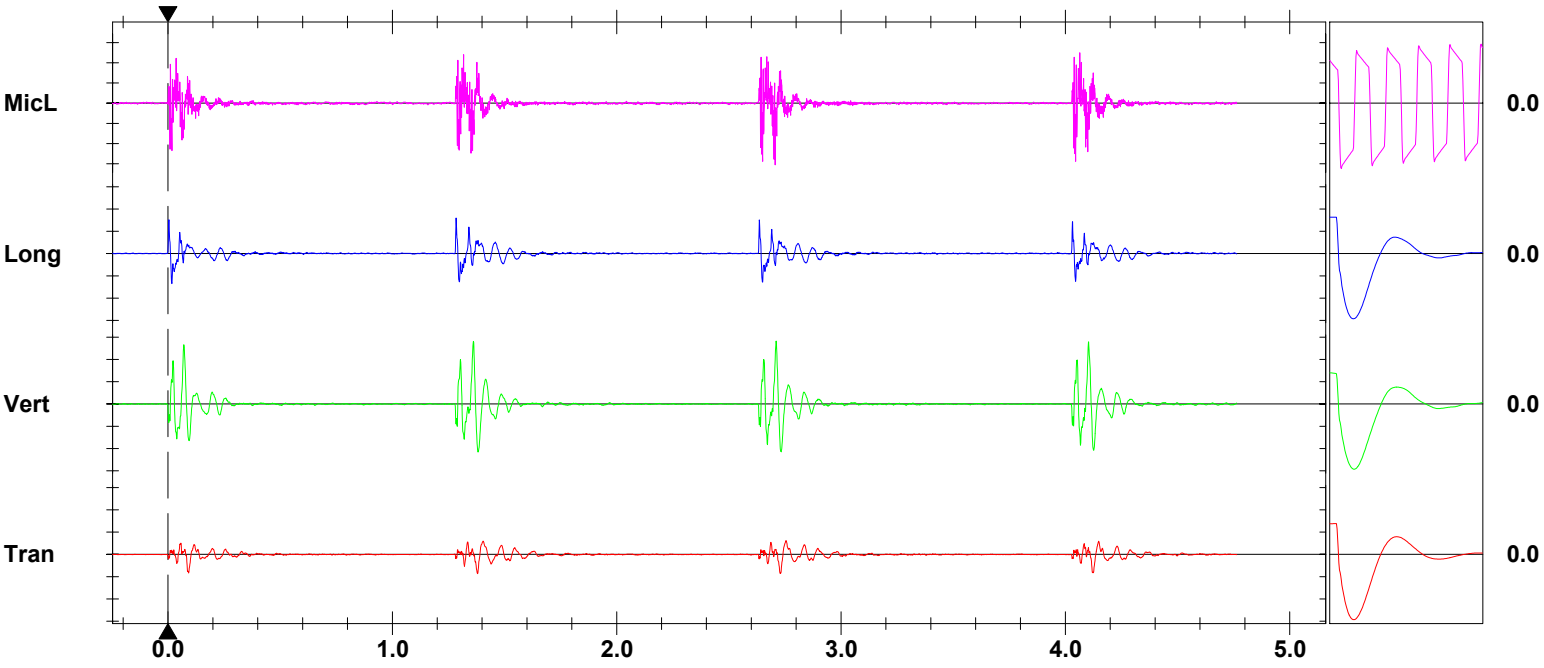

Time Scale: 0.20 sec/div **Amplitude Scale:** Geo: 10.00 mm/s/div Mic: 10.00 pa.(L)/div Sensorcheck
Trigger =

Field Vibration Data

Seismograph Unit # 4

at 9.1 feet from Test Pile #1

Non Driving Event

Event Report

Histogram Start Time	10:31:49 December 21, 2009	**Serial Number**	BE13056 V 8.12-8.0 MiniMate Plus
Histogram Finish Time	11:04:05 December 21, 2009	**Battery Level**	6.2 Volts
Number of Intervals	968 at 2 seconds	**Calibration**	December 7, 2007 by Instantel Inc.
Range	Geo :254 mm/s	**File Name**	O056D15P.910
Sample Rate	1024sps		
Job Number:	1		

Notes
Location:
Client:
User Name:
General:

Extended Notes

Post Event Notes

Microphone Linear Weighting
PSPL 4.50 pa.(L) on December 21, 2009 at 10:52:05
ZC Freq 9.3 Hz
Channel Test Passed (Freq = 20.5 Hz Amp = 672 mv)

	Tran	Vert	Long	
PPV	0.127	0.127	0.254	mm/s
ZC Freq	>100	>100	>100	Hz
Date	Dec 21 /09	Dec 21 /09	Dec 21 /09	
Time	10:31:51	10:31:51	10:49:51	
Sensorcheck	Check	Check	Check	
Frequency	37.9	1024.0	68.3	Hz
Overswing Ratio	1.5	0.0	1.0	

Peak Vector Sum 0.254 mm/s on December 21, 2009 at 10:49:51

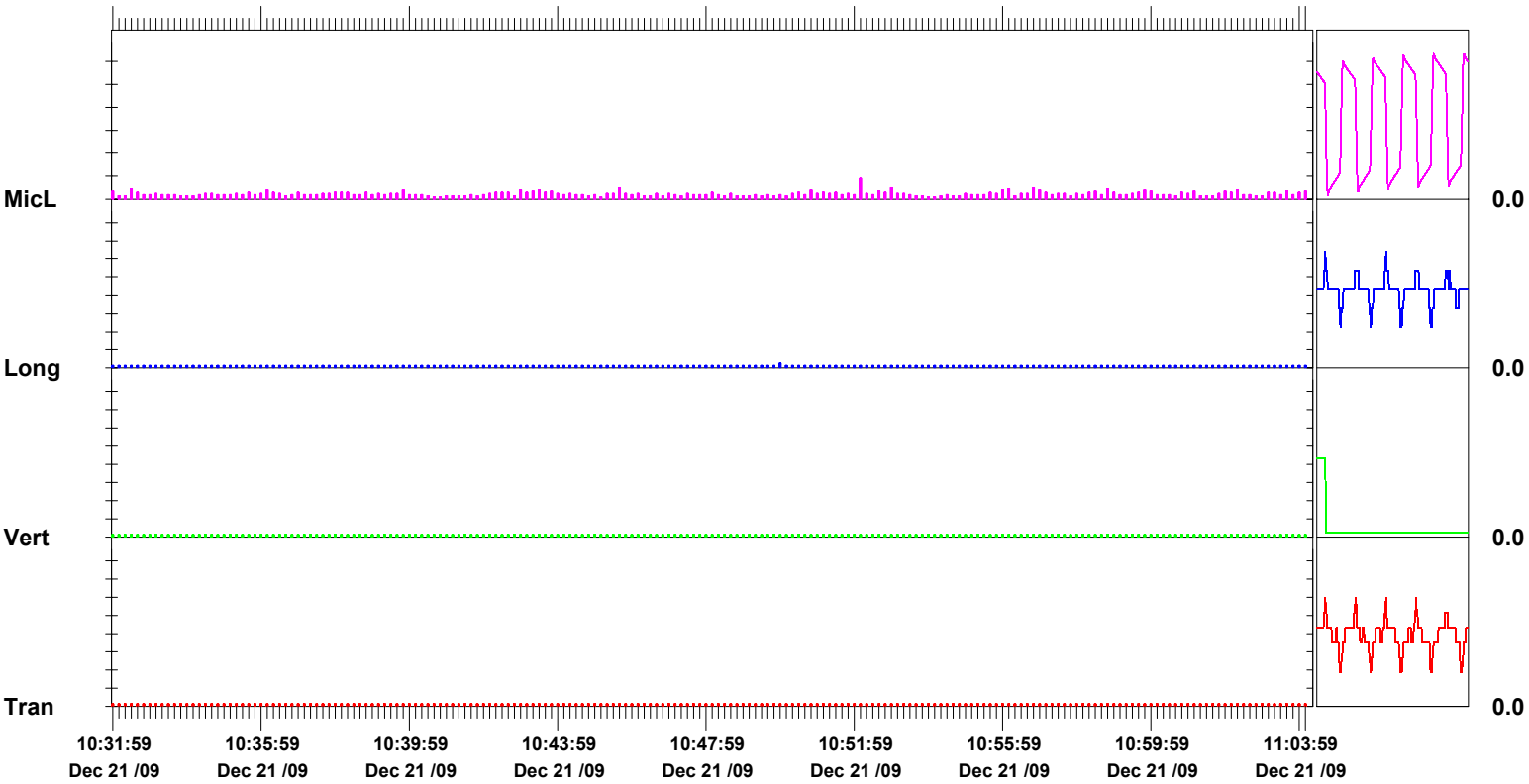

Time Scale: 10 seconds /div **Amplitude Scale:** Geo: 1.000 mm/s/div Mic: 5.00 pa.(L)/div Sensorcheck

Event Report

Histogram Start Time	11:31:38 December 21, 2009	**Serial Number**	BE13056 V 8.12-8.0 MiniMate Plus
Histogram Finish Time	11:54:52 December 21, 2009	**Battery Level**	6.1 Volts
Number of Intervals	697 at 2 seconds	**Calibration**	December 7, 2007 by Instantel Inc.
Range	Geo :254 mm/s	**File Name**	O056D15S.0Q0
Sample Rate	1024sps		
Job Number:	1		

Notes
Location:
Client:
User Name:
General:

Extended Notes

Post Event Notes

Microphone Linear Weighting
PSPL 4.50 pa.(L) on December 21, 2009 at 11:38:32
ZC Freq 4.5 Hz
Channel Test Passed (Freq = 20.1 Hz Amp = 729 mv)

	Tran	Vert	Long	
PPV	0.127	0.127	0.254	mm/s
ZC Freq	>100	>100	>100	Hz
Date	Dec 21 /09	Dec 21 /09	Dec 21 /09	
Time	11:31:40	11:31:40	11:45:00	
Sensorcheck	Check	Check	Check	
Frequency	44.5	48.8	11.3	Hz
Overswing Ratio	1.5	1.0	1.0	

Peak Vector Sum 0.254 mm/s on December 21, 2009 at 11:45:00

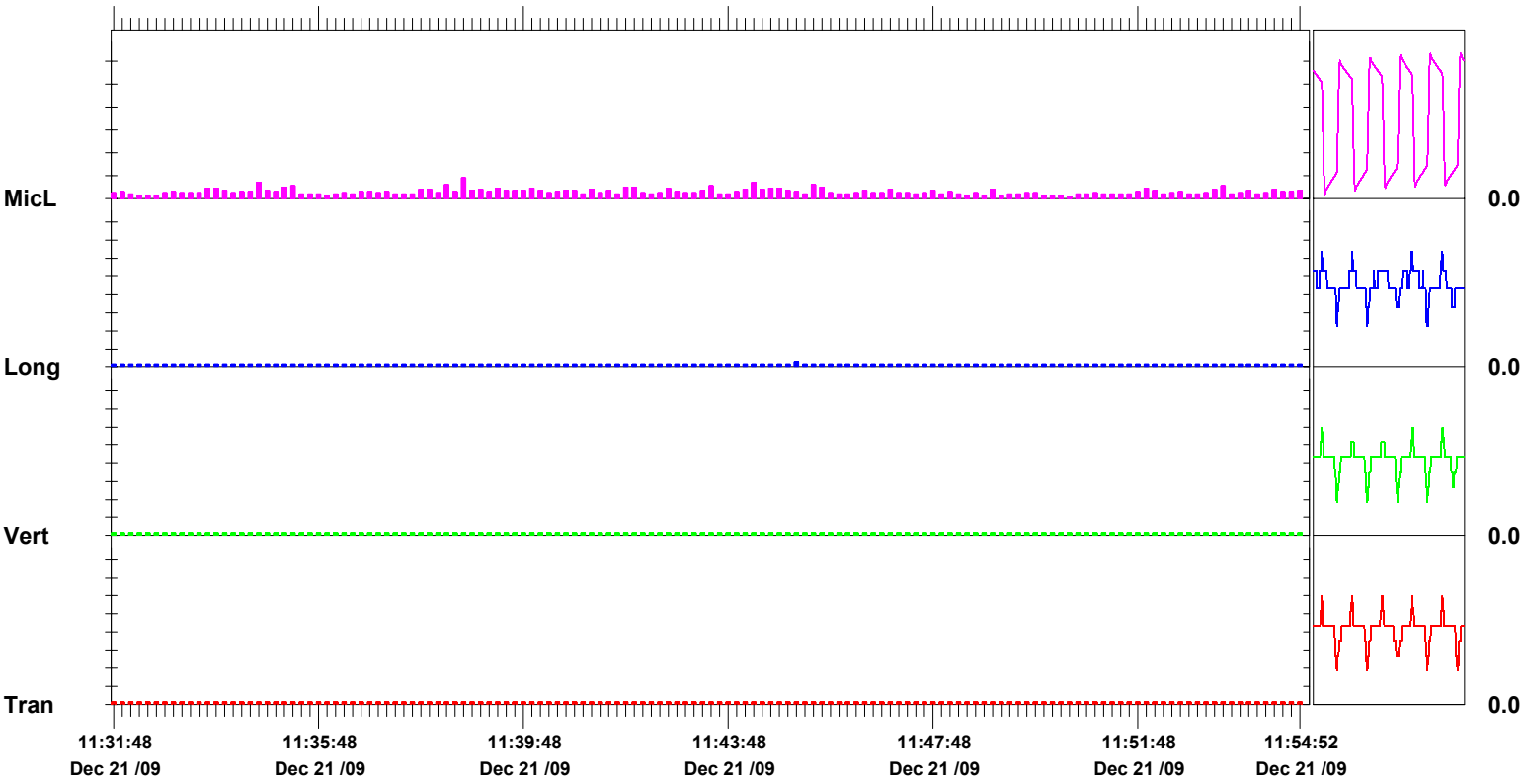

Time Scale: 10 seconds /div **Amplitude Scale:** Geo: 1.000 mm/s/div Mic: 5.00 pa.(L)/div Sensorcheck

Field Vibration Data

Seismograph Unit # 5

at 25.3 feet from Test Pile #1

Event Report

Histogram Start Time	14:17:39 October 29, 2009	**Serial Number**	BE13072 V 8.12-8.0 MiniMate Plus
Histogram Finish Time	14:25:24 October 29, 2009	**Battery Level**	6.2 Volts
Number of Intervals	232 at 2 seconds	**Calibration**	December 7, 2007 by Instantel Inc.
Range	Geo :254 mm/s	**File Name**	O072CYFU.DF0
Sample Rate	1024sps		
Job Number:	1		

Notes
Location:
Client:
User Name:
General:

Extended Notes

Post Event Notes

Microphone	Linear Weighting
PSPL	28.3 pa.(L) on October 29, 2009 at 14:23:51
ZC Freq	>100 Hz
Channel Test	Passed (Freq = 20.1 Hz Amp = 578 mv)

	Tran	Vert	Long	
PPV	11.8	16.6	13.8	mm/s
ZC Freq	18	15	21	Hz
Date	Oct 29 /09	Oct 29 /09	Oct 29 /09	
Time	14:18:11	14:18:11	14:18:13	
Sensorcheck	Passed	Passed	Passed	
Frequency	7.3	7.3	7.3	Hz
Overswing Ratio	3.7	3.8	4.0	

Peak Vector Sum 20.0 mm/s on October 29, 2009 at 14:18:11

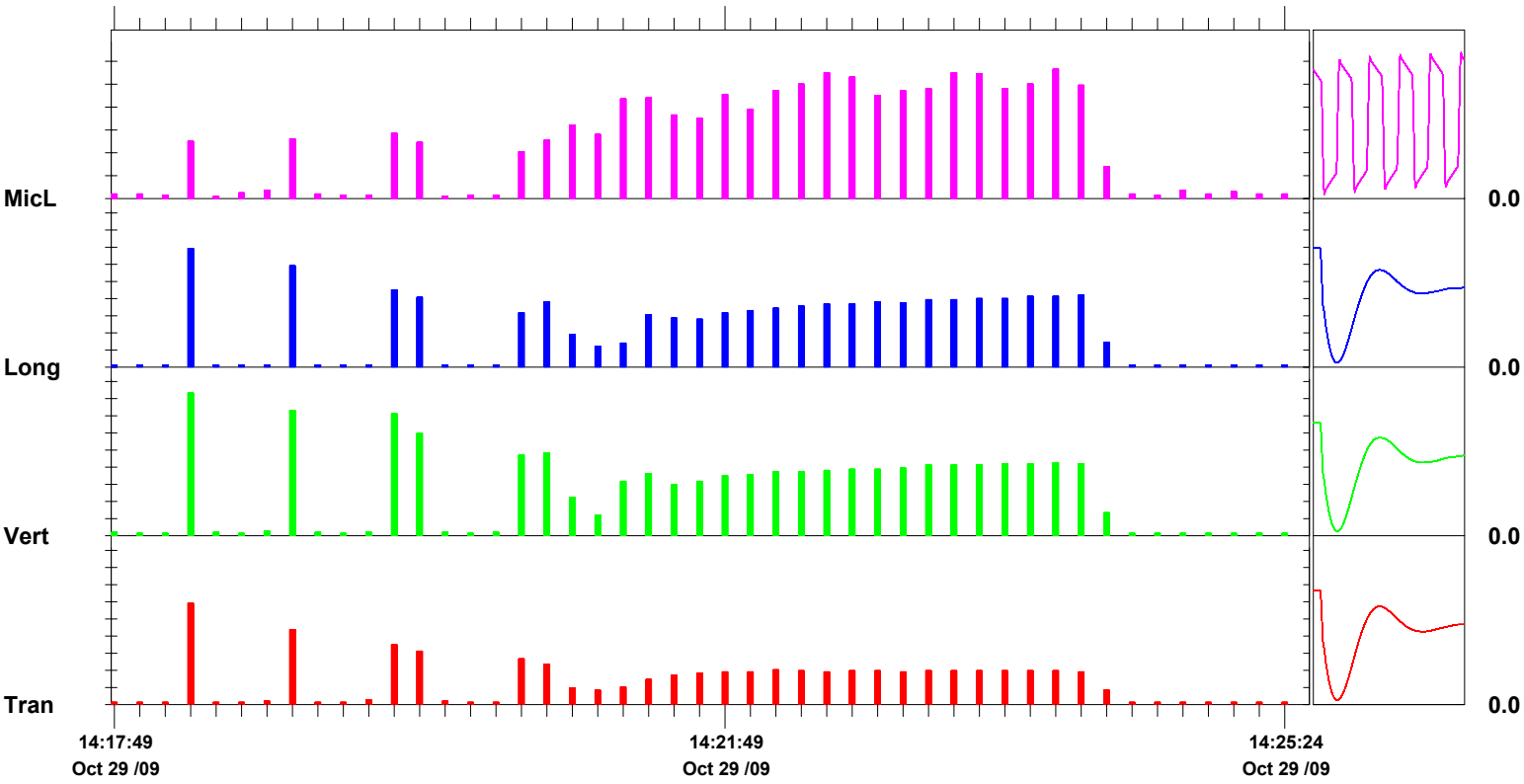

Time Scale: 10 seconds /div **Amplitude Scale:** Geo: 2.00 mm/s/div Mic: 5.00 pa.(L)/div Sensorcheck

Event Report

Date/Time	Long at 14:18:10 October 29, 2009	**Serial Number**	BE13072 V 8.12-8.0 MiniMate Plus
Trigger Source	Geo: 1.27 mm/s	**Battery Level**	6.2 Volts
Range	Geo :254 mm/s	**Calibration**	December 7, 2007 by Instantel Inc.
Record Time	8.0 sec at 1024 sps	**File Name**	O072CYFU.EA0
Job Number:	1		

Notes
Location:
Client:
User Name:
General:

Extended Notes
Combo Mode October 29, 2009 14:17:38

Post Event Notes

Microphone Linear Weighting
PSPL 12.5 pa.(L) at 0.008 sec
ZC Freq >100 Hz
Channel Test Passed (Freq = 20.1 Hz Amp = 578 mv)

	Tran	Vert	Long	
PPV	11.8	16.6	13.8	mm/s
ZC Freq	18	15	21	Hz
Time (Rel. to Trig)	0.109	0.106	1.188	sec
Peak Acceleration	0.159	0.239	0.278	g
Peak Displacement	0.0957	0.153	0.103	mm
Sensorcheck	Passed	Passed	Passed	
Frequency	7.3	7.3	7.3	Hz
Overswing Ratio	3.7	3.8	4.0	

Peak Vector Sum 20.0 mm/s at 0.109 sec

USBM RI8507 And OSMRE

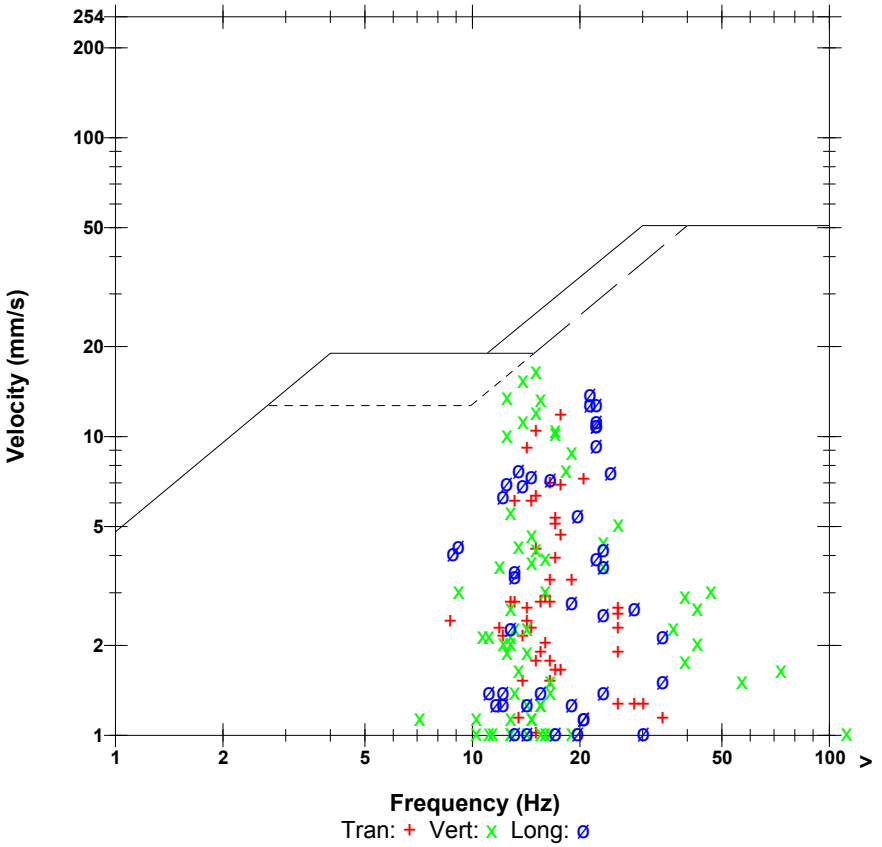

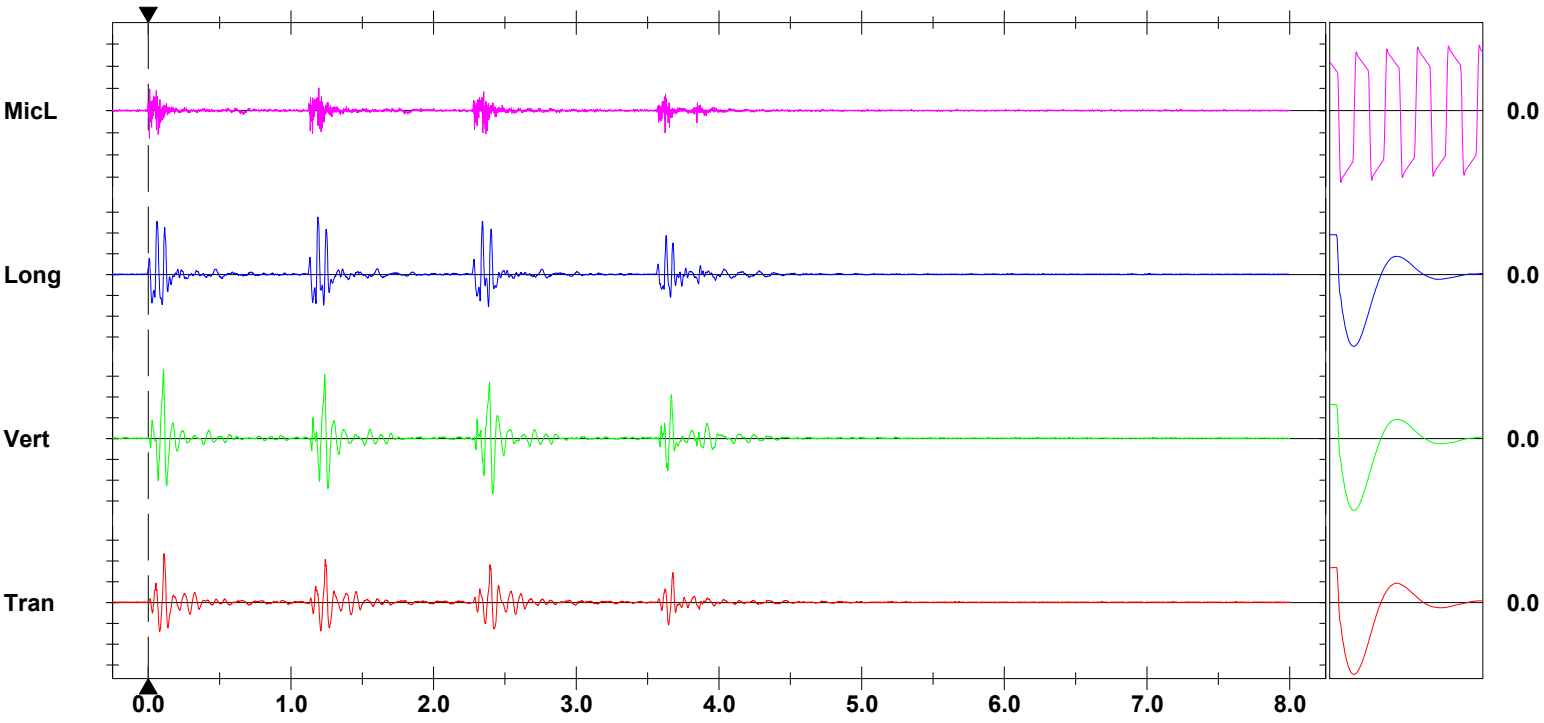

Time Scale: 0.50 sec/div **Amplitude Scale:** Geo: 5.00 mm/s/div Mic: 10.00 pa.(L)/div Sensorcheck
Trigger =

Event Report

Date/Time	Long at 14:18:50 October 29, 2009	**Serial Number**	BE13072 V 8.12-8.0 MiniMate Plus
Trigger Source	Geo: 1.27 mm/s	**Battery Level**	6.3 Volts
Range	Geo :254 mm/s	**Calibration**	December 7, 2007 by Instantel Inc.
Record Time	8.0 sec at 1024 sps	**File Name**	O072CYFU.FE0
Job Number:	1		

Notes
Location:
Client:
User Name:
General:

Extended Notes
Combo Mode October 29, 2009 14:17:38

Post Event Notes

Microphone Linear Weighting
PSPL 13.0 pa.(L) at 0.070 sec
ZC Freq >100 Hz
Channel Test Passed (Freq = 20.1 Hz Amp = 578 mv)

	Tran	Vert	Long	
PPV	8.76	14.6	11.8	mm/s
ZC Freq	14	16	22	Hz
Time (Rel. to Trig)	0.120	1.282	0.066	sec
Peak Acceleration	0.133	0.212	0.212	g
Peak Displacement	0.0810	0.144	0.0794	mm
Sensorcheck	Passed	Passed	Passed	
Frequency	7.3	7.3	7.3	Hz
Overswing Ratio	3.7	3.8	4.0	

Peak Vector Sum 15.4 mm/s at 0.118 sec

USBM RI8507 And OSMRE

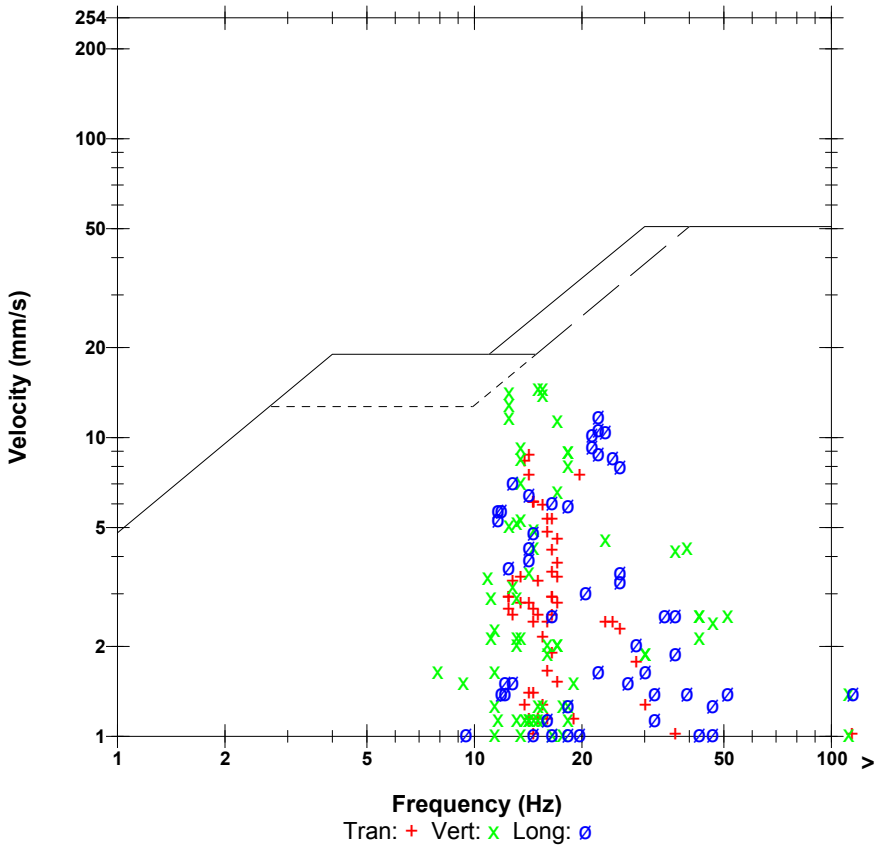

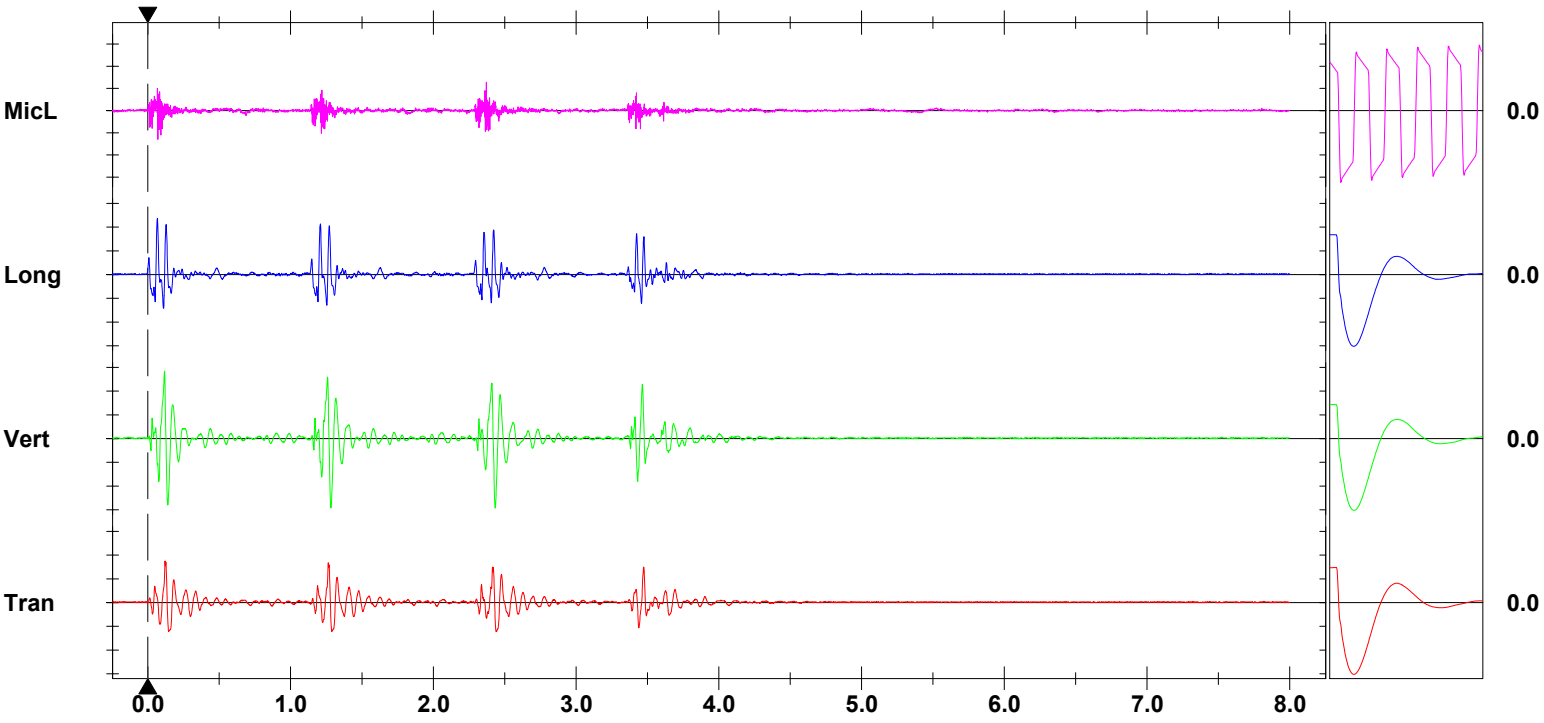

Time Scale: 0.50 sec/div **Amplitude Scale:** Geo: 5.00 mm/s/div Mic: 10.00 pa.(L)/div Sensorcheck
Trigger =

Event Report

Date/Time Long at 14:19:38 October 29, 2009
Trigger Source Geo: 1.27 mm/s
Range Geo :254 mm/s
Record Time 7.099 sec at 1024 sps
Job Number: 1

Serial Number BE13072 V 8.12-8.0 MiniMate Plus
Battery Level 6.2 Volts
Calibration December 7, 2007 by Instantel Inc.
File Name O072CYFU.GQ0

Notes
Location:
Client:
User Name:
General:

Extended Notes
Combo Mode October 29, 2009 14:17:38

Post Event Notes

Microphone Linear Weighting
PSPL 14.3 pa.(L) at 0.092 sec
ZC Freq >100 Hz
Channel Test Passed (Freq = 20.1 Hz Amp = 578 mv)

	Tran	Vert	Long	
PPV	6.98	14.2	9.02	mm/s
ZC Freq	14	15	22	Hz
Time (Rel. to Trig)	0.130	0.144	0.132	sec
Peak Acceleration	0.119	0.186	0.172	g
Peak Displacement	0.0730	0.134	0.0598	mm
Sensorcheck	Passed	Passed	Passed	
Frequency	7.3	7.3	7.3	Hz
Overswing Ratio	3.7	3.8	4.0	

Peak Vector Sum 14.8 mm/s at 0.145 sec

USBM RI8507 And OSMRE

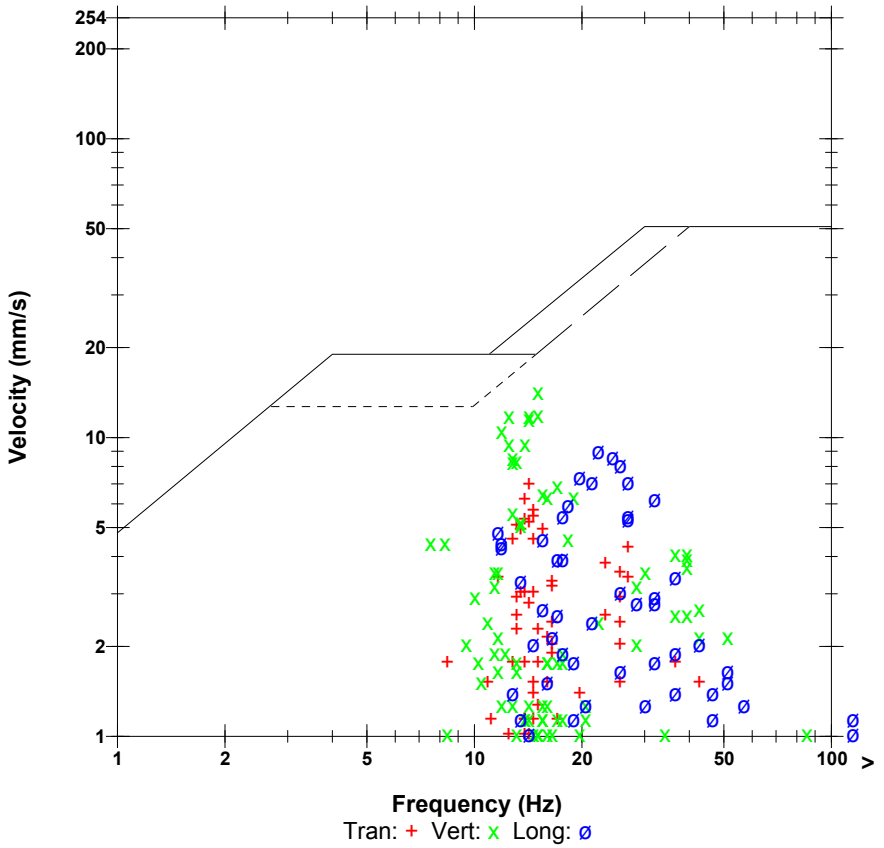

Monitor Log
Oct 29 /09 14:19:38 Oct 29 /09 14:19:45 Event recorded. (Memory Full Exit)

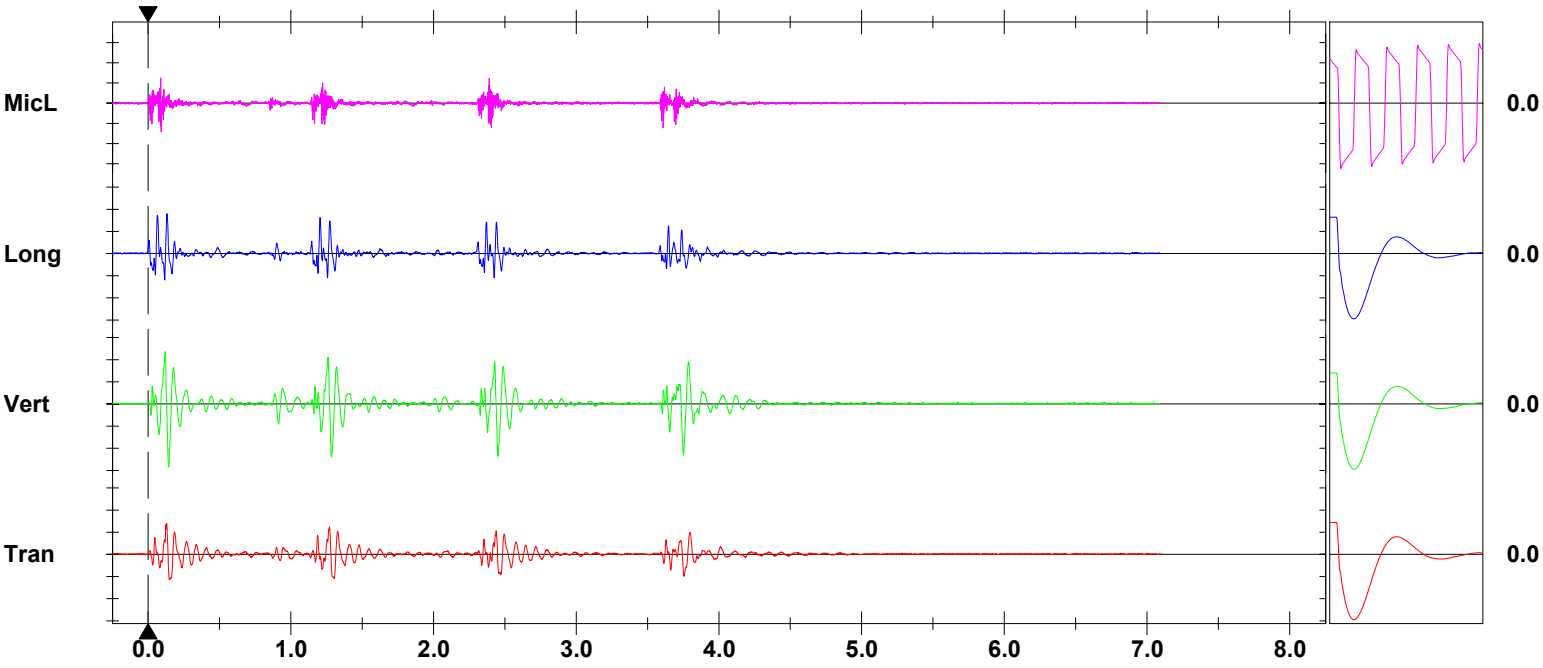

Time Scale: 0.50 sec/div **Amplitude Scale:** Geo: 5.00 mm/s/div Mic: 10.00 pa.(L)/div Sensorcheck
Trigger = ▶——— ———◀

Field Vibration Data

Seismograph Unit # 5

at 24.9 feet from Test Pile #2

Event Report

Histogram Start Time	15:23:53 October 29, 2009	**Serial Number**	BE13072 V 8.12-8.0 MiniMate Plus
Histogram Finish Time	15:38:10 October 29, 2009	**Battery Level**	6.2 Volts
Number of Intervals	428 at 2 seconds	**Calibration**	December 7, 2007 by Instantel Inc.
Range	Geo :254 mm/s	**File Name**	O072CYFX.FT0
Sample Rate	1024sps		
Job Number:	1		

Notes
Location:
Client:
User Name:
General:

Extended Notes

Post Event Notes

Microphone	Linear Weighting
PSPL	31.5 pa.(L) on October 29, 2009 at 15:31:09
ZC Freq	>100 Hz
Channel Test	Passed (Freq = 20.5 Hz Amp = 625 mv)

	Tran	Vert	Long	
PPV	7.62	11.2	20.2	mm/s
ZC Freq	28	23	28	Hz
Date	Oct 29 /09	Oct 29 /09	Oct 29 /09	
Time	15:30:45	15:34:31	15:32:33	
Sensorcheck	Passed	Passed	Passed	
Frequency	7.3	7.3	7.2	Hz
Overswing Ratio	3.7	3.6	4.1	

Peak Vector Sum 22.2 mm/s on October 29, 2009 at 15:33:13

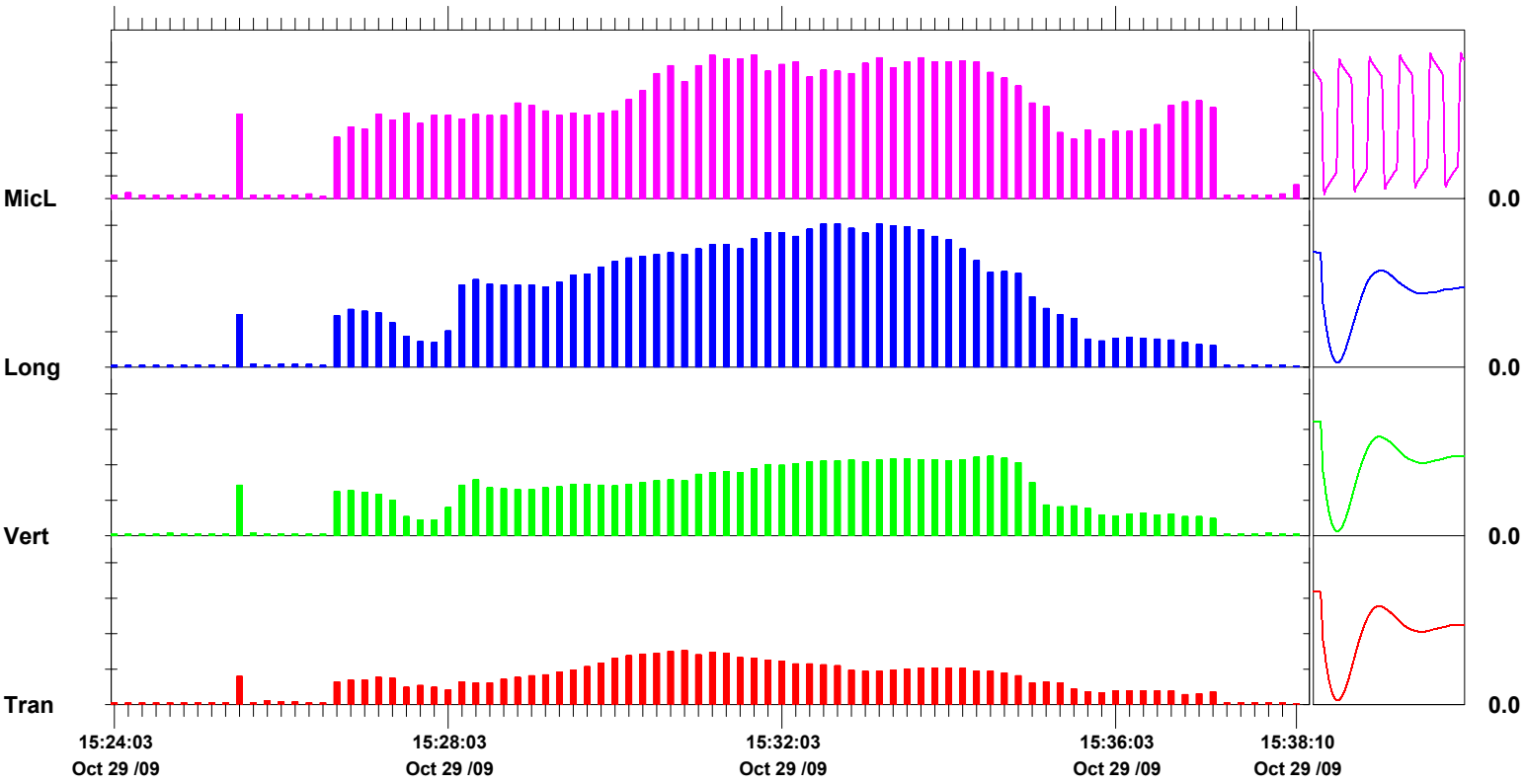

Time Scale: 10 seconds /div **Amplitude Scale:** Geo: 5.00 mm/s/div Mic: 5.00 pa.(L)/div Sensorcheck

Event Report

Date/Time	Long at 15:25:28 October 29, 2009	**Serial Number**	BE13072 V 8.12-8.0 MiniMate Plus
Trigger Source	Geo: 1.27 mm/s	**Battery Level**	6.2 Volts
Range	Geo :254 mm/s	**Calibration**	December 7, 2007 by Instantel Inc.
Record Time	8.0 sec at 1024 sps	**File Name**	O072CYFX.IG0
Job Number:	1		

Notes
Location:
Client:
User Name:
General:

Extended Notes
Combo Mode October 29, 2009 15:23:53

Post Event Notes

Microphone Linear Weighting
PSPL 18.5 pa.(L) at 2.455 sec
ZC Freq >100 Hz
Channel Test Passed (Freq = 20.5 Hz Amp = 625 mv)

	Tran	Vert	Long	
PPV	3.94	7.11	7.37	mm/s
ZC Freq	37	28	21	Hz
Time (Rel. to Trig)	2.454	1.341	2.445	sec
Peak Acceleration	0.106	0.159	0.146	g
Peak Displacement	0.0337	0.0399	0.0628	mm
Sensorcheck	Passed	Passed	Passed	
Frequency	7.3	7.3	7.2	Hz
Overswing Ratio	3.7	3.6	4.1	

Peak Vector Sum 8.83 mm/s at 1.341 sec

USBM RI8507 And OSMRE

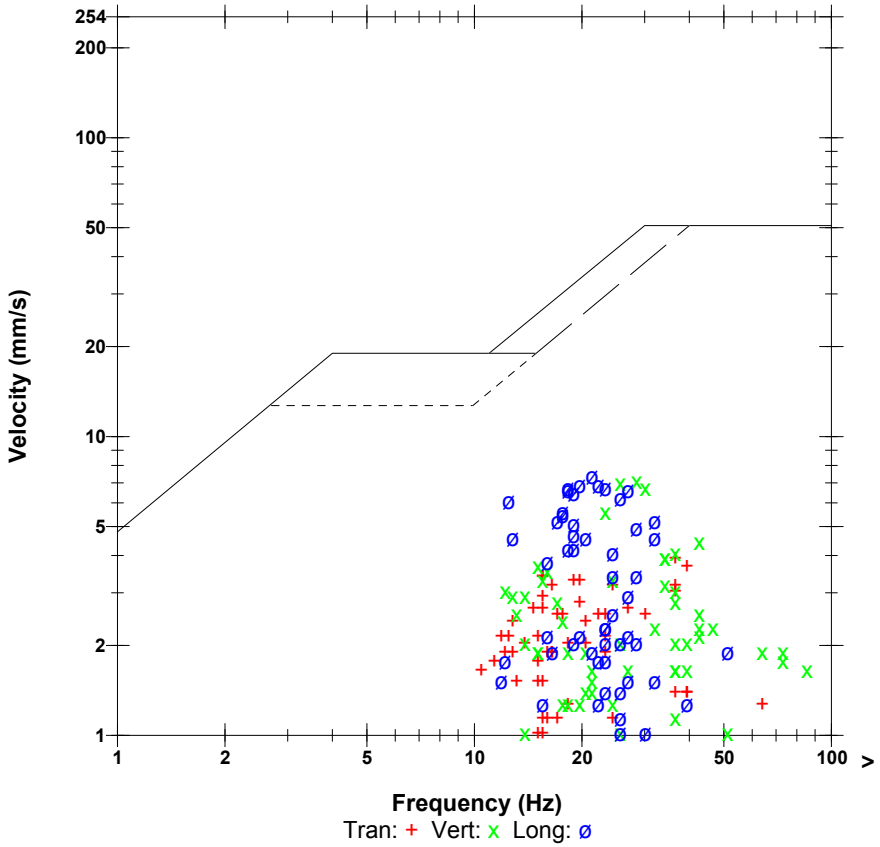

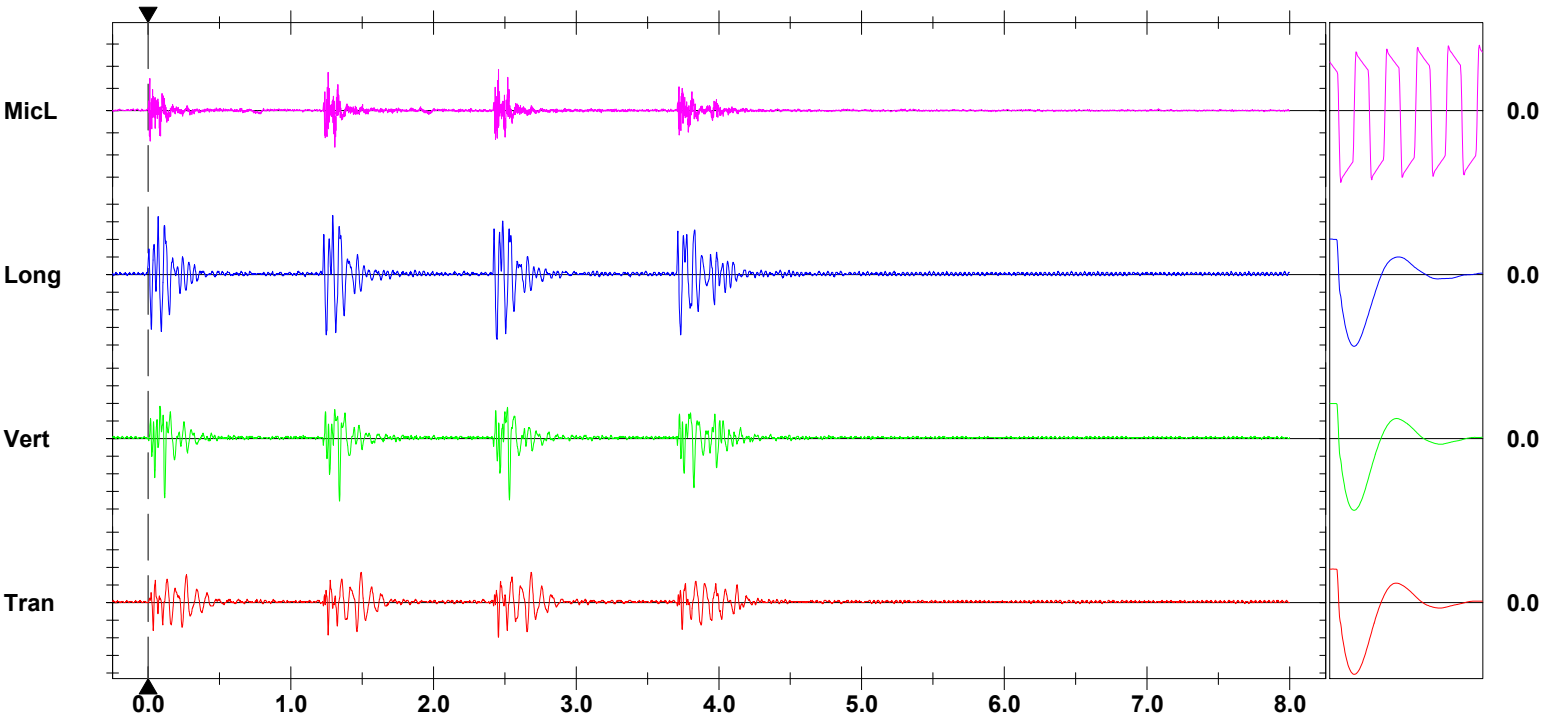

Time Scale: 0.50 sec/div **Amplitude Scale:** Geo: 2.00 mm/s/div Mic: 10.00 pa.(L)/div Sensorcheck
Trigger =

Event Report

Date/Time Long at 15:26:42 October 29, 2009
Trigger Source Geo: 1.27 mm/s
Range Geo :254 mm/s
Record Time 8.0 sec at 1024 sps
Job Number: 1

Serial Number BE13072 V 8.12-8.0 MiniMate Plus
Battery Level 6.3 Volts
Calibration December 7, 2007 by Instantel Inc.
File Name O072CYFX.KI0

Notes
Location:
Client:
User Name:
General:

Extended Notes
Combo Mode October 29, 2009 15:23:53

Post Event Notes

Microphone Linear Weighting
PSPL 15.8 pa.(L) at 2.563 sec
ZC Freq 64 Hz
Channel Test Passed (Freq = 20.5 Hz Amp = 625 mv)

	Tran	Vert	Long	
PPV	3.43	6.35	8.13	mm/s
ZC Freq	37	21	20	Hz
Time (Rel. to Trig)	1.309	1.385	3.837	sec
Peak Acceleration	0.0928	0.133	0.133	g
Peak Displacement	0.0317	0.0437	0.0643	mm
Sensorcheck	Passed	Passed	Passed	
Frequency	7.3	7.3	7.2	Hz
Overswing Ratio	3.7	3.6	4.1	

Peak Vector Sum 8.43 mm/s at 3.837 sec

USBM RI8507 And OSMRE

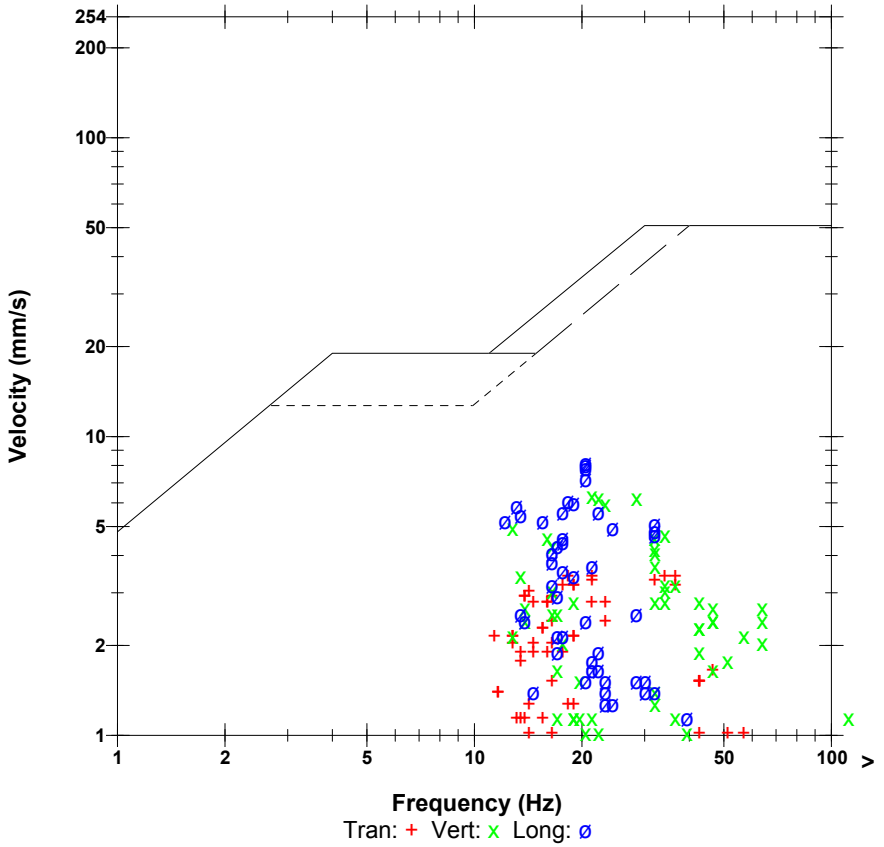

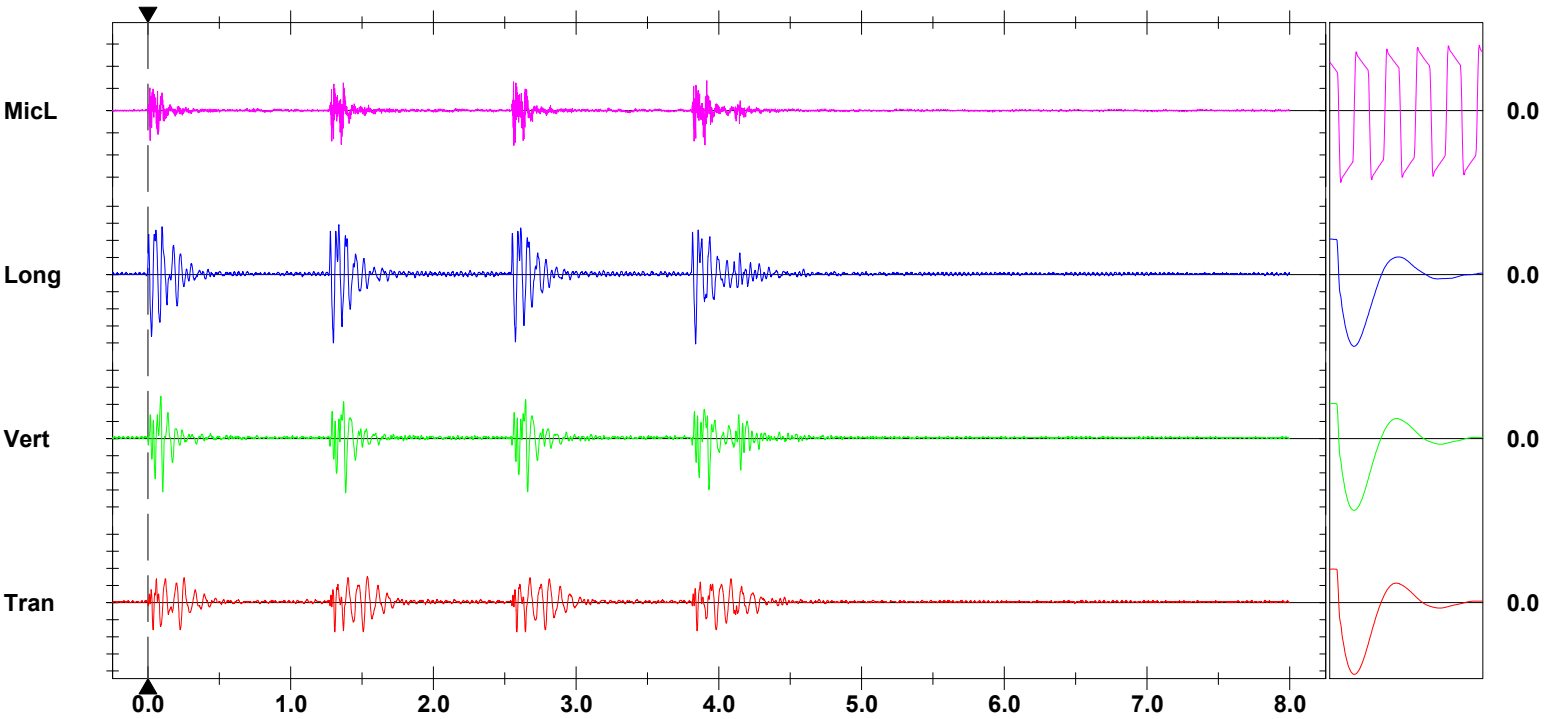

Time Scale: 0.50 sec/div **Amplitude Scale:** Geo: 2.00 mm/s/div Mic: 10.00 pa.(L)/div Sensorcheck
Trigger =

Event Report

Date/Time	Long at 15:26:58 October 29, 2009	**Serial Number**	BE13072 V 8.12-8.0 MiniMate Plus
Trigger Source	Geo: 1.27 mm/s	**Battery Level**	6.3 Volts
Range	Geo :254 mm/s	**Calibration**	December 7, 2007 by Instantel Inc.
Record Time	5.246 sec at 1024 sps	**File Name**	O072CYFX.KY0
Job Number:	1		

Notes
Location:
Client:
User Name:
General:

Extended Notes
Combo Mode October 29, 2009 15:23:53

Post Event Notes

Microphone Linear Weighting
PSPL 15.3 pa.(L) at 2.647 sec
ZC Freq >100 Hz
Channel Test Passed (Freq = 20.5 Hz Amp = 625 mv)

	Tran	Vert	Long	
PPV	3.43	6.10	7.87	mm/s
ZC Freq	18	32	20	Hz
Time (Rel. to Trig)	2.863	4.079	1.306	sec
Peak Acceleration	0.0663	0.119	0.133	g
Peak Displacement	0.0309	0.0486	0.0631	mm
Sensorcheck	Passed	Passed	Passed	
Frequency	7.3	7.3	7.2	Hz
Overswing Ratio	3.7	3.6	4.1	

Peak Vector Sum 8.46 mm/s at 0.050 sec

USBM RI8507 And OSMRE

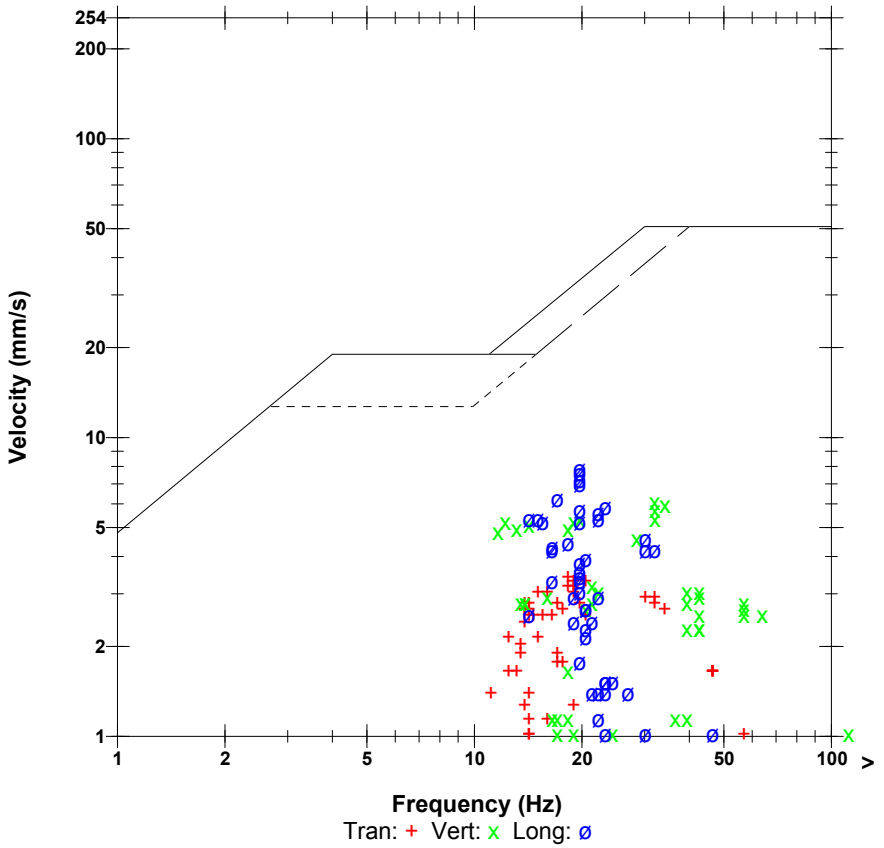

Monitor Log
Oct 29 /09 15:26:58 Oct 29 /09 15:27:04 Event recorded. (Memory Full Exit)

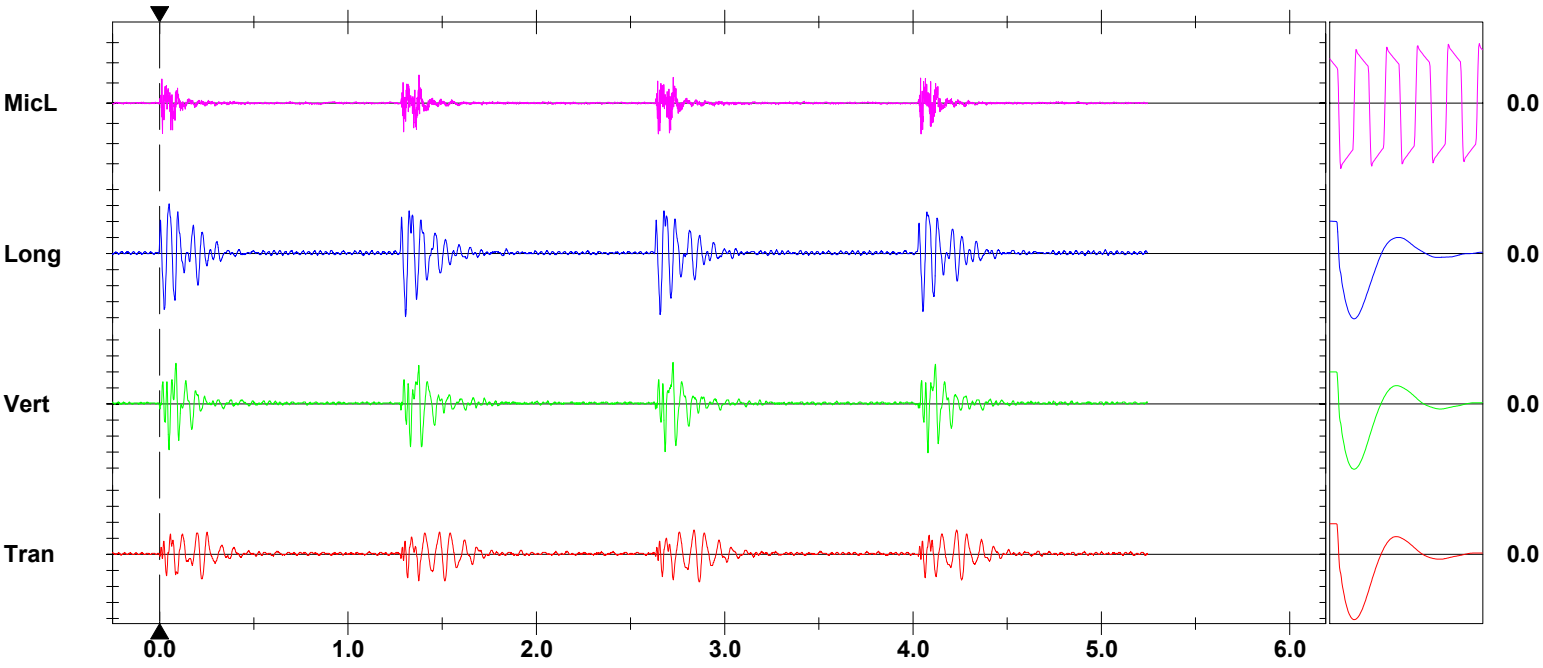

Time Scale: 0.50 sec/div **Amplitude Scale:** Geo: 2.00 mm/s/div Mic: 10.00 pa.(L)/div Sensorcheck
Trigger =

Field Vibration Data

Seismograph Unit # 5

at 25.3 feet from Test Pile #1

Non Driving Event

Event Report

Histogram Start Time	10:32:21 December 21, 2009	**Serial Number**	BE13072 V 8.12-8.0 MiniMate Plus
Histogram Finish Time	11:04:37 December 21, 2009	**Battery Level**	6.2 Volts
Number of Intervals	968 at 2 seconds	**Calibration**	December 7, 2007 by Instantel Inc.
Range	Geo :254 mm/s	**File Name**	O072D15P.9X0
Sample Rate	1024sps		
Job Number:	1		

Notes
Location:
Client:
User Name:
General:

Extended Notes

Post Event Notes

Microphone Linear Weighting
PSPL 3.25 pa.(L) on December 21, 2009 at 10:57:05
ZC Freq 7.8 Hz
Channel Test Passed (Freq = 20.1 Hz Amp = 675 mv)

	Tran	Vert	Long	
PPV	0.254	0.254	0.381	mm/s
ZC Freq	>100	>100	43	Hz
Date	Dec 21 /09	Dec 21 /09	Dec 21 /09	
Time	10:32:53	10:32:25	11:04:37	
Sensorcheck	Check	Check	Check	
Frequency	1024.0	1024.0	1024.0	Hz
Overswing Ratio	0.0	0.0	0.0	

Peak Vector Sum 0.524 mm/s on December 21, 2009 at 11:04:37

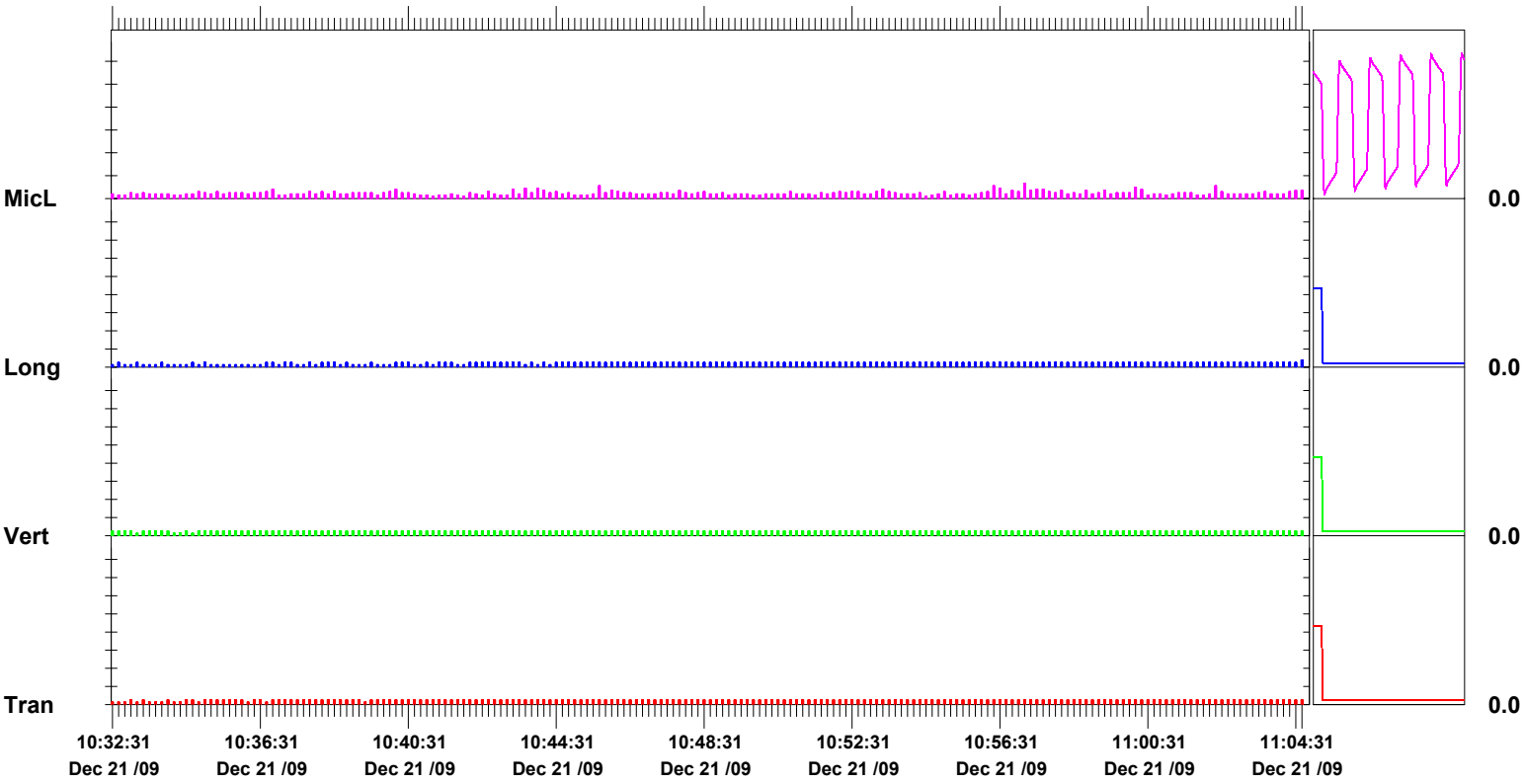

Time Scale: 10 seconds /div **Amplitude Scale:** Geo: 1.000 mm/s/div Mic: 5.00 pa.(L)/div Sensorcheck

Event Report

Histogram Start Time	11:32:29 December 21, 2009	**Serial Number**	BE13072 V 8.12-8.0 MiniMate Plus
Histogram Finish Time	11:55:25 December 21, 2009	**Battery Level**	6.1 Volts
Number of Intervals	688 at 2 seconds	**Calibration**	December 7, 2007 by Instantel Inc.
Range	Geo :254 mm/s	**File Name**	O072D15S.250
Sample Rate	1024sps		
Job Number:	1		

Notes
Location:
Client:
User Name:
General:

Extended Notes

Post Event Notes

Microphone Linear Weighting
PSPL 3.25 pa.(L) on December 21, 2009 at 11:44:33
ZC Freq 3.7 Hz
Channel Test Passed (Freq = 20.5 Hz Amp = 708 mv)

	Tran	Vert	Long	
PPV	0.254	0.254	0.254	mm/s
ZC Freq	>100	>100	>100	Hz
Date	Dec 21 /09	Dec 21 /09	Dec 21 /09	
Time	11:32:31	11:32:31	11:32:31	
Sensorcheck	Check	Check	Check	
Frequency	2.2	1024.0	1024.0	Hz
Overswing Ratio	2044.0	0.0	0.0	

Peak Vector Sum 0.440 mm/s on December 21, 2009 at 11:32:53

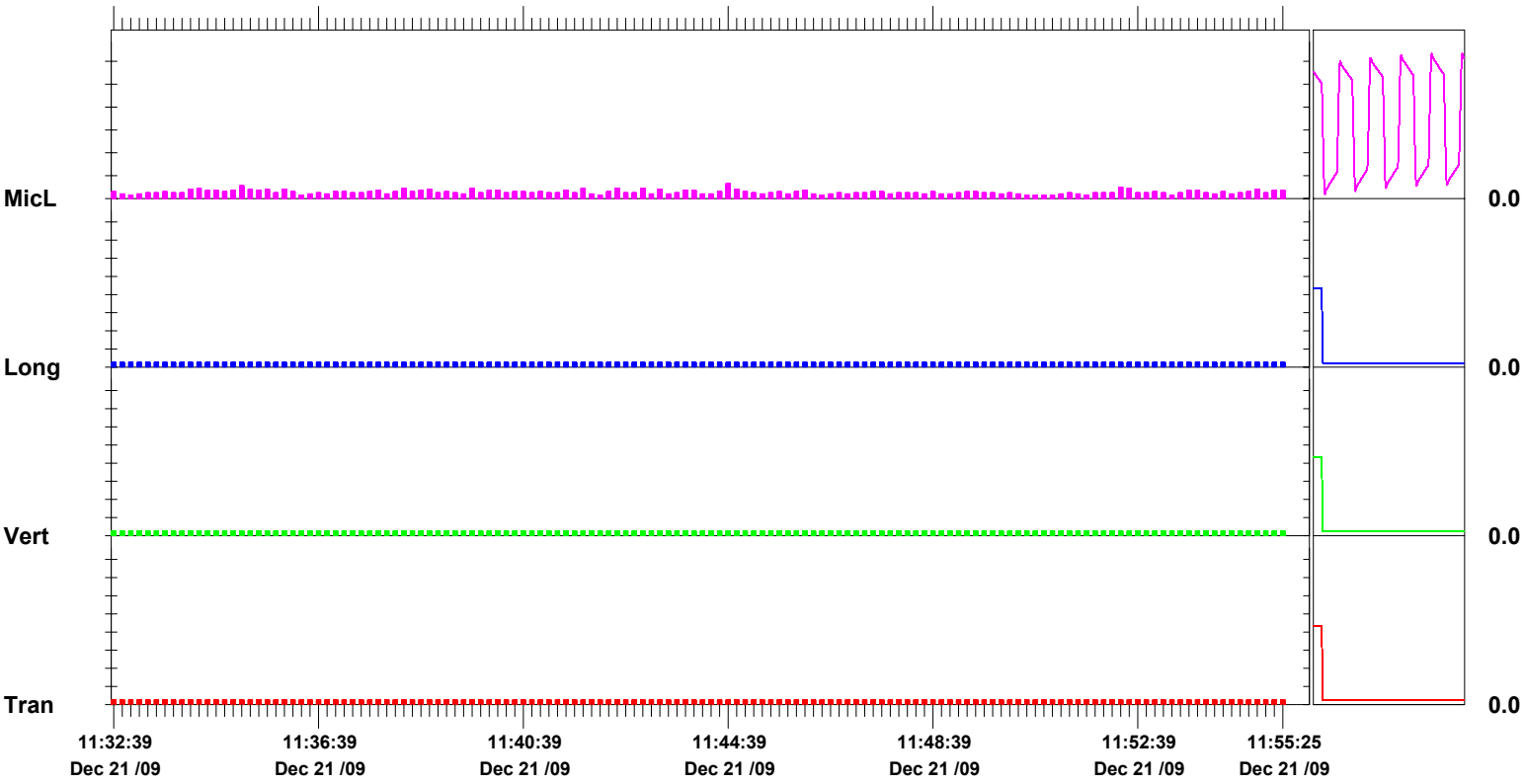

Time Scale: 10 seconds /div **Amplitude Scale:** Geo: 1.000 mm/s/div Mic: 5.00 pa.(L)/div Sensorcheck

Field Vibration Data

Seismograph Unit # 6

at 50.3 feet from Test Pile #1

Event Report

Histogram Start Time	14:17:12 October 29, 2009	**Serial Number**	BE13057 V 8.12-8.0 MiniMate Plus
Histogram Finish Time	14:25:59 October 29, 2009	**Battery Level**	6.3 Volts
Number of Intervals	263 at 2 seconds	**Calibration**	December 7, 2007 by Instantel Inc.
Range	Geo :254 mm/s	**File Name**	O057CYFU.CO0
Sample Rate	1024sps		
Job Number:	1		

Notes
Location:
Client:
User Name:
General:

Extended Notes

Post Event Notes

Microphone Linear Weighting
PSPL 17.3 pa.(L) on October 29, 2009 at 14:23:48
ZC Freq >100 Hz
Channel Test Passed (Freq = 20.1 Hz Amp = 647 mv)

	Tran	Vert	Long	
PPV	5.46	7.11	9.65	mm/s
ZC Freq	16	17	22	Hz
Date	Oct 29 /09	Oct 29 /09	Oct 29 /09	
Time	14:18:54	14:18:12	14:24:06	
Sensorcheck	Passed	Passed	Passed	
Frequency	7.3	7.4	7.2	Hz
Overswing Ratio	4.0	3.9	4.2	

Peak Vector Sum 9.77 mm/s on October 29, 2009 at 14:24:06

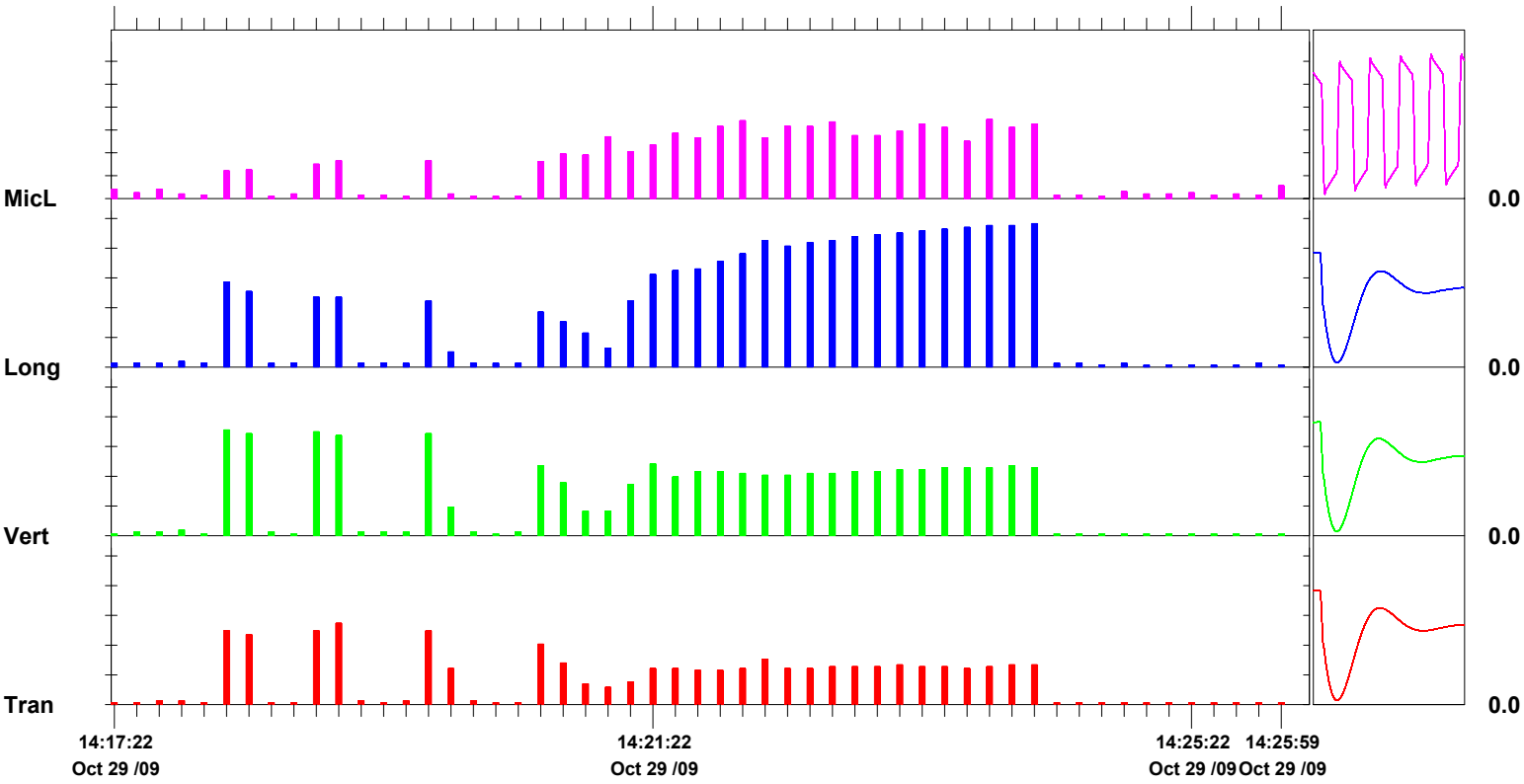

Time Scale: 10 seconds /div **Amplitude Scale:** Geo: 2.00 mm/s/div Mic: 5.00 pa.(L)/div Sensorcheck

Event Report

Date/Time	Long at 14:18:10 October 29, 2009	**Serial Number**	BE13057 V 8.12-8.0 MiniMate Plus
Trigger Source	Geo: 1.27 mm/s	**Battery Level**	6.3 Volts
Range	Geo :254 mm/s	**Calibration**	December 7, 2007 by Instantel Inc.
Record Time	8.0 sec at 1024 sps	**File Name**	O057CYFU.EA0
Job Number:	1		

Notes
Location:
Client:
User Name:
General:

Extended Notes
Combo Mode October 29, 2009 14:17:11

Post Event Notes

Microphone Linear Weighting
PSPL 6.25 pa.(L) at 2.340 sec
ZC Freq >100 Hz
Channel Test Passed (Freq = 20.1 Hz Amp = 647 mv)

	Tran	Vert	Long	
PPV	4.95	7.11	5.71	mm/s
ZC Freq	13	17	20	Hz
Time (Rel. to Trig)	1.260	0.154	0.144	sec
Peak Acceleration	0.0663	0.133	0.0928	g
Peak Displacement	0.0509	0.0695	0.0404	mm
Sensorcheck	Passed	Passed	Passed	
Frequency	7.3	7.4	7.2	Hz
Overswing Ratio	4.0	3.9	4.2	

Peak Vector Sum 8.05 mm/s at 2.443 sec

USBM RI8507 And OSMRE

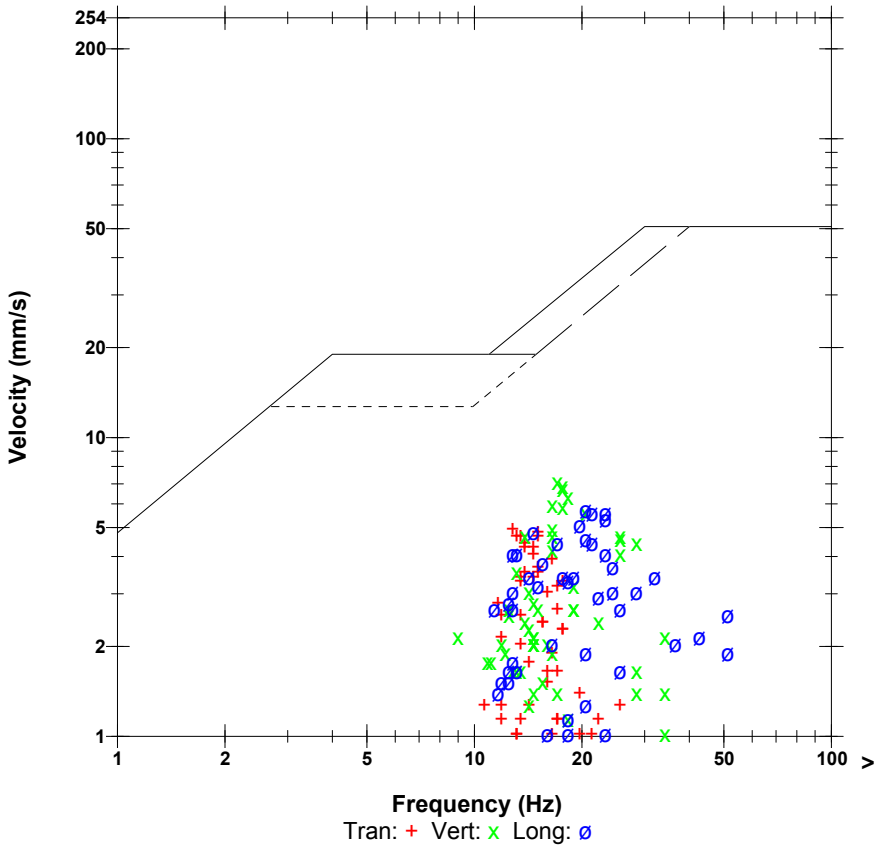

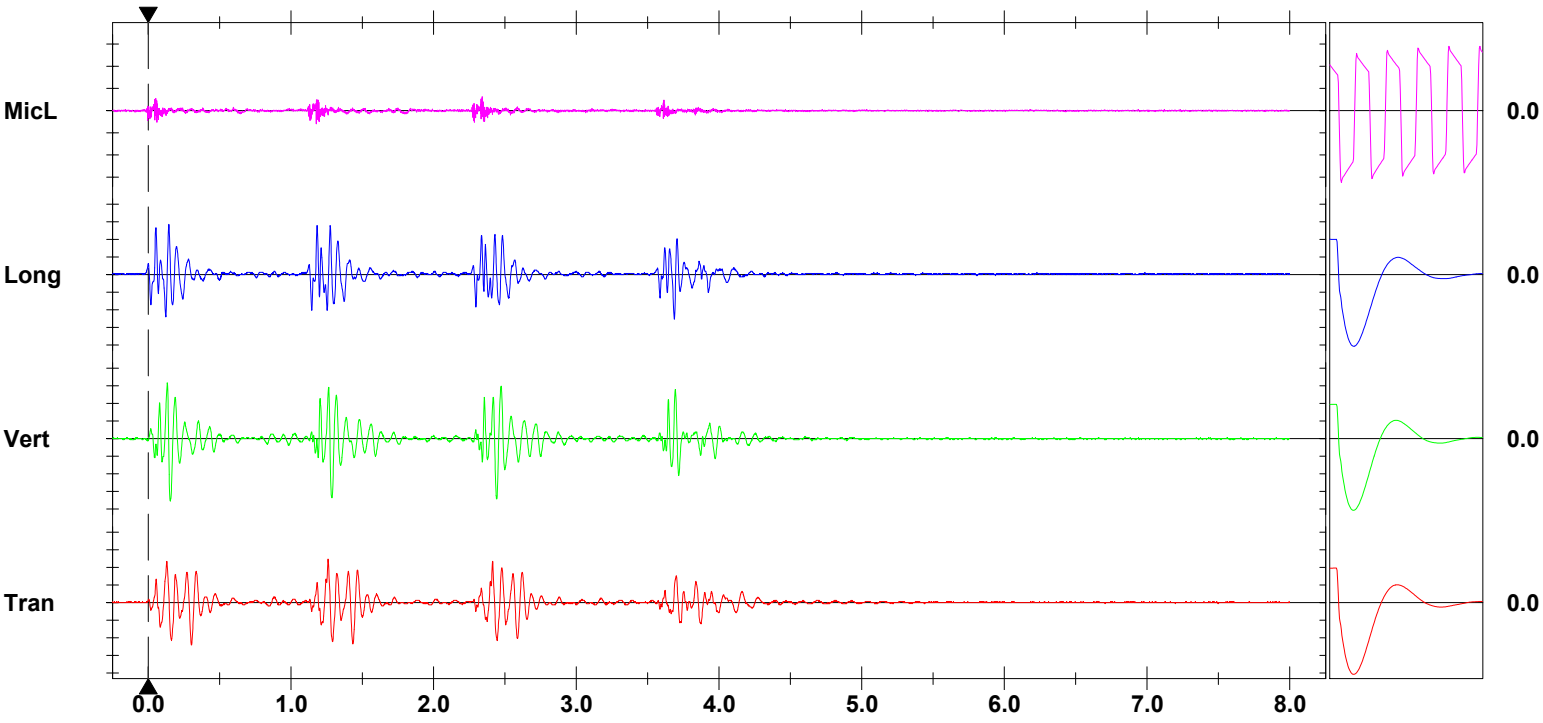

Time Scale: 0.50 sec/div **Amplitude Scale:** Geo: 2.00 mm/s/div Mic: 10.00 pa.(L)/div Sensorcheck
Trigger =

Event Report

Date/Time	Long at 14:18:50 October 29, 2009	**Serial Number**	BE13057 V 8.12-8.0 MiniMate Plus
Trigger Source	Geo: 1.27 mm/s	**Battery Level**	6.3 Volts
Range	Geo :254 mm/s	**Calibration**	December 7, 2007 by Instantel Inc.
Record Time	8.0 sec at 1024 sps	**File Name**	O057CYFU.FE0
Job Number:	1		

Notes
Location:
Client:
User Name:
General:

Extended Notes
Combo Mode October 29, 2009 14:17:11

Post Event Notes

Microphone Linear Weighting
PSPL 8.25 pa.(L) at 2.350 sec
ZC Freq >100 Hz
Channel Test Passed (Freq = 20.1 Hz Amp = 647 mv)

	Tran	Vert	Long	
PPV	5.46	6.98	4.70	mm/s
ZC Freq	16	17	17	Hz
Time (Rel. to Trig)	2.482	0.152	0.193	sec
Peak Acceleration	0.0663	0.106	0.0928	g
Peak Displacement	0.0528	0.0661	0.0412	mm
Sensorcheck	Passed	Passed	Passed	
Frequency	7.3	7.4	7.2	Hz
Overswing Ratio	4.0	3.9	4.2	

Peak Vector Sum 8.69 mm/s at 2.482 sec

USBM RI8507 And OSMRE

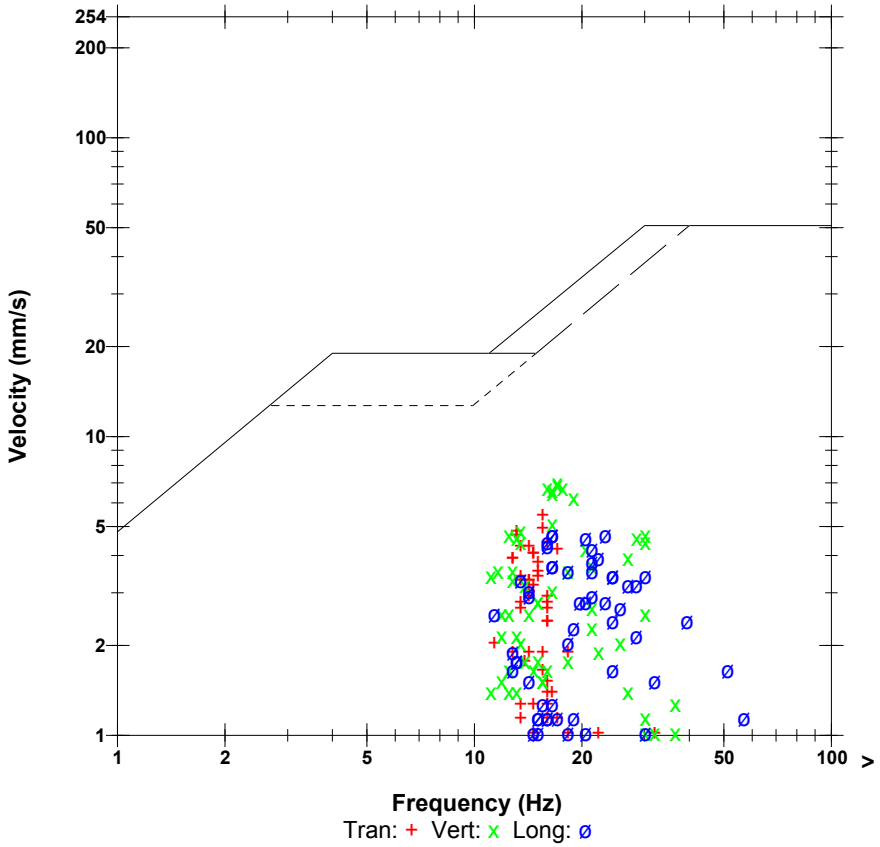

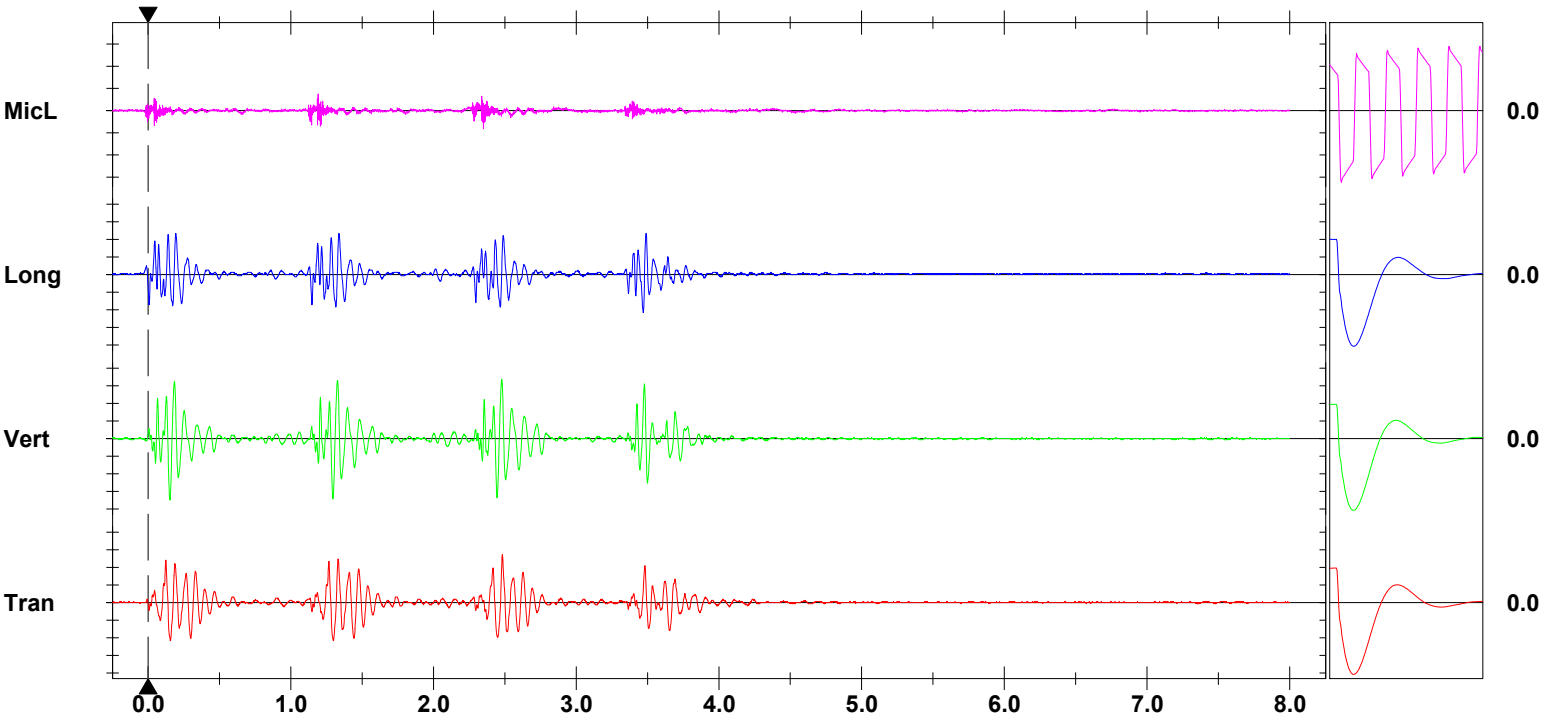

Time Scale: 0.50 sec/div **Amplitude Scale:** Geo: 2.00 mm/s/div Mic: 10.00 pa.(L)/div Sensorcheck
Trigger =

Event Report

Date/Time	Long at 14:19:38 October 29, 2009	**Serial Number**	BE13057 V 8.12-8.0 MiniMate Plus
Trigger Source	Geo: 1.27 mm/s	**Battery Level**	6.3 Volts
Range	Geo :254 mm/s	**Calibration**	December 7, 2007 by Instantel Inc.
Record Time	8.0 sec at 1024 sps	**File Name**	O057CYFU.GQ0
Job Number:	1		

Notes
Location:
Client:
User Name:
General:

Extended Notes
Combo Mode October 29, 2009 14:17:11

Post Event Notes

Microphone Linear Weighting
PSPL 8.25 pa.(L) at 2.374 sec
ZC Freq >100 Hz
Channel Test Passed (Freq = 20.1 Hz Amp = 647 mv)

	Tran	Vert	Long	
PPV	4.95	6.86	4.44	mm/s
ZC Freq	15	17	17	Hz
Time (Rel. to Trig)	3.799	0.155	0.196	sec
Peak Acceleration	0.0663	0.106	0.0795	g
Peak Displacement	0.0471	0.0653	0.0361	mm
Sensorcheck	Passed	Passed	Passed	
Frequency	7.3	7.4	7.2	Hz
Overswing Ratio	4.0	3.9	4.2	

Peak Vector Sum 8.36 mm/s at 0.191 sec

USBM RI8507 And OSMRE

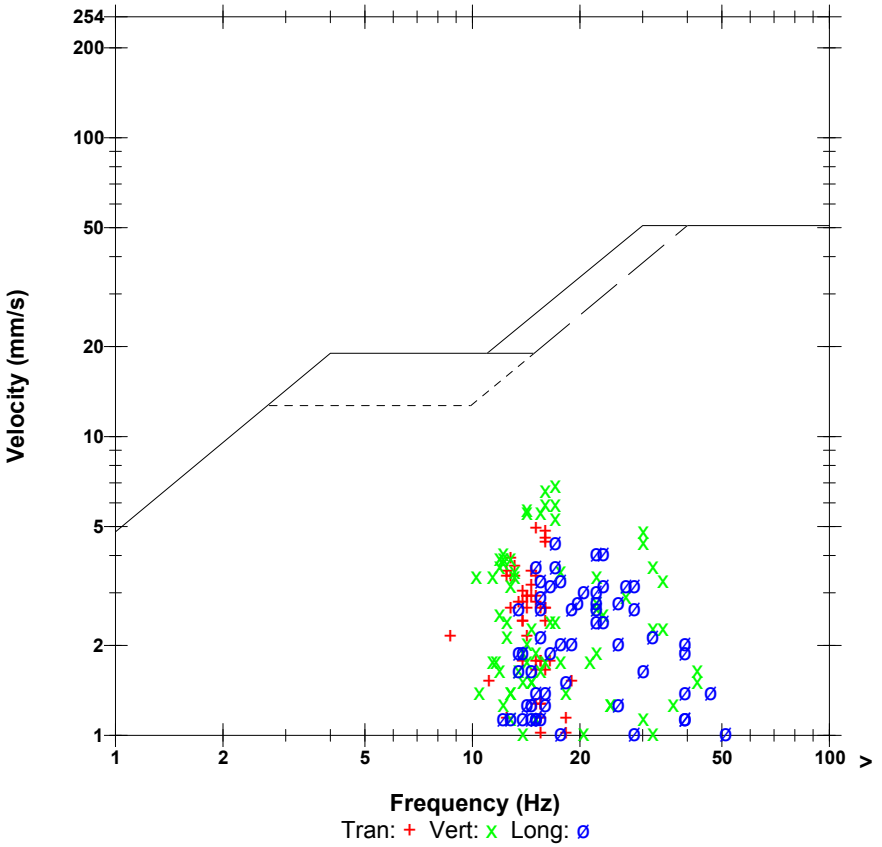

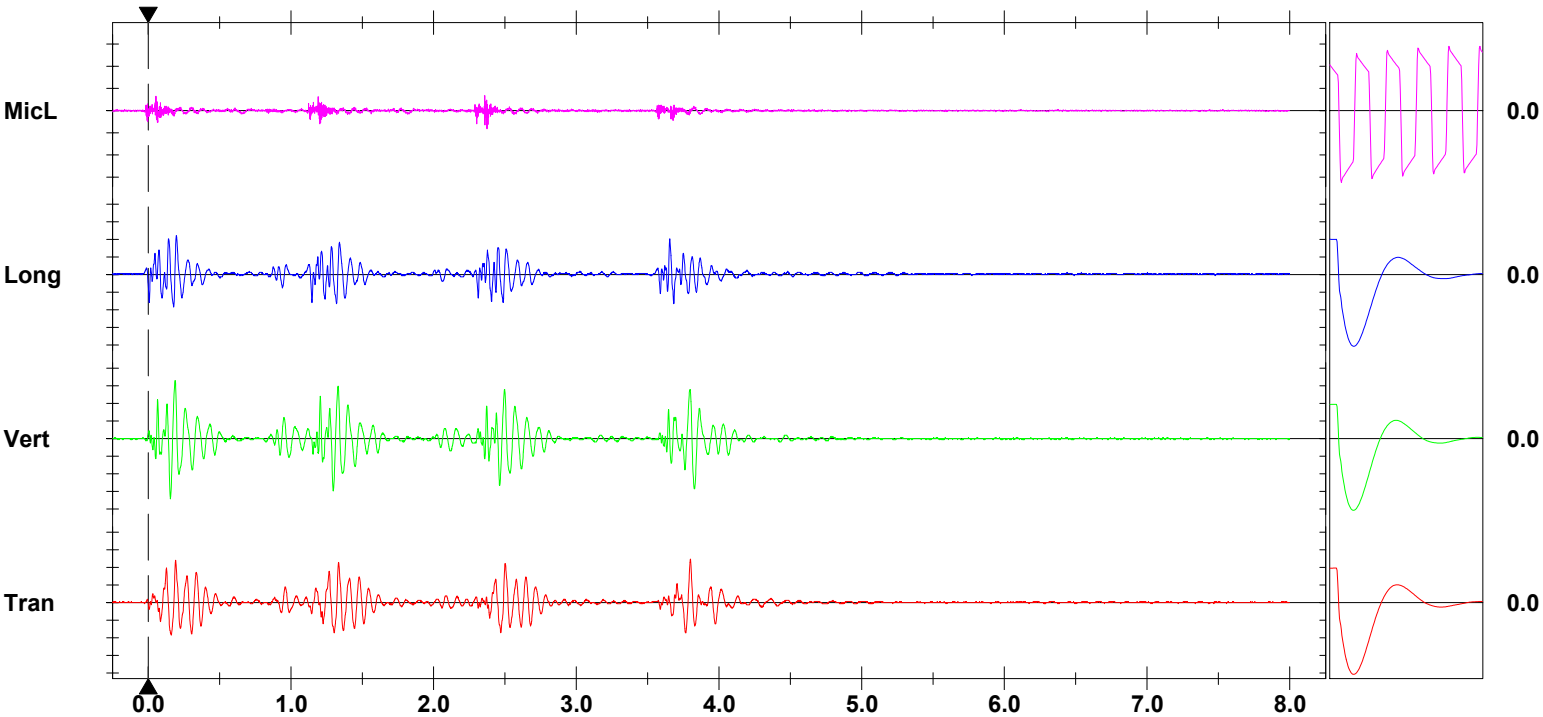

Time Scale: 0.50 sec/div **Amplitude Scale:** Geo: 2.00 mm/s/div Mic: 10.00 pa.(L)/div Sensorcheck
Trigger =

Field Vibration Data

Seismograph Unit # 6

at 49.7 feet from Test Pile #2

Event Report

Histogram Start Time	15:24:12 October 29, 2009	**Serial Number**	BE13057 V 8.12-8.0 MiniMate Plus
Histogram Finish Time	15:38:25 October 29, 2009	**Battery Level**	6.3 Volts
Number of Intervals	426 at 2 seconds	**Calibration**	December 7, 2007 by Instantel Inc.
Range	Geo :254 mm/s	**File Name**	O057CYFX.GC0
Sample Rate	1024sps		
Job Number:	1		

Notes
Location:
Client:
User Name:
General:

Extended Notes

Post Event Notes

Microphone Linear Weighting
PSPL 11.5 pa.(L) on October 29, 2009 at 15:37:00
ZC Freq >100 Hz
Channel Test Passed (Freq = 20.5 Hz Amp = 606 mv)

	Tran	Vert	Long	
PPV	5.97	5.84	7.11	mm/s
ZC Freq	28	24	24	Hz
Date	Oct 29 /09	Oct 29 /09	Oct 29 /09	
Time	15:32:20	15:31:10	15:32:20	
Sensorcheck	Passed	Passed	Passed	
Frequency	7.3	7.4	7.2	Hz
Overswing Ratio	4.1	4.0	4.2	

Peak Vector Sum 7.78 mm/s on October 29, 2009 at 15:33:24

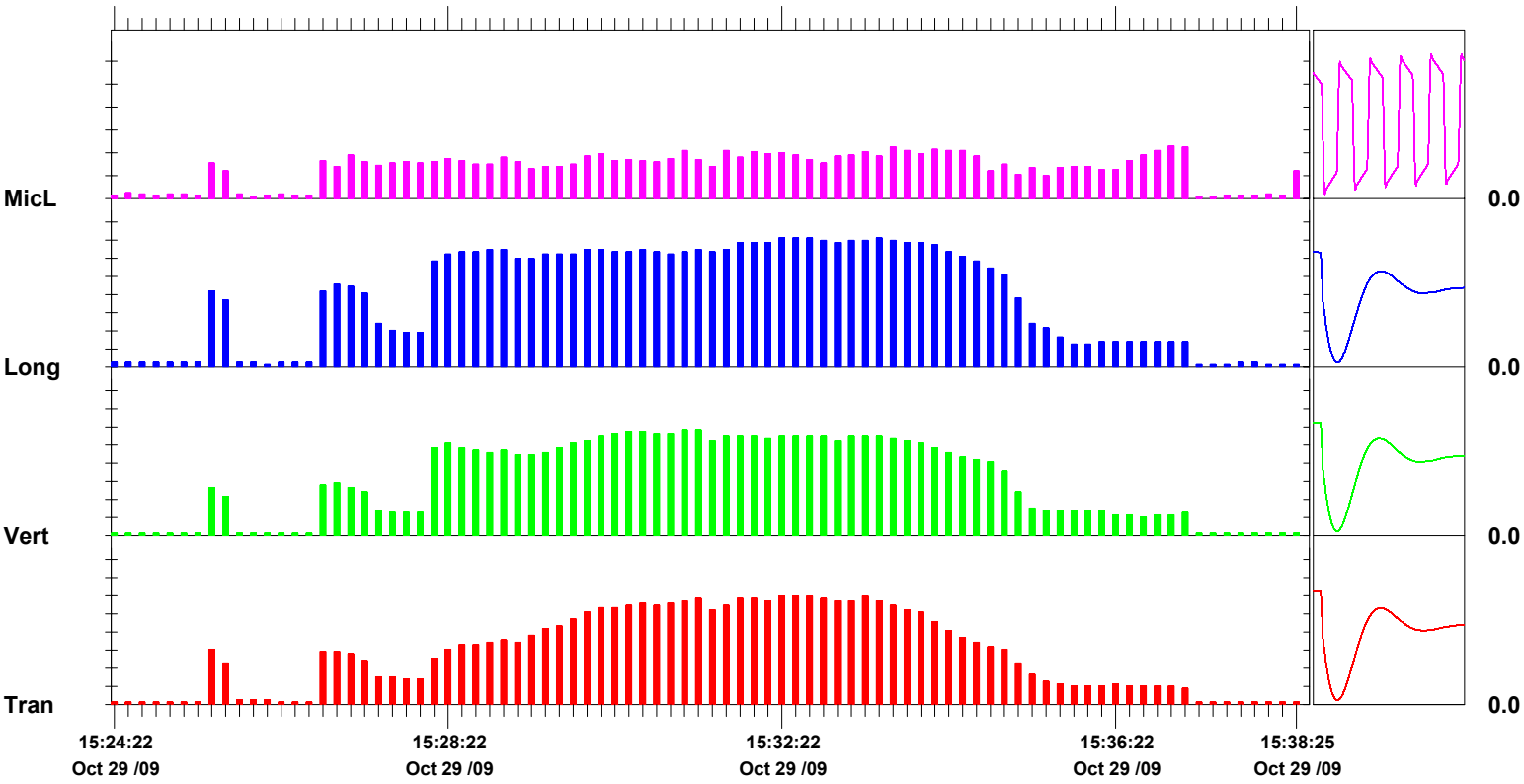

Time Scale: 10 seconds /div **Amplitude Scale:** Geo: 1.000 mm/s/div Mic: 5.00 pa.(L)/div Sensorcheck

Event Report

Date/Time	Long at 15:25:28 October 29, 2009	**Serial Number**	BE13057 V 8.12-8.0 MiniMate Plus
Trigger Source	Geo: 1.27 mm/s	**Battery Level**	6.3 Volts
Range	Geo :254 mm/s	**Calibration**	December 7, 2007 by Instantel Inc.
Record Time	8.0 sec at 1024 sps	**File Name**	O057CYFX.IG0
Job Number:	1		

Notes
Location:
Client:
User Name:
General:

Extended Notes
Combo Mode October 29, 2009 15:24:12

Post Event Notes

Microphone Linear Weighting
PSPL 7.75 pa.(L) at 1.317 sec
ZC Freq >100 Hz
Channel Test Passed (Freq = 20.5 Hz Amp = 606 mv)

	Tran	Vert	Long	
PPV	3.05	2.67	4.19	mm/s
ZC Freq	39	37	23	Hz
Time (Rel. to Trig)	2.477	2.490	2.535	sec
Peak Acceleration	0.0795	0.0663	0.0795	g
Peak Displacement	0.0193	0.0113	0.0293	mm
Sensorcheck	Passed	Passed	Passed	
Frequency	7.3	7.4	7.2	Hz
Overswing Ratio	4.1	4.0	4.2	

Peak Vector Sum 4.64 mm/s at 2.536 sec

USBM RI8507 And OSMRE

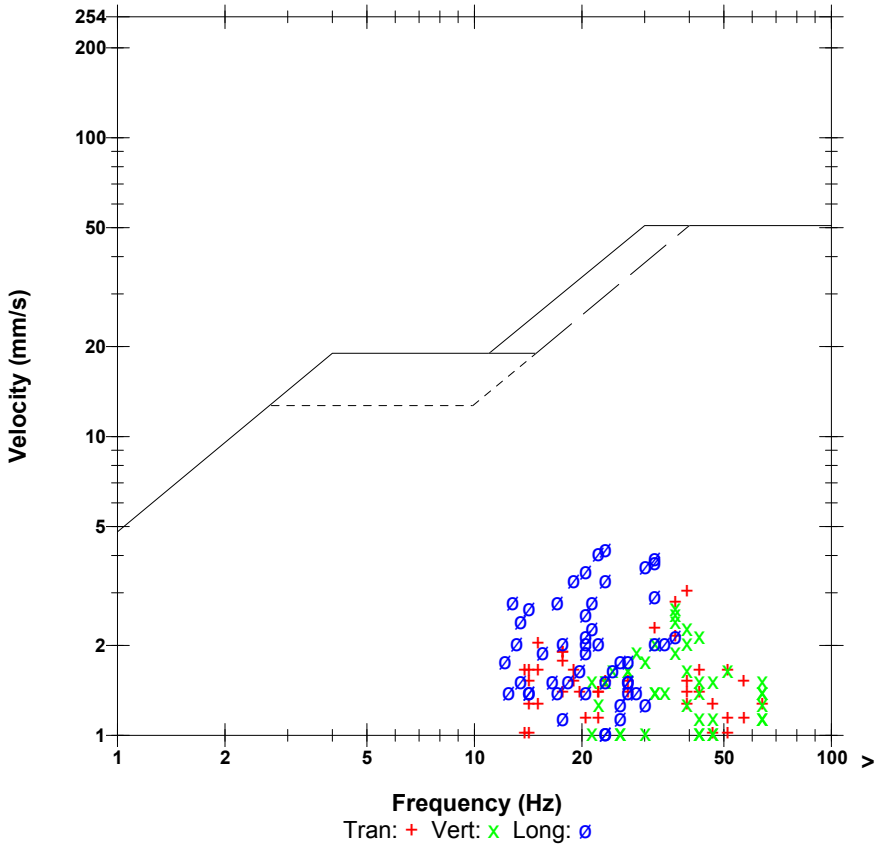

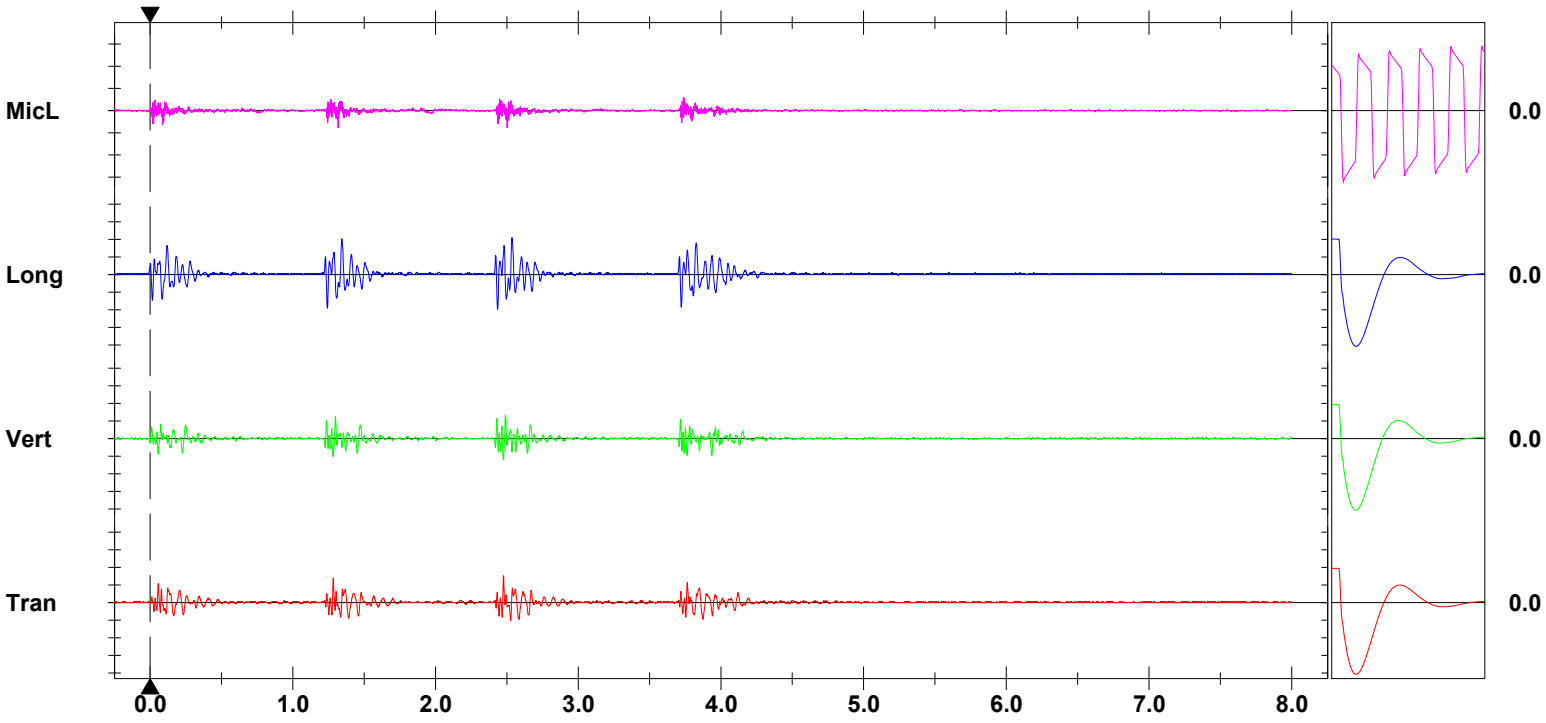

Time Scale: 0.50 sec/div **Amplitude Scale:** Geo: 2.00 mm/s/div Mic: 10.00 pa.(L)/div Sensorcheck
Trigger =

Event Report

Date/Time	Long at 15:26:42 October 29, 2009	**Serial Number**	BE13057 V 8.12-8.0 MiniMate Plus
Trigger Source	Geo: 1.27 mm/s	**Battery Level**	6.3 Volts
Range	Geo :254 mm/s	**Calibration**	December 7, 2007 by Instantel Inc.
Record Time	8.0 sec at 1024 sps	**File Name**	O057CYFX.KI0
Job Number:	1		

Notes
Location:
Client:
User Name:
General:

Extended Notes
Combo Mode October 29, 2009 15:24:12

Post Event Notes

Microphone Linear Weighting
PSPL 8.25 pa.(L) at 3.842 sec
ZC Freq >100 Hz
Channel Test Passed (Freq = 20.5 Hz Amp = 606 mv)

	Tran	Vert	Long	
PPV	2.92	2.79	4.19	mm/s
ZC Freq	37	39	32	Hz
Time (Rel. to Trig)	1.331	2.605	1.289	sec
Peak Acceleration	0.0928	0.0795	0.106	g
Peak Displacement	0.0215	0.0117	0.0319	mm
Sensorcheck	Passed	Passed	Passed	
Frequency	7.3	7.4	7.2	Hz
Overswing Ratio	4.1	4.0	4.2	

Peak Vector Sum 5.49 mm/s at 2.607 sec

USBM RI8507 And OSMRE

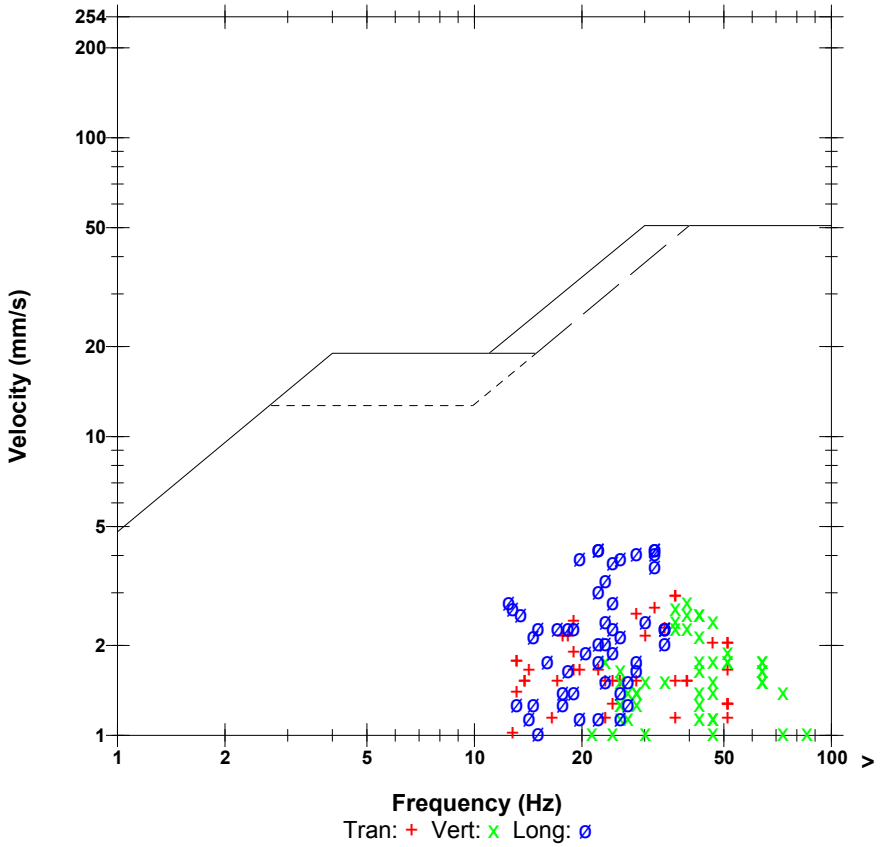

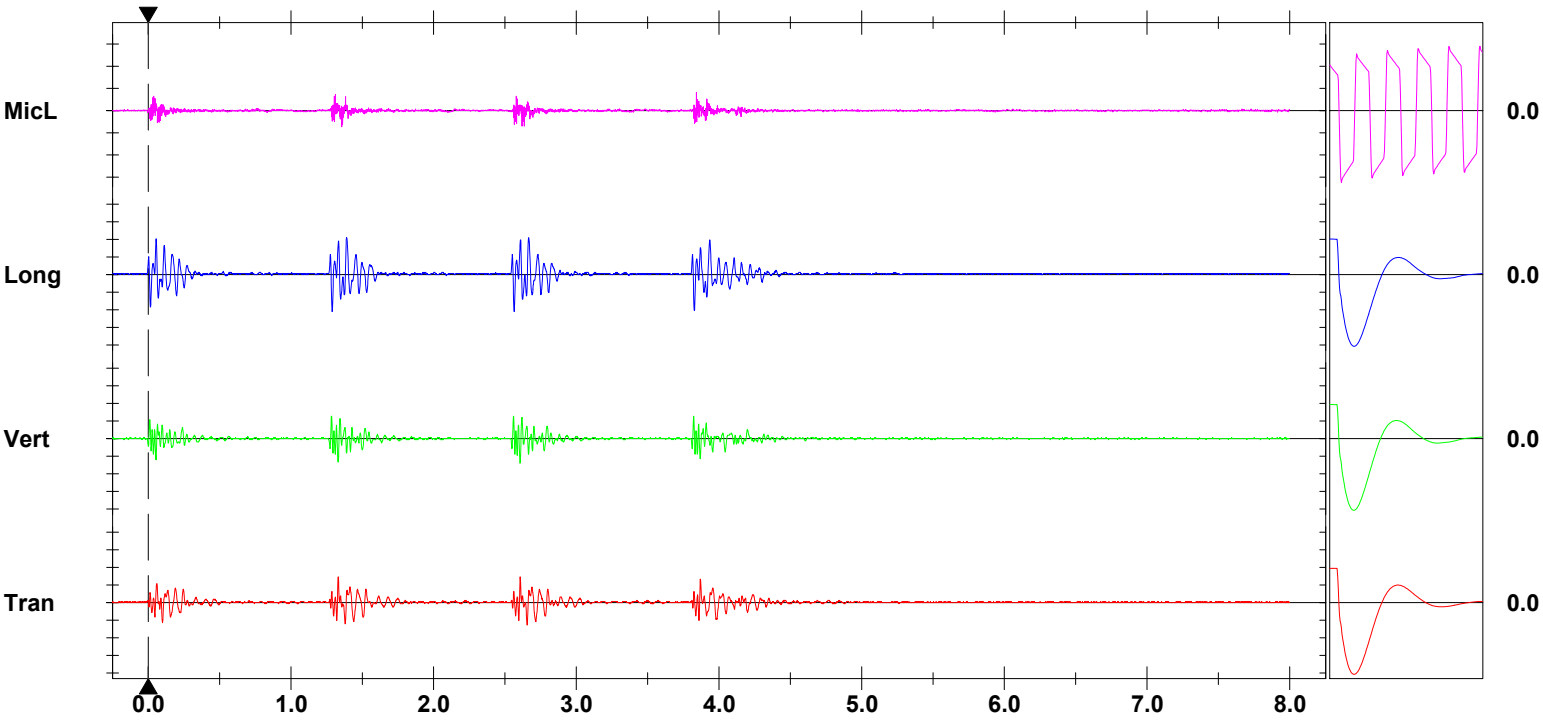

Time Scale: 0.50 sec/div **Amplitude Scale:** Geo: 2.00 mm/s/div Mic: 10.00 pa.(L)/div Sensorcheck
Trigger =

Event Report

Date/Time	Long at 15:26:58 October 29, 2009	**Serial Number**	BE13057 V 8.12-8.0 MiniMate Plus
Trigger Source	Geo: 1.27 mm/s	**Battery Level**	6.3 Volts
Range	Geo :254 mm/s	**Calibration**	December 7, 2007 by Instantel Inc.
Record Time	8.0 sec at 1024 sps	**File Name**	O057CYFX.KY0
Job Number:	1		

Notes
Location:
Client:
User Name:
General:

Extended Notes
Combo Mode October 29, 2009 15:24:12

Post Event Notes

Microphone Linear Weighting
PSPL 9.50 pa.(L) at 5.439 sec
ZC Freq >100 Hz
Channel Test Passed (Freq = 20.5 Hz Amp = 606 mv)

	Tran	Vert	Long	
PPV	2.92	2.92	4.57	mm/s
ZC Freq	37	39	28	Hz
Time (Rel. to Trig)	0.060	1.338	2.690	sec
Peak Acceleration	0.0795	0.0795	0.0928	g
Peak Displacement	0.0215	0.0133	0.0306	mm
Sensorcheck	Passed	Passed	Passed	
Frequency	7.3	7.4	7.2	Hz
Overswing Ratio	4.1	4.0	4.2	

Peak Vector Sum 5.68 mm/s at 1.339 sec

USBM RI8507 And OSMRE

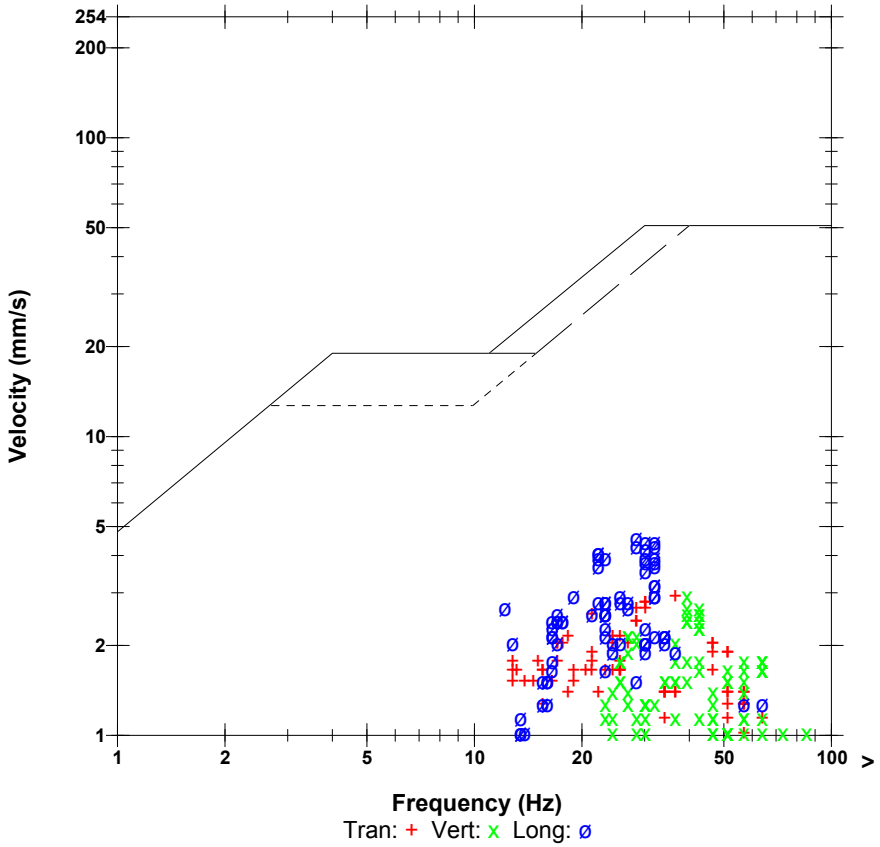

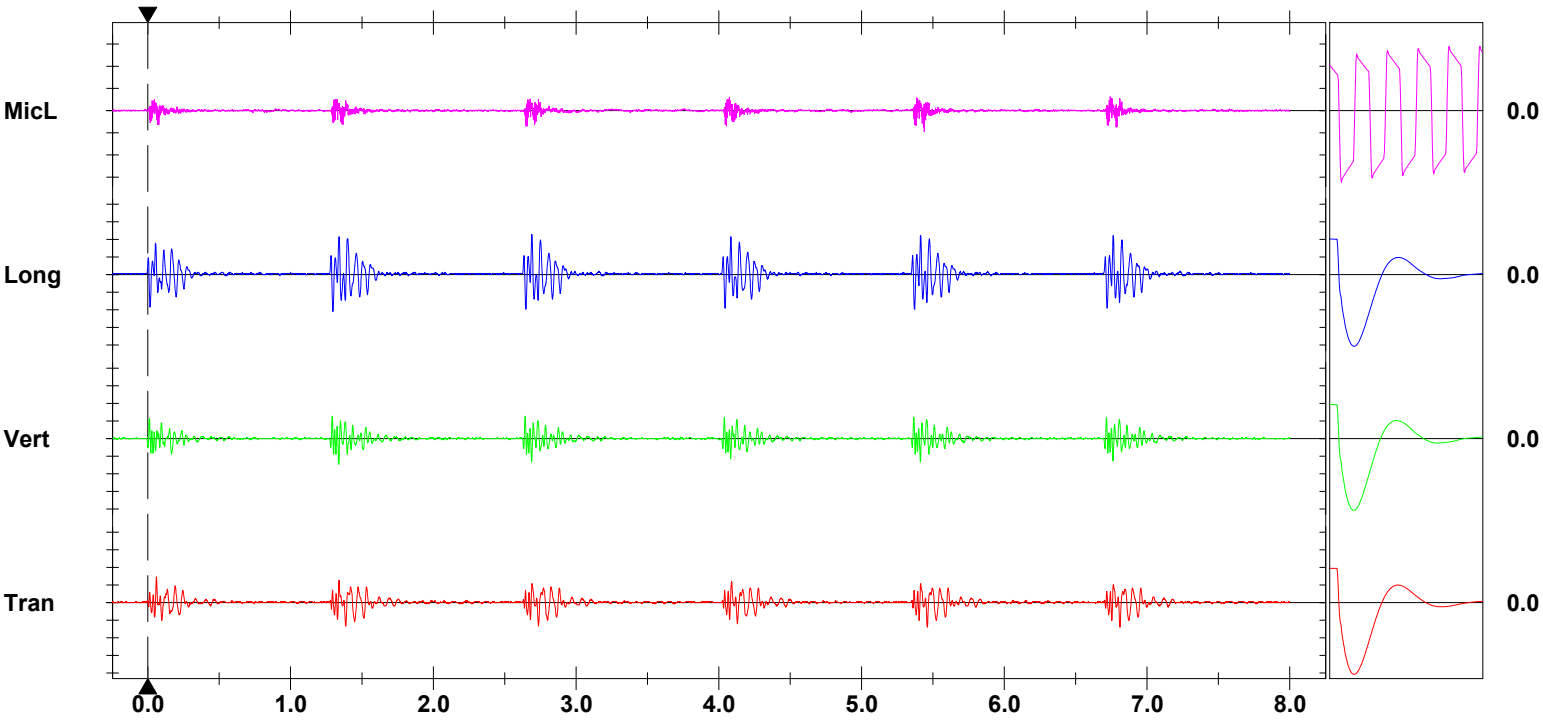

Time Scale: 0.50 sec/div **Amplitude Scale:** Geo: 2.00 mm/s/div Mic: 10.00 pa.(L)/div Sensorcheck
Trigger =

Field Vibration Data

Seismograph Unit # 6

at 50.3 feet from Test Pile #1

Non Driving Event

Event Report

Histogram Start Time	10:32:57 December 21, 2009	**Serial Number**	BE13057 V 8.12-8.0 MiniMate Plus
Histogram Finish Time	11:04:51 December 21, 2009	**Battery Level**	6.2 Volts
Number of Intervals	956 at 2 seconds	**Calibration**	December 7, 2007 by Instantel Inc.
Range	Geo :254 mm/s	**File Name**	O057D15P.AX0
Sample Rate	1024sps		
Job Number:	1		

Notes
Location:
Client:
User Name:
General:

Extended Notes

Post Event Notes

Microphone Linear Weighting
PSPL 3.50 pa.(L) on December 21, 2009 at 11:01:09
ZC Freq 4.0 Hz
Channel Test Passed (Freq = 20.1 Hz Amp = 676 mv)

	Tran	Vert	Long	
PPV	0.127	0.127	0.254	mm/s
ZC Freq	>100	>100	>100	Hz
Date	Dec 21 /09	Dec 21 /09	Dec 21 /09	
Time	10:32:59	10:32:59	10:45:41	
Sensorcheck	Check	Check	Check	
Frequency	1024.0	1024.0	1024.0	Hz
Overswing Ratio	0.0	0.0	0.0	

Peak Vector Sum 0.311 mm/s on December 21, 2009 at 10:49:59

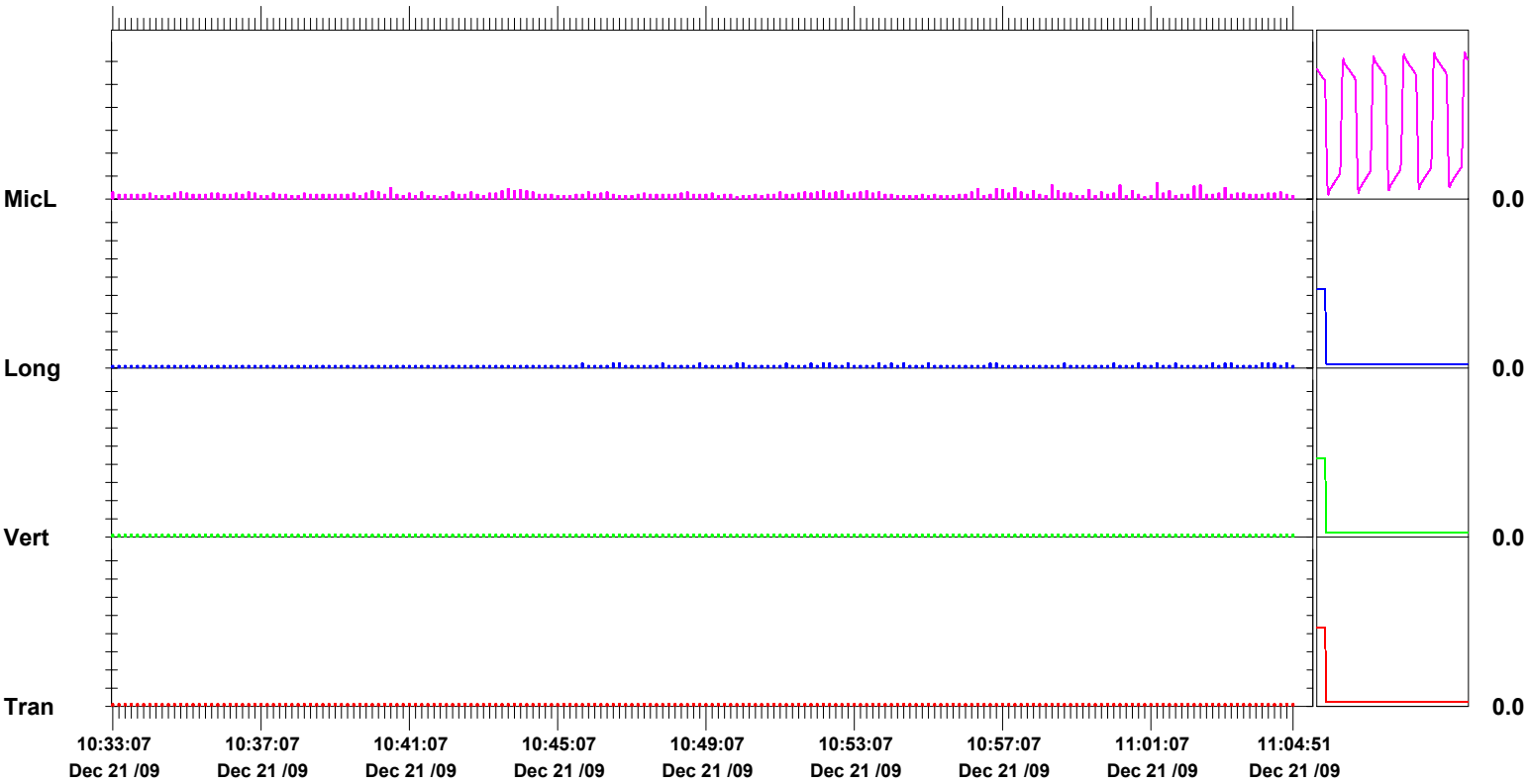

Time Scale: 10 seconds /div **Amplitude Scale:** Geo: 1.000 mm/s/div Mic: 5.00 pa.(L)/div Sensorcheck

Event Report

Histogram Start Time	11:33:02 December 21, 2009	**Serial Number**	BE13057 V 8.12-8.0 MiniMate Plus
Histogram Finish Time	11:55:42 December 21, 2009	**Battery Level**	6.2 Volts
Number of Intervals	680 at 2 seconds	**Calibration**	December 7, 2007 by Instantel Inc.
Range	Geo :254 mm/s	**File Name**	O057D15S.320
Sample Rate	1024sps		
Job Number:	1		

Notes
Location:
Client:
User Name:
General:

Extended Notes

Post Event Notes

Microphone Linear Weighting
PSPL 4.50 pa.(L) on December 21, 2009 at 11:41:50
ZC Freq 15 Hz
Channel Test Passed (Freq = 20.1 Hz Amp = 746 mv)

	Tran	Vert	Long	
PPV	0.127	0.127	0.254	mm/s
ZC Freq	N/A	>100	>100	Hz
Date	Dec 21 /09	Dec 21 /09	Dec 21 /09	
Time	11:33:04	11:33:04	11:33:58	
Sensorcheck	Check	Check	Check	
Frequency	1024.0	60.2	1024.0	Hz
Overswing Ratio	0.0	1.0	0.0	

Peak Vector Sum 0.311 mm/s on December 21, 2009 at 11:33:58

N/A: Not Applicable

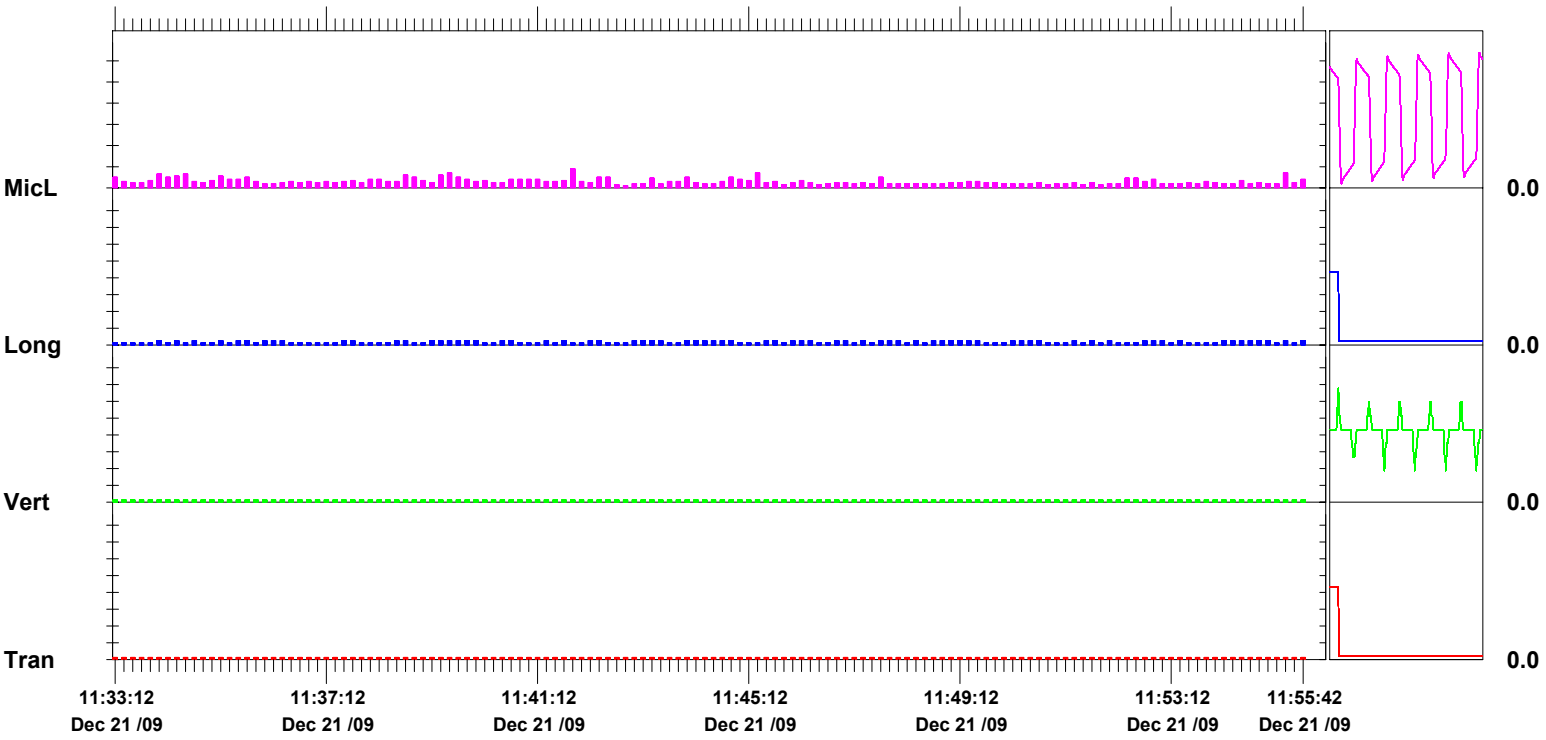

Time Scale: 10 seconds /div **Amplitude Scale:** Geo: 1.000 mm/s/div Mic: 5.00 pa.(L)/div Sensorcheck

Field Vibration Data

Seismograph Unit # 7 in casing

at 13.6 feet from Test Pile #1

Event Report

Histogram Start Time	14:17:11 October 29, 2009	**Serial Number**	BE13075 V 8.12-8.0 MiniMate Plus
Histogram Finish Time	14:25:55 October 29, 2009	**Battery Level**	6.3 Volts
Number of Intervals	261 at 2 seconds	**Calibration**	December 7, 2007 by Instantel Inc.
Range	Geo :254 mm/s	**File Name**	O075CYFU.CN0
Sample Rate	1024sps		
Job Number:	1		

Notes
Location:
Client:
User Name:
General:

Extended Notes

Post Event Notes

Microphone Linear Weighting
PSPL 2.75 pa.(L) on October 29, 2009 at 14:18:09
ZC Freq 27 Hz
Channel Test Check (Freq = 0.0 Hz Amp = 0 mv)

	Tran	Vert	Long	
PPV	29.1	27.8	30.6	mm/s
ZC Freq	16	18	18	Hz
Date	Oct 29 /09	Oct 29 /09	Oct 29 /09	
Time	14:18:09	14:18:09	14:18:49	
Sensorcheck	Passed	Passed	Passed	
Frequency	7.4	7.6	7.2	Hz
Overswing Ratio	3.9	3.5	4.1	

Peak Vector Sum 42.1 mm/s on October 29, 2009 at 14:18:09

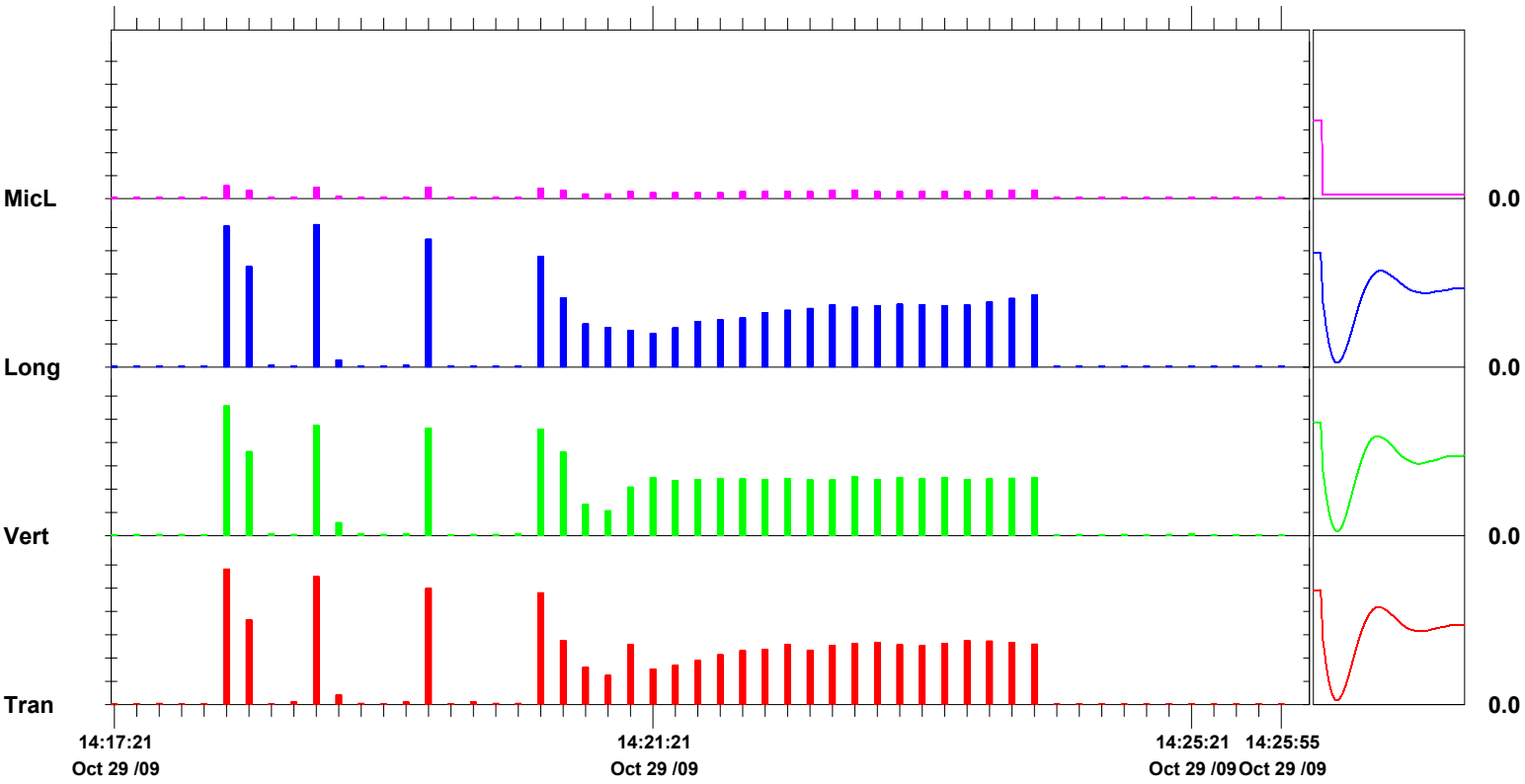

Time Scale: 10 seconds /div **Amplitude Scale:** Geo: 5.00 mm/s/div Mic: 5.00 pa.(L)/div Sensorcheck

Event Report

Date/Time	Vert at 14:18:07 October 29, 2009	**Serial Number**	BE13075 V 8.12-8.0 MiniMate Plus
Trigger Source	Geo: 1.27 mm/s	**Battery Level**	6.2 Volts
Range	Geo :254 mm/s	**Calibration**	December 7, 2007 by Instantel Inc.
Record Time	8.0 sec at 1024 sps	**File Name**	O075CYFU.E70
Job Number:	1		

Notes
Location:
Client:
User Name:
General:

Extended Notes
Combo Mode October 29, 2009 14:17:10

Post Event Notes

Microphone Linear Weighting
PSPL 2.75 pa.(L) at 0.086 sec
ZC Freq 27 Hz
Channel Test Check (Freq = 0.0 Hz Amp = 0 mv)

	Tran	Vert	Long	
PPV	29.1	27.8	30.2	mm/s
ZC Freq	16	18	22	Hz
Time (Rel. to Trig)	0.061	0.074	0.061	sec
Peak Acceleration	0.795	0.504	0.968	g
Peak Displacement	0.172	0.214	0.187	mm
Sensorcheck	Passed	Passed	Passed	
Frequency	7.4	7.6	7.2	Hz
Overswing Ratio	3.9	3.5	4.1	

Peak Vector Sum 42.1 mm/s at 0.061 sec

USBM RI8507 And OSMRE

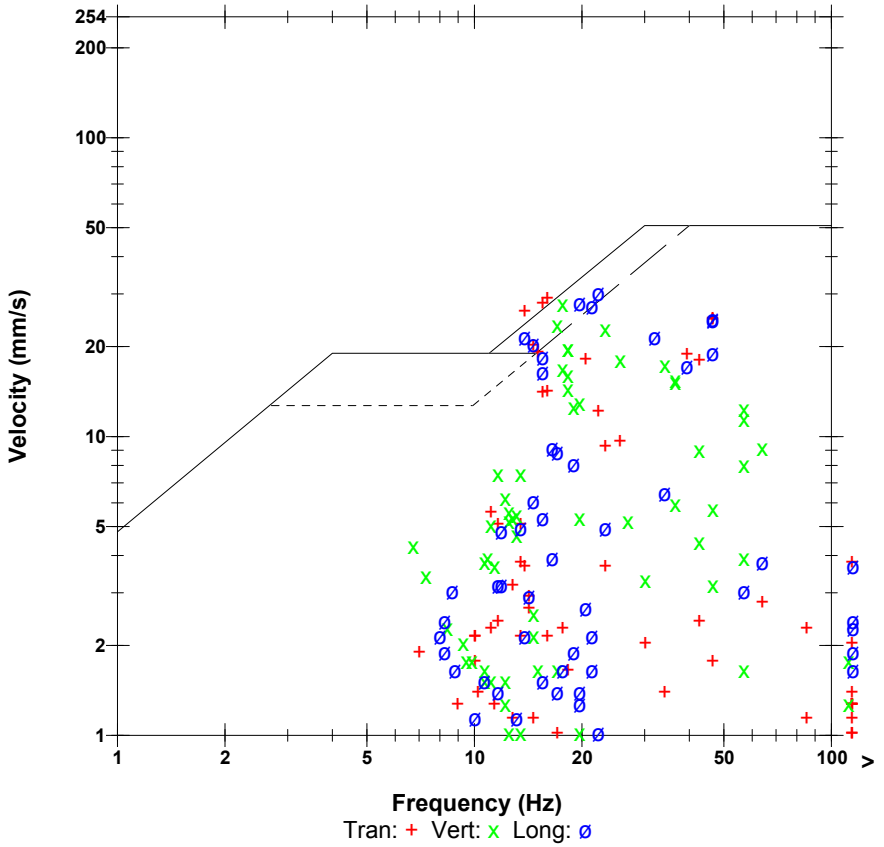

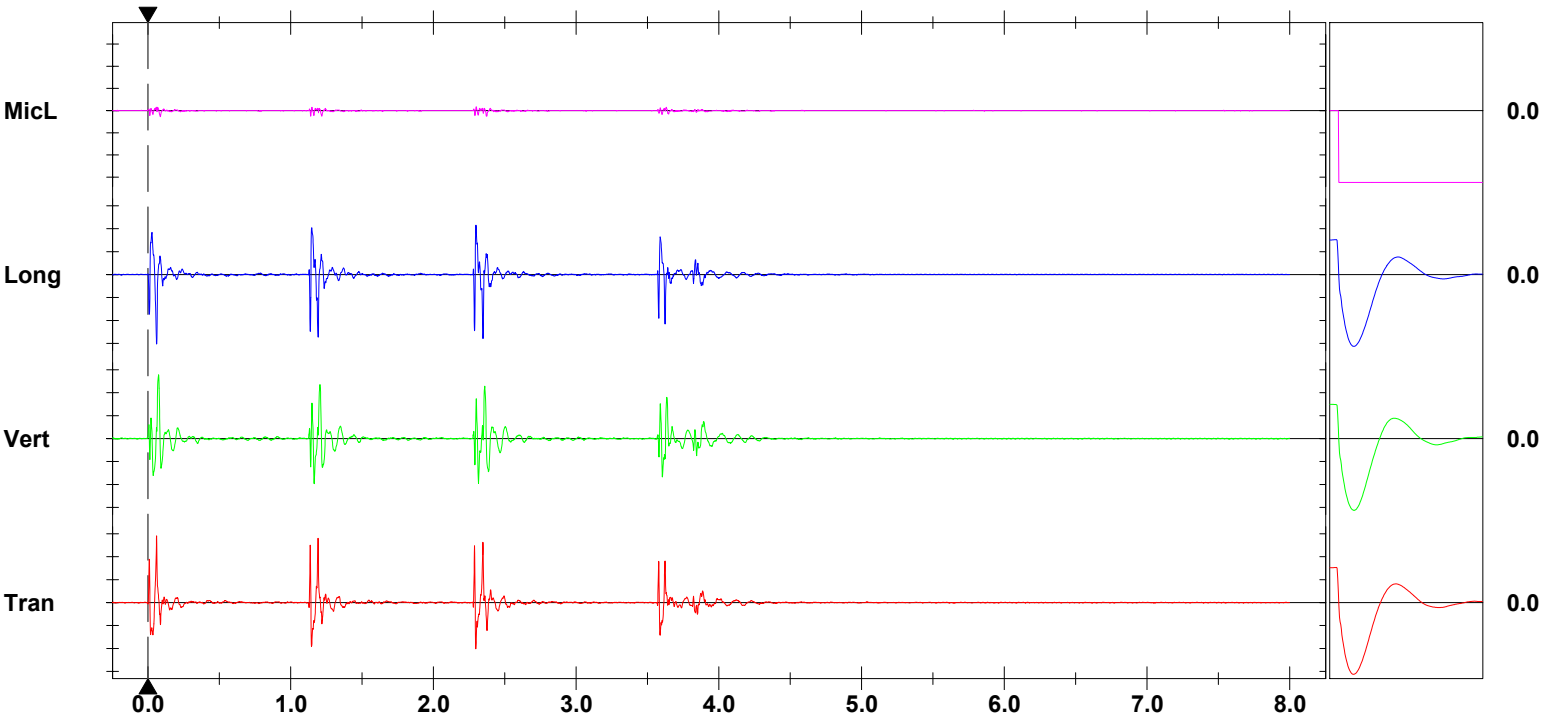

Time Scale: 0.50 sec/div **Amplitude Scale:** Geo: 10.00 mm/s/div Mic: 10.00 pa.(L)/div Sensorcheck
Trigger =

Event Report

Date/Time Vert at 14:18:47 October 29, 2009
Trigger Source Geo: 1.27 mm/s
Range Geo :254 mm/s
Record Time 8.0 sec at 1024 sps
Job Number: 1

Serial Number BE13075 V 8.12-8.0 MiniMate Plus
Battery Level 6.2 Volts
Calibration December 7, 2007 by Instantel Inc.
File Name O075CYFU.FB0

Notes
Location:
Client:
User Name:
General:

Extended Notes
Combo Mode October 29, 2009 14:17:10

Post Event Notes

Microphone Linear Weighting
PSPL 2.50 pa.(L) at 0.094 sec
ZC Freq 28 Hz
Channel Test Check (Freq = 0.0 Hz Amp = 0 mv)

	Tran	Vert	Long	
PPV	27.4	23.6	30.6	mm/s
ZC Freq	18	24	18	Hz
Time (Rel. to Trig)	0.069	0.082	1.213	sec
Peak Acceleration	0.822	0.530	1.15	g
Peak Displacement	0.152	0.159	0.165	mm
Sensorcheck	Passed	Passed	Passed	
Frequency	7.4	7.6	7.2	Hz
Overswing Ratio	3.9	3.5	4.1	

Peak Vector Sum 41.0 mm/s at 1.213 sec

USBM RI8507 And OSMRE

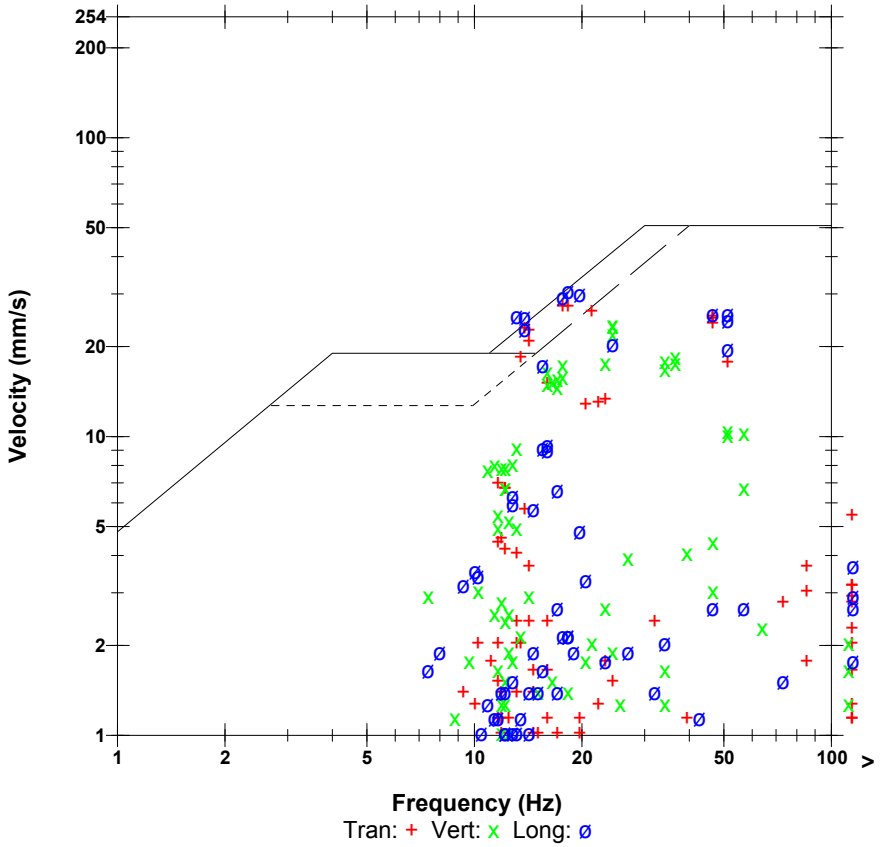

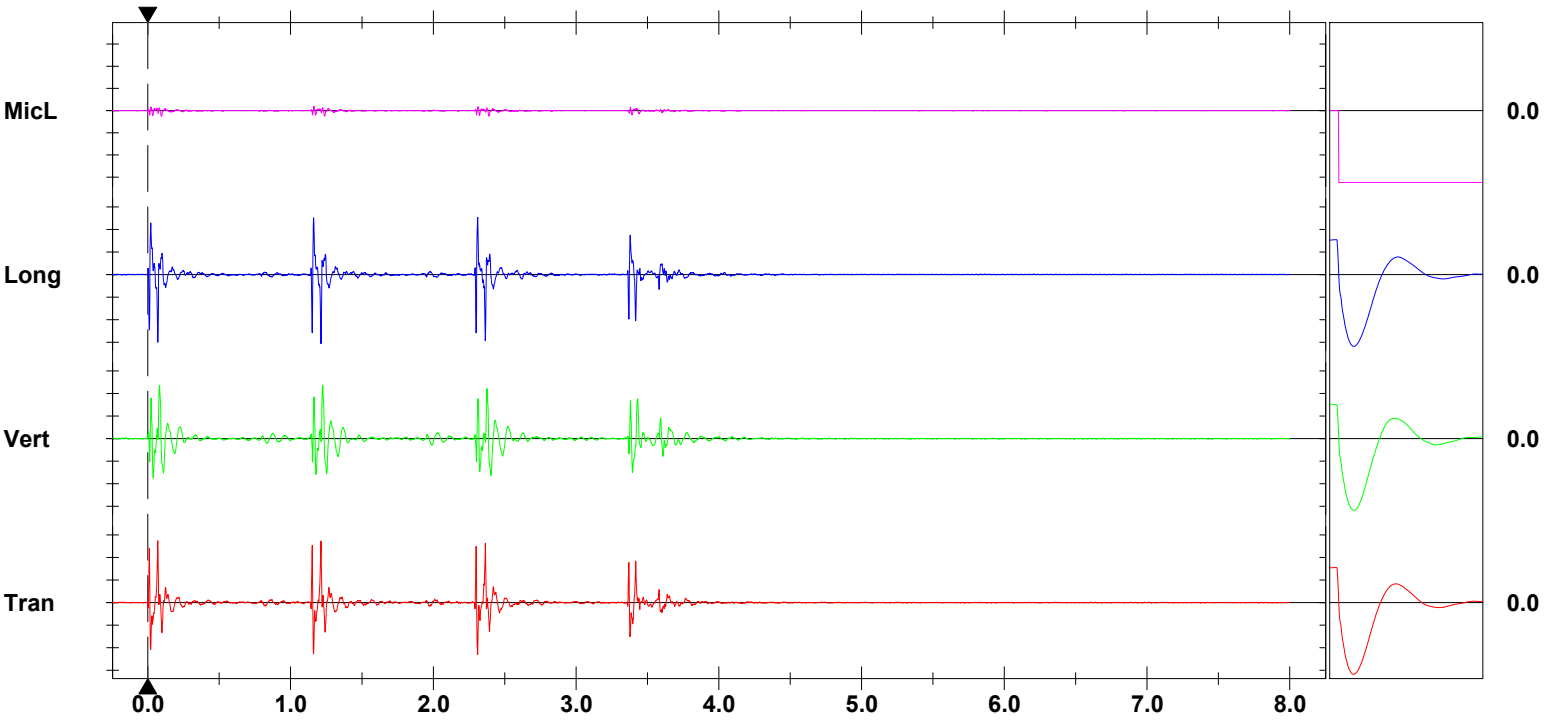

Time Scale: 0.50 sec/div **Amplitude Scale:** Geo: 10.00 mm/s/div Mic: 10.00 pa.(L)/div Sensorcheck
Trigger =

Event Report

Date/Time	Vert at 14:19:35 October 29, 2009	**Serial Number**	BE13075 V 8.12-8.0 MiniMate Plus
Trigger Source	Geo: 1.27 mm/s	**Battery Level**	6.2 Volts
Range	Geo :254 mm/s	**Calibration**	December 7, 2007 by Instantel Inc.
Record Time	8.0 sec at 1024 sps	**File Name**	O075CYFU.GN0
Job Number:	1		

Notes
Location:
Client:
User Name:
General:

Extended Notes
Combo Mode October 29, 2009 14:17:10

Post Event Notes

Microphone Linear Weighting
PSPL 2.50 pa.(L) at 0.033 sec
ZC Freq 47 Hz
Channel Test Check (Freq = 0.0 Hz Amp = 0 mv)

	Tran	Vert	Long	
PPV	24.9	23.1	27.4	mm/s
ZC Freq	21	24	18	Hz
Time (Rel. to Trig)	0.074	0.086	0.074	sec
Peak Acceleration	0.782	0.703	1.10	g
Peak Displacement	0.135	0.182	0.134	mm
Sensorcheck	Passed	Passed	Passed	
Frequency	7.4	7.6	7.2	Hz
Overswing Ratio	3.9	3.5	4.1	

Peak Vector Sum 37.0 mm/s at 0.074 sec

USBM RI8507 And OSMRE

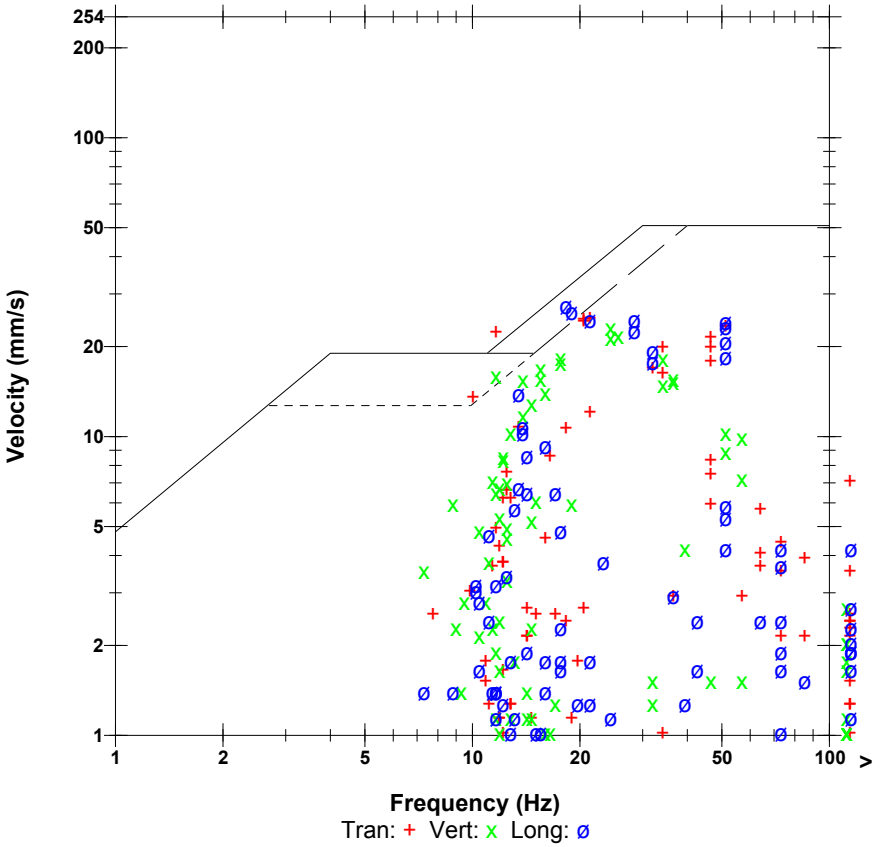

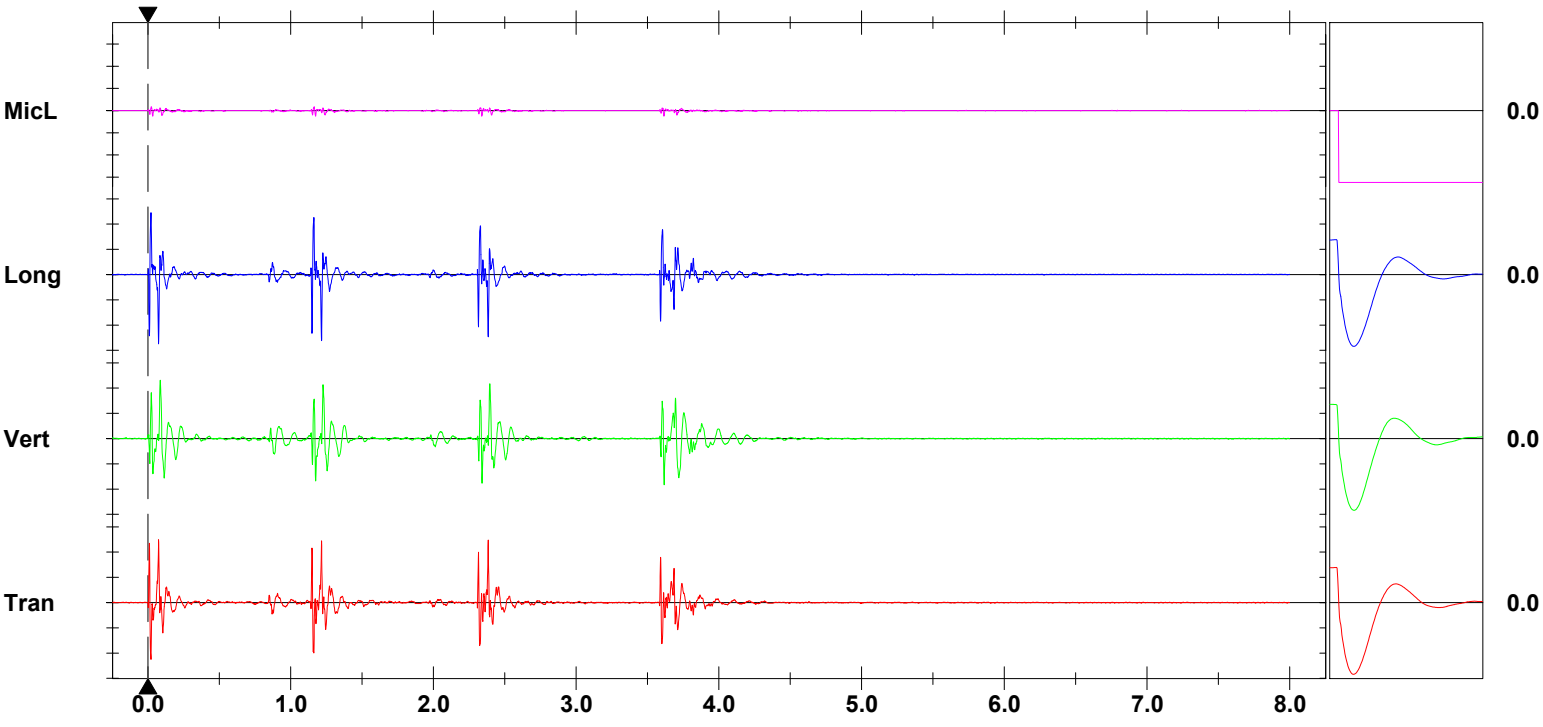

Time Scale: 0.50 sec/div **Amplitude Scale:** Geo: 10.00 mm/s/div Mic: 10.00 pa.(L)/div Sensorcheck
Trigger =

Field Vibration Data

Seismograph Unit # 7 on Concrete Block 5

at 24.1 feet from Test Pile #2

Event Report

Histogram Start Time	15:23:50 October 29, 2009	**Serial Number**	BE13075 V 8.12-8.0 MiniMate Plus
Histogram Finish Time	15:38:08 October 29, 2009	**Battery Level**	6.3 Volts
Number of Intervals	428 at 2 seconds	**Calibration**	December 7, 2007 by Instantel Inc.
Range	Geo :254 mm/s	**File Name**	O075CYFX.FQ0
Sample Rate	1024sps		
Job Number:	1		

Notes
Location:
Client:
User Name:
General:

Extended Notes

Post Event Notes

Microphone Linear Weighting
PSPL 0.500 pa.(L) on October 29, 2009 at 15:26:42
ZC Freq >100 Hz
Channel Test Check (Freq = 0.0 Hz Amp = 0 mv)

	Tran	Vert	Long	
PPV	5.59	17.9	12.8	mm/s
ZC Freq	43	18	30	Hz
Date	Oct 29 /09	Oct 29 /09	Oct 29 /09	
Time	15:33:14	15:27:00	15:33:18	
Sensorcheck	Passed	Passed	Passed	
Frequency	7.4	7.6	7.1	Hz
Overswing Ratio	3.9	3.5	4.2	

Peak Vector Sum 18.6 mm/s on October 29, 2009 at 15:26:58

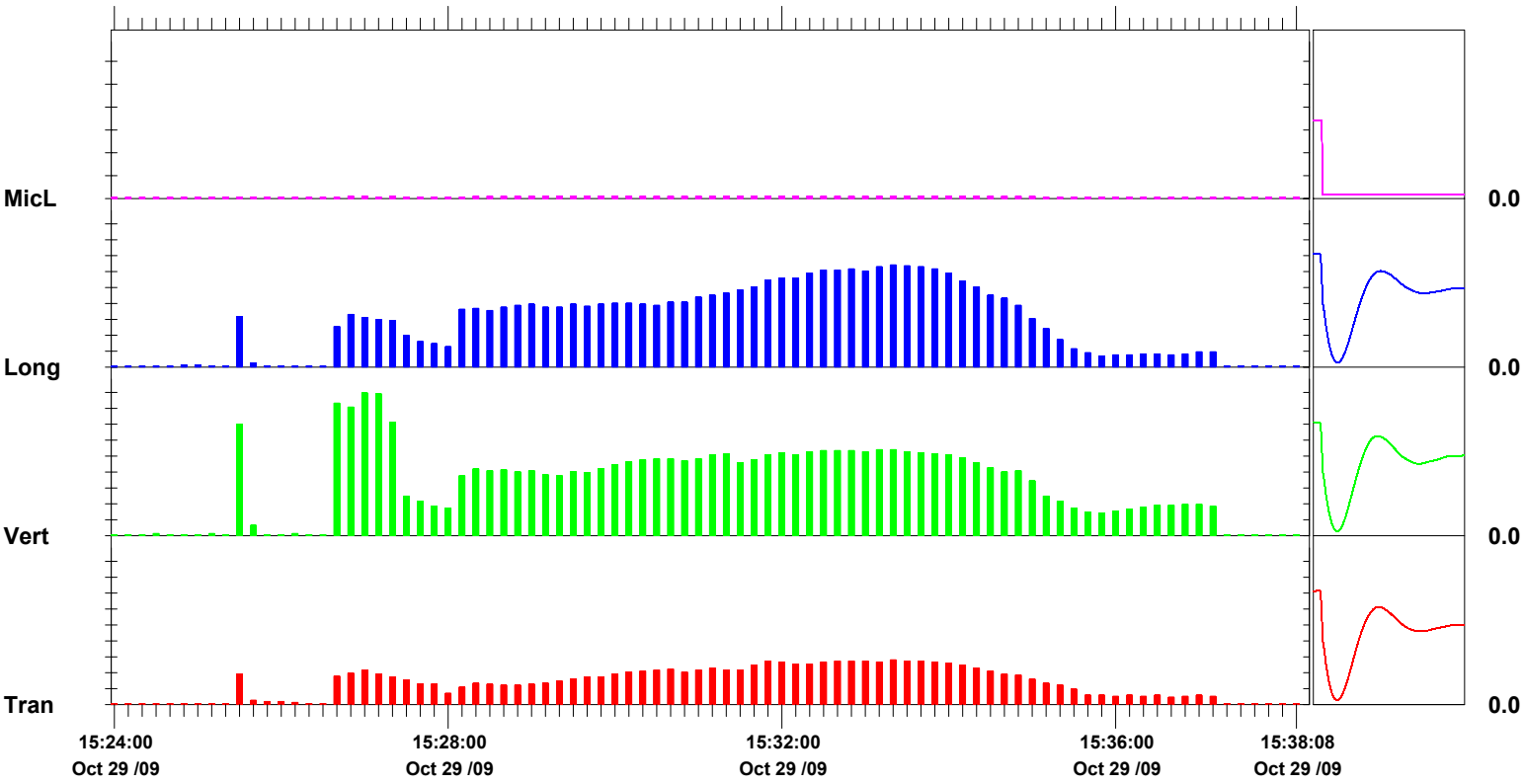

Time Scale: 10 seconds /div **Amplitude Scale:** Geo: 2.00 mm/s/div Mic: 5.00 pa.(L)/div Sensorcheck

Event Report

Date/Time Long at 15:25:26 October 29, 2009
Trigger Source Geo: 1.27 mm/s
Range Geo :254 mm/s
Record Time 8.0 sec at 1024 sps
Job Number: 1

Serial Number BE13075 V 8.12-8.0 MiniMate Plus
Battery Level 6.2 Volts
Calibration December 7, 2007 by Instantel Inc.
File Name O075CYFX.IE0

Notes
Location:
Client:
User Name:
General:

Extended Notes
Combo Mode October 29, 2009 15:23:50

Post Event Notes

Microphone Linear Weighting
PSPL <0.500 pa.(L) at -0.003 sec
ZC Freq N/A
Channel Test Check (Freq = 0.0 Hz Amp = 0 mv)

	Tran	Vert	Long	
PPV	3.81	14.0	6.35	mm/s
ZC Freq	43	18	19	Hz
Time (Rel. to Trig)	0.128	2.521	2.520	sec
Peak Acceleration	0.133	0.225	0.199	g
Peak Displacement	0.0156	0.124	0.0455	mm
Sensorcheck	Passed	Passed	Passed	
Frequency	7.4	7.6	7.1	Hz
Overswing Ratio	3.9	3.5	4.2	

Peak Vector Sum 15.1 mm/s at 2.521 sec

N/A: Not Applicable

USBM RI8507 And OSMRE

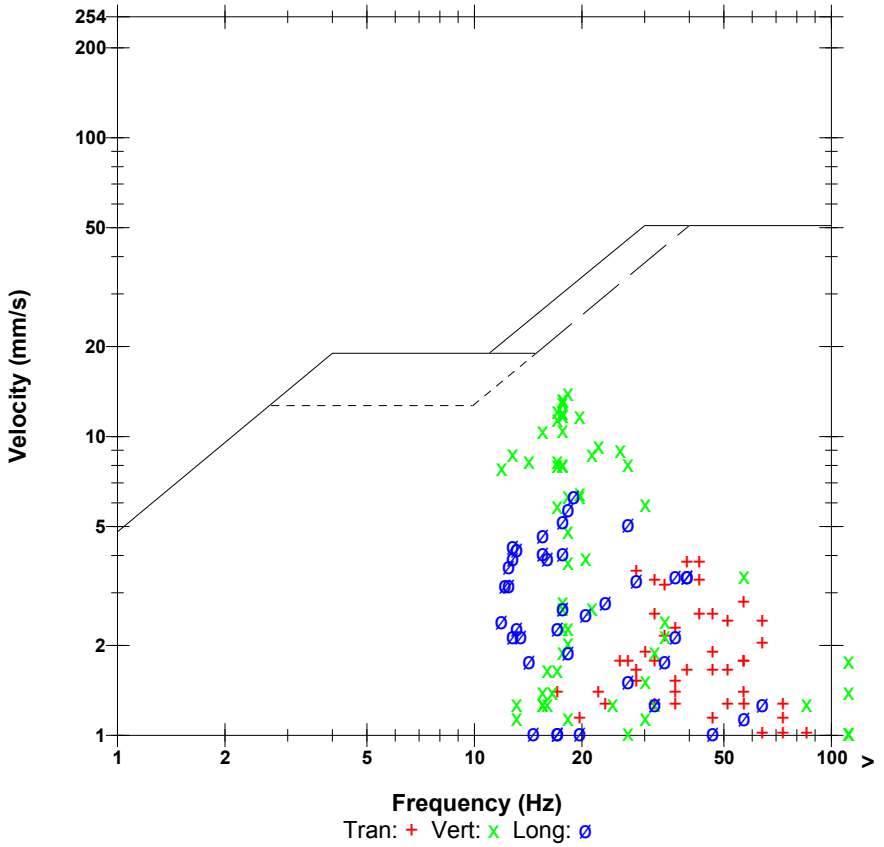

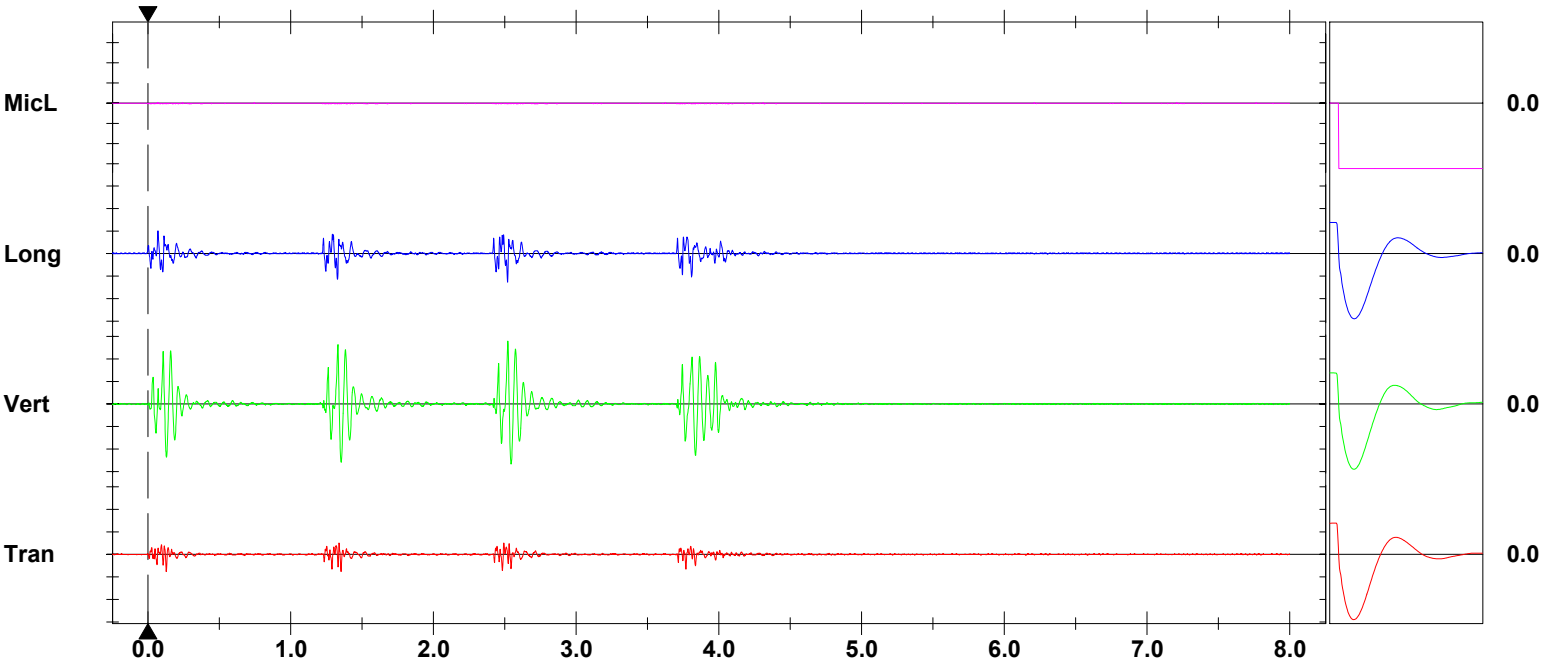

Time Scale: 0.50 sec/div **Amplitude Scale:** Geo: 5.00 mm/s/div Mic: 10.00 pa.(L)/div Sensorcheck
Trigger =

Event Report

Date/Time	Long at 15:26:39 October 29, 2009	**Serial Number**	BE13075 V 8.12-8.0 MiniMate Plus
Trigger Source	Geo: 1.27 mm/s	**Battery Level**	6.3 Volts
Range	Geo :254 mm/s	**Calibration**	December 7, 2007 by Instantel Inc.
Record Time	8.0 sec at 1024 sps	**File Name**	O075CYFX.KF0
Job Number:	1		

Notes
Location:
Client:
User Name:
General:

Extended Notes
Combo Mode October 29, 2009 15:23:50

Post Event Notes

Microphone Linear Weighting
PSPL 0.500 pa.(L) at 1.373 sec
ZC Freq >100 Hz
Channel Test Check (Freq = 0.0 Hz Amp = 0 mv)

	Tran	Vert	Long	
PPV	3.94	16.6	6.60	mm/s
ZC Freq	39	18	20	Hz
Time (Rel. to Trig)	2.612	0.094	1.374	sec
Peak Acceleration	0.119	0.239	0.252	g
Peak Displacement	0.0156	0.133	0.0542	mm
Sensorcheck	Passed	Passed	Passed	
Frequency	7.4	7.6	7.1	Hz
Overswing Ratio	3.9	3.5	4.2	

Peak Vector Sum 17.2 mm/s at 2.649 sec

USBM RI8507 And OSMRE

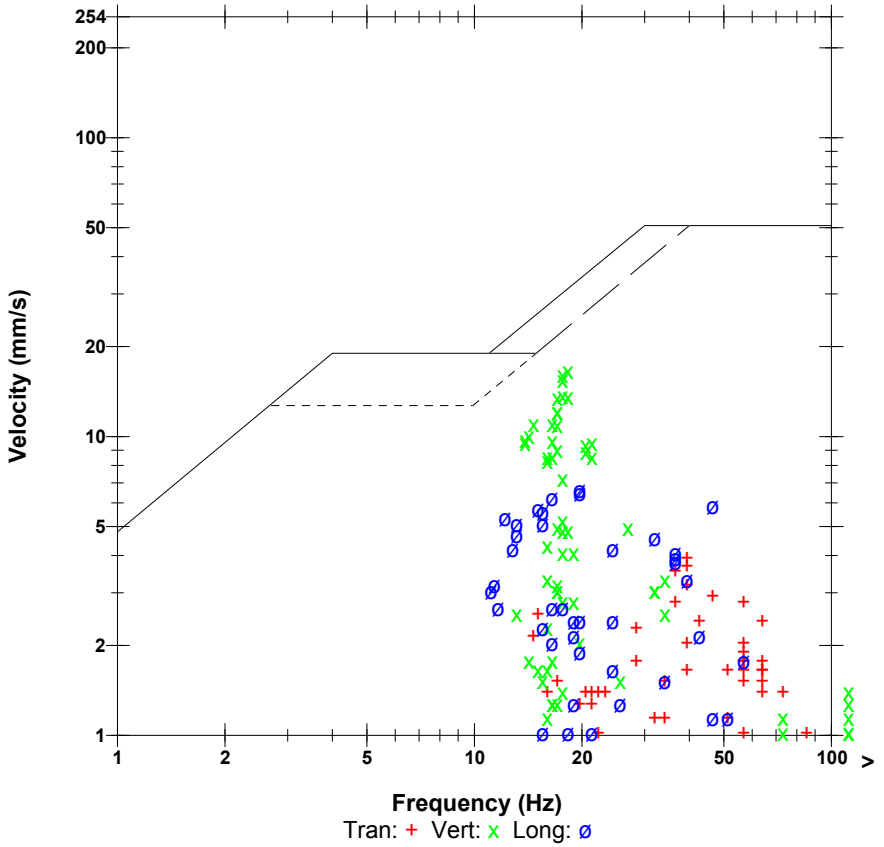

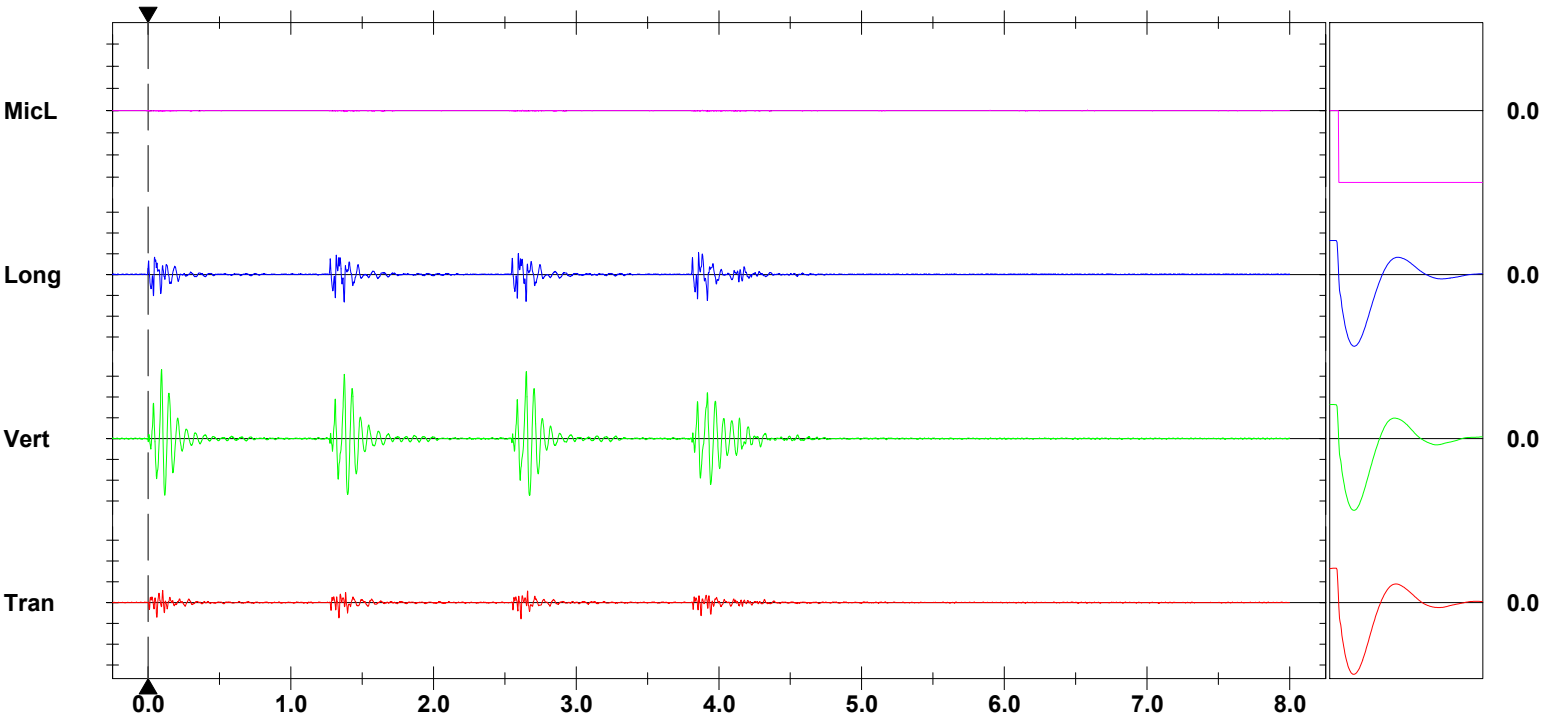

Time Scale: 0.50 sec/div **Amplitude Scale:** Geo: 5.00 mm/s/div Mic: 10.00 pa.(L)/div Sensorcheck
Trigger =

Event Report

Date/Time	Long at 15:26:56 October 29, 2009	**Serial Number**	BE13075 V 8.12-8.0 MiniMate Plus
Trigger Source	Geo: 1.27 mm/s	**Battery Level**	6.3 Volts
Range	Geo :254 mm/s	**Calibration**	December 7, 2007 by Instantel Inc.
Record Time	8.0 sec at 1024 sps	**File Name**	O075CYFX.KW0
Job Number:	1		

Notes
Location:
Client:
User Name:
General:

Extended Notes
Combo Mode October 29, 2009 15:23:50

Post Event Notes

Microphone Linear Weighting
PSPL 0.500 pa.(L) at 2.672 sec
ZC Freq >100 Hz
Channel Test Check (Freq = 0.0 Hz Amp = 0 mv)

	Tran	Vert	Long	
PPV	4.32	17.9	6.22	mm/s
ZC Freq	37	18	22	Hz
Time (Rel. to Trig)	4.132	2.730	0.048	sec
Peak Acceleration	0.106	0.239	0.252	g
Peak Displacement	0.0195	0.137	0.0526	mm
Sensorcheck	Passed	Passed	Passed	
Frequency	7.4	7.6	7.1	Hz
Overswing Ratio	3.9	3.5	4.2	

Peak Vector Sum 18.6 mm/s at 1.381 sec

USBM RI8507 And OSMRE

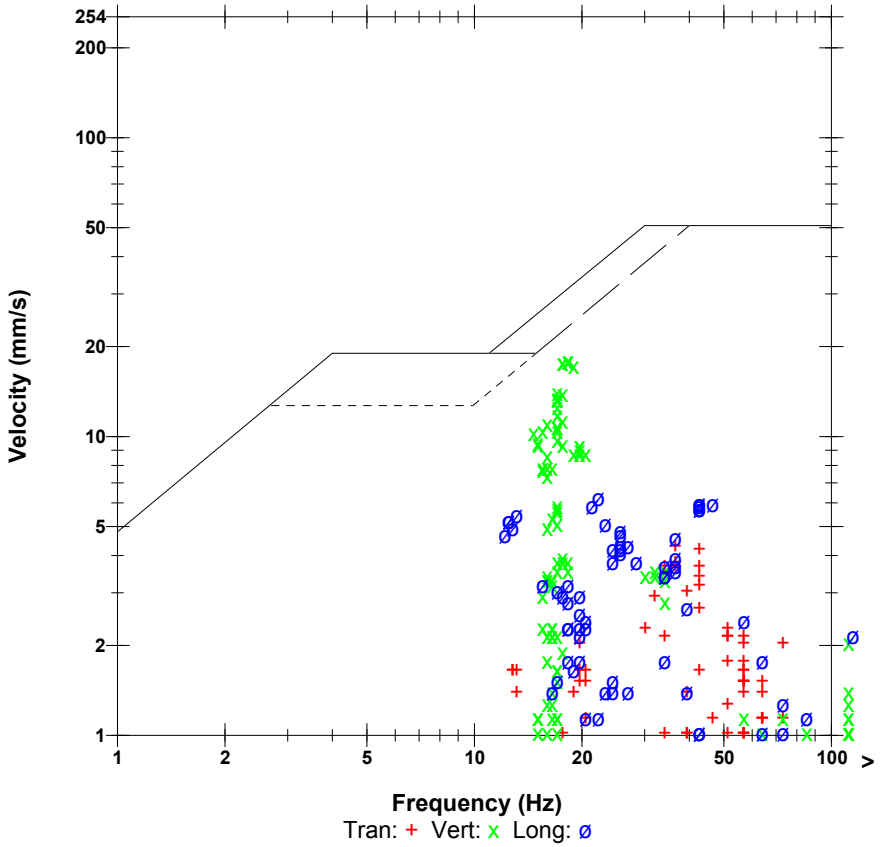

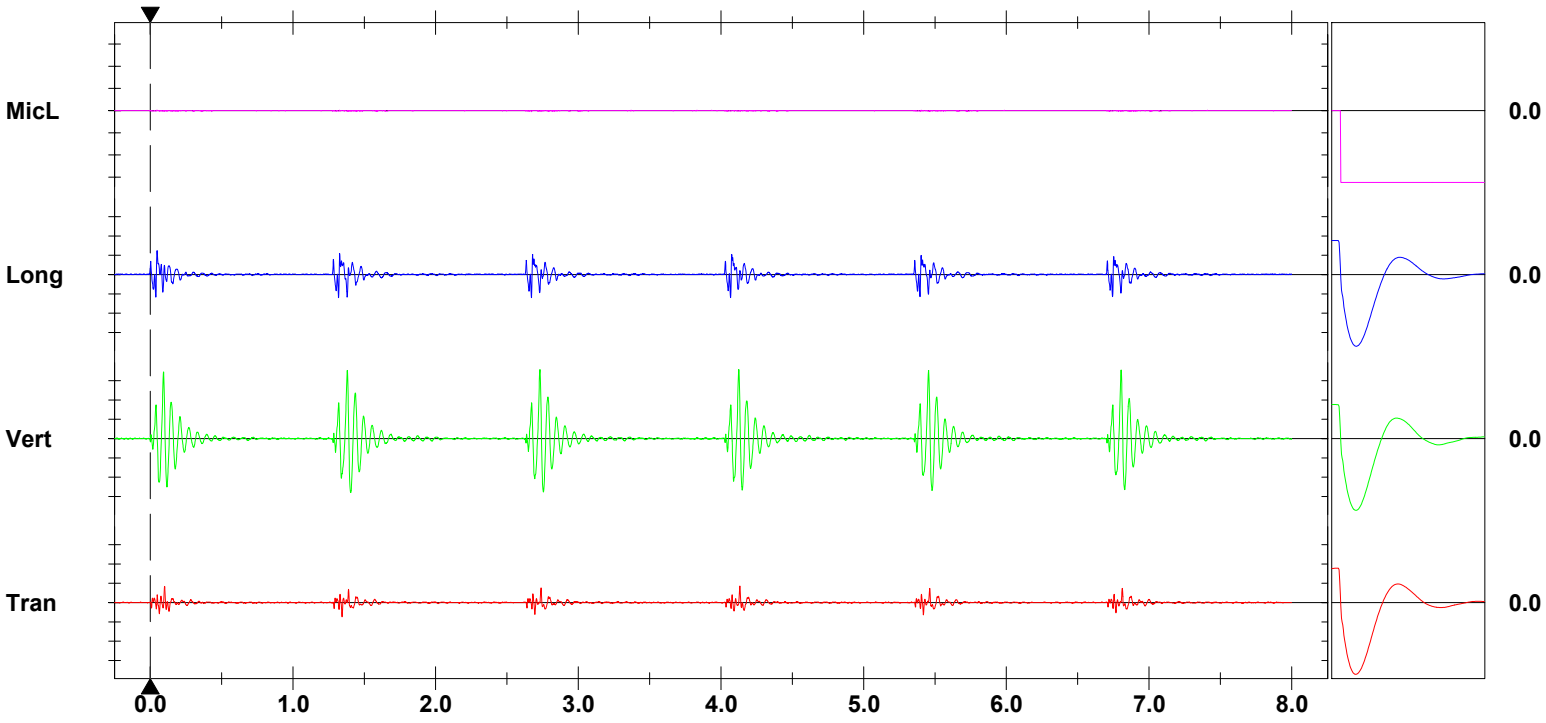

Time Scale: 0.50 sec/div **Amplitude Scale:** Geo: 5.00 mm/s/div Mic: 10.00 pa.(L)/div Sensorcheck
Trigger =

Event Report

Date/Time	Vert at 15:27:04 October 29, 2009	**Serial Number**	BE13075 V 8.12-8.0 MiniMate Plus
Trigger Source	Geo: 1.27 mm/s	**Battery Level**	6.3 Volts
Range	Geo :254 mm/s	**Calibration**	December 7, 2007 by Instantel Inc.
Record Time	3.893 sec at 1024 sps	**File Name**	O075CYFX.L40
Job Number:	1		

Notes
Location:
Client:
User Name:
General:

Extended Notes
Combo Mode October 29, 2009 15:23:50

Post Event Notes

Microphone Linear Weighting
PSPL <0.500 pa.(L) at -0.242 sec
ZC Freq N/A
Channel Test Check (Freq = 0.0 Hz Amp = 0 mv)

	Tran	Vert	Long	
PPV	3.81	17.1	5.84	mm/s
ZC Freq	34	22	32	Hz
Time (Rel. to Trig)	-0.229	-0.237	3.630	sec
Peak Acceleration	0.106	0.239	0.225	g
Peak Displacement	0.0187	0.135	0.0460	mm
Sensorcheck	Passed	Passed	Passed	
Frequency	7.4	7.6	7.1	Hz
Overswing Ratio	3.9	3.5	4.2	

Peak Vector Sum 17.7 mm/s at -0.237 sec

N/A: Not Applicable

USBM RI8507 And OSMRE

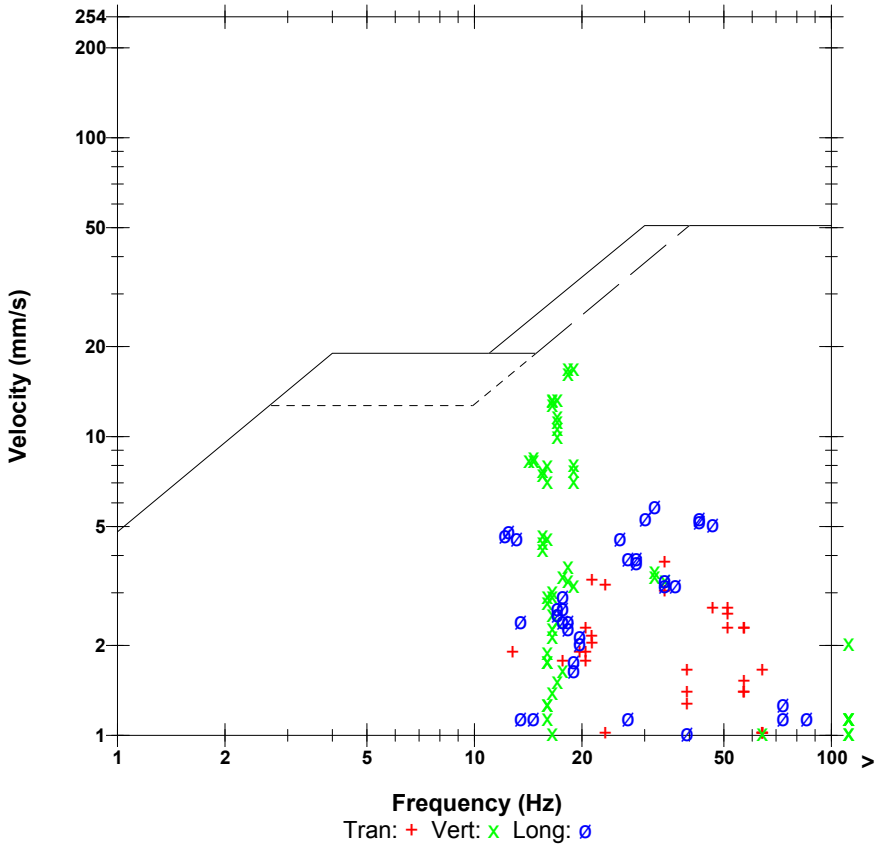

Monitor Log
Oct 29 /09 15:27:04 Oct 29 /09 15:27:08 Event recorded. (Memory Full Exit)

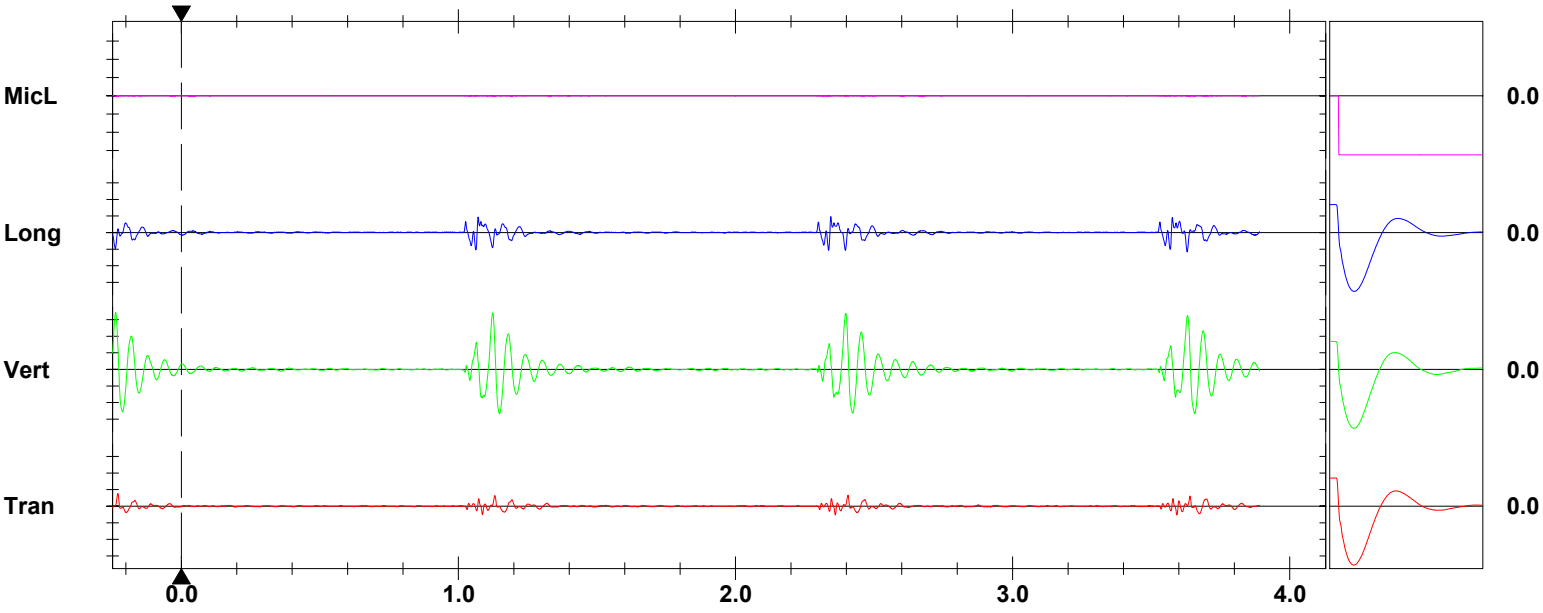

Time Scale: 0.20 sec/div **Amplitude Scale:** Geo: 5.00 mm/s/div Mic: 10.00 pa.(L)/div Sensorcheck
Trigger =

Field Vibration Data

Seismograph Unit # 7 in casing

at 13.6 feet from Test Pile #1

Non Driving Event

Event Report

Histogram Start Time	10:31:14 December 21, 2009	**Serial Number**	BE13075 V 8.12-8.0 MiniMate Plus
Histogram Finish Time	11:03:45 December 21, 2009	**Battery Level**	6.2 Volts
Number of Intervals	975 at 2 seconds	**Calibration**	December 7, 2007 by Instantel Inc.
Range	Geo :254 mm/s	**File Name**	O075D15P.820
Sample Rate	1024sps		
Job Number:	1		

Notes

Post Event Notes

Microphone Linear Weighting
PSPL 11.0 pa.(L) on December 21, 2009 at 10:56:02
ZC Freq 20 Hz
Channel Test Passed (Freq = 20.5 Hz Amp = 702 mv)

	Tran	Vert	Long	
PPV	0.127	0.254	0.254	mm/s
ZC Freq	>100	47	>100	Hz
Date	Dec 21 /09	Dec 21 /09	Dec 21 /09	
Time	10:31:16	11:03:44	11:03:44	
Sensorcheck	Check	Check	Check	
Frequency	1024.0	33.0	1024.0	Hz
Overswing Ratio	0.0	1.3	0.0	

Peak Vector Sum 0.381 mm/s on December 21, 2009 at 11:03:44

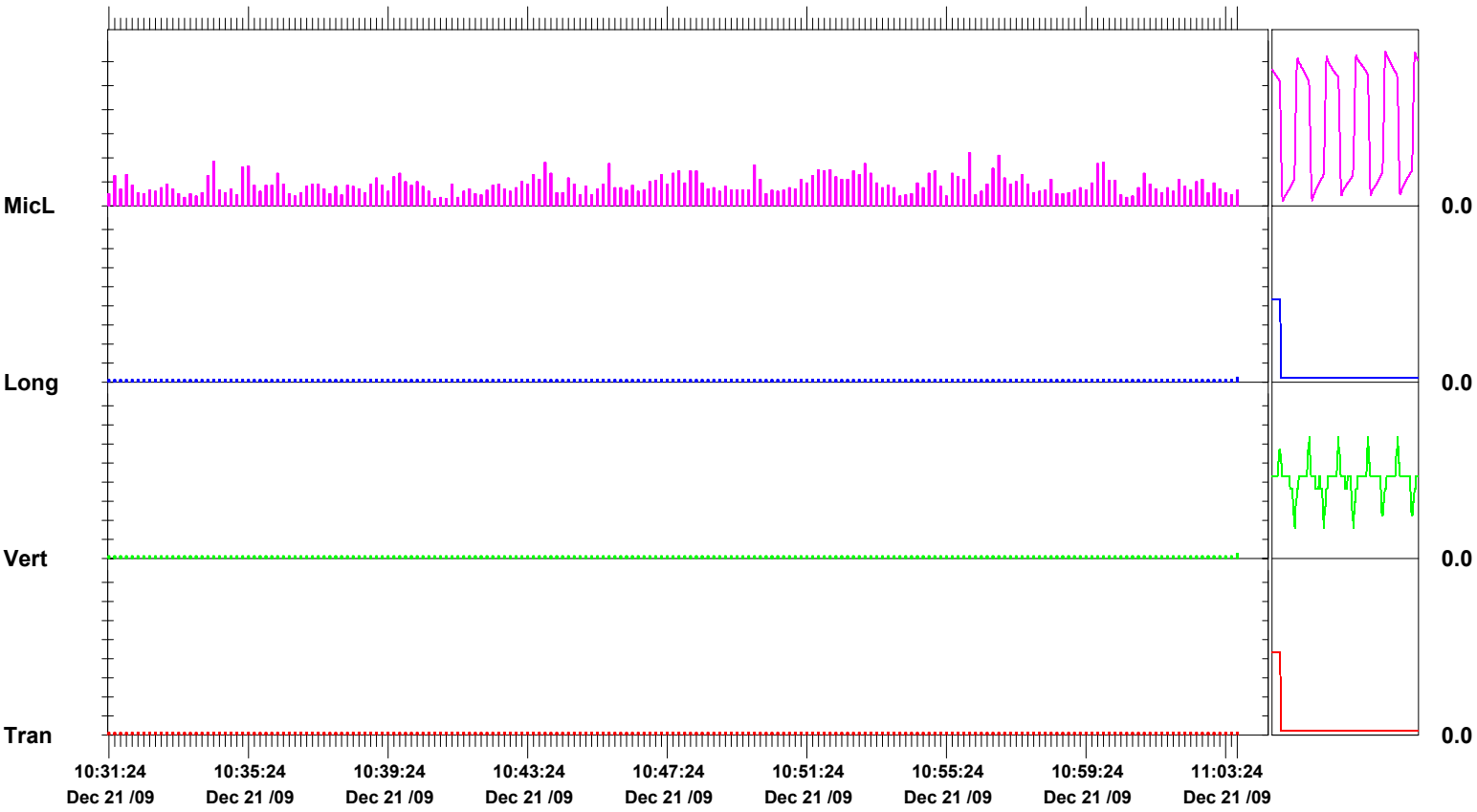

Time Scale: 10 seconds /div **Amplitude Scale:** Geo: 1.000 mm/s/div Mic: 5.00 pa.(L)/div Sensorcheck

Event Report

Histogram Start Time	11:31:13 December 21, 2009	**Serial Number**	BE13075 V 8.12-8.0 MiniMate Plus
Histogram Finish Time	11:54:39 December 21, 2009	**Battery Level**	6.2 Volts
Number of Intervals	703 at 2 seconds	**Calibration**	December 7, 2007 by Instantel Inc.
Range	Geo :254 mm/s	**File Name**	O075D15S.010
Sample Rate	1024sps		
Job Number:	1		

Notes

Post Event Notes

Microphone Linear Weighting
PSPL 2.75 pa.(L) on December 21, 2009 at 11:38:09
ZC Freq 4.5 Hz
Channel Test Passed (Freq = 20.5 Hz Amp = 695 mv)

	Tran	Vert	Long	
PPV	0.127	0.127	0.127	mm/s
ZC Freq	>100	>100	N/A	Hz
Date	Dec 21 /09	Dec 21 /09	Dec 21 /09	
Time	11:31:15	11:31:15	11:31:15	
Sensorcheck	Check	Check	Check	
Frequency	1024.0	48.8	1024.0	Hz
Overswing Ratio	0.0	1.0	0.0	

Peak Vector Sum 0.220 mm/s on December 21, 2009 at 11:31:21

N/A: Not Applicable

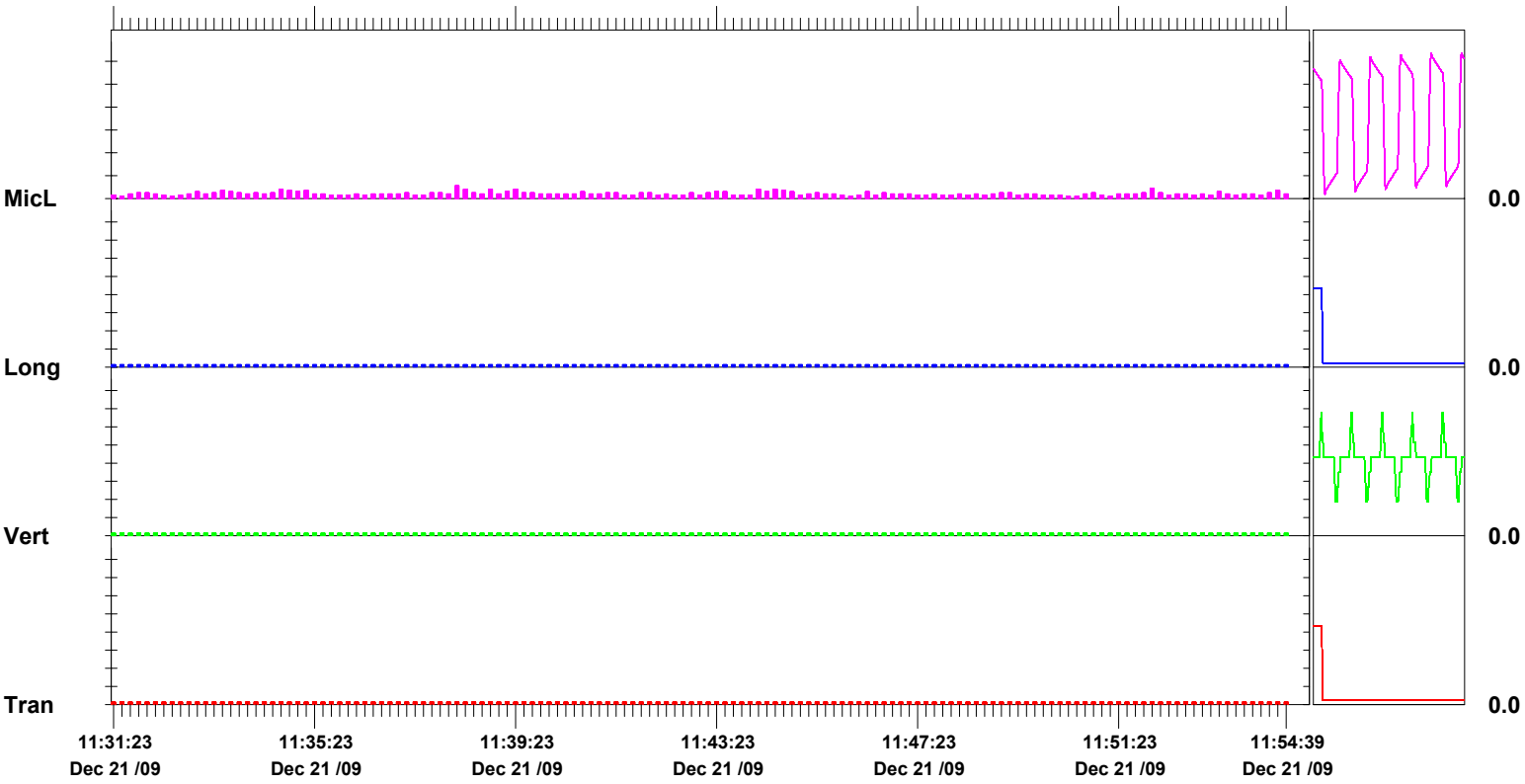

Time Scale: 10 seconds /div **Amplitude Scale:** Geo: 1.000 mm/s/div Mic: 5.00 pa.(L)/div Sensorcheck

Field Vibration Data

Seismograph Unit # 8 in casing

at 26.7 feet from Test Pile #1

Event Report

Histogram Start Time	14:17:12 October 29, 2009	**Serial Number**	BE13054 V 8.12-8.0 MiniMate Plus
Histogram Finish Time	14:18:28 October 29, 2009	**Battery Level**	6.3 Volts
Number of Intervals	37 at 2 seconds	**Calibration**	December 7, 2007 by Instantel Inc.
Range	Geo :254 mm/s	**File Name**	O054CYFU.CO0
Sample Rate	1024sps		
Job Number:	1		

Notes
Location:
Client:
User Name:
General:

Extended Notes

Post Event Notes

Microphone	Linear Weighting
PSPL	0.500 pa.(L) on October 29, 2009 at 14:18:14
ZC Freq	>100 Hz
Channel Test	Check (Freq = 0.0 Hz Amp = 0 mv)

	Tran	Vert	Long	
PPV	4.70	11.2	8.25	mm/s
ZC Freq	20	17	20	Hz
Date	Oct 29 /09	Oct 29 /09	Oct 29 /09	
Time	14:18:14	14:18:14	14:18:16	
Sensorcheck	Passed	Passed	Passed	
Frequency	7.6	7.3	7.1	Hz
Overswing Ratio	3.8	4.0	4.1	

Peak Vector Sum 11.4 mm/s on October 29, 2009 at 14:18:14

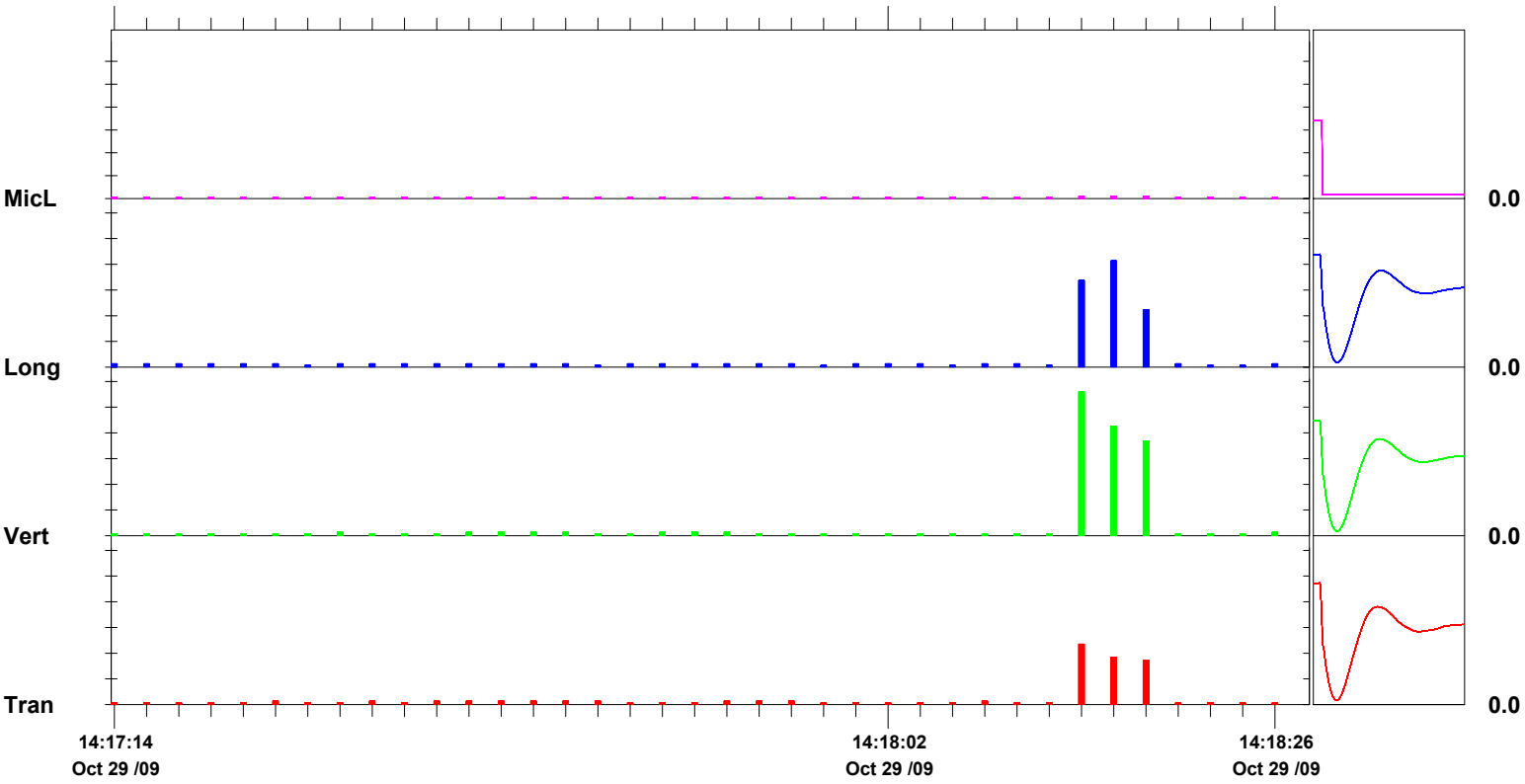

Time Scale: 2 seconds /div **Amplitude Scale:** Geo: 2.00 mm/s/div Mic: 5.00 pa.(L)/div Sensorcheck

Event Report

Date/Time Tran at 14:18:12 October 29, 2009
Trigger Source Geo: 1.27 mm/s
Range Geo :254 mm/s
Record Time 8.0 sec at 1024 sps
Job Number: 1

Serial Number BE13054 V 8.12-8.0 MiniMate Plus
Battery Level 6.3 Volts
Calibration December 7, 2007 by Instantel Inc.
File Name O054CYFU.EC0

Notes
Location:
Client:
User Name:
General:

Extended Notes
Combo Mode October 29, 2009 14:17:11

Post Event Notes

Microphone Linear Weighting
PSPL 0.500 pa.(L) at 0.001 sec
ZC Freq >100 Hz
Channel Test Check (Freq = 0.0 Hz Amp = 0 mv)

	Tran	Vert	Long	
PPV	4.70	11.2	8.25	mm/s
ZC Freq	20	17	20	Hz
Time (Rel. to Trig)	1.150	0.093	2.344	sec
Peak Acceleration	0.106	0.172	0.133	g
Peak Displacement	0.0311	0.0994	0.0567	mm
Sensorcheck	Passed	Passed	Passed	
Frequency	7.6	7.3	7.1	Hz
Overswing Ratio	3.8	4.0	4.1	

Peak Vector Sum 11.4 mm/s at 0.093 sec

USBM RI8507 And OSMRE

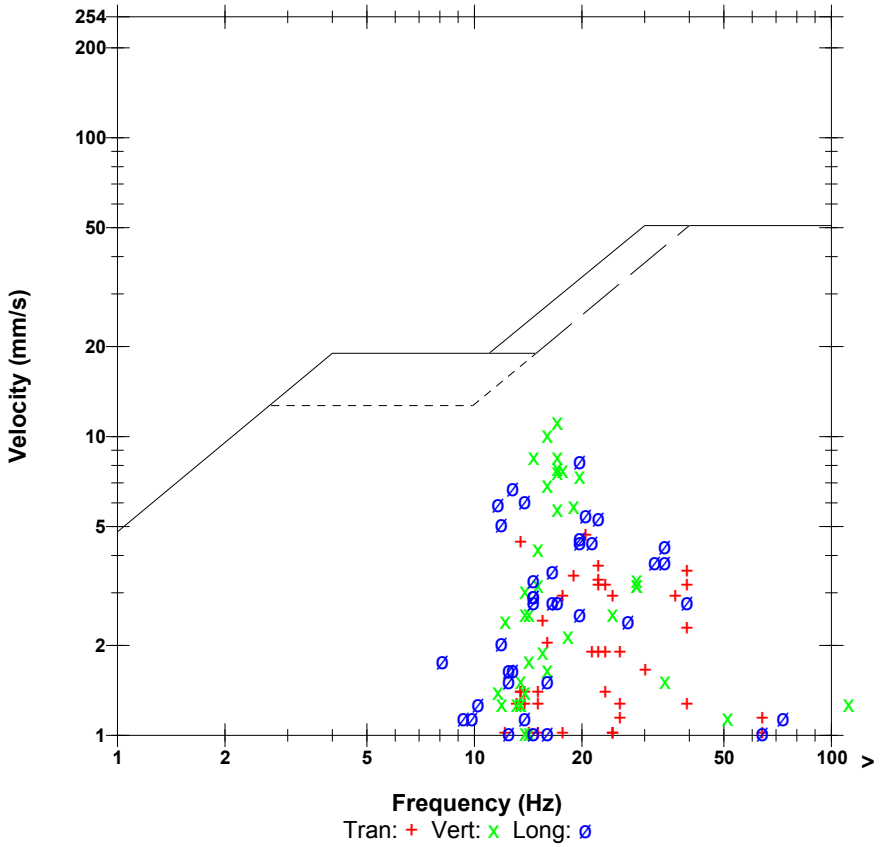

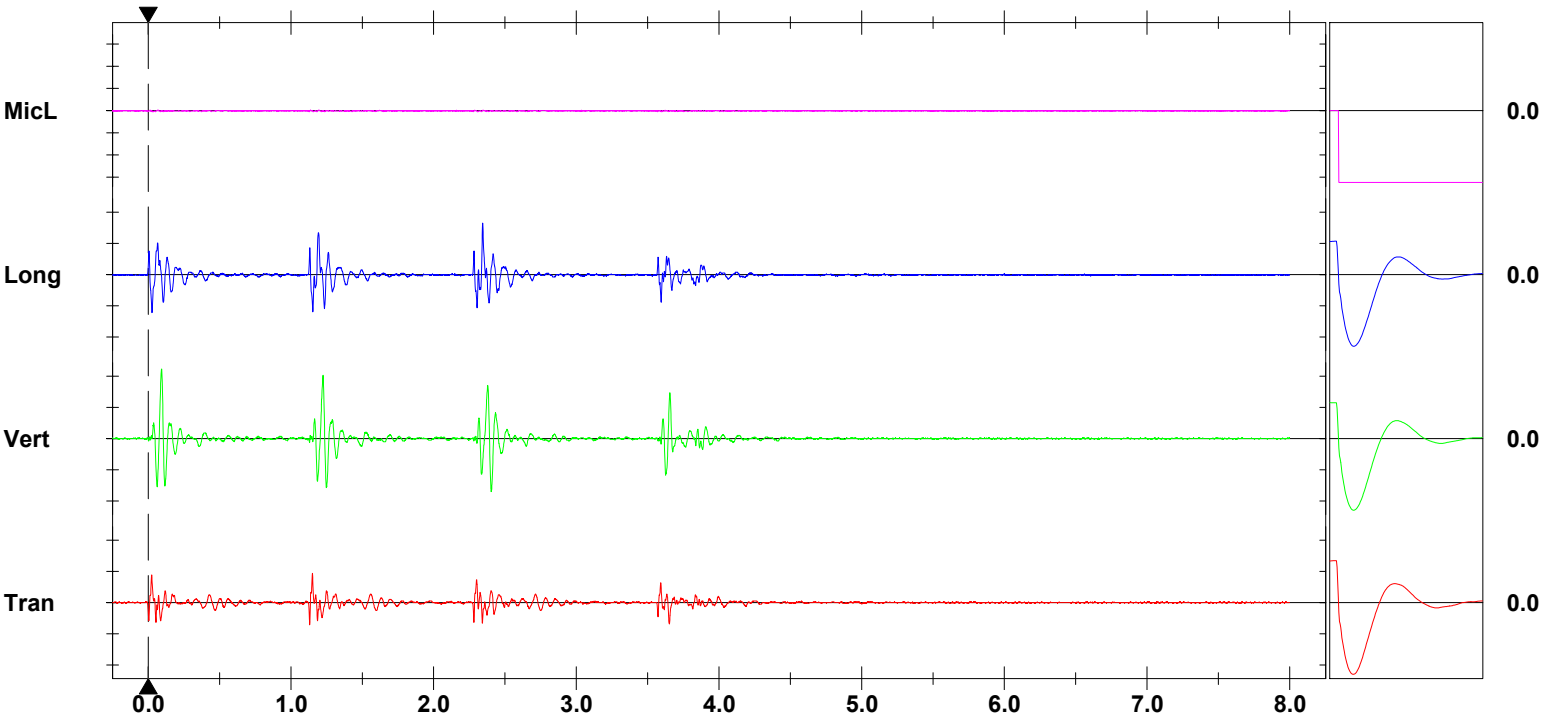

Time Scale: 0.50 sec/div **Amplitude Scale:** Geo: 5.00 mm/s/div Mic: 10.00 pa.(L)/div Sensorcheck
Trigger =

Event Report

Histogram Start Time	14:21:52 October 29, 2009	**Serial Number**	BE13054 V 8.12-8.0 MiniMate Plus
Histogram Finish Time	14:26:12 October 29, 2009	**Battery Level**	6.4 Volts
Number of Intervals	130 at 2 seconds	**Calibration**	December 7, 2007 by Instantel Inc.
Range	Geo :254 mm/s	**File Name**	O054CYFU.KG0
Sample Rate	1024sps		
Job Number:	1		

Notes
Location:
Client:
User Name:
General:

Extended Notes

Post Event Notes

Microphone Linear Weighting
PSPL 1.00 pa.(L) on October 29, 2009 at 14:22:24
ZC Freq 73 Hz
Channel Test Check (Freq = 0.0 Hz Amp = 0 mv)

	Tran	Vert	Long	
PPV	7.49	5.84	7.75	mm/s
ZC Freq	30	15	34	Hz
Date	Oct 29 /09	Oct 29 /09	Oct 29 /09	
Time	14:24:12	14:23:40	14:23:34	
Sensorcheck	Passed	Passed	Passed	
Frequency	7.7	7.2	7.2	Hz
Overswing Ratio	3.9	3.8	4.1	

Peak Vector Sum 10.3 mm/s on October 29, 2009 at 14:23:52

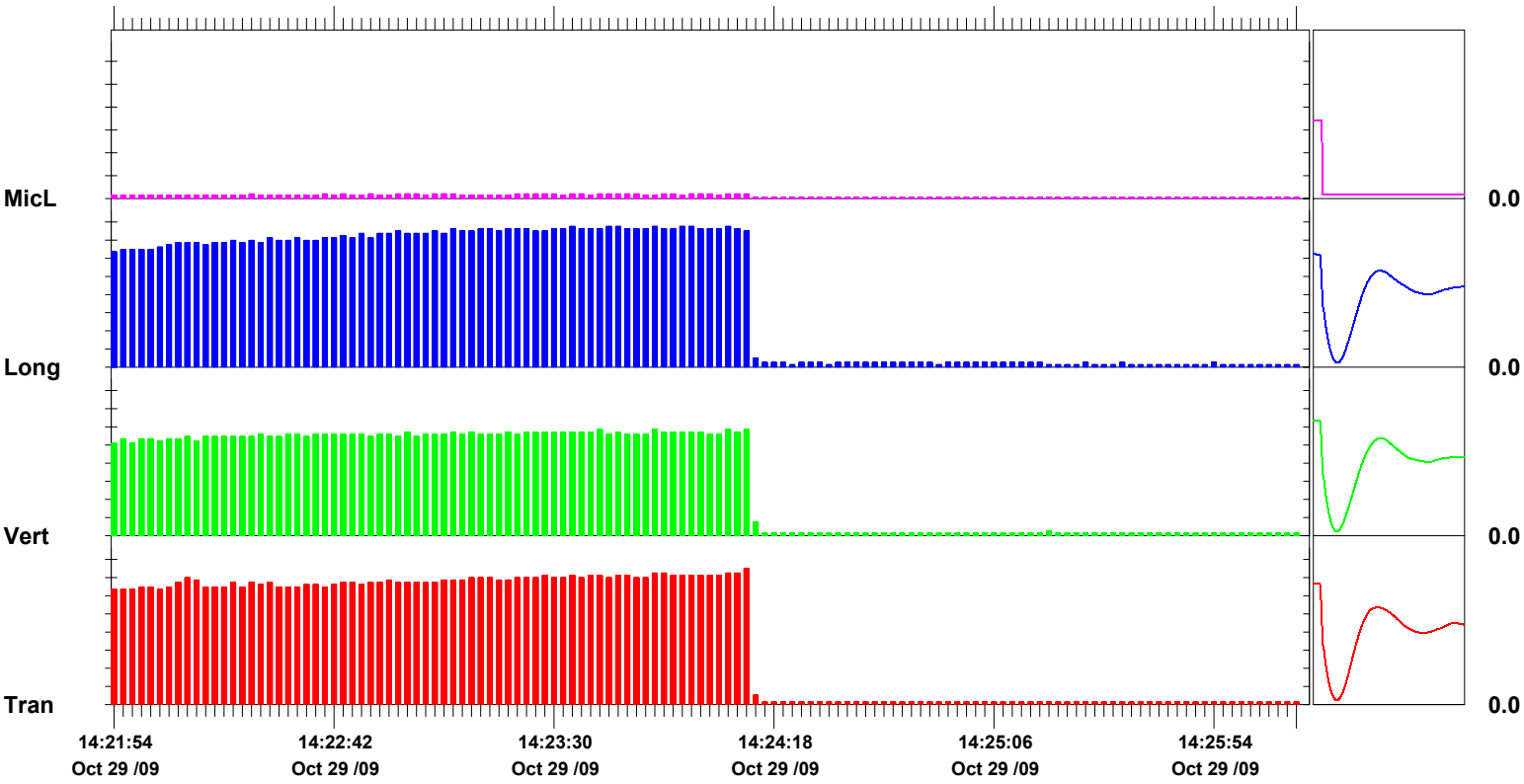

Time Scale: 2 seconds /div **Amplitude Scale:** Geo: 1.000 mm/s/div Mic: 5.00 pa.(L)/div Sensorcheck

Event Report

Date/Time	Tran at 14:21:53 October 29, 2009	**Serial Number**	BE13054 V 8.12-8.0 MiniMate Plus
Trigger Source	Geo: 1.27 mm/s	**Battery Level**	6.3 Volts
Range	Geo :254 mm/s	**Calibration**	December 7, 2007 by Instantel Inc.
Record Time	8.0 sec at 1024 sps	**File Name**	O054CYFU.KH0
Job Number:	1		

Notes
Location:
Client:
User Name:
General:

Extended Notes
Combo Mode October 29, 2009 14:21:52

Post Event Notes

Microphone Linear Weighting
PSPL 0.750 pa.(L) at 0.017 sec
ZC Freq 73 Hz
Channel Test Check (Freq = 0.0 Hz Amp = 0 mv)

	Tran	Vert	Long	
PPV	6.48	5.33	6.48	mm/s
ZC Freq	28	15	34	Hz
Time (Rel. to Trig)	6.664	1.935	2.869	sec
Peak Acceleration	0.146	0.133	0.186	g
Peak Displacement	0.0362	0.0554	0.0279	mm
Sensorcheck	Passed	Passed	Passed	
Frequency	7.7	7.2	7.2	Hz
Overswing Ratio	3.9	3.8	4.1	

Peak Vector Sum 8.81 mm/s at 4.768 sec

USBM RI8507 And OSMRE

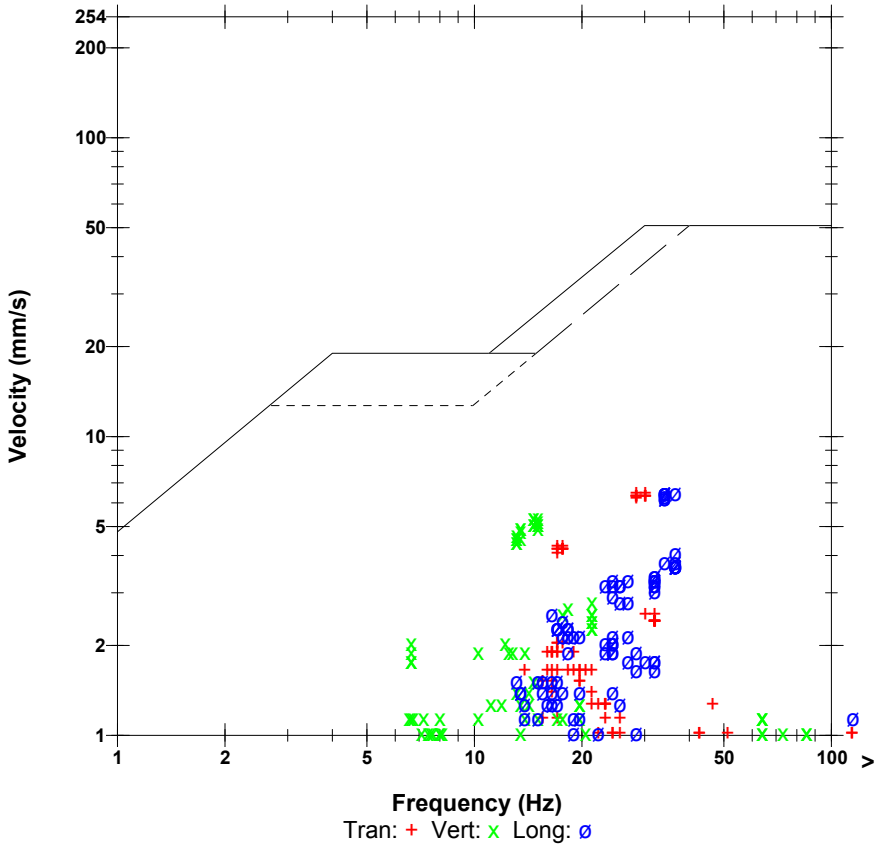

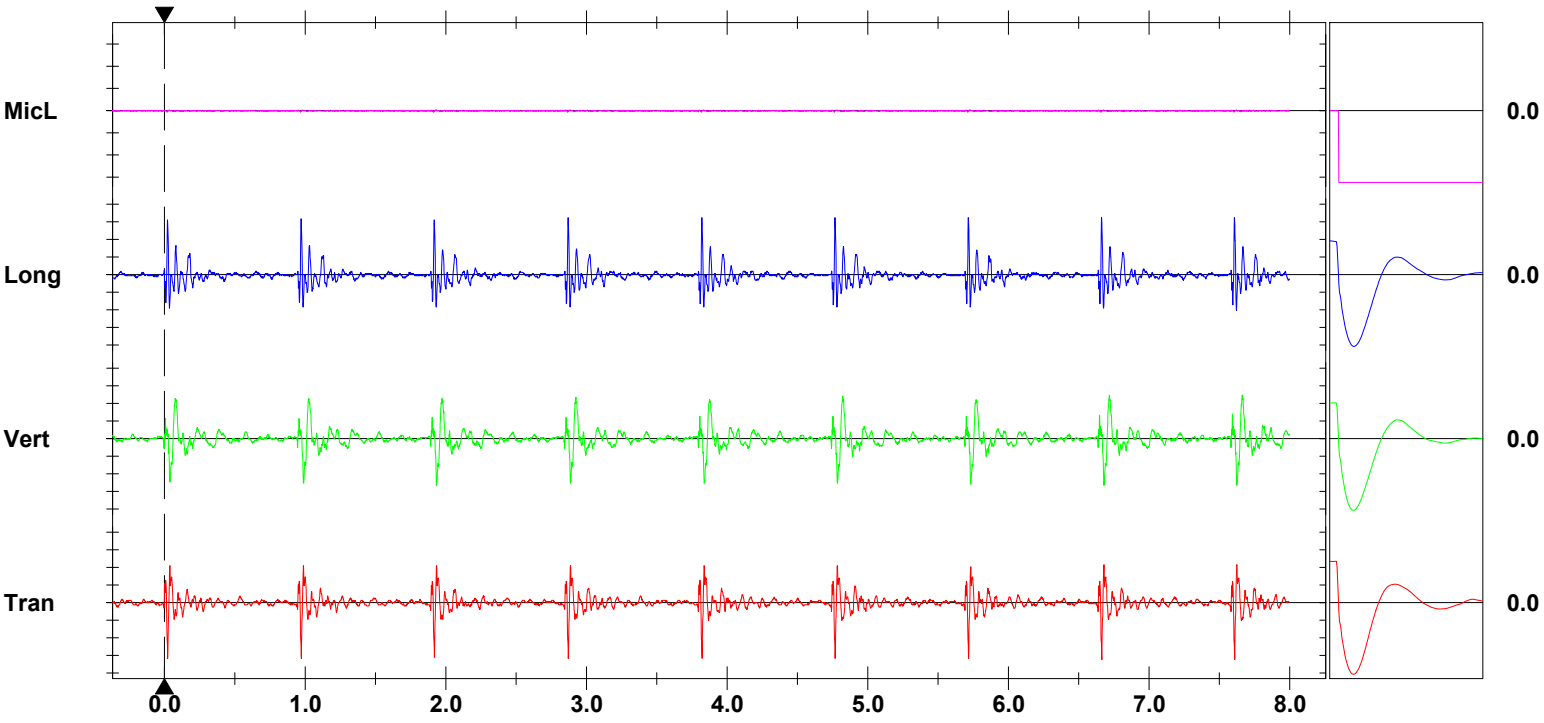

Time Scale: 0.50 sec/div **Amplitude Scale:** Geo: 2.00 mm/s/div Mic: 10.00 pa.(L)/div Sensorcheck
Trigger =

Event Report

Date/Time Tran at 14:22:01 October 29, 2009
Trigger Source Geo: 1.27 mm/s
Range Geo :254 mm/s
Record Time 8.0 sec at 1024 sps
Job Number: 1

Serial Number BE13054 V 8.12-8.0 MiniMate Plus
Battery Level 6.3 Volts
Calibration December 7, 2007 by Instantel Inc.
File Name O054CYFU.KP0

Notes
Location:
Client:
User Name:
General:

Extended Notes
Combo Mode October 29, 2009 14:21:52

Post Event Notes

Microphone Linear Weighting
PSPL 0.750 pa.(L) at 0.016 sec
ZC Freq >100 Hz
Channel Test Check (Freq = 0.0 Hz Amp = 0 mv)

	Tran	Vert	Long	
PPV	6.98	5.46	6.86	mm/s
ZC Freq	27	15	34	Hz
Time (Rel. to Trig)	7.499	6.605	6.589	sec
Peak Acceleration	0.146	0.133	0.186	g
Peak Displacement	0.0376	0.0556	0.0313	mm
Sensorcheck	Passed	Passed	Passed	
Frequency	7.7	7.2	7.2	Hz
Overswing Ratio	3.9	3.8	4.1	

Peak Vector Sum 9.57 mm/s at 7.498 sec

USBM RI8507 And OSMRE

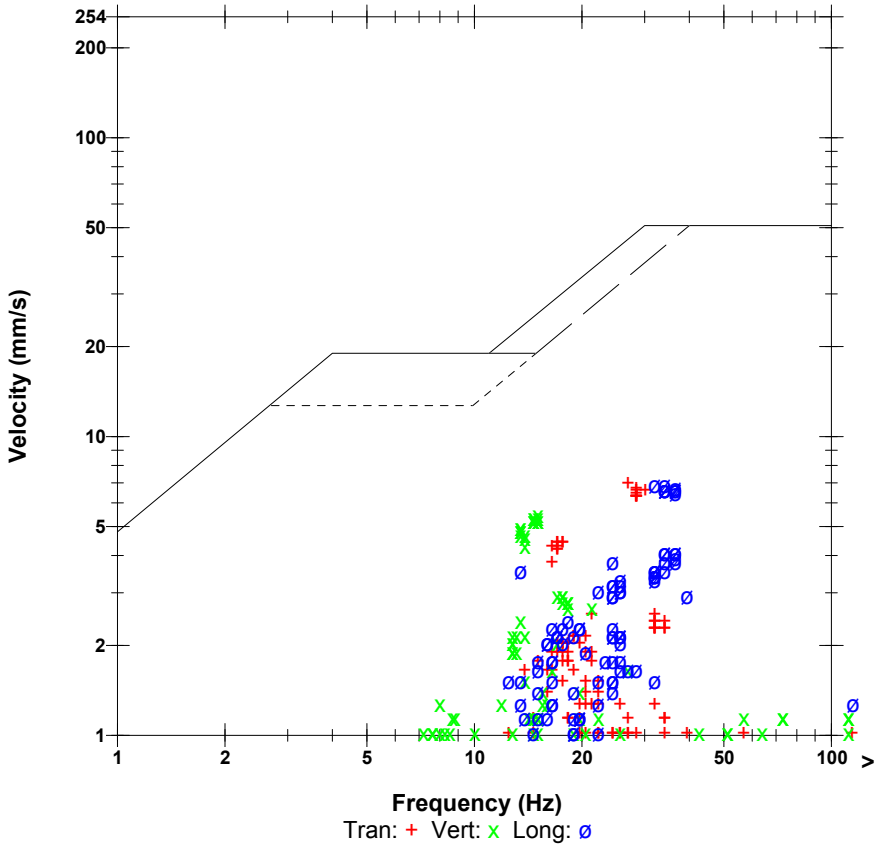

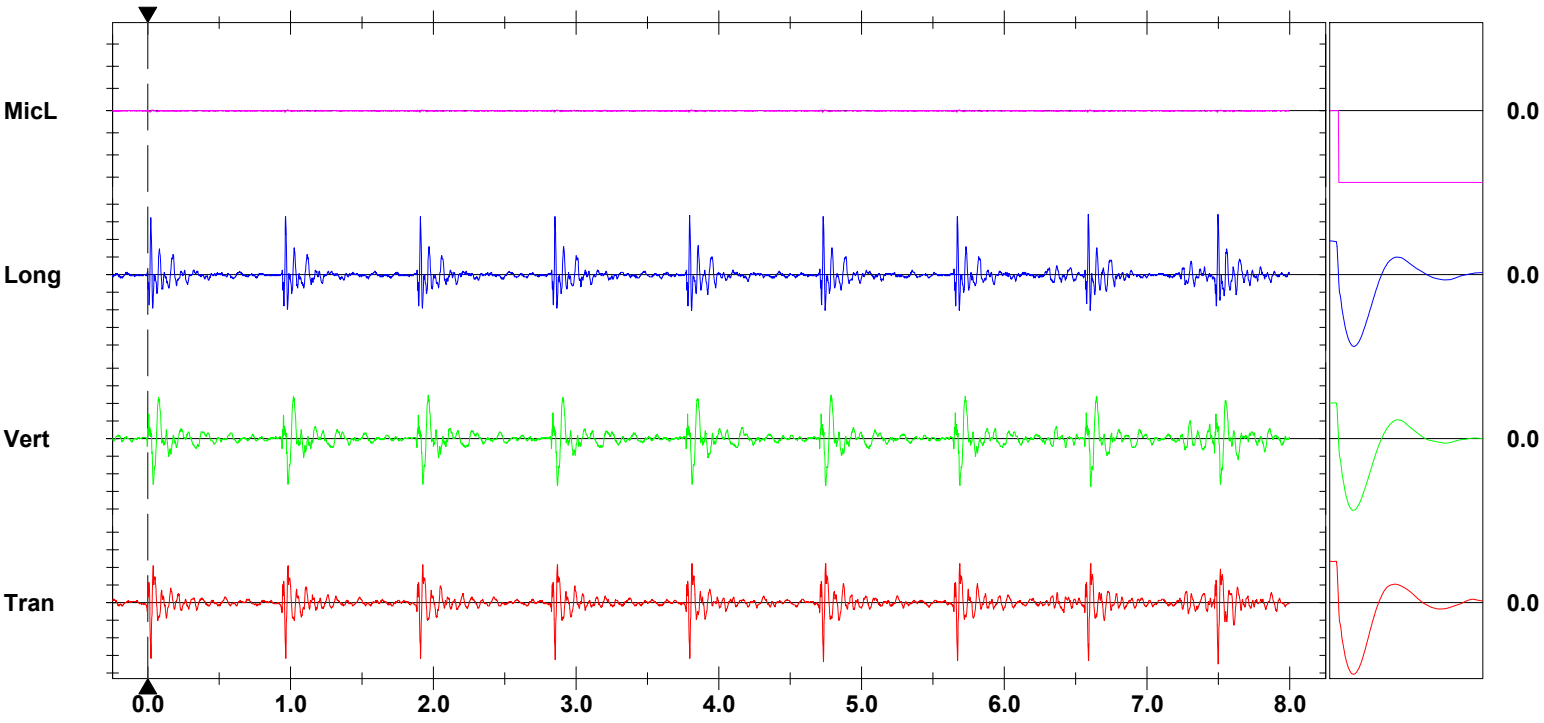

Time Scale: 0.50 sec/div **Amplitude Scale:** Geo: 2.00 mm/s/div Mic: 10.00 pa.(L)/div Sensorcheck
Trigger =

Event Report

Date/Time Tran at 14:22:10 October 29, 2009
Trigger Source Geo: 1.27 mm/s
Range Geo :254 mm/s
Record Time 6.203 sec at 1024 sps
Job Number: 1

Serial Number BE13054 V 8.12-8.0 MiniMate Plus
Battery Level 6.3 Volts
Calibration December 7, 2007 by Instantel Inc.
File Name O054CYFU.KY0

Notes
Location:
Client:
User Name:
General:

Extended Notes
Combo Mode October 29, 2009 14:21:52

Post Event Notes

Microphone Linear Weighting
PSPL 0.750 pa.(L) at 0.016 sec
ZC Freq 64 Hz
Channel Test Check (Freq = 0.0 Hz Amp = 0 mv)

	Tran	Vert	Long	
PPV	6.86	5.46	6.86	mm/s
ZC Freq	28	15	34	Hz
Time (Rel. to Trig)	0.942	3.770	0.940	sec
Peak Acceleration	0.146	0.146	0.186	g
Peak Displacement	0.0374	0.0557	0.0337	mm
Sensorcheck	Passed	Passed	Passed	
Frequency	7.7	7.2	7.2	Hz
Overswing Ratio	3.9	3.8	4.1	

Peak Vector Sum 9.44 mm/s at 0.942 sec

USBM RI8507 And OSMRE

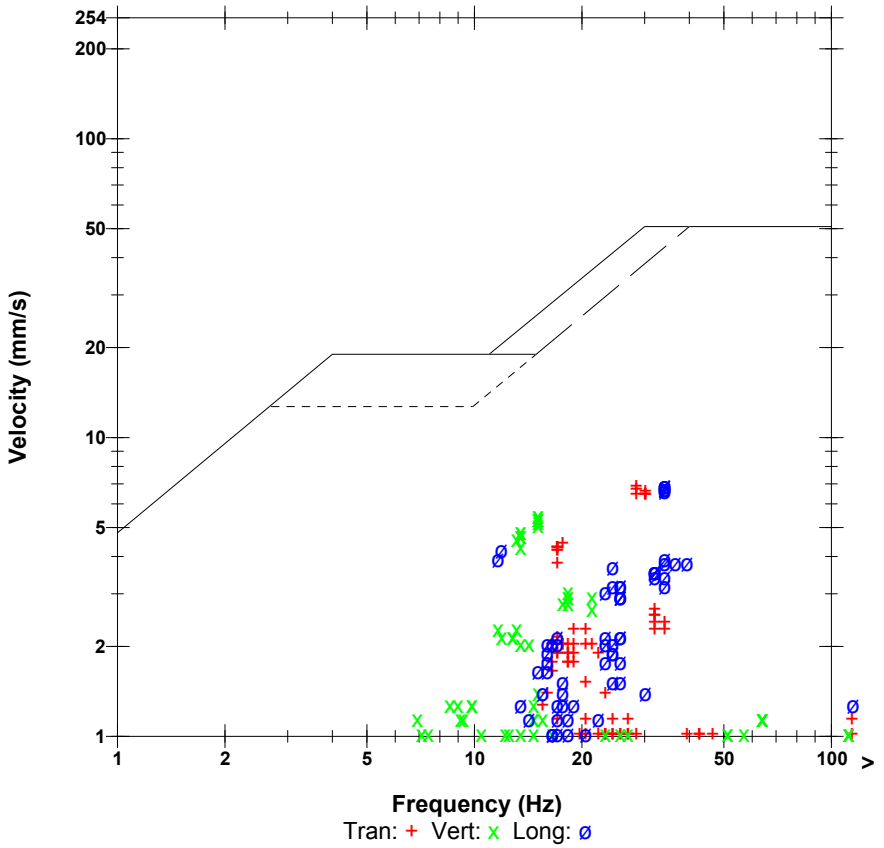

Monitor Log
Oct 29 /09 14:22:10 Oct 29 /09 14:22:16 Event recorded. (Memory Full Exit)

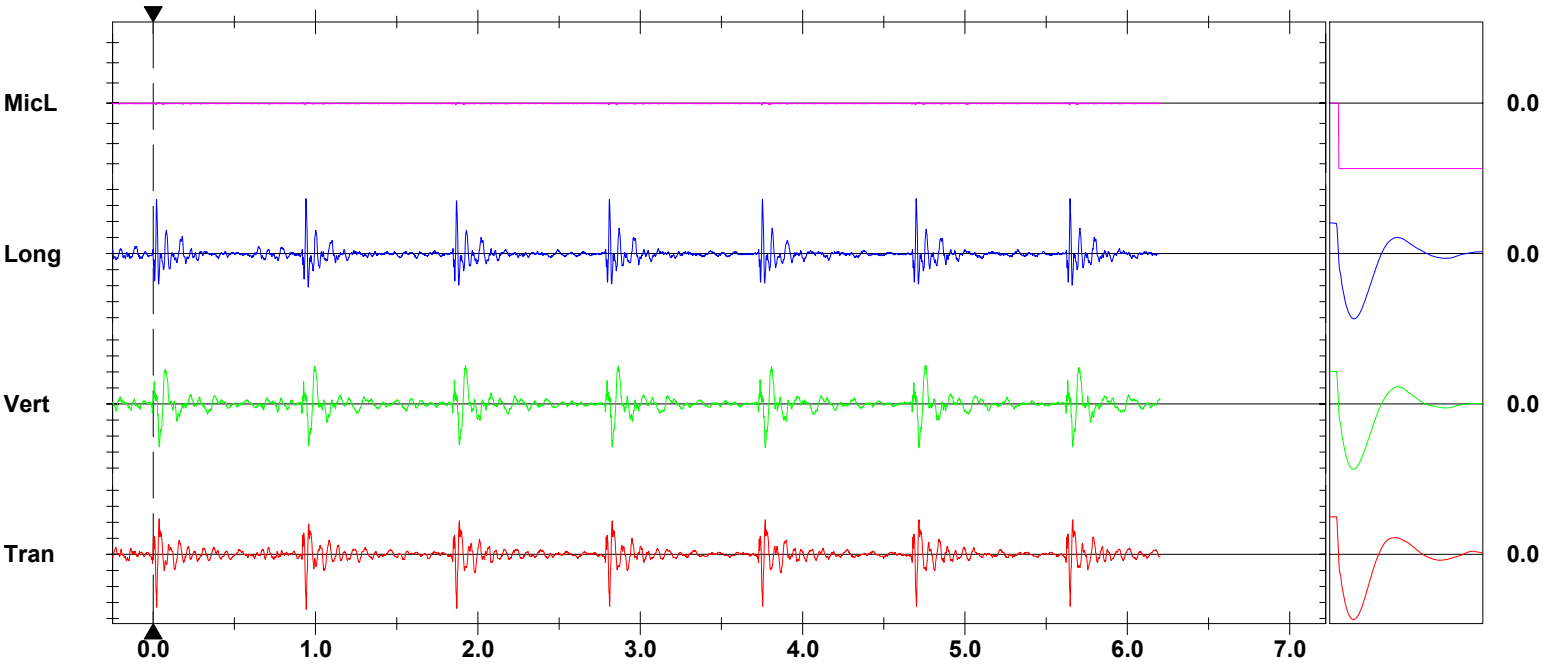

Time Scale: 0.50 sec/div **Amplitude Scale:** Geo: 2.00 mm/s/div Mic: 10.00 pa.(L)/div Sensorcheck
Trigger =

Field Vibration Data

Seismograph Unit # 8 on Concrete Block 2

at 9.2 feet from Test Pile #2

Event Report

Histogram Start Time	15:24:26 October 29, 2009	**Serial Number**	BE13054 V 8.12-8.0 MiniMate Plus
Histogram Finish Time	15:37:55 October 29, 2009	**Battery Level**	6.3 Volts
Number of Intervals	404 at 2 seconds	**Calibration**	December 7, 2007 by Instantel Inc.
Range	Geo :254 mm/s	**File Name**	O054CYFX.GQ0
Sample Rate	1024sps		
Job Number:	1		

Notes
Location:
Client:
User Name:
General:

Extended Notes

Post Event Notes

Microphone Linear Weighting
PSPL 1.00 pa.(L) on October 29, 2009 at 15:25:34
ZC Freq 39 Hz
Channel Test Check (Freq = 0.0 Hz Amp = 0 mv)

	Tran	Vert	Long	
PPV	14.0	37.3	24.3	mm/s
ZC Freq	34	20	24	Hz
Date	Oct 29 /09	Oct 29 /09	Oct 29 /09	
Time	15:31:18	15:25:34	15:25:34	
Sensorcheck	Passed	Passed	Passed	
Frequency	7.3	7.3	7.2	Hz
Overswing Ratio	3.9	3.9	4.1	

Peak Vector Sum 39.4 mm/s on October 29, 2009 at 15:25:34

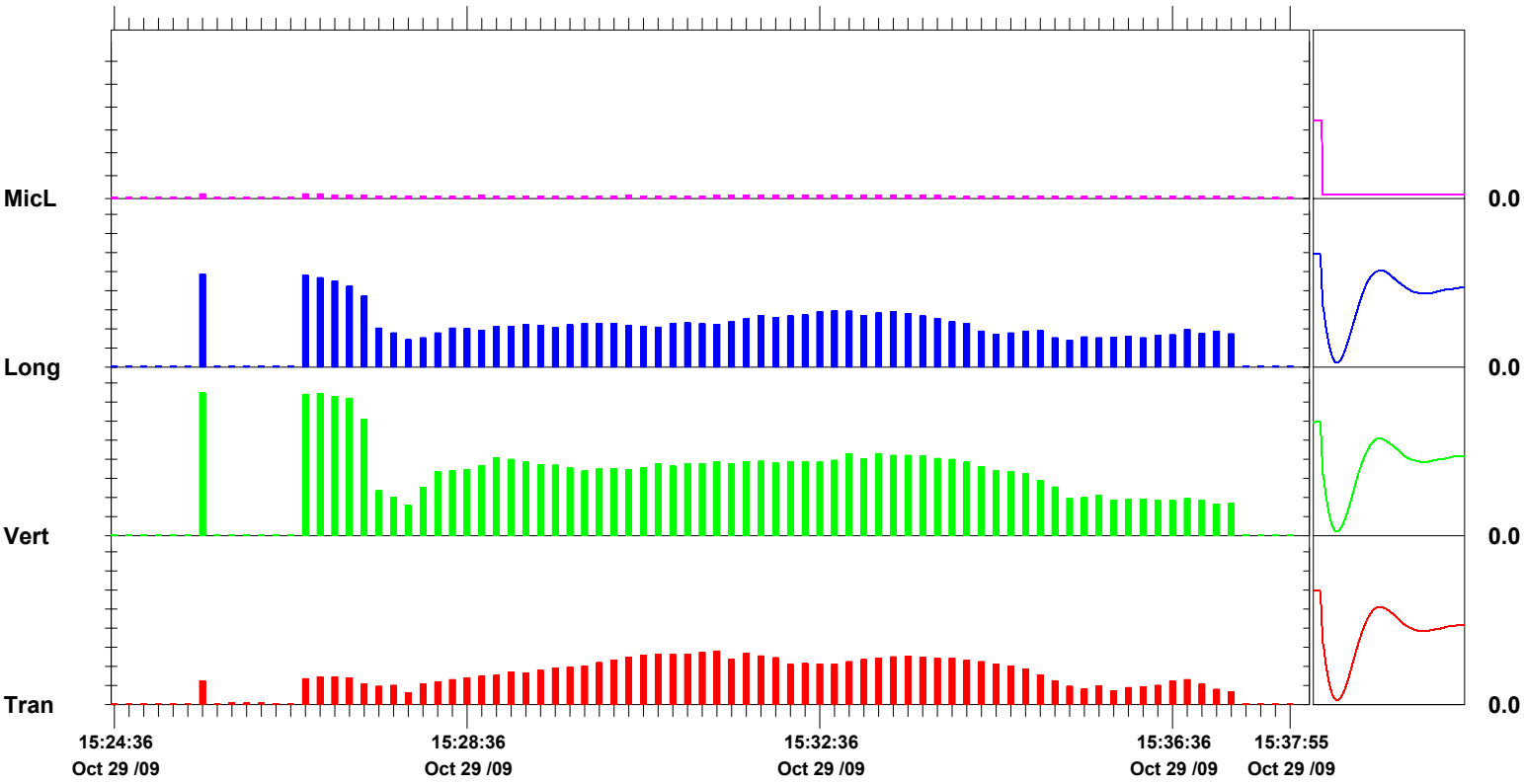

Time Scale: 10 seconds /div **Amplitude Scale:** Geo: 5.00 mm/s/div Mic: 5.00 pa.(L)/div Sensorcheck

Event Report

Date/Time	Long at 15:25:31 October 29, 2009	**Serial Number**	BE13054 V 8.12-8.0 MiniMate Plus
Trigger Source	Geo: 1.27 mm/s	**Battery Level**	6.4 Volts
Range	Geo :254 mm/s	**Calibration**	December 7, 2007 by Instantel Inc.
Record Time	8.0 sec at 1024 sps	**File Name**	O054CYFX.IJ0
Job Number:	1		

Notes
Location:
Client:
User Name:
General:

Extended Notes
Combo Mode October 29, 2009 15:24:26

Post Event Notes

Microphone Linear Weighting
PSPL 1.00 pa.(L) at 1.241 sec
ZC Freq 39 Hz
Channel Test Check (Freq = 0.0 Hz Amp = 0 mv)

	Tran	Vert	Long	
PPV	6.22	37.3	24.3	mm/s
ZC Freq	39	20	24	Hz
Time (Rel. to Trig)	2.491	2.502	2.512	sec
Peak Acceleration	0.225	0.729	0.756	g
Peak Displacement	0.0510	0.258	0.136	mm
Sensorcheck	Passed	Passed	Passed	
Frequency	7.3	7.3	7.2	Hz
Overswing Ratio	3.9	3.9	4.1	

Peak Vector Sum 39.4 mm/s at 2.502 sec

USBM RI8507 And OSMRE

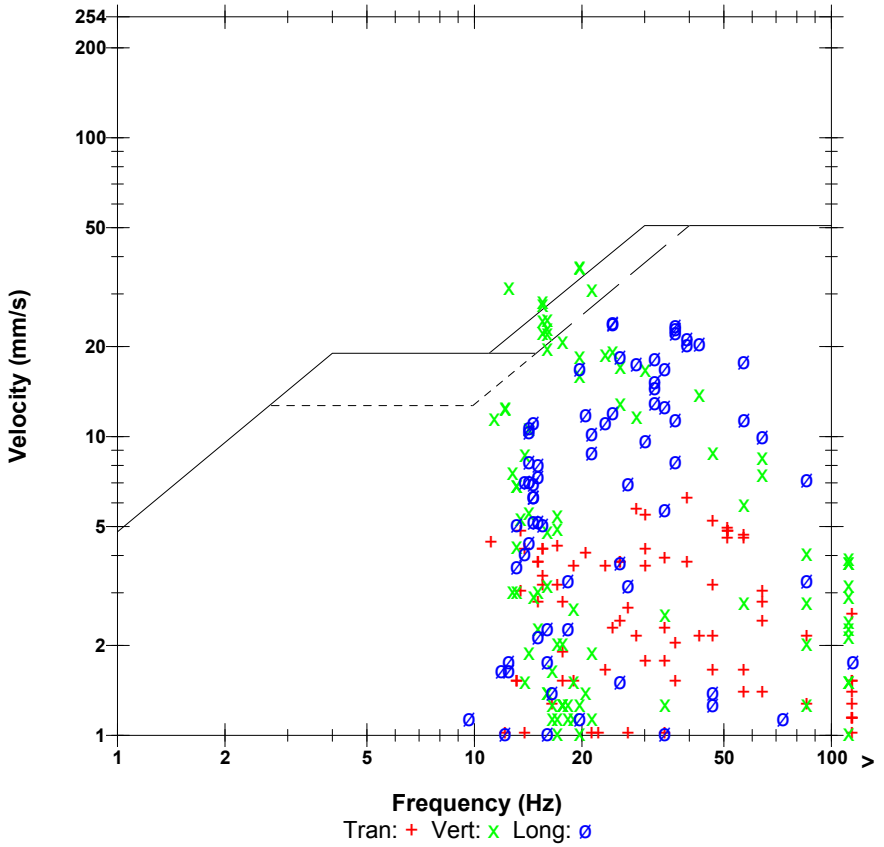

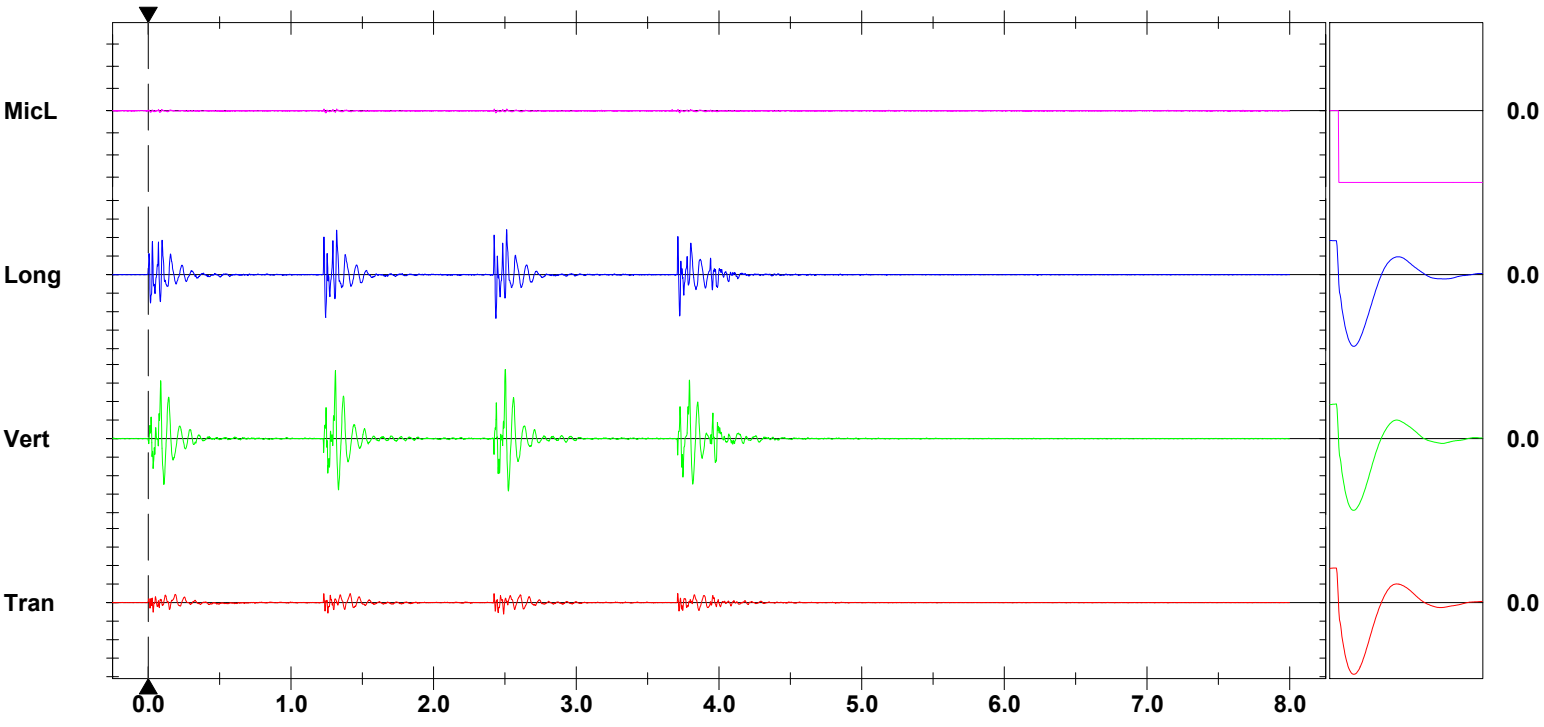

Time Scale: 0.50 sec/div **Amplitude Scale:** Geo: 10.00 mm/s/div Mic: 10.00 pa.(L)/div Sensorcheck
Trigger =

Event Report

Date/Time	Vert at 15:26:45 October 29, 2009	**Serial Number**	BE13054 V 8.12-8.0 MiniMate Plus
Trigger Source	Geo: 1.27 mm/s	**Battery Level**	6.4 Volts
Range	Geo :254 mm/s	**Calibration**	December 7, 2007 by Instantel Inc.
Record Time	8.0 sec at 1024 sps	**File Name**	O054CYFX.KL0
Job Number:	1		

Notes
Location:
Client:
User Name:
General:

Extended Notes
Combo Mode October 29, 2009 15:24:26

Post Event Notes

Microphone Linear Weighting
PSPL 1.00 pa.(L) at 0.016 sec
ZC Freq 47 Hz
Channel Test Check (Freq = 0.0 Hz Amp = 0 mv)

	Tran	Vert	Long	
PPV	7.24	37.2	24.0	mm/s
ZC Freq	37	18	22	Hz
Time (Rel. to Trig)	2.618	2.630	1.364	sec
Peak Acceleration	0.199	0.756	0.742	g
Peak Displacement	0.0437	0.269	0.154	mm
Sensorcheck	Passed	Passed	Passed	
Frequency	7.3	7.3	7.2	Hz
Overswing Ratio	3.9	3.9	4.1	

Peak Vector Sum 38.6 mm/s at 1.354 sec

USBM RI8507 And OSMRE

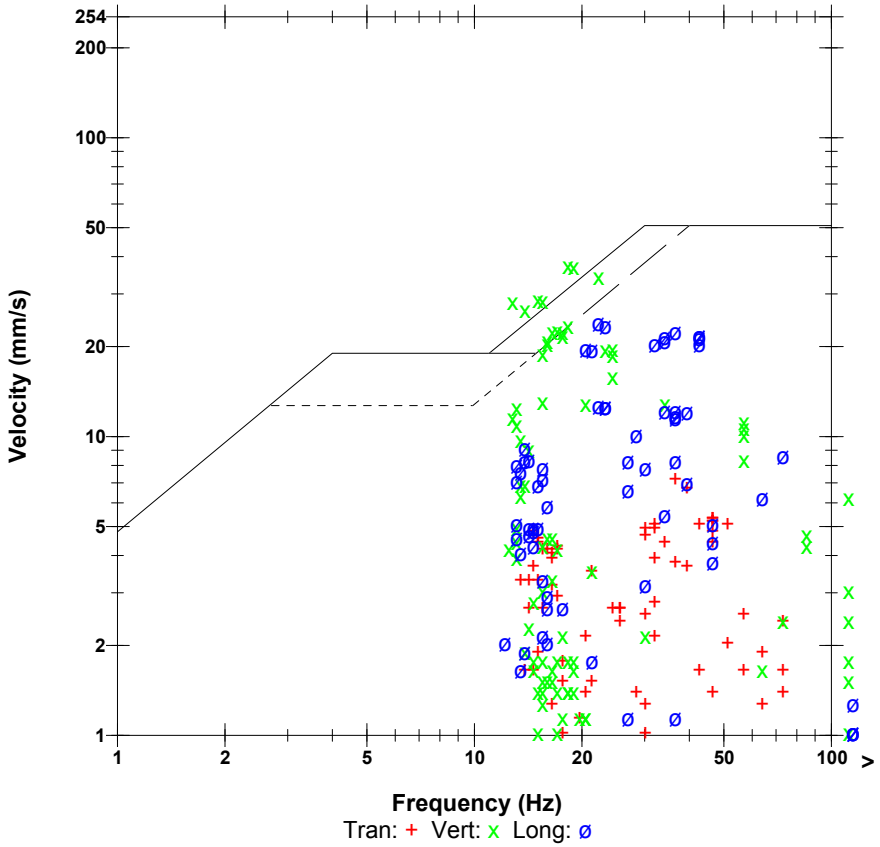

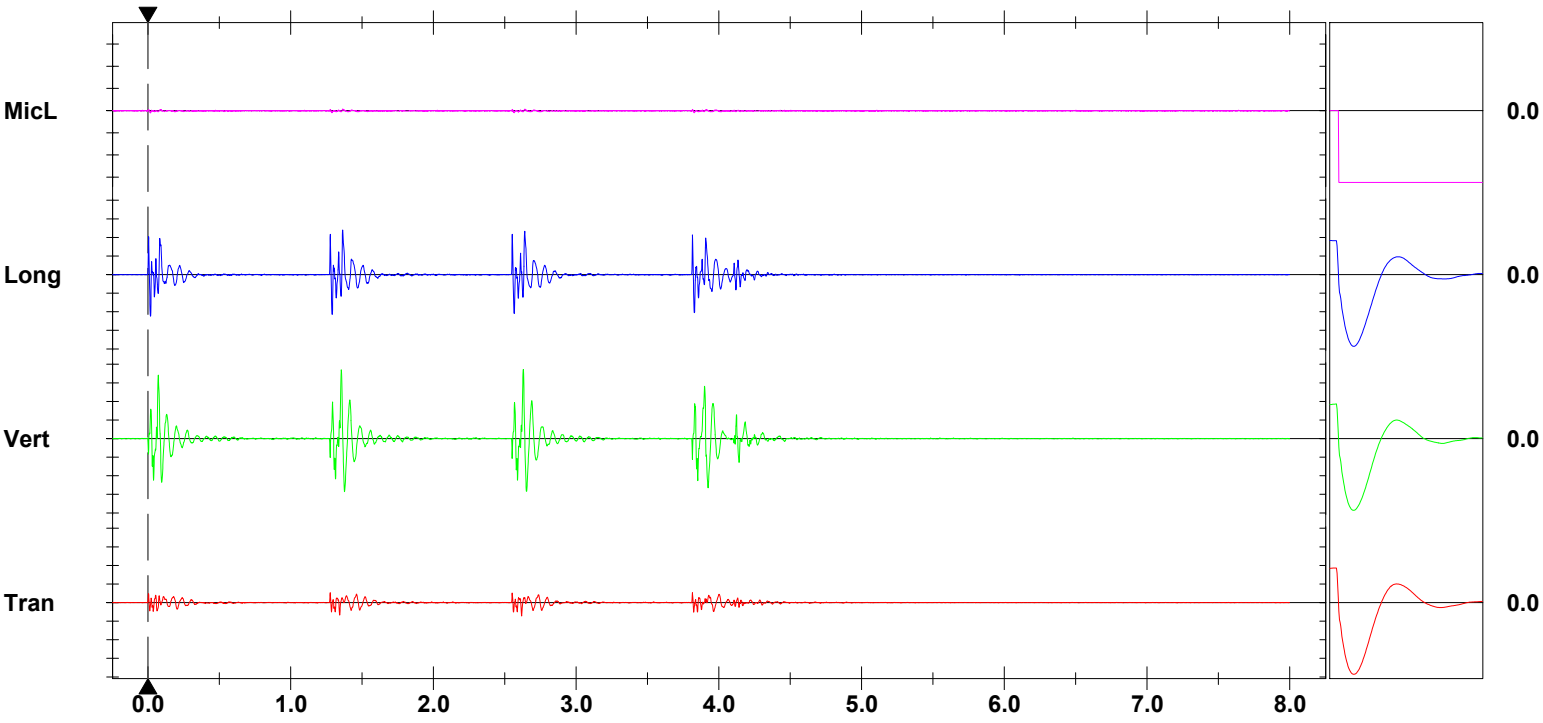

Time Scale: 0.50 sec/div **Amplitude Scale:** Geo: 10.00 mm/s/div Mic: 10.00 pa.(L)/div Sensorcheck
Trigger =

Event Report

Date/Time Vert at 15:27:01 October 29, 2009
Trigger Source Geo: 1.27 mm/s
Range Geo :254 mm/s
Record Time 5.743 sec at 1024 sps
Job Number: 1

Serial Number BE13054 V 8.12-8.0 MiniMate Plus
Battery Level 6.4 Volts
Calibration December 7, 2007 by Instantel Inc.
File Name O054CYFX.L10

Notes
Location:
Client:
User Name:
General:

Extended Notes
Combo Mode October 29, 2009 15:24:26

Post Event Notes

Microphone Linear Weighting
PSPL 0.750 pa.(L) at 0.014 sec
ZC Freq 43 Hz
Channel Test Check (Freq = 0.0 Hz Amp = 0 mv)

	Tran	Vert	Long	
PPV	7.24	36.4	22.5	mm/s
ZC Freq	28	18	20	Hz
Time (Rel. to Trig)	1.349	1.359	1.371	sec
Peak Acceleration	0.199	0.636	0.676	g
Peak Displacement	0.0457	0.256	0.158	mm
Sensorcheck	Passed	Passed	Passed	
Frequency	7.3	7.3	7.2	Hz
Overswing Ratio	3.9	3.9	4.1	

Peak Vector Sum 38.2 mm/s at 1.359 sec

USBM RI8507 And OSMRE

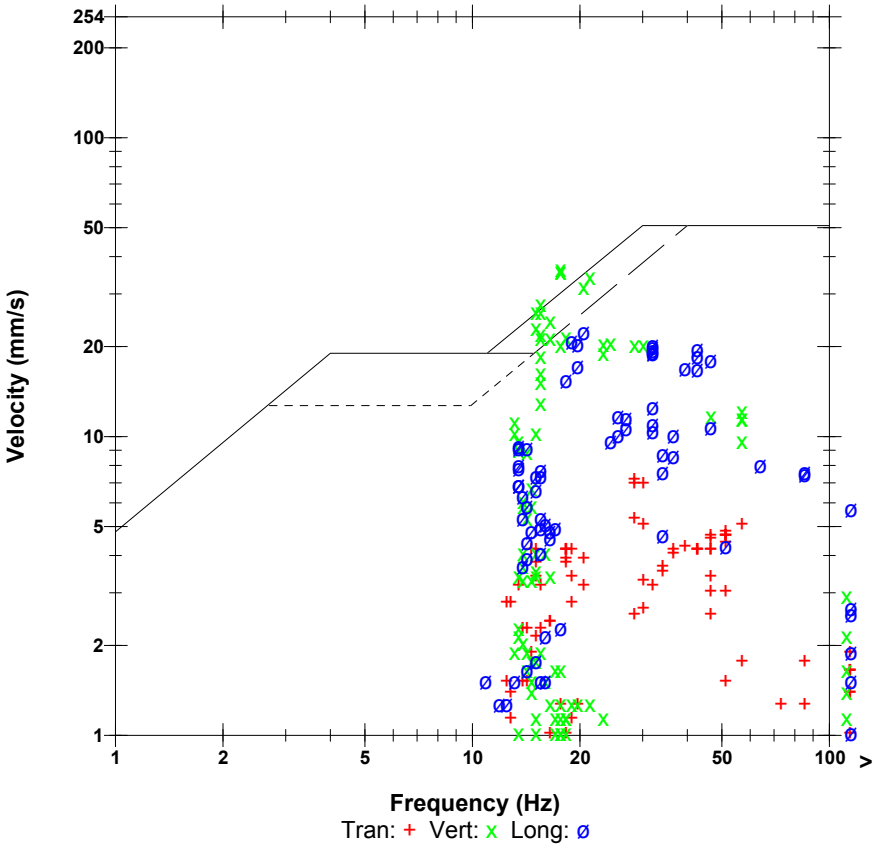

Monitor Log
Oct 29 /09 15:27:01 Oct 29 /09 15:27:07 Event recorded. (Memory Full Exit)

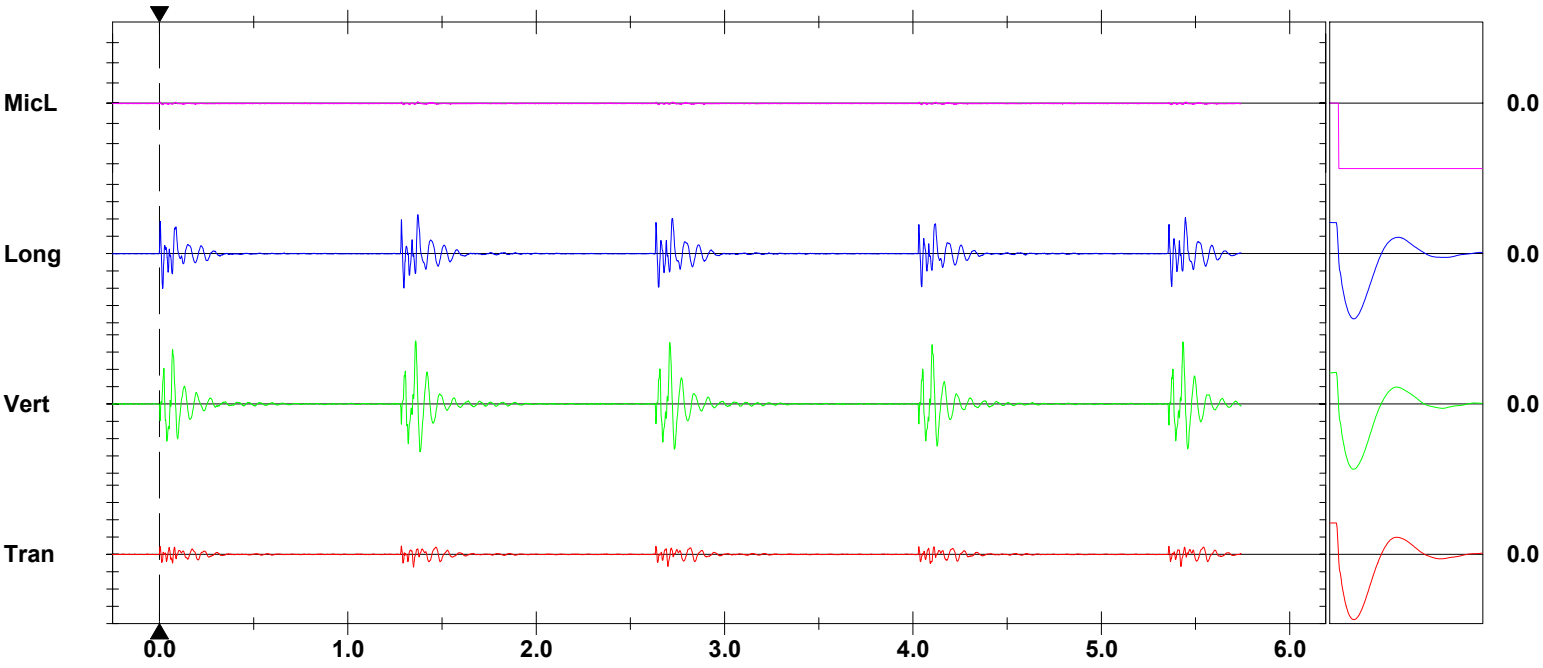

Time Scale: 0.50 sec/div **Amplitude Scale:** Geo: 10.00 mm/s/div Mic: 10.00 pa.(L)/div Sensorcheck
Trigger =

Field Vibration Data

Seismograph Unit # 8 in casing

at 26.7 feet from Test Pile #1

Non Driving Event

Event Report

Histogram Start Time	22:33:58 December 21, 2009	**Serial Number**	BE13054 V 8.12-8.0 MiniMate Plus
Histogram Finish Time	23:04:43 December 21, 2009	**Battery Level**	6.3 Volts
Number of Intervals	922 at 2 seconds	**Calibration**	December 7, 2007 by Instantel Inc.
Range	Geo :254 mm/s	**File Name**	O054D16M.OM0
Sample Rate	1024sps		
Job Number:	1		

Notes
Location:
Client:
User Name:
General:

Extended Notes

Post Event Notes

Microphone	Linear Weighting
PSPL	11.8 pa.(L) on December 21, 2009 at 22:48:18
ZC Freq	30 Hz
Channel Test	Passed (Freq = 20.5 Hz Amp = 739 mv)

	Tran	Vert	Long	
PPV	0.127	0.254	0.127	mm/s
ZC Freq	>100	>100	>100	Hz
Date	Dec 21 /09	Dec 21 /09	Dec 21 /09	
Time	22:34:00	22:38:06	22:34:00	
Sensorcheck	Check	Check	Check	
Frequency	1024.0	1024.0	17.4	Hz
Overswing Ratio	0.0	0.0	1.5	

Peak Vector Sum 0.254 mm/s on December 21, 2009 at 22:38:06

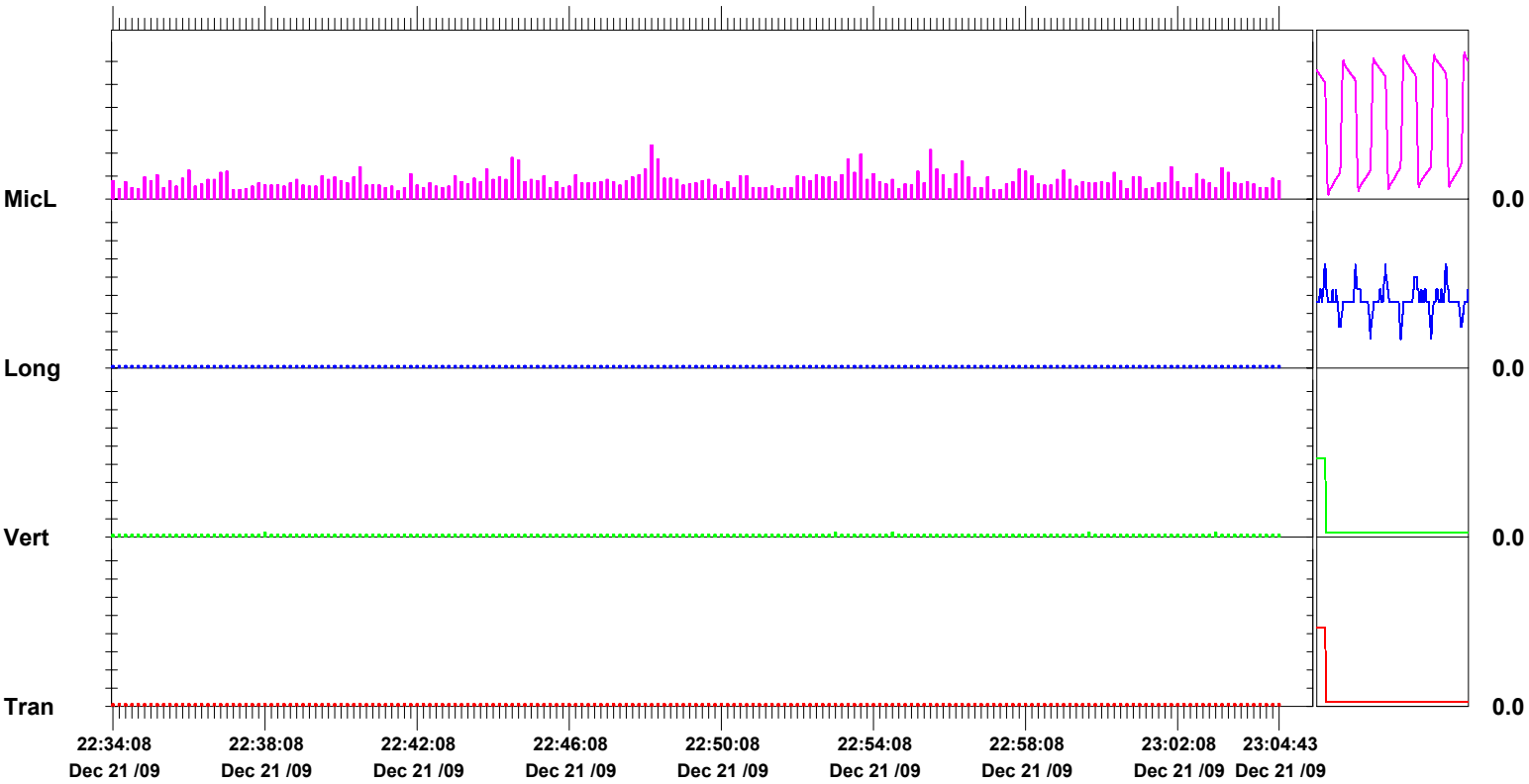

Time Scale: 10 seconds /div **Amplitude Scale:** Geo: 1.000 mm/s/div Mic: 5.00 pa.(L)/div Sensorcheck

Event Report

Histogram Start Time	23:31:30 December 21, 2009	**Serial Number**	BE13054 V 8.12-8.0 MiniMate Plus
Histogram Finish Time	23:55:34 December 21, 2009	**Battery Level**	6.3 Volts
Number of Intervals	722 at 2 seconds	**Calibration**	December 7, 2007 by Instantel Inc.
Range	Geo :254 mm/s	**File Name**	O054D16P.CI0
Sample Rate	1024sps		
Job Number:	1		

Notes
Location:
Client:
User Name:
General:

Extended Notes

Post Event Notes

Microphone Linear Weighting
PSPL 2.00 pa.(L) on December 21, 2009 at 23:35:22
ZC Freq 13 Hz
Channel Test Passed (Freq = 20.5 Hz Amp = 752 mv)

	Tran	Vert	Long	
PPV	0.127	0.254	0.127	mm/s
ZC Freq	>100	>100	>100	Hz
Date	Dec 21 /09	Dec 21 /09	Dec 21 /09	
Time	23:31:32	23:43:16	23:31:32	
Sensorcheck	Check	Check	Check	
Frequency	1024.0	1024.0	33.0	Hz
Overswing Ratio	0.0	0.0	2.0	

Peak Vector Sum 0.254 mm/s on December 21, 2009 at 23:43:16

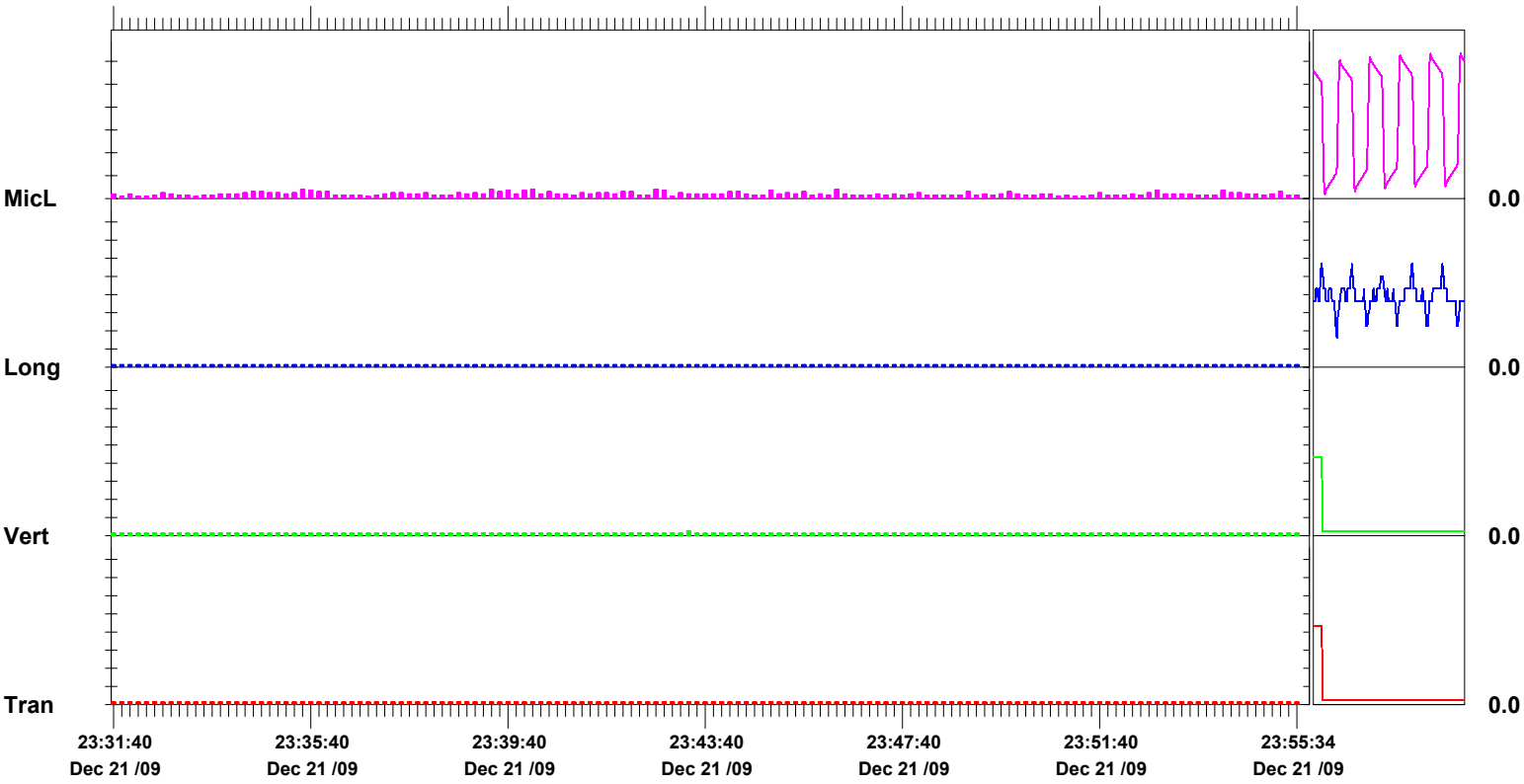

Time Scale: 10 seconds /div **Amplitude Scale:** Geo: 1.000 mm/s/div Mic: 5.00 pa.(L)/div Sensorcheck

Wisconsin Highway Research Program
University of Wisconsin-Madison
1415 Engineering Drive
Madison, WI 53706
608/262-3835
www.whrp.org